ICES COOPERATIVE RESEARCH REPORT

RAPPORT DES RECHERCHES COLLECTIVES

NO. 225

North Atlantic-Norwegian Sea Exchanges: The ICES NANSEN Project

Edited by

Dr B. Hansen and Dr S. Østerhus

ISSN 2707-7144
ISBN 978-87-7482-442-8

International Council for the Exploration of the Sea
Conseil International pour l'Exploration de la Mer

Palægade 2–4 DK-1261 Copenhagen K Denmark

November 1998

https://doi.org/10.17895/ices.pub.5517

North Atlantic–Norwegian Sea Exchanges: the ICES NANSEN Project

Contents

ICES NANSEN (North Atlantic–Norwegian Sea Exchanges) Project

Introduction

Bogi Hansen and Svein Østerhus

Editors

The ICES NANSEN (North Atlantic - Norwegian Sea Exchanges) project was initiated by Council Resolution 1985/4:9 to study the exchanges of water, heat, and other properties across the Greenland-Scotland Ridge between the Atlantic Ocean and the areas northeast of the ridge. Across this ridge, warm, saline water makes its way north-eastward in the upper layers while cold, fresher water returns south-westward partly in the upper layers along the Greenland coast and partly as deep overflows at several locations across the ridge. These exchanges are of major importance for the global thermohaline circulation as well as for the regional climate of the Nordic Seas and the Arctic with their surrounding landmasses. ICES has long recognised the importance of these flows by mounting the Overflow '60 and Overflow '73 experiments which focused mainly on the cold, deep overflows. The NANSEN Project was initiated to study in more detail the Atlantic water flow north-eastward over the ridge as well as the return flows, with most emphasis on the eastern part of the area.

The field work within NANSEN started in 1986 and continued with cruises every year, operated by a number of ICES member countries as co-ordinated by the ICES Working Group on Oceanic Hydrography until the field phase was declared finished by the end of 1990. Hydrographic data from the project are stored at the ICES Oceanographical Data Centre while the British Oceanographic Data Centre (BODC) has stored the current meter data.

Results from the project have been published in various journals. This *Cooperative Research Report* is a collection of papers that originally were presented at ICES Statutory Meetings, especially at the NANSEN session of the Hydrography Committee during the 1991 meeting in La Rochelle, France. In addition, the first paper in the volume is an attempt to summarise our present understanding of the problems addressed by the NANSEN project based on results from the project as well as from other studies, old and new.

North Atlantic–Norwegian Sea Exchanges: the ICES NANSEN Project

B. Hansen[1], S. Østerhus[2], W. J. Gould[3], and L. J. Rickards[4]

[1]Fiskirannsóknarstovan, PO Box 3051, FO-110 Tórshavn, Faroe Islands. [2]Geophysical Institute, Allegaten 70, Bergen, Norway. [3]Southhampton Oceanography Centre, Empress Dock, Southampton, SO14 3ZH, UK. [4]British Oceanographic Data Centre, CCMS Proudman Oceanographic Laboratory, Bidston Observatory, Birkenhead, Merseyside, L43 7RA, UK.

The North Atlantic has a large northward transport of heat that extends to high latitudes. This heat flux and its interaction with the prevailing westerly winds moderates the climate of western Europe. In the Arctic and Subarctic seas the warm Atlantic water is converted to colder water masses that return southward via gaps in the Scotland-Greenland Ridge. ICES has long recognised the importance of these cold return flows by mounting the Overflow '60 and Overflow '73 experiments. The NANSEN Project was initiated to study in more detail the Atlantic water flow northward over the ridge as well as the return flows, focusing on the eastern part of the area. The project was co-ordinated by the ICES Working Group on Oceanic Hydrography. Several of cruises were made by various ICES Member Countries in the latter half of the 1980s in connection with the project. In this paper an overview of the data sets acquired during the project is given and the state of knowledge on the exchanges especially across the eastern part of the Greenland-Scotland Ridge is reviewed based on results from NANSEN and from other sources. The accumulated evidence allows us to describe the exchanges in fair detail; the origins of the waters, the patterns of their flow towards and over the ridge and their ultimate fate. Quantitative estimates for the volume transport of the overflows seem reasonably well established, and flux estimates of the Atlantic inflows to the Nordic Seas are approaching acceptable levels of confidence. There is also increasing information on temporal variations of the exchanges although dynamical changes are still not well understood. It should be stressed that both the overflow and the Atlantic inflow to the Nordic Seas occur through several different branches which may be produced and affected by different processes and that the ocean regions where they ultimately deliver their water mass character are different as well.

Keywords: Thermohaline circulation, Northeast Atlantic, Atlantic inflow, Overflow

North Atlantic–Norwegian Sea Exchanges: the ICES NANSEN Project

Contents

Introduction

The submarine ridges that lie between Greenland and the northern tip of the United Kingdom constitute a partial barrier to the flow of water between the North Atlantic and the ocean areas north of the barrier. Across these ridges, known collectively as The Greenland-Scotland Ridge, warm, saline water makes its way northeastward in the upper layers while cold, fresher water returns southwestward partly in the upper layers along the Greenland coast and partly at depth at several locations across the ridge. This deep "overflow" of cold, dense water results from cooling and subsequent sinking of upper layer waters in the areas north of the Greenland-Scotland Ridge and, after passing the ridge and entrainment of surrounding Atlantic water, it forms the deeper component of the North Atlantic Deep Water (NADW). The water exchange across the ridges thus plays a key role in the global thermohaline circulation.

The International Council for the Exploration of the Sea (ICES) has for many years had an interest in the area and has sponsored two major initiatives to study the overflow: "Overflow '60" (Tait, 1967) and "Overflow '73". The overflow is, however, only part of the problem, since northeastward transport of salt in the upper layers is a prerequisite for sufficiently dense upper waters to initiate deep water formation. Also, the heat transported by the Atlantic inflows to the Nordic Seas determines both the oceanic and atmospheric climate of the region. Sponsored by "Nordisk Kollegium for Fysisk Oceanografi", a Nordic programme to study the Atlantic water flow over the ridge was initiated in the mid-1980s and the ICES Hydrography Committee encouraged intensified research on the whole question of the water exchange across the Greenland-Scotland Ridge (Council Resolution 1985/4:9). The resulting activity was co-ordinated within the Oceanic Hydrography Working Group of ICES as the NANSEN (North Atlantic - Norwegian Sea Exchanges) Project. For logistical reasons, the NANSEN Project was focused on the eastern part of the area, the Iceland-Scotland Gap, but results from the Denmark Strait have been included also especially with regard to the Atlantic water inflow. The outstanding problems to be addressed by the Project were:

1. The origins and characteristics of the upper ocean water masses feeding the Norwegian Sea.

2. The pathways and temporal variations of these inflows.

3. The characteristics and long-term variations of the outflows to the North Atlantic.

4. Quantification of the exchanges of water, salt and heat between the North Atlantic and the ocean areas north of the Greenland-Scotland Ridge.

This *Cooperative Research Report* is intended to document some of the results obtained during the Project that were presented in scientific papers which were presented at ICES Statutory Meetings, especially at the NANSEN session of the Hydrography Committee during the 1991 meeting in La Rochelle, France. At that meeting a preliminary overview was presented (Dooley *et al.*, 1991). This paper is an update of that overview. It also attempts to summarise our present understanding of the problems addressed by the NANSEN Project based on results from the Project as well as from other studies, old and new.

In this paper, a complete coverage of the Atlantic water inflow to the Nordic Seas has been attempted. With regard to the outflows, the focus has been on the Iceland - Scotland region with only a brief summary of the outflows over the westernmost part of the ridges, i.e. the East Greenland Current and the Denmark Strait overflow, since these were only touched upon sporadically during the Project.

Implementation and results of the NANSEN Project

The fieldwork within NANSEN started in 1986 and continued with cruises every year until the field phase was declared finished by the end of 1990. At an early stage it was decided that the ICES Oceanographic Data Centre would store the hydrographic data while the British Oceanographic Data Centre (BODC) would store the current meter data.

Hydrographic station data. Station data from all NANSEN cruises were compiled by the ICES Oceanographic Data Centre. This included the post-cruise submission of ROSCOP forms that served as a means of tracking and cataloguing of the data sets following their submission to ICES. Table 1 is a list of cruises compiled from the information stored in the ICES ROSCOP catalogue, and indicates the ships which took part, either informally or formally, in the NANSEN Project.

Not all the data have been submitted to ICES, but still the data set currently (beginning of 1998) contains a somewhat larger number of stations than the

Table 1. Cruises flagged at ICES as NANSEN cruises. Also shown are the number of hydrographic stations using water bottle (WB) or CTD observations, and the actual number submitted to the ICES Oceanographic Data Centre

IOC	Ship	Period	Number of stations with		Number at ICES
Code			WB	CTD	
26	Magnus Heinason	25 Apr to 04 May 86		11	0
26	Magnus Heinason	05 Jun to 16 Jun 86		101	57
26	Magnus Heinason	07 Aug to 19 Aug 86		51	0
58	Haakon Mosby	01 Jun to 17 Jun 86		65	65
26	Magnus Heinason	23 Apr to 06 May 87		100	0
26	Magnus Heinason	03 Jul to 14 Jul 87		187	175
26	Magnus Heinason	26 Aug to 08 Sep 87		54	0
06	Gauss 2	02 Jul to 14 Aug 87		83	82
46	Bjarni Saemundsson	03 Sep to 22 Sep 87	64		64
64	Tydeman	11 Sep to 05 Oct 87		20	20
58	Eldjarn	16 Mar to 11 Apr 87		63	63
58	G.O.Sars	28 Jul to 16 Aug 87		105	105
58	Haakon Mosby	27 Jun to 10 Jul 87		165	165
74	Challenger	09 May to 05 Jun 87		88	87
74	Cirolana	19 Jun to 20 Jul 87		123	123
74	Frederick Russell	04 Aug to 24 Aug 87		206	206
74	Frederick Russell	27 Aug to 19 Sep 87		166	117
74	Scotia	17 Jun to 07 Jul 87	12	34	11
74	Scotia	09 Sep to 29 Sep 87	101	67	89
26	Magnus Heinason	23 Apr to 02 May 88		101	0
26	Magnus Heinason	20 May to 01 Jun 88		164	20
26	Magnus Heinason	11 Aug to 28 Aug 88		95	0
06	Gauss	15 Jun to 16 Jul 88		83	71
58	Haakon Mosby	29 Apr to 02 May 88		119	119
74	Challenger	Feb to 07 Mar 88	87	62	0
74	Challenger	06 Jun to 23 Jun 88	142	147	146
74	Gorsethorn	23 Oct to 06 Nov 88	13	11	21
58	Haakon Mosby	26 May to 06 Jun 89		61	61

Table 2. Moorings deployed within the NANSEN programme as reported to BODC.

Latitude		Longitude		Botto m	Instrument heights	Start	Dur.
dd	mm.m	ddd	mm.m h	metres	metres	dd.mm.yy	days
60	13.3N	8	37.3W	892	174, 17	10.06.88	no data
60	13.5N	8	37.0W	900	170, 15	02.03.88	99
60	15.6N	8	45.1W	1115	171, 20	06.09.87	?
60	17.4N	8	46.8W	710	440, 171, 20	06.09.87	177
60	17.4N	8	46.1W	712	430, 170, 15	02.03.88	99
60	17.8N	8	47.7W	692	446, 183, 17	10.06.88	no data
60	49.8N	5	31.5W	595	290, 40	04.07.87	83
60	40.9N	4	56.5W	978	690, 440	04.07.87	83
60	01.2N	3	02.1W	108	76, 28	22.06.88	102
60	07.6N	2	21.8W	112	80, 11	22.06.88	no data
60	07.7N	2	22.0W	110	76, 14	20.09.87	73
60	50.9N	0	30.6W	112	79, 10	26.04.90	no data
60	53.0N	0	44.8E	146	112, 10	26.04.90	154
60	53.2N	2	28.7E	128	93	27.04.90	64
60	53.2N	2	28.7E	128	10	27.04.90	64
61	40.1N	19	11.7W	1983	1499, 1204, 702	02.08.87	275
61	44.3N	15	23.9W	2291	2281	16.07.90	403
61	49.9N	15	37.4W	2306	2296, 1975	16.07.90	397
61	16.8N	8	04.5W	767	22	08.10.89	?
61	16.8N	8	04.0W	769	22	22.10.89	no data
61	18.9N	8	15.3W	520	200, 10	27.05.87	307
61	19.1N	8	14.9W	499	10	07.10.89	38
61	20.2N	8	12.3W	703	401, 301, 211, 10	28.05.87	362
61	20.5N	8	13.7W	695	311,310,210,110,10	07.10.89	38
61	21.0N	8	10.0W	840	?	07.10.89	no data
61	21.1N	8	09.8W	840	411.410,310,210,110,10	08.10.89	37
61	21.7N	8	08.6W	824	550, 300, 60	28.05.87	no data
61	24.2N	8	10.2W	769	306, 110	09.10.89	no data
61	24.2N	8	10.2W	769	10	09.10.89	no data
61	24.2N	8	05.3W	734	459, 259, 9	28.05.87	no data
61	25.1N	8	07.3W	?	210, 110, 10	08.10.89	no data
61	26.0N	8	03.0W	504	201, 8	27.05.87	?
61	26.5N	8	05.5W	435	10	05.10.89	40
61	26.7N	8	13.3W	746	32, 22	16.03.86	50
61	26.9N	8	00.4W	315	8	27.05.87	no data
61	27.1N	8	17.4W	745	22	09.10.89	38
61	30.5N	8	22.9W	737	20	31.05.87	?
61	33.2N	8	47.2W	724	20	30.05.87	?
61	06.8N	7	51.1W	762	23	22.05.88	?
61	22.0N	7	52.1W	745	23	22.05.88	?
62	53.7N	35	51.5W	2640	660, 110	09.09.86	289
62	54.1N	35	06.4W	2706	803, 100	28.06.87	367
62	54.4N	35	06.6W	2706	835, 60, 19	04.07.88	359
62	38.4N	34	30.4W	2835	803,100	28.06.87	117
62	39.2N	34	30.9W	2827	775, 60, 19	04.07.88	358
62	47.0N	34	48.1W	2756	325, 63	02.07.89	246
62	47.0N	34	48.1W	2756	20	02.07.89	133
62	43.1N	16	49.2W	1800	1135, 1790, 1465	15.07.90	402
62	23.5N	7	40.3W	100	100, 100	23.10.89	20
62	59.7N	6	12.1W	1415	1310,1209,1108,907,404	15.05.87	7

Latitude		Longitude		Botto m	Instrument heights	Start	Dur.
dd	mm.m	ddd	mm.m h	metres	metres	dd.mm.yy	days
62	50.1N	5	11.7W	1002	847, 498, 50	03.06.86	18
63	36.3N	37	01.9W	1648	401, 100	27.06.87	98
63	23.0N	36	05.3W	2153	365, 63, 20	03.07.89	246
63	25.8N	36	34.2W	2046	510, 110	09.09.86	289
63	28.9N	36	17.9W	1984	60, 19, 362	03.07.88	360
63	29.1N	36	17.4W	1986	401, 100	27.06.87	369
63	33.4N	36	30.3W	1767	365, 63, 20	03.07.89	247
63	37.2N	36	43.8W	1660	362, 60, 19	03.07.88	360
63	39.4N	36	51.5W	1445	265, 63, 20	04.07.89	63
63	41.7N	36	59.2W	1260	262, 60, 19	03.07.88	242
63	42.4N	36	58.3W	1220	301, 100	26.06.87	370
63	00.0N	35	20.1W	2634	405, 63, 20	02.07.89	246
63	07.0N	35	33.3W	2572	703, 100	28.06.87	368
63	07.1N	35	32.5W	2569	674, 60, 19	04.07.88	340
63	12.1N	35	43.7W	2463	437, 63, 20	02.07.89	399
63	16.7N	35	53.6W	2355	601, 100	27.06.87	368
63	16.7N	35	52.2W	2345	612, 60, 19	04.07.88	360
63	37.3N	32	55.6W	2738	1104	12.07.90	383
63	37.3N	32	55.6W	2738	602, 100, 18	12.07.90	383
63	08.6N	17	17.8W	1028	1018	15.07.90	395
63	04.3N	6	10.5W	1688	1591,1490,1389,1188,686	15.05.87	8
63	09.0N	6	04.3W	1893	1791,1690,1589,1386,884	15.05.87	7
63	30.1N	5	35.4W	2012	1802, 1052, 1052, 102	03.06.86	no data
63	10.5N	4	59.6W	2357	2097, 1847, 1350, 401	03.06.86	19
64	43.2N	34	06.3W	1142	202, 60, 18	12.07.90	382
64	01.9N	33	21.2W	2345	822, 60, 18	12.07.90	no data
64	16.3N	33	37.8W	2001	752, 370,18	12.07.90	369
64	25.8N	33	46.8W	1731	202, 60	12.07.90	382
64	25.8N	33	46.8W	1731	18	12.07.90	100
64	33.0N	33	55.6W	1494	502, 100, 18	12.07.90	371
64	45.0N	30	33.0W	2200	1002, 521, 20	09.03.90	122
64	54.8N	30	40.1W	2005	850, 99, 18	09.03.90	122
65	17.9N	31	06.9W	1080	400, 99, 18	09.03.90	122
65	09.9N	30	47.0W	1500	620, 269, 18	09.03.90	122
65	15.3N	30	50.9W	1200	450, 99, 19	09.03.90	122
68	22.0N	10	52.8E	1020	949,873,748,499,249,5	23.09.89	31
68	26.5N	10	59.5E	1080	953, 877, 502	22.09.89	33
68	27.0N	10	39.5E	1545	1455	24.09.89	32
68	28.6N	10	33.2E	2035	1952, 1872, 991, 8	23.09.89	30
68	18.2N	11	04.3E	210	154, 78, 4	24.09.89	29
68	40.9N	12	12.5E	985	502	21.09.89	33
62	49.0N	6	08.0W	500	450, 400, 300, 30	30.06.87	8
62	33.0N	4	40.0W	550	500, 450, 350, 30	29.06.87	8
62	45.0N	4	28.0W	1000	950, 900, 700, 500	29.06.87	8
62	13.0N	3	23.0W	600	550, 500, 300, 30	29.06.87	8
62	27.0N	6	10.1W	89	49	05.06.86	11
62	40.6N	6	09.6W	195	150, 20	05.06.86	11
62	15.4N	6	03.4W	101	51	02.07.87	10
62	14.3N	5	01.9W	197	90	02.07.87	8
62	12.5N	4	05.9W	353	50	02.07.87	8

Overflow'60 and Overflow'73 data sets. At about half of these stations nutrient measurements were also made. The distribution of all submitted NANSEN stations is shown in Figure 1, from which it can be clearly seen that most of them were worked within 200 nautical miles of the Faroe Islands. The NANSEN data set is more compact than the Overflow data sets that were more focused in time but broader in scale, in order to meet its scientific objectives. The submitted Overflow and NANSEN hydrographic data sets are available from ICES.

Moored instrument data. Data from 100 moored current meter stations have been submitted to the BODC in its capacity as data centre for current meter data for NANSEN. Table 2 lists main features of these stations and their location is shown in Figure 2. As is the case of the station data, most mooring positions were within 200 nautical miles of the Faroe Islands. The data are available from BODC.

Main features of bottom topography, and water exchange

The overview presented in this chapter is intended to give the reader a framework to help structure the more detailed discussion to follow. The information presented here on currents and water masses will be elaborated and justified in the following chapters. Supplementary information on bathymetry and general features may be found in the reviews by Hansen (1985), Johannesen (1986), Perry (1986), Vogt (1986) and Hopkins (1991).

Bottom topography. Iceland and the Faroe Islands divide the Greenland-Scotland Ridge into three gaps which have different widths and sill depths (Figure 3): From northwest to southeast the first gap is the fairly wide Denmark Strait with a sill depth of about 620 m (Figure 4). Between Iceland and the Faroe Islands is the Iceland-Faroe Ridge, a broad ridge with minimum depths along the crest of 300-500 m, generally deepening from the Icelandic to the Faroese end. The deepest passages across the Iceland-Faroe Ridge are in the form of four channels, with sill depths between 420 m close to Iceland and 480 m close to the Faroes.

Between the Faroes and Scotland the bottom topography is more complex. The relatively broad, deep Faroe-Shetland Channel is blocked at its southwestern end by the Wyville Thomson Ridge with sill depth around 600m. The Wyville Thomson Ridge joins the Scottish shelf at its southern end and at the northern end joins the Faroe Bank rather than the Faroe Plateau. These two are separated by the narrow, deep Faroe Bank Channel with sill depth around 850 m. This channel, which is a continuation of the Faroe-Shetland Channel, thus exceeds all other passages across the Greenland-Scotland Ridge by more than 200 m in sill depth (Figure 4).

The ocean regions southwest of the Greenland-Scotland Ridge are divided into three basins/channels by two shallower structures (Figure 3). The Mid Atlantic (Reykjanes) Ridge separates the Irminger Basin from the Iceland Basin, which is separated from the Rockall Channel by the Rockall-Hatton Plateau. Northeast of the Greenland-Scotland Ridge are the Nordic Seas: The Norwegian Sea, the Iceland Sea and the Greenland Sea which in their deep parts are separated from one another by deep submarine ridges. Through the Fram Strait, the Nordic Seas are connected to the Arctic Ocean. Collectively, the Nordic Seas and the Arctic Ocean are known as the Arctic Mediterranean.

The effect of the Greenland-Scotland Ridge on the surrounding waters may be illustrated by Figure 5, showing a section across the Iceland-Faroe Ridge. On the Atlantic side of the ridge, temperature and salinity are high ($T>5°C$, $S>35.0$) down to 1000 m or more except for a narrow boundary region close to the ridge which is influenced by the overflows. On the northeastern side of the ridge, the whole of the Arctic Mediterranean is filled with cold ($T< 0°C$), low-salinity ($S \approx 34.9$) water from about sill-level down to bottom. This is water which by various processes, to be described in more detail later, has been cooled and has descended from the upper layers of the Arctic Mediterranean down to intermediate ($\approx$ 1000 m) and deep levels.

In the upper layers (down to $\approx$ 500 m) the Arctic Mediterranean is much less homogeneous. In the eastern areas, especially, Atlantic water, that has crossed the ridge, penetrates far to the north while the rest of the area is dominated by cold, low-salinity water. In the Iceland-Faroe region these two water masses meet in the Iceland-Faroe Front (Figure 5). The front, clearly, is locked topographically to the ridge, which thus influences also the upper layer fundamentally.

Water exchanges across the ridge. The major flows in the upper layer are shown in Figure 6 that is based on the accumulated evidence to be discussed in detail below. The Atlantic water inflow to the Arctic Mediterranean has several branches. The North Atlantic Current sends one branch toward the north; part of which passes the ridge west of Iceland (the North Icelandic Irminger Current) and one branch that flows through the southeastern part of the Iceland Basin and over the Rockall-Hatton Plateau toward the Faroes. West of the Faroes this flow splits further into one branch passing south of the Faroes into the Faroe-Shetland Channel (the Shetland Current) and one branch that takes a more northerly route. A part of the

northern branch recirculates in the Iceland Basin, while part of it crosses the Iceland-Faroe Ridge and becomes the Faroe Current. In addition to these three "oceanic" branches, there is also a persistent flow of Atlantic water northeastward over the continental slope, termed the Continental Slope Current.

Northeast of the ridges, the Atlantic water meets the colder and less saline water in the upper layers of the East Icelandic Current. In the surface, this encounter occurs in two regions close to the ridge, north of Iceland and in the Iceland-Faroe Front. The different branches of Atlantic water affect different parts of the Arctic Mediterranean. The Atlantic water that passed west of Iceland and part of the water that came through the Iceland-Faroe Gap are absorbed into the upper layers of the Iceland Sea and the southwestern part of the Norwegian Sea, providing heat and salt to these areas. The rest of the Atlantic water continues northwards in the Norwegian Atlantic Current to affect the Barents Sea and the northern parts of the Nordic Seas as well as the Arctic Ocean.

The waters below sill-level on both sides of the Greenland-Scotland Ridge contain a variety of water masses of different, and partly unknown, origin and circulation that is difficult to describe. In the present context, the cold waters that flow over the ridge into the Atlantic, the overflow, are of most interest. The overflow, like the Atlantic inflow, has several branches which transport water of different origin and characteristics (Figure 7) and the mechanisms driving the overflow may be different as well for the different branches. Thus, the overflow through the deep passages (e.g. the Faroe Bank Channel) is driven by the large density difference across the ridge below $\approx$ 500m. The overflow over shallower areas (e.g. the Iceland-Faroe Ridge) may be considered as a feature of the upper ocean frontal interface close to the ridge crest (Figure 5).

After passing the ridges, some of the overflow water is admixed into the surrounding Atlantic water masses while the rest flows as density driven bottom currents which extend all the way into the Western Basin of the North Atlantic along with entrained Atlantic water. In a later section we discuss various transport estimates from the literature. For the overflow, in contrast to the upper layer inflows, we find that fairly reliable estimates are available.

The two circulation maps (Figures 6 and 7) indicate the water masses transported by the upper layer inflows and the deep overflows. As always, the classification is to some extent arbitrary as are the names used to identify the different water masses. We have chosen to distinguish between two different Atlantic water masses and three different kinds of overflow water. Figure 8 shows the TS ranges of these water masses and Table 3 summarises their properties. The origins and paths of these water masses are discussed below for the Atlantic and overflow waters separately. Fluxes and temporal variations of water mass properties will be discussed in separate sections.

The origins of the Atlantic water flowing into the Nordic Seas

As demonstrated by Figure 6, two separate source regions may be defined for the Atlantic water that crosses the Greenland-Scotland Ridge. One of these is the area where the North Atlantic Current enters the eastern Atlantic. This region feeds the two inflow branches to the Nordic Seas that pass between Greenland and Iceland and between Iceland and the Faroes. It also contributes to the branch that flows between the Faroes and Shetland. The other source region is off the European continental shelf south of the entrances to the Greenland-Scotland inflow region. This source feeds the Continental Slope Current that passes through the Faroe-Shetland Channel. The water masses produced in these two regions are not so different that they could not be combined, but considerable differences may be expected in the processes responsible both for production and for subsequent transport to the ridge area. This, as well as tradition, motivates a distinction between the two different sources of Atlantic water.

Table 3. Typical properties of the main water masses exchanged across the Greenland-Scotland Ridge.

Acronym	Name	Temperature range	Salinity range
MNAW	Modified North Atlantic Water	7.0 - 8.5 °C	35.15 - 35.30
NAW	North Atlantic Water	9.5 - 10.5 °C	35.35 - 35.45
MEIW	Modified East Icelandic Water	1 - 3 °C	34.70 - 34.90
NSAIW	Norwegian Sea Arctic Intermediate Water	-0.5 - +0.5 °C	34.87 - 34.90
NSDW	Norwegian Sea Deep Water	< -0.5 °C	34.91

The oceanic source region may appropriately be considered to start west of the Mid-Atlantic Ridge, in the area between the Subarctic Front and the Azores front. In this region, which according to Käse and Krauss (1996) is "the largest and most intensive stirring area in the North Atlantic", various processes contribute to mix the subtropical water masses carried by the North Atlantic Current with water of subpolar origin. Thus, when the North Atlantic Current crosses the Mid-Atlantic Ridge, it carries with it a large volume of water with temperature and salinity intermediate in character between subtropical and subpolar. Its composition varies more or less continuously across the current with increasing cooler/fresher subpolar influence as the Subarctic Front is approached.

The current and the frontal region in the Mid-Atlantic Ridge area have recently been studied in a number of works (Sy, 1988; Arhan, 1990; Sy *et al.*, 1992; Belkin and Levitus, 1996). The northernmost branch of the North Atlantic Current, known as the North Subarctic Front, exhibits interannual variability, shifting 200 - 300 km in a few months. Apart from this, it remains fairly stable and "slips into the Northeast Atlantic above the eastern part of the Charlie-Gibbs Fracture Zone" (Belkin and Levitus, 1996). These results are consistent with the scheme of Sy (1988), who found that the North Atlantic Current crosses the Mid-Atlantic Ridge between 50°N and 52°N.

Further towards the Greenland-Scotland Ridge, this water is progressively cooled and freshened by air/sea interaction, a process which is enhanced by the deep winter-time convection which occurs over wide areas in the Northeastern Atlantic away from frontal regions (Harvey, 1982; Fuchs *et al.*, 1984). Assuming a net annual heat loss of 60 W m^{-2} (Isemer and Hasse, 1987), a net freshwater input from the atmosphere of 25 cm per year (Schmitt *et al.*, 1989) and a homogenisation down to 500 m, an annual decrease of about 1°C for temperature and 0.02 for salinity may be expected.

There is no standard name for the water mass originating in the oceanic source region. Certainly, North Atlantic Central Water (NACW) has gone into the mixture, but so has water from north of the Subarctic Front (Käse and Krauss, 1996). Some authors prefer the name Sub Polar Mode Water (SPMW) (McCartney and Talley, 1982), but the definition of this water includes also quite different waters (e.g. Labrador Sea Water) and we do not find it very appropriate to denote the Atlantic water inflow to the Nordic Seas. A more informative name is the Eastern North Atlantic Water (ENAW) of Harvey (1982) whose θ-S trace falls within the properties of the water crossing the ridge (Figure 8). The ENAW (or the alternative name, NEAW) could, however, as well be used to denote the Atlantic water from the continental source region and we consider it rather to be a mixture of water from the two source regions, i.e., a product rather than a source.

As seen in Figure 8, we have chosen to adopt the name "Modified North Atlantic Water" (MNAW), which for many years has been used for the oceanic Atlantic water in the Iceland-Scotland region (Martin, 1976). As shown by Becker and Hansen (1998, this volume), the earlier concept of a local modification is not supported by observations. If the "modification" is considered to occur in the source region and on the way towards the ridge then the use of the word is appropriate. The name MNAW is also appropriate for the Atlantic water crossing into the Nordic Sea between Greenland and Iceland, even though the usage has not been as common, since this water comes from the same source region (although closer to the Subarctic front).

The θ-S ranges shown for MNAW in Table 3 and Figure 8 represent the properties of the water shortly before crossing the Greenland-Scotland Ridge and are based on long-term observations (Malmberg and Kristmansson, 1992; Hansen and Kristiansen, 1994) as well as some more sporadic observations (Ellett *et al.*, 1983). The ranges illustrate typical conditions although not extremes (like the Great Salinity Anomaly, e.g.). For comparison, Figure 8 shows also defining lines of western and eastern North Atlantic Water (Harvey, 1982).

The continental source region is by definition the production area of the Continental Slope Current. The existence of persistent Poleward flow over the continental slope region, constrained by the bottom slope, was hypothesised in the late 1970s (Swallow *et al.*, 1977; Ellett *et al.*, 1979). Since then a number of studies have supported the idea of a more or less continuous flow over the continental slope. This originates from south of the Rockall Channel toward the northeast, and passed the exit of the Faroe-Shetland Channel (Booth and Ellett, 1983; Gould *et al.*, 1985; Huthnance, 1986; Booth, 1988; Pingree and Le Cann, 1989; Turrell *et al.*, 1992).

A detailed discussion on the ultimate origin of this flow and its continuity along the continental slope is beyond the scope of this review. However, there are indications that its origin lies at least as far south as the Armorican Slope region off the west coast of northern France (Pingree and Le Cann, 1989). Clearly, it contains a large component of water with a similar origin to that produced in the oceanic source region, but it has higher salinities than the waters further offshore (Harvey, 1982). Harvey (1982) and Ellett *et al.* (1986) argue, that admixture of Mediterranean (or rather Gulf of Gibraltar) water is responsible for this and Reid (1979) even found it likely to "be the Mediterranean core that contributes the characteristics of the Norwegian Current".

The Mediterranean outflow has, however, a fairly high density and others have questioned the importance of Mediterranean Water as source for the Continental Slope Current in the depth range of interest (Pollard and Pu, 1985; Hill and Michelson-Jacob, 1993; van Aken and Becker, 1996). Its necessity may also be questioned, since, clearly, a persistent Poleward flow may advect high-salinity water from the upper layers to the south which do have sufficiently high salinities (Harvey, 1982). Whatever the reason, the water of the Continental Slope Current is the saltiest (and warmest) water exchanged over the ridge.

As for the oceanic source region, we have chosen to adopt the traditional name "North Atlantic Water" (NAW) (Tait, 1957) for the water mass transported by the Continental Slope Current. The property ranges assigned to it in Figure 8 and Table 3 represent conditions in the Rockall Trough, prior to passage over the Wyville Thomson Ridge. They are based on a number of sources (Ellett and Martin, 1973; Booth and Ellett, 1983; Ellett *et al.*, 1983 and Ellett *et al.*, 1986) and again reflect typical, rather than extreme, variability.

The paths of Atlantic water inflow to the Nordic Seas

The main features of the northeastward flow of Atlantic water toward and across the Iceland-Scotland ridge area was described already by Helland Hansen and Nansen (1909) in their monograph on the Norwegian Sea (Figure 9). Although different in detail, many of the main features of their description are consistent with our present knowledge as reviewed above. Throughout this Century, and especially through the two Overflow experiments and the NANSEN project, a number of open questions have been resolved and firm observational evidence has replaced what was originally based largely upon intuition.

In this section we will discuss the paths of the different Atlantic water current branches from the source regions toward the Greenland-Scotland Ridge. After that we discuss separately how these waters pass the ridge through each of the main gaps. Finally we consider the flow of the Atlantic water after it has passed the ridge and summarise the upper layer circulation in the whole region.

The North Icelandic Irminger Current. After the North Atlantic Current has crossed the Mid-Atlantic Ridge between 50°N and 52°N it divides into branches. In Dietrich's (1975) circulation scheme, the Irminger Current branches off shortly after that, flowing north - to northeastward well east of the Mid-Atlantic Ridge almost all the way to Iceland before crossing to the western side of the ridge. The remainder of the North Atlantic Current continues in a more easterly direction toward the Iceland-Scotland Gap in his interpretation.

Bersch (1995) found support for this path of the Irminger Current from altimeter data. On a map of root mean square variability of sea surface height for the period November 1986 to June 1989, he shows two bands of increased variability in this region. The westernmost of these, he associated with the Irminger Current and it follows Dietrich's (1975) path fairly well. He also reported, however, results from CTD and shipmounted ADCP observations that located the Subarctic Front west of the mid-Atlantic Ridge at about 59°N and linked to that a strong northward flow. Associating this frontal jet with the Irminger Current would appear natural.

The location of the Subarctic Front in the upper layers usually coincides fairly well with the steepening of the 35.00 isohaline as shown in Figure 10 from van Aken and Becker (1996). Further to the north, Hermann crossed the front with a section along 62°N from the Faroes to Greenland annually from 1948 to 1959 (e.g. Hermann, 1949) and since then it has been occupied more sporadically, e.g. by Krauss in 1988 (Krauss, 1995). The front apparently stays close to the Mid-Atlantic Ridge at this latitude, but consistently on the western side of the ridge.

Krauss (1995) also deployed a series of satellite-tracked buoys, drogued at 100m depth, on both sides of the ridge which confirmed the above. Buoys deployed west of the Mid-Atlantic Ridge, continued toward the Denmark Strait in the Irminger Current while buoys deployed east of the ridge first moved southwestward over the eastern slope of the ridge before drifting northeastward toward the Iceland-Scotland Gap.

Thus, the Subarctic Front and the North Atlantic Current cross the Mid-Atlantic Ridge into the Eastern Basin close to the Charlie-Gibbs Fracture Zone. However, there is considerable evidence indicating that the Front, and associated with it the Irminger Current, cross the ridge again further to the north and become locked to its western flank

When approaching the Denmark Strait, the Irminger Current again divides into two branches, one branch turning west- and then southwestward to run parallel to the East Greenland Current, and one branch that flows northward over the west Icelandic shelf. This second branch is termed the "North Icelandic Irminger Current" (Stefánsson, 1962). It transports Atlantic water northward across the ridge and contributes to the import of Atlantic water to the Arctic Mediterranean (Figure 11).

Most drifters, seeded into the Irminger Current southwest of Iceland, seem to take the western branch

toward East Greenland (Krauss, 1995; Malmberg and Briem, 1993), but the occurrence of Atlantic water north of Iceland (Stefánsson, 1962) requires a flow from the Irminger Current into North Icelandic waters. Malmberg and Briem (1993) speculate that this flow may be confined to the deeper layers in contrast to the westward flow shown by their shallow drifters (15-m drogues). They note, however, the large variability in circulation patterns shown both by drifter experiments, but also in standard hydrography and studies on larval drift.

In his monograph on North Icelandic Waters, Stefánsson (1962) shows a number of TS sections off the northwestern corner of Iceland (Kögur section) containing the Atlantic water as a high-salinity core on the shelf. However there are only small amounts of water with S > 35.0 extending further offshore or deeper than 200 m (Figure 12). Kristmannsson (1998, this volume) has reported results from long-term current meter measurements at two depths on a mooring located in this section (Figure 11). Figure 13 shows progressive vector diagrams (PVDs) from these measurements for the period mid-1985 to late-1990. From the current measurements, the flow eastward is fairly barotropic, although somewhat bottom intensified.

On its path eastward, the North Icelandic Irminger Current feeds the North Icelandic shelf area with relatively warm, saline water. This water, however, rapidly loses its Atlantic character (heat and salt) so that the percentage of Atlantic water reduces to less than 30% by the time it reaches the northeastern corner of Iceland (Langanes, Figure 11) (Stefánsson, 1962).

Although probably the weakest of the Atlantic inflow branches to the Arctic Mediterranean in terms of transport, the north Icelandic Irminger Current may well be the one for which we have the most quantitative knowledge and the best long-term estimate of transport. This will be returned to in a later section.

The Hatton Slope Current. After the Irminger Current has branched off, the remainder of the North Atlantic Current continues toward the Iceland-Scotland Gap. In general usage, this branch keeps the name, the North Atlantic Current. The frontal jet associated with the current may be inferred from hydrographic sections crossing the Rockall-Hatton Plateau (Figure 14). An example is shown in Figure 10 where the baroclinic flow is centered over the deep slope region northwest of the plateau. The figure appears to be fairly typical (Malmberg and Magnusson, 1982; Becker and Hansen, 1998, this volume; van Aken and Becker, 1996). A general situation may therefore be relatively warm and saline water from the open Atlantic over the Rockall-Hatton Plateau, bounded by a frontal jet on the boundary between the plateau and the Iceland Basin.

That the baroclinic structure is indeed associated with a residual north to northeastward flow in the upper layer, was confirmed by current measurements reported by van Aken (1995). In parallel with other similar areas (e.g. the north Faroese slope and the Scottish slope in the Faroe-Shetland Channel), we expect the baroclinic jet associated with the front to be only the outer limit of a more barotropic flow over shallower parts of the slope. This conjecture seems to be supported by the available evidence from drifters (Booth and Meldrum, 1987; Otto and van Aken, 1996). We consider this flow to be a continuation of the North Atlantic Current, but during the discussion we will refer to it as the "Hatton Slope Current" to avoid confusion.

In Figure 6 the link between the Hatton Slope Current and the North Atlantic Current further west has not been drawn as a direct line as in the scheme of Krauss (1986). Rather, we assume a more circuitous route, as is partly implied by Dietrich *et al.* (1975). van Aken and Becker (1996) and Otto and van Aken (1996) suggest that although there is some direct flow, the main water transport makes a retroflection southwest of the Rockall-Hatton Plateau. This is also evident in their horizontal maps of temperature and salinity in the core of the Atlantic water layer (SPMW in their notation) based on several cruises, partly from the NANSEN project (Figure 15). Certainly a number of drogued buoys have been observed to drift from the southern Rockall Channel in a northwestward direction, west of the Rockall-Hatton Plateau, before turning northeastward. From there it flows either over the plateau or joins the Hatton Slope Current (Booth and Meldrum, 1987; Pingree, 1993). The opposite has also been observed (Otto *et al.*, 1992), and the large eddy-activity in the region southwest of the Rockall-Hatton Plateau (Otto and van Aken, 1996; Pingree, 1993) makes conclusions from drifter observations difficult.

The most convincing argument for a retroflection is perhaps the observation by Ellett (1993) that the waters at 350 m depth at Ocean Weather Station (OWS) I were warmer and more saline than those at the same depth at J further south (Figure 14). This indicates that a water mass with some arctic water influence reaches to the southern OWS. This does not, however, have to be water from west of the Irminger Current as implied by Ellett's (1993) circulation scheme, in which the Irminger Current also makes this retroflection and only branches off from the North Atlantic Current at the northwestern corner of the Rockall-Hatton Plateau. Rather, the colder and less saline water reaching south to OWS J is probably water that has moved southward east of the Irminger Current as shown by Krauss's (1995) drifters. Hydrographic sections do show such a water mass in between warmer water (Ellett, 1993).

The flow over the Rockall-Hatton Plateau is not clearly understood. The bottom topography (Figure 14) shows a fairly steep slope northwest of Rockall Bank and one might expect a "slope current" toward northeast over the slope region. Dooley and Henderson (1980) confirmed the existence of fairly regular eastward flow over the 500-m isobath north of Rockall Bank, but at least part of this flow might be associated with a quasi-closed anticyclonic circulation over the shallower parts of the Rockall Bank (Dooley, 1984). Indeed, Otto and van Aken (1996) using results from drifter studies find only weak and even southward flow over the central and northern part of the Rockall-Hatton Plateau. Pingree (1993), however, does find evidence of continuous northeastward flow over the plateau. Clearly the flow over the Rockall-Hatton Plateau merits further study, but the above studies suggest that, at least at times, there is a northeastward flow over the plateau, although probably less persistent and weaker than the slope current which is found over the northwestern slope of the plateau.

In the Rockall Channel, hydrographic observations have been carried out routinely for a long time. With the geostrophic method, they were originally (Ellett and Martin, 1973) used to infer an overall northeastward flow over the western half of the channel, a southwestward recirculation in the eastern half and, again, northeastward flow over the Scottish slope. Modern use of more direct current observations has shown the dangers of using the geostrophic method over steep bottom topography and the original circulation scheme has been somewhat modified (Ellett *et al.*, 1986) as shown in Figure 16. Later observations with drifters (Booth and Meldrum, 1987; Pingree, 1993) have verified the general features of Figure 16 although the central parts of the channel show large variability and small residual flow vectors like many other ocean areas over flat bottom.

When approaching the banks west of the Faroes (Figure 14), the Hatton Slope Current splits up into two branches, one branch crossing the Iceland-Faroe Ridge and one branch that flows into the Faroe-Shetland Channel. The ubiquitous presence of Atlantic water over the Iceland-Faroe Ridge and north and west of the Faroes is a result of the northern branch and one possible origin of it is the Hatton Slope Current as suggested by Helland-Hansen and Nansen (1909) in Figure 9. Using hydrographical observations obtained in the NANSEN Project, Becker and Hansen (1998, this volume) compare temperature-salinity relationships in the Iceland Basin and over the Rockall-Hatton Plateau to those in Faroese waters and find a continuity in water mass distribution that supports this scheme.

A number of drifting buoy tracks also follow this pattern (Krauss, 1995; Otto *et al.*, 1992; Pingree, 1993; Booth and Meldrum, 1987). In addition there is a general slow northeastward flow over most of the deep part of the Iceland Basin and, although some of this water apparently is recirculated, part of it continues over the Iceland-Faroe Ridge as shown especially by Krauss's (1995) drifter experiment in May 1988.

The southern branch from the Hatton Slope Current, shown in Helland-Hansen and Nansen's (1909) circulation picture (Figure 9), is also fairly well established. Much of the Atlantic water found over the Wyville Thomson Ridge and in the Faroe-Shetland Channel may certainly have been brought there by the Continental Slope Current (to be discussed). However, water mass analysis in the northern part of the Rockall Channel indicate input also of water from the north or west (Ellett *et al.*,1983). A few drifters have also been observed to leave the Hatton Slope Current, crossing the plateau eastward to continue into the Faroe-Shetland Channel (Otto *et al.*, 1992; Krauss, 1995). Most convincing, however, is the 9 month long current meter record from 275 m depth on the northern part of the Wyville Thomson Ridge, reported by Ellett (1998, this volume). Except for short periods, this record, which should represent the upper layer, showed persistent eastward flow from the Rockall-Hatton Plateau over the Wyville Thomson Ridge.

The Atlantic water crossing the Wyville Thomson Ridge between the Faroe Bank and the Scottish shelf thus seems to derive both from water of southerly origin associated with the Continental Slope Current and from a branch of the Hatton Slope Current. van Aken and Becker (1996) suggest a branching in the opposite direction with water from the Rockall Channel flowing northward to join the Hatton Slope Current west of Faroe Bank. We find the available observational evidence to be in conflict with this suggestion which seems to be mostly based on geostrophic calculations and budget considerations. Possible exchanges between the two branches through the Faroe Bank Channel will be discussed later.

The Continental Slope Current. As previously discussed, the core of the Continental Slope Current carries the warmest and most saline water crossing the Greenland-Scotland Ridge and is apparently not linked as directly to the North Atlantic Current as the other branches of Atlantic flow that were discussed above. This justifies the treatment of the Continental Slope Current as a separate branch, but it must be realised that the boundary between these two flows is not always well defined. Already at the entrance to the Rockall Channel, water from the North Atlantic Current will at times enter the channel and flow parallel to the Continental Slope Current. Using drifter observations, Pingree (1993) finds a "watershed" around 51°N with drifters released north of this position in deep water moving either into the Rockall Channel or in a more northerly path over the Rockall-Hatton Plateau. Ellett

and Martin (1973), however, find that in certain periods there is no surface water in the Rockall Channel with characteristics derived directly from the west and that the ratio of input from the west and from the south varies on long timescales.

Even in periods when all the surface water in the southern Rockall Channel derives from the south, there may be an inflow of water from the Hatton Slope Current into the northern parts of the Rockall Channel (Ellett *et al.*, 1983). As the flow propagates northeastward across the Wyville Thomson Ridge and in the Faroe-Shetland Channel, where the two branches flow parallel to one another and partly mix, there is always a more or less continuous transition in water mass characteristics from the slope region into deep water.

The Atlantic water flow through the Iceland-Faroe Gap. The presence of Atlantic water over the Iceland-Faroe Ridge has been known for a long time (Nielsen, 1904). During the three multiship surveys of the Overflow '60 expedition (Tait *et al.*, 1967), it was found to dominate the upper layers over the whole ridge area (bounded by the 500 m isobath) except for the region close to Iceland (Figure 17). A standard section over the western flank of the ridge (shown on Figure 48) which was occupied by German vessels on 14 occasions in 1959 – 1971 demonstrates the ubiquitous presence of Atlantic water in the uppermost 300 m along this line. With increasing depth, the boundary towards colder waters slopes (Figure 5) so that the water just over the ridge crest has not much of Atlantic character (Figure 17). However, the upper waters seem to be consistently Atlantic water as demonstrated by the fact that none of the many drifters released east of Iceland by the SACLANT group (Poulain *et al.*, 1996) turned westward over the ridge.

From the above discussion it may be noted that the Atlantic water that crosses the Iceland-Faroe Ridge into the Norwegian Sea originates from the Hatton Slope Current, from the more sluggish northeastward flow across the central Iceland Basin (Krauss, 1995) and, perhaps, from more central parts of the Rockall-Hatton Plateau. Using water mass characteristics, Becker and Hansen (1998, this volume) trace the Atlantic water over the southeastern Iceland-Faroe Ridge and north of the Faroes back to the Hatton Slope Current and the water over the central Rockall-Hatton Plateau. This is in general agreement with Helland-Hansen and Nansen's (1909) scheme (Figure 9), but does not clarify the flow pattern over the ridge.

Some attempts have been made to use the geostrophic method to investigate the circulation over the ridge. Using the Overflow '60 data set, Bogdanov *et al.* (1967) found the Atlantic water to be flowing from Iceland towards the Faroes over the western flank of the Iceland-Faroe Ridge in conflict with Helland-Hansen and Nansen's scheme (Figure 9). van Aken (1988), using an inverse method, found northgoing flow on both sides of the ridge at the Faroese end. Both these works are critically based on assumptions which have not been tested by observations and which may not be valid in such areas with large topographical changes and strong barotropic flows. Based on experience from other areas (c.f. later discussion on Faroe-Shetland Channel) we hesitate to put too much faith in their conclusions.

Long-term current meter moorings on the ridge have not been frequent, but during the Overflow '73 experiment a number of short term moorings were deployed (Koltermann *et al.*, 1976). Based on these and other information, Meincke (1983) produced current maps for the near-surface and the bottom layer (Figure 18). More recently, the SACLANT group deployed three moorings east of the ridge for 3–4 months in 1988-89. Their observations confirm Meincke's general picture at all depths (Hopkins *et al.*, 1992) and so do preliminary results from three long-term ADCP moorings north of the Faroes deployed during the Nordic WOCE (Anon., 1992) programme (Figure 19).

The available Eulerian current measurements on the Iceland-Faroe Ridge are thus largely consistent with Helland-Hansen and Nansen's (1909) picture (Figure 9) based on water mass tracing, although the data set is small, especially west of the ridge. To this picture of the flow pattern over the ridge, Lagrangian measurements from drifter experiments have yielded a new dimension. Hansen *et al.* (1998, this volume) show four drifters, deployed during NANSEN, crossing the ridge. Figure 20 indicates in a schematic way the behaviour of three of these. Apparently, drifters may cross the Iceland-Faroe Ridge at several locations along it (though probably constrained by local topography). They may cross the ridge directly (drifter A on Figure 20) or they may make an almost complete anticyclonic circulation over it (drifter B).

The track of drifter B in Figure 20 might be interpreted as a temporal change in the flow field from northwesterly to southeasterly rather than a complete circulation cell. However, another drifter on the ridge in the same period shows unambiguously the existence of the circulation cell (Hansen *et al.*, 1998, this volume). Other drifter experiments (Krauss, 1995; Otto and van Aken, 1996) support these general conclusions. To some extent, Meincke's (1983) near-surface current map in Figure 18 covers the behaviour of both drifter A and B on Figure 20, but this is apparently because the flow map is an amalgam of two different situations that may occur in different periods. In some periods, water passes more or less directly over the ridge. At other times, there is an extensive anticyclonic circulation over the ridge (though perhaps

somewhat displaced toward the Atlantic side as compared to Figure18).

The time that a drifter takes to cross the ridge may also vary considerably. The track of drifter A on Figure 20 took about one month, while drifter B took about three months. Other drifters have been known to take more than half a year for the crossing (Hansen *et al.*, 1998, this volume). There is, however, one path across the ridge which seems to be somewhat faster. This is the track of drifter C in Figure 20 which crossed the ridge in about two weeks. A few examples indicate that when a drifter enters the slope region west of the Faroes, it will follow the bottom topography in a fairly regular path similar to this track, crossing the ridge where it slopes up toward the northern Faroe shelf.

This indicates the presence of a slope current along the northwestern and northern slope of the Faroe Plateau. The available evidence is not sufficient to establish its persistence and the origin of its water is not quite clear either. One possibility is that the Hatton Slope Current crosses the northern end of the fairly narrow Faroe Bank Channel more or less directly, briefly loosing the topographical steering during the crossing. Case C in Figure 20 is an alternative path where a branch from the Hatton Slope Current detours south into the Faroe Bank Channel before returning to the region north of the Faroes. Thirdly, water that has crossed the Wyville Thomson Ridge south of the Faroe Bank may join the northward flow along the western slope of the Faroe Plateau. Evidence from drifter experiments (Booth and Meldrum, 1984; Booth and Meldrum, 1987) and salinity distribution (Hansen, unpubl. data) indicate, however, that the third alternative is not a dominant contributor to the north Faroese slope current. As discussed in more detail later, the upper-layer flow of the Faroe Bank Channel is not well known and, apparently, quite variable.

The Iceland-Faroe Front. Having crossed the Iceland-Faroe Ridge, the Atlantic water meets colder and less saline waters in the Iceland-Faroe Front (Figure 5). A statement commonly encountered is that this front separates the Atlantic water from that of the East Icelandic Current. The typical situation is somewhat more complicated and is better represented by a scheme like that in Figure 21 with two fronts: The Iceland-Faroe Front and the Jan Mayen Front. The Iceland-Faroe Front separates the Atlantic water from colder and fresher water which at least in some areas is recirculated Atlantic Water either from the North Icelandic Irminger Current or from the Faroe Current (see later). The Jan Mayen Front separates this water from the water of the East Icelandic Current.

Close to Iceland the two fronts may join together (Read and Pollard, 1992), but Smart (1984) also shows a situation where the Jan Mayen Front is depicted as a continuation of the Kolbeinsey Current Front north of Iceland. This separates the North Icelandic Irminger Current from the open Iceland Sea waters. Niiler *et al.* (1992) have used AVHRR images to trace frontal structures over large distances. However, a fairly persistent mixed-layer in the uppermost 25–50 m (Hopkins *et al.*, 1992) tends to confuse the temperature signature of the front in the surface during much of the year and salinity is a better frontal indicator close to the surface. The near-surface expression of the Iceland-Faroe Front is usually well represented by the path of the 35.00 isohaline and Hansen and Meincke (1979) show examples of its behaviour in May-June for several years in the 1950s. In the detailed "SeaSoar" (undulating CTD) survey, carried out as part of the NANSEN project, Read and Pollard (1992) associated the Jan Mayen Front with the 34.8 isohaline.

In this scheme, the East Icelandic Current recirculates towards the north and does not penetrate much south of Iceland in the surface layer (Figure 21). This might seem somewhat inconsistent with the scheme of Helland-Hansen and Nansen (1909) shown in Figure 9. This figure is, however, from a greater depth and their observations were at a time when the low-salinity water in the upper layers of the East Icelandic Current penetrated further to the southeast than during the NANSEN period so the discrepancy is to some extent exaggerated. In spite of variations, the surface expression of the east Icelandic Current has always been found to be limited towards the south by the recirculation. Poulain *et al.* (1996) have found that drifters released northeast of Iceland have a sluggish motion with several drifters meandering in the salinity minimum tongue for more than a year.

The further discussion focuses on the Iceland-Faroe Front that is the boundary of the Atlantic water that has passed through the Iceland-Faroe Gap. Throughout this Century this Front has been the subject of many cruises and publications. Of the early results, one may note especially the standard hydrographic observations, obtained during herring surveys in the 1950s, the ICES Overflow '60 hydrographic surveys (Tait *et al.*, 1967) and the Russian-Icelandic surveys that were reported annually to the ICES Hydrography Committee.

During the NANSEN Project more detailed studies of the front were initiated (Gould *et al.*, 1987) which were continued in the following years. Thus the current literature teems with results based on standard CTD surveys (Hallock, 1985; Hopkins *et al.*, 1992; Tokmakian, 1994) or more modern techniques such as undulating CTD's, towed thermistor chains, shipborne ADCP's, airborne XBT's, moored ADCP's and current meters, drifters, and remote sensing, both as infrared radiometry and satellite altimetry (Smart, 1984; Gould *et al.*, 1987; Dobson, 1988; Østerhus and Golmen, 1988; Griffiths, 1990; Scott and McDowall, 1990;

Essen, 1992; Griffiths *et al.*, 1992; Niiler *et al.*, 1992; Perkins, 1992; Pistek and Johnson, 1992; Read and Pollard, 1992; Allen *et al.*, 1994; Tokmakian, 1994, Allen *et al.*, 1996). In addition to the observational effort, a number of theoretical studies have focused on meso- and small-scale processes of the front, both from an analytical (Willebrand and Meincke, 1980) and from a numerical point of view (Varnas *et al.*, 1993; Griffiths, 1995; Miller *et al.*, 1995; Fox and Maskell, 1996).

The depiction of the Iceland-Faroe Front, shown in Figure 21, is based on these works. The front extends from the southeast coast of Iceland where the Iceland-Faroe Ridge impinges upon the Icelandic shelf. Stefánsson (1972) has shown that it is fairly well localised close to the coast although seasonal variations can be seen, probably deriving from freshwater runoff. From there it generally has a northeasterly going track until about 10°W. At that longitude one often observes a "bump" in the 35.0 isohaline which implies that the most northerly extension of the Atlantic water in this region will normally be around 10°W.

At its "start", close to Iceland, the front is generally sharp with abrupt cross-frontal temperature and salinity changes (Stefánsson, 1972). As the front progresses eastward, it becomes more diffuse so that north of the Faroes, cross-frontal gradients may be considerably smaller. Associated with this, there is a progressive change in the vertical slope of the front. Close to Iceland, the overall slope from near-surface to near-bottom at 400 m depth may exceed 0.015, which may have decreased by more than a factor of 5 northeast of the Faroes (Read and Pollard, 1992). In spite of this overall change, high-gradient frontal filaments persist as shown by AVHRR images (Niiler *et al.*, 1992) and Østerhus and Golmen (1988) found cross-frontal gradients approaching 0.5 °C km^{-1} at 6°W in a "Sea-Soar" survey on their 1986 NANSEN cruise.

If we ignore the bottom boundary layer associated with the overflow, the intersection of the front with the sea bed seems generally to be constrained to the ridge, somewhat west of the crest (Tait *et al.*, 1967) as demonstrated on Figures 5 and 17. At the junction between the ridge and the Faroe Plateau, the bottom expression of the front continues eastward on the northern Faroe slope, at about crest depth, somewhat shallower than 500 m (Meincke, 1978). When the front has progressed to the sharp eastern corner of the Faroe Plateau (Figure 21), it looses bottom contact. At this stage, its near-surface expression has already become much more diffuse.

In spite of this fairly regular behaviour, the Iceland-Faroe Front is not a smoothly varying boundary. On the contrary, it is typically distorted by meanders and eddies of 30-50 km scale (Hansen and Meincke, 1979). Since the Overflow '60 hydrographic survey of the frontal region (Tait *et al.*, 1967), a number of observational studies have focused on the variability of the front. To some extent, these detailed observational and theoretical studies might be said to fall outside the scope of this review which focuses on inter-oceanic exchanges. The frontal variability does, however, imply a cross-frontal exchange of heat and salt which has to be evaluated in budget considerations. In addition, the overflow across the Iceland-Faroe Ridge seems to be closely interlinked with the frontal processes.

Briefly summarised, the frontal meanders seem to derive from baroclinic instability as suggested by Willebrand and Meincke (1980) and they move eastward along the front. Thus Pistek and Johnson (1992), using altimetry and drifters, followed three strong sea surface height signatures with current speeds up to 50 cm s^{-1} and radii of curvature of 25 km which propagated with average speed of 3.3 km day^{-1} and were discernible for 2–3 months. Eddies derive from unstable meanders and are found on both sides of the front. In a detailed survey, Allen *et al.* (1994) thus found cyclonic cold-core eddies southwest of the front and anticyclonic warm-core eddies northeast of it. The scales of these varied from 15 to 70 km. They estimated an average eddy-production of about one per day along the Iceland-Faroe Front.

Hallock (1985) notes that the eddy-like convolutions of the frontal surface are most pronounced in the (70 km wide) uppermost 100m layer. Effects of the eddies can usually be seen down to the typical 400m depth of the crest of the ridge or deeper (Hansen and Meincke, 1979). Below 100 m depth, Hallock (1985) finds a less convoluted frontal surface, but with strong evidence of intrusive interleaving.

The Faroe Current. The water that crosses the Iceland-Faroe Ridge close to the Faroese end of it, proceeds eastward more or less parallel to the northern Faroese slope. Water that has crossed the ridge closer to Iceland, turns into a more southeasterly direction towards the Faroes. This implies a focusing of the Atlantic water that has crossed the ridge into a more concentrated flow, which has been termed the "Faroe Current" (Hansen and Meincke, 1984). Around 6°W, a section across the flow (Figure 22) has a typical wedge like shape. The section in Figure 22 was obtained during a NANSEN cruise where a number of short-term moorings were deployed parallel to this section and Figure 23 shows progressive vector diagrams for the near-surface and deeper flow (Hansen *et al.*, 1998, this volume).

Although only covering 10 days, these observations clearly indicate the barotropic character of the current within the Atlantic water wedge. The outer moorings were, evidently, affected by the passage of an eddy or frontal meander. Over most of the slope, the flow

direction was constrained by the bottom topography. These observations were used to make a short-term estimate of the Atlantic water transport of the Faroe Current that will be discussed in more detail later. About half of the transport was estimated to be in the inner, bottom-constrained part of the wedge.

The Nordic WOCE ADCP programme includes three mooring sites crossing the Faroe Current (Figure 19). Mesoscale activity clearly affects the progressive vector diagrams in that figure especially at the northernmost mooring site but the overall picture demonstrates the regularity of the flow. The depth variation of velocity is shown in Figure 24. At the innermost site, site NWNA, with 300 m depth to bottom, the flow has a strongly barotropic character, but also at site NWNB (bottom depth 963 m) there is appreciable flow, even deeper than 500 m.

Figures 19, 23 and 24 do not, however, represent only Atlantic water. The extent of Atlantic water on the section varies considerably as seen in Figure 25 which compares salinity sections along 6°W obtained at two different times. Roughly, the Atlantic water may be delimited by the 35.05 isohaline. Thus the cross-sectional area of Atlantic water on the section may vary by an order of magnitude, although the two situations on Figure 25 represent extremes.

As the Atlantic water progresses farther east, it approaches the eastern corner of the Faroe Plateau and east of about 4°W the Faroe Current either has to continue eastward without the bottom contact which has steered it or turn the corner and proceed into the Faroe-Shetland Channel. Apparently, it does both, as indicated already by Helland-Hansen and Nansen (1909) in Figure 9. This has been clearly demonstrated by the large drifter programme in the Norwegian Sea, carried out by the SACLANT centre in 1991–95 (Poulain *et al.*, 1996) which shows diverging paths east of the Faroe Plateau as indicated in Figure 21. The drifter tracks have to be interpreted with caution due to the difficulty in assessing which of the eastward-going drifters are in Atlantic water, and which are in the recirculating loop of the Norwegian Basin (Figure 21). Added to the information on the frontal zone as established by Smart (1984) (Figure 21) and the typical horizontal salinity distribution (Figure 9), the evidence for a branching of the Atlantic water flow is strong.

The bifurcation process was studied during a joint Nordic two-ship cruise within the NANSEN Project in 1987 as reported by Hansen *et al.* (1998, this volume) and Østerhus and Sælen (1988). Figure 26 shows progressive vector diagrams from a number of simultaneous current meter moorings deployed for about 10 days. Only instruments which were in Atlantic water through most of the period, have been included. The diagrams confirm the bifurcation thesis with the water over the deep parts of the slope (site N2) continuing eastward into the Norwegian Sea while water over the inner part of the slope (site F3 at 350 m bottom depth) continued into the Faroe-Shetland Channel.

Close to the eastern corner of the Faroe Plateau (site N3 in Figure 26), the flow of the Atlantic water changed from mainly northward to mainly southward in the middle of the period. During the deployment period, two CTD surveys were carried out which confirm the variable character of the flow. During the first survey (Figure 27a, b), a tongue of low-temperature (and low-salinity) water penetrates southwestward into the Faroe-Shetland Channel at intermediate depths. A week later (Figure 27c, d), the tongue seems to have been retracted, leaving a low-temperature (and low-salinity) eddy in the channel.

This type of behaviour had been observed previously. Thus, Hermann (1953), using hydrographic observations, noted the frequency and variability of a low-salinity tongue protruding southward into the Faroe-Shetland Channel and eddies propagating into the channel from the north are also a well known phenomenon (Hansen and Meincke, 1979). This usually gives rise to a salinity minimum in the waters north and east of the Faroes. Meincke (1978) mapped the depth and properties of this layer from a survey in 1977. Close to bottom, due north of the Faroes, he found it at 500 m depth, ascending to 200 - 300 m over the eastern corner of the Faroe Plateau and sinking again to some 400 m in the Faroe-Shetland Channel.

The situation encountered during the NANSEN experiment in 1987 (Figures 26 and 27) may be interpreted as a meander from the Iceland-Faroe Front being advected onto the eastern corner of the Faroe Plateau and affected by the local topography. We do not know how typical this situation is, but it may be concluded that the bifurcation east of the Faroes at least to some extent is in a statistical sense. There may be more or less stationary paths over the deep parts with Atlantic water going eastward into the Norwegian Sea. Likewise, the shallow areas east of the Faroes have persistent southward flow of Atlantic water (Hansen, 1992) and Figure 26 indicates that this may perhaps extend out to site F3. But, between these stable paths the flow clearly may change on time scales of days between the two directions.

The water, brought south into the Faroe-Shetland Channel by these highly variable processes is generally a mixture with Atlantic water dominating the upper layers and increasing amounts of low-salinity water at deeper levels (Meincke, 1978). The low-salinity core clearly derives from north of the Iceland-Faroe Front. This water also contributes to the overflow over the Iceland-Faroe Ridge and its origin will be discussed in

more detail in a later section. Here we note that in the Faroe-Shetland Channel it has been given various names (e.g. NI/AI, EIW, AIW). We will, as argued later, use the name "Modified East Icelandic Water (MEIW)", proposed by Read and Pollard (1992). This water mass is shown in the TS diagram of Figure 8 and its properties are listed in Table 3.

The Atlantic water flow through the Faroese Channels. Two channels, the Faroe-Shetland Channel and the Faroe Bank Channel separate the Faroe Plateau from the British Isles and the shallower regions defined by the Wyville Thomson Ridge and the Faroe Bank. Collectively they are called the "Faroese Channels" and, in some respects, they may be considered one channel (Figure 28).

The Faroe-Shetland Channel is probably one of the most intensively studied oceanic regions in the world, having been observed regularly for more than a century (Turrell, 1995). Nevertheless, many problems have only recently been resolved with the advent of modern instrumentation while some important questions, such as the typical magnitude of Atlantic water transport through the channel, are still to a large extent open. Since 1903, temperature and salinity have been monitored routinely along two standard sections, crossing the channel (Figure 28), mostly by Scottish research vessels. Since the late 1980s, the southwestern section and part of the northeastern are also occupied regularly by a Faroese research vessel and since 1994, five ADCP moorings have been more or less constantly instrumented within the Nordic WOCE/VEINS programme (Figure 19).

Detailed analyses of the standard sections worked to the mid-1950s were reported by Tait (1957). Typical sections across the channel may look like Figure 29. Over the slope and outer shelf on the Scottish side of the channel, a high-salinity core is usually found. This water is associated with the Continental Slope Current (Turrell *et al.*, 1992) and has passed into the Faroe-Shetland Channel from the Rockall Channel. Except for surface heating, this core is usually associated with a temperature maximum.

Through the years, a number of experiments have been carried out to study the flow over the slope and shelf on the Scottish side of the channel (Dooley *et al.*, 1976; Dooley and Meincke, 1981). Some observations, financed by the oil industry, have not reached the open literature, but Gould *et al.* (1985) report observations from four moorings on a section crossing the slope from 400m to 1100m bottom depth, covering a period of about one year. Focusing more on the inner slope and shelf area, Turrell *et al.* (1992) report observations from six moorings over a period of about 4 months. In addition to these, the just completed Nordic WOCE moored ADCP programme has yielded some preliminary results (Figures 19 and 24). As a whole, these measurements confirm the persistent character of the Continental Slope Current on the Shetland side of the Faroe-Shetland Channel. For the area northwest of the Hebrides, Turrell *et al.*, 1992 found the high-salinity core to be located over the 300 m depth contour, but found the along-slope current speed to increase offshore from this, from 10 cm s^{-1} over 200m depth to 20 cm s^{-1} over 500m depth.

Over the Faroese slope on the northwestern side of the channel, the upper layers are colder and less saline. Much of this water has crossed the Iceland-Faroe Ridge and passed north of the Faroe Islands before entering the Faroe-Shetland Channel, as previously described (Figure 21). Below about 500 m, the temperature decreases with depth on both sides of the channel and falls below zero while salinity tends toward the characteristic 34.91 – 34.92 salinity of the Norwegian Sea Deep Water, NSDW (Figure 8). Parts of this deep water will continue westward and overflow either the Wyville Thomson Ridge or through the Faroe Bank Channel.

The Faroe Bank Channel has not been studied as intensively as the Faroe-Shetland Channel, but through the Century a large number of research vessels have sampled its waters and since its importance in the overflow was realised, sections across the channel have been obtained more frequently. From the late 1980s, a standard section has been worked regularly by the Faroese Fisheries Laboratory. Figure 30 shows a typical temperature and salinity section across the Faroe Bank Channel. Except for a seasonally heated surface layer, the uppermost 500m are typically very homogeneous. Below this homogeneous Atlantic water layer, temperature and salinity decrease and the deepest parts of the channel are the overflow waters, rushing northwestward toward the North Atlantic.

The sections across the two channels (Figure 29 and Figure 30) appear rather similar with warm, saline Atlantic water in the upper layers and cold, low-salinity water below. There are differences, however, and and these can be seen clearly in Figure 31. In the surface layer, the Faroe Bank Channel and the northwestern Faroe-Shetland Channel will typically have very similar temperature and salinity characteristics, which is reasonable, since they both have almost the same source region in the eastern Atlantic (Figure 6). With increasing depth, differences develop, however. The Atlantic water in the Faroe Bank Channel retains the vertically homogeneous character of its source regions in the Iceland Basin and over the Rockall-Hatton Plateau which stems from the deep winter convection in these areas. The water in the northwestern Faroe-Shetland Channel, however, decreases in temperature with depth almost linearly from the surface downward

while salinity also decreases and often will have a minimum at intermediate (≈ 500 m) depths.

The TS-diagram in Figure 31 illustrates the reason for this. In the Faroe Bank Channel, there are typically only two water masses through most of the channel, the Atlantic (MNAW) and the overflow waters. In the northwestern Faroe-Shetland Channel, the curvature of the TS-diagram indicates the presence of a third water mass which is found increasingly with depth from the surface down to intermediate levels. The occurrence of this water in the Faroe-Shetland Channel was noted already by Jacobsen (1943) who also identified its origin in the low-salinity tongue (Figure 27) protruding into the Faroe-Shetland Channel over the eastern corner of the Faroe Plateau from the north as previously described.

Through the years, attempts have been made to derive the horizontal circulation of the channels, especially the Faroe-Shetland Channel, using the geostrophic method with hydrographic observations. Thus, Jacobsen (1943) produced circulation maps for various levels of the Faroe-Shetland Channel, assuming a depth of no motion at 800 meters or at bottom over the slopes. Tait (1957) used the depth of the 35.00 isohaline instead of a fixed 800 m as a level of no motion over the deep parts of the channel in his transport calculations.

Today we know that the flow over the slopes on both sides of the Faroe-Shetland Channel has a large barotropic component (Figure 24). Neither the 800 m level, the depth of the 35.00 isohaline or the bottom will in general represent levels of no motion for the geostrophic component of the flow. A more refined attempt was tried by van Aken (1988), using an inverse method. His results have some realistic features while others are in conflict with the observations (e.g. Figure 19).

Using geostrophic calculations to deduce horizontal currents from hydrography without additional observational evidence is of limited value in this complex area. Dooley and Meincke (1981) tried to overcome this difficulty by combining hydrographic observations obtained during Overflow'73 with simultaneous current meter observations. This clearly improved the results, but the current measurements were not sufficient to replace intuition in some areas and their circulation map includes a significant amount of Atlantic water flow from the Faroe-Shetland Channel into the Faroe Bank Channel which is not supported by other evidence from hydrographic observations (Becker and Hansen, 1998, this volume) and drifters (Poulain *et al.*, 1996).

The circulation map of Helland Hansen and Nansen (1909) was largely based on analysis of horizontal distributions of temperature and salinity. Using observations acquired during the NANSEN Project, Becker and Hansen (1998, this volume) employed an extension of this method to study the "bend" region of the joint channel, i.e. the area south of the southern tip of the Faroe Plateau where the two channels meet (Figure 28). Figure 32 shows the depth of the σ_θ=27.5 surface as well as the salinity on this surface. The steep sloping of this isopycnal surface in the bend region from 300 m depth in the Faroe Bank Channel up to the surface in the Faroe-Shetland Channel would seem to exclude a significant upper layer (0–300 m) exchange between the two channels over the deep regions (bottom depth > 500 m).

Dynamically, Figure 32 implies a front crossing the channel in the bend region. In the surface, this front is not well expressed in temperature or salinity, but with increasing depth, both parameters exhibit abrupt changes across the front and at 300 – 400 m depth, the front is clearly evident on horizontal temperature or salinity maps (Figure 31). Hansen and Jákupsstovu (1992) termed this feature the "Midwater Front" and used a series of annual surveys in April-May to document variations of it. The front was found at all occasions studied, although differently located. Combined with the evidence from drifters (Poulain *et al.*, 1996; Krauss, 1995) this strongly indicates that the mixture of Atlantic water and MEIW, which flows southwestward over the slope on the Faroese side of the Faroe-Shetland Channel, recirculates within the channel and joins the northeastward flow into the Norwegian Sea as indicated by Helland Hansen and Nansen (1909).

On the shallower parts of the Faroese shelf, long-term current meter moorings have documented a persistent anticyclonic circulation around the islands (Hansen, 1992). Associated with this circulation, some flow may occur over the shallow parts of the Faroese slope which rounds the tip and flows from the Faroe-Shetland Channel into the Faroe Bank Channel and continues northward to make a complete circle of the Faroe Plateau, but the progressive vector diagrams in Figure 19 indicates that this must be small. Hansen and Jákupsstovu (1992) report indications that the Midwater Front may shed eddies of water from the Faroe-Shetland Channel into the Faroe Bank Channel (Figure 31). These processes aside, there is no indication of a significant transport from the Faroe-Shetland Channel into the Faroe Bank Channel of either Atlantic water or of water that derives from north of the Iceland-Faroe Front.

As regards the Atlantic water flow through the upper layer of the Faroe Bank Channel, there remains the question whether this is southward and feeds into the Faroe-Shetland Channel as indicated by Helland-Hansen and Nansen (1909) in Figure 9. Hansen and Jákupsstovu (1992), using the annual Faroese surveys,

find that the dynamic balance between the different flows converging on this area may be different from one survey to another. These different circulation schemes may perhaps also be responsible for the different behaviour of drifters (track C and track D on Figure 20) in the southern Faroe Bank Channel.

The preliminary results from the Nordic WOCE ADCP measurements in the Faroe Bank Channel shed some light on this problem as shown by the progressive vector diagram for 220 m depth from a year-long deployment in 1996 – 1997 (Figure 33). The figure shows typical flow directions which may persist for months to be replaced by radically different flows. This supports the view that the upper layer flows in the Faroe Bank Channel and their coupling to the Rockall Channel and the Faroe-Shetland Channel are variable so that different circulation schemes may apply at different times analogous to – and possibly coupled to – what was found for the Atlantic water flow over the Iceland-Faroe Ridge. The time scales of these variations are not well known and neither do we know whether they have any seasonal character or what mechanisms drive them.

The spreading of Atlantic water in the Nordic Seas. After passing the Greenland-Scotland Ridge, the different branches of Atlantic water progress into the Nordic Seas and from there into the Arctic. The details of the paths and associated water mass changes on route have been reviewed by various authors (Johannesen, 1986; Hopkins, 1991) and are beyond the scope of this work. A few comments are, however, appropriate on the more local behaviour of the Atlantic water after it has passed through the various gaps of the ridge. How much of the heat and salt, transported by the Atlantic water across the ridge, is delivered into the surrounding waters in the immediate vicinity? and do the different branches, that continue out of the ridge area, recombine, or do they stay separate? Stated differently: Do the various Atlantic inflows to the Nordic Seas produce one pot of heat and salt which is distributed over the Arctic Mediterranean or do the different branches affect different parts of the areas northeast of the ridge?

In response to these questions, there seems to be a clear trend of changing behaviour from the western- to the easternmost of the Atlantic branches, crossing the Greenland-Scotland Ridge. The water of the North Icelandic Irminger Current becomes more or less completely absorbed into the areas due north of Iceland (Stefánsson, 1962). In the Iceland-Faroe Gap, the frontal variability and eddy production induces a transport of heat and salt across the Iceland-Faroe Front. Willebrand and Meincke (1980) estimated the eddy-mediated transport of heat northeastward across a 440 km length of the front to be 1.6 10^{13} W. Later estimates have tended to give slightly smaller, but comparable values for this process (Allen *et al.*, 1994) while Hallock (1985) estimated a heat-flux due to intrusive interleaving of approximately half this size. For comparison, the conversion of 1 Sv from Atlantic water to overflow (cooling by 8°C) delivers about 3.2 10^{13} W.

In contrast, the Continental Slope Current in the Faroe-Shetland Channel probably looses relatively smaller amounts of its heat and salt content to the surrounding waters since the horizontal temperature and salinity gradients are much smaller. It should be noted, though, that the recirculated Atlantic water in the Faroe-Shetland Channel has been intermixed with water from north of the Iceland-Faroe Front so that, even though heat and salt content are not rapidly lost, their properties (i.e. temperature and salinity) are vastly changed.

Compared to the North Icelandic Irminger Current, the two Atlantic water branches leaving the Iceland-Scotland Gap can be traced much further. The northern branch is the Atlantic water that continues eastward from the eastern tip of the Faroe Plateau around 63°N. Since this is an extension of the Faroe Current, we use that name also for the continued flow into the Norwegian Sea. The southern branch follows the continental slope and includes water from the Continental Slope Current and recirculated water from the Iceland-Faroe Gap. We use the name "Shetland Current" for this flow.

In the literature (Sælen, 1959; Sælen, 1963; Mosby, 1970; Johannesen, 1986; Hopkins, 1991), the Faroe Current and the Shetland Current have generally been lumped together into one flow through the Norwegian Basin, the "Norwegian Atlantic Current", but the SACLANT drifters (Poulain *et al.*, 1996) clearly indicate that the two branches to a large extent stay separated all the way north to the area just south of the entrance to the Barents Sea. The inner branch seems to be topographically locked to the main slope off the Norwegian shelf. The outer branch, the Faroe Current may perhaps be tied to a "secondary slope" at bottom depths of 2000 – 2500 m. It is bounded towards the northwest by a front in the upper layers (Smart, 1984) which represents the outer boundary of the Atlantic water in the southern Norwegian Sea.

Summarising, the answer to the question posed, is that different regions in the Arctic Mediterranean are indeed affected differently by the three Atlantic inflows to the Nordic Seas. The Icelandic Irminger Current has direct effects only on the Iceland Sea. The Faroe Current apparently feeds the two recirculating cells in the Norwegian Basin and the Lofoten Basin (Figure 21) and thus probably delivers much of the heat and salt to these areas plus a possible input to the Iceland Sea and the southern Greenland Sea close to Jan Mayen. The North Sea and the Barents Sea, on the other hand, probably receive their main input from the Shetland

Current which includes the Continental Slope Current. A quantification of these, very qualitative, statements does not seem possible with the available information and it also seems premature to draw conclusions as to the relative contribution to the continuing flow feeding the Greenland Sea and the Arctic Ocean from the two main inflow regions, the Iceland-Faroe Gap and the Faroe-Shetland Gap.

The circulation of the upper layer. To a large extent, the synopsis of this chapter is the circulation scheme presented in Figure 6. Most of the features on the figure have been discussed, but some additional comments are appropriate. One of these relates to the circulation in the Iceland Basin. Through this century a number of investigators have discussed the upper layer circulation of the Iceland Basin as reviewed by Hansen (1985). Although geostrophic calculations (e.g. Dietrich, 1957; Wegner, 1972) have given diverging results, the main consensus has been a cyclonic circulation as implicit in Helland-Hansen and Nansen's (1909) Figure 9. Becker and Hansen (1998, this volume) found support for that in their analysis of water mass characteristics in the Iceland Basin, based on NANSEN observations.

As yet, the number of moored current meter measurements from the upper layers of the Iceland Basin seems too small to draw any conclusions on this question, but both of the major drifter experiments from the area (Krauss, 1995; Otto and van Aken, 1996) do support a cyclonic recirculation. They both indicate clearly a southward flow on the eastern side of the Mid-Atlantic Ridge which for continuity reasons requires some kind of recirculation in the northwestern corner of the basin.

We are not aware of any drifter experiment that has shown complete circuits in the basin, but Otto and van Aken (1996) see indications of it. Also, van Aken and de Boer (1995) argue that the water mass characteristics of the upper water over the Iceland slope indicates admixture of overflow water from the Iceland-Faroe region. The more or less centrally symmetric recirculation cell in the older literature probably has to be somewhat deformed, however. In Krauss's (1995) experiment, a number of buoys appear to cross the central basin in a fairly straight line toward the Iceland-Faroe Ridge. The northeastgoing flow thus seems to be broader than the return, which we have indicated in Figure 6.

On the northeastern side of the ridge, we have, as argued, adopted the circulation system of Figure 21 for the Norwegian Basin. The cyclonic circulation cell in this basin carries a mixture of Atlantic and northern water masses (mainly Arctic Intermediate Water) back towards the Iceland-Faroe Ridge. In Figure 6 we have used the name "Recirculated Faroe Current" for this flow and for the water which it transports we have adopted Read and Pollard's (1992) name "Norwegian North Atlantic Water (NNAW)". This water is involved in the production of the overflow across the Iceland-Faroe Ridge and will be discussed and will be touched upon within that discussion.

The origins of the overflow waters

The word "overflow" is used to denote the cold, dense water masses crossing in a layer close to the crest of the Greenland-Scotland Ridge in various areas, flowing from the Arctic Mediterranean to the North Atlantic. Together with the surface flow of the East Greenland Current, the overflow comprises the total outflow from the Arctic Mediterranean through the Greenland-Scotland Gap. Much of the overflow water has been produced (that is has left the surface) far away from the ridge, but some of the water overflowing the Iceland-Faroe Ridge has left the surface layers quite close to the ridge. These two sources are discussed separately and we discuss also the intermediate and deep waters of the southern Norwegian Sea (Figure 34) which acts as a buffer region for the Iceland-Scotland overflow.

Remotely produced overflow waters. Traditionally the waters that contribute to the overflow are divided into "intermediate" and "deep" water masses. The boundary between these two is not well defined, but roughly stated, the intermediate waters have been produced by convective or other sinking processes no deeper than about a thousand meters, while deep waters are those that have descended to deeper levels.

Deep-water formation has been discussed during most of this century. It is now recognised (Aagaard *et al.*, 1985) that there are two distinct mechanisms for creating deep water. One is the traditional scheme in which water in the Greenland Sea sinks from surface or near-surface layers to large depths by open ocean deep convection. The second mechanism involves dense water being formed in the shallow shelf regions surrounding the Arctic Ocean.

Both deep-water formation mechanisms require that the upper water has a sufficiently high salt content which may be acquired by advection of saline water from the surroundings or by brine rejection from forming ice. In addition to salt, cooling is required in both cases forced by air-sea temperature differences and enhanced by winds. Thus deep water is mostly formed in winter. It appears that both deep convection and shelf-production of deep water are intermittent in time and fairly localised geographically, which makes observation and quantification of production rates difficult. Apparently, however, deep convection in the Greenland Sea has been much reduced during the last two decades. This is implied by increasing bottom temperatures and salinities (Meincke *et al.*, 1997) as well as by tracer

studies (Schlosser *et al.*, 1991; Rhein, 1996). In the deep parts of the Greenland Sea, water from the Arctic Ocean has thus been replacing locally formed Greenland Sea Deep Water (GSDW) (Meincke *et al.*, 1997).

In the Arctic Ocean, the low salinity of the surface waters prevents deep convection, but not the formation of dense waters over the surrounding shelves (Aagaard *et al.*, 1985; Midttun, 1985). This water flows outward over the shelf and descends the slope down to intermediate or deep levels, determined by its density, as modified by entrainment of surrounding water, in relation to the in situ density structure.

Rudels *et al.* (1998, this volume) discuss in detail the contribution of Arctic Ocean waters to the overflow. In contrast to older conjectures (e.g. Swift, 1986) they find that the outflow through the Denmark Strait contains intermediate water as well as some upper deep water from the Arctic Ocean in addition to the Polar water in the upper parts of the East Greenland Current. The densest Arctic Ocean deep waters are too deep to overflow and are turned either at the Jan Mayen Fracture Zone or at the entrance to the Denmark Strait (Rudels and Quadfasel, 1991; Buch *et al.*, 1992). As indicated in Figure 7, these waters may, however, continue into the Norwegian Basin. In this way both European Basin Deep Water (EBDW) and Canadian Basin Deep Water (CBDW) may contribute to the formation of Norwegian Sea Deep Water (NSDW) (Rudels *et al.*, 1998, this volume).

Intermediate water is in the traditional view produced in the open areas of the Iceland Sea and the Greenland Sea (Swift and Aagaard, 1981; Swift, 1986) from where it flows towards the Denmark Strait and into the Norwegian Sea (Blindheim, 1990). In addition to this, intermediate water is formed by sinking in frontal regions within the Norwegian Sea as shown by Blindheim and Ådlandsvik (1995). Changing nomenclature and large interannual variability in thermohaline characteristics have added much to the confusion surrounding these water masses.

In the classification by Swift (1986), two main types of intermediate water are produced in the Iceland and Greenland Seas: "Upper Arctic Intermediate Water" (UAIW) ($T<2°C$, $34.7<S<34.9$) and "Lower Arctic Intermediate Water" (LAIW) ($0°C<T<3°C$, $S>34.9$). Comparing these to available data, Blindheim (1990) identified the UAIW as a salinity minimum around 0°C in the Norwegian Sea and called it simply Arctic Intermediate Water (AIW). This is the same water mass that Martin (1993) has identified in the Faroe-Shetland Channel and denoted as "Norwegian Sea Intermediate Water" to avoid confusion with older literature. We follow Blindheim and Ådlandsvik (1995) and use the name "Norwegian Sea Arctic Intermediate Water" (NSAIW) to denote water of temperature around 0°C in the overflow.

Observations in the Faroe-Shetland Channel have indicated a considerable salinity variation for the water around 0°C and Martin (1993) has found a positive correlation between the salinity of this water and that of the NAW lagged by 7 years. Apart from the uncertainty introduced by the older salinity observations, the salinity of this water in the Faroe-Shetland Channel may already have been modified. Blindheim and Ådlandsvik (1995) and Fogelquist *et al.* (in press) give a more restricted salinity range of 34.87 – 34.90 for NSAIW and we have adopted this range in Table 3.

The deep and intermediate water masses all derive from the Atlantic inflow to the Nordic Seas and they have descended from the upper layers in a more or less vertical process, be it convection, cascading down the slope or frontal sinking. Some of the Atlantic water remains, however, in the boundary current that circles the Arctic Mediterranean. This water is continuously being cooled and freshened by contact with the atmosphere and dilution by fresher waters. Originally, it occupies the upper layers, but when it encounters fresher surface waters like the upper layers of the Arctic Ocean or the East Greenland Current it dives beneath these.

In Figure 7 two kinds of water of this type may be traced to the Denmark Strait overflow. This is the remains of the Atlantic water that has entered the Arctic Ocean. Rudels *et al.* (1998, this volume) call this "Modified Atlantic Water". In the Fram Strait this water is joined by "Recirculated Atlantic Water" which has bypassed the Arctic Ocean. In the classical description (Swift *et al.*, 1980) this water has not figured prominently as an overflow contributor. However, Rudels *et al.* (1998, this volume) assign about half of the Denmark Strait overflow to this source. Mauritzen (1996) argues that more than 80% of the total overflow over the Greenland-Scotland Ridge derives from this direct pathway. In her model most of the cooling and freshening of the Atlantic water occurs within the Norwegian Sea.

The Iceland-Faroe Ridge overflow water. Part of the water overflowing the Iceland-Faroe Ridge has been remotely produced but there is also a component which, it is believed, acquires its main character in a region close to the ridge by mixing of different water masses and sinking in the frontal zone. This water is most clearly identified as a salinity minimum with salinity below 34.90 and a temperature usually around 2–3°C. It is typically seen on sections crossing the Iceland-Faroe Ridge (Figure 35); it is commonly found north of the Faroes (Figures. 22 and 25) and also in the Faroe-Shetland Channel (Figure 29), as has been previously discussed.

Table 4. Properties listed by various authors for water masses involved in the formation of Modified East Icelandic Water (MEIW).

Authors	MNAW		NNAW		NNIW		EIW		NSAIW	
Stefánsson 1962					1.5–2.0	34.82–34.90				
Meincke (1978)							1.5	34.63		
Müller *et al.* (1979)	8.5	35.24					-0.5–1.0	34.72		
Read and Pollard (1992)	7.5–8.0	35.20–35.25	3.0	34.98			0.4	34.74	0.0	34.90

In the literature the term "NI/AI water" has been commonly used to denote this water. Somewhat confusingly, this term has been used as abbreviation both for "North Icelandic (NI) Winter water/Irminger Sea (AI) water" (Meincke, 1974) and for "North Icelandic (NI) Winter water/Arctic Intermediate (AI) water" (Müller *et al.*, 1979). To confuse the uninitiated reader even more, this water mass, when it reaches the Faroe-Shetland Channel, is commonly denoted as "Arctic Intermediate Water (AIW)". We have chosen to follow Read and Pollard (1992) and use the name: "Modified East Icelandic Water (MEIW)".

The temperature and salinity of MEIW makes it very similar to the "North Icelandic Winter Water" (NIWW) ($2°C<T<3°C$, $34.85<S<34.90$). According to Stefánsson (1962) this water is homogenised in winter north of Iceland from a mixture of MNAW from the North Icelandic Irminger Current and water from the upper layers of the Iceland Sea plus some coastal water influenced by runoff. Using observations from the Overflow'60 experiment Stefánsson (1962) tried to estimate the contribution of NIWW to the Iceland-Faroe Ridge overflow. He found quite a large NIWW content in the overflow over the northwestern part of the ridge, close to Iceland, which approached zero towards the Faroese end.

This kind of analysis is, however, made ambiguous by the fact that there are other water masses in the vicinity whose properties either in pure form or as mixtures are close to those of NIWW. Thus a colder and fresher water mass, "East Icelandic Water" (EIW), was included in analyses carried out on the basis of the overflow'73 experiment (Müller, 1978; Müller *et al.*, 1979) and a German survey in 1977 (Meincke, 1978). This water is carried towards the ridge area by the East Icelandic Current. Read and Pollard (1992) introduced yet another water mass which they called "Norwegian North Atlantic Water (NNAW)" and considered to be formed in the recirculating gyre of the Norwegian Basin (Figures 6 and 21) as a mixture of MNAW and NSAIW, mainly.

In most treatises, the resulting overflow water mass, MEIW, is (explicitly or implicitly) considered to be formed outside the ridge area and carried towards it by the southgoing flows east of Iceland. Based on their densely spaced SeaSoar survey of the Iceland-Faroe Ridge, Read and Pollard (1992), however, did not find MEIW entering into the Iceland-Faroe region as a distinct water mass, but they observed its production as a mixture of the source waters: MNAW, NSAIW, EIW and NNAW.

Read and Pollard (1992) illustrated the spreading of the MEIW by the distribution of the 2°C isotherm at 100, 200 and 300 m depth levels (Figure 36). In the northern part of the area, MEIW is seen forming a cold tongue along the Jan Mayen Front and then sinking and progressing southwards towards the Faroes in-between MNAW and NNAW. As previously described, Meincke (1978) has traced the associated salinity minimum around the Faroes and into the Faroe-Shetland Channel.

Figure 37 shows è-S-diagrams from an area north of the Faroes, through which the cold low-salinity tongue of MEIW (Figure 36) passes. The core properties of MEIW in this area are defined by the salinity minimum at 1–3°C which has salinities in the range 34.70 – 34.90. With the rapidly changing conditions in this frontal area, well defined water mass properties are hard to estimate, but these ranges are consistent with other information and have been adopted in Table 3 and Figure 8.

In Figure 38 we illustrate the formation of MEIW in è-S space schematically and properties of source waters cited by various authors are listed in Table 4. The temperature and salinity ranges of MEIW include NIWW as defined by Stefánsson (1962), but in addition it can clearly be formed out of different mixtures of source waters. It is seen in Figure 13 that the observations discussed by Read and Pollard (1992) were at a time (summer 1990) when the North Icelandic Irminger Current had been relatively weak for about two years. This might perhaps explain why they did not observe NIWW directly. In general we may expect variations both in absolute and relative strengths of the inputs of NIWW and the fresher and colder EIW to the frontal area which may perhaps explain the large variations observed for MEIW. The fact that the MEIW propagates as a narrow tongue, layered between

radically different waters, will, however, always lead to significant mixing and modification of the original water and thus the name "Modified East Icelandic Water" should be generally appropriate.

The deep and intermediate waters of the southern Norwegian Sea. The Norwegian Basin in the southern Norwegian Sea feeds the overflow passing between the Faroes and Shetland and also a part of the overflow over the Iceland-Scotland Ridge. It acts as a mixing and buffering area for these waters before their approach to the ridge. The deep parts of this basin are filled by "Norwegian Sea Deep Water (NSDW)". Water mass analysis indicates that the deepest component of the NSDW results from Greenland Sea Deep Water (GSDW) and Eurasian Basin Deep Water (EBDW) in a fairly even mixture (Aagaard *et al.*, 1985; Swift and Koltermann, 1988). This mixture is thought to enter the Norwegian Basin through the Jan Mayen Channel (Figure 34) with sill depth around 2200 m just north of Jan Mayen (Sælen, 1990).

The deepest layers in the Norwegian Basin are vertically homogeneous in salinity as well as in potential temperature. Figure 39a (Østerhus *et al.*, 1996) shows that from about 2000 m, down to bottom, the basin was in 1994 homohaline (constant salinity) with a salinity close to 34.910. From about 2800 m, downward, it was adiabatic (constant potential temperature) as well, probably due to convection driven by heat flow from the ocean floor (Østerhus *et al.*, 1996).

Above the adiabatic layer in the Norwegian Basin, potential (and in situ) temperature increases upward, but salinity remains fairly constant, perhaps with a slight minimum around 2200 m depth and a slight maximum around a depth of 1200–1500 m (Figure 39b). Swift and Koltermann (1988) list a number of possible causes for this salinity maximum, but Rudels and Quadfasel (1991) suggest that this may be the remnants of Canadian Basin Deep Water (CBDW) from the Arctic penetrating all the way to the area north of Iceland and from there flowing into the Norwegian Sea after having been admixed with NSDW and GSDW on route as indicated on Figure 7.

Above the salinity maximum at 1500 m, Figure 39b shows decreasing salinities as we ascend into first the NSAIW and then, at about 500 m depth, into MEIW. During a period of vigorous deep-water formation in the central Greenland Sea, the deep parts of the Norwegian Basin will be continually supplied with dense bottom water which will induce an upwelling in the basin. At the same time intermediate water sinks from above and is advected from the surrounding areas. In-between these is the zone which is continually flushed by the overflow and where properties are intermediate due to mixing. Where to place the boundary between the NSDW and the NSAIW becomes a matter of definition.

One common definition has been to use the temperature (or the potential temperature) -0.5°C as the upper boundary for NSDW (e.g. Müller *et al.*, 1979). This temperature is commonly found close to (but usually above) the 1000 m depth level. Fogelquist *et al.* (in press) have found that this is the depth from which the densest overflow in the Faroe Bank Channel is drawn and that this water has an apparent age of 20 years as compared to 30 years for the adiabatic bottom layer of the Norwegian Basin. We have adopted this definition for NSDW in Table 3 and Figure 8 which makes NSDW and NSAIW blend continuously into one another.

In Figure 7 the intermediate and deep layers of the Norwegian Basin are represented by a black box from which the overflow of NSDW and NSAIW derives. The homogeneity implied by this may be misleading. Halocarbon concentrations observed by Fogelquist *et al.* (in press) show significantly higher values over the deep eastern flank of the Iceland-Faroe Ridge than at comparable depths in the middle of the basin. These observations may be linked to a boundary current that has been suggested to flow southeastwards over this flank.

Thus, Sælen (1990) suggests that the flow through the Jan Mayen Channel from the Greenland Sea turns to the right when it enters the Norwegian Basin and flows as a boundary current. Hopkins *et al.* (1992) report results from current meter observations from depths around 900 m at three sites east of Iceland and the Iceland-Faroe Ridge. These observations (Figure 34), which are just below sill-depth of the Faroe Bank Channel show persistent flow along the topography with velocities of 3–6 km/day consistent with a cyclonic circulation. The observed halocarbon distribution over the eastern flank of the Iceland-Faroe Ridge could then be due either to enhanced vertical mixing in this boundary current or to an input from north of Iceland as indicated by the residual flow vector east of Iceland shown on Figure 34.

The paths of the overflow

Through the gap between Iceland and Scotland the three overflow water masses, MEIW, NSAIW and NSDW (Figure 7) may be traced along two paths towards the ridge. The MEIW and part of the other two water masses flow over the Iceland-Faroe Ridge. The rest flows through the deep parts of the Faroe-Shetland Channel and spills over the Wyville Thomson Ridge or continues northwestwards through the Faroe Bank Channel. From these three overflow sites, the water may follow different paths and be incorporated into different water masses, but an important component

flows as a deep boundary current westwards on the northern flank of the Iceland Basin to cross the Mid-Atlantic Ridge and join the Denmark Strait overflow (Figure 7).

The deep flow through the Faroe-Shetland Channel. The main outlet of overflow water from the southern Norwegian Sea is through the Faroe-Shetland Channel. A map of the bottom topography (Figure 28) shows the Faroe-Shetland Channel intruding between the Faroes and Shetland. From the Norwegian Sea, the channel shallows towards the southwest until it reaches a sill southeast of the Faroes which is a little more than 1000 m deep. From there the channel again deepens into a basin of more than 1200 m depth between the Wyville Thomson Ridge, the Faroe Bank and the Faroe Plateau. The Faroe Bank Channel is the outlet from this basin.

A section across the Faroe-Shetland Channel will typically show cold (< 3°C) water of salinity below 35.0 from about 500 m depth down to the bottom (Figure 29). This is the water that may potentially contribute to the overflow. Through the years a number of publications have listed results from hydrographic investigations on this water, especially based on data from the two standard sections (Figure 28) in the channel (Tait, 1955, 1957a, 1957b; Martin, 1966, 1976, 1988, 1993).

Figure 40 shows four θ-S diagrams from a cruise in May 1996. Two of these are from either end of the Faroe-Shetland Channel (FSCW and FSCE). The θ-S-diagram from the eastern end of the Faroe-Shetland Channel (FSCE) is very similar to the diagram from the Norwegian Basin (NB) and both these diagrams show the two intermediate water masses MEIW and NSAIW in addition to the deep water NSDW. In the western end of the channel (FSCW) the MEIW is not seen at all in Figure 40 and the low-salinity signal of NSAIW is much less pronounced. Being a snapshot from one cruise, Figure 40 should not be over-interpreted, but it does illustrate two typical features. One is that the deepest water of the Faroe-Shetland Channel deviates little from its origin in the Norwegian Sea. The second typical feature is a weakening of the signature from the two intermediate water masses MEIW and NSAIW. To some extent this may be due to mixing, but it may also be related to the deep circulation of the Faroe-Shetland Channel.

In the classical studies on the Faroe-Shetland Channel, cited above, much effort was invested into geostrophic calculations of currents and volume transport. As has been discussed, the assumptions that have been made in these calculations are not supported. For information on deep flows direct current measurements are necessary. Most available deep current measurements from the Faroe-Shetland Channel have been fairly short-term except for the Nordic WOCE observations that as yet are only preliminary. Combining the available evidence, there are indications of a partial recirculation of the cold water as indicated in Figure 41, but more observations are necessary on this question. Also, more research is needed on the link between this flow and the Norwegian Sea. To what extent and how is the deep flow in the Faroe-Shetland Channel coupled to the boundary current which apparently flows southeastwards over the eastern flank of the Iceland-Faroe Ridge?

The overflow across the Wyville Thomson Ridge. Having passed the sill southeast of the Faroe Plateau (Figure 28), a part of the deep-water approaches and overflows the Wyville Thomson Ridge. Our knowledge of the Wyville Thomson Ridge overflow is to a large extent due to the work of David Ellett. From its first observation (Ellett and Roberts, 1972, 1973), through its mapping and quantitative assessment (Ellett, 1976, 1988, 1991; Ellett and Martin, 1973; Ellett and Edwards, 1978; Ellett *et al.*, 1986; Edwards *et al.*, 1979) to the last estimates (Ellett, 1998, this volume), he and co-workers have given us a comprehensive, although not complete, picture of this overflow and its impact on the waters west of the ridge.

A map of the bottom topography (Figure 42) shows that the Wyville Thomson Ridge is fairly flat with depths mostly between 500 and 600 m along its total extent from the Faroe Bank to the Hebridean slope area. It has a shallow depression in the middle where the sill depth of about 600 m is found (Ellett, 1988). Overflow through this depression, as well as over the ridge crest northwest of it, will be trapped by a narrow gully between Faroe Bank and the Ymir Ridge (Figure 42). During the Overflow '73 experiment a series of CTD sections traced the flow of cold water through this channel (Müller *et al.*, 1979) and monitoring of the overflow has mainly focused on this path.

Using results from current meter deployments during NANSEN, Ellett (1998, this volume) has reported observations for 10 consecutive months in 1987–1988 from a current meter moored 15 meters above bottom at 710 m depth (Figure 42). This showed a persistent westward flow over the northern flank of the gully with 10-day average velocities of 25 – 50 cm s^{-1} and only occasional reversals. The temperature at this instrument was usually in the 5 – 7 °C range which is sufficiently cold to indicate a cold-water component from northeast of the Wyville Thomson Ridge. It also indicates that it must have a large Atlantic water component either from east of the ridge or entrained on the way to the current meter. Ellett (1998, this volume) suggests that this steady flow is entrained by a deep branch of the Continental Slope Current which is turned westwards by the Wyville Thomson Ridge.

In addition to this steady flow, the current meter observations show a much more distinct overflow event with stronger than normal currents that lasted more than a week and had 10-day mean temperatures falling below three degrees. This event extended above an upper current meter that was 170 m above bottom level. CTD sections also demonstrate that cores of cold overflow water may be found much higher up on the southern Faroe Bank slope (Figure 43) which probably has overflowed the ridge close to the Faroe Bank, but this is clearly an intermittent feature (Ellett, 1998, this volume). Others have found evidence for intermittent overflow over the southeastern part of the ridge also. Altogether the Wyville Thomson Ridge overflow is intermittent both spatially and temporally and a thorough monitoring of it would require long-term observations at many sites.

The overflow through the Faroe Bank Channel. The existence of cold bottom water in the Faroe Bank Channel (Figure 30) was first suggested by Knudsen (1911). However, he seems not to have imagined a continuation of this flow into the Atlantic Ocean and not until the seminal paper by Cooper (1955) was the importance of this flow recognised. By then, bathymetric surveys had demonstrated the considerable depth of the channel and Hermann (1959) and Tait (1961) presented a number of hydrographic sections across the channel, sampled by Scottish and Danish research vessels, which all of them showed the cold deep overflow water. Both these authors also presented results of bottom current measurements in the channel using the "Carruthers Pisa" current meter (Tait 1958). These measurements were, however, in the bottom boundary layer and did not give any indication of the strong currents now known to dominate the overflow core.

In volume 12 of the Deep-Sea Research journal, two papers helped focus the research on the Faroe Bank Channel. Harvey (1965) discussed the topography of the channel based on surveys in 1941–43 and 1960–63 finding a sill depth of about 840 m and, using a neutrally buoyant ("Swallow") float, Crease (1965) demonstrated that the deep flows may exceed 1 m s^{-1}. In 1967 Sætre published results from current measurements covering a few days in 1964-65 on anchored buoys using the newly developed Aanderaa current meters and hydrographic observations. These measurements showed persistent currents of speeds up to 140 cm s^{-1} in the deep layer of the channel and established the Faroe Bank Channel as a major overflow path.

Since then the Faroe Bank Channel has been visited by a large number of the research vessels operating in the North Atlantic and it was included into the observations of both the "Overflow" expeditions. During the NANSEN programme the Faroe Bank Channel was studied by Swedish scientists (Borenäs and Lundberg, 1988) and by the Institute of Oceanographical Sciences in the UK which mounted a major observational effort to study the channel as evidenced by Tables 1 and 2. These studies involved hydrography, shipborne ADCP and moored current measurements (Saunders, 1990, 1992). The NANSEN programme also inspired the establishment of a Faroese standard section across the channel (Figure 28) which in the following decade (1988-1997) has been sampled on 40 CTD cruises. In the Nordic WOCE programme these CTD sections have been combined with an upward-looking ADCP moored close to the bottom near the sill of the channel (Figure 41).

The temperature and salinity section on Figure 30 shows a fairly typical cross section close to the sill. As was shown in Figure 31, the boundary between the upper Atlantic water layer and the overflow water is typically sharp. Figure 44 shows an average temperature profile based on 40 CTD observations at one of the Faroese standard stations close to the sill and also an average velocity profile based on preliminary Nordic WOCE ADCP observations. Both profiles indicate a bottom layer of about 250 m thickness. Average velocities exceeding 1 m s^{-1} are found in a layer of about 100 m thickness with the velocity core some 100 m above bottom. In Figure 45 is shown the daily averaged current component towards 304° (out into the Atlantic) in this core for a period of about one year. The persistence of the flow is demonstrated by the fact that not one of the days in this figure had southeastgoing flow, but there are clearly variations in the flow.

A typical feature, seen in Figure 30, is the pinching of isolines on the southwestern (Faroe Bank) side of the channel and the corresponding vertical spreading of isolines towards the Faroe side. Johnson and Sanford (1992) suggested that this was due to a helical velocity pattern in the overflow which they had observed using XCP' s and Johnson and Ohlsen (1994) found this behaviour in laboratory experiments simulating the channel flow. The measurements by Johnson and Sanford (1992) indicate that the overflow core is separated from the bottom by a boundary layer of 30m thickness in which both log-layer and Ekman layer dynamics are seen.

A number of theoretical studies have treated the Faroe Bank Channel overflow. In his 1965 paper Crease made a simple model in which the overflow was driven by the downstream pressure gradient and limited by a bottom stress quadratically dependent upon velocity and by entrainment from the Atlantic layer above. His velocity estimate was somewhat high, but his estimate of the bottom stress was not very much higher than that measured by Johnson and Sanford (1992). Hydraulic control theory was employed to the Faroe Bank Channel by Rydberg (1980) and by Borenäs and

Lundberg (1988), but has been questioned by Saunders (1990) and Johnson and Sanford (1992).

In the classical literature the core of the Faroe Bank Channel overflow is generally cited as being composed of NSDW. With the identification of NSAIW in the bottom water of the Faroe-Shetland Channel this water mass could also be expected to enter the Faroe Bank Channel. Indeed Figure 40 shows a slight salinity minimum somewhat colder than 0°C. This θ-S trace, as well as most others from the middle of the Faroe Bank Channel, shows only small indications of MEIW. This is usually attributed to mixing and, certainly, strong mixing may be expected. Johnson and Sanford (1992) used high-resolution XCP profiles to estimate gradient Richardson numbers in the channel which supported the conclusion by Saunders (1990) that the shear was sufficient to allow shear instabilities in the high-gradient layer above the overflow core.

As previously argued, the recirculation in the Faroe-Shetland Channel implies that the deep water of the Faroe Bank Channel, although deriving from the Faroe-Shetland Channel, may not necessarily be just an averaged version of that water. Fogelquist *et al.* (in press) report results of halocarbon measurements and hydrography which indicated a maximum concentration of MEIW of about 20% in a thin layer in the thermocline. They concluded that the deepest water in the channel is a fairly even mixture of NSDW and NSAIW deriving from about 1000 meters depth in the southern part of the Norwegian Sea.

When the overflow water has passed the sill of the Faroe Bank Channel, the continuing flow is often represented as a stationary, single-cored density-driven plume hugging the Iceland-Faroe Ridge and only slowly descending (Price and O'Neil Baringer, 1994; Lindblad, 1997). Reality seems to be more complicated. There are sections crossing the southern Iceland-Faroe Ridge which show only one core centered at some 800–900 m (Saunders, 1990; Lee, 1967), but often this core is supplemented by one much deeper which seems to follow the deepest path into the Iceland Basin (Saunders, 1992; Lee, 1967; Lindblad, 1997). From the Overflow '60 observations Hermann (1967) plotted two overflow paths from the Faroe Bank Channel as shown on Figure 46. In addition we have added a path (dotted arrow on the figure), following a gully in the ocean floor, where there is some indication of overflow as will be argued later.

The overflow plume from the Faroe Bank Channel is not always single-cored and it is probably not very stationary either. This is documented by the downstream observations just cited and Figure 47 illustrates non-stationarity close to the sill. This figure is based on an R/V Magnus Heinason cruise within NANSEN and it shows that after exiting the channel, the overflow water did not flow as a continuous stream but rather it released a bolus of cold water. This behaviour should not be unexpected. When the overflow has passed out of the channel the dynamic constraints on it change abruptly. The bottom descends sharply into the depths of the Iceland Basin and from a channel the flow enters a slope region without a supporting wall on the left-hand side. Under these conditions, highly variable flows must be expected and associated with these a strong mixing which may explain why the minimum temperature in the overflow cores on the slope of the Iceland-Faroe Ridge is so much higher (usually 1 – 2°C) than in the channel.

Pure overflow water without any entrained Atlantic water is generally not observed after the flow has exited the Faroe Bank Channel. The same applies to the overflows across the Wyville Thomson and the Iceland-Faroe ridges and it has therefore been customary to define "Iceland-Scotland Overflow Water (ISOW)" as a water mass that contains entrained water in addition to NSAIW, NSDW and MEIW. This water mass has been defined in terms of temperature ($\theta < 3$°C) or salinity ($S > 34.94$), but perhaps most generally in terms of density ($\sigma_\theta > 27.8$).

The overflow across the Iceland-Faroe Ridge. Overflow across the Iceland-Faroe Ridge was observed more than a century ago by Danish oceanographers. Using results from the "Ingolf expedition" Knudsen (1898) observed the overflow and suggested that it was intermittent (occurring "in jerks") while Nielsen (1904) argued that it must be continuous. During the next half century, the problem seems only to have been sporadically studied until interest in it re-surged in the 1950s. Dietrich (1956) reported results of measurements from four sections across the ridge and Hermann (1959) and Steele (1959) published sections and maps of bottom temperature. All these observations showed strong evidence of overflow.

In 1960 ICES co-ordinated the first overflow expedition (Overflow '60) in which 9 ships from 5 nations made three quasisynoptic hydrographic surveys of the Iceland-Faroe Ridge (Tait *et al.*, 1967). In the following years hydrographic observations were supplemented by current measurements (Steele, 1967; Meincke, 1972), leading up to the second overflow expedition (Overflow '73) in August/September 1973. Then, thirteen research vessels carried out individual scientific programs while simultaneously contributing to the general topic of water mass exchange across the Greenland-Scotland Ridge (Meincke, 1974).

It would probably be an exaggeration to claim that a theoretically based comprehensive description resulted from these and later, more sporadic, studies on the Iceland-Faroe Ridge overflow, but they did provide a more complete picture of the process. Figure 49

summarises results from 14 occupations by German research vessels of a section west of the ridge crest in the period 1959–1971 (Meincke, 1972). Figure 49a shows average temperature as well as its standard deviation along the section. Cold water is found all along the ridge as a 100–150 m thick layer with temperatures down to 3°C. The high standard deviations indicate a high variability in this layer, but different in different regions.

Figure 49a demonstrates that water from east of the Iceland-Faroe Ridge may be found all along the ridge just west of its crest, but more regularly in some locations (low average temperature combined with low standard deviation) than in others. This does not imply that the overflow occurs as a broad southwestward flowing stream all over the ridge. Some of the cold water in Figure 49a may retreat back eastwards and the water that does overflow has a velocity which is more alongslope than downslope. This was argued already by Steele (1961) and confirmed by current measurements (Meincke, 1972; Koltermann *et al.*, 1976) as summarised in Figure 18b. That figure indicates five overflow branches that follow depressions across the ridge. Except for the deepest one closest to the Faroes, they are consistent with Figure 46 where the main overflow paths established during Overflow '60 were shown (Hermann, 1967).

During the Overflow '73 experiment a detailed study was made of an overflow event occurring in a small region (Müller *et al.*, 1974). Combined results from hydrography and current measurements showed that the overflow in that region may occur as thin narrow bands spilling over the sills of cross channels (Figure 50). Later studies have also seen local overflow events (Perkins *et al.*, 1994), but establishing more generally where, and where not, overflow occurs would be a very resource demanding task which has not been completed and Figures 18b and 46 may not be the final answer.

The water mass composition of the overflow may be illustrated by Figures 49b, 49c and 49d (from Meincke, 1972). The Atlantic water component remains high even in the deepest layer, indicating large entrainment. In the figure, NSAIW and NSDW have been lumped together into one water mass ("NS" in Meincke's notation) as was common at the time and Meincke used the name and properties of North Icelandic Winter Water while we have used the more general term: MEIW. It is seen that the deepest part of the overflow layer is dominated by NSAIW+NSDW while MEIW is more dominant in the upper part of the layer. As noted by Stefánsson (1962), the ratio between these two overflow source waters changes along the ridge with the largest influence of NSAIW+NSDW in the Faroese end of the ridge.

The distributions in Figure 49 are based on an analysis which assumes source water masses with well defined and constant temperature and salinity. These assumptions are not valid, but the qualitative features of the distributions are robust and have remained in the results from the Overflow '73 (Müller *et al.*, 1978) and in later studies (Fogelquist *et al.*, in press). From the Overflow '60 experiment Hermann (1967) concluded that MEIW and NSAIW+NSDW (in our notation) each contributed about half of the overflow across the ridge. Using Halocarbon concentrations and hydrography, measured during a cruise in 1994, Fogelquist *et al.* (in press) found these three water masses in about equal proportions in the flow over the ridge.

To classify the Iceland-Faroe Ridge overflow as intermittent may not be proper, taking into account the regular occurrence of overflow water on the western side of the ridge, but it certainly is highly variable, both spatially and temporally and there has been some discussion as to what drives the variability. After the Overflow '73 experiment attempts were made to link observed variations to atmospheric forcing (Meincke, 1975) and in a follow-up experiment "MONA" (Monitoring the Overflow into the North Atlantic) six long-term current meter moorings were deployed during the summer of 1975.

Four of these instruments were successfully recovered in the summer of 1976. One of these was on the Iceland-Faroe Ridge (Figure 48) and similarities were observed between spectra of oceanographic and atmospheric variables with some evidence of coherence (Meincke, 1976; Meincke and Kvinge, 1978). In spite of this statistical evidence for a coupling between atmospheric parameters and overflow, these authors could not provide physical evidence for it. Later Willebrand and Meincke (1980) concluded that the oceanic variations observed at the MONA mooring on the Iceland-Faroe Ridge were generated by (presumably baroclinic) instabilities of the Iceland-Faroe Front. Only occasionally, during the passage of strong atmospheric cyclones would wind generation be likely to play a dominant role (Meincke, 1975).

The spreading of overflow waters in the North Atlantic. The cold overflow water that has crossed the Iceland-Scotland Ridge continues along various paths. A considerable part of the overflow through the Faroe Bank Channel and across the Iceland-Faroe Ridge joins to form a deep boundary current flowing westwards south of Iceland. This current has been studied by a number of authors through the years (Steele, 1961; Steele *et al.*, 1962; Shor *et al.*, 1977; Shor, 1978; de Boer *et al.*, 1998, this volume; van Aken, 1998, this volume; Saunders, 1996).

From these studies a fairly consistent picture can be drawn of a broad flow, hugging the southern Icelandic slope, carrying overflow water which, compared to its surroundings, is cold and saline, high in oxygen and

low in nutrients. During and after the NANSEN programme, oceanographers from the Netherlands and from Germany studied this flow using hydrography, nutrient chemistry and moored instruments. As an example, Figure 51 shows a meridional section crossing the Iceland Basin. The overflow water is identified as a cold, saline layer extending from 1200–1500 m depth on the Icelandic slope all the way to the bottom of the Iceland Basin on this section. This is confirmed by an optimal parameter water mass analysis (de Boer, 1998, this volume) as seen in Figure 51c.

This figure conflicts with the picture, sometimes presented, of a fairly narrow, single-cored overflow current, confined to mid-depths on the Icelandic slope. In the eastern part of the Iceland Basin Figure 51 shows that even in the deepest parts of the section, overflow water may be a major component. Three potential sources for this bottom water may be imagined as schematically illustrated in Figure 52. It may have recirculated the Iceland Basin as suggested by Harvey and Theodorou (1986), it may have overflowed the Wyville Thomson Ridge or it may derive directly from the Faroe Bank Channel overflow.

Long-term current meter observations have verified that the deep circulation of the Iceland Basin is cyclonic (van Aken, 1998, this volume) at least at depths around 2000 m and this may bring along both recirculated overflow water and overflow from the Wyville Thomson Ridge which has circled the Rockall-Hatton Plateau. The overflow across the Wyville Thomson Ridge is in Figure 52 indicated as having two different paths. One of these paths goes into the depths of the Rockall Channel and continues southwestwards on the eastern flank of the Rockall-Hatton Plateau. In this region overflow influence was inferred from water mass characteristics and sediment distribution before the Wyville Thomson Ridge overflow had been directly observed (Ellett and Roberts, 1973). Some of this water may continue out into the open waters of the Northeastern Atlantic, but there is also evidence of a continuation around the Rockall-Hatton Plateau into the Iceland Basin. Thus, Figure 10 shows a salinity maximum between 2000 and 2500 m depth on the northwestern flank of the plateau with properties similar to those in the Rockall Channel (van Aken and Becker, 1996).

The alternative path of Wyville Thomson Ridge overflow around Bill Baileys Bank, shown on Figure 52, was suggested as a possibility by Ellett (1988) and this is strengthened by the occasional occurrence of, presumably high-velocity, boluses of overflow water high on the southern flank of the Faroe Bank (Figure 43). Geological evidence has verified the existence of this flow (Kuijpers *et al.*, In the Press) with indications of occasional strong currents, but as to their persistence we have no information.

The third path of overflow water to the southeastern depths of the Iceland Basin is directly from the Faroe Bank Channel. The high velocity of the overflow core in the Channel (Figure 44) might be thought to keep the flow on the western flank of the Iceland-Faroe Ridge by the Coriolis force. Certainly, part of the water does follow this path, but there are also indications that part of the plume turns towards the southwest, as shown on Figures 46 and 52, following gullies in the bottom (Bathymetry of the Northeast Atlantic, sheet 2, Roberts *et al.*).

This situation was observed during Overflow '73. R/V Shackleton made a series of hydrographic sections on which fairly pure (up to 70%) overflow water (NSAIW+NSDW) could be traced from the exit of the Faroe Bank Channel to the area due north of Lousy Bank (Figure 53) (Müller *et al.*, 1979). Geological studies support the existence of this path (Kuijpers *et al.*, In the Press). Figure 47 has a slight indication of a divergence in the Faroe Bank Channel overflow plume and the strong mixing and non-stationary behaviour of the plume, demonstrated by this figure, may be involved in the bifurcation.

This is also indicated by the high variability in the eastern Iceland Basin bottom layer observed by de Boer *et al.* (1998, this volume). They concluded that in this layer there is a strong competition between overflow water and a water mass (Lower Deep Water, LDW) of southern origin with high contents of Antarctic Bottom Water indicated by large concentrations of dissolved silica. Variations in the ratio of these two components were found on all time-scales from interannual to weeks and days, arguing proximity to a variable source.

The evidence, cited above, indicates that some of the Iceland-Scotland overflow may descend more or less directly to large depths in the southern part of the Iceland Basin. The remainder enters the boundary current on the south Icelandic slope. Hydrographic sections published by different authors show this flow, but the details differ considerably. In addition to the bottom layer, de Boer *et al.* (1998, this volume) found two cores of overflow water on the Icelandic slope (Figure 51), centered at 1600m and 2200m. These two cores may, as argued by de Boer *et al.*, derive from two different overflow sources (the Iceland-Faroe Ridge versus the Faroe Bank Channel). However, the high variability observed for the Iceland-Faroe Ridge overflow and for the Faroe Bank Channel overflow after exiting the channel (Figure 47) also may produce overflow boluses of different magnitudes and velocities which may mix and move quite differently.

Long-term current measurements have been obtained by van Aken (1998, this volume) and Saunders (1996). Figure 52 shows average flow vectors close to the bottom in Saunders' experiment. He found strong (10–

20 cm s^{-1}) and persistent flow, generally along the topography, in a region between 1300 and 2100m over the Icelandic slope. Current speed was variable with significant energy near periods of one week. We might perhaps expect the variability to be smoothed out with increasing distance from the source, but even in the Charlie-Gibbs Fracture Zone Saunders (1994) found the overflow flux to vary strongly on time-scales from 10 days to the record length of his observations.

As the boundary current continues westwards south of Iceland, it loses momentum to friction and entrainment and descends to larger depths. When it reaches the Mid-Atlantic Ridge, it is deflected to a more southerly direction and flows over the eastern flank of that ridge until part of it escapes into the Irminger Basin of the Western North Atlantic. In the literature, the path across the Mid-Atlantic Ridge is generally cited as the Charlie-Gibbs Fracture Zone and experiments have confirmed an overflow flux through it (Worthington and Volkmann, 1965; Harvey and Shor, 1978; Saunders, 1994). Figure 54 illustrates this flow as measured by Saunders (1994).

The two transform valleys in the Charlie-Gibbs Fracture Zone are the first deep (>2500 m) passages across the Mid-Atlantic Ridge encountered by the overflow. The deepest part of the overflow water has to go through these valleys to enter the Irminger Basin, but farther to the north there are shallower passages. The very rugged topography makes it difficult to map these in detail. However the IOS map of the Northeast Atlantic (Laughton *et al.*, 1982, sheet 1) has one passage with a sill depth of 2100–2200 m at about 55°N and Harvey and Shor (1978) mention passages even farther north. We do not have any evidence for or against flow through this or any other passage north of the Charlie-Gibbs Fracture Zone, but there seems to be no reason to assume that all overflow has descended below this level on its way. Also the shape of the isohalines on Figure 54 might well indicate that some of the water has escaped before reaching the Charlie-Gibbs Fracture Zone.

Flux estimates

The exchanges across the Greenland-Scotland Ridge involve inflows to and outflows from the Arctic Mediterranean of water, heat, salt and various substances. Through the years, many people have tried to estimate the magnitudes of these exchanges, both for specific branches and for the Arctic Mediterranean as a whole. For most purposes, the properties, temperature, salinity etc., of the exchanged waters are fairly well established (Table 3) and the large uncertainties mainly derive from difficulties in establishing volume transports. We therefore focus on that problem.

Two main strategies have been employed to determine exchange magnitudes. One of these relies on measurement of volume transports while the other strategy aims at balancing various exchanges in a consistent budget. Below, these are discussed separately and we differentiate also between transport measurements of Atlantic water and overflow. Under the heading of measurement, we classify direct current measurements but also the "classical dynamic method" which relies on geostrophic computations from temperature and salinity observations with additional assumptions.

Measured volume transport of the Atlantic inflows to the Nordic Seas. As discussed, two origins may be defined for the Atlantic water crossing the Greenland-Scotland Ridge. The oceanic origin is the North Atlantic Current when it crosses the Mid-Atlantic Ridge. Lately, a number of studies have estimated the volume transport across the Mid-Atlantic Ridge and summarising these, Käse and Krauss (1996) listed values between 18 and 26 Sv (1 Sv = 10^6 m^3 s^{-1}) for the North Atlantic Current. Using an inverse model, Paillet and Mercier (1997) found somewhat larger transports. Added to this wide range of values comes the difficulty in estimating the amount of water recirculated in the upper layers or deeper. These measurements cannot therefore be used to estimate the amount of Atlantic water crossing the Greenland-Scotland Ridge except to note that they do not in practice set any upper bounds to the exchange.

The transport of Atlantic water from the continental source has also been estimated by several authors as listed by Turrell *et al.* (1992) and in a relative sense, the range is larger than for the oceanic source. West of the Hebrides, Booth and Ellett (1983) only found 0.5 Sv while Pingree and Le Cann (1989) arrived at 2 Sv; both values based on direct current measurements. One difficulty lies in deciding what part of the flow to consider. The flow over the deepest part of the slope may perhaps not cross the ridge.

The most direct transport measurements are those performed in or close to the gaps of the Greenland-Scotland Ridge and measurements have been performed in all three gaps. North of Iceland, Stefánsson (1962) used the dynamic method (geostrophy) to derive an average transport of 0.6 Sv for the North Icelandic Irminger Current. Kristmannsson (1998, this volume), using current measurements, found varying values between 1 and 2 Sv of water warmer than 4°C (Figure 55). Since this is somewhat colder than the original Atlantic water (Figure 8), 1 Sv is probably a fair guess for the typical transport.

North of the Faroes, Hermann (1949) found a transport of 4.5 Sv through one section, although only part of this

value represented Atlantic water. Tait (1957) reported transport of Atlantic water through several sections of considerably smaller magnitudes while Sukhovey (as cited by Rossov, 1972) estimated a transport of almost 10 Sv between Iceland and the Faroes. These numbers were all based on the dynamic method while Hansen *et al.* (1998, this volume) used a dense net of short-term current meter moorings to arrive at their estimate of 2.9 Sv for the Atlantic water flow in the Faroe Current through 6°W.

In the third gap, the Faroe-Shetland Channel, many studies have reported volume transport estimates based on the dynamic method (Jacobsen, 1943; Hermann, 1949; Timofeyev, 1963) or geostrophy combined with an inverse method (van Aken, 1988). Estimates, based on direct current measurements, have been published by Dooley and Meincke (1981). They combined a few, fairly short, current meter records with geostrophy and by Gould *et al.* (1985) and Turrell *et al.* (1992) who used fairly dense sets of current meter records which, however, covered only a part of the channel cross-section

A comparison of these studies demonstrates a wide range in transport estimates for the Atlantic water flow through the Faroe-Shetland Channel. The classical dynamic method tends to give smaller values than direct current measurements. This is exemplified by contrasting Tait's (1957) value of 2.3 Sv, determined as an average of 69 geostrophically computed sections, to Gould and co-authors' (1985) value of 7.5 Sv, computed from a set of year-long current meter records (Figure 56).

Tait's transport value rests on at least two fundamentally wrong assumptions. One is the assumption of no flow close to bottom over the slopes which neglects the barotropic flow in these regions, in conflict with all the observational evidence available today (e.g. Figure 24). Secondly, Tait's assumption of no horizontal flow at the 35.0 isohaline in mid-channel neglects the recirculation which may induce south-going flow throughout the water column on the Faroese side of the channel (NWSA and NWSB on Figures 19 and 24). A dynamic computation between two stations only extends to the depth of the shallower one and in a strongly sloping region like the Faroe-Shetland Channel there will be large areas of the cross-section where the method cannot be used unless it is based on a very dense station-net.

Taking all this into account, the discrepancy between Tait (1957) and Gould *et al.* (1985) is not surprising. In the Faroe-Shetland Channel, as well as north of Iceland and north of the Faroes, we choose to ignore all transport estimates based purely upon geostrophic calculations. We also are reluctant to accept van Aken's (1988) inverse method estimate since his circulation, as argued previously, is not consistent with observations. The same applies to Dooley and Meincke's (1981) estimate, probably due to a too limited set of current observations.

In recent years, transport estimates have been based on measurements of sea surface heights from satellite (Samuel *et al.*, 1994). Since the geoid is not well enough known, estimation of absolute sea-level height and hence absolute transport by this method requires calibration. By itself the method also neglects baroclinic flows. Samuel *et al.* (1994) tried to overcome these difficulties by combining their satellite altimeter observations of sea surface height with a numerical model which implies that their transport value is critically dependent upon the model and, strictly spoken, not a measured value.

The most reliable transport measurements therefore may be expected from direct current measurements combined with hydrographic surveys. Of those published, Gould *et al.* (1985) is clearly based on the best material consisting of data from four moorings with a total of 12 successful current meters deployed across the Shetland slope for about one year. Their mean value of 7.5 Sv cannot, however, be taken at face value as the Atlantic water flux through the Faroe-Shetland Channel. One problem is that their section covered only a small, albeit perhaps the most important, part of the total cross-section of the channel (Figure 56). In that sense, their value is an underestimate. In their transport estimate, Gould *et al.* (1985) included all the water flowing towards the northeast. From Figures 6 and 19, this may contain a fair amount of Atlantic water that has passed over the Iceland-Faroe Ridge and recirculated into the Faroe-Shetland Channel. Also, a fair amount of MEIW may be included (Figure 56). In that sense their value is an overestimate.

Turrell *et al.* (1992) have reported a volume transport of 1.8 Sv through a section somewhat upstream from Gould and co-authors' section. Turrell and co-authors' section did not cover as much of the slope, it had less dense current meter coverage and lasted only from June to September 1989, during a season when the transport according to Gould *et al.* is fairly low. Turrell and co-authors' value therefore is not in conflict with Gould and co-authors' estimate.

Summarising transport measurements on the ridge, the published literature does not allow a reliable estimate of the total Atlantic water inflow to the Nordic Seas. For the North Icelandic Irminger Current, Kristmannsson's (1998, this volume) work indicates a number on the order of 1 Sv, though with fairly large error bars, but the Atlantic water flux through the Iceland-Scotland Gap is not found in the literature. Estimates of this flux may be expected in the near future, however. The long-term ADCP moorings combined with regular CTD cruises in the Nordic WOCE deployments (Figure 19) are ideally suited for flux calculations and Figure 57 shows a preliminary estimate of Atlantic water inflow from the Nordic WOCE group.

This estimate is based on fairly short deployments at some sites and may need revision. Observations are continuing within the EC-MAST-funded "VEINS" programme. Therefore a more reliable estimate should be available within the next year or two. In Figure 57, the flux through the Iceland-Scotland Gap exceeds that through the Faroe-Shetland Channel. Since the Atlantic water in the Faroe-Shetland Channel is considerably warmer than the northern branch, the heat transported by both branches on either side of the Faroes was found to be almost identical (Hansen *et al.*, 1998).

Downstream from the Greenland-Scotland Ridge, the volume transport of Atlantic water has been estimated in several studies. Blindheim (1993) found an annual mean transport close to 5 Sv for 1990 and 1991 based on dynamic computations of a section occupied monthly, and crossing from the Norwegian coast into the deep Norwegian Basin. He used the 1000m depth as a level of no motion and a fairly speculative method on the shallower slope. The classical dynamic method is probably more applicable to Blindheim's section than to the Faroe-Shetland Channel, but we still hesitate to put too much faith in the result, also taking into account the large temporal variability due to mesoscale activity.

Transport estimates based on recent direct current measurements along the "Svinøy section" have been reported by Orvik and Mork (1996) who find an annual mean of 5.3 Sv. Hjøllo and Mork (1996) similarly found a transport of 3.3 Sv using current measurements of about one months duration in 1969. Both these values seem, however, to include water, not of Atlantic origin and neither one of their sections covers the whole width of the Atlantic water inflow.

Measurements of sea-level height have also been used to estimate the transport of Atlantic water in the Norwegian Sea. Samuel *et al.*, (1994) and Pistek and Johnson (1992) both found transport values between 2.5 and 3 Sv using satellite altimetry. As previously discussed, Samuel *et al.* results are critically dependent upon the numerical model they used while Pistek and Johnson used geostrophic calculations with an assumed reference level for their calibration and thus their results are limited the uncertainties of the dynamic method. An alternative approach was tried by McClimans (pers.comm.). He used measurements from coastal tide gauges and found a surprisingly good correlation to Gould *et al.* (1985) measurements. This technique seems to offer promise for historical assessment of transport variations and together with satellite altimetry also for future monitoring, but both techniques will require calibration and verification against high-quality direct current observations and possibly also observational input on the baroclinic structure.

Measured volume transport of overflow waters. Estimates of the Wyville Thomson Ridge overflow have been published by Ellett and Edwards (1978), Saunders (1990) and Ellett (1998, this volume). The first two of these found quite similar values of about 0.3 Sv cold water plus entrained Atlantic water, but these values were based on very short observational periods and, taking into account the already cited intermittent character of the Wyville Thomson Ridge overflow, they must be interpreted with care. In contrast to this, Ellett's (1998, this volume) estimate of about 0.1 Sv of cold (NSDW + NSAIW) is based on current meter observations lasting up to 10 months (Figure 42).

This latter estimate does, however, only cover a fairly narrow path through the descending gully (Figure 42). We know that not all the overflow follows this path (Figure 43), but we have no way of quantifying the rest. On the observational evidence available at present we estimate that the Wyville Thomson Ridge overflow probably lies within the range of 0.1–0.3 Sv of cold water. Some of this may be NSDW, but the main component will be NSAIW.

Estimates of the volume transport of water through the Faroe Bank Channel were made by Crease (1965), based on a few hours observation of a neutrally buoyant float and theoretical arguments. He did not give one resulting number, but rather calculations that pointed to a value in the 1–2 Sv range. Later authors have stayed within that same range (Table 5). Most of the estimates have been based on a very limited set of observations or upon unproved theoretical assumptions. Most frequently cited are the estimates by Borenäs and Lundberg (1988) ranging from 1.4 to 1.9 Sv and the estimate by Saunders (1990) of 1.9±0.4 Sv. Both these estimates refer to water colder than 3°C and thus include a certain amount of entrained Atlantic water. Saunders (1990) gives a mean temperature of 0.4°C for his overflow water and states that it is 90% "NS-water" which in our notation must be translated to NSAIW+NSDW.

Table 5. Estimates of the volume transport (flux) of overflow through the Faroe Bank Channel by various authors. The flux values are not always comparable since overflow has been defined differently by different authors. Short-term moorings are those that are at most a few days to weeks of length, while long-term moorings extend over several months.

Authors	Flux	Method
Hermann (1967)	1.4 Sv	Hydrography
Sætre (1967)	1.5 Sv	Short-term moorings + hydrography
Rydberg (1980)	1.2 Sv	Hydraulic theory + hydrography
Dooley and Meincke (1981)	1.4 Sv (incl. MEIW)	Short-term moorings + hydrography
Borenäs and Lundberg (1988)	1.7 Sv (T < 3°C)	Ship borne observations + hydraulic theory
Saunders (1990)	1.9 Sv (T < 3°C)	Long-term moorings + ship borne observations
Saunders (1992)	1.3 Sv (T < 3°C)	Hydrography + shipborne ADCP

These two sets of estimates, which are compatible, are also, unfortunately, based on a rather meager set of observations. Saunders (1990) bases his estimate on a combination of CTD and shipborne ADCP work with results from long-term current meter moorings. Of the three current meters that were in the cold overflow water, two were only 10 m above the bottom, that is well within the bottom boundary layer according to Johnson and Sanford (1992). The third was at the top of this layer (30 m above bottom). Certainly, Saunder's mean along-channel velocities were considerably smaller (56–69 cm s^{-1}) than the ADCP values shown in Figure 44, but they are on a different section. Saunder's (1990) estimate thus has to be largely based on the snapshot shipborne observations as are Borenäs and Lundberg's (1988). These estimates are, no doubt, the best transport values available in the literature, but their accuracy should not be overrated.

For the overflow across the Iceland-Faroe Ridge, Dietrich (1956) estimated a volume flux of 6 Sv. He did not, however, consider the effect of geostrophy turning the flow from down-slope to along-slope and Steele (1961) reduced this value to 1.5–3.0 Sv. From the results of the Overflow '60 expedition, Hermann (1967) estimated 1.1 Sv and this number, or rather 1 Sv, continues to be cited as the Iceland-Faroe Ridge overflow volume transport (Dickson and Brown, 1994). In his summary paper on the exchanges across the Greenland-Scotland Ridge, Meincke (1983) also uses this value.

A value of 1 Sv for the Iceland-Faroe Ridge overflow flux is the best available direct estimate at present, but again the number should not be considered too definite. It seems mostly to be based on Hermann's (1967) Overflow '60 estimate and, although this was a very comprehensive study, it was only for a limited period with only short-term current measurements. Part of this water, perhaps up to 50% (Hermann, 1967), is MEIW and, although usually classified as overflow, it should be noted that not all of this water satisfies the $\sigma_\theta > 27.8$ criterion (Figure 8).

The transport of the boundary current flowing southwestwards over the south Icelandic slope was estimated by Steele *et al.* (1962) based on geostrophy and the drift of Swallow floats and by Shor (1978) using hydrography and short-term (a few days) current measurements. Both these studies found a total flux on the order of 5 Sv with 1.4–2 Sv of "pure" overflow water (i.e. without the entrained component). Using hydrography and long-term current measurements, van Aken (1995) estimated 3.5 Sv of water with $\sigma_\theta > 27.8$ flowing through a section along 20°W extending from the Icelandic slope to 60°N.

Taking into account the limited observational basis, these three estimates agree reasonably well. Van Aken's estimate is very close to the value of 3.2±0.5 Sv ($\sigma_\theta > 27.8$), given by Saunders (1996) based on hydrographic surveys and results from 13 current meters on seven moorings with up to 13 months of data. Saunders estimated that half of his transport value (1.6±0.15) Sv was "NS-water" (NSAIW+NSDW) and 25% was "AI/NI-water" (MEIW). However, as argued by van Aken (1995), this is only if surface MNAW with a temperature of 8°C is assumed to be the entrained water accounting for the remaining 25% in the mixture. If the MNAW is entrained from a deeper level with lower temperature, the proportions will change.

A further problem in making flux estimates of this kind is the combination of long-term current measurements with a few hydrographic sections especially if high-velocity events are correlated with larger extension of the overflow water cross-section. Also, both velocity

and proportion of overflow water change with height over bottom (Figure 51c) and evaluating the flux of "pure" overflow requires information on profiles of both which is generally not available. Finally, as has been shown above (Figures 52 and 53), some of the overflow descends into the Iceland Basin close to the Rockall-Hatton Plateau and it is not evident that this component has to pass the moorings in Figure 52. Saunders' (1996) flux estimate is clearly the best value available, but whether his error bars are realistic is more doubtful, especially as regards the flux of "pure" overflow.

The final set of flux estimates for Iceland-Scotland overflow water derives from the Charlie-Gibbs Fracture Zone. Worthington and Volkmann (1965) used geostrophic calculations supplemented by Swallow float drift and short-term (30 hour) moored current measurements to arrive at an estimate of about 5 Sv. Estimates based on long-term current measurements combined with hydrography have, however, reduced this value to 2 Sv (Harvey and Shor, 1978) and 2.4±0.5 Sv (Saunders, 1994). Both these studies defined overflow water in terms of salinity (S>34.96 and S>34.94 respectively) which with a freshening (Saunders, 1996) should make them roughly comparable and equivalent to other definitions (σ_θ> 27.8, Saunders, 1994). This would imply that the maximum content of "pure" overflow water in the Charlie-Gibbs Fracture Zone according to these studies would be about 50% or 1.2 Sv.

In Figure 58 we have summarised what were considered to be the "best" estimates of overflow flux in each region focusing upon the "NS" component (NSAIW+NSDW) which should be conserved irrespective of entrainment. As noted by Dickson and Brown (1994) there are certain inconsistencies, but they are not irreconcilable and do not necessarily imply temporal flux variations of interannual to decadal scales. As mentioned, we find the error bars cited in many studies to be overly optimistic taking into account that the flux estimates are based on inter- and extrapolations from data sets which even in the best cases are severely limited.

Secondly, the measurements south of Iceland and in the Charlie-Gibbs Fracture Zone may not necessarily cover the total flow, as previously argued and indicated in Figure 58. Thus, the flux of overflow water crossing the Mid-Atlantic Ridge into the Western Basin may well exceed both estimates from these two regions. Indeed, if the maximum estimates in each of the three overflow areas are added, a total of 2.9 Sv NSAIW+NSDW are obtained which with entrainment should be more than adequate to supply the water that Dickson and Brown (1994) found missing southeast of Greenland. On the other hand, there is no reason to assume that all the overflow from the Iceland-Scotland Gap is transported into the Western basin. Some of it may upwell east of the Mid-Atlantic Ridge and van Aken (1998) has found Iceland-Scotland overflow water in the Eastern Basin, south of the Charlie-Gibbs Fracture Zone as indicated by the southernmost arrow on Figure 7.

Budget estimates of the exchanges. Using budget considerations to evaluate exchanges involves applying the restrictions implied by the fundamental conservation laws for water (mass), salt and heat (energy) to observations. For the Arctic Mediterranean these considerations were applied at an early stage (e.g. Rossov, 1961), but the milestone was established by Worthington (1970) who brought in the overflow as a main factor in the balance (Figure 59). Alternatives have been suggested to Worthington's budget by later studies (McCartney and Talley, 1984; Mauritzen, 1996), but a generally accepted budget for the Arctic Mediterranean has not emerged.

In addition to the flows that have been discussed in this paper, a complete budget requires information on the fluxes through the Bering Strait and the Canadian Archipelago. More important are the flows through the Denmark Strait, both the overflow and the upper layer flow in the East Greenland Current. The Denmark Strait overflow has been studied by several authors. Dickson and Brown (1994) summarise these results to a typical value of 2.9 Sv of cold water through the Denmark Strait. This is somewhat less than Worthington's (1970) estimate. For the East Greenland Current, flux estimates seem more uncertain. The transport of Polar Water south through the Fram Strait appears to be on the order of 1 Sv plus 2 Sv of recirculated Atlantic water and Arctic Intermediate Water (Foldvik *et al.*, 1988). It is not clear how much of this remains in the East Greenland Current when it flows over the Greenland-Scotland Ridge. Malmberg (1985) found a similar value for the transport over the East Greenland shelf while Hopkins (1991) found a somewhat larger flux. These transport values of the East Greenland Current through the Denmark Strait are thus fairly consistent with Worthington's (1970) estimate, but they are mainly based on geostrophic calculations and budget estimates and more direct current measurements would be required for an independent reliable flux estimate.

In the simplest scheme, the exchanges across the Greenland-Scotland Ridge may be considered a balance between three flows: The Atlantic inflow, the surface outflow in the East Greenland Current and the overflows. If representative temperatures and salinities of each of these flows are assumed to be known, their fluxes become the three primary unknowns to be solved from the conservation equations. The equations bring in, however, two additional parameters, the fresh-water flux and the heat exchange with the atmosphere and especially the heat exchange has proven to be difficult to estimate. In his budget (Figure 59) Worthington (1970) calculated the heat loss to about 260 TW (10^{12}

W), but this value depends critically upon parameterization of various processes involved in the heat transfer. Simonsen and Haugan (1996) compared different combinations of parameterizations frequently applied and found the atmospheric heat exchange for the Nordic Seas to vary from a loss of 304 TW to a gain of 52 TW, using identical climatological data. With such a large spread in values there seems to be little hope at present for a determination of fluxes from budget considerations.

In view of this, it is remarkable, how well Worthington's (1970) numbers fit to the best observational evidence available today. Certainly, the flow paths and the relative strengths of the various inflow and outflow branches in Figure 59 differ from current wisdom. However, the total flux of Atlantic water inflow (9 Sv) is very close to Figure 55 plus Figure 57 and the accepted value for the total overflows are also close to Worthington's estimate of 6 Sv (Dickson and Brown, 1994). And, the heat flux calculated from the preliminary Nordic WOCE observations through the sections on Figure 57 was found to be 259 TW (10^{12} W), very close to Worthington's value.

Temporal variations

As shown on Figure 8, the temperature and salinity of the Atlantic inflow waters have fairly wide ranges. Partly this is due to temporal variations on both seasonal and longer time scales. In the overflow the deep water component is much more constant, but that is not the case for all of the intermediate waters.

Seasonal variations in the Atlantic inflows to the Nordic Seas. Seasonal variation of surface temperature and salinity has been documented for wide areas (Malmberg and Magnússon, 1982; Reverdin *et al.*, 1994), but for the sub-surface parts of the Atlantic inflow waters, a comprehensive overview of seasonal variations is harder to find. For the MNAW in the Iceland-Scotland gap, Hansen and Kristiansen (1994) found a seasonal range of about 1°C in temperature for the 100–300 m depth layer in the Faroe Bank Channel with a maximum in September. They found no consistent seasonal salinity variation in this water.

After having passed the ridge, the Atlantic inflow water has been reported to exhibit much larger variations in many regions due to seasonal variations in the flow dynamics. Thus, Stefánsson (1962) found a strengthening of the North Icelandic Irminger Current in summer on the basis of seasonal variations in water mass properties and Kristmannsson (1998, this volume) also finds a systematic seasonal variation in volume transport with a minimum in early spring (Figure 55). Coupled with a similar temperature variation, this gives a seasonal variation in heat transport with minimum in spring.

A similar behaviour has been reported for the Faroe Current by Hansen and Kristiansen (1994) who found indications of a seasonal variations in the width of the current with maximum extent in late summer based on CTD observation on a standard section along 6°W, initiated during NANSEN.

In the Faroe-Shetland Channel there are also clear indications of seasonally changing dynamics. On the Faroese side of the channel Hansen and Kristiansen (1994) found a seasonal variation of the salinity of the uppermost 200m layer. This observation has been confirmed by analysis of more extensive data sets (Turrell, pers. comm; Reverdin *et al.*, 1994). This water is a mixture of MNAW and MEIW. Since no seasonal salinity variation could be found in the Atlantic water entering the Iceland-Faroe Gap, Hansen and Kristiansen (1994) concluded that the ratio of MNAW to MEIW is larger in summer than in winter which is consistent with a relative strengthening of the Faroe Current in summer.

On the Shetland side of the Faroe-Shetland Channel the current meter observations, reported by Gould *et al.* (1985) indicate a seasonal variation of the along-slope transport over the Shetland slope with maximum flow in winter and a summer minimum (Figure 56). In addition to Atlantic water that has reached their observational area from the west, Gould and co-authors' transport time series includes recirculated Atlantic water from the Iceland-Faroe Gap as well as MEIW from the north of the Iceland-Faroe Front. It is therefore not clear how much of Gould and co-authors' seasonal variation may stem from increased MEIW recirculation through the Faroe-Shetland Channel during winter. Also, one should not conclude too much about seasonal variation from a one-year data set. Altogether, these observations indicate a seasonal north-south shift of the Atlantic inflow with relatively more of the water going through the Faroe-Shetland Channel in winter as compared to the two other gaps. This might also involve seasonal variations of the total Atlantic water transport over the ridge, but the observational evidence is not sufficient either to verify or to reject such an hypothesis.

Long-term variations in the Atlantic inflows to the Nordic Seas. Long-term changes of the temperature and salinity of the various Atlantic inflow branches have been documented by a number of authors. They have mainly focused on salinity and Figure 60 shows observed salinity changes for three kinds of Atlantic water crossing the ridge. One of these time series is from a site southwest of Iceland in the origin of the North Icelandic Irminger Current, one is from the Faroe Bank Channel and one is in the core of the

Continental Slope Current in the Faroe-Shetland Channel. This last series represents NAW while the other two represent MNAW.

The three time series in Figure 60 represent the whole range of Atlantic water crossing the ridge and the figure indicates a certain coherency in low-frequency salinity changes over the whole ridge. Thus all the series show the mid-1970s "Great" salinity anomaly (Dooley *et al.*, 1984; Dickson *et al.*, 1988) occurring at about the same time. The two series that extend to the beginning of the century also indicate "the Earlier Salinity Anomaly" (Dickson *et al.*, 1984) which seems to have culminated around 1910.

In addition to changes in water mass properties, there is evidence for long-term variations in the Atlantic inflow dynamics. North of Iceland, long-term hydrographic investigations have demonstrated large variations in the amount of Atlantic water present on the shelf with both interannual and decadal timescales (Malmberg *et al.*, 1994). These measurements indicate a dramatic decrease of Atlantic water influence in the 1960s with a partial recovery in the early 1990s (Figure 61). Kristmannsson's (1998, this volume) current measurements also demonstrate interannual variability. As seen on Figure 13, the flow during 1986-87 was apparently about twice as fast as for the following two years.

It has been noted (Figure 25) that the Faroe Current may vary significantly in cross-sectional area and width. Analysing CTD observations from the 6°W standard section, Hansen and Kristiansen (1994) found indications of a decrease in the width of the current from the mid-1980s to the mid-1990s (Figure 62) in parallel with the salinity decrease of the water feeding that current (FBC-MNAW on Figure 60). This apparent weakening of Atlantic water influence north of the Faroes is consistent with Kristmannsson's (1998, this volume) current observations for the same period (Figure 13).

Summarising, we find evidence of long-term changes, not only of Atlantic water properties, but also of inflow strength and influence, especially in the northwestern part of the ridge area. Most of the evidence is qualitative, however, and any conclusions as to variations of total Atlantic water inflow would be premature. Comparing observations from a large number of sites around the Norwegian Sea, Blindheim *et al.* (in prep.) have documented a general freshening of the Norwegian Sea as a whole since about 1960 which involves both the Atlantic water and the MEIW spreading from the Iceland-Faroe region into the Norwegian Sea. The mechanisms behind the changes have not been clarified in detail, but wind seems to be one of the main forces. Thus, Blindheim *et al.* (in prep.) find a high correlation between the location of the 35.0 isohaline along 65°45'N and the North Atlantic Oscillation Index which indicates that strong westerlies cause a reduction of the Atlantic water domain in the Norwegian Sea and increase of the Arctic water domain. To what extent these changes involve flux variations in the Atlantic inflow has not been resolved, however.

Variations in the overflow. By its nature, the production of overflow water is necessarily seasonally dependent to a high degree. As regards the remotely produced waters, the seasonal variations will be much smoothed on their way towards the ridge. The production of MEIW, on the other hand, occurs so close to the ridge that seasonal variations could be expected. Thus, NIWW exhibits a clear seasonal cycle (Stefánsson, 1962). It has been noted that an observed seasonal salinity variation in the upper layers of the Faroe-Shetland Channel can be interpreted as a variation in the relative influence of MNAW and MEIW. How this reflects MEIW production is not clear, however, and as a whole, there is no observational evidence for a seasonal variation of the overflow either in property or intensity.

On longer time-scales, the diminished production of Greenland Sea Deep Water (GSDW), cited above, might be thought to have effects on the production of NSDW and indeed that seems to be the case. Thus Østerhus *et al.*, 1996 report a warming of the deepest layers of the Norwegian Basin during the last decade. This is seen in Figure 39 where high quality observations from 1982 are compared to observations in 1994. From the early 1980s, to 1994, the temperature of the adiabatic layer increased by 0.015–0.020°C while the thickness of the layer decreased. Salinity, on the other hand, appears to have decreased by 0.001, if it changed at all. The temperature increase might be just a reflection of the temperature increase of the GSDW, but the evidence indicates rather a stagnation with a much reduced input of new water to the adiabatic layer (Østerhus *et al.*, 1996). This conclusion is borne out by tracer measurements indicating an equilibration with the atmosphere in the early- to mid-sixties (Fogelquist *et al.*, in press) and by the observation, that the deep current of new NSDW through the Jan Mayen Channel has stopped (Østerhus and Gammelsrød, in press).

While a possible freshening from 1982 to 1994 of the deep adiabatic layer is so small to be at the limit of detectability, Figure 39b indicates clearly a freshening of the upper layer of the NSDW. The salinity maximum decreased in salinity and deepened in the period between 1982 and 1994. This conclusion is supported by salinity measurements at Ocean Weather Station M which have similar salinities at 1000 m and 1500 m depth from 1950 to the mid 1980s, when the 1000 m level suddenly became fresher than the 1500 m level (Østerhus *et al.*, 1996).

In the Faroe-Shetland Channel much of the classic work has focused on long-term trends, but problems with historic salinity observations have made deep-water changes difficult to assess. A re-examination of all the data from the standard sections (Turrell *et al.*, 1993) have allowed more definite conclusions which confirm a freshening of intermediate and deep waters. In the 500 to 800m depth interval the freshening started before the mid-seventies anomaly (FSC-MEIW on Figure 60). Below this, the NSAIW in the Faroe-Shetland Channel has freshened since 1980 as originally suggested by Martin (1988, 1993) and a freshening has been observed at deeper layers from 800 m downwards (Turrell *et al.*, in press). These changes have been linked to the reduced supply of NSDW. Turrell *et al.* (in press) concluded that a change has occurred in the composition of the deep waters of the Faroe-Shetland Channel. Hence, this also includes the overflow through the Faroe Bank Channel such that the percentage content of NSDW decreased from being 60% in the period 1970–1985 to 40% in the early 1990s. The changes would be expected to affect the properties downstream from the overflow sites in support of Swift's (1984) suggestion of a freshening.

A reduced production of deep and intermediate waters in the Arctic Mediterranean should in the long term decrease the volume flux of the Faroe Bank Channel overflow. In the extreme case of a total production stop, a continued overflow of 2 Sv (Saunders, 1990) would lower the interface to the upper layer on the order of 10 m per year. This assumes the change to affect the whole of the Arctic Mediterranean (6 million km^2 at the sill level of the Faroe Bank Channel).

Figure 63 shows the depth of the 3°C isotherm and the -0.5°C isotherm during a 10-year period based on CTD observations at a standard station in the Faroe Bank Channel (Hansen and Kristiansen, in press). The figure indicates a decreased influence of the coldest water (< -0.5°C) and this tendency was found to be statistically significant although the number of observations is too low to allow definite conclusions. For intermediate water (-0.5°C < t < 3°C) no systematic change was observed. If there has been a lowering of the 3°C isotherm, it is sufficiently small to vanish in the variability and the figure rather indicates a constant interface which implies an intermediate water compensation to the reduced deep water formation in line with Turrell and co-authors' (in press) conclusion.

Conclusions

The problem studied in the NANSEN programme, the exchanges across the Greenland-Scotland Ridge, is one of the major challenges of modern oceanography. The overflows of cold, dense water across the Greenland-Scotland Ridge are of critical importance for the production of North Atlantic Deep Water. Hence the global thermohaline circulation while the Atlantic water inflows to the Arctic Mediterranean to a large extent determine the climate of the surrounding waters and land areas as well as providing the salt input necessary for deep water production.

This problem has naturally been the focus of a number of national and international studies and programmes and the NANSEN programme should not be seen as a self-contained project, but rather as one link in a continuous effort to describe and quantify the exchanges. Through the review and discussion presented in this paper we hope to have documented that the qualitative features of the exchanges are fairly well known. The water masses involved, their origins and paths may be mapped as summarized in Figures 6, 7 and 8. We have emphasised the complexity of the system. Neither the Atlantic water inflows to the Arctic Mediterranean nor the overflows into the Atlantic occur as single branches, but are rather promoted by a series of branches carrying water that may have different properties and origins, be produced by different processes and which may affect different water masses.

The NANSEN programme did not provide a complete quantitative budget for the exchanges. However, it helped quantify the fluxes of the overflow and the Atlantic water inflow. It also laid the foundation for programmes such as Nordic WOCE and VEINS which have given preliminary results that, in the next few years, may be expected to have developed into a reliable total budget for the exchanges.

The NANSEN programme has also helped our understanding of what is probably the most important question of all within this problem, the temporal variations of the exchanges. This question needs to be answered both for those studying fish stocks and other biological changes in the region and for regional and global climate simulation and prediction. As yet, quantitative answers are few and do not provide a consistent picture. A major effort is needed both in the form of observations and in numerical modelling, but we have obtained a qualitative description which should allow us to identify where and how the main changes occur and how to monitor them.

References

Aagaard, K., Swift, J. H., and Carmack, E. C. 1985. Thermohaline Circulation in the Arctic Mediterranean Seas. Journal of Geophysical Research, 90 (C5): 4833–4846.

Allen, J. T., and Smeed, D. A. 1996. Potential Vorticity and Vertical Velocity at the Iceland-Færoes Front. Journal of Physical Oceanography, 26: 2611–2634.

Allen, J. T., Smeed, D. A., and Chadwick, A. L. 1994. Eddies and mixing at the Iceland-Færoes Front. Deep-Sea Research, 41: 51–79.

Anon. 1992. Nordic WOCE. Project Description. II. 43 pp.

Arhan, M. 1990. The North Atlantic Current and Subarctic Intermediate Water. Journal of Marine Research, 48: 109–144.

Becker, G., and Hansen, B. 1998. Modified North Atlantic Water. ICES Cooperative Research Report, this volume.

Belkin, I. G., and Levitus, S. 1996. Temporal variability of the Subarctic Front near the Charlie-Gibbs Fracture Zone. Journal of Geophysical Research, 101 (C12): 28317–28324.

Bersch, M. 1995. On the circulation of the northeastern North Atlantic. Deep-Sea Research, 42 (9): 1583–1607.

Blindheim, J., and Ådlandsvik, B. 1995. Episodic formation of intermediate water along the Greenland Sea Arctic Front. ICES CM 1995/Mini:6. 11 pp.

Blindheim, J. 1990. Arctic intermediate water in the Norwegian Sea. Deep-Sea Research, 37 (9): 1475–1489.

Blindheim, J. 1993. Seasonal Variations in the Atlantic Inflow to the Nordic Seas. ICES CM 1993/C:39. 13 pp.

Blindheim, J., Borovkov, V., Hansen, B., Malmberg, S. Aa., Turrell, W. R., and Østerhus, S. Upper layer cooling and freshening in the Norwegian Sea in relation to atmospheric forcing. Submitted to Deep Sea Research

Bogdanov, M. A., Zaitsev, G. N., and Potaichuk, S. I. 1967. Water mass dynamics in the Iceland Faroe Ridge area. Rapports et Procès-Verbaux des Réunions du Conseil International pour l'Exploration de la Mer, 157: 150–156.

Booth, D. A., and Ellett, D. J. 1983. The Scottish continental slope current. Continental Shelf Research, 2: 127–146.

Booth, D. A., and Meldrum, D. T. 1984. Drifting Buoys in the Northeast Atlantic and Norwegian Sea. ICES CM 1984/C:27. 9 pp.

Booth, D. A., and Meldrum, D. T. 1987. Drifting buoys in the Northeast Atlantic. Journal du Conseil International pour l'Exploration de la Mer, 43: 261–267.

Booth, D. A. 1988. Eddies in the Rockall Trough. Oceanologica Acta, 11: 213–219.

Borenæs, K. M., and Lundberg, P. A. 1988. On the Deep-Water Flow Through the Faroe Bank Channel. Journal of Geophysical Research, 93 (C2): 1281–1292.

Buch, E., Malmberg, S. Aa., and Kristmannsson, S. S. 1992. Arctic Ocean deep water masses in the Western Iceland Sea. ICES CM 1992/C:2. 19 pp.

Cooper, L. H. N. 1955. Deep water movements in the North Atlantic as a link between climatic changes around Iceland and biological productivity of the English Channel and Celtic Sea. Journal of Marine Research, 14: 347–362.

Crease, J. 1965. The flow of Norwegian Sea Water through the Faroe Bank Channel. Deep-Sea Research, 12: 143–150.

de Boer, C. J. 1998. Water mass distribution in the Iceland Basin calculated with an Optimal Parameter Analysis. ICES Cooperative Research Report, this volume.

de Boer, C. J., van Aken, H. M., and van Bennekom, A. J. 1998. Hydrographic variability of the overflow water in the Iceland Basin. ICES Cooperative Research Report, this volume.

Dickson, R. R., and Brown, J. 1994. The production of North Atlantic Deep Water: Sources, rates, and pathways. Journal of Geophysical Research, 99: 12,319–12,341.

Dickson, R. R., Malmberg, S. A., Jones, S. R., and Lee, A. J. 1984. An investigation of the earlier Great Salinity Anomaly of 1910–14 in waters west of the British Isles. ICES CM 1984/Gen:4. 30 pp.

Dickson, R. R., Meincke, J., Malmberg, S. A., and Lee, A. J. 1988. The "Great Salinity Anomaly" in the Northern North Atlantic 1968–1982. Progress in Oceanography, 20: 103–151.

Dietrich, G. 1957. Stratification and Circulation of the Irminger sea in June 1955. Annales Biologiques du Conseil International pour l'Exploration de la Mer, 12: 36–38.

Dietrich, G., Kalle, K., Krauss, W., and Siedler, G. 1975. Allgemeine Meereskunde. Borntrager, Berlin. 593 pp.

Dietrich, von G. 1956. Überstrømung des Island-Farøer-Ruckens in Bodennahe nach Beobachtungen mit dem Forschungsschiff "Anton Dohrn" 1955/56. Deutsche Hydrographische Zeitschrift, 9 (2): 78–89.

Dobson, E. B. 1988. Dynamic topography as measured by the GEOSAT altimeter in regions of small surface height signatures. Proceedings of IGARSS '88 Symposium, Edinburgh, Scotland, 13–16 Sept. 1988. Ref. ESA SP-284 (IEEE 88CH2497-6): 635–638.

Dooley, H. D., and Crease, J. 1978. Observed and Geostrophic Currents south and east of Faroe during Overflow '73. ICES CM 1978/C:53. 12 pp.

Dooley, H. D., and Henderson, E. W. 1980. Low Frequency Currents North of Rockall Bank. ICES CM 1980/C:25. 11 pp.

Dooley, H. D., and Meincke, J. 1981. Circulation and Water Masses in the Faroese Channels during Overflow '73. Deutsche Hydrographische Zeitschrift, 34: 41–55.

Dooley, H. D., Martin, J. H. A., and Ellett, D. J. 1984. Abnormal hydrographis conditions in the Northeast Atlantic during the 1970s. Rapports et Procès-Verbaux des Réunions du Conseil International pour l'Exploration de la Mer, 185: 179–187.

Dooley, H. D. 1984. Aspects of oceanographic variability on Scottish fishing grounds. Ph.D. thesis, University of Aberdeen.

Dooley, H., Gould, W. J., Hansen, B., and Rickards, L. J. 1991. North Atlantic-Norwegian Sea Exchanges The ICES NANSEN Project: an overview. ICES CM 1991/C:24. 9 pp.

Dooley, H., Martin, J. H. A., and Payne, R. 1976. Flow across the continental slope off northern Scotland. Deep-Sea Research, 23: 875–880.

Edwards, A., Ellett, D. J., Kruseman, P., and Prangsma, G. J. 1979. Temperature - salinity variability in the northern Rockall Trough during JASIN 1978. ICES CM 1979/C:34. 24 pp.

Ellett, D. J., and Edwards, A. 1978. A volume transport estimate for Norwegian Sea overflow across the Wyville Thomson Ridge. ICES CM 1978/C:19. 12 pp.

Ellett, D. J., and Martin, J. H. A. 1973. The physical and chemical oceanography of the Rockall Channel. Deep-Sea Research, 20: 585–625.

Ellett, D. J., and Roberts, D. G. 1972. The overflow of Norwegian Sea Deep Water across the Wyville Thomson Ridge. ICES CM 1972/C:27. 14 pp.

Ellett, D. J., and Roberts, D. G. 1973. The overflow of Norwegian Sea Deep Water across the Wyville Thomson Ridge. Deep-Sea Research, 20: 819–835.

Ellett, D. J. 1976. Bottom topography along the track of the Wyville Thomson Ridge overflow. ICES CM 1976/C:13. 7 pp.

Ellett, D. J., Dooley, H. D., and Hill, H. W. 1979. Is there a North-east Atlantic Slope Current? ICES CM 1979/C:35. 11 pp.

Ellett, D. J., Edwards, A., and Bowers, R. 1986. The hydrography of the Rockall Channel-an overview. Proceedings. Royal Society, 88B: 61–81.

Ellett, D. J., Kruseman, P., Prangsma, G. J., Pollard, R. T., van Aken, H. M., Edwards, A. Dooley, H. D., and Gould, W. J. 1983. Water masses and mesoscale circulation of North Rockall Trough waters during JASIN 1978. Philosophical Transactions of the Royal Society of London. Series A, 308: 231–252.

Ellett, D. J. 1988. Bottom Topography to the West of the Wyville Thomson Ridge. Deutsche Hydrographische Zeitschrift, 41: 23–33.

Ellett, D. J. 1991. Norwegian Sea Deep Water overflow across the Wyville Thomson Ridge during 1987–88. ICES CM 1991/C:41. 11 pp.

Ellett, D. J. 1993. The north-east Atlantic: A fan-assisted storage heater? Weather, 48: 118–126.

Ellett, D. J. 1998. Norwegian Sea Deep Water overflow across the Wyville Thomson Ridge during 1987–88. ICES Cooperative Research Report, this volume.

Essen, H. H. 1992. Ocean currents in the Iceland-Faeroe area, measured by a bottom-mounted

ADCP. SACLANTCEN Memoirs, SM-265. 43 pp.

Fogelquist, E., Blindheim, J., Tanhua, T., Buch, E., and Østerhus, S. Greenland-Scotland Overflow studied by hydro-chemical multivariate analysis. Submitted

Foldvik, A., Aagaard, K., and Tørresen, T. 1988. On the velocity field of the East Greenland Current. Deep-Sea Research, 35 (8): 1335–1353.

Fox, A. D. and Maskell, S. J. 1996. A nested primitive equation model of the Iceland-Faeroe front. Journal of Geophysical Research, 101 (C8): 18259–18278.

Fuchs, G., Jancke, K., and Meincke, J. 1984. Observations of winter convection in the Northeastern Atlantic. ICES CM 1984/C:18. 9 pp.

Gould, W. J., Loynes, J., and Backhaus, J. 1985. Seasonality in Slope Current Transports N.W. of Shetland. ICES CM 1985/C:7. 13 pp.

Gould, W. J., Read, J. F., and Smithers, J. 1987. SeaSoar profiles in the Iceland Scotland area, May 1987. Institute of Oceanographic Sciences Deacon Laboratory Report, 253. 50 pp.

Griffiths, C. 1995. A fine resolution numerical model of the Iceland-Faræ front with open boundary conditions. Journal of Geophysical Research, 100 (C8): 15,915–15,931.

Griffiths, G. 1990. The temperature, salinity and velocity structure of the Iceland-Faeroes Front and North Atlantic Water inflow to the GIN Sea. Institute of Oceanographic Sciences Deacon Laboratory, Cruise Report, 216. 42 pp.

Griffiths, G., Hartman, M. C., and Alderson, S. G. 1992. Shipboard ADCP observations during RRS Charles Darwin cruise 51. Institute of Oceanographic Sciences Deacon Laboratory, Report, 293. 97 pp.

Hallock, Z. R. 1985. Variability of Frontal Structure in the Southern Norwegian Sea. Journal of Physical Oceanography, 15: 1245–1254.

Hansen, B., and Jákupsstovu, S. H. í 1992. Availability of blue whiting (Micromesistius poutassou) in Faroese waters in relation to hydrography. ICES Marine Science Symposia, 195: 349–360.

Hansen, B., and Kristiansen, R. 1994. Long-Term changes in the Atlantic water flowing past the Faroe Islands. ICES CM 1994/S:4. 16 pp.

Hansen, B., and Kristiansen, R. Variations of the Faroe Bank Channel overflow. In press.

Hansen, B., and Meincke, J. 1979. Eddies and meanders in the Iceland-Faroe Ridge area. Deep-Sea Research, 26A: 1067–1082.

Hansen, B., and Meincke, J. 1984. Long-term coastal sea surface temperature observations at the Faroe Islands. Rapports et Procès-Verbaux des Réunions du Conseil International pour l'Exploration de la Mer, 185: 162–169.

Hansen, B. 1985. The circulation of the northern part of the Northeast Atlantic. Rit Fiskideildar, 9: 110–126.

Hansen, B. 1992. Residual and tidal currents on the Faroe Plateau. ICES CM 1992/C:12. 18 pp.

Hansen, B., Jónsson, S., Lundberg, P., Turrell, W. R., and Østerhus, S. 1998. Exchanges of water, heat and salt between the Arctic Mediterranean and the World Ocean through the Greenland-Scotland Gap measured in the Nordic WOCE programme. The 1998 Conference of the World Ocean Circulation Experiment. Ocean Circulation and Climate. Halifax, Canada 24–29 may 1998.

Hansen, B., Malmberg, S. A., Sælen, O. H., and Østerhus, S. 1998. Measurement of flow north of the Faroe Islands June 1986. ICES Cooperative Research Report, this volume.

Hansen, B., Meldrum, D., and Ellett, D. 1998. Satellite-tracked drogue paths over Faroe Bank and the Iceland-Faroe Ridge. ICES Cooperative Research Report, this volume.

Hansen, B., Sælen, O. H., and Østerhus, S. 1998. The passage of Atlantic water east of the Faroes. ICES Cooperative Research Report, this volume.

Harvey, J. G., and Shor, A. N. 1978. Norwegian Sea overflow water in the Charlie-Gibbs Fracture Zone. ICES CM 1978/C:62. 11 pp.

Harvey, J. G., and Theodorou, A. 1986. The circulation of Norwegian Sea overflow water in the eastern North Atlantic. Oceanologica Acta, 9 (4): 393–402.

Harvey, J. 1965. The topography of the South-Western Faroe Channel. Deep-Sea Research, 12: 121–127.

Harvey, J. 1982. θ-S relationships and water masses in the eastern North Atlantic. Deep-Sea Research, 29 (8A): 1021–1033.

Helland Hansen, B., and Nansen, F. 1909. The Norwegian Sea, Its Physical Oceanography. Based on the Norwegian Researches 1900–1904. Report on Norwegian Fishery and Marine-Investigations, Bergen, 2 (2).

Hermann, F. 1949. Hydrographic Conditions in the South-Western Part of the Norwegian Sea. Annales Biologiques du Conseil International pour l'Exploration de la Mer, 5: 19–21.

Hermann, F. 1953. Hydrographic conditions in the southern part of the Norwegian Sea, 1952. Annales Biologiques du Conseil International pour l'Exploration de la Mer, IX: 22–25.

Hermann, F. 1959. Hydrographic Observations in the Faroe Bank Channel and over the Faroe-Iceland Ridge June 1959. Journal du Conseil International pour l'Exploration de la Mer, 118. 5 pp.

Hermann, F. 1967. The T-S Diagram Analysis of the Water Masses over the Iceland-Faroe Ridge and in the Faroe Bank Channel (Overflow '60). Rapports et Procès-Verbaux des Réunions du Conseil International pour l'Exploration de la Mer, 157: 139–149.

Hill, A. E. and Mitchelson-Jacob, E. G. 1993. Observations of a poleward-flowing saline core on the continental slope west of Scotland. Deep-Sea Research, 40: 1521–1527.

Hjøllo, S. S., and Mork, M. 1996. Atlantic inflow to the Norwegian Sea as deduced from current meter observations and numerical modelling. ICES CM 1996/O:7. 7 pp.

Hopkins, T. S. 1991. The GIN Sea-A synthesis of its physical oceanography and literature review 1972–1985. Earth-Science Reviews, 30: 175–318.

Hopkins, T. S., Baldasserini, G., Minnett, P., Povero, P., and Zanasca, P. 1992. Icelandic Current Experiment GIN Sea Cruise 88. Data Report Hydrography and Circulation. SACLANTCEN Memoirs, SM-260 (1). 214 pp.

Hopkins, T. S., Povero, P., Pistek, P., and Varnas, A. W. 1992. Upper layer environmental parameters from CTD data GIN '87 cruises. SACLANTCEN Memoirs, SM-252. 46 pp.

Huthnance, J. M. 1986. The Rockall slope current and shelf-edge processes. Proc. Roy. Soc. Edinb., 88B: 83–101.

Huthnance, J. M. 1986. The Rockall slope current and shelf-edge processes. Proc. Roy. Soc. Edinb., 88B: 83–101.

Isemer, H. J., and Hasse, L. 1985. The Bunker climate atlas of the North Atlantic Ocean. Springer Verlag. Berlin.

Jacobsen, J. P. 1943. The Atlantic Current through the Faroe-Shetland Channel and its Influence on the Hydrographical Conditions in the Northern Part of the North Sea, the Norwegian Sea, and the Barents Sea. Rapports et Procès-Verbaux des Réunions du Conseil International pour l'Exploration de la Mer, 112: 5–47.

Johannesen, O. M. 1986. Brief overview of the physical oceanography. In The Nordic Seas, pp. 103–127. Ed. by B.G. Hurdle. Springer, New York.

Johnson, G. C., and Ohlsen, D. R. 1994. Frictionally Modified Rotating Hydraulic Channel Exchange and Ocean Outflows. Journal of Physical Oceanography, 24: 66–78.

Johnson, G. C., and Sanford, T. B. 1992. Secondary Circulation in the Faroe Bank Channel Outflow. Journal of Physical Oceanography, 22 (8): 927–933.

Knudsen, M. 1898. Den Danske Ingolf-expedition. Bianco Lunos Kgl. Hof-Bogtrykkeri (F. Dreyer), København, 1 (2): 21–154.

Knudsen, M. 1911. Danish Hydrographical Investigations at the Faroe Islands in the spring of 1910. Meddelelser fra Kommisionen for Havundersøgelser. Serie Hydrografi, II (1). 21 pp.

Koltermann, K. P., Meincke, J., and Müller, T. 1976. Overflow '73 - Data Report 'Meteor' and 'Meerkatze 2'. Berichte der Institut für Meereskunde an der Universität Kiel, 23. 88 pp.

Krauss, W. 1986. The North Atlantic Current. Journal of Geophysical Research, 91 (C4): 5061–5074.

Krauss, W. 1995. Currents and mixing in the Irminger Sea and in the Iceland Basin. Journal of Geophysical Research, 100 (C6): 10,851–10,871.

Kristmansson, S. S. 1998. Flow of Atlantic Water into the northern Icelandic shelf area, 1985–1989. ICES Cooperative Research Report, this volume.

Kuijpers, A., Andersen, M. S., Kenyon, N. H., Kunzendorf, H., and van Weering, T. C. E. Quaternary sedimentation and Norwegian Sea overflow pathways around Bill Bailey Bank, Northeastern Atlantic. In press.

Käse, R. H., and Krauss, W. 1996. The Gulf Stream, the North Atlantic Current, and the Origin of the Azores Current. In The Warmwatersphere of the North Atlantic Ocean, pp. 291–337. Ed. by W. Krauss. Gebrüder Borntrager, Berlin.

Lee, A. J. 1967. Temperature and Salinity Distributions as shown by Sections Normal to the Iceland-Faroe Ridge (Overflow '60). Rapports et Procès-Verbaux des Réunions du Conseil International pour l'Exploration de la Mer, 157: 100–135.

Lindblad, K. 1997. Near-source behaviour of the Faroe Bank Channel Deep-water plume. Gøteborg University, Department of Oceanography, Gøteborg, Sweden. 41 pp.

Malmberg, S. Aa. 1983. Hydrographic Investigations in the Iceland and Greenland Seas in late Winter 1971 – "Deep Water Project". Jøkull, 33: 133–140.

Malmberg, S. A., and Briem, J. 1993. Satellite tracked drogue experiments in Icelandic waters 1992. ICES CM 1993/C:45. 11 pp.

Malmberg, S. A., and Kristmannsson, S. S. 1992. Hydrographic conditions in Icelandic waters, 1980–1989. ICES Marine Science Symposia, 195: 76–92.

Malmberg, S. A., and Magnússon, G. 1982. Sea Surface Temperature and Salinity in South Icelandic Waters in the period 1868–1965. Rit Fiskideildar, 6. 31 pp.

Malmberg, S. A. 1985. The water masses between Iceland and Greenland. Rit Fiskideildar, 9: 127–140.

Malmberg, S. A., Valdimarsson, H., and Mortensen, J. 1994. Long time series in Icelandic waters. ICES CM 1994/C:8. 17 pp.

Martin, J. H. A. 1966. The Bottom Waters of the Faroe-Shetland Channel. In Some Contemporary Studies in Marine Science, pp. 469–478. Ed. by H. Barnes. George Allen and Unwin Ltd, London.

Martin, J. H. A. 1976. Long term changes in the Faroe-Shetland Channel associated with intrusions of Iceland-Faroe Ridge water during the period 1955–75. ICES CM 1976/C:22. 11 pp.

Martin, J. H. A. 1988. Temporal salinity changes in the 0-degree centigrade water in the Faroe-Shetland Channel. ICES CM 1988/C:38. 9 pp.

Martin, J. H. A. 1993. Norwegian Sea intermediate water in the Faroe-Shetland Channel. ICES Journal of Marine Science, 50: 195–201.

Mauritzen, C. 1996. Production of dense overflow waters feeding the North Atlantic across the Greenland-Scotland Ridge. Deep-Sea Research, 43 (6): 769–835.

Mc Cartney, M. S, and Talley, L. D. 1982. The Subpolar Mode Water of the North Atlantic Ocean. Journal of Physical Oceanography, 12: 1169–1188.

Mc Cartney, M. S., and Talley, L. D. 1984. Warm-to-Cold Water Conversion in the Northern North Atlantic Ocean. Journal of Physical Oceanography, 14: 922–935.

Meincke, J., and Kvinge, T. 1978. On the atmospheric forcing of Overflow-events. ICES CM 1978/C:9. 14 pp.

Meincke, J. 1972. Recent Observations of the Overflow across the Greenland-Scotland Ridge. ICES CM 1972/C:7. 9 pp.

Meincke, J. 1972. The Hydrographic Section along the Iceland-Faroe Ridge carried out by R.V. "Anton Dohrn" in 1959–1971. Berichte der Deutschen Wissenschaftlichen Kommission für Meeresforschung, 22: 372–384.

Meincke, J. 1974. 'Overflow 73 - Large-scale Features of the Overfolw across the Iceland-Faroe Ridge. ICES CM 1974/C:7. 10 pp.

Meincke, J. 1975. Overflow '73 – Evidence for atmospheric forcing of Arctic water overflow events. ICES CM 1975/C:29. 13 pp.

Meincke, J. 1976. Coupling between bottom currents and weather pattern on the Iceland-Faroe ridge. ICES CM 1976/C:30. 9 pp.

Meincke, J. 1978. On the Distribution of Low Salinity Intermediate Waters around the Faroes. Deutsche Hydrographische Zeitschrift, 31: 50–64.

Meincke, J. 1983. The modern current regime across the Greenland Scotland Ridge. In Structure and Development of the Greenland Scotland Ridge, New Methods and Concepts, Ed. by M. H. P.Bott, S. Saxov, M. Talwani & J. Thiede. Proc. NATO Adv. Res. Inst., Padua Univ., 11–15 May, 1981. Plenum Press, New York.

Meincke, J., Rudels, B., and Friedrich, H. J. 1997. The Arctic Ocean-Nordic Seas thermohaline system. ICES Journal of Marine Science, 54: 283–299.

Midttun, L. 1985. Formation of dense bottom water in the Barents Sea. Deep-Sea Research, 32 (10): 1233–1241.

Miller, A. J., Poulain, P. M., Robinson, A. R., Arango, H. G., Leslie, W. G., and Varnas, A. W. 1995. Quantitative skill of quasi-geostrophic forecasts of a baroclinically unstable Iceland-Faroe Front. Journal of Geophysical Research, 100 (C6): 10,833–10,849.

Mosby, H. 1970. Atlantic water in the Norwegian Sea. Geophysica Norvegica, 28 (1). 60 pp.

Müller, T. J., Schott, F. A., Siedler, G., and Koltermann, K. P. 1974. Overflow '73 – Observations in a Small-Scale Overflow Event on the Iceland-Faroe Ridge. ICES CM 1974/C:6. 8 pp.

Müller, T. J. 1978. TS-Characteristics and Water Masses during Overflow '73. ICES CM 1978/C:10. 23 pp.

Müller, T. J., Meincke, J., and Becker, G. A. 1979. Overflow' 73: The Distribution of Water Masses on the Greenland-Scotland Ridge in August / September 1973. Berichte der Institut für Meereskunde an der Universität Kiel, 62. 172 pp. pp.

Nielsen, J. N. 1904. Hydrography of the waters by the Faroe Islands and Iceland during the cruises of the danish research steamer "Thor" in the summer 1903. Meddelelser fra Kommisionen for Havundersøgelser. Serie Hydrografi, I (4). 42 pp.

Niiler, P. P., Piacsek, S., Neuberg, L., and Warn-Varnas, A. 1992. Sea Surface Temperature Variability of the Iceland-Faeroe Front. Journal of Geophysical Research, 97 (C11): 17777–17785.

Orvik, K. A., and Mork, M. 1996. Atlantic water transport from long term current measurements in the Svinøy section. ICES CM 1996/O:8. 9 pp.

Otto, L., and van Aken, H. M. 1996. Surface circulation in the Northeast Atlantic as observed with drifters. Deep-Sea Research, 43 (4): 467–499.

Otto, L., van Aken, H. M., and Koster de, R. X. 1992. Use of drifters in the "Dutch-Warp" programme, 1990 and 1991. Programme description and preliminary results. Nederlands Instituut voor Onderzoek der Zee Data-Report, 2. 22 pp.

Paillet, J., and Mercier, H. 1997. An inverse model of the eastern North Atlantic general circulation and thermocline ventilation. Deep-Sea Research, 44 (8): 1293–1328.

Perkins, H. 1992. Large-scale structure of the Iceland-Faeroe Front. SACLANTCEN Report, SR-189. 21 pp.

Perkins, H., Sherwin, T. J., and Hopkins, T. S. 1994. Amplification of Tidal Currents by Overflow on the Iceland-Faeroe Ridge. Journal of Physical Oceanography, 24: 721–735.

Perry, R. K. 1986. Bathymetry. In The Nordic Seas, pp. 211–235. Ed. by B.G. Hurdle. Springer, New York.

Pingree, R. D., and Le Cann, B. 1989. Celtic and Armorican slope and shelf residual currents. Progress in Oceanography, 23: 303–338.

Pingree, R. D. 1993. Flow of surface waters to the west of the British Isles and in the Bay of Biscay. Deep-Sea Research, 40: 369–388.

Pistek, P., and Johnson, D. R. 1992. A Study of the Iceland-Faeroe Front using GEOSAT altimetry and current-following drifters. Deep-Sea Research, 39: 2029–2051.

Pistek, P., and Johnson, D. R. 1992. Transport of the Norwegian Atlantic Current as determined from Satellite Altimetry. Geophysical Research Letters, 19 (13): 1379–1382.

Pollard, R. T., and Pu, S. 1985. Structure and circulation of the upper Atlantic Ocean northeast of the Azores. Progress in Oceanography, 14: 443–462.

Poulain, P. M., Warn-Varnas, A., and Niiler, P. P. 1996. Near-surface circulation of the Nordic seas as measured by Lagrangian drifters. Journal of Geophysical Research, 101 (C8): 18237–18258.

Price, J. F., and O'Neil Baringer, M. 1994. Outflows and deep water production by marginal seas. Progress in Oceanography, 33: 161–200.

Read, J. F., and Pollard, R. T. 1992. Water Masses in the Region of the Iceland-Faeroes Front. Journal of Physical Oceanography, 22: 1365–1378.

Reid, J. L. 1979. On the contribution of the Mediterranean Sea outflow to the Norwegian-Greenland Sea. Deep-Sea Research, 26A: 1199–1223.

Reverdin, G., Cayan, D., Dooley, H. D., Ellett, D. J., Levitus, S., Penhoat, Y. du, and Dessier, A. 1994. Surface salinity of the North Atlantic: Can we reconstruct its fluctuations over the last one hundred years?. Progress in Oceanography, 33: 303–346.

Rhein, M. 1996. Convection in the Greenland Sea, 1982 – 1993. Journal of Geophysical Research, 101 (C8): 18183–18192.

Rossov, V. V. 1961. On the water end heat balance of the Norwegian and Greenland Seas. Okeanologiya, 1 (5): 944–947.

Rossov, V. V. 1972. On the Water Exchange between the North Atlantic and the Polar Basin and the Water Balance of the North Atlantic Current. ICES CM 1972/C:3. 9 pp.

Rudels, B., and Quadfasel, D. 1991. The Arctic Ocean Component in the Greenland-Scotland overflow. ICES CM 1991/C:30. 21 pp.

Rudels, B., Quadfasel, D., and Friedrich, H. 1998. The Arctic Ocean Deep Water component in the Greenland-Scotland overflow. ICES Cooperative Research Report, this volume.

Rydberg, L. 1980. Rotating hydraulics in deep-water channel flow. Tellus, 32: 77–89.

Samuel, P., Johannessen, J. A., and Johannessen, O. M. 1994. A Study on the Inflow of Atlantic Water to the GIN Sea using GEOSAT Altimeter Data. Submitted to Nansen Centennial Volume. 12 pp.

Saunders, P. M. 1990. Cold Outflow from the Faroe Bank Channel. Journal of Physical Oceanography, 20: 28–43.

Saunders, P. M. 1992. Combining hydrographic and Shipborne ADCP measurements. Deep-Sea Research, 39 (7/8): 1417–1427.

Saunders, P. M. 1994. The flux of overflow water through the Charlie-Gibbs Fracture Zone. Journal of Geophysical Research, 99 (C6): 12343–12355.

Saunders, P. M. 1996. The Flux of Dense Cold Overflow Water Southeast of Iceland*. Journal of Physical Oceanography, 26: 85–95.

Schlosser, P., Bønisch, G., Rhein, M., and Bayer, R. 1991. Reduction of Deepwater Formation in the Greenland Sea During the 1980s: Evidence from Tracer Data. Science, 251: 1054–1056.

Schmitt, R. W., Bogden, P. S., and Dorman, C. E. 1989. Evaporation Minus Precipitation and Density Fluxes for the North Atlantic. Journal of Physical Oceanography, 19: 1208–1221.

Scott, J. C., and Dowall, Mc A. L. 1990. Cross-Frontal Cold Jets Near Iceland: In-Water, Satellite Infrared, and Geosat Altimeter Data. Journal of Geophysical Research, 95 (C10): 18,005–18,014.

Shor, A., Muller, D., and Johnson, D. 1977. Transport of Norwegian Sea Overflow--Preliminary Results of ATLANTIS II Cruise 94, June-July 1977. ICES CM 1977/C:44. 13 pp.

Shor, A. 1978. Bottom Currents on East Katla Ridge, NW Iceland Basin. ICES CM 1978/C:60. 19 pp.

Simonsen, K., and Haugan, P. M. 1996. Heat budgets of the Arctic Mediterranean and sea surface heat flux parameterizations for the Nordic Seas. Journal of Geophysical Research, 101 (C3): 6553–6576.

Smart, J. H. 1984. Spatial variability of major frontal systems in the North Atlantic-Norwegian Sea area: 1980–1981. Journal of Physical Oceanography, 14: 185–192.

Steele, J. H. 1959. Observations of Deep Water Overflow across the Iceland-Faroe Ridge. Deep-Sea Research, 6: 70–72.

Steele, J. H. 1961. Notes on the Deep Water Overflow Across the Iceland-Faroe Ridge. Rapports et Procès-Verbaux des Réunions du Conseil International pour l'Exploration de la Mer, 149: 84–88.

Steele, J. H., Barrett, J. R., and Worthington, L. V. 1962. Deep currents south of Iceland. Deep-Sea Research, 9: 465–474.

Steele, J. H. 1967. Current measurements on the Iceland-Faroe Ridge. Deep-Sea Research, 14: 469–473.

Stefánsson, U. 1962. North Icelandic Waters. Rit Fiskideildar, 3. 269 pp.

Stefánsson, U. 1972. Near-shore Fluctuations of the Frontal Zone Southeast of Iceland. Rapports et Procès-Verbaux des Réunions du Conseil International pour l'Exploration de la Mer, 162: 201–205.

Swallow, J. C., Gould, W. J., and Saunders, P. M. 1977. Evidence for a poleward eastern boundary current in the North Atlantic Ocean. ICES CM 1977/C:32. 11 pp.

Swift, J. H., and Aagaard, K. 1981. Seasonal transitions and water mass formation in the Iceland and Greenland seas. Deep-Sea Research, 28A (10): 1107–1129.

Swift, J. H., and Koltermann, K. P. 1988. The Origin of Norwegian Sea Deep Water. Journal of Geophysical Research, 93 (C4): 3563–3569.

Swift, J. H., Aagaard, K., and Malmberg, S. Aa. 1980. The contribution of the Denmark Strait overflow to the deep North Atlantic. Deep-Sea Research, 27A: 29-42.

Swift, J. H. 1984. A Recent O - S Shift in the Deep Water of the Northern North Atlantic. Climate Processes and Climate sensitivity Geophysical Monograph 29, Maurice Ewing Volume, 5: 39–47.

Sy, A. 1988. Investigation of large-scale circulation patterns in the central North Atlantic: The North Atlantic Current, the Azores Current and the Mediterranean water plume in the area of the Mid-Atlantic Ridge. Deep-Sea Research, 35: 383–413.

Sy, A., Schauer, U., and Meincke, J. 1992. The north Atlantic Current and its associated hydrographic structure above and eastwards of the Mid-Atlantic Ridge. Deep-Sea Research, 39: 825–853.

Sælen, O. H. 1959. Studies in the Norwegian Atlantic Current, Part I. The Sognefjord section. Geophysica Norvegica, 20 (13): 1–28.

Sælen, O. H. 1963. Studies in the Norwegian Atlantic Current, Part II. Investigations during the years of 1954-1959 in an area west of Stad. Geophysica Norvegica, 23 (6): 1–82.

Sælen, O. H. 1990. On the exchange of bottom water between the Greenland and Norwegian Seas. Geophysica, 3: 133–144.

Sætre, R. 1967. Report on the Norwegian Investigations in the Faeroe Channel 1964-65. NATO Subcommittee on Oceanographic Research technical Report, 38. 27 pp.

Tait, J. B. 1955. Long Term Trends and changes in the Hydrography of the Faroe Shetland Channel Region. Deep-Sea Research, 3: 482–498 (suppl.).

Tait, J. B. 1957. Hydrography of the Faroe-Shetland Channel 1927-1952. Scottish Home Department Marine Research, 2. 309 pp.

Tait, J. B. 1957. Recent Oceanographical Investigations in the Faroe-Shetland Channel. Proceedings. Royal Society, 18: 239–289.

Tait, J. B. 1958. Bottom current measurements between Faroe Bank and the Faroe Islands by the carruthers "PISA" Subsurface current indicator. Journal du Conseil International pour l'Exploration de la Mer, 35. 3 pp.

Tait, J. B. 1961. Hydrography of the Faroe Bank Channel. Annales Biologiques du Conseil International pour l'Exploration de la Mer, 16: 28–30.

Tait, J. B. 1967. The Iceland-Faroe Ridge international (ICES) "Overflow" expedition, May-Juni 1960. Rapports et Procès-Verbaux des Réunions du Conseil International pour l'Exploration de la Mer, 157. 71 pp.

Tait, J. B., Lee, A. J., Stefansson, U., and Hermann, F. 1967. Temperature and salinity distributions and water-masses of the region. Rapports et Procès-Verbaux des Réunions du Conseil International pour l'Exploration de la Mer, 157: 38–149.

Timofeyev, V. T. 1963. Interaction of waters from the Arctic Ocean with those from the Atlantic and Pacific. Okeanologiya, 3 (4): 569–578.

Tokmakian, R. 1994. The Iceland-Faroe Front: A Synergistic Study of Hydrography and Altimetry. Journal of Physical Oceanography, 24: 2245–2262.

Turrell, B. 1995. A Century of Hydrographic Observations in the Faroe-Shetland Channel. Ocean Challenge, 6 (1): 58–63.

Turrell, W. R., Devonshire, E., Payne, R., and Slesser, G. 1993. Analysis of the Historic Time-Series Obtained in the Faroe-Shetland Channel. ICES CM 1993/C:29. 21 pp.

Turrell, W. R., Henderson, E. W., and Slesser, G. 1990. Residual transport within the Fair Isle Current observed during the Autumn Circulation Experiment (ACE). Continental Shelf Research, 10 (6): 521–543.

Turrell, W. R., Henderson, E. W., Slesser, G., Payne, R., and Adams, R. D. 1992. Hydrographic observations at the continental shelf edge northwest of Scotland. ICES CM 1992/C:19. 32 pp.

Turrell, W. R., Slesser, G., Adams, R. D., Payne, R., and Gillibrand, P. A. 1999. Decadal variability in Faroe Shetland Channel bottom water. Deep-Sea Res. 46:1–25.

van Aken, H. M., and Becker, G. 1996. Hydrography and through-flow in the north-eastern north Atlantic Ocean: the NANSEN project. Progress in Oceanography, 38: 297–346.

van Aken, H. M., and de Boer, C. J. 1995. On the synoptic hydrography of intermediate and deep water masses in the Iceland Basin. Deep-Sea Research, 42: 165–189.

van Aken, H. M. 1988. Transports of water masses through the Faroese Channels determined by an inverse method. Deep-Sea Research, 35: 595–617.

van Aken, H. M. 1995. Mean currents and current variability in the Iceland Basin. Netherlands Journal of Sea Research, 33 (2): 135–145.

van Aken, H. M. 1998. Current measurements in the Iceland Basin. ICES Cooperative Research Report, this volume.

van Aken, H. M. 1998. The hydrography of the mid-latitude northeast Atlantic Ocean: Physical and chemical characteristics. The 1998 Conference of the World Ocean Circulation Experiment. Ocean Circulation and Climate. Halifax, Canada 24–29 May 1998.

Varnas, A. W., Henderson, L., Meurs, Van. P., and Piacsek, S. 1993. Diagnostic modelling studies of the Iceland-Faeroe front. SACLANTCEN Report, SR-204. 33 pp.

Vogt, P. R. 1986. Seafloor topography, sediments, and paleoenvironments. In The Nordic Seas, pp. 237–410. Ed. by B.G. Hurdle. Springer, New York.

Wegner, G. 1972. Geostrophic Surface Currents in the northern North Atlantic Ocean in the International Geophysical Year 1957/58. ICES CM 1972/C:4. 10 pp.

Willebrand, J., and Meincke, J. 1980. Statistical analysis of fluctuations in the Iceland-Scotland frontal zone. Deep-Sea Research, 27A: 1047–1066.

Worthington, L. V., and Volkmann, G. H. 1965. The Volume Transport of the Norwegian Sea Overflow Water in the North Atlantic. Deep-Sea Research, 12: 667–676.

Worthington, L. V. 1970. The Norwegian Sea as a mediterranean basin. Deep-Sea Research, 17: 77–84.

Østerhus, S., and Gammelsrød, T. The Abyss of the Nordic Seas is warming. In press.

Østerhus, S., and Golmen, L. G. 1988. Comparison of ADCP data against moored current meter data and calculated geostrophic currents. ICES CM 1988/C:28. 12 pp.

Østerhus, S., and Sælen, O. H. 1988. Hydrographic conditions north and east of the Faeroe Islands 1986–87. Seminar on fisheries and hydrography, Norðurlandahúsið 29 Aug – 3 Sep 1988, Tórshavn, Faroe Islands. 20 pp.

Østerhus, S., Turrell, W. T., Hansen, B., Blindheim, J., and van Bennekom, J. 1996. Changes in the Norwegian Sea Deep Water. ICES CM 1996/O:11. 3 pp.

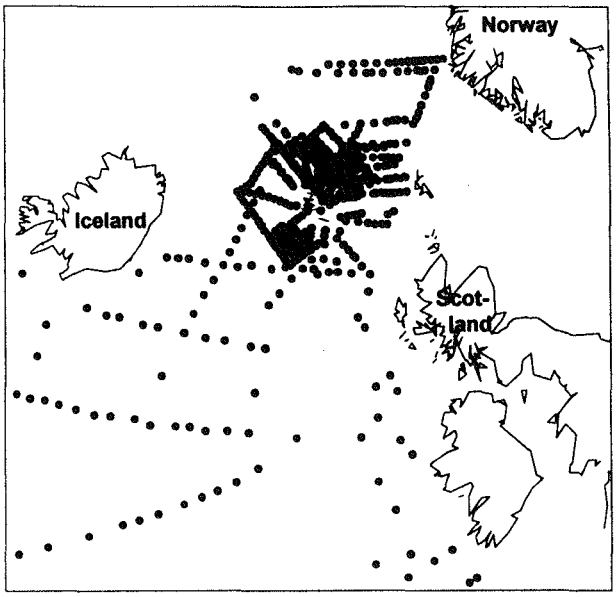

Figure 1. Hydrographic stations in the Iceland-Scotland area occupied during the NANSEN Project 1986–1989 as reported to the ICES Oceanographic Data Centre.

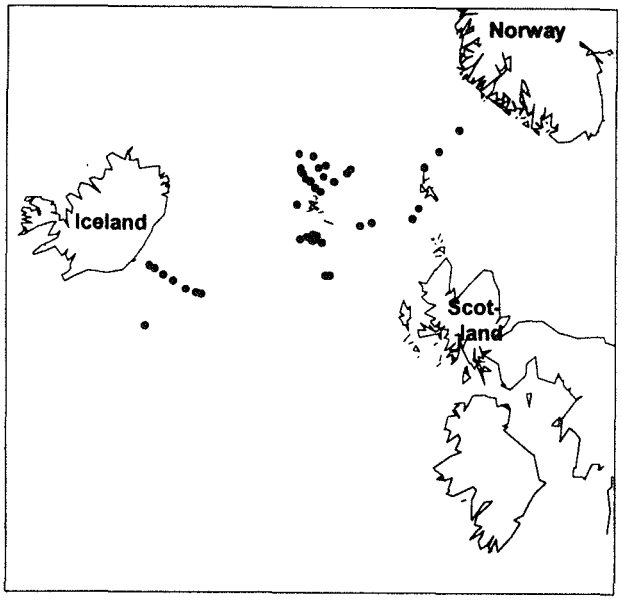

Figure 2. Positions of current meters moored in the Iceland-Scotland area during the NANSEN Project 1986 – 1989 as reported to BODC.

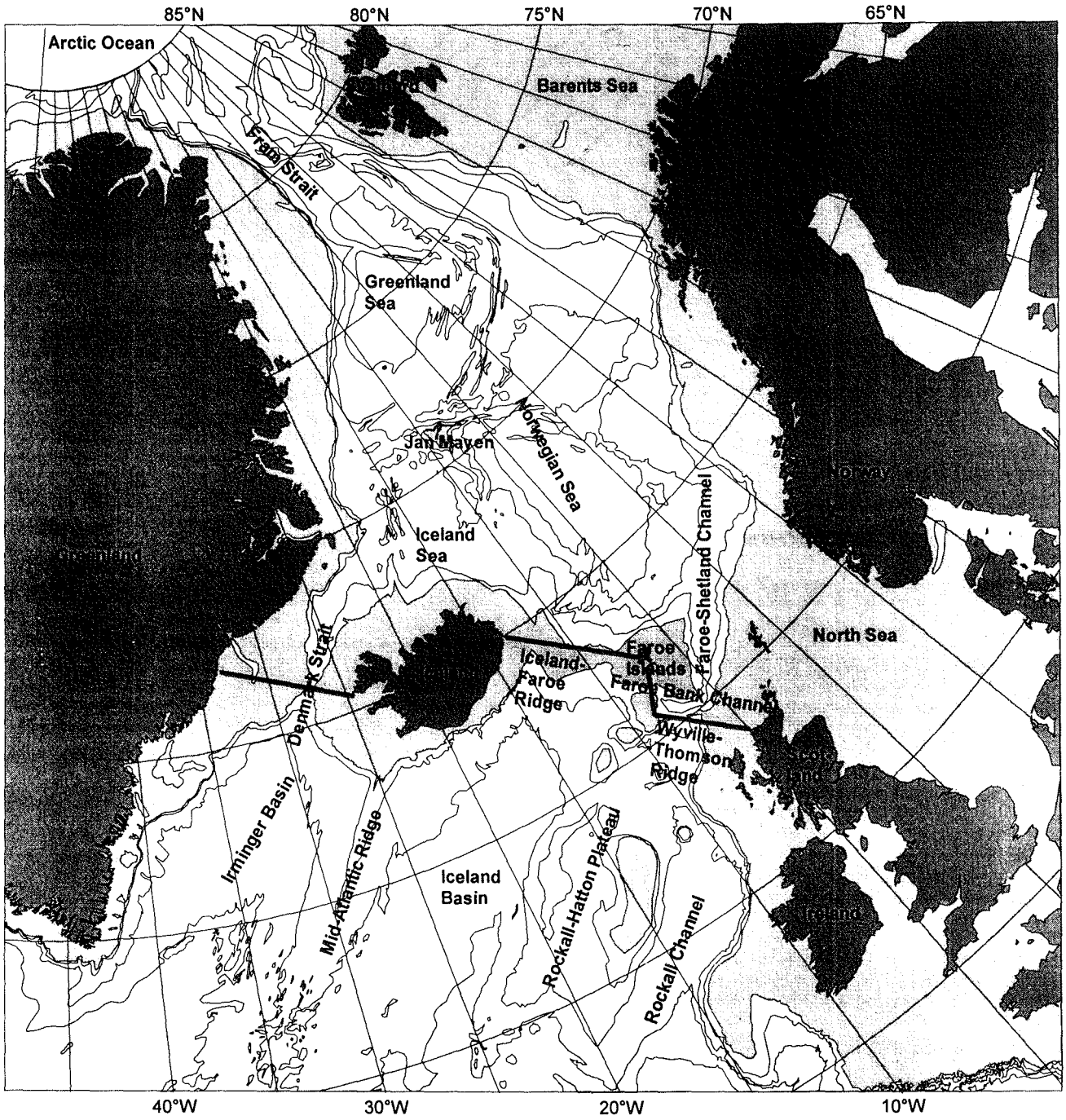

Figure 3. Bathymetry of the Greenland-Scotland region. Thick line following the Greenland-Scotland Ridge indicates location of section shown in Figure 4.

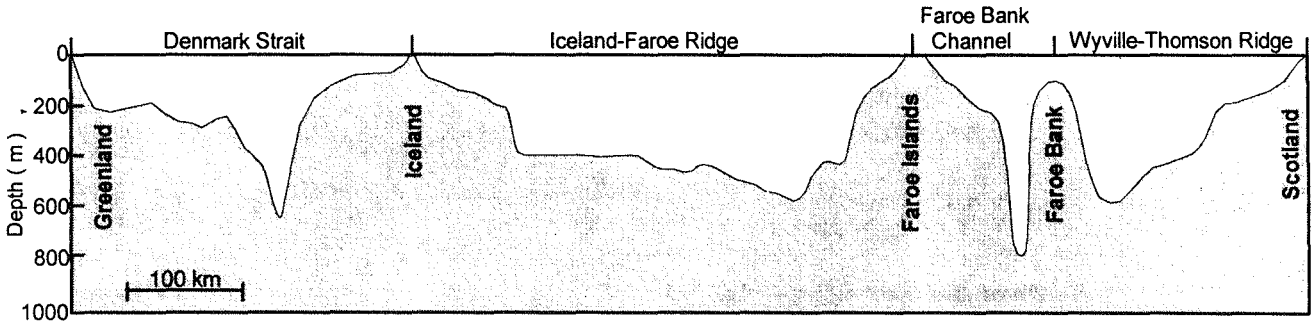

Figure 4. Bottom depth along the oceanic part of a section following the crest of the Greenland-Scotland Ridge. Section location shown on Figure 3.

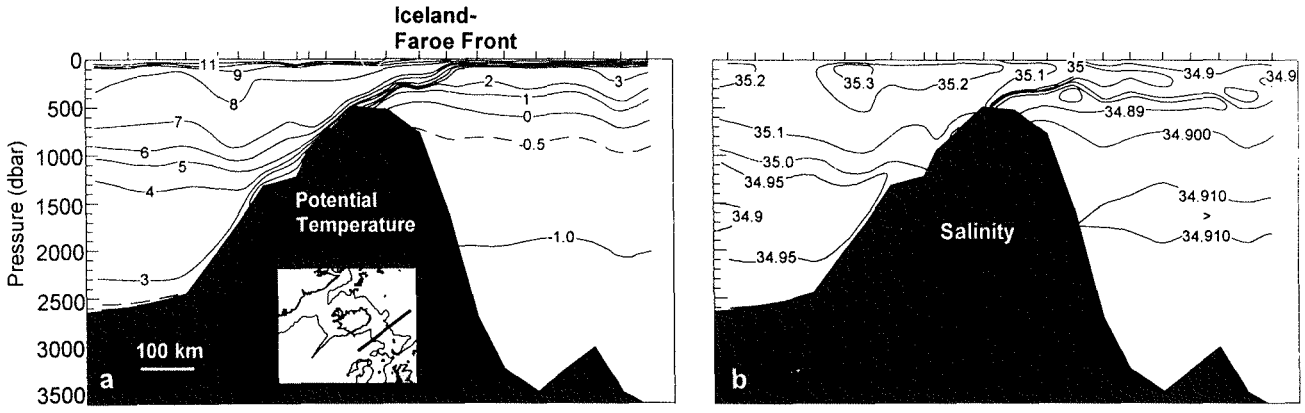

Figure 5. Potential temperature (a) and salinity (b) on a vertical section crossing the Iceland-Faroe Ridge. From R/V Johan Hjort Nordic WOCE cruise 1994 (From Fogelquist *et al.*, 1998). Section location is shown on inset map.

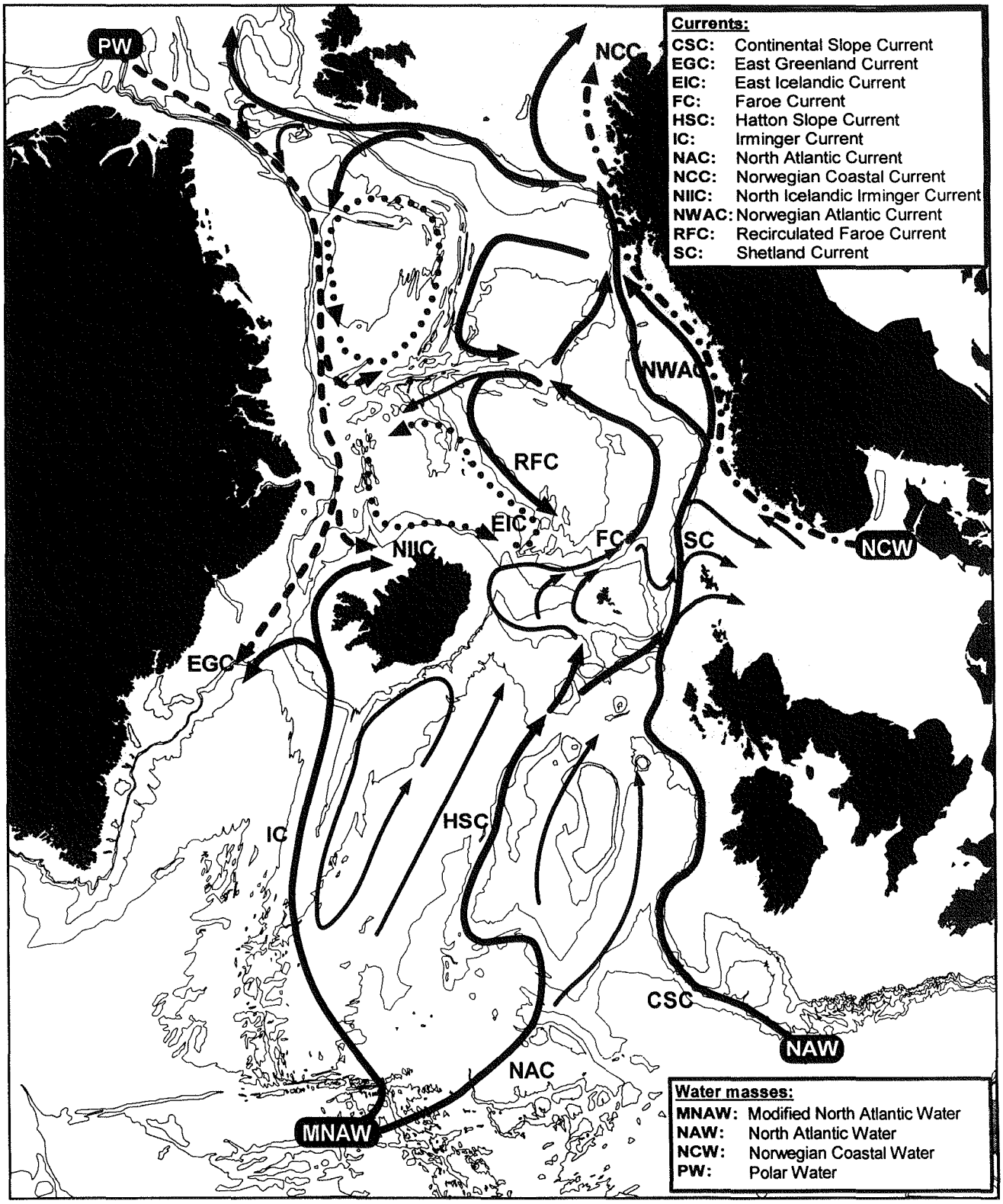

Figure 6. Main features of the upper-layer circulation in the eastern North Atlantic and the Nordic Seas. Continuous arrow show Atlantic water flow. Broken and dotted arrows indicate flow of other water masses. Water masses transported by the main current branches are indicated.

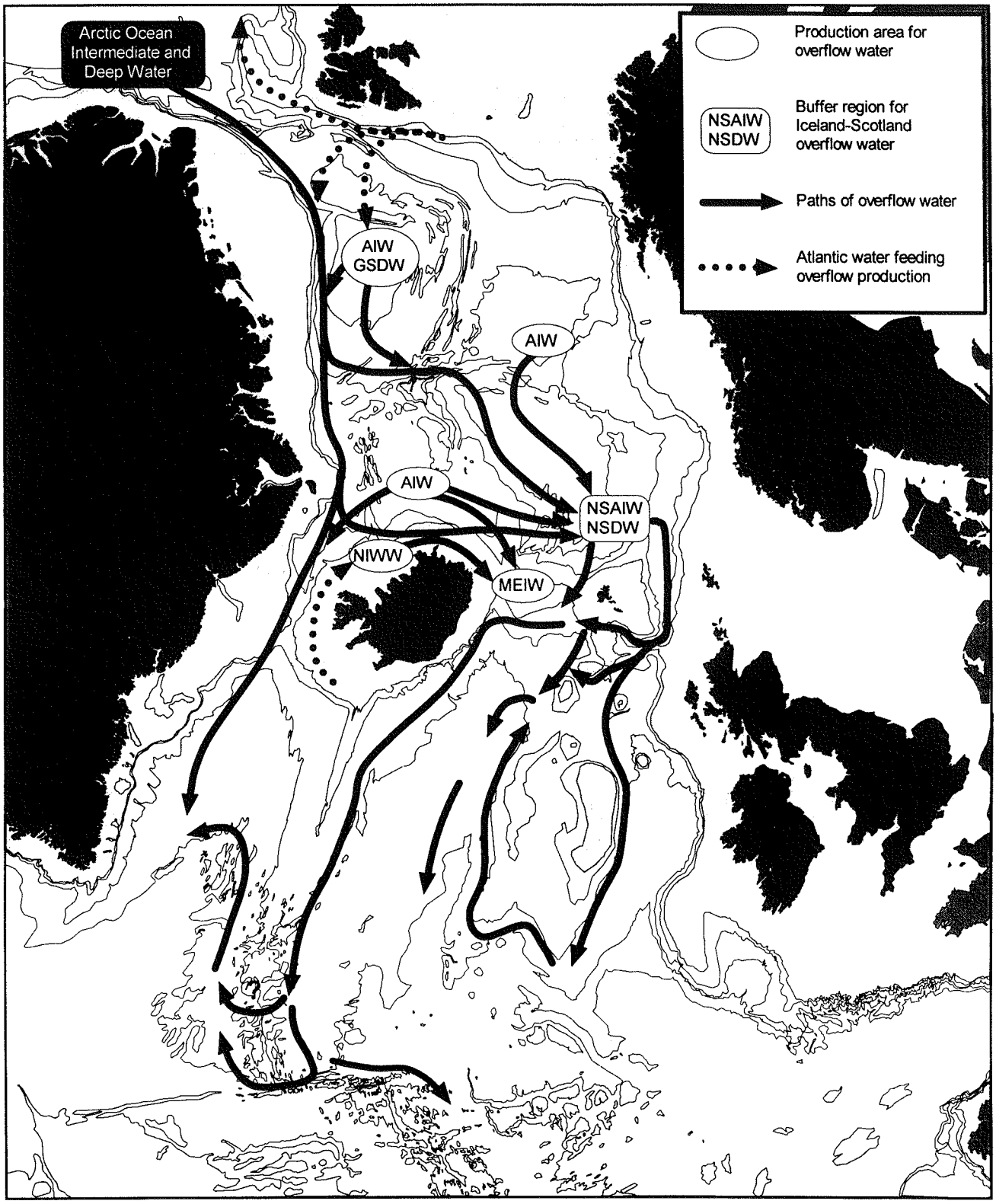

Figure 7. General location of main overflow sites and paths of the overflow through the eastern North Atlantic.

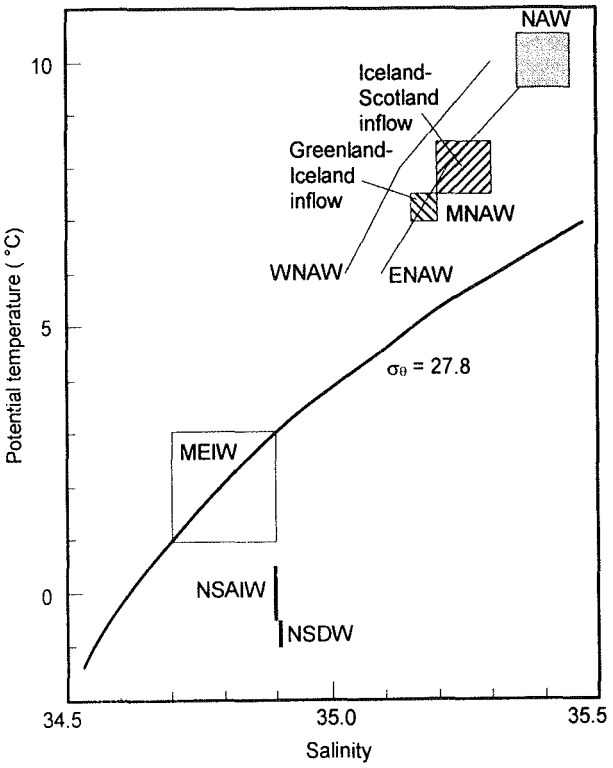

Figure 8. Potential temperature and salinity ranges of the main water masses exchanged across the Greenland-Scotland Ridge. For MNAW, the inflow between Greenland and Iceland is somewhat colder and fresher than the Iceland-Scotland inflow. The traces defining WNAW and ENAW are those discussed by Harvey (1982). The σ_θ=27.8 line is often used to define overflow water in the Atlantic.

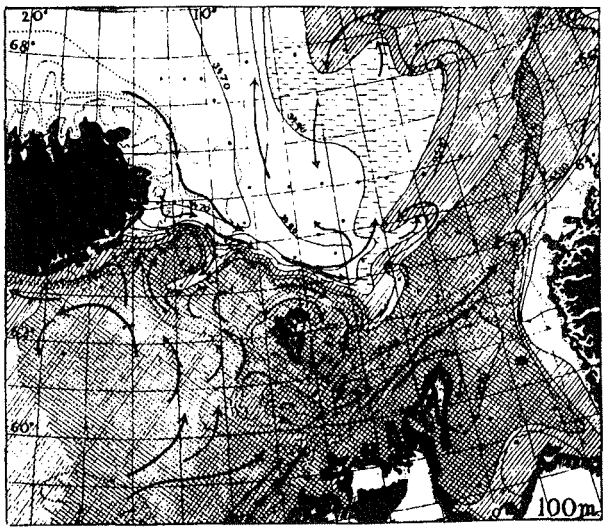

Figure 9. Main circulation pattern and horizontal salinity distribution at 100 depth in May 1904 according to Helland-Hansen and Nansen (1909).

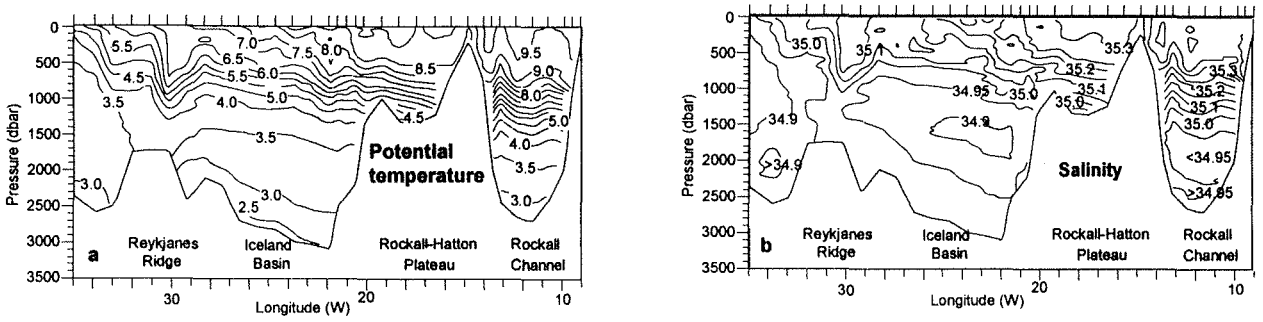

Figure 10. Potential temperature (a) and salinity (b) on a section from the Rockall Channel to the Irminger Basin (location on Figure 14) by R/V Tyro in April 1991. Adapted from van Aken and Becker (1996).

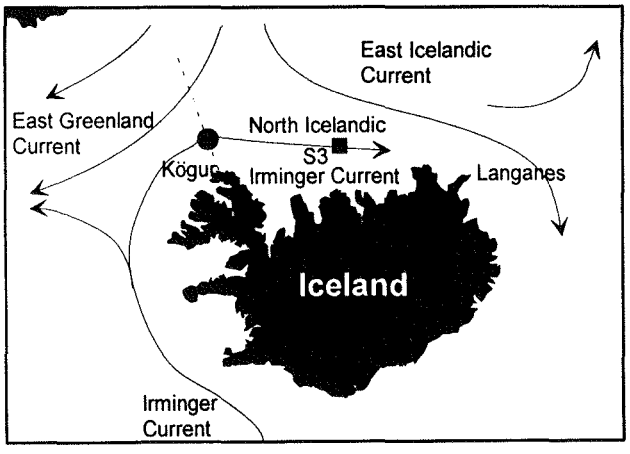

Figure 11. The path of the North Icelandic Irminger Current and its encounter with the flows from the north (arrows). The Kögur standard section is shown as a dotted line. The filled circle on the section shows a long-term mooring site. The black square shows location of standard station S3. Adapted from Kristmansson (1998, this volume).

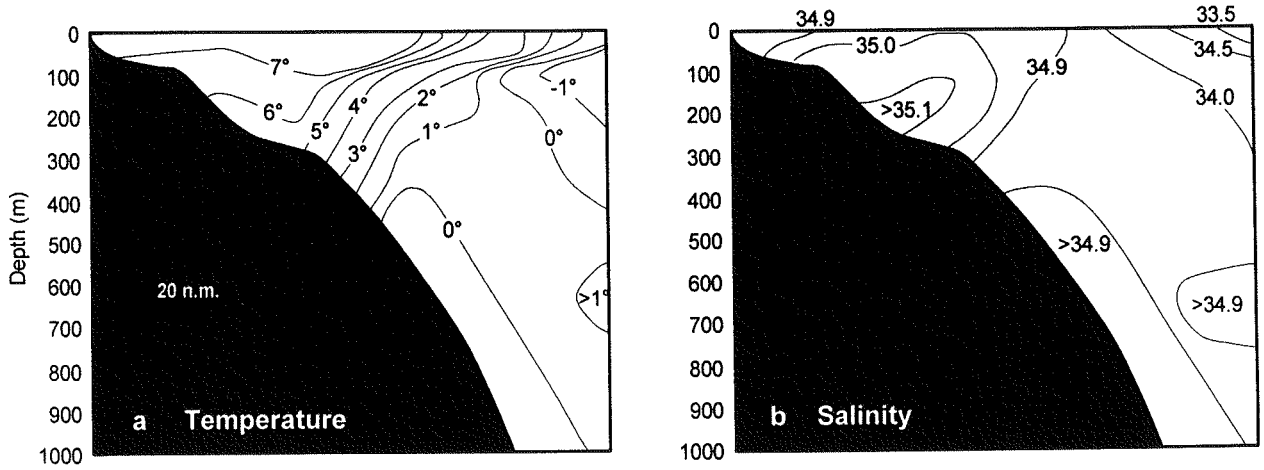

Figure 12. Temperature (a) and salinity (b) along the Kögur section (Figure 11) on 30 – 31 July 1950. Adapted from Stefánsson (1962).

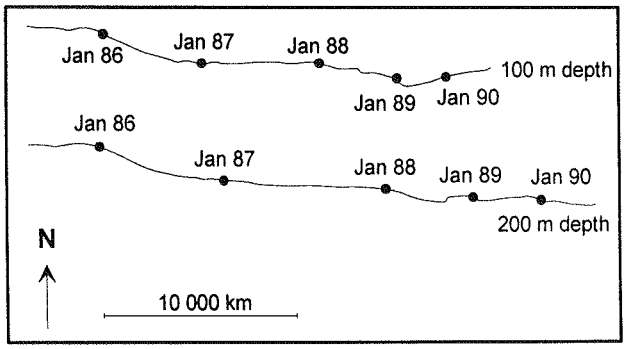

Figure 13. Progressive vector diagrams for current at 100 and 200 m depth on mooring located in the North Icelandic Irminger Current (black circle on Figure 11, at a bottom depth of 250 m). Adapted from Kristmansson (1998, this volume).

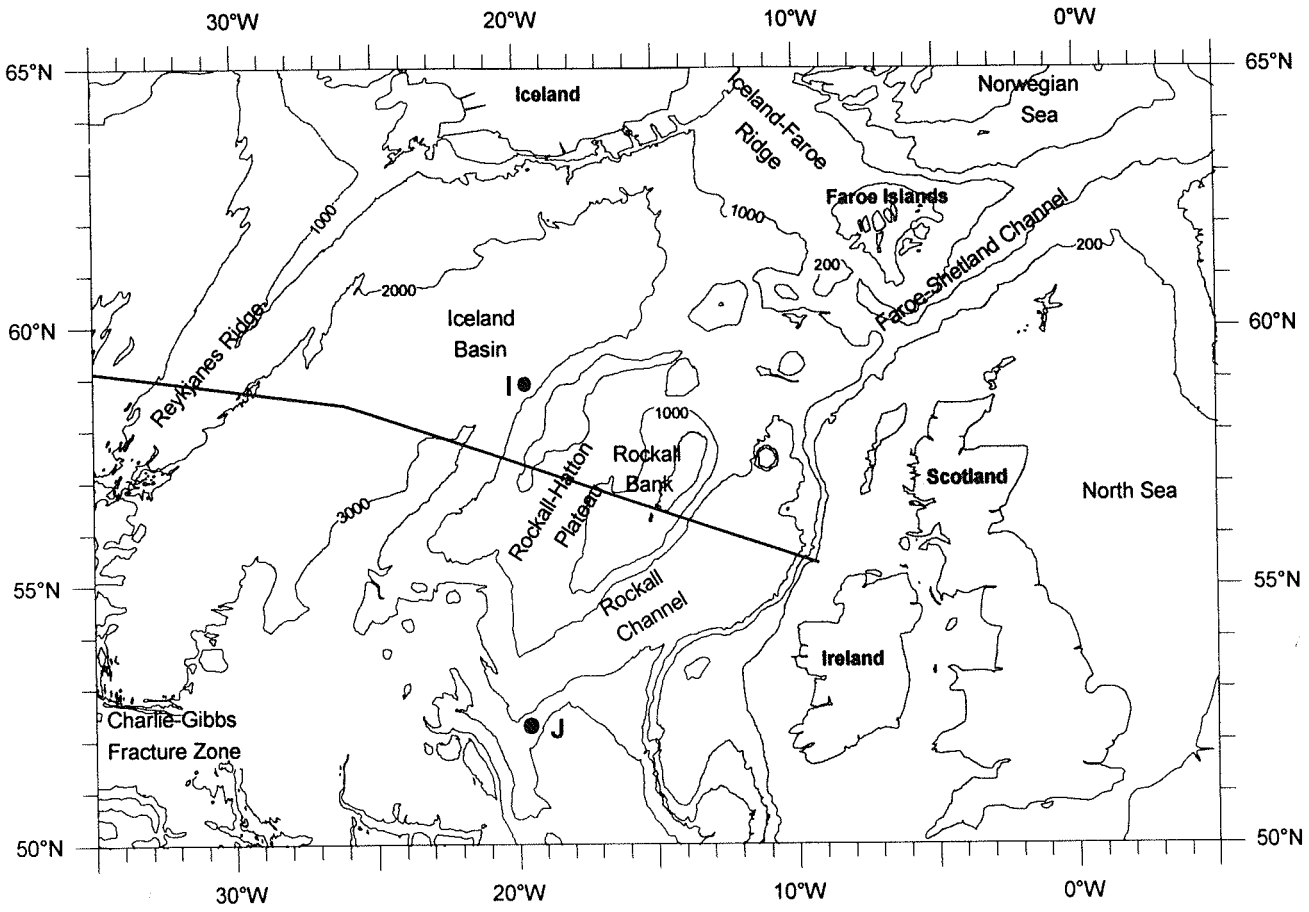

Figure 14. Bottom topography of the region southwest of the Iceland-Scotland Gap. Location of two Ocean Weather Stations is shown. Thick line shows section referred to in Figure 10.

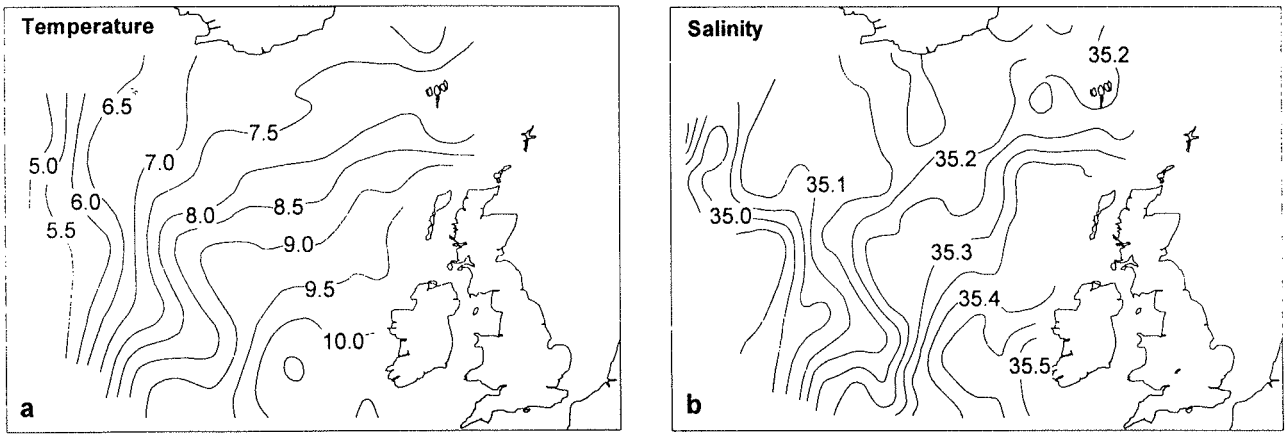

Figure 15. Lateral distribution of hydrographic properties in the core of the Sub Polar Mode Water, characterized by the sub-surface potential vorticity minimum; (a) potential temperature, (b) salinity. Adapted from van Aken and Becker (1996).

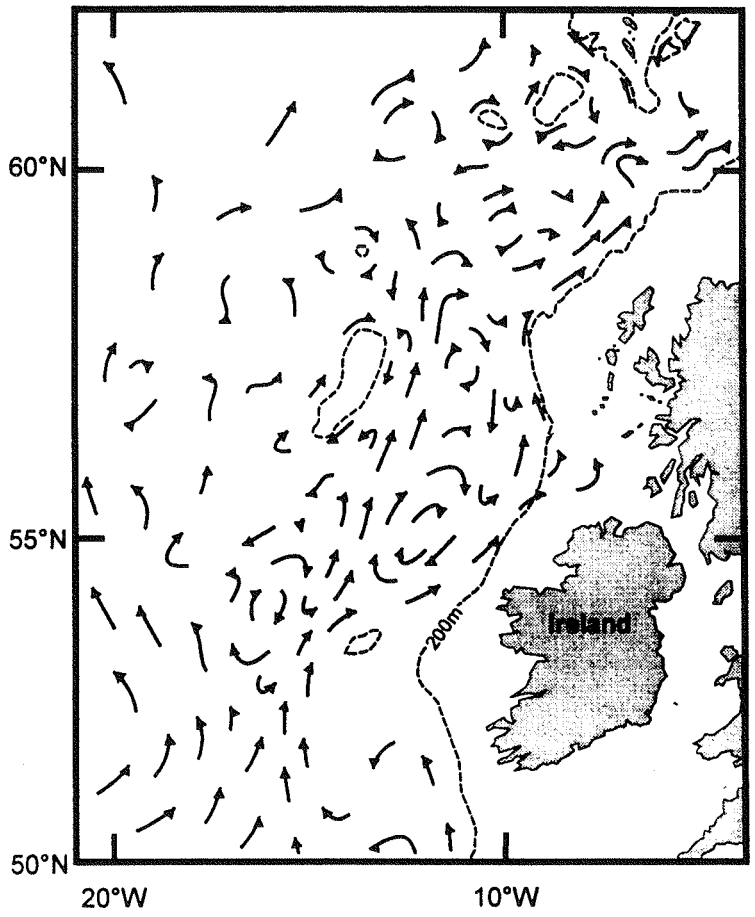

Figure 16. The circulation of the Rockall Channel according to Ellett *et al.* (1986).

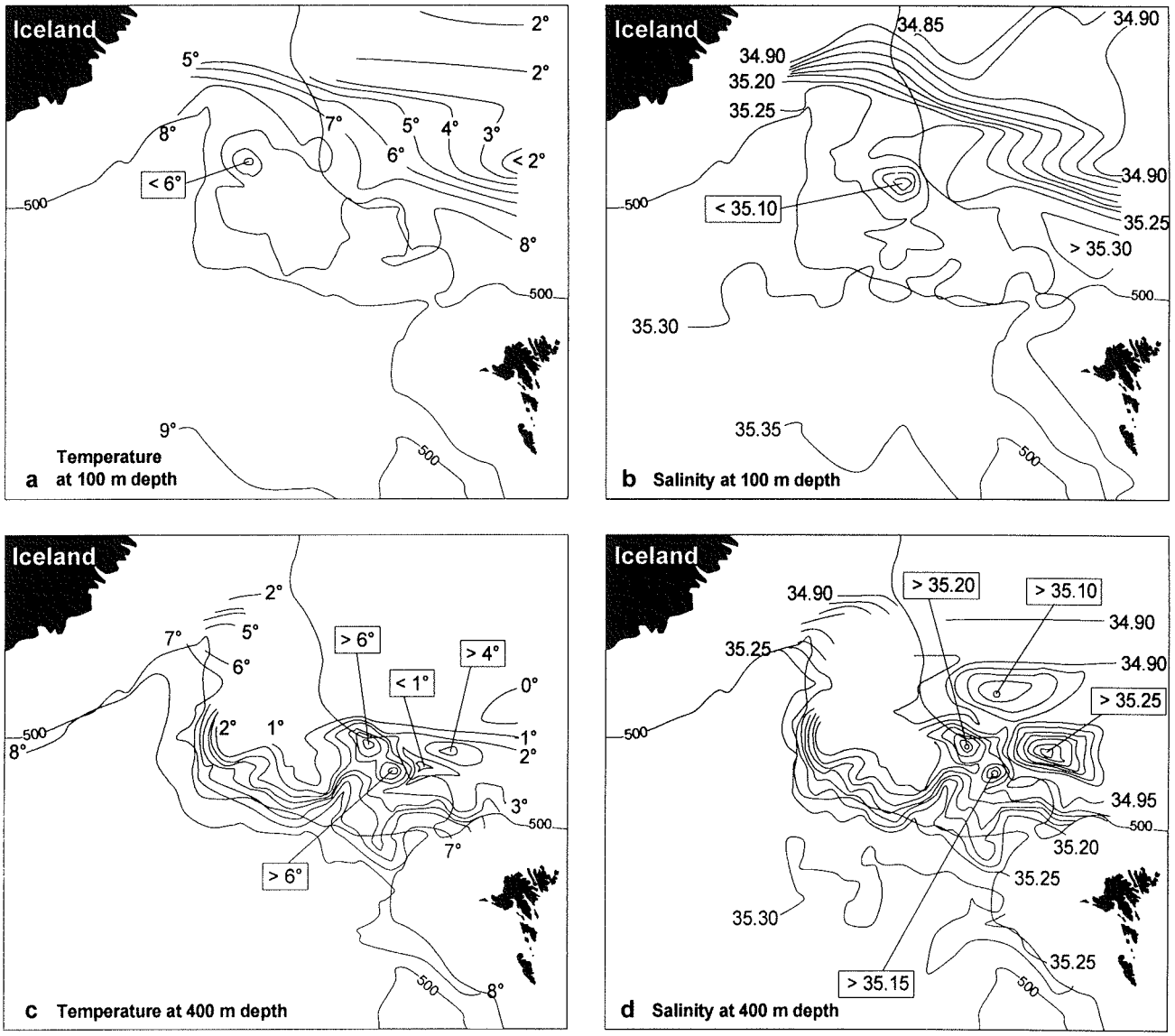

Figure 17. Horizontal temperature and salinity distribution at two depth levels over the Iceland-Faroe Ridge in May-June 1960 based on the first survey of the international multiship Overflow '60 expedition. Adapted from Tait *et al.* (1967).

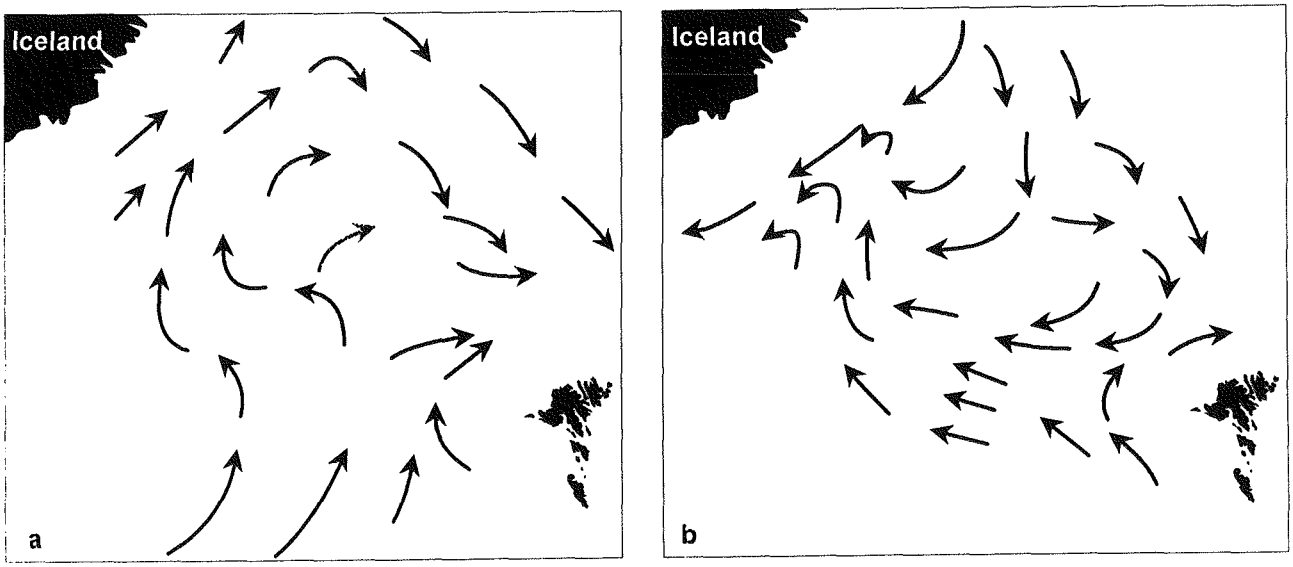

Figure 18. Near-surface (a) and bottom (b) currents over the Iceland-Faroe Ridge according to Meincke (1983).

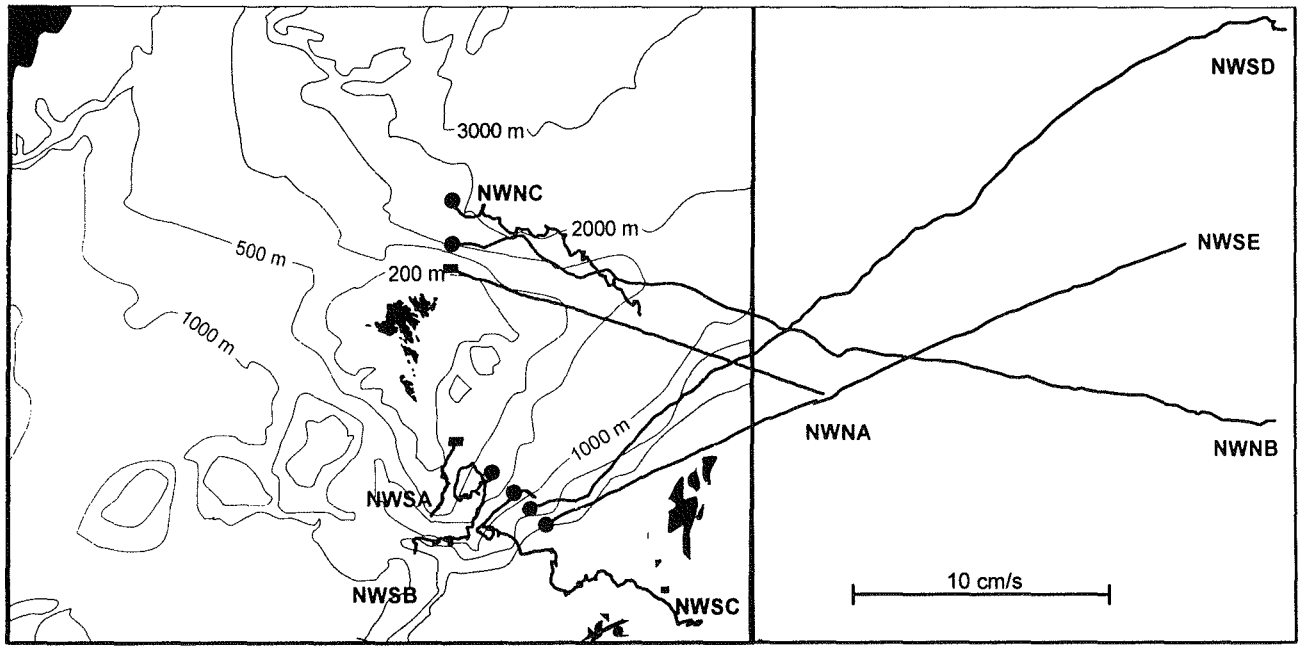

Figure 19. Progressive vector diagrams for currents at approximately 200 m depth based on preliminary results from the Nordic WOCE ADCP mooring programme (Hansen *et al.*, 1998). The observations are from different periods and have different length, but have been adjusted so that the length of each trace reflects velocity in a relative manner.

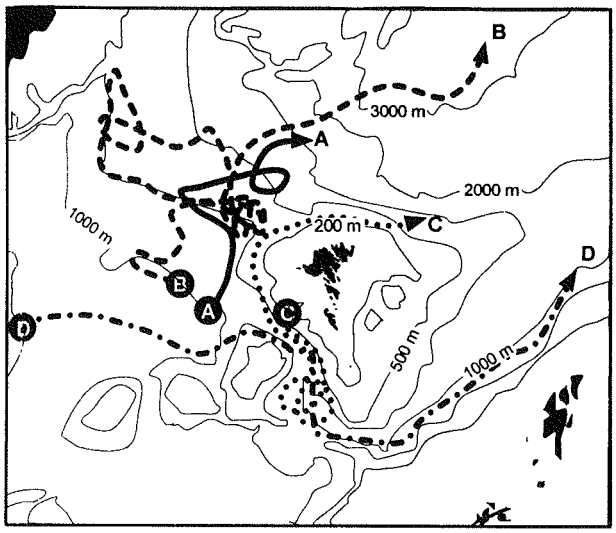

Figure 20. Simplified tracks of four drifters crossing the Iceland-Scotland Gap. Based on Hansen *et al.* (1998, this volume) and Krauss (1995).

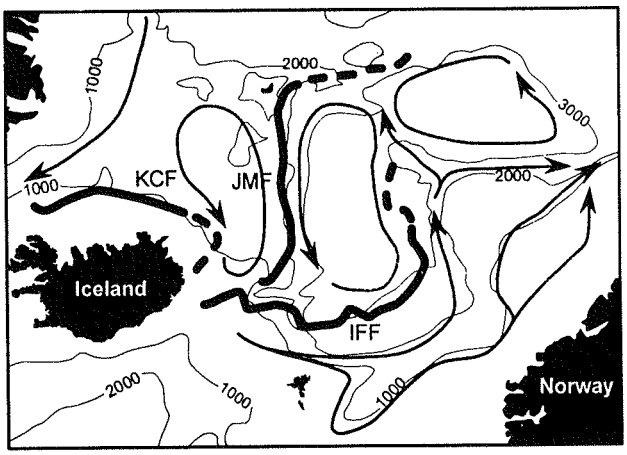

Figure 21. Typical location of surface fronts (thick lines) and main currents (arrows) in the area northeast of the Iceland-Faroe Ridge. KCF: Kolbeinsey Current Front. JMF: Jan Mayen Front. IFF: Iceland-Faroe Front.. Mainly based on Smart (1984) and Poulain *et al.* (1996).

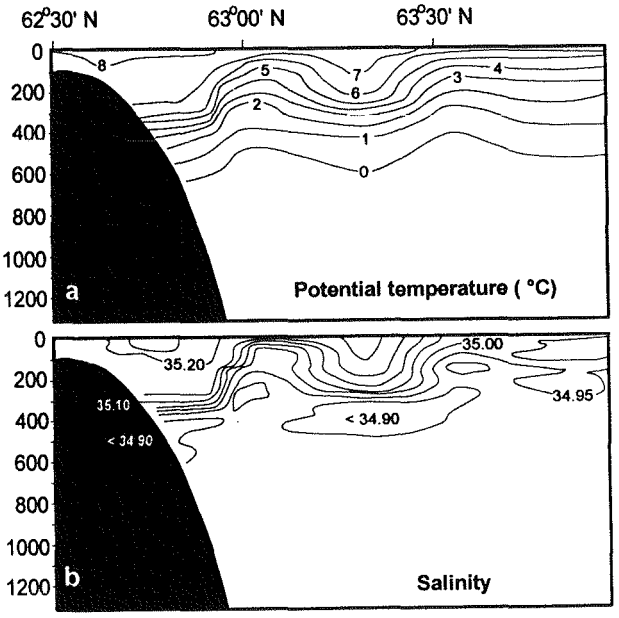

Figure 22. Potential temperature (a) and salinity (b) on a vertical section (section N on Figure 28) north from the Faroes in June 1986, obtained by R/V Haakon Mosby. From Hansen *et al.*, 1998, this volume.

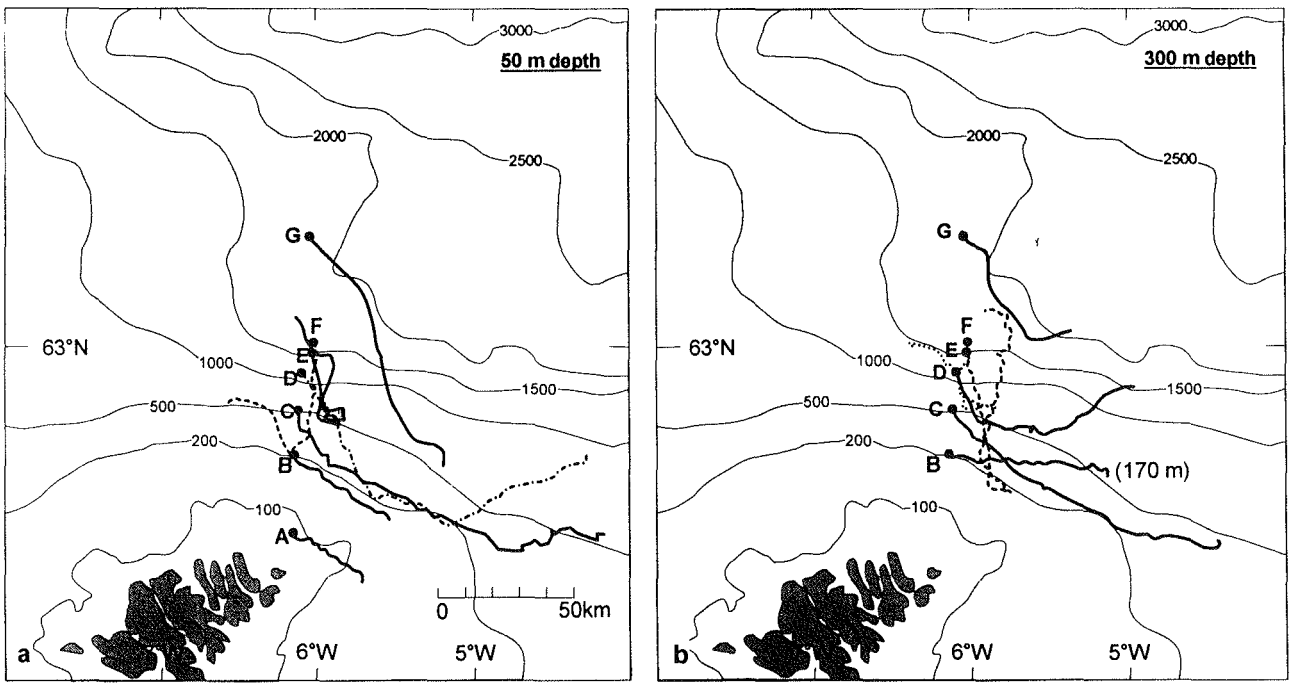

Figure 23. Location of current meter moorings and progressive vector diagrams at the 50 m level and deeper (300 m at all sites except at B where the deeper current meter was at 170 m depth) north of the Faroes in a 10 day period in June 1986. Adapted from Hansen *et al.*, 1998, this volume.

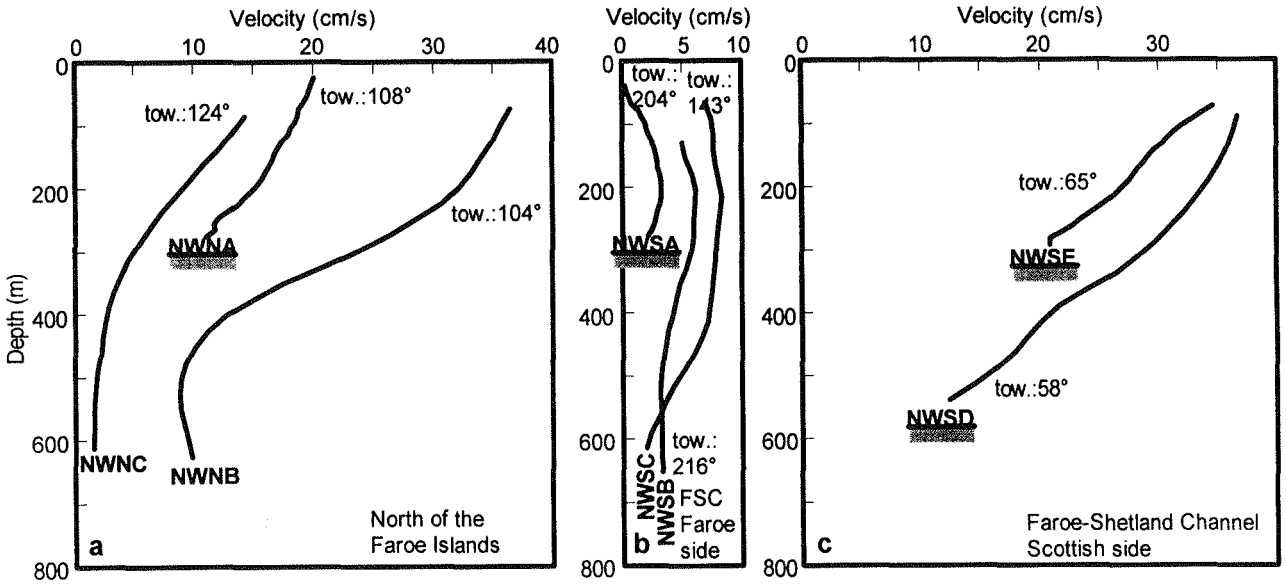

Figure 24. Vectorially averaged velocity profiles for selected Nordic WOCE deployments. Current velocities have been projected on directions following the bottom topography and shown for each profile. For sites shallower than 800 m, the bottom depth is indicated.

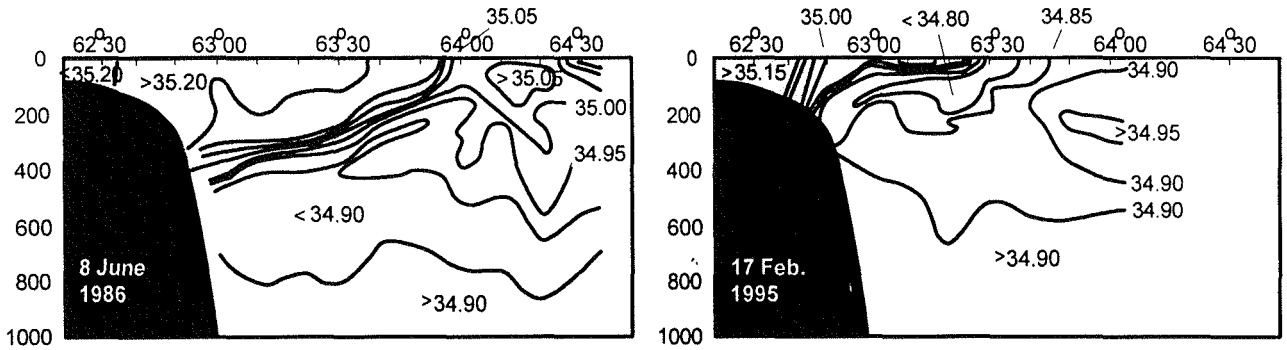

Figure 25. Salinity on a vertical section along 6°W (section N on Figure 28) at two different occasions.

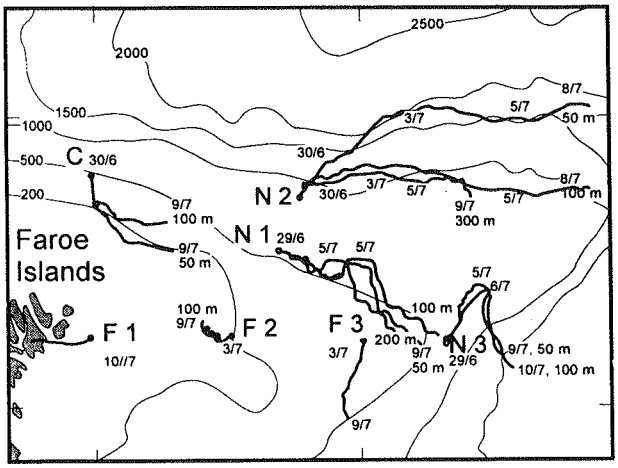

Figure 26. Mooring sites and progressive vector diagrams from current meters located in Atlantic water in June-July 1987. Numbers show observational depths and dates. Adapted from Hansen *et al.* (1998, this volume).

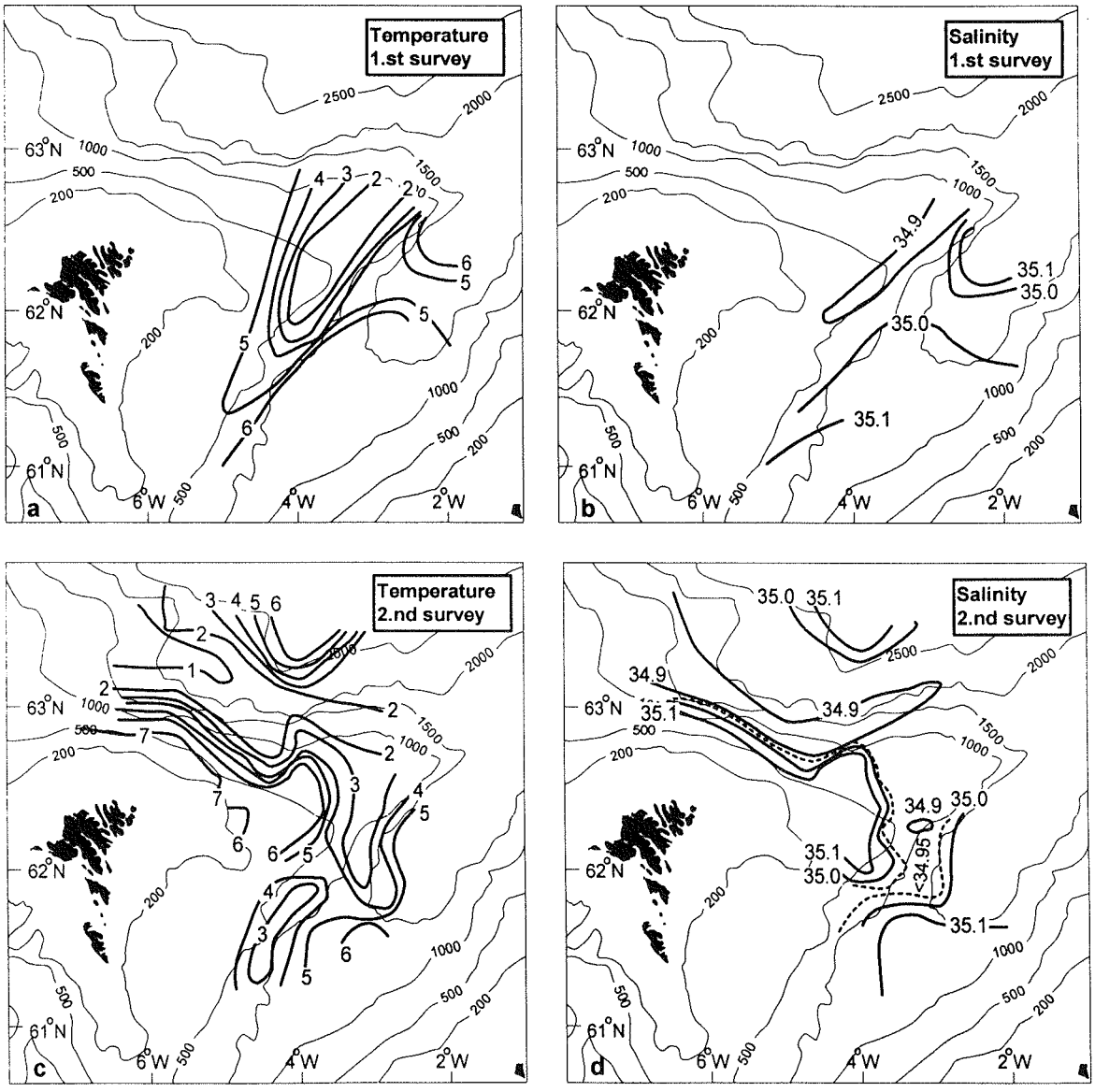

Figure 27. Temperature and salinity at 300 m depth east of the Faroes in the period 27 June to 1 July (a, b, 1.st survey) and 5 July to 13 July (c, d, 2.nd survey) 1987. From Hansen *et al.* (1998, this volume).

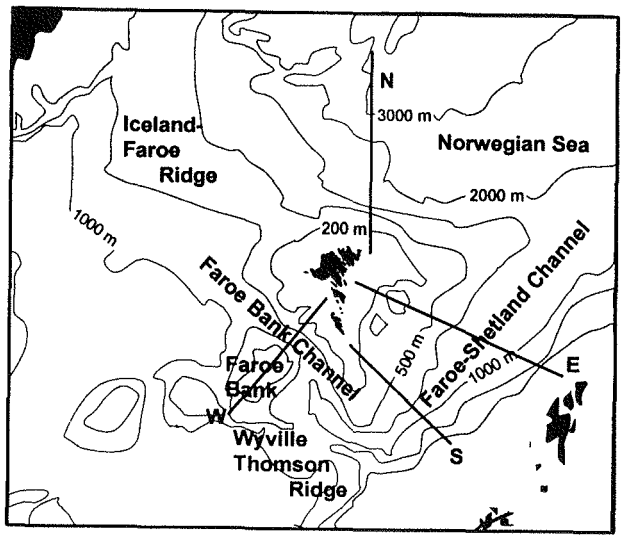

Figure 28. Bottom topography in the Iceland-Shetland region. Lines show tracks of standard sections in the area.

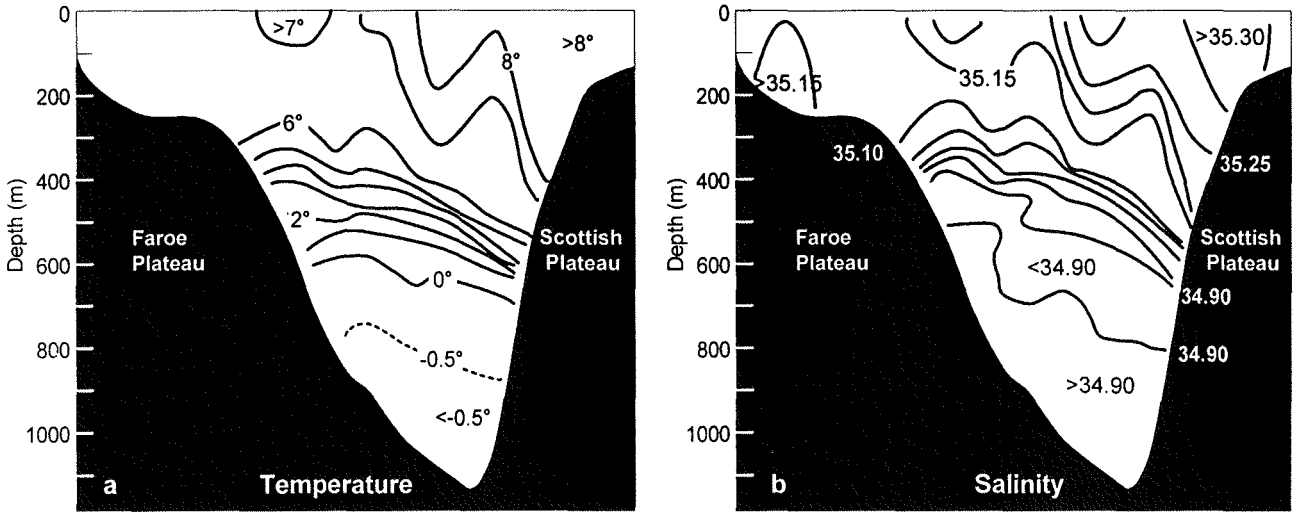

Figure 29. Temperature (a) and salinity (b) on a section (section S on Figure 28) across the Faroe-Shetland Channel in February 1995.

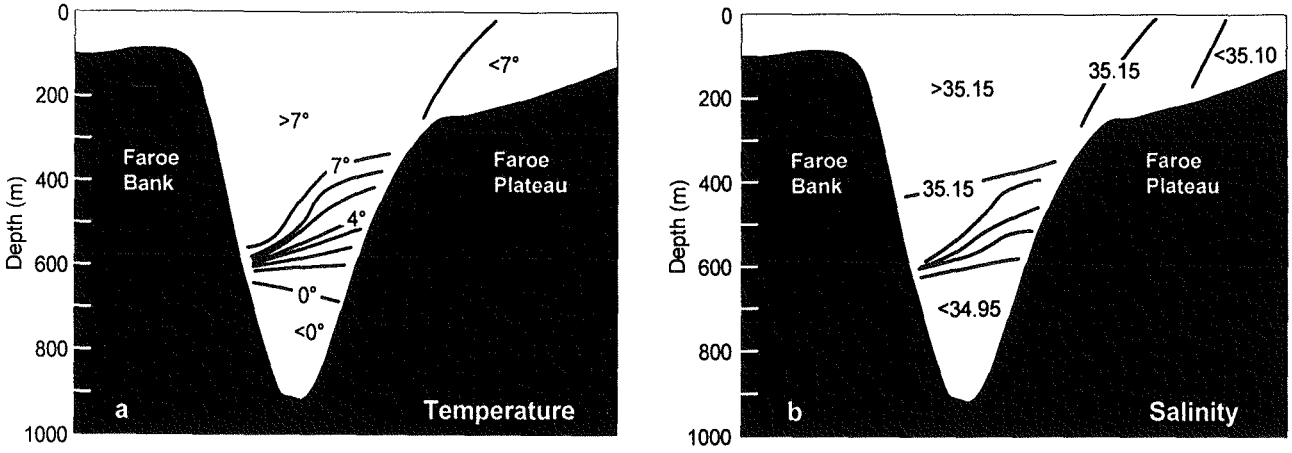

Figure 30. Temperature (a) and salinity (b) on a section (section W on Figure 28) across the Faroe Bank Channel in February 1993.

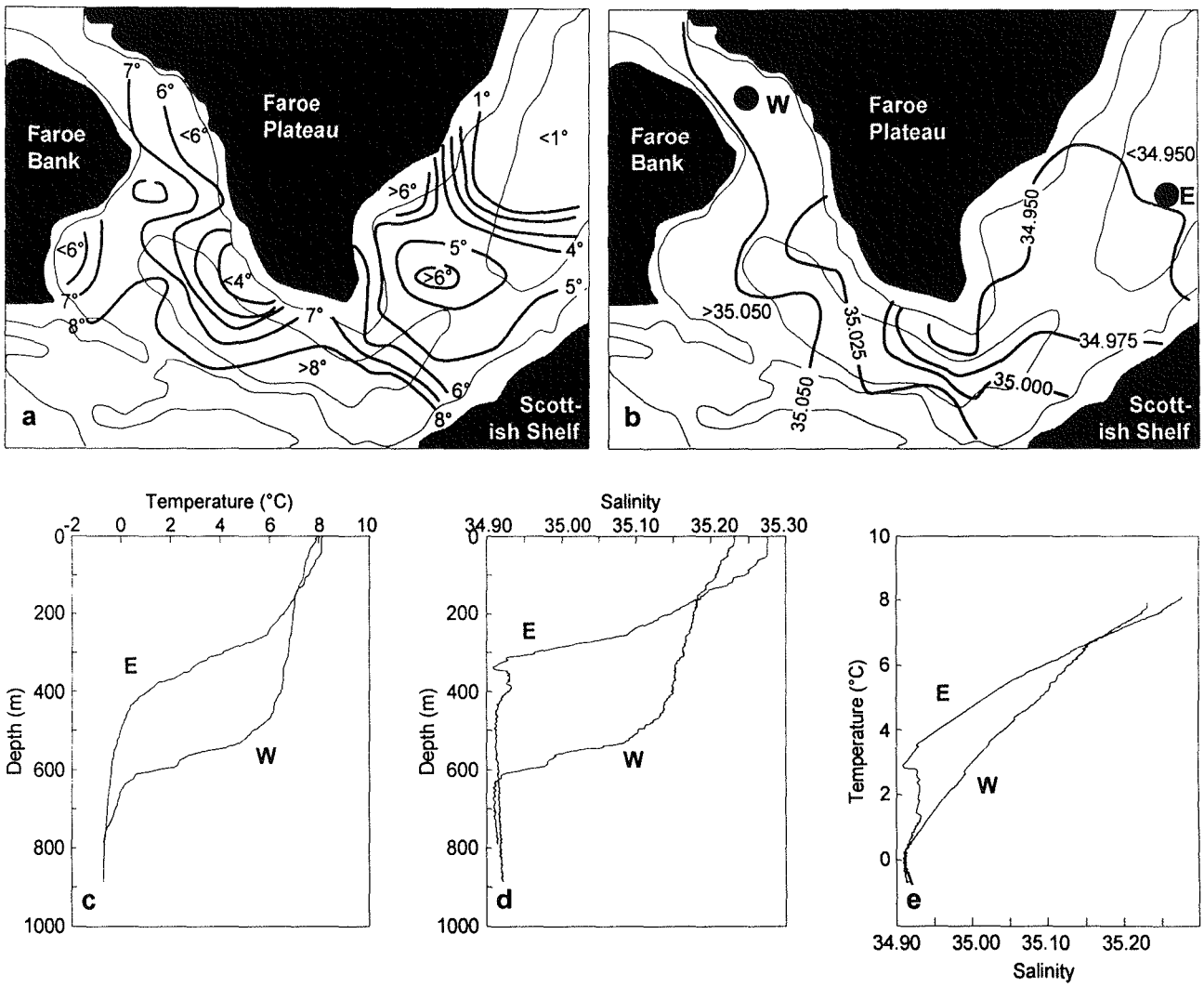

Figure 31. Temperature (a) and salinity (b) at 300 m depth in the Faroese Channels, profiles of temperature (c), salinity (d) and TS diagram (e) at two locations (E and W) shown in (b) from the R/V Magnus Heinason April-May 1989 NANSEN cruise.

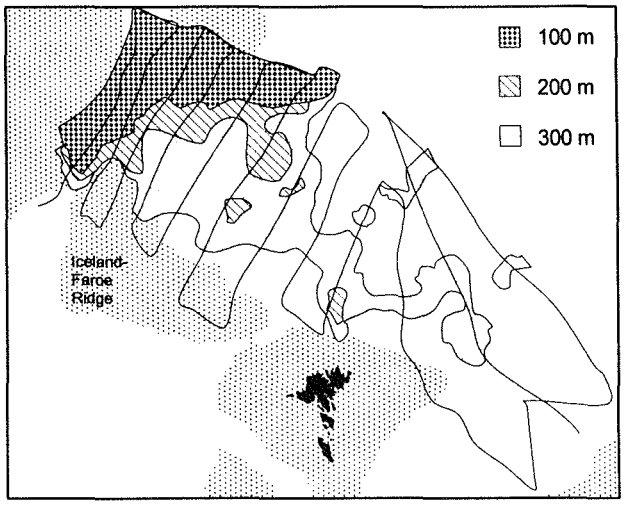

Figure 36. Spreading of water colder than 2°C over the Iceland-Faroe Ridge. Areas where bottom depth is less than 500m are dotted. Areas with hatching indicate the extension of water colder than 2°C at depths of 100m, 200m and 300m. Cruise track of the vessel is also shown. Adapted from Read and Pollard (1992).

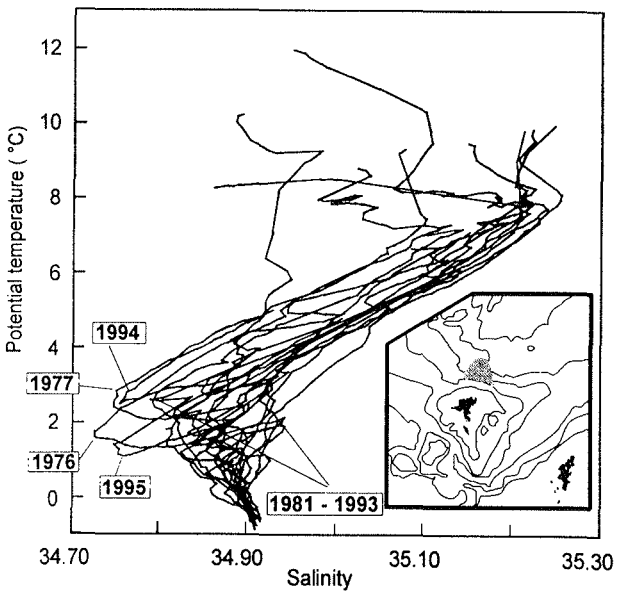

Figure 37. θ-S diagrams from CTD stations north of the Faroes (region shown as hatched area on inserted map) in the May-August period 1976-77 and 1981–1995, one trace for each year.

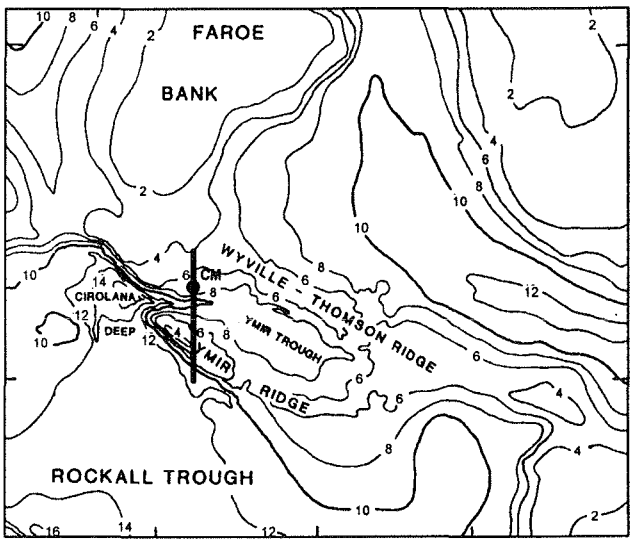

Figure 42. Bottom topography of the Wyville Thomson Ridge. The section in Figure 43 is shown as well as a current meter mooring, discussed in the text (circle marked "CM").

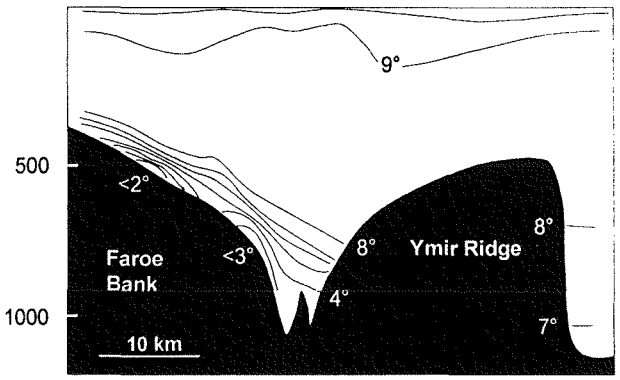

Figure 43. CTD section west of the Wyville Thomson Ridge (location shown in Figure 42) acquired in June 1988. Based on Ellett (1998, this volume).

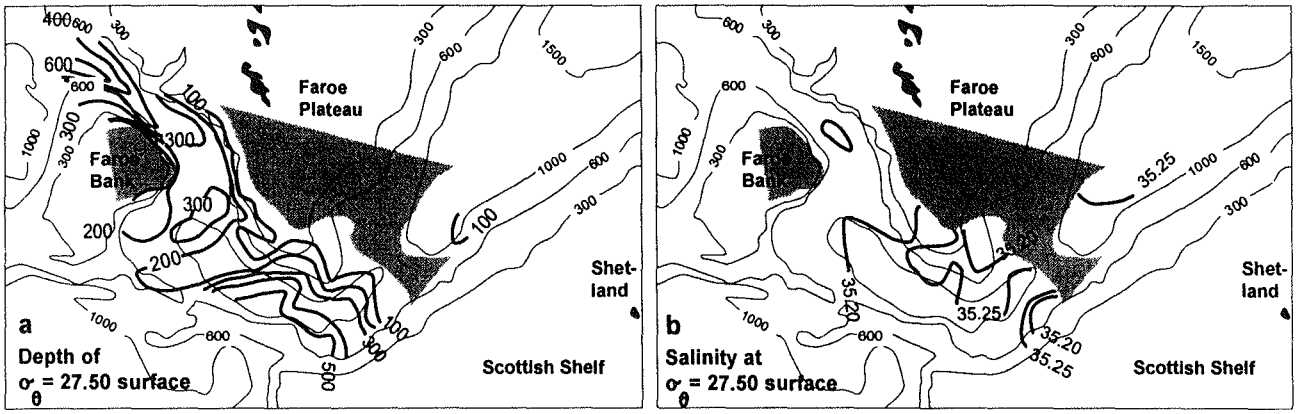

Figure 32. Depth (in m) of the σ_θ=27.5 surface (a) and salinity on this surface (b) in the Faroese Channels during the R/V Magnus Heinason April-May 1987 NANSEN cruise. Hatching indicates areas where σ_θ>27.5 throughout the water column. Adapted from Becker and Hansen (1998, this volume).

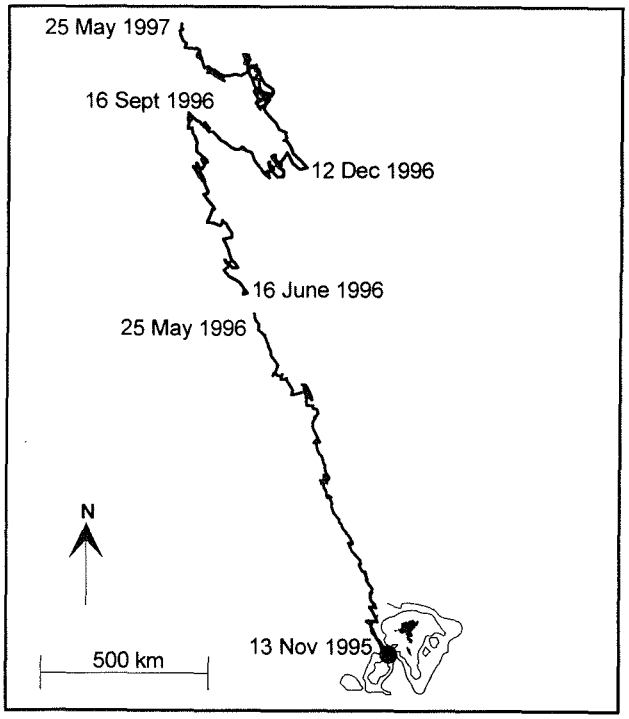

Figure 33. Progressive vector diagram for the current at approximately 220 m depth in the Faroe Bank Channel, based on preliminary results from the Nordic WOCE ADCP mooring programme.

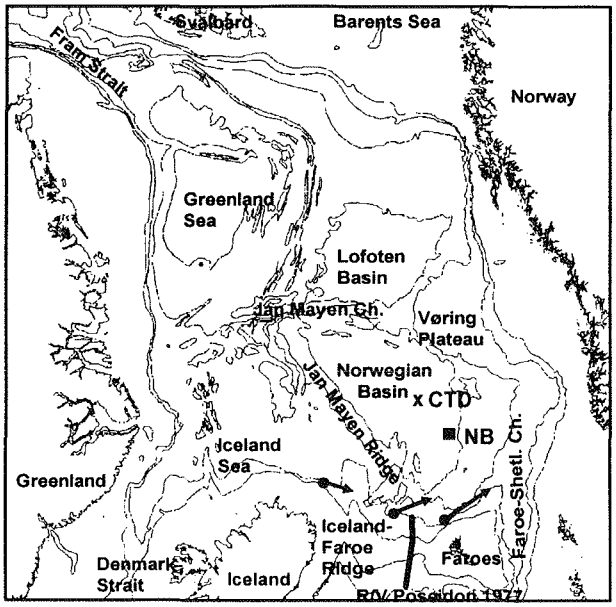

Figure 34. Bottom topography of the Nordic Seas showing the major basins and some important topographical features. Arrows indicate residual flow direction at three moorings, discussed by Hopkins *et al.* (1992) as referred to in the text. The "x" marked "CTD" shows stations occupied by R/V Hudson in 1982 and by R/V Håkon Mosby in 1994, referred to in Figure 39. The black square marked "NB" shows a CTD station occupied by R/V Magnus Heinason in 1996, referred to in Figure 40. The section taken by R/V Poseidon in 1977 across the Iceland-Faroe Ridge is shown in Figure 35.

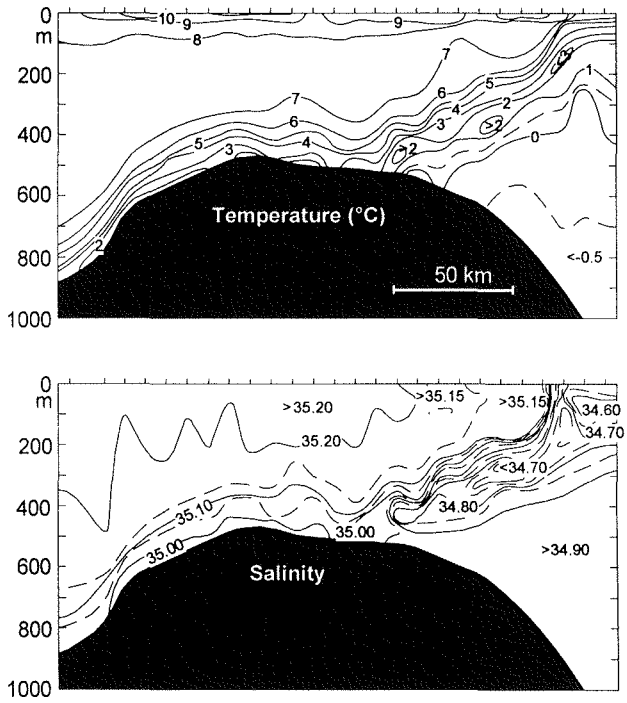

Figure 35. Temperature (a) and salinity (b) on a section crossing the Iceland-Faroe Ridge occupied by R/V Poseidon in 1977 (location shown on Figure 34). Adapted from Meincke (1978).

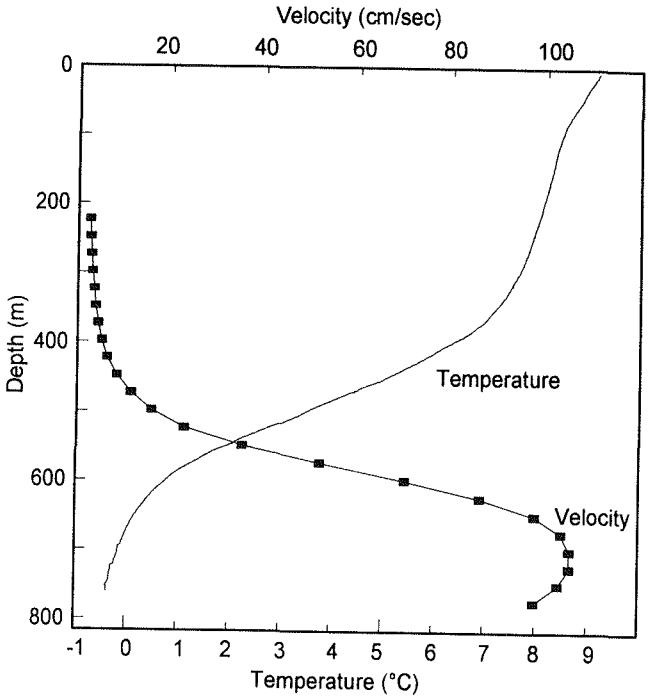

Figure 44. Black rectangles show average velocity profile from Faroe Bank Channel derived from preliminary results from a Nordic WOCE ADCP moored at 61°25.038'N 8°17.366'W in the period 15 June 1996 to 25 May 1997 by vectorial averaging. The depth scale ends at the bottom depth (817 m) of the mooring. Continuous line shows average temperature profile derived from CTD observations at a Faroese standard station at 61°20'N 7°53'W from 1988 to 1997. In the upper layers, 47 CTD observations were included in the average with fewer observations below 700 m depth.

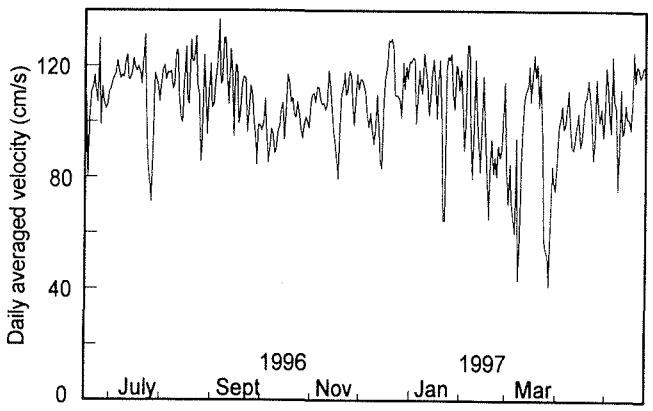

Figure 45. Daily averaged current velocity component towards 304° in a 25 meter layer centered at a depth of 698 m, 119 m above the bottom in the Faroe Bank Channel from June 1996 to may 1997. Based on preliminary results from the Nordic WOCE program.

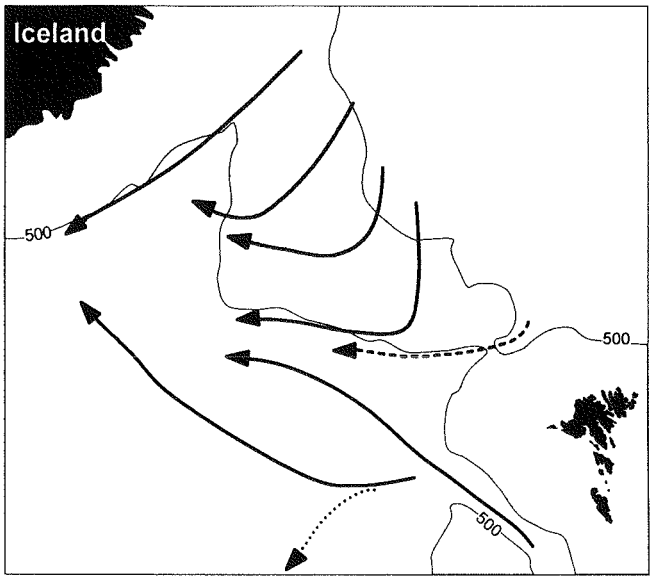

Figure 46. Overflow paths across the Iceland-Faroe Ridge and from the Faroe Bank Channel according to Hermann, 1967 (continuous arrows) and Meincke, 1983 (broken arrow). Dotted arrow indicates alternative path, discussed in text.

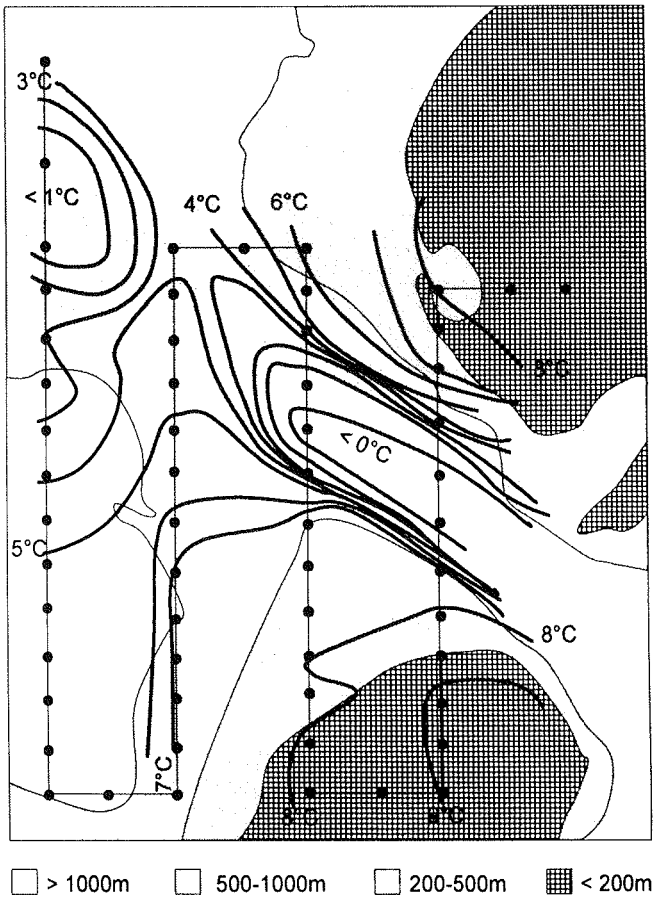

Figure 47. Temperature 50 m above bottom outside the Faroe Bank Channel as observed by R/V Magnus Heinason in July 1987. Cruise track is shown as a continuous line with CTD stations as black circles. From Hansen and Kristiansen (in press)

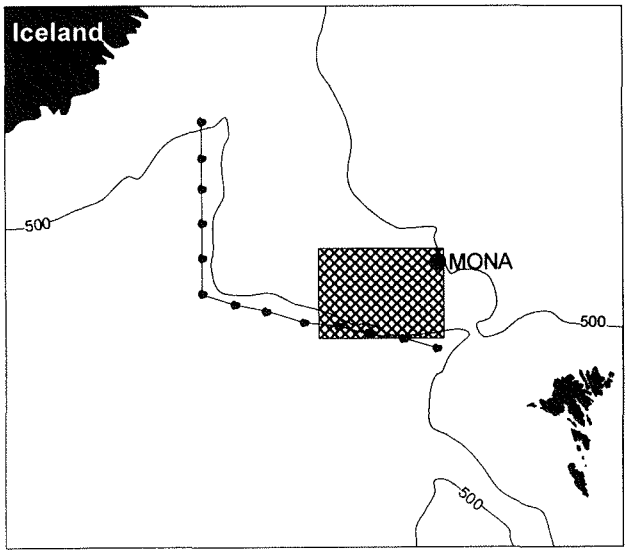

Figure 48. Black circles connected by line indicate a hydrographic section west of the Iceland-Faroe Ridge (Meincke, 1972) discussed in Figure 49. Large black circle indicates position of a mooring deployed during the MONA project. Hatched rectangle indicates area depicted in Figure 50.

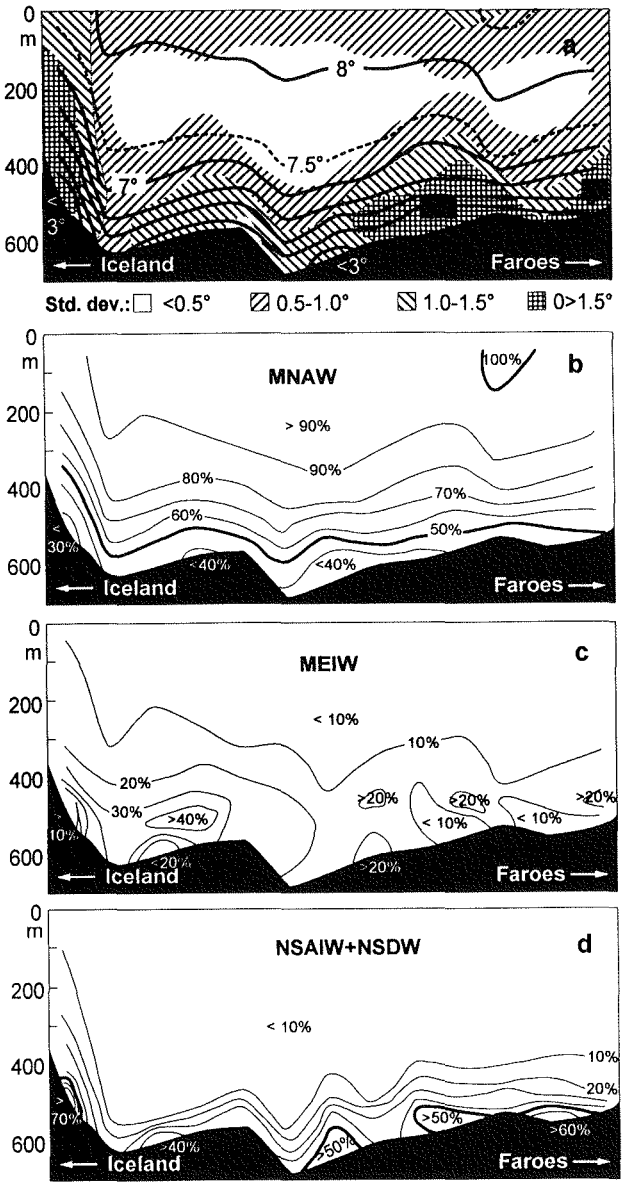

Figure 49. Average temperature and water mass composition along section shown in Figure 48 based on Meincke (1972). a: Average temperature is shown by isotherms, standard deviation of temperature indicated by hatching. b: Average content of Modified North Atlantic Water. c: Average content of Modified East Icelandic Water. d: Average content of Norwegian Sea Arctic Intermediate Water and Norwegian Sea Deep Water.

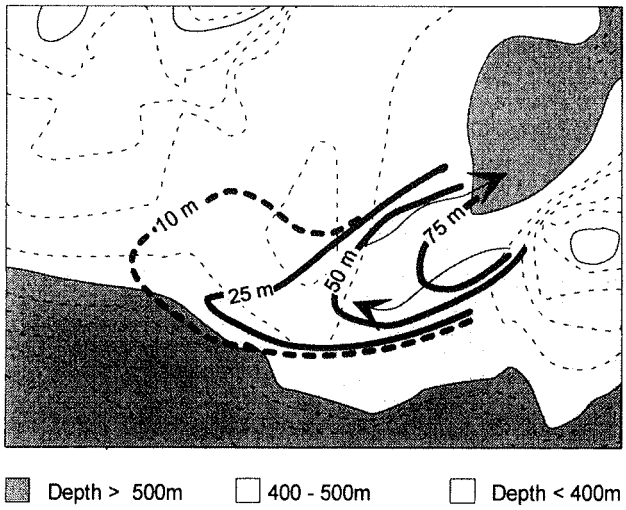

Figure 50. An overflow event on the Iceland-Faroe Ridge during the Overflow '73 experiment. Thin, broken lines show bottom depth in a small area (shown on Figure 48) on the ridge. Thick lines indicate the thickness of the layer of water colder than 2°C. Arrows show main flow direction according to current measurements. Based on Müller *et al.* (1974).

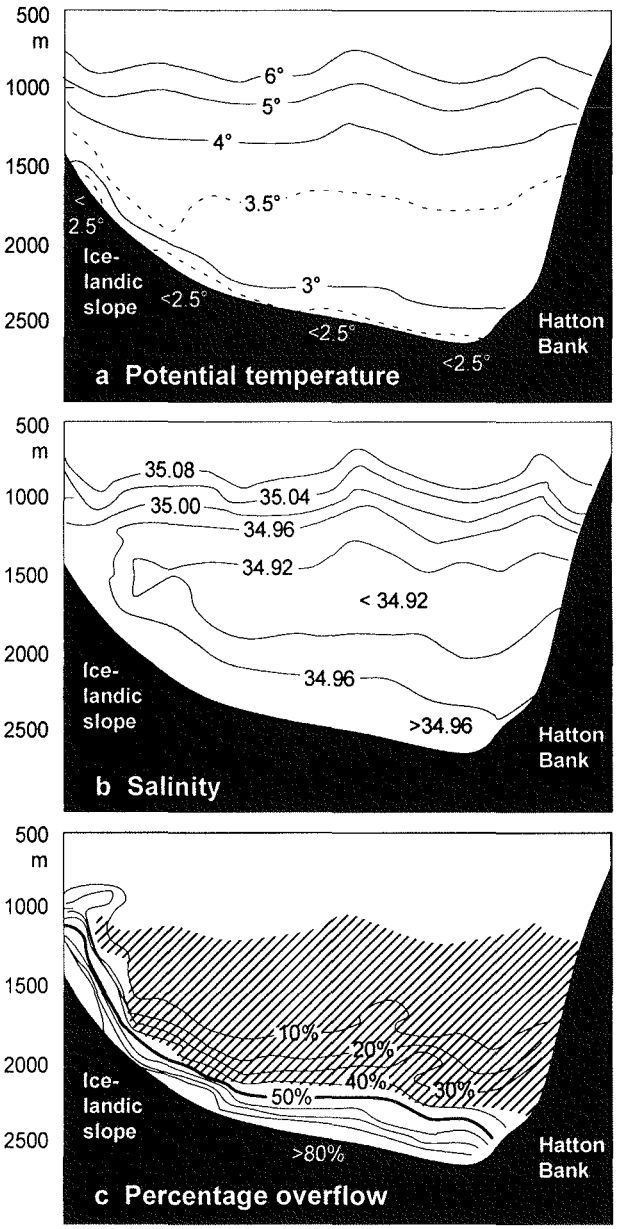

Figure 51. Water mass characteristics on a zonal section along 17°W, crossing the Iceland Basin as measured by R/V Tyro in 1990. a: Potential temperature. b: salinity. c: percentage of overflow water indicated by isolines, shaded area shows water with more than 50% Labrador Sea Water. Based on de Boer *et al.* (1998, this volume) and de Boer (1998, this volume). Section location is shown on Figure 52.

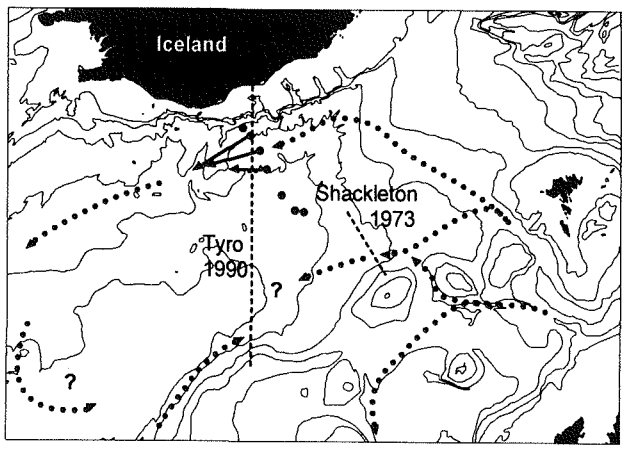

Figure 52. Overflow passage through the Iceland Basin. Overflow paths are indicated by dotted curved arrows. Black circles with arrows south of Iceland shows average velocity 10 m above the bottom according to Saunders (1996). Also shown are the locations of two sections referred to in Figures 51 and 53.

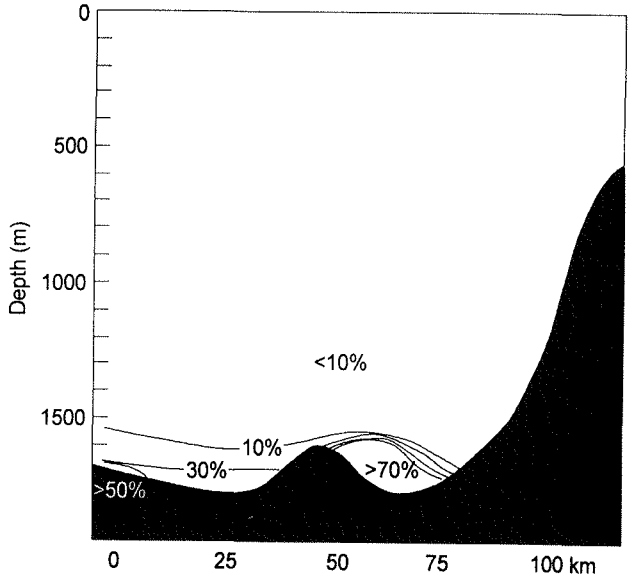

Figure 53. Percentage content of "NS-water" (NSAIW+NSDW) on a section north from Lousy Bank (location on Figure 52) as observed by R/V Shackleton in 1973. Based on Müller *et al.* (1979).

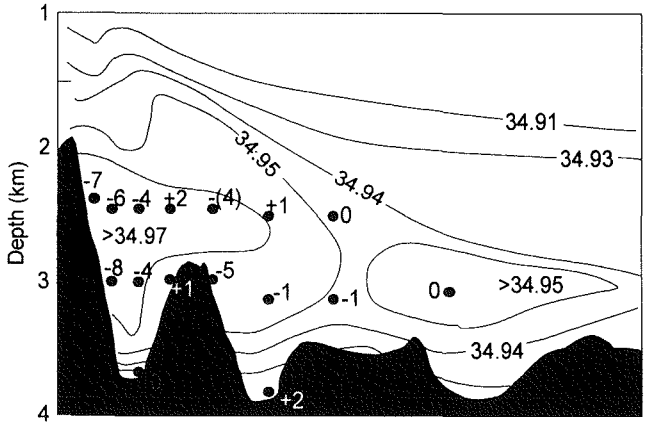

Figure 54. Salinity and current speed on a section along 35 °W through the Charlie-Gibbs Fracture Zone according to Saunders (1994). Current meters are indicated by black circles. Adjacent numbers give eastward velocity component averaged over the observation period. Based on Saunders (1994).

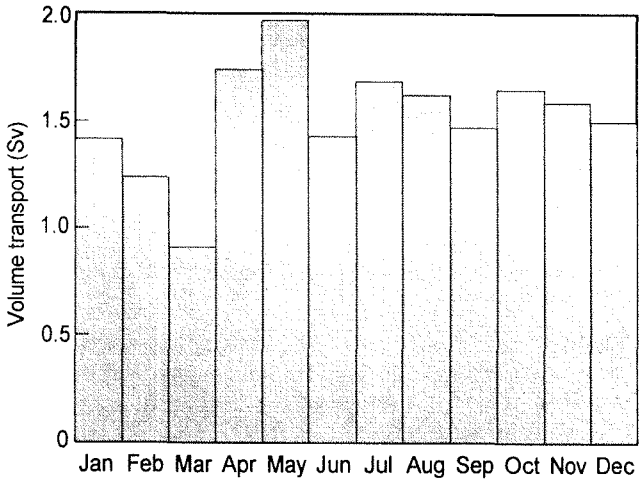

Figure 55. Mean monthly eastward warm-water transport (T > 4 °C) at Kögur (Figure 11) for the period June 1985 to August 1990. Adapted from Kristmannsson (1998, this volume).

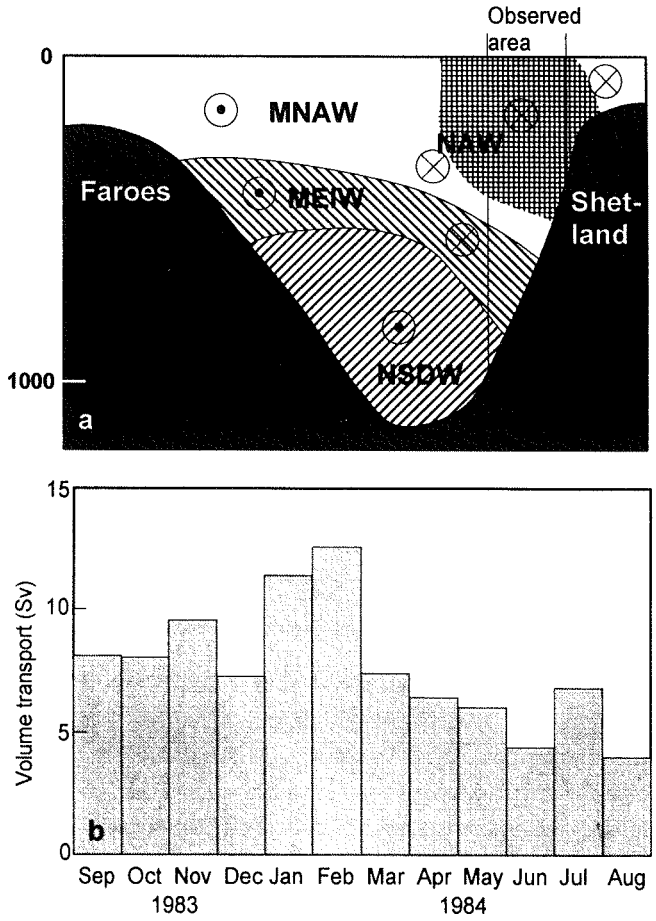

Figure 56. Gould *et al.*'s (1985) current meter measurements on the Shetland slope. The channel cross-section (a) shows the area covered by the moorings as well as a schematic distribution of the main water masses with arrows indicating typical flow through the section. Monthly mean volume transports (b) include all water flowing through the section towards northeast. Adapted from Gould *et al.* (1985).

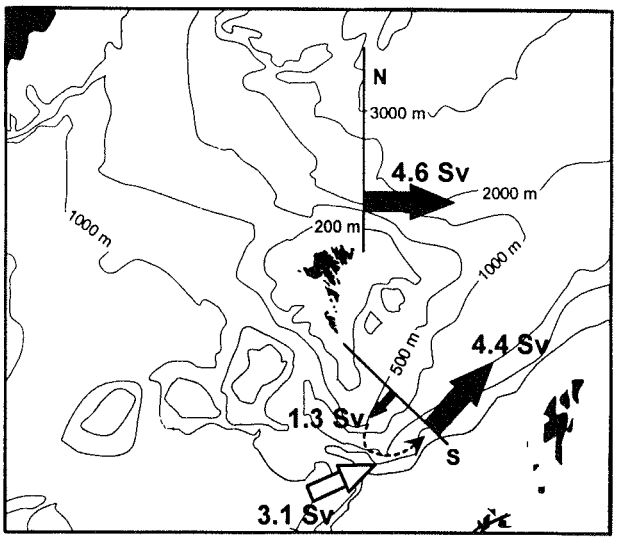

Figure 57. Preliminary estimate of the flux of Atlantic water through the Iceland-Scotland Gap based on Nordic WOCE ADCP moorings and CTD sections for the period October 1994 – May 1997. Numbers associated with black arrows indicate measured fluxes. The number associated with the open arrow (3.1 Sv) is the flux of Atlantic water into the Faroe-Shetland Channel from the southwest which is necessary to balance the measured fluxes in the channel assuming that the southwestwards flowing water on the Faroe side of the channel recirculates as indicated by the broken arrow.

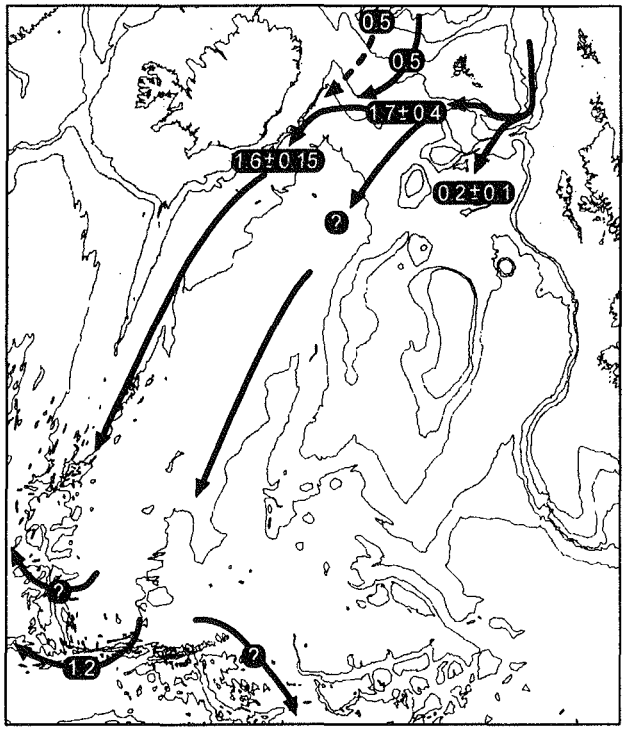

Figure 58. "Best" estimates of Iceland-Scotland overflow fluxes in different areas. Continuous arrows indicate flux of NSAIW+NSDW, dotted arrow indicates flux of MEIW.

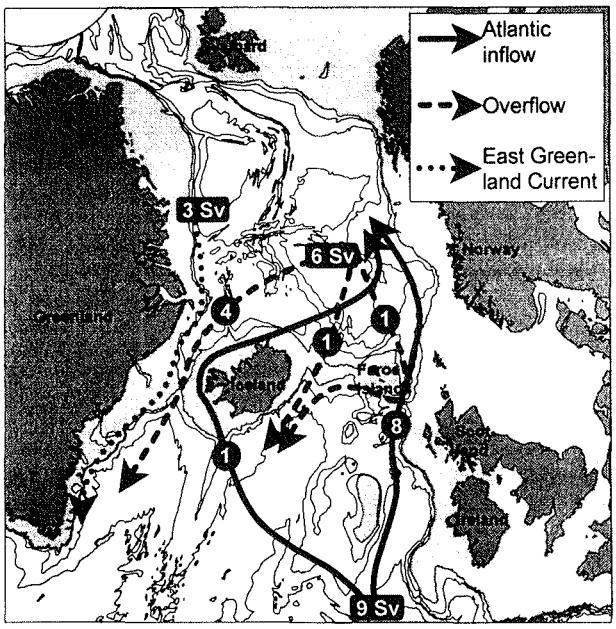

Figure 59. Exchange fluxes across the Greenland-Scotland Ridge in Worthington' s (1970) budget.

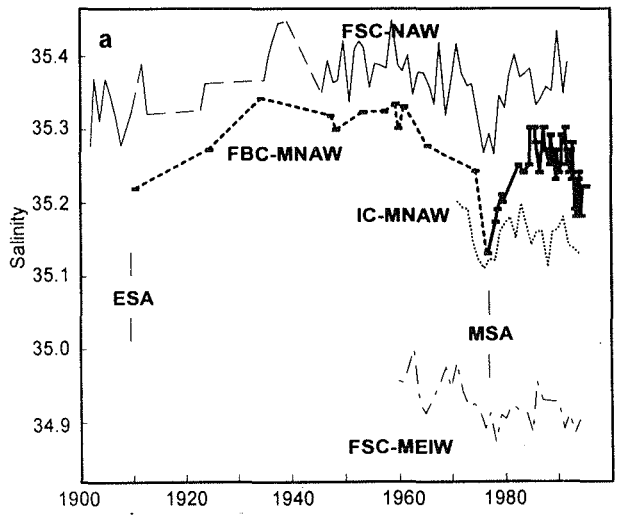

Figure 60. Long-term salinity changes of water passing the Greenland-Scotland Ridge. FSC-NAW is measured in the Continental Slope Current over the upper Shetland Slope (from Turrell *et al.*, 1993). FBC-MNAW is the average of the 100-300 m layer in the middle of the Faroe Bank Channel (from Hansen and Kristiansen, 1994). IC-MNAW is from a station southwest of Iceland (from Malmberg *et al.*, 1994). FSC-MEIW is the salinity at intermediate depths and temperatures on the Faroese side of the Faroe-Shetland Channel (from Turrell, 1995). Also are indicated two periods with anomalously low salinity, the Mid-seventies Salinity Anomaly (MSA) and the Earlier Salinity Anomaly (ESA).

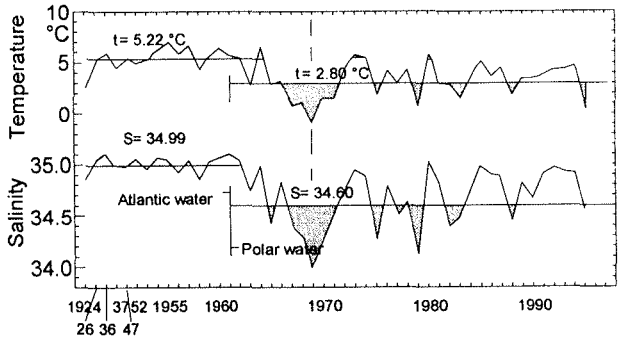

Figure 61. Temperature and salinity at 50 m depth at a hydrographic station in North Icelandic waters (location S3 on Figure 11) in May/June 1924, 1926, 1936, 1937, 1947 and 1952–1994. From Malmberg *et al.*, 1994.

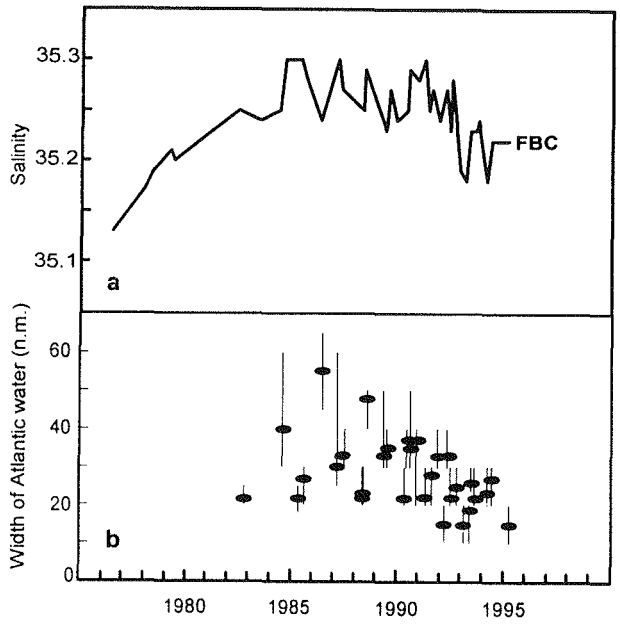

Figure 62. Variation of the salinity of the MNAW in the 100–300 m layer in the middle of the Faroe Bank Channel (a) and variation of the width (b) of Atlantic water in the Faroe current on a section along 6°W (section N on Figure 28) defined as distance (in n.m.) from 62°30'N to the latitude where the vertically averaged Atlantic water content from 25m to 500m depth (or bottom where shallower) falls to 50%. From Hansen and Kristiansen, 1994.

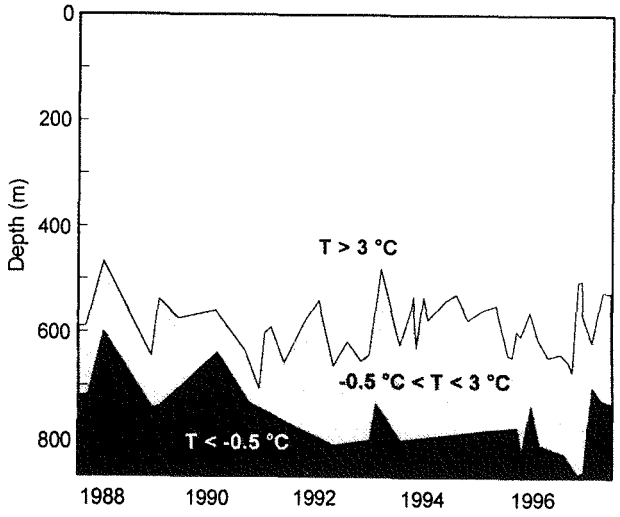

Figure 63. Depth of the 3°C isotherm and the -0.5°C isotherm at a standard station in the middle of the Faroe Bank Channel based on Faroese CTD observation 1988 – 1997. From Hansen and Kristiansen (in press).

Measurement of flow north of the Faroe Islands, June 1986

B. Hansen[1], S. A. Malmberg[2], O. H. Sælen and S. Østerhus[3]

[1]Fiskirannsóknarstovan, PO Box 3051, FR–110 Tórshavn, Faroe Islands. [2]Hafrannsóknastofnunin, Skúlagata 4, Reykjavík, Iceland. [3]Geofysisk Institut A, Allegaten 70, Bergen, Norway.

Based on a paper presented to the ICES Hydrography Committee as ICES CM 1986/C:12

A line of moorings with current meters were deployed northwards from the Faroe Islands for ten days in the beginning of June 1986. Simultaneous hydrography was observed by Faroese and Norwegian ships. A preliminary report of the current measurements will be given in this contribution describing the flow in the upper layers and giving a preliminary estimate of the transport of Atlantic water between Iceland and the Faroes into the Norwegian Sea. A total of 2.9 Sv (10^6 m^3 s^{-1}) of Atlantic water was found to flow between the Faroes and the surface front at about 63°30'N.

Keywords: Current measurements, Faroe Islands, Iceland-Faroe Ridge, water transport

Introduction

The flow of water out of the Atlantic into the Norwegian Sea is of considerable interest both from a basic oceanographic point of view and as a part of the climatic problem. Attempts to arrive at a quantitative estimate of the transport value have been made for several decades without a satisfactory conclusion. Estimates based on balance constraints (Worthington, 1970; McCartney and Talley, 1984) have given values higher by a factor of 2 to 5 than those arrived at by direct measurement, using either geostrophy (Tait, 1957) or current meter data (Dooley and Meincke, 1981), which is not surprising taking into account the large uncertainties inherent in previous attempts at direct estimation (Hansen, 1985). Recently this picture has changed somewhat by the publication by Gould *et al.* (1985) of a transport value amounting to 7.5 Sv (10^6 m^3 s^{-1}) flowing northeastwards over the slope north of Shetland. This estimate, based on yearlong direct current measurements, is very close to Worthingtons original estimate of 8 Sv flowing between Iceland and Shetland, but, as the authors point out, their section is over a limited part of the Faroe-Shetland Channel not covering the southwestward going flow in the Faroe side of the channel, their transport value included other water than Atlantic and they considered only "positive" flow, i.e. flow towards the northeast. Most of these simplifications would tend to increase the transport, so the cited number is probably an overestimate.

Thus there is still a discrepancy between the measured transport and the balance estimate by Worthington, although there may be consistency with the smaller balance estimates by McCartney and Talley (1984). There is, however, another possibility, namely that there is, in addition to the Faroe-Shetland Channel flow, a flow between Iceland and the Faroes considerably larger, than has been generally assumed.

The warm water over the Iceland-Faroe Ridge derives from the Iceland Basin. The path of the Atlantic water, as it approaches the Iceland-Faroe Ridge, is not much better known today, than it was early in this century (Figure 1). The horizontal distribution of temperature and salinity along the ridge axis appears quite homogeneous on the ridge proper (Meincke, 1972), but changes when approaching the shallower areas in both the Icelandic and the Faroese end of the ridge. On the Faroese end a high salinity core is often found, which appears to be a continuation of a core north of Faroe Bank.

Further towards the east this core is much more evident, and an oft repeated north south section about 6 degrees west (Tait, 1957 and contributions by F. Hermann and K. P. Andersen in the ICES Annales Biologiques for the years 1948–1957) always shows this core (Figure 2a) with steeply sloping isolines indicating a strong flow. Thus there is some evidence of both a concentrated flow along the northern flank of Faroe Bank continuing on the northern Faroe slope and also a broader flow over the ridge, both of these concentrating east of the ridge at about 6 degrees W. This pattern is in good agreement with Helland Hansen and Nansens (1909) circulation map (Figure 1).

Over the northeastern flank of the Ridge Figure 1 agrees well with the dynamic current computations from the Overflow-60 dataset (Bogdanov *et al.*, 1967), but not over the southwestern flank. The dynamic method is, however, very difficult to use on a ridge, and Figure 1 is

in substantial agreement with the available information from drift bottle experiments and direct current measurements. This flow has been denoted the Faroe Current by Hansen and Meincke (1984). Its core seldom exceeds 35.3 in salinity and 9°C in temperature. Probably it represents fairly undiluted water from the eastern part of the Iceland Basin and the term MNAW (Modified North Atlantic Water) seems to have originated with this watermass.

The Subarctic Front is inclined and the frontal boundary surface deepens as one goes southwards and westwards. It hits the Iceland-Faroe Ridge on the top and the Faroe slope at depths of 300 to 500 m (Figure 2a). Below the Faroe Current there is a layer of water from the East Icelandic Current giving a salinity minimum between the overlying MNAW and the NSDW (Norwegian Sea Deep Water), which is found in increasing amounts from about 500 m and downwards. The water of the salinity minimum varies in composition. Usually it is found to be mostly NI/AI water (North Icelandic/Arctic Intermediate) but also EIW (East Icelandic Winter) water has been found (Meincke, 1978).

East of about 5 degrees W the surface isolines tend to diverge horizontally (Figure 1), and a cold tongue protruding far towards the Faroese shelf is a common, although irregular, feature, which may be connected to the well documented meandering and instabilities of the Subarctic Front (Hansen and Meincke, 1979, Willebrand and Meincke, 1980). Hydrographic sections from the Faroes northwards thus generally show a wedge of high salinity water presumably fairly undiluted Atlantic water (Figure 2a). North of the surface front terminating the wedge one usually finds in addition a layer of water, which by its salinity contains a fair amount of Atlantic water. This layer is also evident in the typical section of Figure 2a.

The further fate of the Atlantic water is not very clear. Presumably a part of it continues into the Norwegian Sea (Figure 1) but certainly part of it turns towards the south and flows southwards east of the Faroes into the Faroe-Shetland Channel.

In recent western literature the transport over the Iceland-Faroe Ridge is generally regarded as insignificant compared to the Faroe-Shetland Channel transport (e.g. Coachman and Aagaard, 1974 p. 90). The arguments remain obscure, however. Certainly a visual comparison of two contemporary sections through the two flows (Figure 2) does not support this view especially taking into account, that part of the flow through the Faroe-Shetland Channel has come through the northern section.

A few estimates of the transport may be found in the literature. Thus Hermann (1948) estimated the total transport through the section of Figure 2a, north from the Faroes to be 4.5 Sv, of which, however, only part was Atlantic water. Tait (1957) also cites a number of geostrophic transports through this section of considerably smaller magnitude, while Sukhovey (as cited by Rossov, 1972) estimated a transport of almost 10 Sv between Iceland and the Faroes. There does not seem to have been any attempt to evaluate the transport based on observed current, and with the amount of current meter data published for this area, that is hardly realistic at present.

Thus there was a need for an experiment to measure the transport of this flow including hydrographic sections with current meter moorings. Such an attempt was made in 1982 as a collaboration between the University of Copenhagen (G. Kullenberg) and the Fisheries Laboratory in Tórshavn. That attempt, unfortunately, resulted only in lost current meters, but taught the lesson, that any future experiment should include careful planning to avoid such loss due to fisheries.

With this in mind the Nordisk Kollegium for Fysisk Oceanografi (NKFO) at its meeting in Reykjavík September 1984 decided to establish an ad hoc working group to plan a project in this area. The first result of this group was the planning of a pilot experiment to evaluate the importance of the Faroe current to the water and heat transport into the Norwegian Sea.

Material

This project took place during the first half of June 1986. Its main aim was to get a preliminary estimate of the transport value. To realise that aim a total of seven moorings were deployed more or less along a line following the 6°05'W longitude (Figure 3). The moorings had from 2 to 4 current meters each which were all of them Aanderaa meters except for the two shallowest moorings which also had some SD2000 Sensordata (Gytre) instruments.

The complete mooring section was out for 10 days from 5 June to 14 June. This period is short for an estimate of a typical transport value. However. from previous experience, the risk of instrument loss from fisheries is so great that it was decided rather to get as many as possible of the instruments back and consider the transport value as only a preliminary number.

In addition to the moorings, two research vessels did hydrographic surveys in the area in the observational period. The Faroese ship R/V Magnus Heinason steamed back and forth along the mooring section taking CTD stations and chemistry and alerting the fishing fleet to the moorings while the Norwegian R/V Haakon Mosby covered a larger area doing CTD and seasoar sections in addition to other work. The current meters were contributed from most Nordic countries and

scientists from Norway, Sweden, Finland, Denmark, Faroes and Iceland were on the two ships.

The care taken with the moorings paid off in that all of them were recovered successfully and nearly all the current meters had functioned properly, so a fairly complete current section was obtained allowing an estimate of the transport value during the period.

Results

We will not present the total amount of hydrographic data observed during the project, but will consider only those observations that were along the current meter section. R/V Haakon Mosby made one hydrographic section and Figure 4 shows potential temperature, salinity and density from this section. The other vessel, R/V Magnus Heinason, made altogether 6 CTD sections along the same line (Figure 5). Three of these are shown in Figure 6.

The data from the current meters have been edited and calibrated. The measurements below 500 m depth will not be discussed here at all. Figure 7 shows progressive vector diagrams from all the moorings at 50 m depth and 300 m depth respectively (170 m for mooring B). Furthermore 25-hour running means have been calculated.

Discussion

The CTD sections (Figure 4 and Figure 6) show a typical hydrographic situation consistent with available published data (Tait, 1957 and Annales Biologiques from different years) with high salinity water from the Atlantic in a wedge-shaped region along the Faroe slope. The water in this wedge was fairly homogeneous and bounded by a sharp frontal surface going from the Faroe slope at depths about 400 m and reaching the surface between 63°30'N and 64°00'N.

Below the wedge the salinity minimum indicated water from the East Icelandic Current interleaved between the Atlantic water and the Norwegians Sea Deep Water characterised by its stable salinity values around 34.92. Fairly undiluted water from the East Icelandic Current was evident in the surface in the northernmost part of some of the hydrographic sections in Figure 6. Between this water and the surface front further south the uppermost 200 m showed a mixture of this water and water from the Atlantic with up to 50% of Atlantic water.

Another expected feature was the large variability both spatially and temporally. This is evident in Figure 6 and indeed makes an unambiguous representation of isolines impossible. Most important for the present discussion are the larger scale movements. Comparing Figure 7 to Figures 4 and 6, it is seen that the flow was fairly barotropic in the upper 300 m throughout the measurement period. In the beginning of the period the flow was directed towards the east or southeast past all the current meters in the southern part of the section while it was more towards the south in the northern part. Around 7 June this changed. The innermost and outermost moorings (A,B,C and G) continued to have the same flow, but moorings E and F experienced a reversal of the flow while the current turned 90° at mooring D. This was consistent with the hydrography as the temperature and salinity and hence also density sloped in the "opposite" direction between mooring D and F in the later part of the period. A detailed analysis is difficult from only one section, but apparently an eddy or meander (Hansen and Meincke, 1979) propagated through the section. It is evident as a cold water dome north of mooring F (station 7) in Figure 4. As it decayed or moved out of the section it moved southwards so that its northern flank was between moorings D and F (Figure 6). Thus the reversal of flow in this region probably indicates only the cyclonic flow around this feature.

Using the computed 25-hour running mean flow velocities we have estimated the water transport. To this end the current meter section was divided into subareas around each instrument (Figure 8). The dividing lines between the subareas have as a rule been put midway between the meters vertically and horizontally. The northernmost subareas around mooring G are extended to 63°40'N which is considered a mean position of the surface front for the period (Figure 6). The bottom subarea was limited by the 500m depth, which is close to the sill depth of the Iceland-Faroe Ridge. The transport through each subarea was obtained as the product of the area and the mean flow velocity perpendicular to the section (east component).

Summing all values gave a total transport of water amounting to *4.7* Sv (10^6 $m^3 \cdot s^{-1}$) for the cross section from Faroes out to 63° 40'N and down to 500 meters depth.

This is however not the number we are seeking as it contains not only the Atlantic flow. The innermost subarea around mooring A contains water of mainly Atlantic origin, but most of this water is within the mixing front separating the shelf waters from the outer waters. As this water probably is recirculated on the shelf to a large degree we will not include this subarea in the transport value.

Furthermore the other subareas contain other watermasses not deriving from the Atlantic. A complete solution of this problem requires a water mass analysis beyond the scope of this preliminary report. We can get, however, a fairly good estimate of the percentage of Atlantic water by considering only the salinity. There

are indeed at least three separate water masses involved, but two of these have quite similar salinities of about 34.90 as compared to the higher salinity of the Atlantic water. We have considered water of salinities above 35.20 to be 100% Atlantic water, water of salinity below 34.90 to have no Atlantic water and in between these two limits the percentage of Atlantic water was considered a linear function of salinity. With this procedure we have used the salinities of the CTD sections (Figures 4 and 6) to estimate typical percentages for each subarea. The percentages chosen, shown in Figure 8, are to some degree subjective, but in the present context good enough for a transport estimate. Multiplying the percentages by the transport through each subarea we get an estimate of the Atlantic water transport.

In Figure 9 the transport has been summed for each vertical subsection (labelled as the moorings, Figure 8) and plotted against time. The figure also shows the transport of Atlantic water through the whole section. The short-period variations in the hydrography are reflected in the transport values for each subsection, but as the different subsections did not vary coherently, the total transport was relatively more stable around a mean value of *2.9* Sv for the one week, where all the current meters were operating.

This value is at present the best estimate we can give for the Atlantic flow through the current meter section. We must note, however, that this section does not include all the Atlantic flow. It has been noted already that north of the surface front there is a layer of mixed water containing appreciable amounts of Atlantic water. In Figure 8 this has been indicated by the subarea H. The value 40% for the proportion of Atlantic water again is a subjective estimate based on the salinities of Figures 4 and 6. The choice of a typical velocity for this subarea is a more difficult problem. Considering the layer as a whole it can hardly go anywhere except eastwards, but at present we can only guess at velocities. If we use the velocity of mooring G for this area also (about 10cm s^{-1}), we get an additional 0.9 Sv of Atlantic water through subsection H. The origin of this water is, however, not quite clear. Most likely, it is recirculated water from the Norwegian Sea and therefore we do not include it into the total transport.

Conclusion

We find a flow amounting to 2.9 Sv through the section covered by the current meter moorings for the observational period. The shortness of that period, little more than one week, urges that the value found be used with the greatest caution. There seems, however, to be no evidence that the situation was not normal and we feel justified in stating that:

The flow of Atlantic water between Iceland and the Faroes is not insignificant compared to the transport through other pathways. Rather it may be of the same order of magnitude as the flow through the Faroe Shetland Channel and the inconsistency may be resolved, which has been between measured transport of Atlantic water into the Norwegian Sea and balance estimates of this quantity. Combining our estimate for the transport between Iceland and Faroes with recent estimates of the transport between Faroes and Shetland (Gould et al., 1985) the total flow of Atlantic water appears to be sufficient to satisfy the published balance estimates (Worthington, 1970; McCartney and Talley, 1984).

It would be of great interest to have these conclusions checked by experiments of longer duration.

Acknowledgement

This project was planned on the initiative of and partly financed by Nordisk Kollegium for Fysisk Oceanografi.

References

Bogdanov, M. A., Zaitsev, G. N., and Potaichuk, S. I. 1967. Water mass dynamics in the Iceland Faroe Ridge area. Rapports et Procès-Verbaux des Réunions du Conseil International pour l'Exploration de la Mer, 157: 150–156.

Coachman, L. K., and Aagaard, K. 1974. Physical oceanography of Arctic and Subarctic seas. In Nelson, H., and Herman, Y. (Eds.), Arctic geology and oceanography, Springer Verlag: 1–96.

Dooley, H., and Meincke, J. 1981. Circulation and water masses in the Faroese Channels during Overflow-73. Deutsche Hydrografische Zeitschrift, 34: 41–55.

Gould, W. J., Loynes, J., and Backhaus, J. 1985. Seasonality in slope current transports N.W. of Shetland. ICES C.M. 1985/C:7, 13 pp.

Hansen, B. 1985. The Circulation of the Northern part of the North Eastern Atlantic. Rit Fiskideildar, 9: 110–126.

Hansen, B., and Meincke, J. 1979. Eddies and Meanders in the Iceland Faroe Ridge area. Deep-Sea Research, 26A: 1067–1082.

Hansen, B., and Meincke, J. 1984. Long-term coastal sea surface temperature observations at the Faroe Islands. Rapports et Procès-Verbaux des

Réunions du Conseil International pour l'Exploration de la Mer, 185: 162–169.

Helland-Hansen, B., and Nansen, F. 1909. The Norwegian Sea. Rept. Report on Norwegian Fishery and Marine Investigations, II (2), 390 pp.+suppl.

Hermann, F. 1948. Hydrographic conditions in the southwestern part of the Norwegian Sea. Annales Biologiques du Conseil International pour l'Exploration de la Mer, V: 19–21.

McCartney, M. S., and Talley, L. D. 1984. Journal of Physical Oceanography, 14: 922–935.

Meincke, J. 1972. The hydrographic section along the Iceland Faroe Ridge carried out by R.V. "Anton Dohrn" in 1959–1971. Berichte der Deutschen Wissenschaftlichen Kommision für Meeresforschung, 22: 372–384.

Meincke, J. 1978. On the Distribution of Low Salinity Intermediate Waters around the Faroes. Deutsche Hydrografische Zeitschrift, 31 (2): 50–64.

Rossov, V. V. 1972. On the water exchange between the North Atlantic and the Polar Basin and the water balance of the North Atlantic Current. ICES CM 1972/C:3, 9 pp.

Tait, J. B. 1957. Hydrography of the Faroe-Shetland Channel 1927–52. Marine Research Scotland 1957, 2.

Willebrand, J., and Meincke, J. 1980. Statistical analysis of fluctuations in the Iceland Scotland frontal zone. Deep-Sea Research, 27: 1047–1066.

Worthington, L. V. 1970. The Norwegian Sea as a Meditteranean Basin. Deep-Sea Research. 17: 77–84.

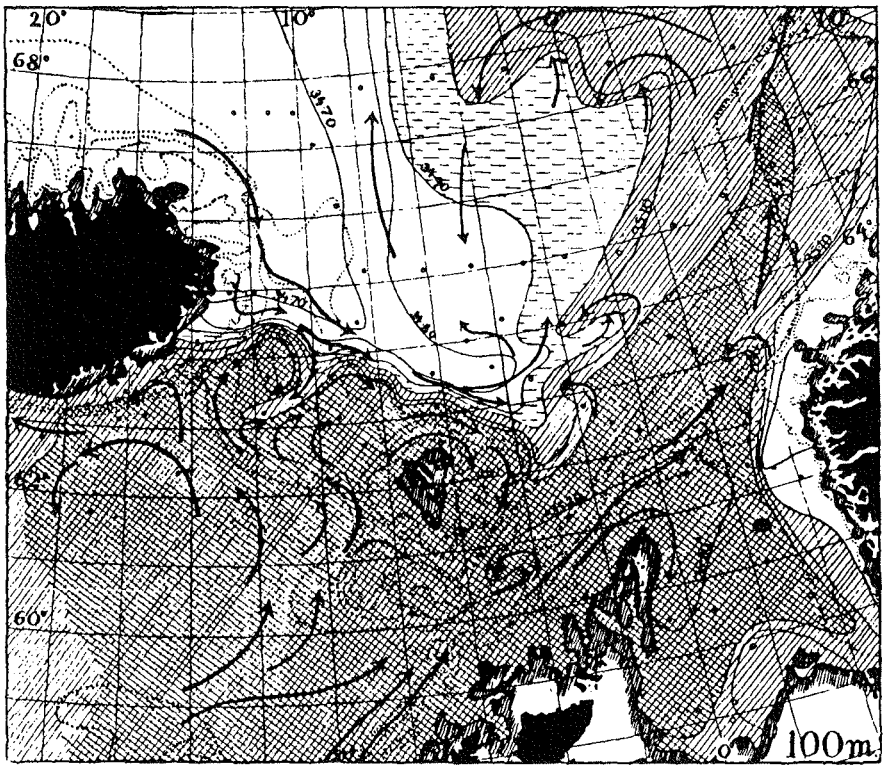

Figure 1. Horizontal distribution of salinity at 100 m, May 1904. The arrows indicate the circulation pattern according to Helland, Hansen and Nansen (1909).

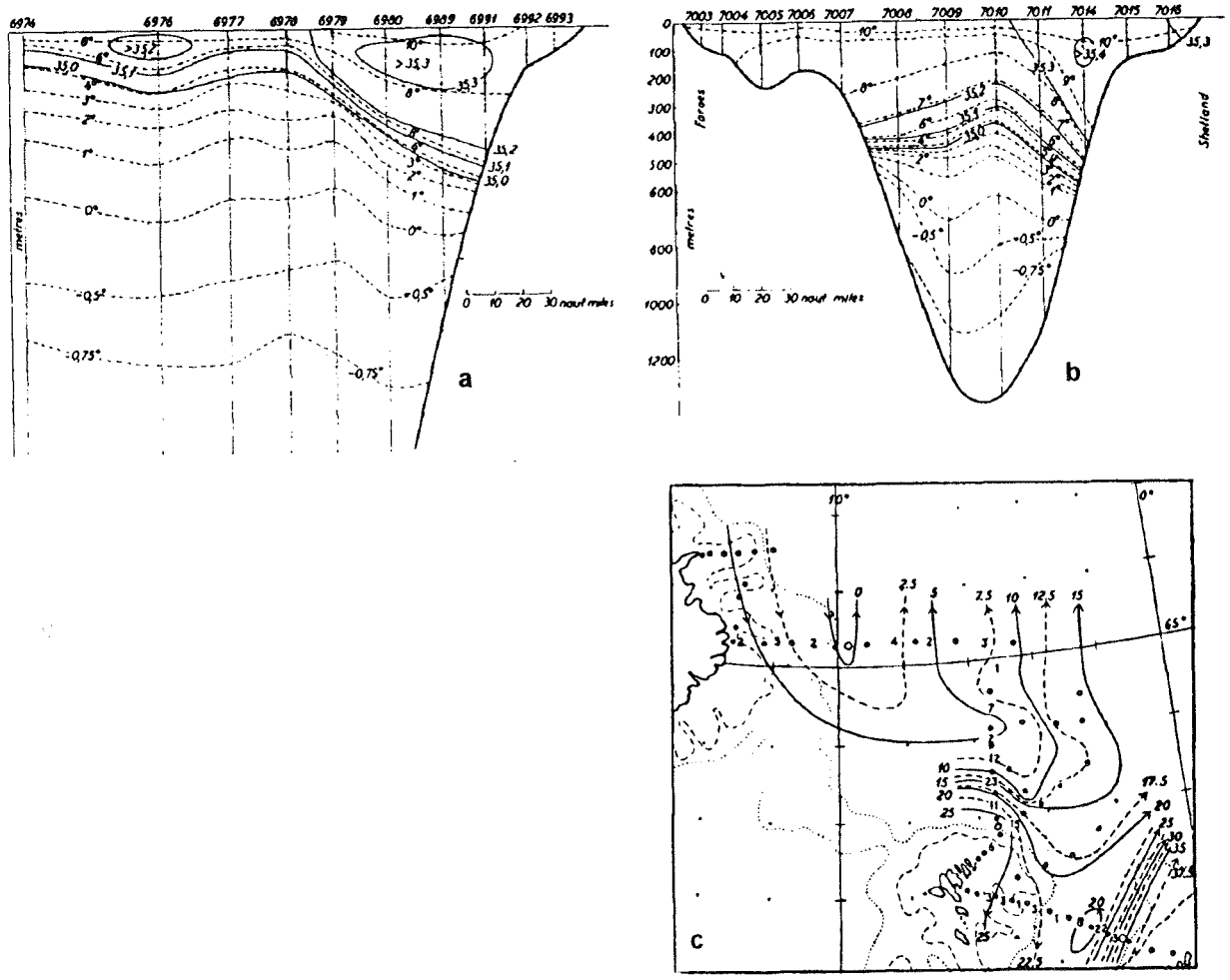

Figure 2. Hydrographic investigations in August 1948 by R/V Dana (Hermann, 1948). a.: vertical section from the Faroes northwards. b.: Faroe-Shetland section. c.: station map showing dynamic topography relative to 1000 m. Numbers between stations are geostrophic velocities in cm s^{-1}.

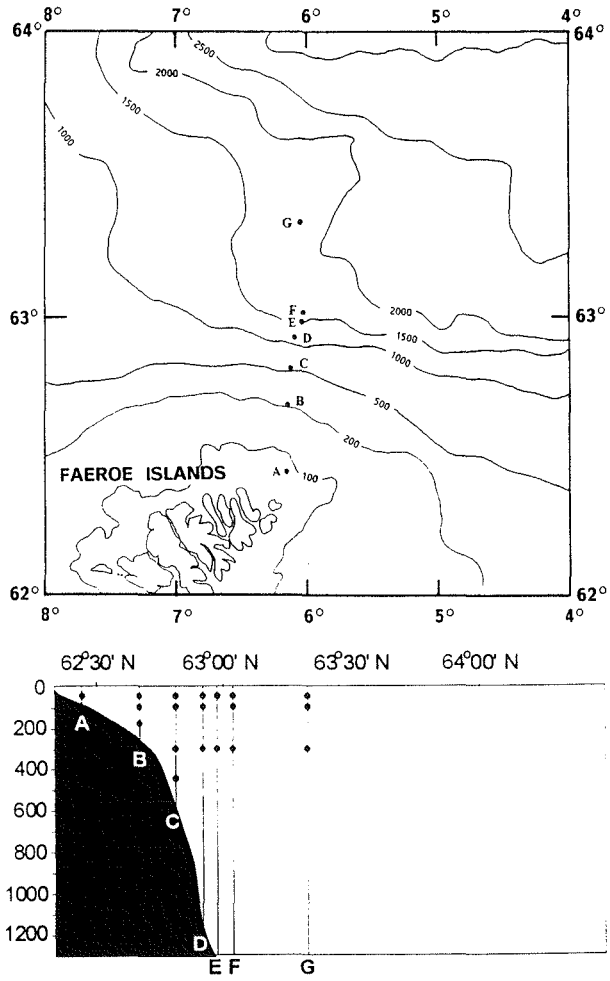

Figure 3. Current meters recovered north of the Faroes June 1986 (only instruments above 500 m depth are shown). On the vertical section (bottom part of figure), the current meters are indicated by filled circles.

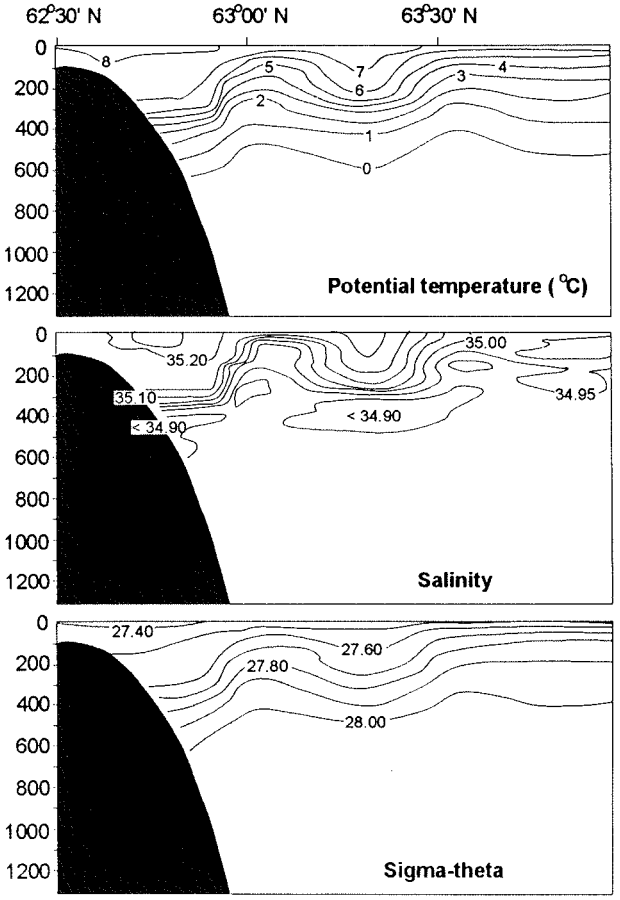

Figure 4. CTD section made by R/V Haakon Mosby on 3 June along the current meter moorings.

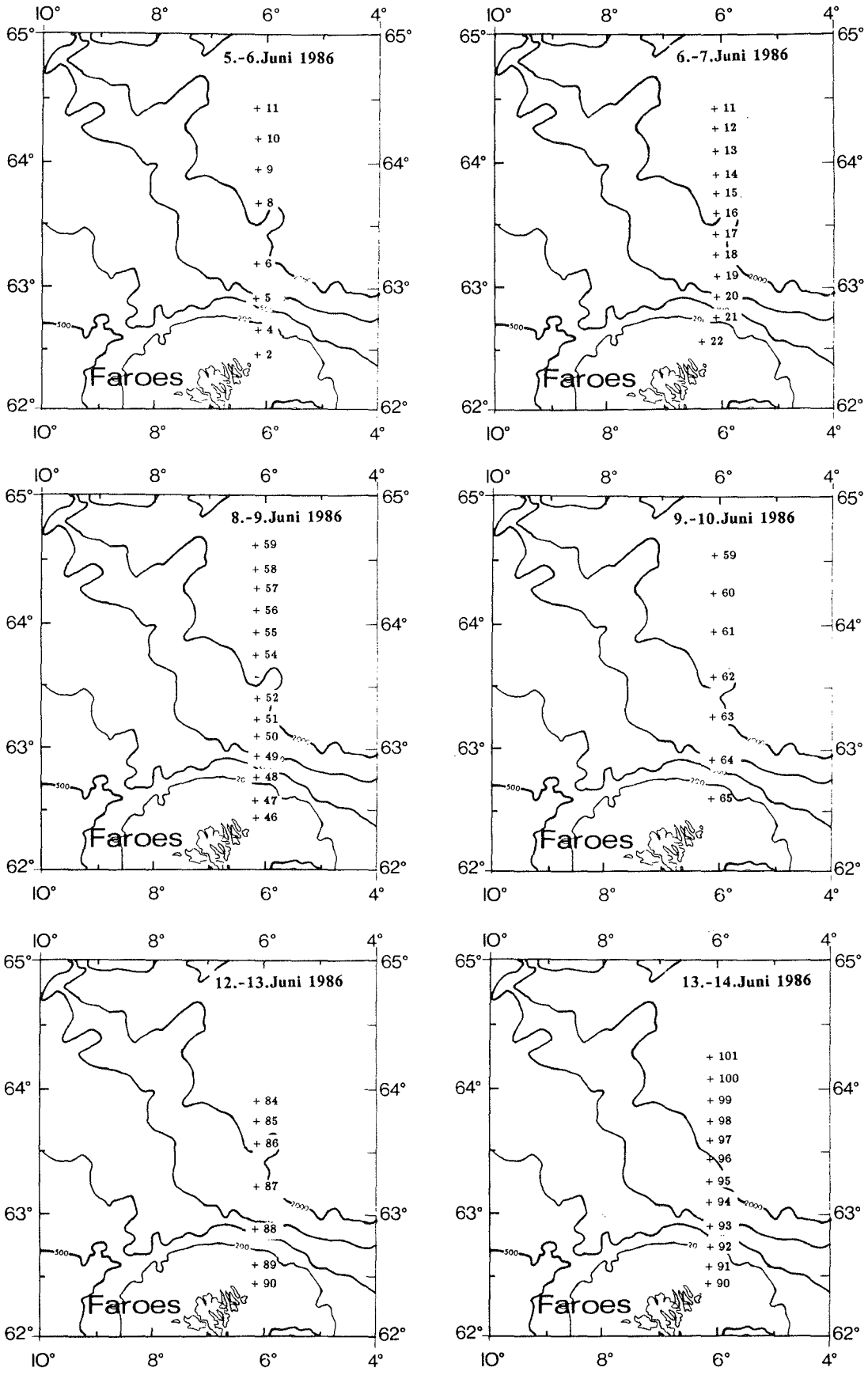

Figure 5. CTD stations made by R/V Magnus Heinason along the current meter moorings. Sections are shown in Figure 6.

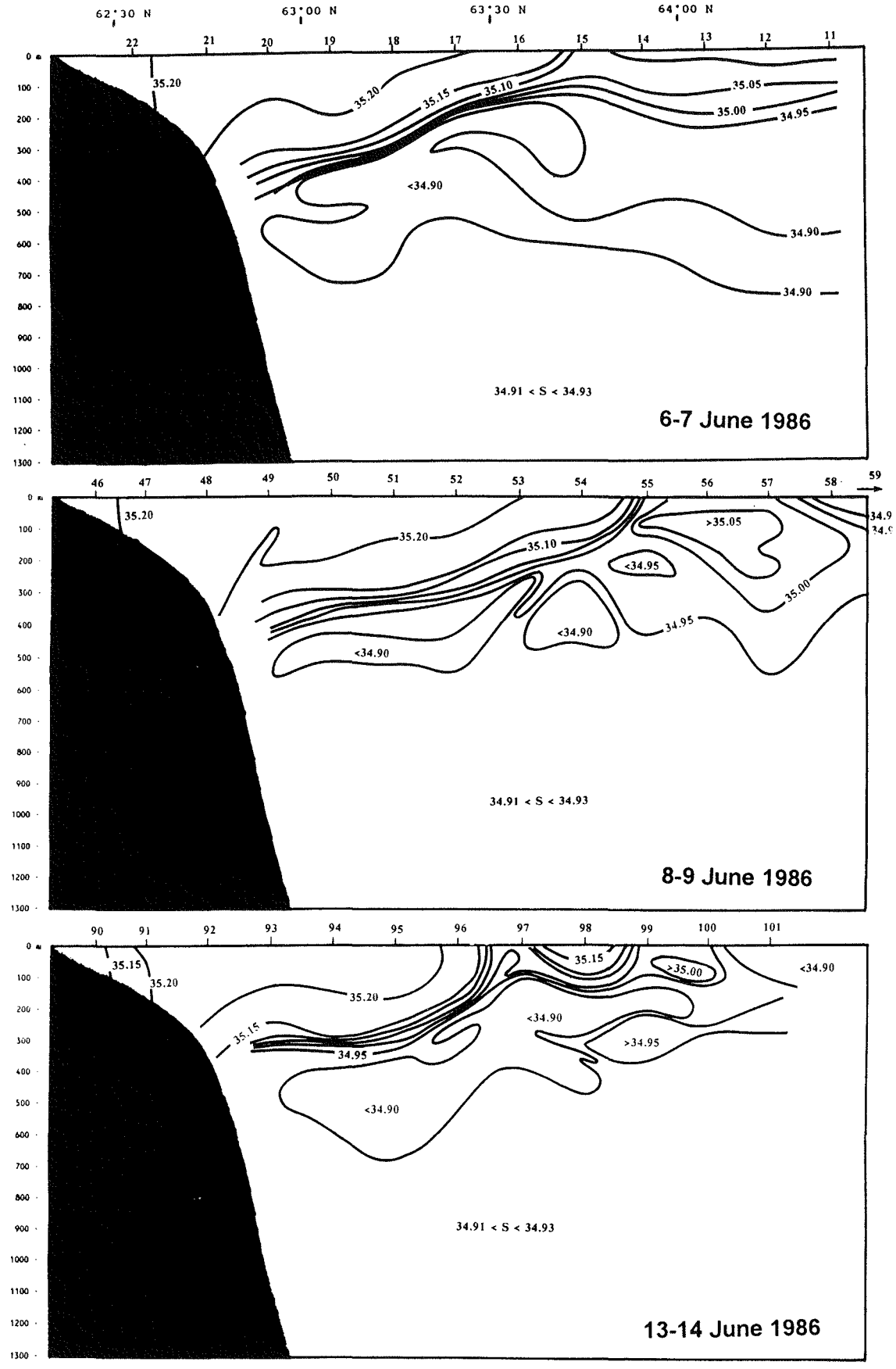

Figure 6. CTD sections made by R/V Magnus Heinason at three different times. Numbers above the sections are stationnumbers shown in Figure 5.

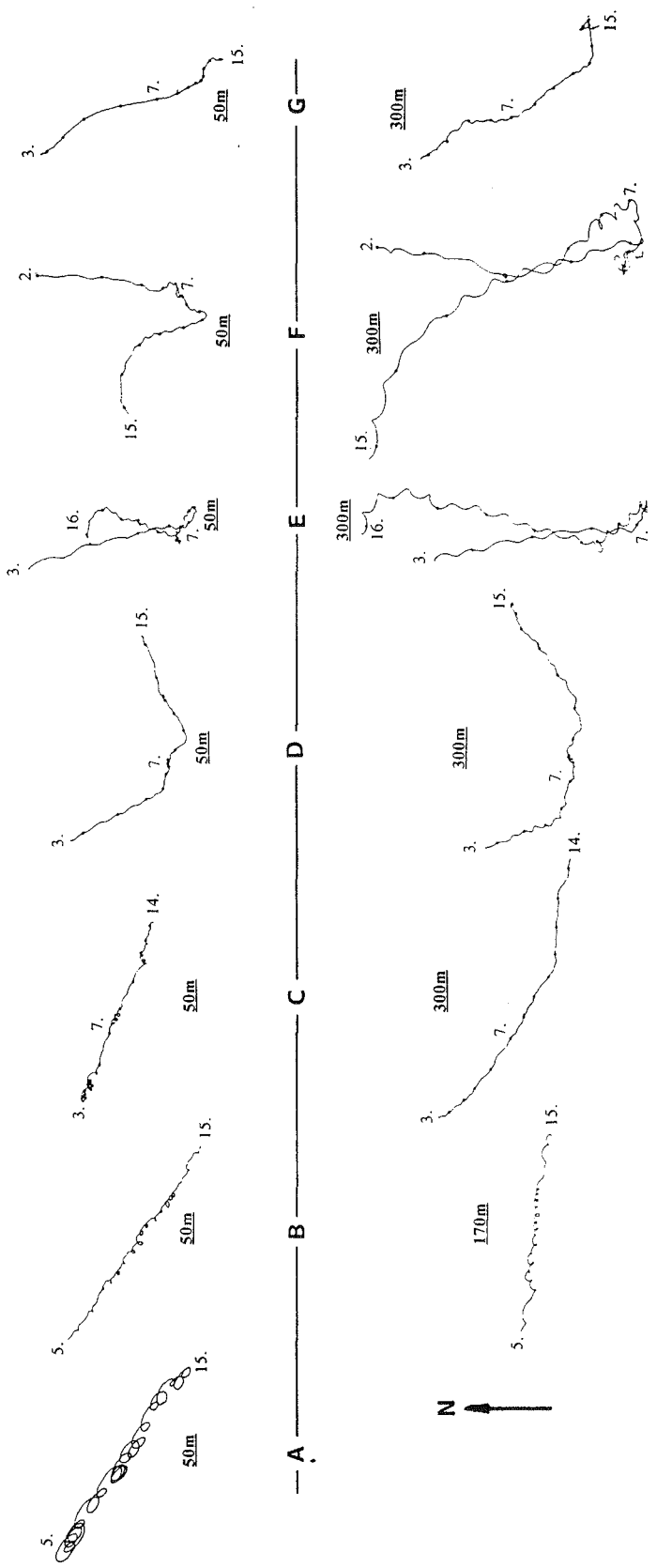

Figure 7. Progressive vector diagrams of current from the uppermost current meter and the meter at 300 m (or the deepest) for each mooring. Mooring locations are seen in Figure 3. Numbers indicate the date in June.

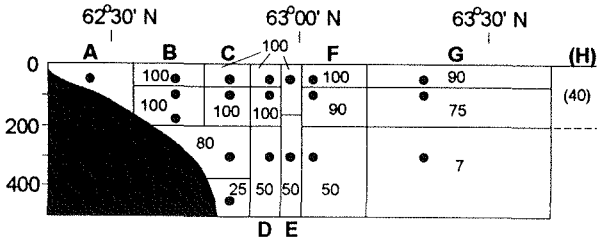

Figure 8. Subareas chosen around each current meter which were used for transport calculation. Numbers in each area represent the percentage of Atlantic water in that area during the measurement period (see text).

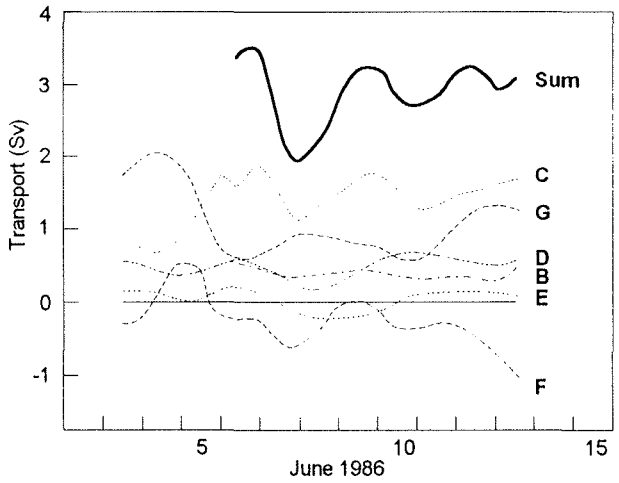

Figure 9. The transport of Atlantic water through each subsection (shown in Figure 8) during the measurement period. Sum denotes the total transport trough sections B to G (H not included).

Modified North Atlantic Water

G. Becker[1] and B. Hansen[2]

[1]Deutsches Hydrographisches Institut, [2]Fiskirannsóknarstovan, PO Box 3051, FR-110 Torshavn, Faroe Islands.

Based on a paper presented to the ICES Hydrography Committee as ICES CM 1988/C:17

In recent literature the term Modified North Atlantic Water (MNAW) has been used to denote the Atlantic water in the region of the Iceland-Faroe Ridge and around the Faroes in contrast to the classical North Atlantic Water (NAW) in the Faroe-Shetland Channel which is somewhat warmer and more saline. The paper uses data mainly from the 1987 NANSEN experiment to trace water of similar θS characteristics from the western edge of the Rockall Plateau to the area between Iceland and Scotland. Modified North Atlantic Water thus appears to be relatively unmodified water from the North Atlantic Current flowing eastward over the Rockall Plateau directly into the Faroe Bank Channel and into the western part of the Faroe-Shetland Channe. It also flows over the Iceland-Faroe Ridge to the area north of the Faroes and thence to the eastern part of the Faroe-Shetland Channel mixed with colder and fresher water from east of the Iceland-Faroe Ridge.

Keywords: Faroe region, Iceland Basin, North Atlantic, water masses

Introduction

The term "Modified North Atlantic Water (MNAW)" has been in general use since the early seventies to describe a water mass of Atlantic origin which is found over large areas in the region between Iceland and Scotland surrounding the Faroe Islands to all sides. In earlier literature (e.g. Tait, 1957; Hermann, 1967) it was common practice to denote all the Atlantic water in this region by the term North Atlantic Water (NAW or NA). It was recognised, however, that the waters in the northern parts of the area were considerably fresher and also colder than the classical θS values for NA water (Tait, 1957). In his 1976 paper on long term changes Martin (1976) distinguished between these two water masses in the Faroe-Shetland Channel. As results from the Overflow-73 entered the literature, MNAW was used to denote water found between Iceland and the Faroe Islands, in the Faroe-Shetland Channel and in the Faroe Bank Channel. Thus the Water mass synopsis from the Overflow-73 experiment (Müller *et al.*, 1979) shows MNAW to be the dominant water in the upper parts of most of the oceanic region between Iceland and Scotland excluding only the area over the Shetland slope dominated by NAW. It also became clear that water with similar characteristics was to be found in the northern parts of the Rockall Trough (Ellett *et al.*, 1983). These authors further introduce a separate water mass IMNAW (Intermediate MNAW) which they consider to be a mixture of NAW and Subarctic Intermediate Water (SAIW). Van Aken and Eisma (1987) also found IMNAW in the Faroe-Shetland Channel although they preferred the name Lower Atlantic Water (LAW) and consider it a mixture of NAW and Labrador Sea Water (LSW).

As to the origin of MNAW the early papers are not quite clear. In one of the first published references to MNAW, Martin (1976) states: "... its most likely passage into the Faroe-Shetland Channel is over the Iceland-Faroe Ridge and east of the Faroes". And indeed there seems to be a general consensus that at least part of the MNAW in the Faroe-Shetland Channel comes from the area north of the Faroes and to that area it has come over the Iceland-Faroe Ridge. Less agreement is to be found on the origin of the MNAW west of the Faroes. Thus Dooley and Meincke (1981) consider the MNAW in the Faroe Bank Channel to derive from the Faroe-Shetland Channel while Hansen (1979, 1985) finds a westerly origin more probable which was supported by Van Aken and Eisma (1987). In the Northern Rockall Trough Ellett *et al.* (1983) considered the MNAW to have entered the area from the north and northwest.

The ultimate origin of MNAW is no doubt the North Atlantic Current. Recent investigations (Krauss, 1986; Sy, 1988) confirm that a major branch of that current impinges onto the Rockall Plateau. The upper waters in the southern Rockall Trough on the other hand seem to have a more southerly origin at least in recent years (Ellett and Martin, 1973). Thus, a natural explanation of the MNAW salinity being less than NAW salinity is the more direct descent of MNAW from the North Atlantic Current while the NAW has received larger amounts of Meditteranean Overflow Water partly transported by the Continental Slope Current (Booth and Ellett, 1983).

A more precise determination of the MNAW origin is, however, lacking. The term "Modified" implies that this water is in some ways changed since its Atlantic origin and that idea is implicit in much of the early literature. Thus Meincke (1978) states: "MNA water is originally North Atlantic water which was slightly modified on its devious route into the Faroe region". If the MNAW circles the Faroe Islands then the modification could be to a large extent in the Faroe area maybe especially the Iceland-Faroe Ridge region. Alternatively; if the MNAW west of the Faroes derives from the west then the modification must be in the region of the Rockall Plateau or the Iceland Basin if indeed there is any modification.

The aim of this note was to explore to what extent the MNAW in the Iceland-Scotland region can be traced from the North Atlantic Current to the Iceland-Scotland area and what modifications occur on the route. We do not presume to give much more than a snapshot view on this problem as our discussion will be based mostly on three cruises made within a period of six months in 1987 and one cruise in the summer of 1988. All of these cruises took place in the framework of the ICES NANSEN project (North Atlantic – Norwegian Sea ExchaNge).

Observations

The main results of this paper are based on two cruises of the German research vessel Gauss to the Iceland Basin, the first in August 1987 and the second in June/July 1988 and on two cruises in Faroese waters by the Faroese research vessel Magnus Heinason one in April-May of 1987 and one in July 1987. Station positions on these cruises are shown in Figure 1. (The Gauss 1988 stationmap was almost identical to that from 1987 and it is not shown).

From the Gauss cruises we shall be using mainly water bottle data taken by rosette sampler and analysed within 48 hours onboard ship on an Autosal A salinometer. From the two Magnus Heinason cruises we shall use CTD data obtained by a Neil Brown Mark III CTD calibrated with water bottle samples taken on approximately every third station and analysed on an Autosal salinometer ashore some months later. The accuracy of the Magnus Heinason CTD data is within about 0.01 in salinity which is sufficient for the present purpose. The Gauss water bottle salinities are considerably more precise (order of or better than 0.002)

Results

θS-characteristics of the southern Iceland Basin. We shall look first at the Iceland Basin and the Rockall Plateau and we will use especially the bottle data from the Gauss August 1987 cruise. Figure 1a shows the location of those stations on that cruise that will be used. A complete discussion of results from the Gauss cruise will appear elsewhere. Here we shall concentrate on the θS characteristics of the upper layers along the southern edge of the Iceland Basin and over the Rockall Plateau. In Figure 2 is shown a composite θS diagram for all the Gauss stations from 1987 discussed in this paper (Figure 1a). This diagram, like all the following θS diagrams in the paper, exclude the uppermost 100 meters to minimise surface effects.

The θS curves of Figure 2 show considerable scatter with a range of salinities for each temperature, but there is also a large number of stations with remarkably similar θS curves. One way to systematise this data is to divide the θS diagram into regions and in Figure 3a, region B is defined to include the many similar stations while region A includes stations fresher and region C stations more saline than region B.

This defines three different water mass types (A, B and C) and for each station one may by visual comparison classify which type of water mass the station belongs to. This has been done to the Gauss 1987 data and the stations sorted into the three types. That this can be done in a fairly consistent way is demonstrated by Figure 3b,c,d. One may furthermore consider the geographical location of the stations belonging to each type and in Figure 4 it is shown that the three different water masses are to be found in three coherent regions of the Iceland Basin and the Rockall Plateau. It should be stressed that the water mass classification presented is rather ad hoc and not based on any generic arguments. Thus the three curves of Figure 3a defining the water masses are also ad hoc and could doubtless be chosen differently, but Figure 4 demonstrates the usefulness of this classification. The three curves separating the water masses A, B and C are also plotted on Figures 3b,c,d and on all the θS diagrams which will be seen in the following. Their defining values are to be found in Table 1. It is interesting to note that the regions are more or less parallel to the boundaries of the Iceland Basin and to the assumed flow direction of the Atlantic water (Ryder, 1901; Helland Hansen and Nansen, 1909).

The simplest interpretation of this is that a fairly broad current enters the area and follows the topography more or less towards the northeast. Across this flow the salinity increases towards the Southeast for fixed temperature but along the flow direction, the water seems to be advected with little modification below about 100 m depth. The division into regions can be further related to the current structure by looking at

Table 1 Definition of three water masses of the Iceland Basin and Rockall Plateau.

	Salinity at 4°C	Salinity at 7°C	Salinity at 8°C
Water mass A	<34.92	<35.11	<35.07
Water mass B	34.92–34.96	35.11–35.15	35.07–35.20
Water mass C	34.96–35.05	35.15–35.20	35.20–35.25

Figure 5a,b which shows repeated salinity sections from 1987 and 1988 across the Rockall Plateau and into the Iceland Basin. The salinities in Figures 5a,b demonstrate a high salinity core in the flow. In 1987 the core depth was about 400 m, coinciding with region C of Figure 4 while the outer edge of the core and the most baroclinic part was in region B. In the summer of 1988 the high salinity core was less pronounced and about 100 m shallower.

The Area north and east of the Faroes. The fact that at least part of this flow seems to head towards the Faroes and the Iceland-Faroe Ridge makes it appropriate to compare the θS characteristics of the waters surrounding the Faroes to the waters just discussed.

The water flowing over the Iceland-Faroe Ridge from the Atlantic into the Norwegian Sea must come either from the eastern edge of the Iceland Basin with the well defined θS relationship of watermass B (Figure 3c) or from the area close to Faroe Bank, that is the region north of Faroe Bank and between Faroe Bank and the Faroe Plateau. This may be studied by comparing the θS characteristics of the three watermass types defined from the Gauss data to the results from the July 1987 Magnus Heinason cruise (Figure 1b). In Figure 6 the θS characteristics in this area (section 2, Figure 1b) is shown for this period. In this and following figures we show θS curves from Magnus Heinason as continuous traces with the watermasses A, B and C plotted on the same diagrams for comparison. The point to note is that the water north and east of Faroe Bank falls into the category of water mass type C previously defined as long as we consider temperatures above 5 or 6°C. At lower temperatures several of the stations are clearly influenced by Overflow water from the Norwegian Sea as is typical for this area. The upper waters (above 6°C) in this area thus could have come from the western edge of the Rockall Plateau with little or no modification.

Proceeding onto the Iceland-Faroe Ridge Figure 7a,b shows θS curves along sections 3 and 4 (Figure 1b). Above 7°C this water has the same characteristics as the water just discussed (watermass C) and thus seems to derive from the region just north of Faroe Bank or from the Faroe Bank Channel rather than from the open parts of the Iceland Basin. That interpretation is consistent with the flow map of Hansen and Meincke (1978) and recent drifter experiments and was proposed early in this century already by Helland Hansen and Nansen (1909). Below 7°C the water over the Iceland-Faroe Ridge becomes increasingly fresher compared to watermass C at the same temperature. This is especially the case for the eastern flank of the ridge as is seen on some of the stations in Figure 7b. In the Iceland Basin due west of the Iceland-Faroe Ridge, the 7°C isotherm is found at depths between 500 and 1000 m. Thus we would not expect water much colder than this to overflow the ridge eastwards as the Iceland-Faroe Ridge has a sill depth around 500 m.

The water over the Iceland-Faroe Ridge colder than 7 °C is usually considered a mixture of water masses from three origins: The Atlantic water crossing the ridge, the Norwegian Sea Deep Water (NSDW) (colder than –0.5 °C, salinity between 34.90 and 34.92) and water from the East Icelandic Current which is usually termed NI/AI water and has intermediate temperatures (2–4°C) and low salinities (around 34.8). Both of these colder watermasses are found on section 4 in almost pure form and mixing with one another and with the Atlantic water. The decrease in salinity on section 3 and 4 relative to section 2 at temperatures around 5–6°C indicate presence of NI/AI water especially.

Further east, sections 5 and 6 (Figure 8a,b) extend from the Faroes towards the north and east respectively. Again for temperatures above 7°C most of the stations have θS relations very similar to those close to Faroe Bank and on the western edge of the Rockall Plateau. They indicate continuation of water mass C as an eastward flow north of the Faroes and a branching of this flow southward into the Faroe-Shetland Channel in accordance with the accepted flow picture. Below 7°C we find again admixtures of NI/AI water.

The Faroe Channels. The θS characteristics of the upper parts of the Faroe-Shetland Channel and of the Faroe Bank Channel are seen in Figure 9a,b,c,d from the April-May 1987 cruise of Magnus Heinason (Figure 1c). Above 7°C we find again water of the same character although we find also more saline water (probably containing some NAW). Below 7 °C there is a clear difference between the eastern Faroe-Shetland Channel and the Faroe Bank Channel, however, as the NI/AI water which is clearly present in the Faroe-Shetland Channel is not as evident in the Faroe Bank Channel. On the easternmost section (section 7), Figure

9a shows clearly the occurrence of NI/AI water by the bend of the θS curves around 4 °C. The same feature is apparent in section 8 (Figure 9b) also from the eastern Faroe-Shetland Channel although to a smaller degree. But the two westernmost sections: 9, and 10 from the western Faroe-Shetland Channel and from the Faroe Bank Channel (Figure 9c and d) do not show this water unambiguously.

Discussion

In this paper we have traced a watermass (watermass C) from the western edge of the Rockall Plateau where a core of the North Atlantic Current impinges on the Plateau to the Iceland-Faroe Ridge region and the area north and east of the Faroes. For temperatures above 5-6 °C no significant modification is apparent in the θS curves from the source region to the Iceland-Faroe Ridge area. Having passed the Iceland-Faroe Ridge this water is mixed with both NSDW and especially NI/AI water and this mixture is advected eastward north of the Faroes and south into the Faroe-Shetland Channel.

From its ubiquitous presence in the Faroe region it is clear that this water (water mass C) is indeed MNAW and its high temperature definition in Figure 3a (salinity from 35.20 to 35.25 at 8°C) fits well with numbers found in the literature. There is, of course, the question which part of the θS curve should be called MNAW. Traditionally MNAW has been given fixed values for temperature and salinity which is more appropriate for a water type than for a water mass.

Following that tradition, only the high temperature part of the θS curve would be MNAW and we would need to introduce further names like IMNAW or LAW, but as long as the origin and formation of these water masses is not clear (and that question is beyond the scope of this paper), we will use the term MNAW to denote the water over the Rockall Plateau. Another question is to what degree it is appropriate to compare, as we have done, the Gauss data from the Iceland Basin and the Rockall Plateau to the Magnus Heinason data from the area around the Faroes. This presupposes an assumption of stationarity which may not be justified. With speeds on the order of 10 cm s^{-1} the water would need 2–3 months to flow from the western edge of the Rockall Plateau to the Faroese region and the fact that the two Faroese cruises precede the Gauss 1987 cruise by a couple of months makes the difference in timing worse. Comparing the results from the different cruises in regions where they overlap (Figure 10) indicates, however, that the data sets are consistent. There is indeed a tendency for the Magnus Heinason data to have higher salinities especially around 7°C, but the difference is not large and will rather strengthen the conclusions drawn.

In the Faroe Bank Channel and the area south of it, MNAW was also clearly present. It was mentioned in the introduction that a major part of this water has been suggested to derive from the Faroe-Shetland Channel. This is not consistent with our data for the period April-May 1987. The MNAW in the Faroe-Shetland Channel was mixed to a considerable degree with NI/AI water (Figure 9a and b) while the same was not the case for the Faroe Bank Channel (Figure 9c and d). This is an argument against a recirculation of MNAW around the Faroes, especially when taking into account that NI/AI water is mixed with the MNAW from fairly shallow depths down to some 500 m in the eastern Faroe-Shetland Channel as may be seen in Figure 11. The two stations in that figure show a picture which is fairly typical (Hansen, 1979) with vertically homogeneous water down to 400–500 m in the Faroe Bank Channel and the western part of the Faroe-Shetland Channel, but with vertically decreasing temperature and salinity in the eastern part of the Faroe-Shetland Channel due to the increasing amounts of NI/AI water.

A more convincing argument is obtained by considering the horizontal distribution of water properties. In Figure 12a and b the horizontal distribution of temperature and salinity at 300 m is shown for April-May 1987. In the Faroe Bank Channel and most of the western part of the Faroe-Shetland Channel the water at that depth was almost pure MNAW with temperatures above 7°C and salinities above 35.20, but due south of the southern tip of the Faroe Plateau there was a fairly sharp front and east of it temperature and salinity decreased below 4°C and 35.00 respectively at 300 m.

This front appears to be a persistent feature although its location changes somewhat (Hansen, 1985). Plotting the variation of properties at constant depth is, however, of debatable value if we assume isopycnal flow and indeed the variation of salinity on isopycnal surfaces between the eastern and western part of the area was smaller than on isobaric surfaces. This is seen in Figure 12c where salinity has been plotted on the surface σ_θ=27.50 for April-May 1987 and it would be consistent with a flow from the eastern Faroe-Shetland Channel to the Faroe Bank Channel, but when the depth of this surface is considered (Figure 12d) that becomes improbable. In the Faroe Bank Channel and most of the western part of the Faroe-Shetland Channel, the water was less dense than 27.50 down to depths exceeding 200 meters, but in the eastern Faroe-Shetland Channel almost all the water had densities exceeding this value, and there was no natural continuation from east to west.

For this period we may thus confidently state that the uppermost waters in the Faroe Bank Channel and most of the area due south of it must have come from the west directly rather than over the Iceland-Faroe Ridge and through the Faroe-Shetland Channel. This should not be taken to mean that there was no recirculation around the Faroes. On the shelf there is a persistent anticyclonic

flow around the islands. Also there is some evidence of eddying of the front south of the Faroe Plateau with blobs of water from the Faroe-Shetland Channel being released into the region west of the front. An example of that is evident in Figure 12. The bottom water of the Faroe Bank Channel is furthermore a direct continuation of NSDW from the Faroe-Shetland Channel and in the boundary between this flow and the upper water there is no doubt some entrained MNAW transported westwards. Nonetheless the major part of the upper water in the Faroe Bank Channel and the area south of it clearly came from the west.

Conclusion

In this paper we have used the similarity between θS curves of different regions to trace the flow pattern. Alternative explanations are of course possible if one takes into account water mass modifications other than mixing with surrounding waters, but the similarity argument is consistent with the data presented and is certainly the simplest interpretation of that data. On this assumption we find the MNAW in the Iceland-Scotland region to be fairly unmodified water from the North Atlantic Current, advected from the western Rockall Plateau over the Plateau towards the Faroe Bank region as water mass C in Figure 4. From that region the MNAW is advected into the western Faroe-Shetland Channel and into the Faroe Bank Channel and it is advected over the Iceland-Faroe Ridge and thence into the eastern Faroe-Shetland Channel.

References

Booth, D. A., and Ellett, D. J. 1983. The Scottish Continental Slope Current. Continental Shelf Research, 2 (2/3): 127–146.

Dooley, H., and Meincke, J. 1981. Circulation and water masses in the Faroese Channels during Overflow-73. Deutsche Hydrografische Zeitschrift, 34: 41–55.

Ellett, D. J., Kruseman, P., Prangsma, G. J., Pollard, R. T., van Aken, H. M., Edwards, A., Dooley, H. D., and Gould, W. J. 1983. Water masses and mesoscale circulation of North Rockall Trough waters during JASIN 1978. Philosophical Transactions of the Royal Society of London. A 308: 231–252

Ellett, D. J., and Martin, J. H. A. 1973. The physical and chemical oceanography of the Rockall Channel. Deep-Sea Research, 20: 585–625.

Hansen, B. 1979. Residual flow and temperature on the Faroe Plateau during the first half of 1978 in relation to the circulation. ICES CM 1979/C:18, 17 pp.

Hansen, B. 1985. The circulation of the northern part of the North Eastern Atlantic. Rit Fiskideildar, 9: 110–126.

Hansen, B., and Meincke, J. 1978. Eddies and Meanders in the Iceland-Faroe Ridge area. ICES CM 1979/C:35, 20 pp.

Harvey, J. G. 1982. θ-S relationships and water masses in the Eastern North Atlantic. Deep–Sea Research, 29: 1021–1033.

Helland–Hansen, B., and Nansen, F. 1909. The Norwegian Sea. Report on Norwegian Fishery and Marine Investigations, II (2), 390 pp.+suppl.

Hermann, F. 1967. The T-S diagram analysis of the water masses over the Iceland-Faroe Ridge and in the Faroe Bank Channel. Rapports et Procès-Verbaux des Réunions du Conseil International pour l'Exploration de la Mer, 157: 139–149.

Krauss, W. 1986. The North Atlantic Current. Journal of Geophysical Research, 91: 5061–5074.

Martin, J. H. A. 1976. Long term changes in the Faroe-Shetland Channel associated with intrusions of Iceland-Faroe Ridge Water during the period 1955–75. ICES CM 1976/C:22, 11pp.

Meincke, J. 1978. On the distribution of low salinity intermediate waters around the Faroes. Deutsche Hydrografische Zeitschrift, 31: 50–64.

Müller, T. J., Meincke, J., and Becker, G. A. 1979. Overflow–73: The distribution of water masses on the Greenland Scotland Ridge in August/September 1973 – A data report. Berichte der Institut für Meereskunde an der Universität Kiel, 62: 172 pp.

Ryder, C. 1901. Nogle undersøgelser over hav-strømmene i farvandene mellem Norge, Skotland og Grønland. Nautisk Meteorologisk Aarbog 1901, Copenhagen.

Sy, A. 1988. Investigation of large-scale circulation patterns in the central North Atlantic: The North Atlantic Current, The Azores Current, and the Meditterranean Water plume in the area of the Mid-Atlantic Ridge. Deep-Sea Research, 35: 383–413.

Tait, J. B. 1957. Hydrography of the Faroe-Shetland Channel 1927–1952. Marine Research Scotland 1957, No.2, 309 pp.

van Aken, H. M. 1988. Transports of water masses through the Faroese Channels determined by an inverse method. Deep-Sea Research, 35: 595-617.

van Aken, H. M. and Eisma, D. 1987. The circulation between Iceland and Scotland derived from water mass analysis. Netherlands Journal of Sea Research, 21(1): 1–15.

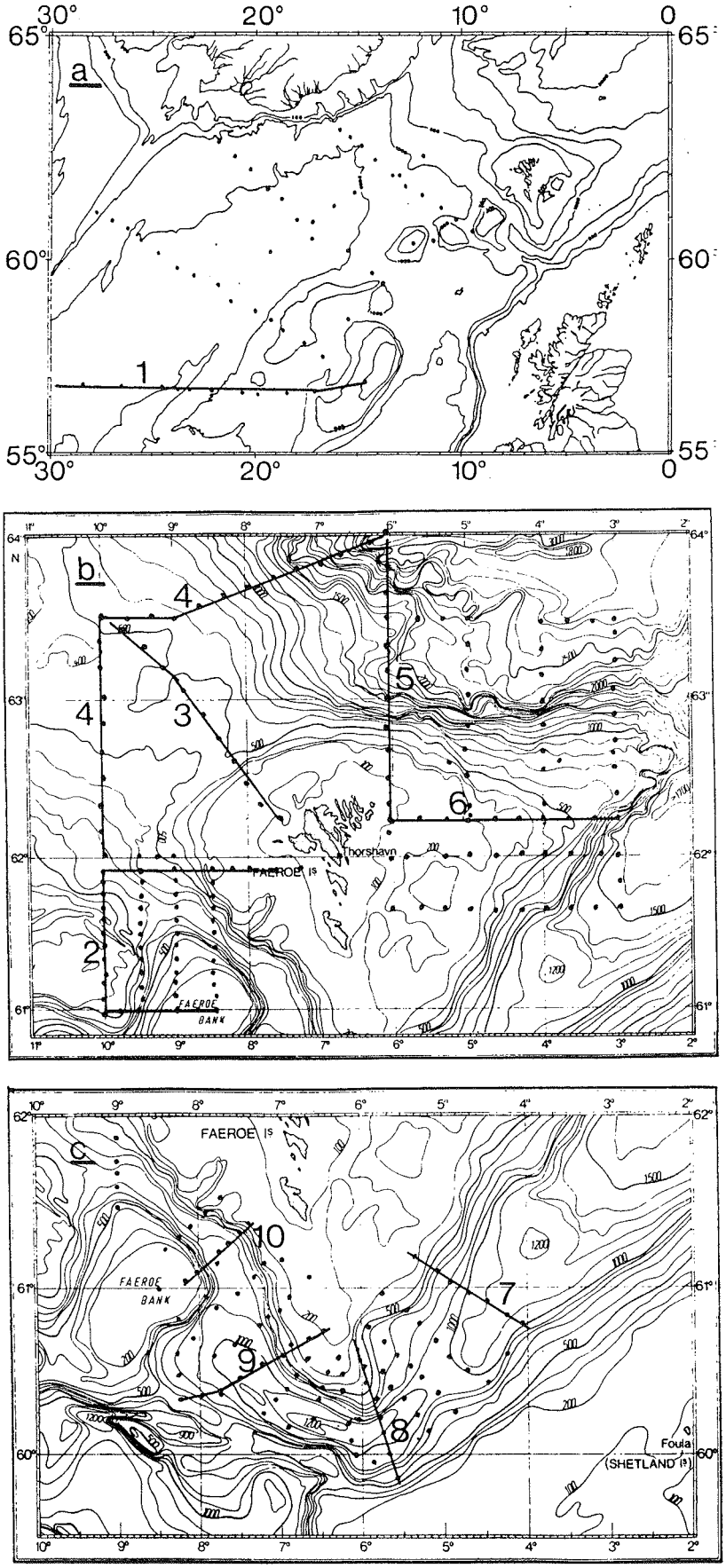

Figure 1a.: Stations on the Gauss August 1987 cruise discussed in this paper. b.: Stations of the Magnus Heinason July 1987 cruise. c.: Stations of the Magnus Heinason April-May 1987 cruise. The numbers denote sections discussed in the paper.

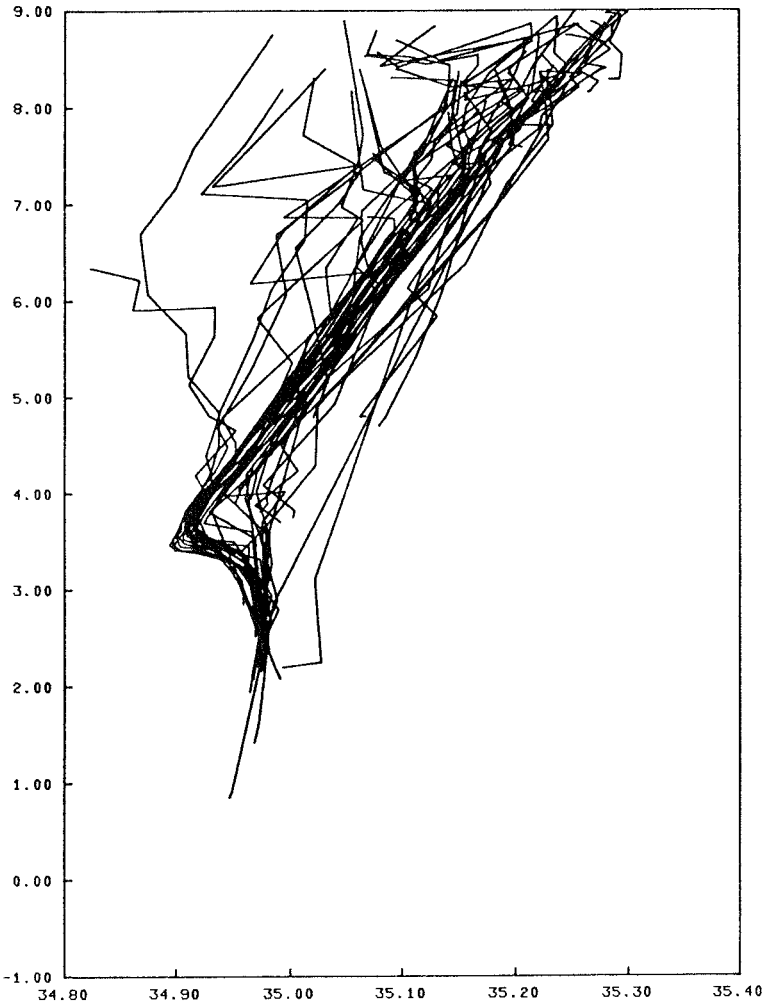

Figure 2. θS diagram of water bottle data below 100 m depth from the stations on Figure 1a.

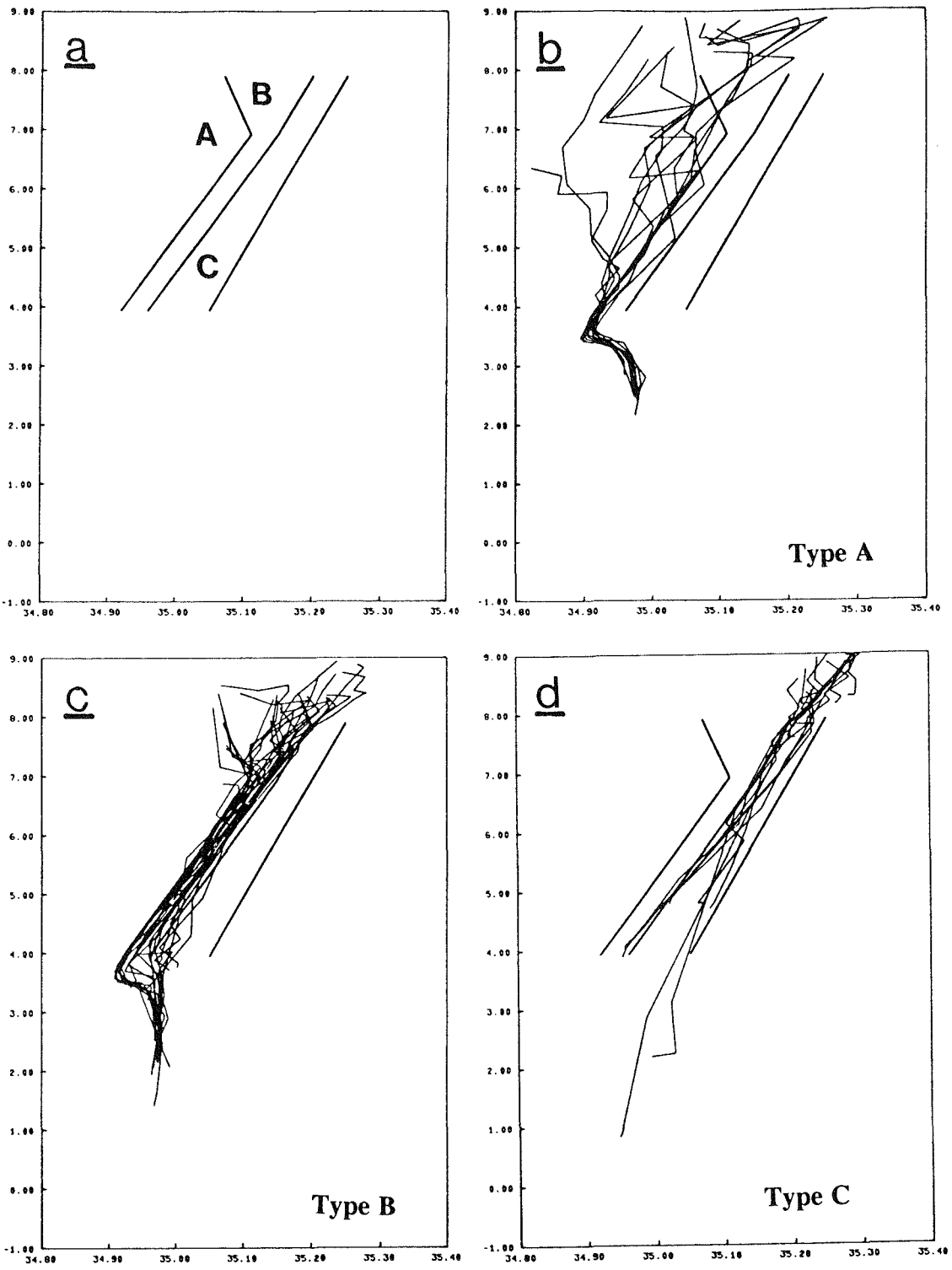

Figure 3 a.: Classification of the upper waters. b.: θS curves for Gauss 1987 stations of water mass type A. c.: θS curves for Gauss 1987 stations of water mass type B. d.: θS curves for Gauss 1987 stations of water mass type C.

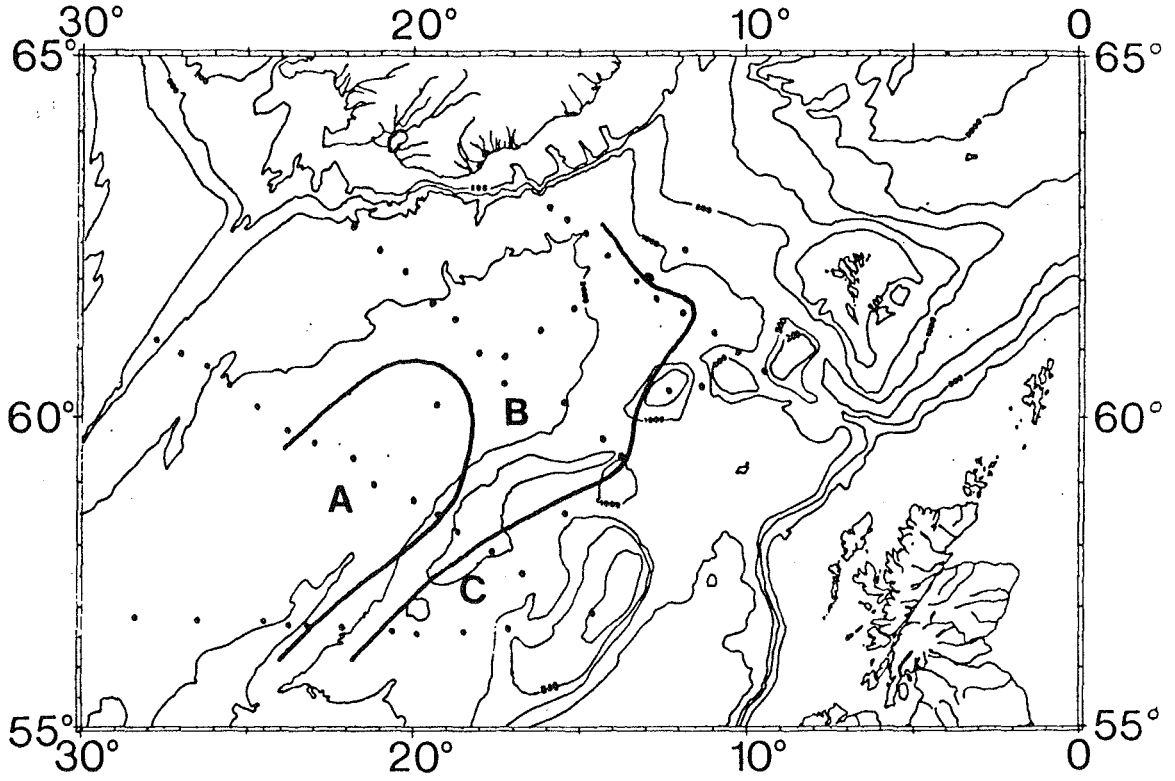

Figure 4. Geographical distribution of water masses A, B and C. in August 1987.

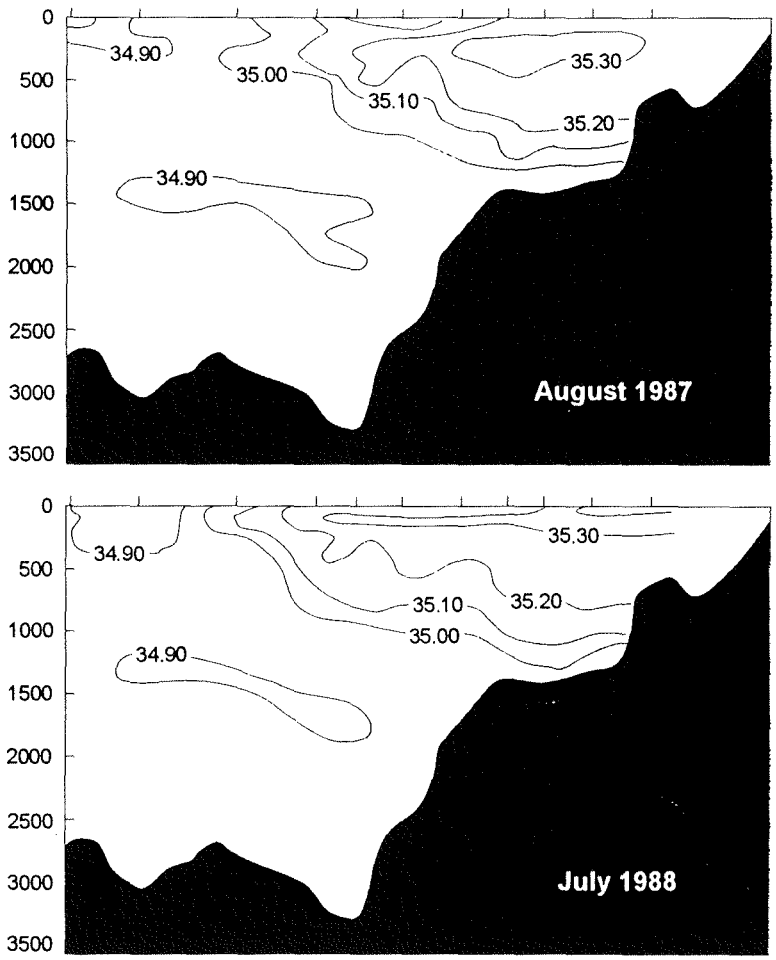

Figure 5 a.: Salinity across the Iceland Basin section 1, August 1987. b.: Salinity across the Iceland Basin section 1, July 1988.

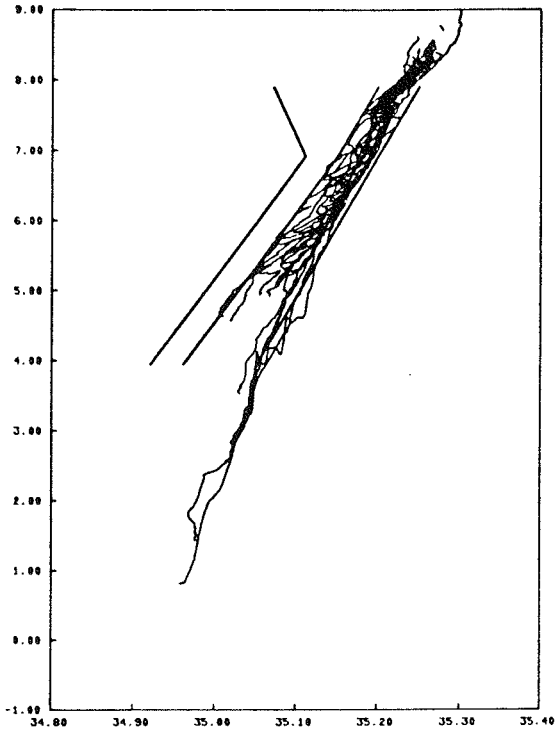

Figure 6. θS curves from CTD stations along section 2 in Figure 1b compared to Iceland Basin water mass types.

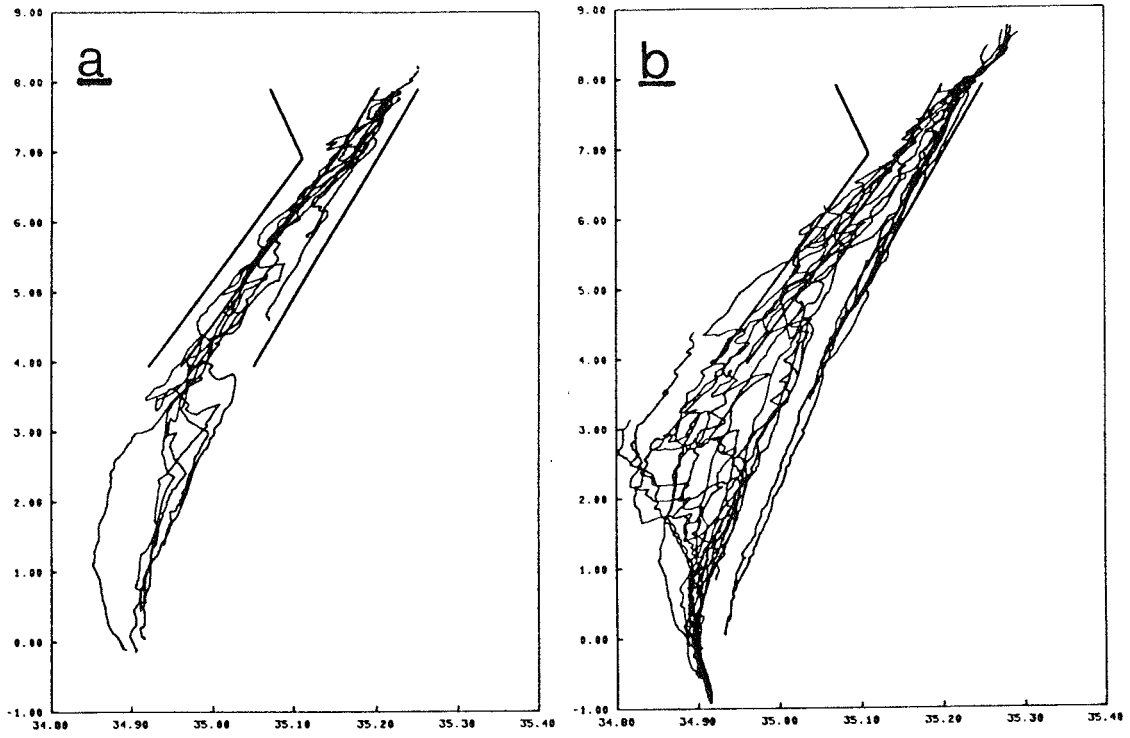

Figure 7 a.: θS curves along section 3. b.: θS curves along section 4.

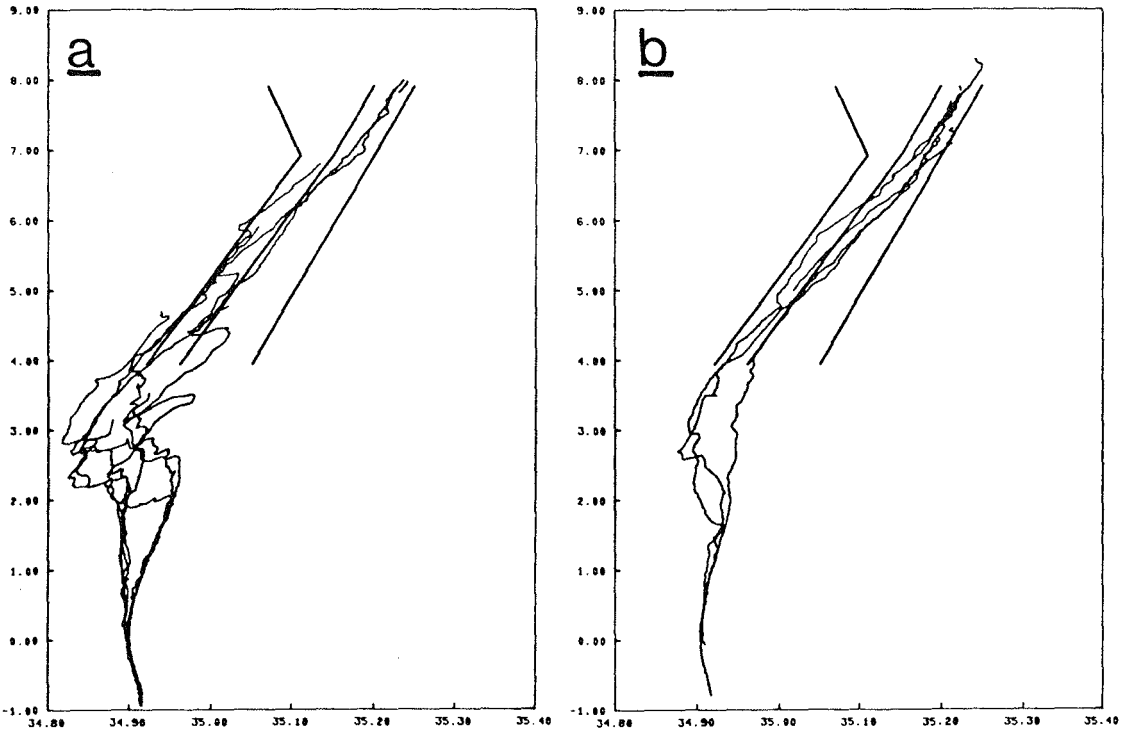

Figure 8 a.: θS curves along section 5. b.: θS curves along section 6.

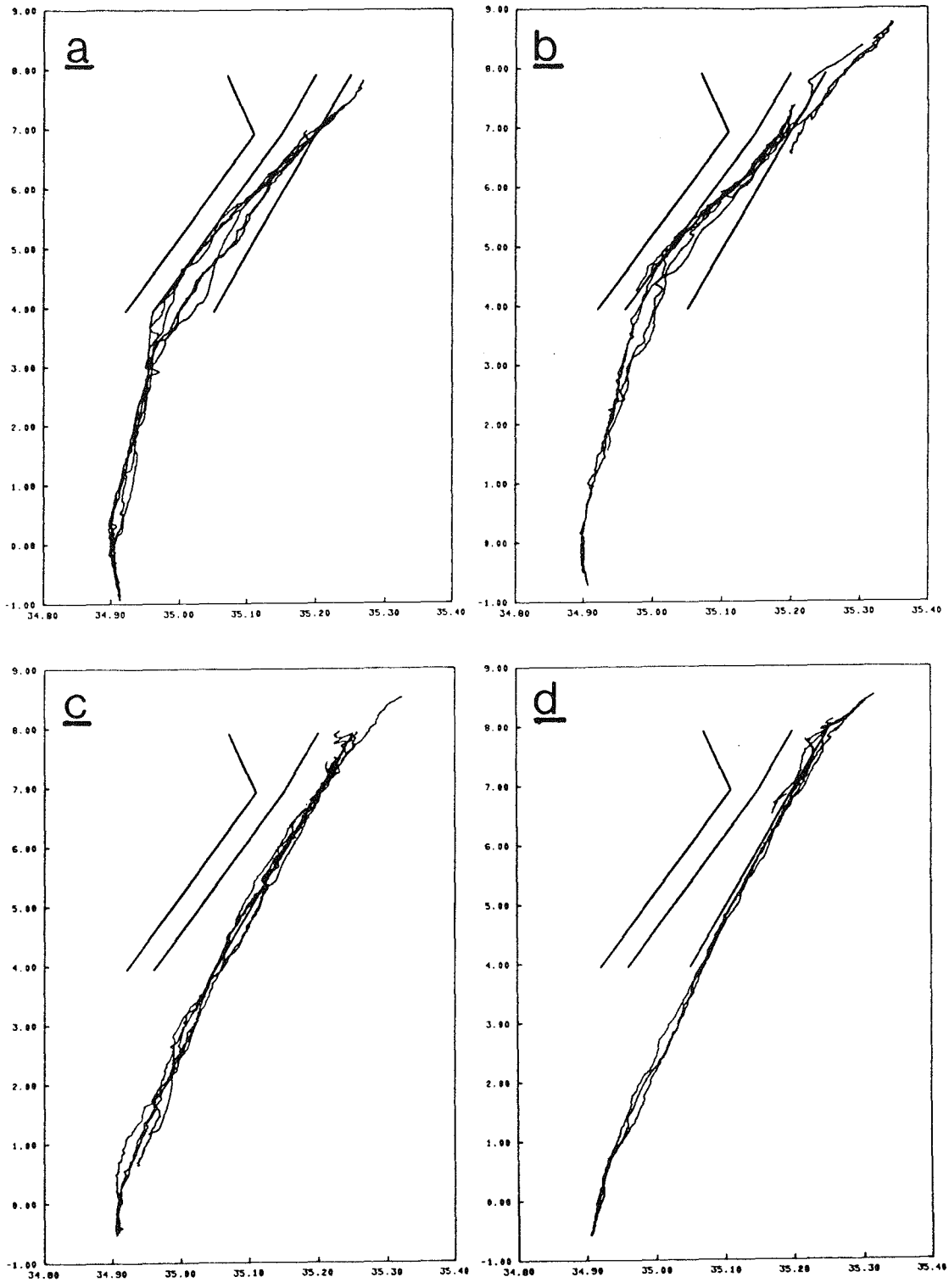

Figure 9 a.: θS curves along section 7. b.: θS curves along section 8. c.: θS curves along section 9. d.: θS curves along section 10.

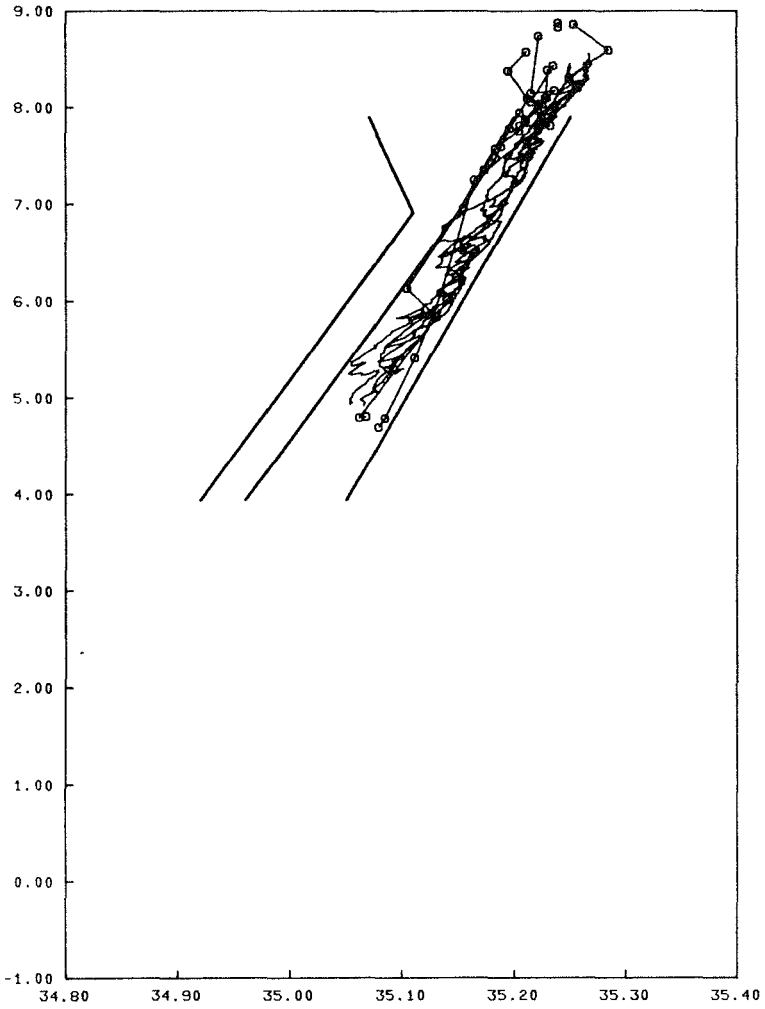

Figure 10. Comparison of Gauss water bottle data (circles connected by straigth lines) from August 1987 with Magnus Heinason July 1987 data (continuous curves) from the area northwest of Faroe Bank.

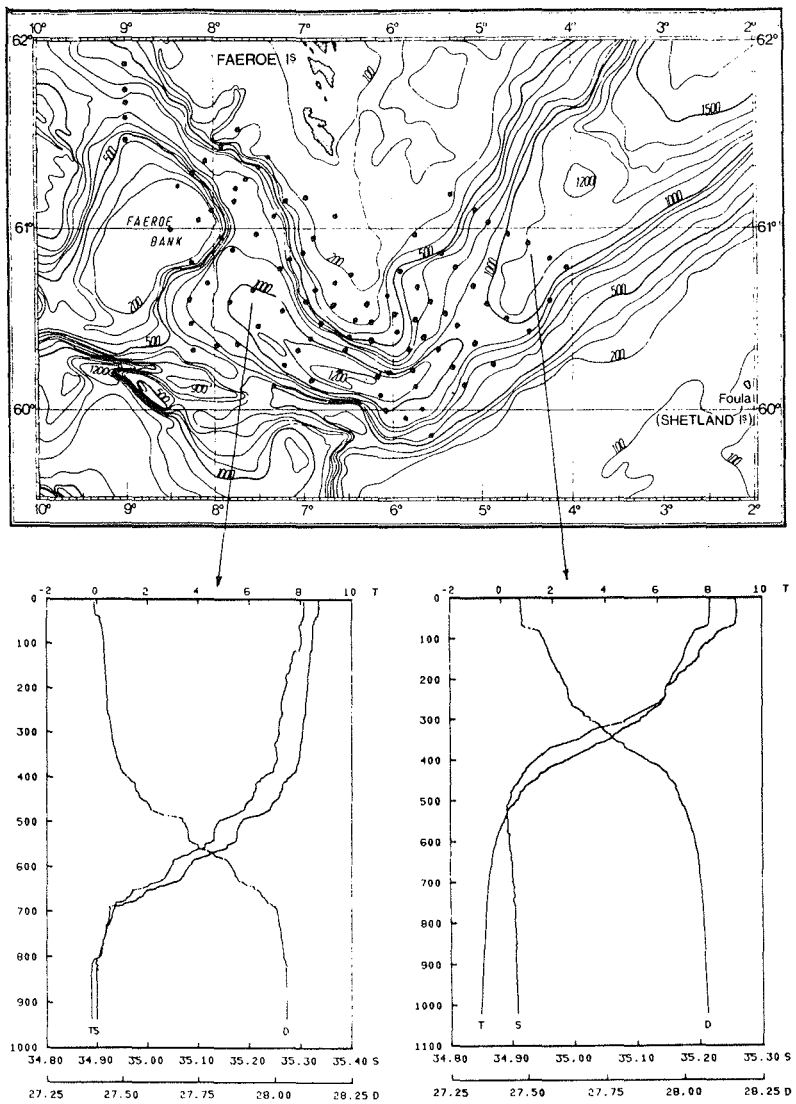

Figure 11. Vertical profiles of temperature (T), salinity (S) and σ_T (D) at two stations in the western and eastern part of the Faroe-Shetland Channel respectively.

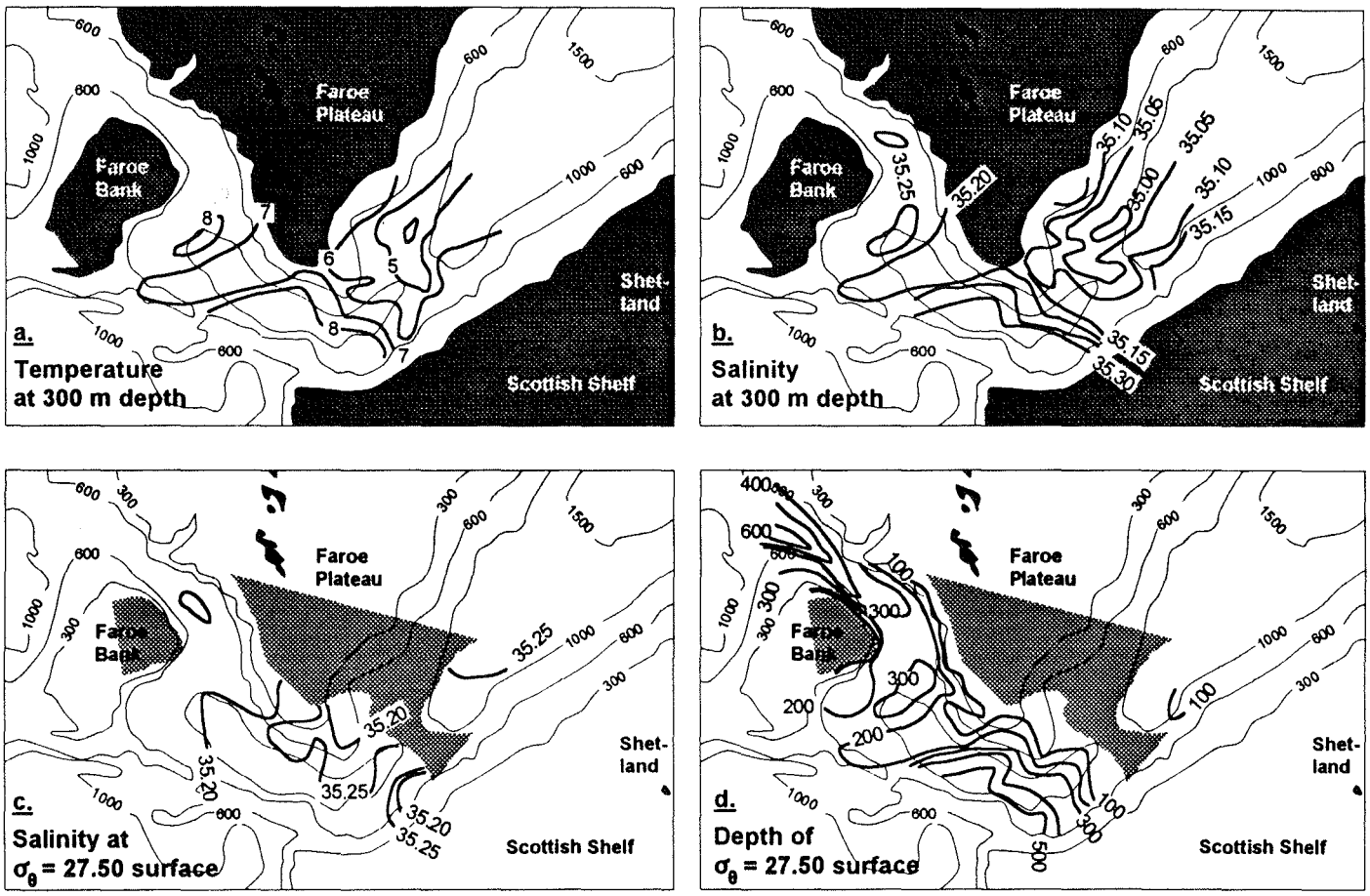

Figure 12. Horizontal distributions of properties in April-May 1987 based upon CTD observations at stations shown in Figure 1c. a.: Temperature at 300 m depth. b.: Salinity at 300 m depth. c.: Salinity at the σ_θ=27.50 surface. d.: Depth of the σ_θ=27.50 surface. Hatched areas in c and d have σ_θ exceeding 27.50 at all depths.

The passage of Atlantic Water east of the Faroes

Bogi Hansen[1], Odd H. Sælen[2], and Svein Østerhus[2]

[1]Fiskirannsóknarstovan, P.O.Box 3051, FR-110 Tórshavn, Faroe Islands.[2] Geophysical Institute, University of Bergen, Bergen, Norway.

Based on a paper presented to the ICES Hydrography Committee as ICES CM 1988/C:29

Current measurements made during the joint Nordic Expedition north of the Faroes in June 1986 showed that a considerable amount of Atlantic water in that period flowed through a section running north from the Faroes into the Norwegian Sea. As a continuation of that project an experiment in July 1987 with two ships studied the further fate of the water. The combined results from CTD and current meter moorings confirm the concept of a flow division with part of the water continuing east and northeast into the Norwegian Sea proper while part flows southward into the Faroe-Shetland Channel. The divergency seems, however, to be more a result of highly variable flows on timescales of days to weeks rather than of stationary divergent flows.

Keywords: Faroe region, Norwegian Sea, Atlantic water

Introduction

It has been known from the beginning of this century that there is a more or less continuous flow between Iceland and the Faroes of warm saline water from the Atlantic to the Norwegian Sea (Nielsen, 1904; Helland-Hansen and Nansen, 1909). Together with the flow through the Faroe-Shetland Channel, this flow is the major transport of Atlantic water into the cold seas north of the submarine ridge system from Greenland to Scotland and the amount of water (and heat) exchanged is an important parameter. Estimates of the transport value have varied almost within an order of magnitude, but in recent years there have been indications that the number is rather in the high end of these estimates making it even more important to determine its size.

Traditionally the Faroe-Shetland Channel has been assumed to carry by far the major part of the transport, but there is no real evidence to support that assumption and the transport of Atlantic water over the Iceland-Faroe Ridge may well be significant. Therefore, attempts to estimate it should be given high priority.

This line of arguments was the main reason for the *"Nordisk Kollegium for Fysisk Oceanografi"* to initiate a Nordic project on the Atlantic flow over the Iceland-Faroe Ridge. This project has later been coordinated with the more general *NANSEN* (North Atlantic - Norwegian Sea ExchaNge) project within ICES. Within the Nordic project, three field experiments have been carried out in the summers of 1986, 1987 and 1988. In 1986 the experiment aimed at establishing a snapshot value for the transport. Using CTD data and a line of 7 current meter moorings along 6°05' W north from the Faroes, it was possible to arive at an estimate of approximately 3 Sv (10^6 m^3 s^{-1}) of Atlantic water flowing eastward north of the Faroes. As the observational period was not much longer than a week this number is only an indication of the typical transport, but its size confirms that the area between Iceland and the Faroe Islands is one of the key areas for exchange between the Atlantic and the northern seas.

It would have been a natural continuation of the 1986 experiment to acquire longer time series of current measurements in order to establish a more representative transport value, but the heavy fishing activity in the area makes that a risky business as past experience proves and it probably requires other measurement techniques rather than moorings. It was therefore decided to aim the 1987 fieldwork at studying the further fate of the Atlantic water after its passage over the Iceland-Faroe Ridge. This paper presents preliminary results from that attempt.

The Atlantic water north of the Faroes has by tradition been termed *Modified North Atlantic Water* (MNAW) although it appears (Becker and Hansen, 1988) that this is fairly unmodified water from the North Atlantic Current flowing over the Rockall Plateau before turning northward just west of the Iceland-Faroe Ridge. Having crossed the ridge this water is mixed with water from the East Icelandic Current which by tradition is called NI/AI water (North Icelandic/Arctic Intermediate) and the *Norwegian Sea Deep Water* (NSDW). Thus the eastgoing flow north of the Faroes contains these three water masses. Usually the Atlantic water is concentrated as a wedge against the Faroe Plateau. The boundary

reaches the bottom on the Faroe slope at depths around 500 m and slopes upward so that it reaches the surface usually between 63°30' N and 64° N. Further north one finds in addition Atlantic water in a surface layer mixed with NI/AI water with increasing amounts of this latter water mass with depth until the NSDW starts to dominate the water at depths exceeding about 500 m.

When the Atlantic water and the other accompanying water masses have passed the Faroes and approach the northeastern corner of the Faroe Plateau one generally observes a divergence of isolines and the question arises whether the water continues directly towards the east into the Norwegian Sea proper or deflects into the Faroe-Shetland Channel. Nielsen (1904) held to the former view and he stated: *The East-Icelandic polar current which moves through the Jan Mayen-Channel in a southern or southeastern direction, and the warm Atlantic water flowing towards the northeast meet to the north of the Faroe-Iceland-ridge, and the resulting movement goes towards the east, till, on the western side of the current passing through the Faroe-Shetland-channel, it turns again and assumes its former direction towards the north-east and north, in order to join, later, the rotation movement in the Norwegian Sea.*

Helland-Hansen and Nansen (1909), however, disagreed with Nielsen: *This may perhaps sometimes happen; but as a rule it is not the case. The observations from May and August 1902 to 1904, show clearly a southward bend of the equilines, proving that water from the Norwegian Sea enters the channel from the north, and that the Atlantic water is moving southwards along the eastern side of the Fœroes.*

Kiilerich (1928) largely agreed with this latter view, but stated that occasionally it behaved as described by Nielsen (1904). He did not cite any evidence, however. Martin (1966), on the other hand, states: *Probably most of the Atlantic water diluted north of the Faroes, flows directly into the Norwegian Sea, the remainder flowing south westwards into the eddy systems of the Faroe-Shetland Channel.*

The ultimate fate of the Atlantic water passing the Iceland-Faroe Ridge seems clear. That part of it which goes into the Faroe-Shetland Channel is to a large extent recirculated into the Norwegian Sea by the eastgoing flow in the channel (Hansen, 1985; Van Aken and Eisma, 1987; Becker and Hansen, 1988), but as the citations above demonstrate, it is not quite clear what fraction this is. Unfortunately most of the elder data from this region does not have sufficient spatial coverage to answer that question and also a definite answer requires current measurements as well as the classical hydrographic data.

The 1987 Nordic expedition was designed to study this problem of the Atlantic flow northeast of the Faroes in more detail.

Observations

The results of this paper are mainly based on data from the cruises of two research vessels working in the area north and east of the Faroes. The Norwegian vessel Håkon Mosby in the period 27 June to 10 July 1987 and the Faroese vessel Magnus Heinason in the period 3 July to 13 July 1987. Both ships did CTD work and deployed current meter moorings. We shall discuss only the data obtained from the region north and east of the Faroes. As the hydrography of this region changes on short timescales it was found convenient to divide the CTD survey into two parts with part 1 from 27 June to 1 July including the first part of the Håkon Mosby data and part 2 from 3 July to 10 July with the rest of the Håkon Mosby data and all the Magnus Heinason data. Figure 1 shows the location of moorings and CTD stations for the two parts of the survey.

The CTD data was on both ships obtained by Neil Brown CTD calibrated by salinity samples taken on every station on the Håkon Mosby and every third station on Magnus Heinason. Both datasets have accuracies of the order of or better than 0.01 in salinity. Of the 8 current meter moorings deployed only one was lost. So four Norwegian moorings were recovered (C, N1, N2 and N3) and most of the instruments on these had functioned properly. The Faroese moorings (F1, F2 and F3) were all recovered, but with only one current meter on each with useable data. The current meters used were Aanderaa meters. Table 1 lists current meter records obtained from these instruments.

Results

We shall not in this paper present all the CTD data obtained. A data report is being prepared. A synopsis of the data is given by Figure 2, Figure 3 and Figure 4 which present a selection of horizontal maps and sections. Horizontal maps of T and S at three different depths are seen in Figure 2 for the first part and in Figure 3 for the second part of the survey. In Figure 4 three sections of potential temperature, salinity and density give an impression of the vertical variation of parameters at three key locations.

Table 1 Data on current meters recovered successfully during the 1987 Nordic expedition.

Mooring	Position		Depth (m)		Period
	Latitude	Longitude	Bott.	Obs.	
C	62°49' N	6°06' W	500	50	29.06–09.07 1987
C	62°49' N	6°06' W	500	100	29.06–09.07 1987
N1	62°32' N	4°39' W	500	50	29.06–09.07 1987
N1	62°32' N	4°39' W	500	100	29.06–09.07 1987
N1	62°32' N	4°39' W	500	200	29.06–09.07 1987
N2	62°46' N	4°26' W	950	50	29.06–09.07 1987
N2	62°46' N	4°26' W	950	100	29.06–09.07 1987
N2	62°46' N	4°26' W	950	300	29.06–09.07 1987
N3	62°14' N	3°33' W	550	50	28.06–09.07 1987
N3	62°14' N	3°33' W	550	100	28.06–09.07 1987
N3	62°14' N	3°33' W	550	300	28.06–09.07 1987
F1	62°15' N	6°03' W	100	50	02.07–11.09 1987
F2	62°14' N	5°02' W	200	100	02.07–10.07 1987
F3	62°12' N	4°06' W	350	300	02.07–10.07 1987

The current meter results are also presented only to the extent relevant to the overall flow patterns pertinent to the problem discussed in this paper. These are presented in Figure 5 as progressive vector diagrams superimposed on a map of the bottom topography. Note that the three Faroese current meter moorings F1, F2 and F3 cover a shorter period than the Norwegian ones (Table 1).

Discussion

We will consider first the northern part of the region. It is only from the second part of the cruise that the CTD station grid is sufficiently dense to give a horizontal picture of the hydrography north of the Faroes and indeed the variability is such that even in this case it is difficult to draw isolines unambiguously. In spite of this difficulty it seems clear that the Atlantic water north of the Faroes is at least partly split up. On section 1 along 6°07' W shown on Figure 4a the Atlantic water has the typical wedge shape, but the wedge appeared narrower on the 1987 cruise than on the 1986 cruise (Hansen *et al.*, 1986) and further east there appears to be an eddy or meander of Atlantic water separated from the rest of the Atlantic water by colder and fresher water.

In the southern part of the region the CTD station grid was sufficiently dense for both parts to give consistent horizontal maps of temperature and salinity especially over the slope and Figure 2 and Figure 3 demonstrate a difference between the two parts. In the first part there was an apparently continuous tongue of cold and relatively low-salinity water extending from the eastern corner of the Faroe Plateau southwestwards over the slope of the plateau. In the second part of the survey, the cold tongue was still found over the eastern slope of the Faroe Plateau. On section 2 (Figure 4b), the core of the tongue appears at approximately 300 meters depth as a salinity minimum with salinities approaching 34.90 indicating a high percentage of NI/AI water from the East Icelandic Current, but now the tongue seems to have split up with a more or less isolated eddy in the southernmost part (Figure 3). Apparently, a tongue containing large amounts of NI/AI water has progressed from the area north of the Faroes splitting the Atlantic water and continued southwards over the slope of the eastern Faroe Plateau.

This tongue seems to be a fairly regular feature (Hermann, 1952), but apparently highly variable in extent. The present data set indicates variability on very short timescales. It appears that during the week separating the two parts, the tongue released an eddy into the Faroe-Shetland Channel and partly retreated. This is reflected also in the results from current meter mooring F3 lying close to the core of the tongue, although further north. In Figure 6 are shown temperature and north component of flow from this instrument and it is seen that the increase in

temperature occurring on 5 July is associated with a reduction of southward going flow.

It is not clear whether this tongue has isolated completely the Atlantic water in the northeastern part of the region from the rest of the Atlantic water. The isolines may converge east of the observational area making this feature a meander rather than an eddy. It is known that this occurs sometimes. During the herring investigations in June 1951 there was thus a meander giving rise to a fairly similar distribution (Hermann, 1951). In any case there can be little doubt that the Atlantic water in the northeastern part of the observational area has passed eastwards north of the Faroes and there is no indication that it flowed into the Faroe-Shetland Channel. The resultant current vectors at N2 (Figure 5) did not indicate any significant southward flow at this site. The uppermost current meter at 50 m depth clearly was in Atlantic water all the time, as is seen from instrument temperature and it is notable that this instrument had the most northward going component of the flow. The instrument a 100 m seems to have been in mixed water; partly Atlantic and partly NI/AI and had a resultant flow due eastward.

Transport of Atlantic water into the Faroe-Shetland Channel thus should be looked for inshore of N2. If we consider the progressive vector diagrams at site N3 situated on the eastern corner of the Faroe Plateau then the two uppermost of these show a variable flow pattern changing from northgoing to southgoing flow. For both of these instruments, temperature stayed above 7°C throughout the period indicating domination by Atlantic water. The deepest instrument (at 300 m) showed steady flow towards the southwest along the topography, but the temperature at that depth only occasionally exceeded 4°C indicating that only little Atlantic water was present.

The site N3 thus, at least for the period investigated, would appear to be on the border of net inflow of Atlantic water to the Faroe-Shetland Channel. West of N3 was the cold tongue previously described and although its deeper parts contained little Atlantic water, still the upper 100-200 meters were dominated by Atlantic water. Of the three current meters on site F3 only the deepest one at 300 m functioned properly. This instrument had a consistent southward component throughout the experiment (Figure 6), but only during the second part was the water flowing past it mainly of Atlantic origin, based on its temperature. Together with the horizontal distributions of temperature and salinity at 50 m depth in Figures 2 and 3, these results indicate, however, a net flow southwards into the Faroe-Shetland Channel in the region around F3. As has been mentioned, however, the flow in this region seems to vary in strength on short timescales.

It remains to discuss the flow over the shelf and inner slope region east of the Faroes. The water in this part clearly was almost pure Atlantic water. Furthermore it is well known from extensive current measurements that the shallow shelf water due east of the Faroes has a net southward component (Hansen, 1985). That flow seems to be more or less a closed circulation around the islands, but the indications of southwestward flow, both due east of the Faroes and also at site F3, argue for a continuous southwestward going flow over the eastern part of the Faroe Plateau from shallow depths out to the slope region.

This flow pattern was suggested already by Helland-Hansen and Nansen (1909) and is implicit in much of the work done since then in the region. Therefore the flow direction at site F2 in Figure 5 was not expected. The most immediate explanation for this discrepancy would be instrument failure and one is tempted to suggest a 180° compass error, but comparing the tidal part of the flow at the three sites F1, F2 and F3 it is seen that they are to a large extent in phase. Thus the flow direction at F2 appears to be real.

We are left with two options. Either the observational period was atypical at least for the region over the eastern Faroe Plateau or else there is a region over the eastern Faroe Plateau with net flow northwestward out of the Faroe-Shetland Channel. There are some indications of atypical flows during the 1987 measurements. It was mentioned that the wedge of Atlantic water north of the Faroes was rather narrower during the 1987 cruise compared to the 1986 cruise. Also the current velocity in the top layer at mooring C was smaller in 1987 than 1986 almost by a factor of two. We have no proof, however, that 1986 was more typical than 1987 so the possibility remains that the flow at F2 is a typical feature. If so then the simplest explanation for it would be a return circulation from the southwest-going flow at site F3.

Conclusion

The results presented indicate that Atlantic water from north of the Faroes is transported both directly into the Norwegian Sea and into the Faroe-Shetland Channel. The transport processes in both directions, however, seem to be highly variable on time scales of weeks or maybe even days and the flow pattern over the eastern Faroe Plateau may be more complicated than has been realised. With the short data set obtained we can not determine to what degree these results are representative but it is well known (Hansen and Meincke, 1979) that not only are eddies and meanders a prominent feature of the frontal zone north of the Faroes, but also in the Faroe-Shetland Channel eddies are common. Further east it has also been known for a long time (Sælen, 1959) that eddies proliferate in the Norwegian Atlantic Current and the northeastern corner of the Faroe Plateau

could be one of the natural production sites for these structures. It had been hoped that transport estimates could be obtained for the two branches of Atlantic water, but the variability of the process requires more data for such an estimate.

References

Becker, G., and Hansen, B. 1988. Modified North Atlantic Water. ICES CM 1988/C:17.

Hansen, B. 1985. The circulation of the northern part of the North Eastern Atlantic. Rit Fiskideildar, 9: 110–126.

Hansen, B., and Meincke, J. 1979. Eddies and Meanders in the Iceland-Faroe Ridge area. Deep-Sea Research, 26A: 1067–1082.

Hansen, B., Malmberg, S. A., Sælen, O. H., and Østerhus, S. 1986. Measurement of flow north of the Faroe Islands June 1986. ICES CM 1986/C:12, 14 pp.

Helland-Hansen, B., and Nansen, F. 1909. The Norwegian Sea. Report on Norwegian Fishery and Marine Investigations, II (2), 390 pp.+suppl.

Hermann, F. 1951. Hydrographic conditions in the south-western part of the Norwegian Sea, 1951. Annales Biologiques du Conseil International pour l'Exploration de la Mer, VIII: 23–26.

Hermann, F. 1952. Hydrographic conditions in the southern part of the Norwegian Sea, 1952. Annales Biologiques du Conseil International pour l'Exploration de la Mer, IX: 22–25.

Kiilerich, A. 1928. Hydrography. *In* Zoology of the Faroes, Vol.I, part 1. Ed. by A. D. S. Jensen, W. Lundbech, Th. Mortensen, R. Spärck. Høst og Søn, Copenhagen.

Martin, J. H. A. 1966. The bottom waters of the Faroe-Shetland Channel. Some Contemporary Studies in Marine Science, pp. 469–478. Harold Barnes, Ed., George Allen and Unwin Ltd., London.

Nielsen, J. N. 1904. Hydrography of the waters by the Faroe Islands and Iceland. Meddelelser fra Kommisionen for Havundersøgelser. Serie: Hydrografi, I (4), 29 pp.

Sælen, O. H. 1959. Studies in the Norwegian Atlantic Current, Part I: The Sognefjord section. Geofysiske Publikationer, XX (13).

Van Aken, H. M., and Eisma, D. 1987. The circulation between Iceland and Scotland derived from water mass analysis. Netherlands Journal of Sea Research, 21 (1): 1–15.

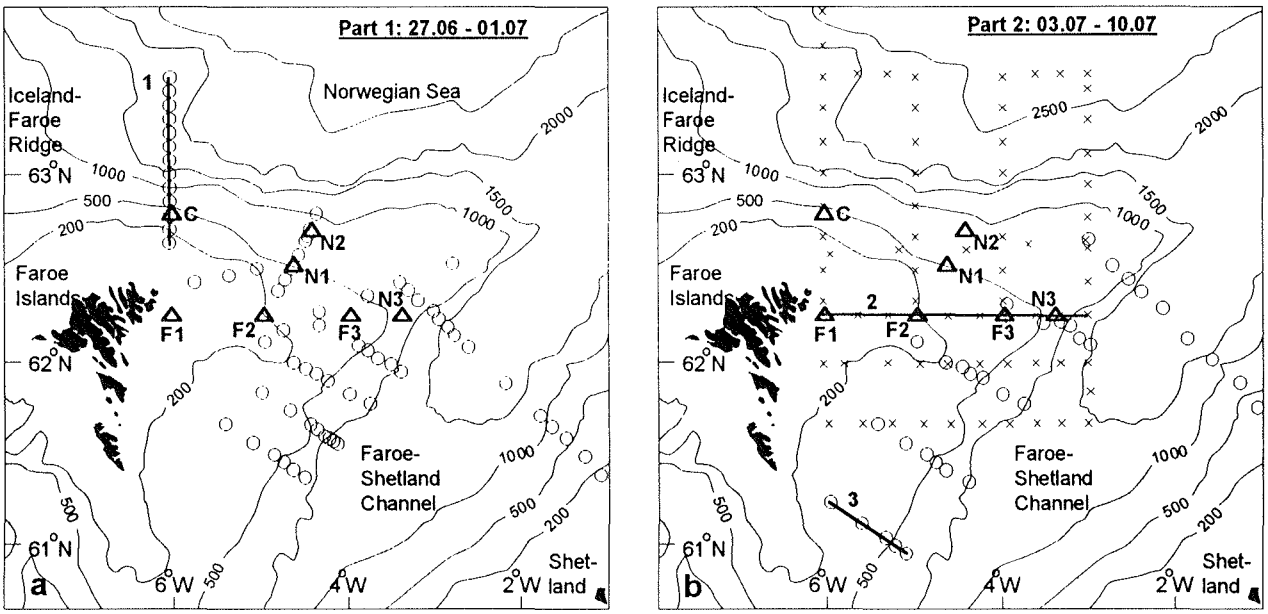

Figure 1. CTD Stations and current meter moorings on the cruises of R/V Håkon Mosby and R/V Magnus Heinason in June-July 1987 north of the Faroes. Open circles: Håkon Mosby CTD stations. Crosses: Magnus Heinason CTD stations. Triangles: Current meter moorings. Numbered lines indicate vertical sections referred to in the paper. a) First part of the survey (27 June - 1 July). b) Second part of the survey (3 July - 10 July).

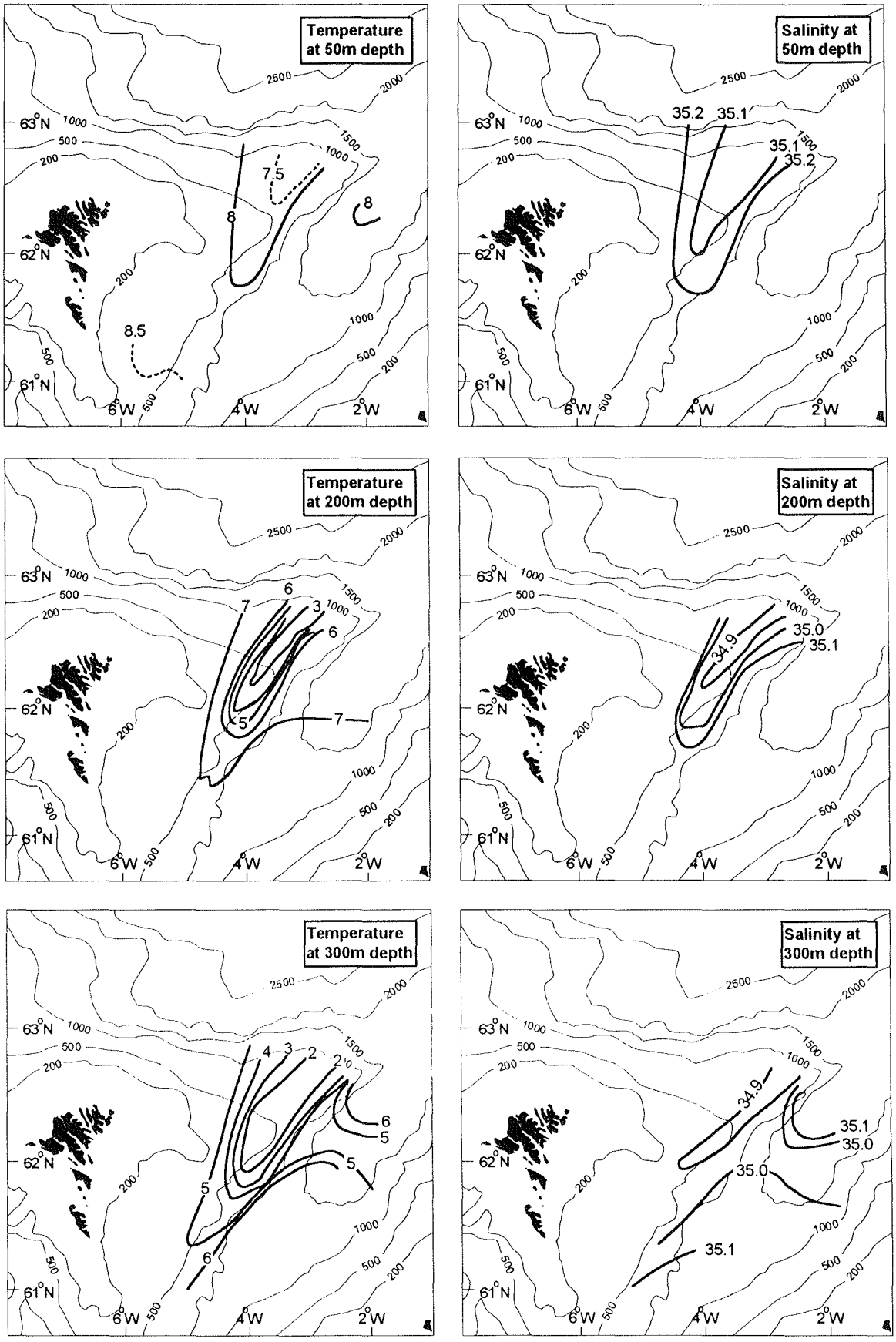

Figure 2. Temperature in °C (left) and salinity (right) from CTD stations during the first part of the survey (27.06 – 01.07 1987) at depths of 50 m, 200 m and 300 m.

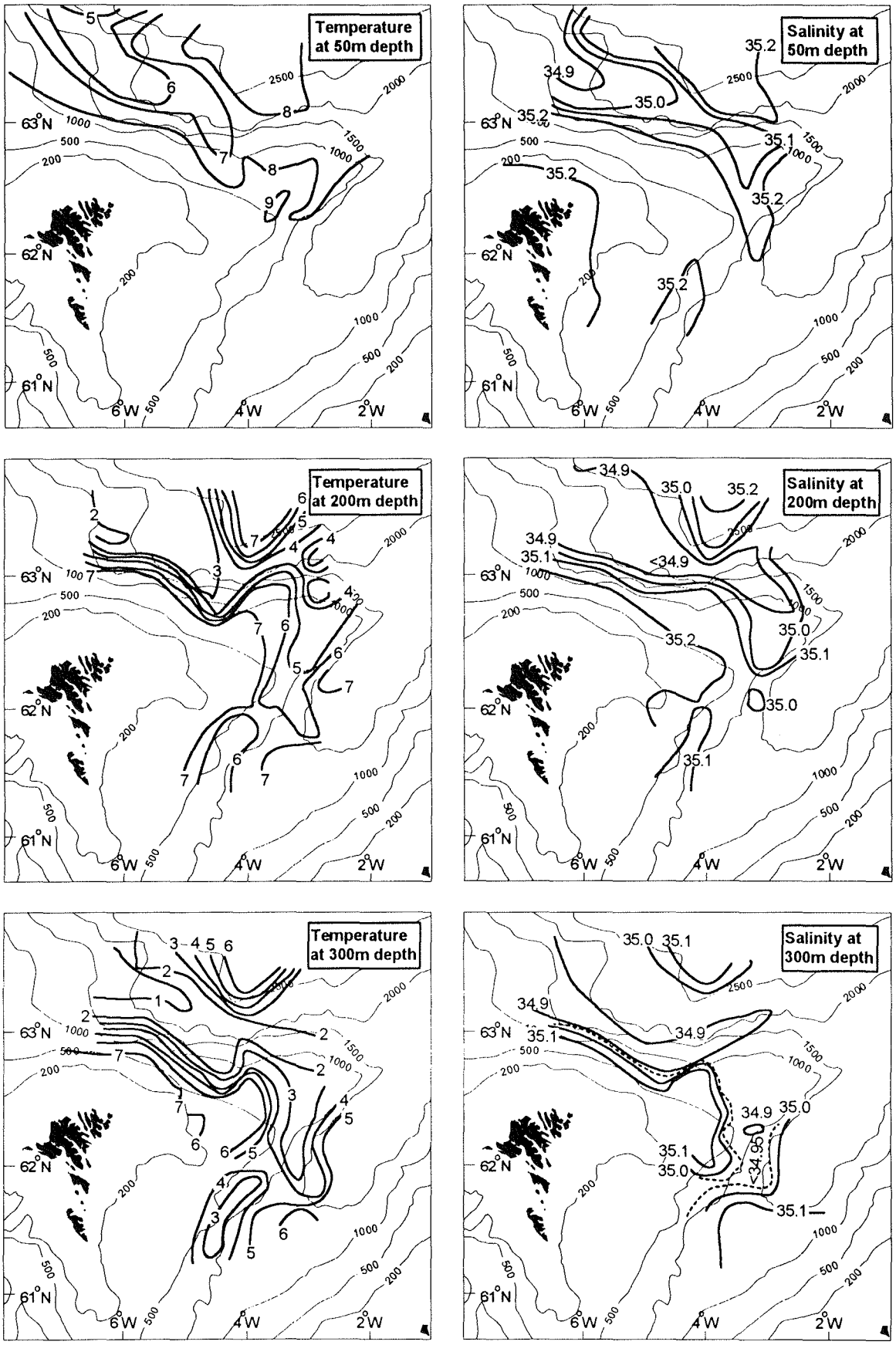

Figure 3. Temperature in °C (left) and salinity (right) from CTD stations during the second part of the survey (03.07 – 10.07 1987) at depths of 50 m, 200 m and 300 m.

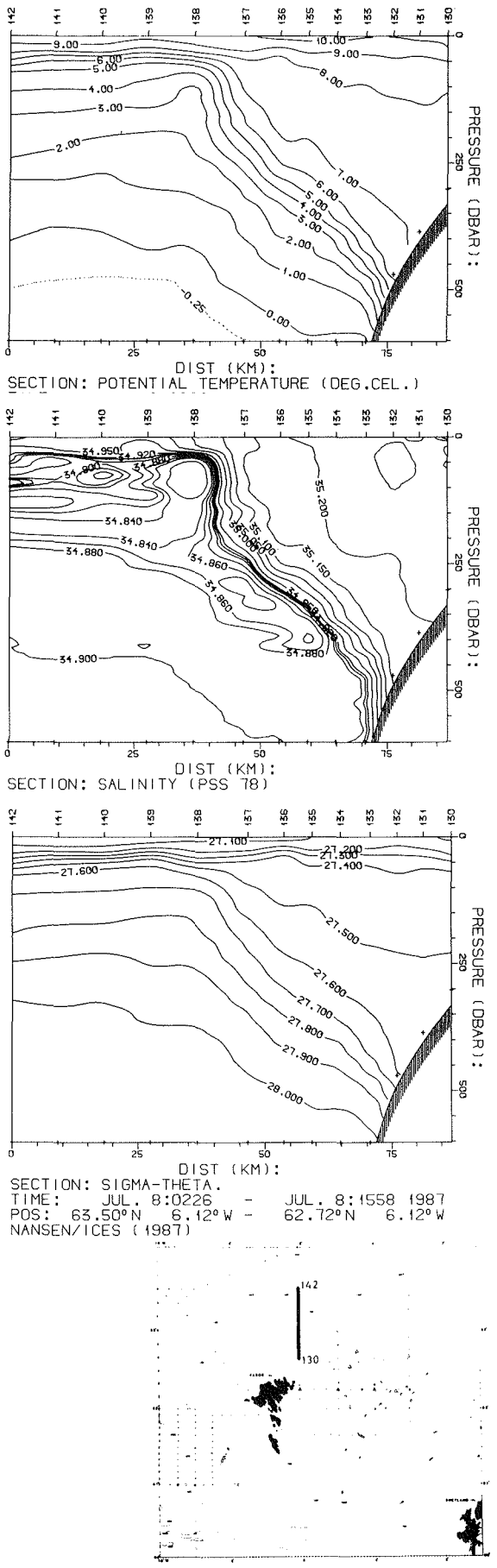

Figure 4a. Vertical sections of potential temperature (above), salinity (middle) and sigma theta (below) along section 1 from R/V Håkon Mosby.

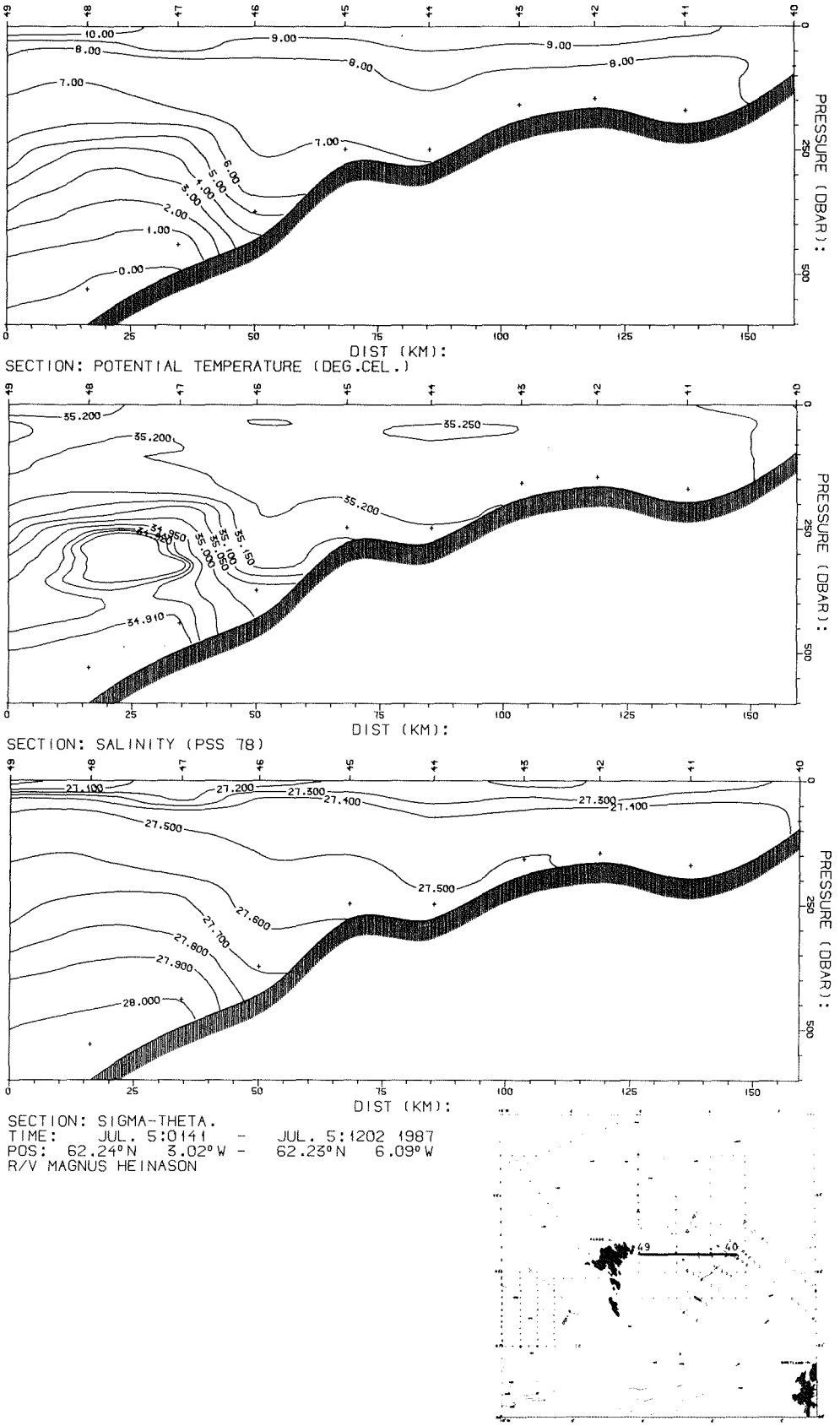

Figure 4b. Vertical sections of potential temperature (above), salinity (middle) and sigma theta (below) along section 2 from R/V Magnus Heinason.

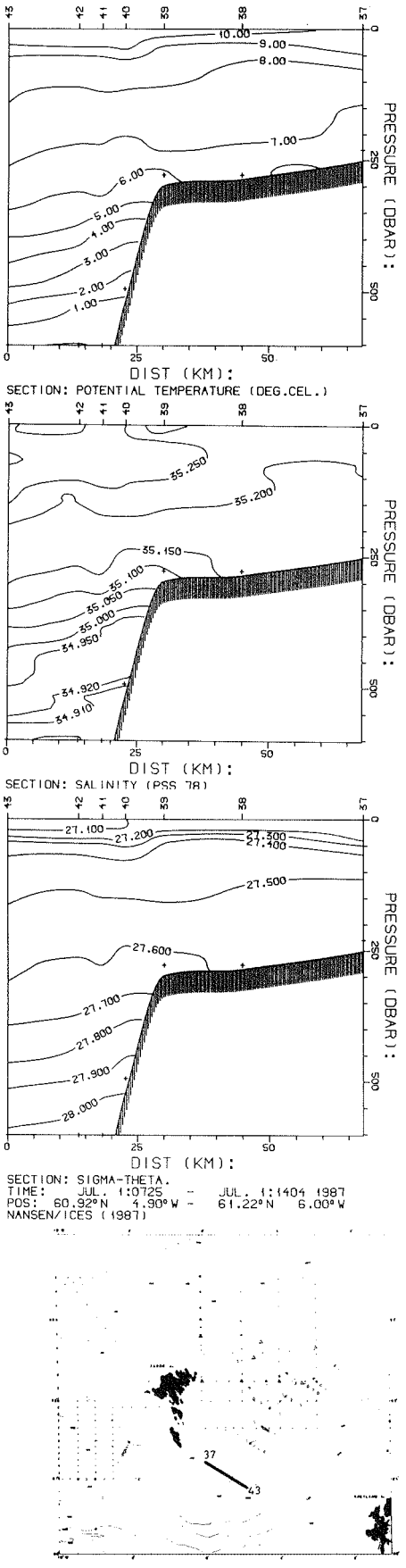

Figure 4c. Vertical sections of potential temperature (above), salinity (middle) and sigma theta (below) along section 3 from R/V Håkon Mosby.

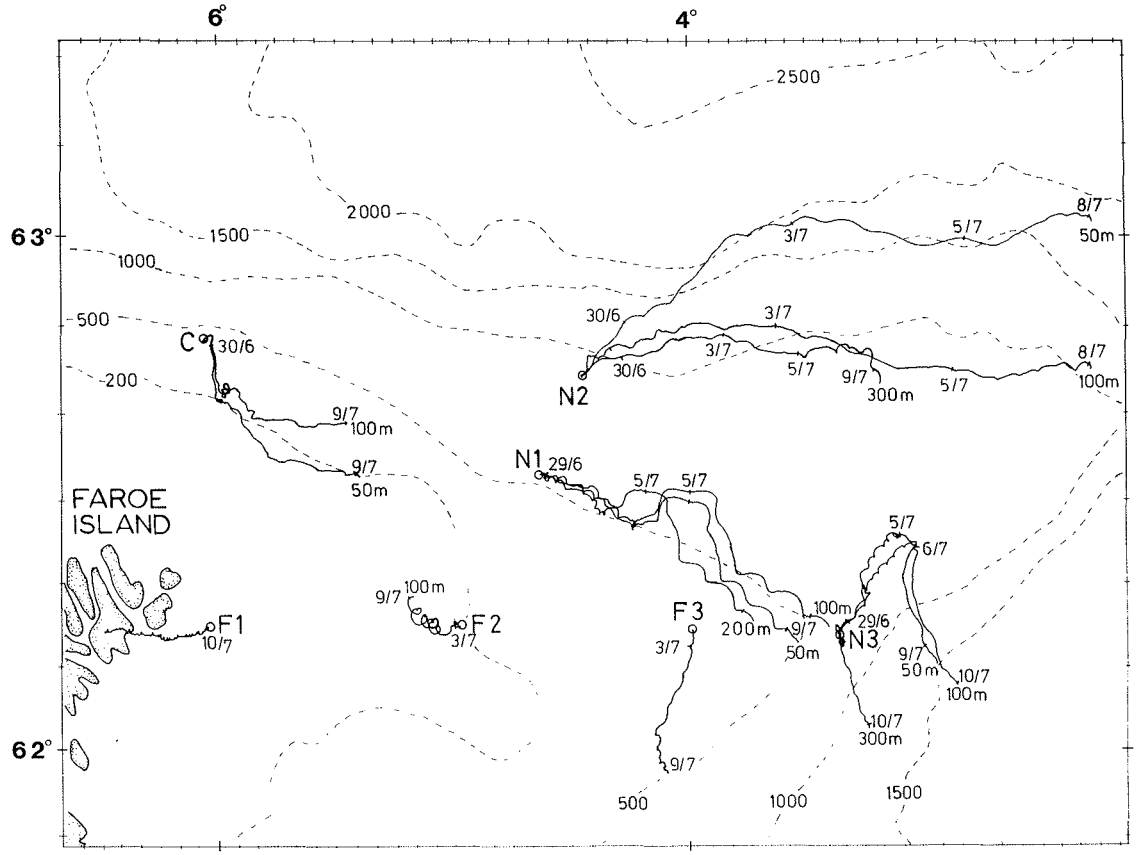

Figure 5. Progressive vector diagrams from current meter measurements north and east of the Faroes in June-July 1987. Dates are indicated.

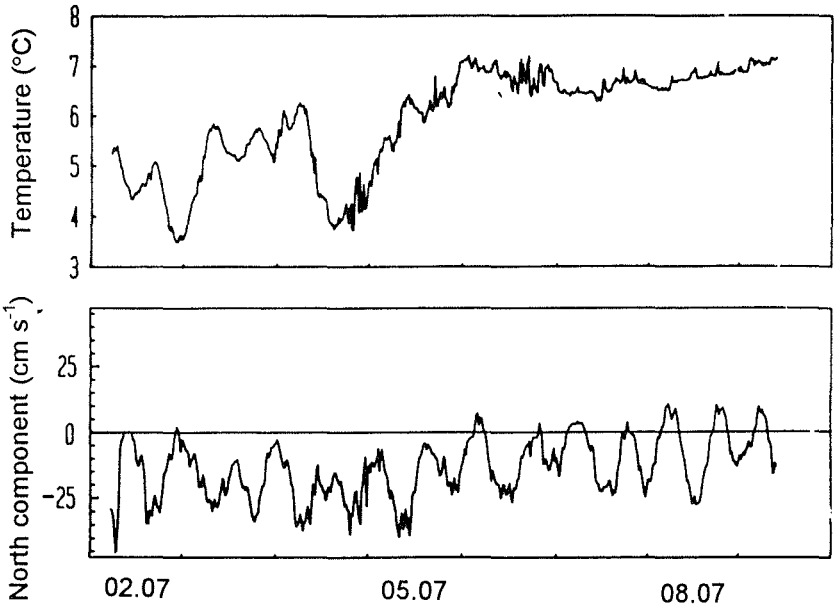

Figure 6. Temperature (upper figure) and north component of current (lower figure) from current meter at 300 m depth moored at site F3 (Figure 1).

Flow of Atlantic Water into the northern Icelandic shelf area, 1985–1989

Stefán S. Kristmannsson

Marine Research Institute, Skúlagata 4, 101 Reykjavík, Iceland.

Based on a paper presented to the ICES Hydrography Committee as ICES CM 1991/C:11

Direct measurements of the shelf current off north-west Iceland were studied. It is in the area of main inflow of warm Atlantic water from the Irminger Current into the Iceland Sea. Current meters were deployed at two depths, one at 100 meters and the other close to bottom at 200 meters. The statistics of the flow are presented and transports estimated. Comparisons with other oceanographic and atmospheric parameters from the region were made.

Keywords: Icelandic region, Irminger Current, Atlantic water, Current measurements

Introduction

This paper describes results of direct measurements of the shelf current off north-west Iceland. The project was started in 1985 to study the flow of warm Atlantic water into the North Icelandic shelf region and monitor the transport and its fluctuation. The main goal was to better understand the flow and the reasons for its variability since the presence of warm Atlantic water is of great importance to the ecology of the North Icelandic shelf region. Also, the presence of the warm water north of Iceland is important to the climate of the area.

The warm Atlantic water branches off the cyclonic flow in the Irminger Sea and flows eastwards through the southern side of the Denmark Strait over the shelf off north-west Iceland and is termed the North Icelandic Irminger Current. The submarine Greenland-Iceland Ridge is certainly a hindrance to the eastward warm water flow of the North Icelandic Irminger Current as is the variable south- and westward flow of different water masses in the area (Malmberg, 1985). The transport of the North Icelandic Irminger Current has been estimated in several studies. Stefánsson (1962) used dynamical calculations and his result was 0.6 Sv (Sv = 10^6 m^3 s^{-1}). Worthington (1970) used continuity arguments in water budget calculations and came up with 1 Sv. In their transport scheme of the northern North Atlantic Dietrich *et.al.* (1975) used 2 Sv for the combined flow of the Irminger Current and the North Icelandic Irminger Current. Results from the first year of the present study indicated a transport of the order of 1 Sv (Kristmannsson *et.al.*, 1989). A more detailed note on the results indicated the transport varying from 0.7 to 2.7 Sv (Kristmannsson *et.al.*, 1987).

Data

Aanderaa RCM4/5 current meters were used in this study. A mooring was deployed near the core of the North Icelandic Irminger Current with bottom depth of 250 m about 75 km from shore (Figure 1). This current meter station is referred to as Kögur in the text. Current meters at nominally 100 m and 200 m depths have recorded the flow since 1 June 1985 (Table 1). The resulting data are almost continuous through August 1990. Initially, the flow was recorded every 20 minutes but after the first year that was increased to 30 minutes and finally, a 60 minutes period has been used since October 1986. The current meters measured the current speed and direction besides the temperature of the water. On a few of them the salinity was also measured but those results are not reported in this paper.

Results

Monthly means of the velocity components, east (along isobaths) and north (across isobaths) and temperature were computed (Tables 2 and 3). They showed a great variability. The monthly mean eastward velocity at 100 m ranged from -2.2 cm s^{-1} (flowing westwards) in April 1988 to 28.8 cm s^{-1} in January 1987 and at 200 m from 0.8 cm s^{-1} to 37.5 cm s^{-1} in the same months. The total means of eastward velocities over the whole measurement period were 14.8 cm s^{-1} and 17.6 cm s^{-1} at the 100 m and 200 m levels, respectively. The cross

Table 1 Kögur 1985-1990. Instrumcnts, Locations, Depths, Deployment Times and Variables measured. (u = current speed, α = direction, T = temperature, p = pressure, S = salinity.)

Site	Latitude °N	Longitude °W	Bottom Depth, m	Meter number	Meter Depth, (m)	Start Time	Duration (days)	Variables measured (freq)
K11	67 10	22 53	250	AA-790201	100	June 1, 1985	110	u,α,T,p,S (20 min)
K12	67 10	22 53	250	AA-387903	200	June 1, 1985	109	u,α,T (20 min)
K21	67 10	22 53	255	AA-790202	105	October 20, 1985	106	u,α,T,p,S (20 min)
K22	67 10	22 53	255	AA-387904	200	October 20, 1985	0	
K31	67 10	22 53	255	AA-790302	125	February 4, 1986	110	u,α,T,p,S(20 min)
K32	67 10	22 53	255	AA-693404	205	February 4, 1986	110	u,α,T (20 min)
K41	67 10	22 53	250	AA-388109	125	May 26, 1986	138	u,α,T (30 min)
K42	67 10	22 53	250	AA-693308	200	May 26, 1986	136	u,α,T,p,S (30 min)
K51	67 10	22 53	254	AA-828501	129	October 12, 1986	341	u,α,T,p,S (60 min)
K52	67 10	22 53	254	AA-790304	204	October 12, 1986	341	u,α,T,p,S (60 min)
K61	67 10	22 53	250	AA-693310	125	September 19, 1987	371	u,α,T,p,S (60 min)
K62	67 10	22 53	250	AA-790305	200	September 19, 1987	363	u,α,T,p,S (60 min)
K71	67 10	22 53	250	AA-939401	125	September 25, 1988	212	u,α,T,p,S (60 min)
K72	67 10	22 53	250	AA-388111	200	September 25, 1988	348	u,α,T (60 min)
K81	67 09	22 52	259	AA-693319	134	September 9, 1989	360	u,α,T,p,S (60 min)
K82	67 09	22 52	259	AA-790306	209	September 9, 1989	360	u,α,T,p,S (60 min)

isobaths (northwards) velocity fluctuated around 0 at both depths, the total means being -1.4 cm s^{-1} and -1.8 cm s^{-1} at 100 m and 200 m, respectively. The standard deviations had similar values as the means in the eastward component but often an order of magnitude higher in the northward component. Spectral decomposition of the flow has shown that the inertial/diurnal tidal frequency motions are the main contributors to the high variability (Kristmannsson *et.al.*, 1987).

The mean temperature at 100 m depth ranged from 1.6 °C in March 1990 to 5.6 °C in September 1988. At 200 m depth it ranged from 0.9 °C in April 1990 to 4.6 °C for a few months. The standard deviations were most often between 1 and 2 °C.

Progressive vector diagrams from both depths were prepared and are shown in Figure 2. They show a striking difference between the former part of the measurement period from June 1985 to January 1988 and the latter part. The flow decreased considerably during this time, e.g. the eastward velocity mean was 18.0 cm s^{-1} at 100 m and 22.6 cm s^{-1} at 200 m in the former period but only 11.1 cm s^{-1} and 13.1 cm s^{-1}, respectively, in the latter period from February 1988 to August 1990. This was reflected in the warm Atlantic Water index for the North Icelandic shelf region over the same years, Figure 4 (from Malmberg and Kristmannsson, 1991). The North Icelandic shelf region is the area to the east of the Kögur section and extends to the section off north-east Iceland (Figure 1a). The warm Atlantic water revealed four distinct periods in 1980 – 1990. The year 1980 was unusually warm followed by a cold period from 1981 to 1983. The latter half of 1983 marked the beginning of a warm period which ended in the fall of 1987. After that there was a three year cold period which ended in the summer of 1990. As an example of the difference between warm and cold periods, the fraction of warm Atlantic water in the spring of 1985 was 56% while in the spring of 1990 it was only 12%.

Table 2 Kögur 100-134m, 6/85-8/90. Monthly means and deviations of current and temperature.
(* denotes incomplete data.)

Period (month)	u, east comp cm s^{-1} mean (st. dev)	v, north comp. cm s^{-1} mean (st. dev)	Temperature °C mean (st. dev)
Jun 85	22.0 (21.0)	-2.4 (10.5)	4.6 (1.0)
Jul 85	14.7 (21.8)	0.1 (13.1)	4.6 (1.2)
Aug 85	19.3 (23.5)	-0.1 (15.6)	4.8 (1.7)
Sep 85*	28.7 (23.6)	-4.1 (14.3)	5.1 (1.9)
Oct 85*	20.8 (21.4)	3.8 (10.5)	3.9 (1.9)
Nov 85	27.1 (24.6)	-2.2 (11.9)	4.4 (2.1)
Dec 85	9.7 (17.4)	-2.0 (6.9)	5.4 (0.5)
Jan 86	6.8 (21.2)	-7.0 (11.5)	4.9 (0.7)
Feb 86	22.1 (18.9)	-8.2 (9.0)	4.7 (1.2)
Mar 86	11.2 (20.7)	-6.0 (9.7)	3.5 (1.0)
Apr 86	18.2 (20.3)	-9.6 (7.9)	4.0 (1.0)
May 86	15.6 (19.5)	-5.3 (10.1)	3.9 (0.9)
Jun 86	15.0 (18.0)	-3.5 (8.6)	3.3 (1.3)
Jul 86	20.3 (19.3)	-6.3 (9.8)	4.3 (1.4)
Aug 86	23.3 (20.4)	-6.7 (10.5)	4.3 (1.8)
Sep 86	12.2 (20.0)	-3.4 (10.5)	4.1 (1.8)
Oct 86	10.1 (22.4)	-3.7 (12.1)	4.3 (1.3)
Nov 86	6.5 (19.7)	0.8 (10.0)	4.1 (0.8)
Dec 86	11.1 (19.1)	2.2 (10.0)	4.1 (0.6)
Jan 87	28.8 (23.7)	-2.7 (12.6)	4.3 (1.4)
Feb 87	18.2 (21.1)	-0.1 (10.9)	4.4 (1.1)
Mar 87	7.9 (20.0)	0.7 (10.9)	3.9 (0.7)
Apr 87	18.8 (19.3)	-4.0 (9.9)	4.1 (0.9)
May 87	24.2 (19.4)	1.9 (12.1)	3.7 (1.5)
Jun 87	17.1 (21.1)	-0.8 (10.6)	4.0 (1.4)
Jul 87	21.3 (20.6)	1.1 (12.4)	4.6 (1.5)
Aug 87	15.5 (20.8)	0.7 (13.5)	4.6 (1.3)
Sep 87	17.9 (21.6)	0.4 (10.6)	4.0 (1.4)
Oct 87	21.5 (22.9)	-2.0 (11.4)	5.2 (1.5)
Nov 87	24.9 (20.2)	-0.1 (10.3)	4.2 (1.8)
Dec 87	26.4 (19.7)	1.8 (11.7)	4.8 (1.5)
Jan 88	18.3 (22.0)	-2.7 (10.8)	5.0 (0.7)
Feb 88	12.4 (22.7)	-1.7 (10.9)	4.2 (1.1)
Mar 88	10.1 (21.1)	-3.1 (10.4)	4.4 (0.8)
Apr 88	-1.1 (19.1)	0.8 (7.1)	3.5 (0.7)
May 88	16.5 (18.2)	-5.5 (9.0)	4.4 (0.9)

Continued

Table 2 Continued

Period (month)	u, east comp cm s^{-1} mean (st. dev)	v, north comp. cm s^{-1} mean (st. dev)	Temperature °C mean (st. dev)
Jun 88	5.4 (18.9)	0.4 (9.2)	4.7 (0.8)
Jul 88	14.4 (18.4)	-0.6 (10.3)	5.1 (1.0)
Aug 88	20.4 (21.8)	-1.5 (12.4)	5.6 (1.0)
Sep 88	4.1 (20.9)	-3.1 (9.2)	5.3 (1.1)
Oct 88	13.1 (24.1)	-3.7 (12.2)	4.3 (1.9)
Nov 88	18.7 (20.2)	-0.5 (10.5)	3.8 (1.9)
Dec 88	26.5 (21.4)	-5.3 (9.9)	3.7 (1.8)
Jan 89	9.4 (18.4)	-1.9 (10.4)	3.8 (0.8)
Feb 89	3.2 (17.6)	-2.7 (10.4)	2.4 (0.7)
Mar 89	6.9 (15.7)	-8.7 (10.9)	2.0 (1.1)
Apr 89*	10.7 (18.0)	-4.9 (7.7)	2.5 (0.9)
Jun 89*			
Jul 89*			
Aug 89*			
Sep 89*	11.5 (21.5)	3.7 (10.9)	3.8 (1.3)
Oct 89	5.1 (19.8)	0.8 (10.1)	3.1 (1.8)
Nov 89	12.6 (20.6)	4.0 (10.3)	4.6 (1.5)
Dec 89	16.5 (20.4)	1.3 (10.4)	3.9 (2.0)
Jan 90	7.6 (19.3)	5.7 (8.7)	3.6 (1.3)
Feb 90	1.0 (16.2)	-0.2 (7.1)	1.8 (0.3)
Mar 90	2.0 (16.0)	1.1 (6.8)	1.6 (0.4)
Apr 90	7.2 (18.6)	2.9 (8.4)	1.8 (1.1)
May 90	18.0 (18.7)	1.3 (9.9)	3.0 (1.8)
Jun 90	15.6 (16.8)	2.4 (10.8)	3.6 (1.4)
Jul 90	21.4 (16.6)	1.9 (11.8)	4.4 (1.5)
Aug 90	10.9 (16.5)	5.1 (10.1)	4.5(1.3)

Table 3 Kögur 200-209m, 6/85-8/90. Monthly means and deviations of current and temperature.
* denotes incomplete data.

Period (month	u, east comp cm s^{-1} mean (st. dev)	v, north comp. cm s^{-1} mean (st. dev)	Temperature °C mean (st. dev)
Jun 85	16.4 (18.2)	0.1 (8.9)	2.8 (1.4)
Jul 85	11.8 (18.4)	0.4 (10.1)	2.3 (1.4)
Aug 85	20.8 (16.8)	-1.0 (8.8)	3.9 (1.8)
Sep 85*	19.6 (18.6)	1.2 (9.5)	4.6 (1.5)
Oct 85*			
Nov 85*			
Dec 85*			

Continued

Table 3 Continued

Period (month)	u, east comp cm s^{-1} mean (st. dev)	v, north comp. cm s^{-1} mean (st. dev)	Temperature °C mean (st. dev)
Jan 86*			
Feb 86*	37.5 (35.5)	-13.2 (14.5)	3.8 (1.6)
Mar 86	17.6 (35.5)	-8.7 (17.0)	1.8 (1.3)
Apr 86	28.0 (34.3)	-13.5 (13.3)	2.5 (1.4)
May 86*	25.5 (33.1)	-9.2 (12.9)	2.6 (1.6)
Jun 86	13.6 (16.9)	-2.0 (8.6)	
Jul 86	19.9 (17.4)	-3.0 (8.6)	
Aug 86	21.1 (17.2)	-2.7 (8.0)	
Sep 86	11.6 (17.8)	-1.5 (9.7)	
Oct 86	12.8 (26.7)	-2.7 (16.5)	2.4 (1.7)
Nov 86	6.1 (28.5)	-1.3 (14.5)	2.6 (1.6)
Dec 86	15.2 (27.4)	0.8 (14.7)	3.5 (1.0)
Jan 87	37.5 (31.6)	-3.3 (15.9)	3.5 (1.9)
Feb 87	23.6 (27.8)	-1.1 (13.1)	3.6 (1.5)
Mar 87	12.1 (29.1)	-1.6 (14.9)	2.7 (1.4)
Apr 87	29.2 (27.0)	-5.0 (13.5)	3.5 (1.1)
May 87	31.0 (26.8)	0.2 (14.8)	2.3 (1.5)
Jun 87	23.3 (28.6)	-1.9 (14.0)	2.6 (1.5)
Jul 87	25.9 (26.4)	-0.7 (14.4)	3.1 (1.6)
Aug 87	21.1 (28.5)	-0.7 (16.9)	3.0 (1.8)
Sep 87	25.4 (30.1)	-0.9 (15.5)	3.0 (1.5)
Oct 87	31.2 (33.2)	-1.8 (16.1)	4.6 (1.8)
Nov 87	33.2 (31.0)	-0.5 (16.1)	3.0 (1.9)
Dec 87	33.4 (28.4)	0.2 (16.1)	3.5 (2.0)
Jan 88	27.1 (32.4)	-4.5 (12.9)	4.4 (1.2)
Feb 88	20.7 (31.7)	-3.3 (14.4)	3.6 (1.3)
Mar 88	16.5 (30.3)	-5.6 (13.3)	3.5 (0.9)
Apr 88	0.8 (26.9)	-0.5 (10.3)	3.2 (0.5)
May 88	23.3 (27.2)	-8.8 (9.9)	3.8 (1.1)
Jun 88	10.1 (27.5)	-1.0 (13.0)	3.2 (1.5)
Jul 88	19.5 (28.1)	-2.7 (15.3)	3.6 (1.5)
Aug 88	26.8 (32.4)	-0.1 (19.1)	4.6 (1.8)
Sep 88*	1.9 (18.7)	7.1 (21.1)	3.5 (0.9)
Oct 88	10.3 (20.3)	-0.5 (12.2)	3.0 (2.0)
Nov 88	12.4 (15.8)	2.0 (10.5)	2.2 (1.9)
Dec 88	18.6 (18.0)	1.1 (11.0)	2.7 (1.6)
Jan 89	7.3 (16.0)	-1.0 (10.0)	2.7 (1.4)

Continued

Table 3 Continued

Period (month)	u, east comp cm s^{-1} mean (st. dev)	v, north comp. cm s^{-1} mean (st. dev)	Temperature °C mean (st. dev)
Feb 89	1.5 (14.7)	-1.4 (10.6)	1.0 (1.0)
Mar 89	6.3 (18.2)	-5.1 (12.1)	1.9 (1.1)
Apr 89	11.6 (16.8)	-1.7 (8.6)	1.9 (1.0)
May 89	14.2 (16.5)	0.0 (9.7)	2.2 (1.6)
Jun 89	19.7 (16.5)	3.5 (10.9)	1.7 (1.6)
Jul 89	8.2 (15.2)	0.8 (11.3)	2.0 (1.9)
Aug 89	9.0 (16.9)	0.3 (9.7)	2.3 (1.9)
Sep 89	11.9 (23.5)	1.2 (15.4)	1.1 (1.3)
Oct 89	4.9 (26.8)	-1.1 (15.1)	1.0 (1.2)
Nov 89	15.1 (29.7)	2.6 (16.2)	3.5 (2.0)
Dec 89	20.9 (29.0)	-3.4 (14.9)	2.7 (1.9)
Jan 90	9.7 (27.8)	0.1 (12.8)	1.8 (1.6)
Feb 90	1.7 (26.6)	-4.1 (12.6)	1.7 (0.5)
Mar 90	2.5 (25.8)	-0.9 (11.0)	1.7 (0.5)
Apr 90	9.1 (26.0)	0.4 (11.7)	0.9 (0.6)
May 90	24.1 (28.3)	-2.8 (13.8)	1.8 (1.6)
Jun 90	22.2 (26.6)	-2.2 (15.7)	1.9 (1.7)
Jul 90	30.6 (24.7)	-3.6 (17.3)	2.9 (1.9)
Aug 90	14.9 (23.8)	1.2 (16.3)	2.4 (1.9)

Discussion

In the following the discussion is based on the eastward velocities. The means of the monthly velocities are shown in Figure 3a and b. It is evident that the yearly cycle has two maxima. Thus the flow at Kögur is at maximum in May through August and in November through January. The former is probably partly due to the increased geostrophic flow in spring as the water close to land warms up in a coastal current. The latter is probably due to increased wind stress vorticity in winter over the Iceland Sea (Malmberg and Kristmannsson, 1991) before much cooling of the water masses takes place, but the Icelandic Low is at maximum in mid-winter. Similarly, the means of the monthly temperature have also two maxima, in August and in December/January. There is a minimum in March and a lesser one in October (Figures 3c and d). Thus the eastward velocity is in concert with warm temperatures.

As can be seen in Tables 2 and 3 the characteristics of the eastward flows and temperatures were similar at the two depth levels. A high correlation (r=0.84) between the monthly eastward velocity values indicated a barotropic nature of the flow and was used to calculate the eastward transport at Kögur (Figure 5). The mean monthly transport of warm water is shown in Figure 6. It is the calculated transport when the water temperature is equal to or higher than 4 °C. There is a maximum eastward warm water transport in April/May followed by a slow decrease with a minimum in March. The mean monthly transport values ranged from 0.9 Sv in March to 2 Sv in May.

A time series of the eastward warm water transport of the monthly deviations is shovm in Figure 7. Again, it was evident that shortly after the beginning of 1988 there was a change from an above-average transport at Kögur to a below-average transport. This result is reflected in the volume fraction of warm Atlantic water in the North Icelandic shelf region (Figure 4), even though the deterioration appeared to have taken place a few months earlier. Thus in the first few months of 1986 there was a large inflow at Kögur coinciding with high indices of warm Atlantic water in the North Icelandic shelf region in the winter and spring of that same year, leading to favorable hydrographic conditions in the area. On the other hand in February to April of 1990 there was a much reduced eastward flow at Kögur (there was no flow of warm Atlantic water in February and March) coinciding with low indices for the winter and spring of 1990 in the North Icelandic shelf region and therefore

very poor hydrographic conditions. However, through the latter half of 1987 there was a great eastward transport at Kögur but low indices of warm Atlantic water in the North Icelandic shelf region in the following few months. Other events of both types can be found and it seems clear that a direct link does not always exist between the inflow of warm Atlantic water at Kögur and its estimated volume fraction in the North Icelandic shelf region, subsequently.

Conclusion

Based on a five year long time series of the flow at Kögur, as demonstrated by the monthly eastward warm water transport and the progressive vector diagrams of mean velocities, it became clear that they were reflected to a high degree in the warm Atlantic water volume fraction of the North Icelandic shelf region of the same period.

The estimated eastward warm water transport at Kögur ranged from 0, in February/March of 1990, to 2.8 Sv in January of 1987.

The yearly cycle of eastward velocity and temperature indicated the effect of the wind regime. Thus in addition to the yearly geostrophic inflow in spring and summer to the North Icelandic shelf region, it seems likely that the strength of the Iceland Low has some effect on the inflow of warm Atlantic water. A significant correlation was found between the wind stress vorticity over the Irminger Sea and the warm Atlantic water index 6 and 9 months later (Malmberg and Kristmannsson 1991). Furthermore, this correlation was stronger between the wind stress vorticity over the Iceland Sea and the warm Atlantic water index up to 9 months later. The strength of the Icelandic Low is at maximum in winter from October through March, e.g. Jónsson (1991), and therefore its associated mean wind stress vorticity. The added energy input from the wind to the water therefore leads to increased eastward flow of the North Icelandic Irminger Current in early winter (Figure 3). However, in the work of Jónsson (1989) from a study further north, in the Greenland Sea, it became clear that a direct connection between wind energy input to the sea and consequent measured current was not found. Rather, there were strong similarities between the power of the wind and the subsequent kinetic energy of the ocean eddies.

Acknowledgements

I wish to thank all who contributed to this project with their kind help and encouragement. Especially, to Johannes Briem who designed the mooring and directed its deployment and did the initial computations of the data series.

References

Dietrich, G., Kalle, K., Krauss, W., and Siedler, G. 1975. General Oceanography, 2nd ed. John Wiley and Sons, New York, 626 pp.

Jónsson, S. 1989. The structure and forcing of the large- and mesoscale circulation in the Nordic Seas, with special reference to the Fram Strait. Ph.D. thesis. Univ.of Bergen, Norway.

Jónsson, S. 1991. Seasonal and Interannual Variability of Wind Stress Curl over the Nordic Seas. Journal of Geophysical Research, 96 (C2): 2649–2659.

Kristmannsson, S. S., Malmberg, S. A. and Briem, J. 1987. Inflow of warm Atlantic water to the subarctic Iceland Sea. ICES C.M. 1987/Mini-Symp./Poster.

Kristmannsson, S. S., Malmberg, S. A. and Briem, J. 1989. Inflow of warm Atlantic water to the subarctic Iceland Sea. Rapports et Procès-Verbaux des Réunions du Conseil International pour l'Exploration de la Mer, 188: 74.

Malmberg, S. A. 1985. The water masses between Iceland and Greenland. Rit Fiskideildar, 9: 127–140.

Malmberg, S. A., and Kristmannson, S. S. 1991. Hydrographic conditions in Icelandic waters 1980 – 1989. ICES 1991/Variability Symp./Paper #6.

Stefánsson, U. 1962. North Icelandic Waters. Rit Fiskideildar, 3, 269 pp.

Worthington, L. V. 1970. The Norwegian Sea as a Mediterranean Basin. Deep-Sea Research, 17: 77–84.

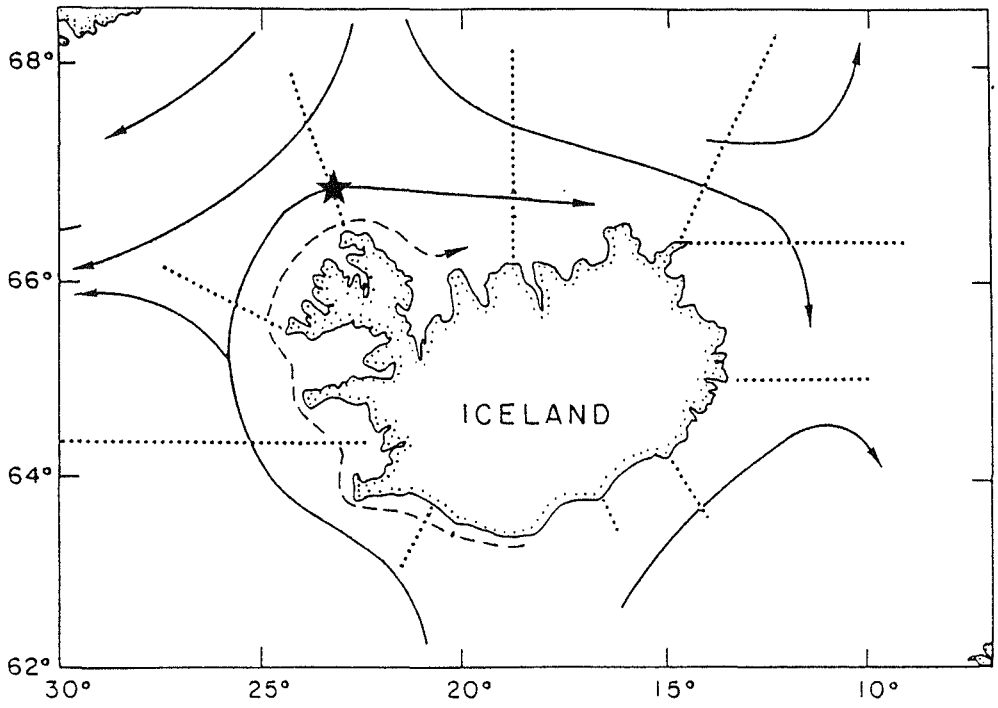

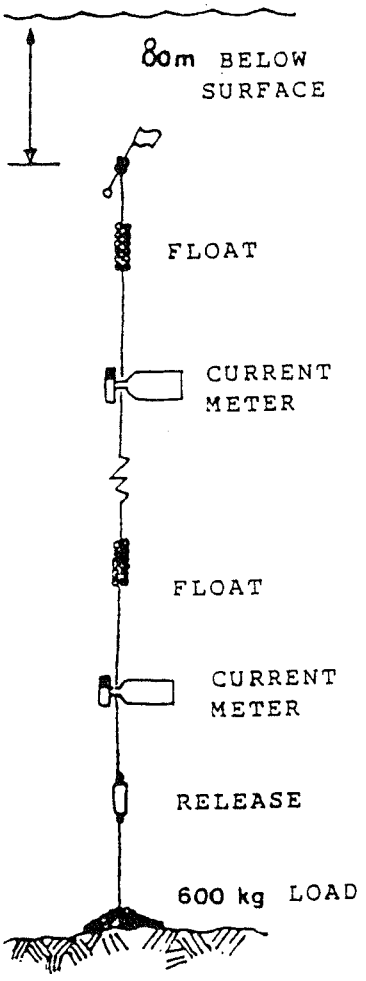

Figure 1. Upper: Main ocean currents and location of standard sections in Icelandic waters. Mooring site is denoted by the star. Lower: Layout of Aanderaa-RCM4 current meter mooring with Océano underwater release mechanism.

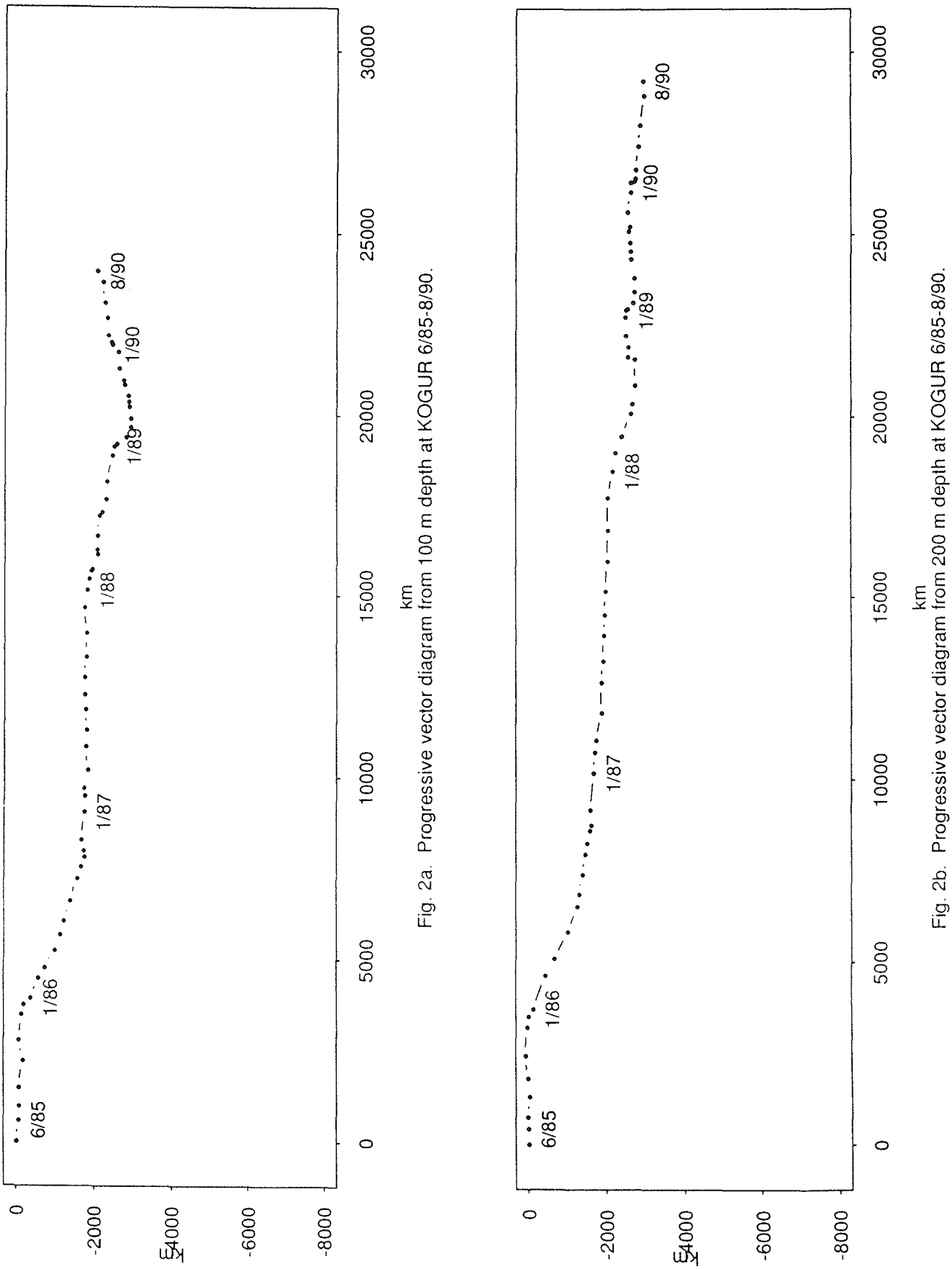

Fig. 2a. Progressive vector diagram from 100 m depth at KOGUR 6/85-8/90.

Fig. 2b. Progressive vector diagram from 200 m depth at KOGUR 6/85-8/90.

Figure 2. Progressive vector diagram at Kögur 6/85-8/90 (month/year) from 100 m depth (upper) and 200 m depth (lower).

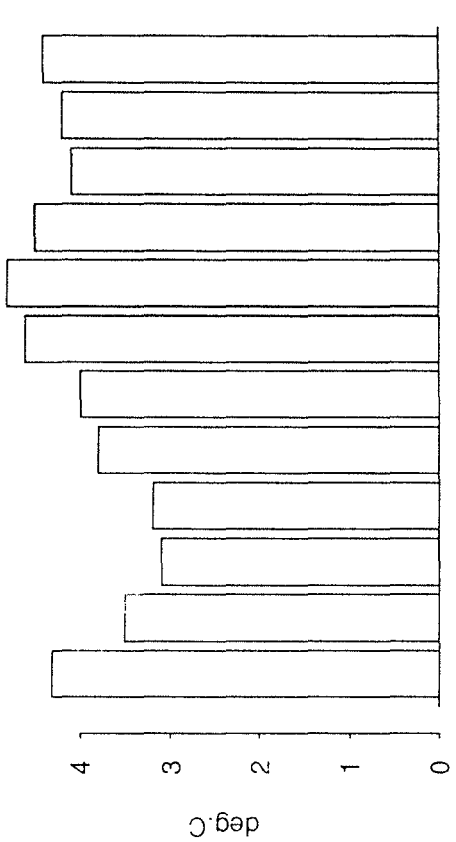

Fig. 3c. Mean temperature at 100 m at KOGUR, (6/85-8/90)

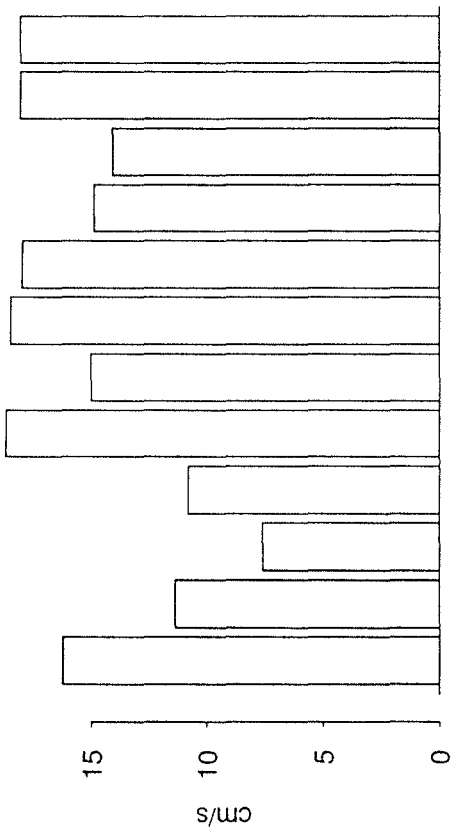

Fig. 3a. Mean eastward monthly velocity at 100 m at KOGUR, (6/85-8/90)

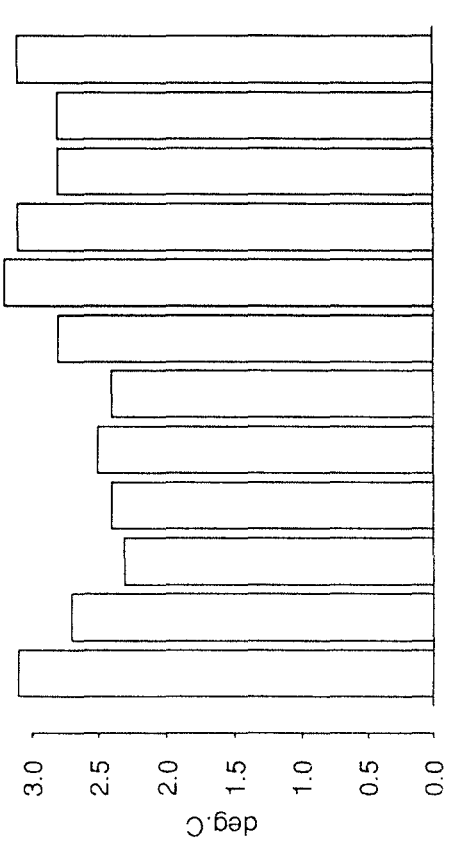

Fig. 3d. Mean temperature at 200 m at KOGUR, (6/85-8/90)

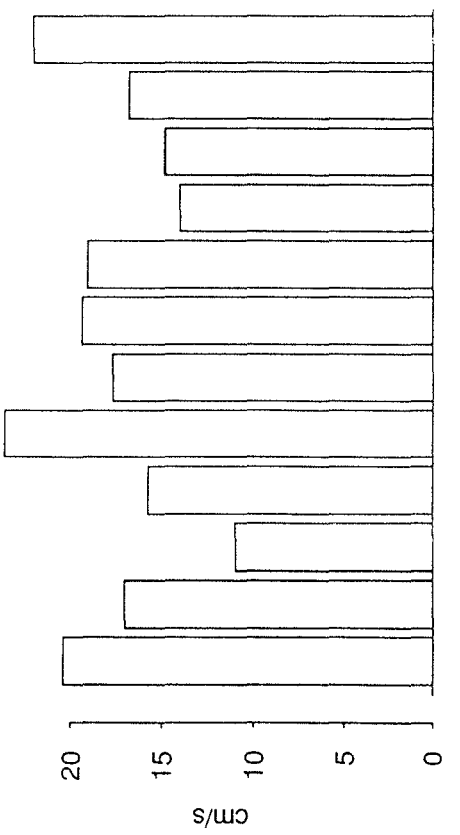

Fig. 3b. Mean eastward monthly velocity at 200 m at KOGUR, (6/85-8/90)

Figure 3. Mean monthly values for the period June 1985 - August 1990 of: eastward velocity at 100 m depth (upper left), eastward velocity at 200 m depth (lower left), temperature at 100 m depth (upper right) and temperature at 200 m depth (lower right).

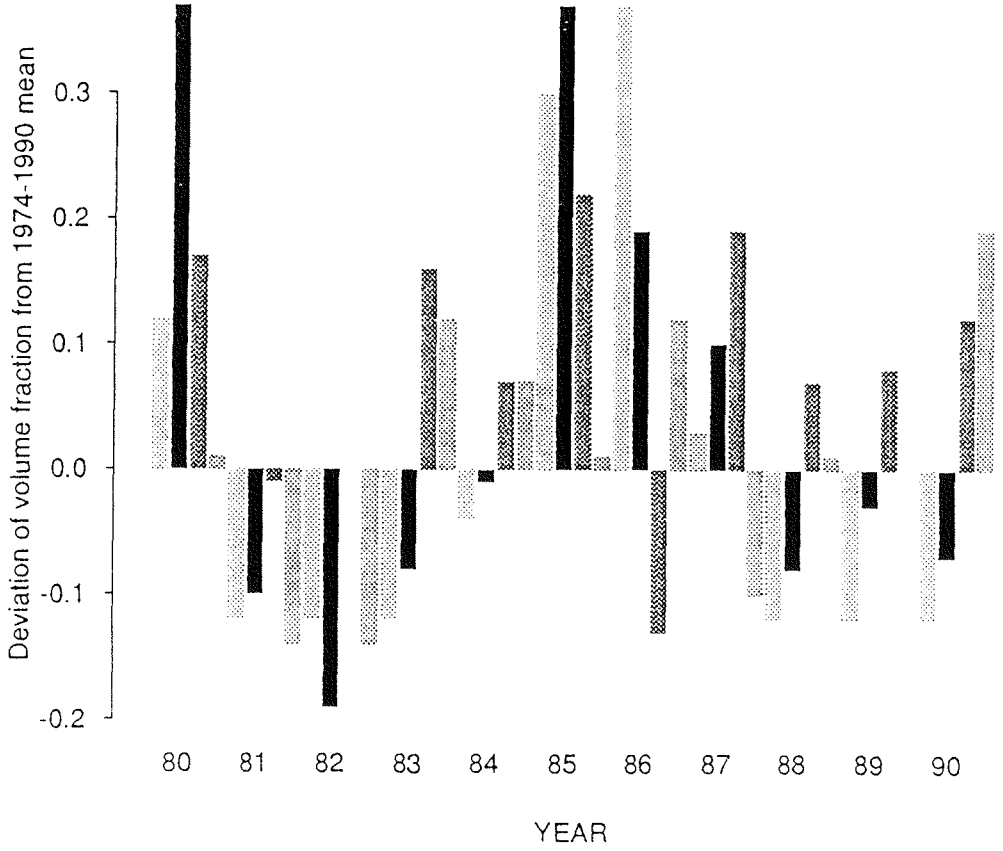

Figure 4. Atlantic Water in North Icelandic Shelf Area (darkest column is the spring value).

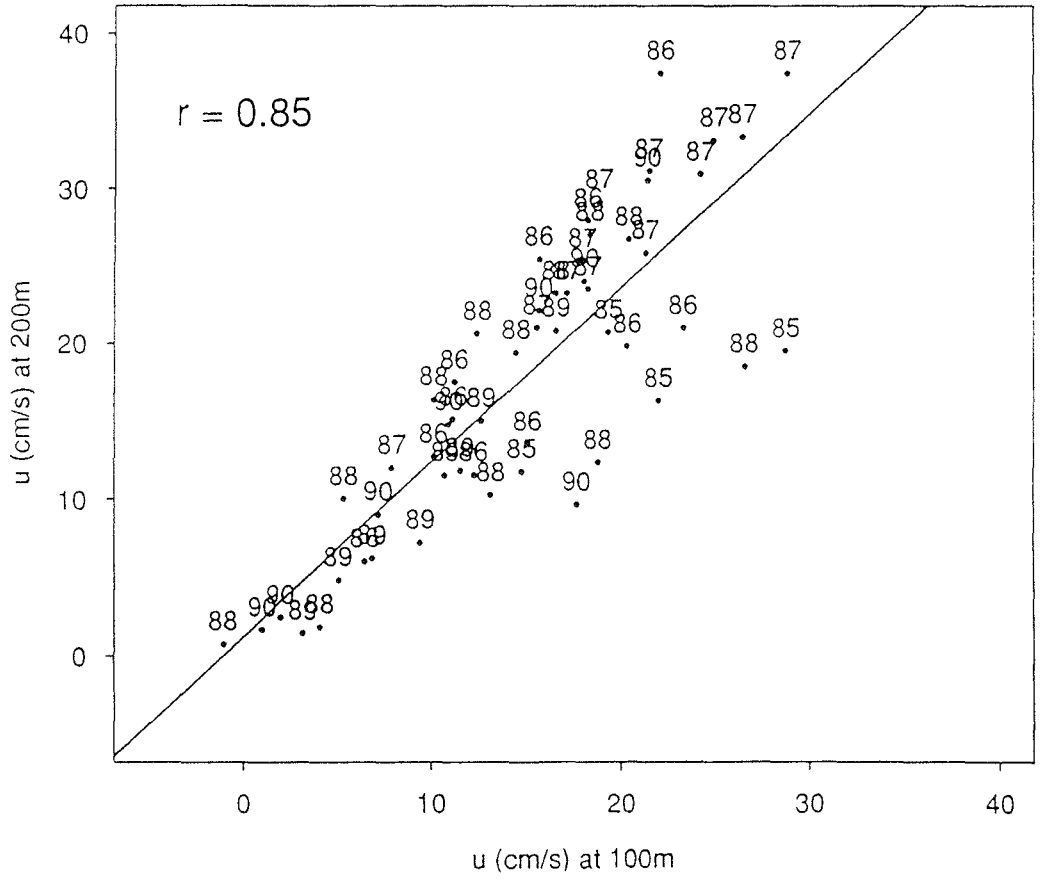

Figure 5. Correlation of monthly velocities in 100 m and 200 m depths at Kögur 6/85-8/90.

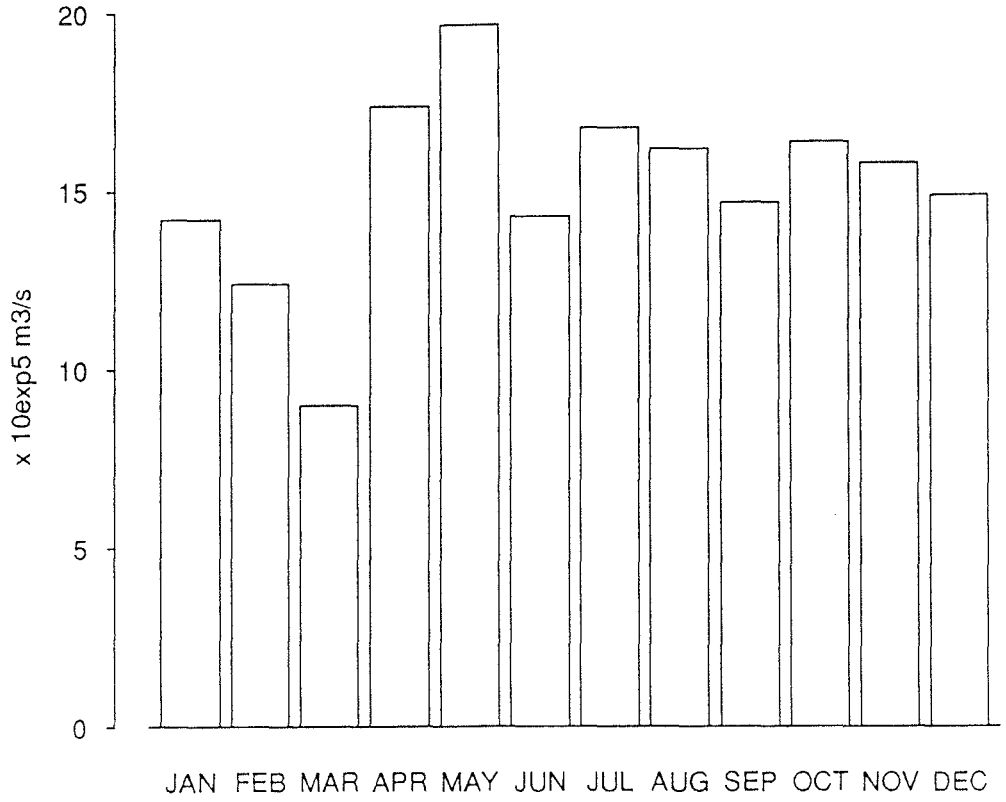

Figure 6. Mean monthly eastward warm water transport (t > 4 °C) at Kögur 6/85-8/90.

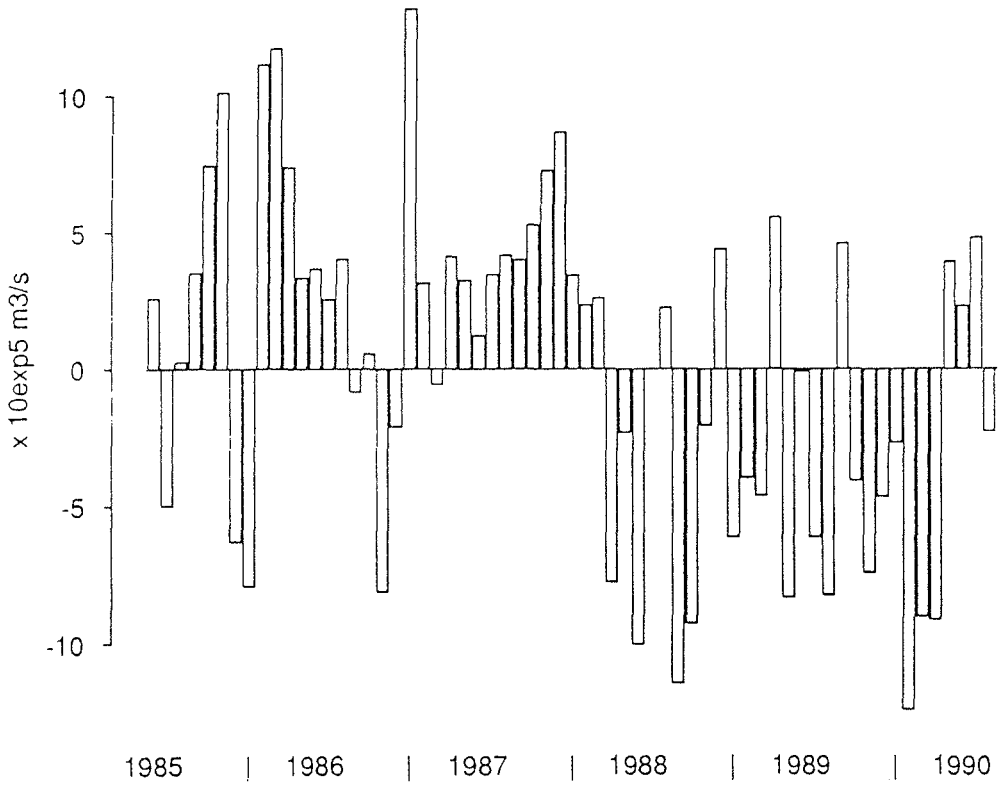

Figure 7. Deviation from monthly mean of warm water eastward transport (t > 4 °C) at Kögur 6/85-8/90.

Hydrographic variability of the overflow water in the Iceland Basin

C. J. de Boer[1], H. M. van Aken[2] and A. J. van Bennekom[2]

[1]Nuwendoorn 40, 1613 LD Grootebroek, The Netherlands. [2]Netherlands Institute for Sea Research, P.O. Box 59, 1790 AB Den Burg/Texel, The Netherlands.

Based on a paper presented to the ICES Hydrography Committee as CM 1991/C:13

During a number of surveys of R.V. Tyro and H.Neth.M.S. Tydeman the deep and bottom waters in the Iceland Basin were studied. As hydrographic parameters nutrient concentrations and oxygen concentrations were measured together with temperature and salinity. Several cores of deep and bottom water were recognised from the distribution of these parameters. The properties of the Overflow Water, flowing into the Iceland Basin from the Norwegian Sea through the Faroese regions, indicated the presence of at least two cores of Overflow Water with different hydrographic properties. Especially the concentration of dissolved silica clearly showed the strong influence of water from the south with properties reminding of Antarctic Bottom Water. This water seems to interact with the deeper core of Overflow Water by lateral dispersion along iso-pycnal surfaces. Repeated observations have shown variations on time scales of days and weeks to inter-annual time scales.

Keywords: Iceland Basin, Overflow, Variability, Antarctic Bottom Water

Introduction

At the Netherlands Institute for Sea Research (NIOZ, Texel) a research programme is carried out on the circulation and hydrography of the Iceland Basin. Within this programme a number of research cruises has been carried out and a data base with historic hydrographic data is established.

This paper discusses the hydrography of the deep and bottom waters south of Iceland. The circulation of these water masses is strongly influenced by the prominent topography; south-west of Iceland the Reykjanes Ridge, south-east the Iceland-Faroe Rise and to the south the Hatton Bank and Rockall Plateau (Figure 1). These 3 features enclose the Iceland Basin which has a maximum depth of over 2500 meter. The Maury Channel forms the deep connection of the Iceland Basin with the more southern basins of the North East Atlantic. The Charlie-Gibbs Fracture Zone connects the Iceland Basin with the western basins of the North Atlantic.

The deep water masses in the Iceland Basin are formed by advection and mixing of several water types originating either from Arctic regions or from southern regions. One of the most prominent water types in the basin is (Norwegian Sea) Overflow Water. This water is formed north of the Iceland-Faroe Rise. It enters the Iceland Basin as a combination of Norwegian Sea Deep Water and Arctic Intermediate Water which flows over the Iceland-Faroe Rise and through the Faroe Bank Channel into the basin (van Aken, 1987).

The Overflow Water is assumed to flow anti-clockwise along the topography of the Iceland Basin as a deep boundary current. In the south it meets water which is influenced by Antarctic Bottom Water (van Bennekom, 1985). Some authors assume that the Overflow Water recirculates for a large part within the Iceland Basin (Harvey *et al.*, 1986). Above these deep water masses Labrador Sea Water is found at ~ 1600 m depth (Lee *et al.*, 1965; Harvey, 1982; van Aken, 1987). Besides the hydrography, the paper discusses also the short and long term variability of these water masses at 60°N, 20°W.

Data

In the past decade NIOZ has carried out a number of hydrographic surveys in the Iceland Basin (1983, 1987, 1989, 1990, 1991). In this study data are used from a survey in 1987 by H.Neth.M.S. Tydeman (from 60°31'N 14°21'W to 62°58'N 16°45'W, see Figure 1 for sections), and a selection of data from JGOFS surveys

Table 1 Position and depth of Overflow Water (1990).

17°W		20°W	
position	**depth**	**position**	**depth**
62°45' N	1600 m	62°00' N	1800 m
62°07' N	2175 m	61°00' N	2500 m
61°00' N	2450 m	60°15' N	2700 m

(Joint Global Ocean Flux Studies) in 1989 and 1990, and from DUTCH-WARP surveys (Deep and Upper Transport, Circulation and Hydrography – WOCE Atlantic Research Programme) in 1990 and 1991. These last 4 surveys have been carried out by R.V. Tyro. From the R.V. Tyro surveys, only the sections at 20°W and 17°W (Figure 1) are used. Available data from 1989 to 1991 from 60°N 20°W have been gathered to study the temporal variability of the hydrographic structure.

Hydrography of the Iceland Basin

Figures 2 to 5 show the distribution of potential temperature (θ), salinity (S), and dissolved silica (Si), along the sections surveyed in 1987, 1989 and 1990. The discussion below will focus on the 1990 survey along 17°W (Figure 5) while references are made to the other sections if considered necessary.

Along 17°W the distribution of potential temperature (Figure 5a) shows 3 cores of Overflow Water (characterised by $\theta \leq 2.5$ °C). The most northern core is found on 62°45'N at a depth of approximately 1600 meter. The two other cores are found on 62°07'N (2175 m) and 61°N (2450 m). The Overflow Water is characterised by a relatively high salinity ($S > 34.975$). The Si concentration of the Overflow Water increases to the south. The presence of 3 distinctive cores at 17°W indicates that mixing has not proceeded so far that the distinction between different overflow locations (Faroe Bank Channel and different locations over the Iceland-Faroe Rise) has been lost. Further eastward, thin (20–80 m) near bottom layers of low θ were found in 1983 (θ = 1.50 °C at 62°13'N 16°10'W, 2150 m; van Bennekom, 1985) and in 1987 (θ = 1.8 °C at 61°59'N 15°45'W, 2200 m, Figure 2). At 20°W the distinction between the 2 southern cores is less well established (Figure 4). From 17°W to 20°W the cores of Overflow Water descend 200 to 300 meters while moving southwards about 60 nautical miles (Table 1).

The distribution of Si along 17°W (Figure 5c) shows the presence of a high Si core in the south on the slope of the Hatton Bank (found on all the sections, Figure 2c, 3c, 4c and 5c). This water overlies the Overflow Water. This core of high Si can be followed southwards along the Hatton Bank to the high Si Antarctic Bottom Water (AABW) observed on the Porcupine Abyssal Plain (van Aken, 1990). Therefore it is assumed that the deep high Si core found on the slope of the Hatton Bank is formed by advection of southern water, probably in a deep boundary current. It is not known yet what drives such a current. The lateral spreading of this core may be caused by iso-pycnal dispersion. The higher Si values of the southern overflow core may be due to entrainment of overlying southern water. The relatively low Si values in the southern water compared to pure AABW (resp. 18 μmol kg^{-1} versus 130 μmol kg^{-1}) indicates a low content of pure AABW in the southern water.

The distributions of Si and salinity (Figure 5b and c) show the presence of Labrador Sea Water at intermediate depths. This water is characterized by a salinity minimum ($S \leq 34.94$) and a silica minimum (Si ≤ 11.5 μmol kg^{-1}). All sections show that the influence of Labrador Sea Water diminishes, and partly vanishes, at the Icelandic slope. This is probably due to either the influence of relatively warm and salty intermediate waters from the Norwegian Sea (Van Aken, 1987) or to increased mixing over the slope. Labrador Sea Water reaches further north at 17°W than at 20°W (Figs 4 and 5).

Above the Labrador Sea Water lies a core with slightly higher Si values (e.g. Figure 5c). This core cannot be recognized in the salinity distribution (Figure 5b) but it coincides with an oxygen minimum and a nitrate maximum (not shown here). The origin of the core is not yet established. It could be Mediterranean Sea Water (Worthington, 1965; Reid, 1979; van Bennekom 1985; Emery, 1986). Emery stated that Mediterranean Sea Water could be found between 500-1500 m with $2.6 \leq \theta \leq 11$ and $35.0 \leq S \leq 36.2$ psu. The core found here doesn't have such a high salinity ($34.95 \leq S \leq 35.05$) but south of the Rockall-Hatton Plateau it has been observed in 1990 at a salinity of S = 35.15 (Van Aken, 1990). Tsuchiya (1989) found a Si maximum associated with residues of Antarctic Intermediate Water at 900 m (8 μmol kg^{-1}) below the Atlantic Water in more southern parts of the Iceland Basin. Because of it's origin this water had a low salinity although a minimum in S wasn't observed. The core found in our section has a higher Si concentration than the values mentioned by Tsuchiya. A third explanation for this core is bio-geochemical processes (coinciding dissolution of silicate

Table 2 Properties of the water mass at 17°W.

Water type	Position (Latitude)	Depth (m)	Pot. Temp. °C	Salinity	Silica (μ Mol kg^{-1})	Nitrate (μMol kg^{-1})	Oxygen
Overflow 1	62°45'N	1600	≤ 2.5	≥ 34.975	(-) 10.5	(-)≤ 16	(+)
Overflow 2	62°07'N	2175	≤ 2.5	≥ 34.975	(-) 10.5	(-)≤ 16	(+)
Overflow 3	61°00'N	2450	≤ 2.5	≥ 34.975	(-) 12.0	(-)≤ 16	(+)
southern W	62°15'N	2000	≤ 3.5	34.95–34.97	(+) 12-16	(+)17–17.5	
L.S.W.	62°30'N*	1200–2300	3.25-3.	≤ 34.94	(-) 11.5	17-18	(?)
? water	62°30'N	1100	4-6	34.95-35.05	(+)≥11.5	(+)≥18	(-)

*South of this latitude.
(+) maximum
(-) minimum

frustules and mineralization of organic matter although these processes are not directly connected). That however does not make evident why the core finds its main expression along the slope of the Hatton Bank. At this moment it is not yet sure what the origin is.

A summary of the results is given in Table 2. The values in this table are based on the data measured on 17°W, where values of the center of the core are used, or if this was not possible, the values of a contour which was assumed to be a characteristic boundary of the water type.

The variability of hydrographic parameters

In this section results are shown on the variability of hydrographic parameters at 60°N 20°W. The data used, have been measured in 1989, 1990 and 1991. In 1989 one, in 1990 three and in 1991 two casts have been executed at this position. The time lapse between two casts in the same year is of the order of a week. Figure 6 shows the 6 profiles of the potential temperature, Figure 7 the profiles of salinity and Figure 8 the profiles of dissolved silica.

The water mass between 800 and 1300 meter and the core at 1100 meter has a large temporal variability in potential temperature and salinity, but a low variability in the Si concentration, even near the Si maximum at 1100 m.

The water mass between 1300 and 2300 m contains a core of LSW centred around a salinity minimum (Figure 7) and a thermostad (Figure 6). This layer shows little short term variability, but a systematic difference between 1991 and the preceding years. This may reflect the inter-annual changes in LSW characteristics, due to varying sea surface properties in winter in the Labrador Sea. Whereas the potential temperature in the thermostad hardly varies between the years, temperature variations increase towards the upper and lower boundaries of the LSW complex (Figure 6). The depth and the value of the LSW salinity minimum varies slightly from year to year (Figure 7), while the variation in Si is mainly important in the lower half of the LSW (Figure 8).

Below the LSW core the situation becomes more complicated. Below a depth of 2400 m the dissolved silica shows a large variability, both in time and in the vertical (Figure 8). This reflects the competition in potential density layers between the low Si Overflow Water (7.5–8 μmol kg^{-1}; van Bennekom 1985) and the high Si southern water. At about 60°N both water types meet in the lowest 350 m of the water column. This competition is also seen in the variability maximum in salinity (Figure 7). Variations in Si and salinity appear to be coherent, with high Si values coinciding with low salinity (compare Figures. 7 and 8). Contrary to the variability maximum at 2600 m, the salinity values at 2400 m are identical within 0.006 psu (Figure 7). In contrast with salinity and Si, the temperature variation has a minimum at 2600 m, while at 2400 m the temperature variation has a maximum due to the inter-annual changes between 1990 and 1991 (Figure 6).

Near the bottom, the variation in all hydrographic parameters diminishes again, most probably because the high density of the Overflow Water was not encountered in the southern water within the Iceland Basin. This prevents iso-pycnal dispersion of southern water into the lower, high-density parts of the Overflow cores.

Conclusions

South of Iceland several cores of Overflow Water exist. While flowing from 17°W to 20°W they descend about 200 meter and move southwards (about 45–60 nautical miles). During the descent they slowly loose part of their individual character due to entrainment and mixing. In the south the Overflow Water meets water with a southern origin, characterised by a high Si value and a relatively low salinity. This core can be traced back to

the Porcupine Abyssal Plain, where bottom water with a high AABW content is found. The concentration of the core of this southern water along the lower stretches of the slope of the Hatton bank suggests the existence of a deep boundary current, transporting this water northward into the Iceland Basin. In the centre of the Iceland Basin, this water lies above the Overflow Water. Above the southern water and the Overflow Water lies a core of Labrador Sea Water which does not reach the Icelandic slope. This is probably due to the fact that there, on top of the core with Overflow Water, Intermediate Water from the Norwegian Sea is advected from sills on the Iceland-Faroe Rise. Labrador Sea Water is characterised by it's salinity and Si minima. Above this water lies a core, which has a Si and nitrate maximum and an oxygen minimum, concentrated along the slope of the Hatton Bank. It is not yet sure what is the source of this water type.

The six profiles at 60°N, 20°W, measured in 1989, 1990 and 1991 show that the character of the temporal variation changes throughout the water column. Especially the deepest 350 meter have a great variability in Si, where Si changes are coherent with salinity changes. At the bottom this variability decreases rapidly. The differences in silica can be as much as 3 μmol kg^{-1} within a few days and between different years the changes can be as high as 8 μmol kg^{-1}. The change in variability in the lowest 350 m is probably due to changes in the intensity of iso-pycnal exchange between Overflow Water and the water of more southern origin. There are several layers within the water column which have a very low variability (in salinity less than 6 mpsu difference) over the six casts.

For the future it is necessary to investigate the decreasing variability of the Overflow Water near the bottom, because this can teach us more about the structure of the Overflow Water flowing through the Iceland Basin and about the mixing processes modifying this water type. We also want to know more about the high silica water type at 1100 meter; it's occurrence, source and role in the hydrography. Therefore we will analyse the other sections we made on the Tyro cruises from 1990 and 1991, and, if possible, other data from recent surveys in the Iceland Basin.

Acknowledgements

The research, presented here, was supported by the Working Group on Meteorology and Physical Oceanography (MFO) with financial aid from the Netherlands Organization for Advancement of Research (NWO) and by the Netherlands Foundation for Marine Research (SOZ/NWO). We thank R. de Vries, R. Kloosterhuis and K. Bakker for the determinations of dissolved silica.

References

Emery, W. J., and Meincke, J. 1986. Global water masses: summary and review. Oceanologica Acta, 9: 383–391.

Hansen, B. 1985. The circulation of the northern part of the Northeast Atlantic. Rit Fiskideildar, 9: 110–126 .

Harvey, J. 1982. θ – S relationships and water masses in the eastern North Atlantic. Deep Sea Research, 29 (8a): 1021–1033.

Harvey, J. G., and Theodorou, A. 1986. The circulation of Norwegian Sea Overflow Water in the eastern North Atlantic. Oceanologica Acta, 9: 393–402.

Lee, A., and Ellett, D. 1965. On the contribution of Overflow Water from the Norwegian Sea to the hydrographic structure of the North Atlantic Ocean. Deep Sea Research, 12: 129–142.

Reid, J. L. 1979. On the contribution of the Mediterranean Sea outflow to the Norwegian-Greenland Sea. Deep Sea Research, 26A: 1199–1223.

Tsuchiya, M. 1989. Circulation of the Antarctic Intermediate Water in the North Atlantic Ocean, Journal of Marine Research, 47: 747–755.

Van Aken, H. M. 1987. The circulation between Iceland and Scotland derived from water mass analysis. Netherlands Journal of Sea Research 21(1): 1–15.

Van Aken, H. M. 1990. DUTCH-WARP 1990, R.V. Tyro cruise 90/3, Part I: WOCE section AR7E. NIOZ, Texel: pp 17 + Figures.

Van Bennekom, A. J. 1985. Dissolved silica as an indicator of Antarctic Bottom Water penetration, and the variability in the bottom layers of the Norwegian and Iceland Basin. Rit Fiskideildar, 9: 101–109.

Worthington, L. V. 1965. The Volume transport of the Norwegian Sea Overflow Water in the North Atlantic. Deep Sea Research, 12: 667–676.

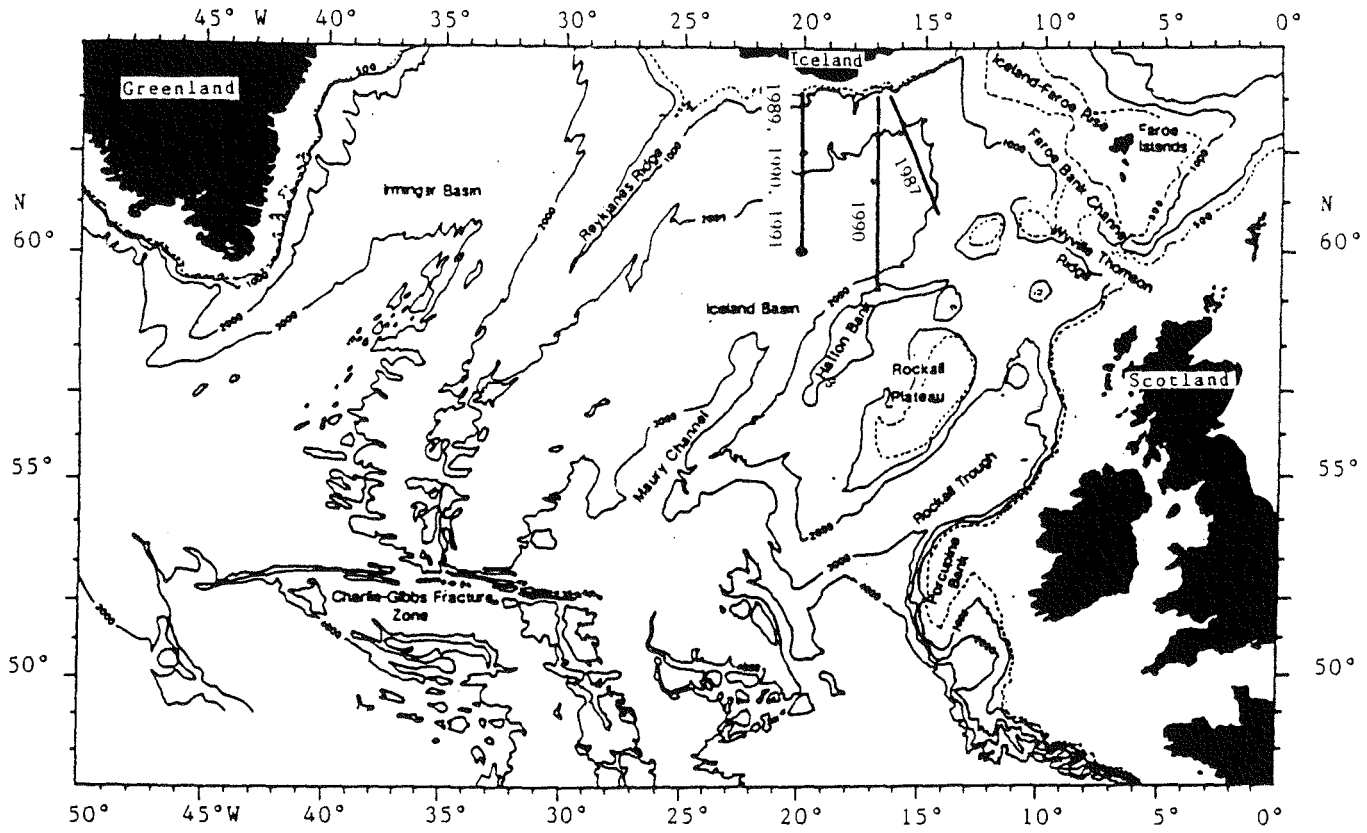

Figure 1. Topography of the Iceland Basin with the hydrographic sections discussed in this paper.

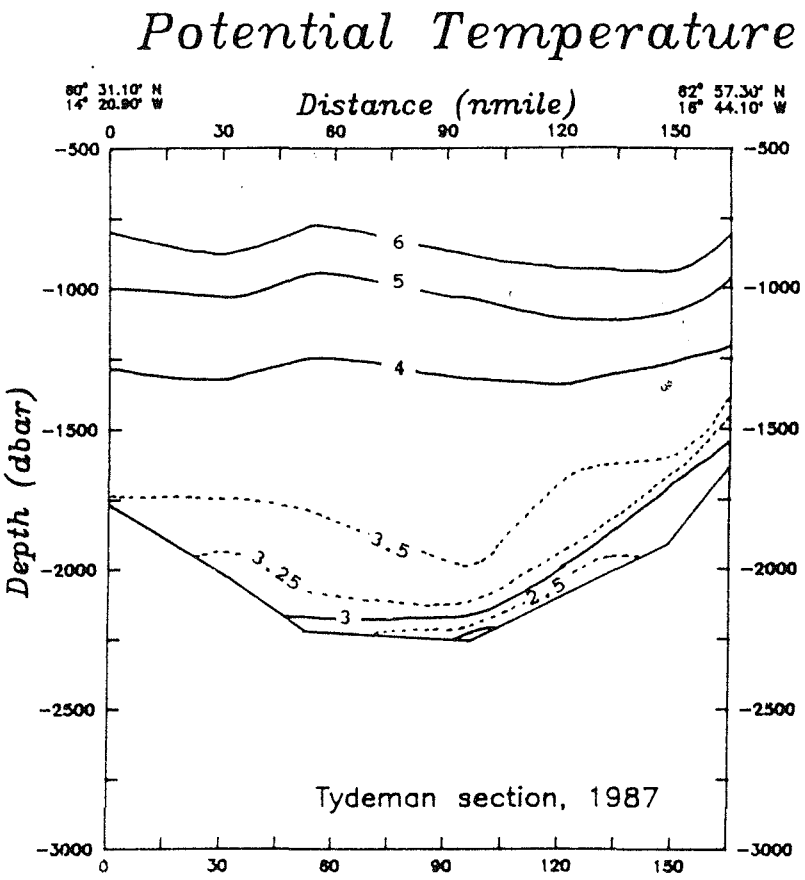

Figure 2a

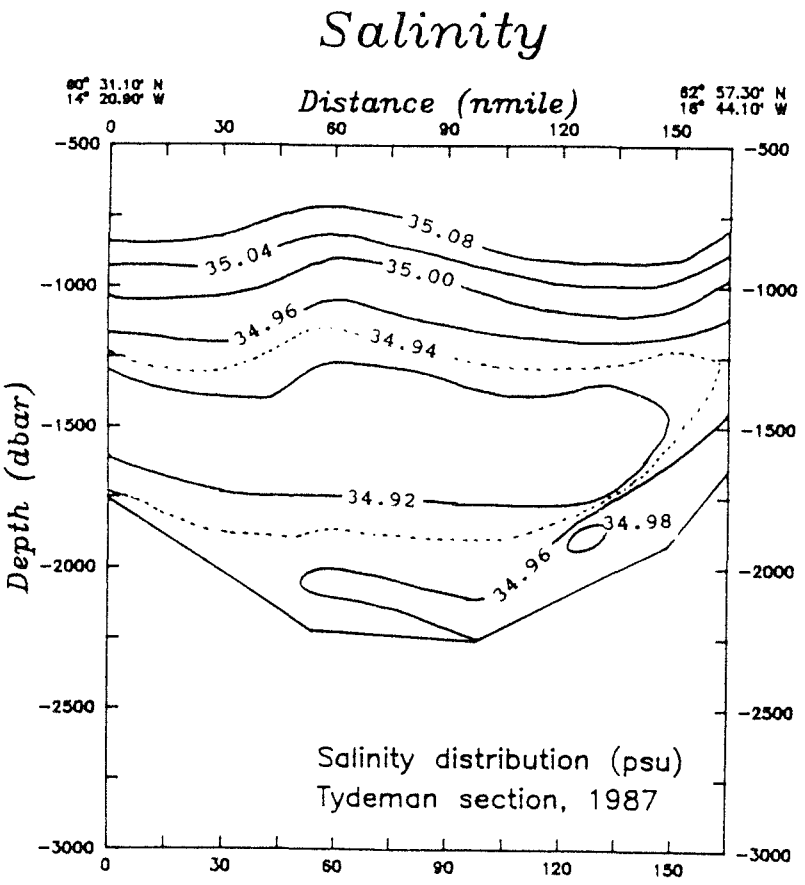

Figure 2b

Figure 2. Distribution of hydrographic parameters along the Tydeman section from 1987; (a) potential temperature (°C), (b) salinity (psu) and (c) dissolved silica (μmol kg^{-1}).

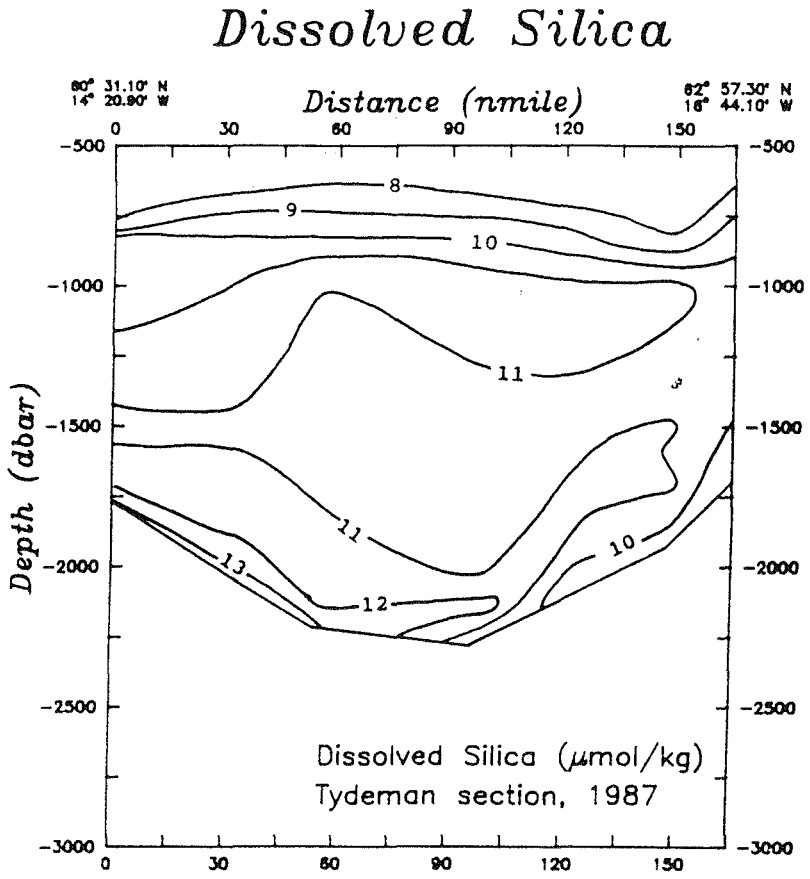

Figure 2c

Figure 2 Continued. Distribution of hydrographic parameters along the Tydeman section from 1987; (a) potential temperature (°C), (b) salinity (psu) and (c) dissolved silica (μmol kg^{-1}).

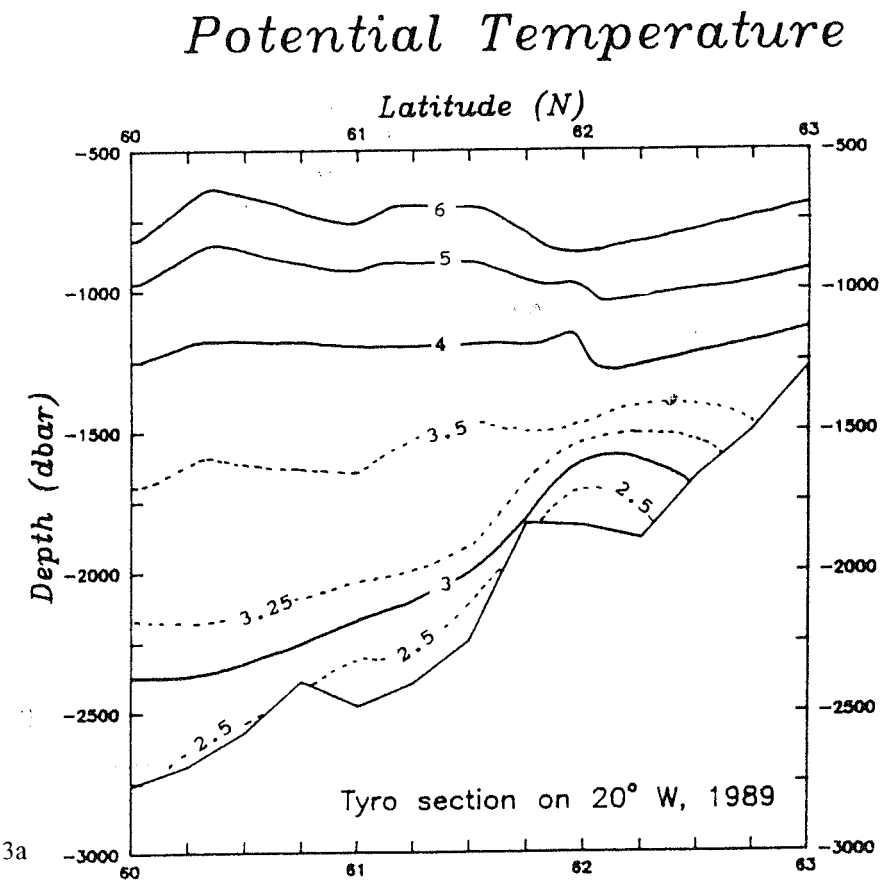

Figure 3a

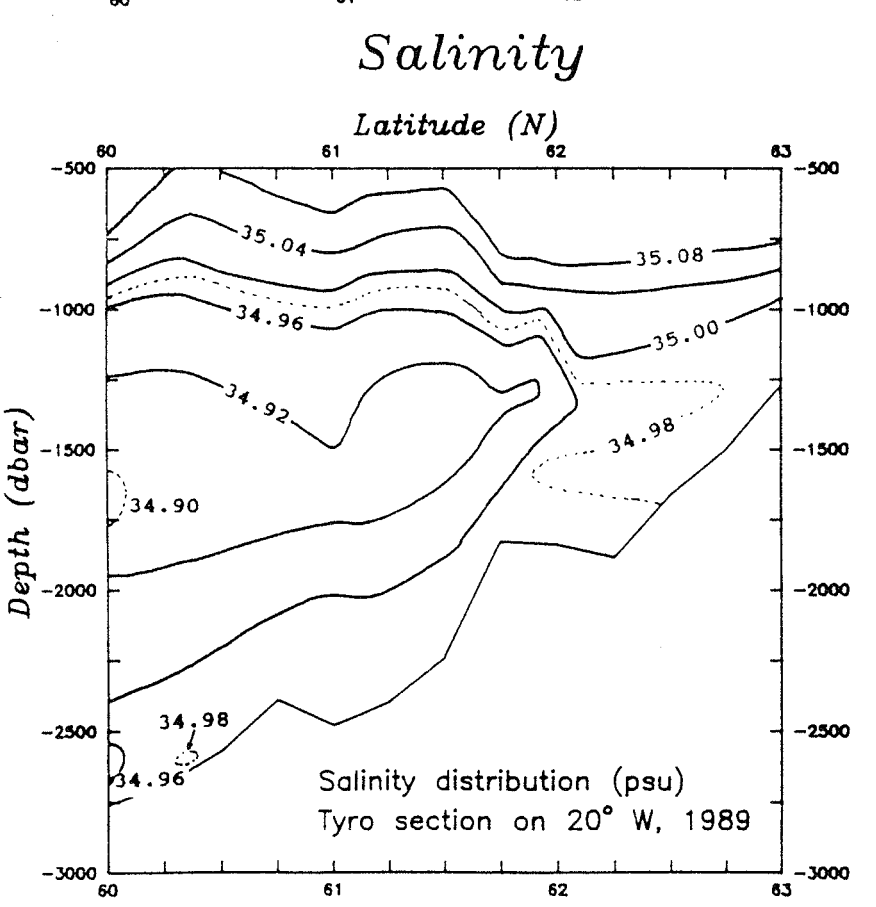

Figure 3b

Figure 3. As Figure 2 along 20°W from Tyro, 1989.

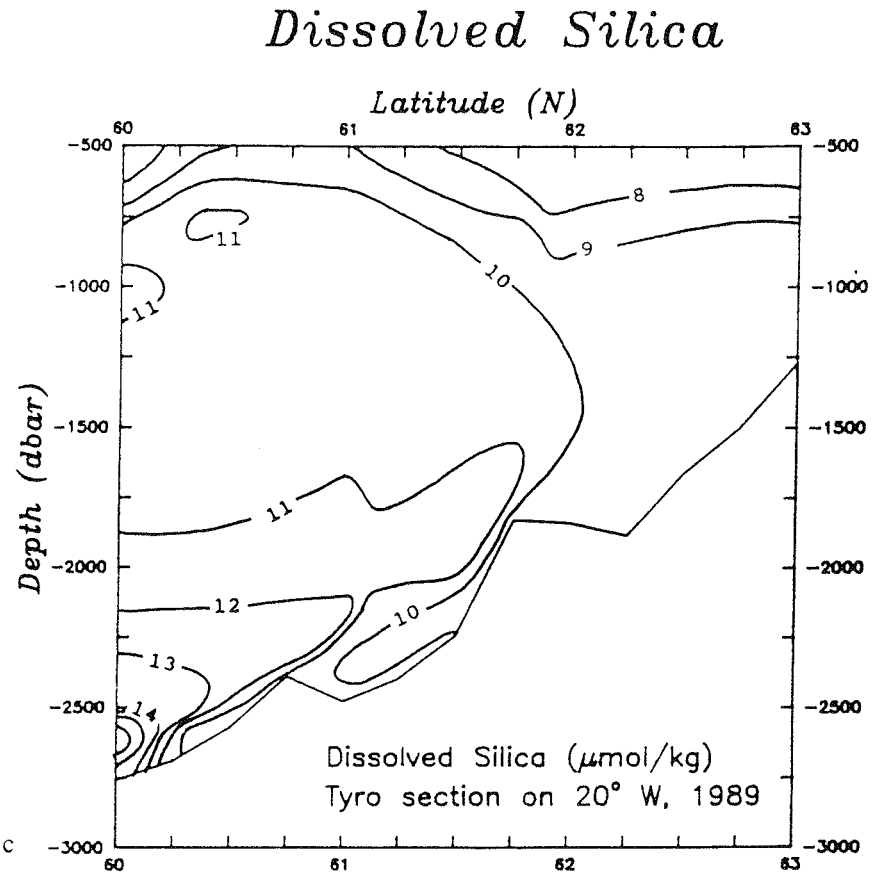

Figure 3c

Figure 3 Continued. As Figure 2 along 20°W from Tyro, 1989.

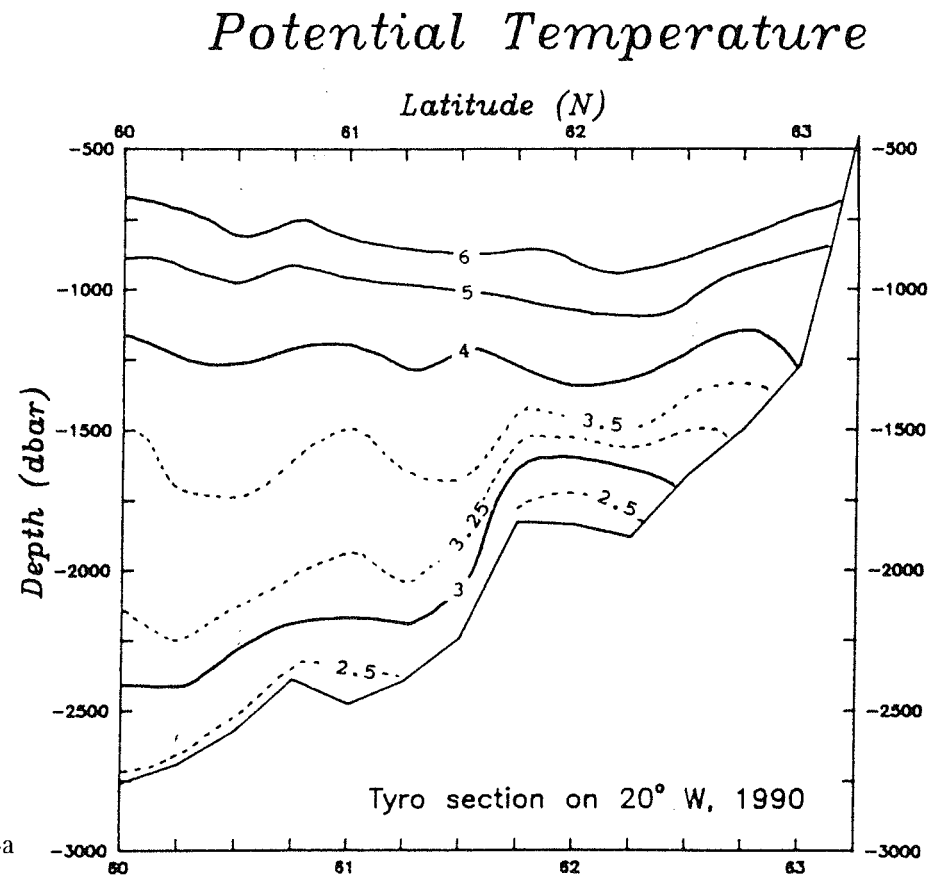

Figure 4a

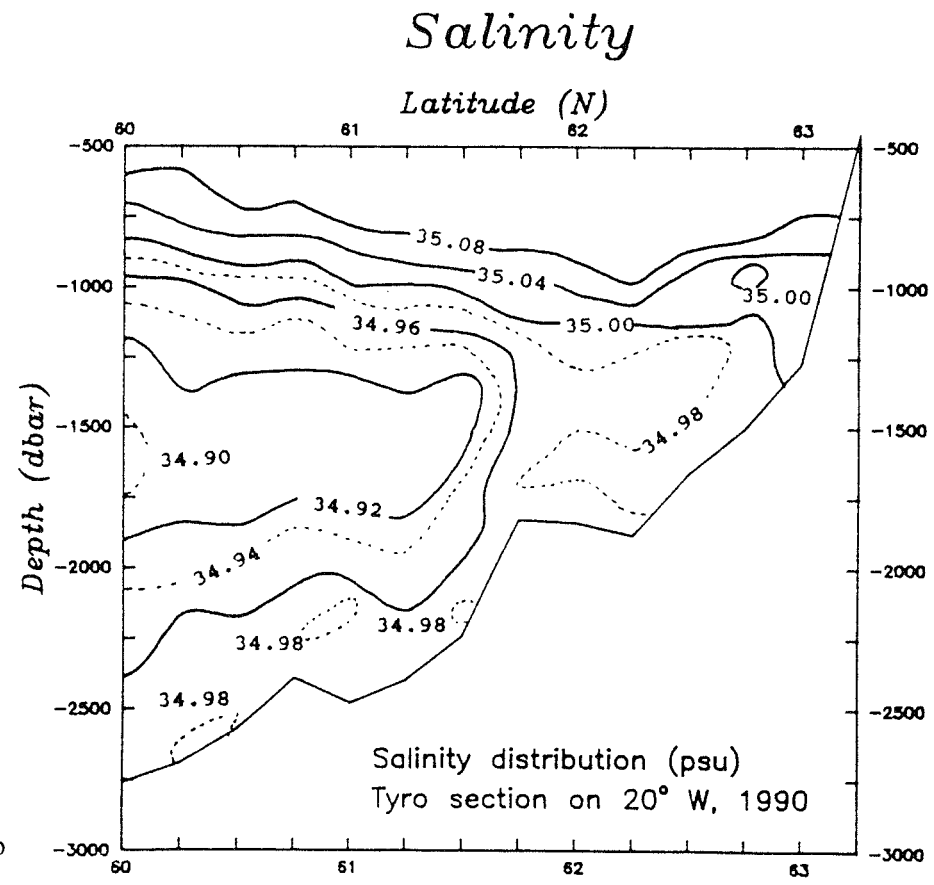

Figure 4b

Figure 4. As Figure 2 along 20°W from Tyro, 1990.

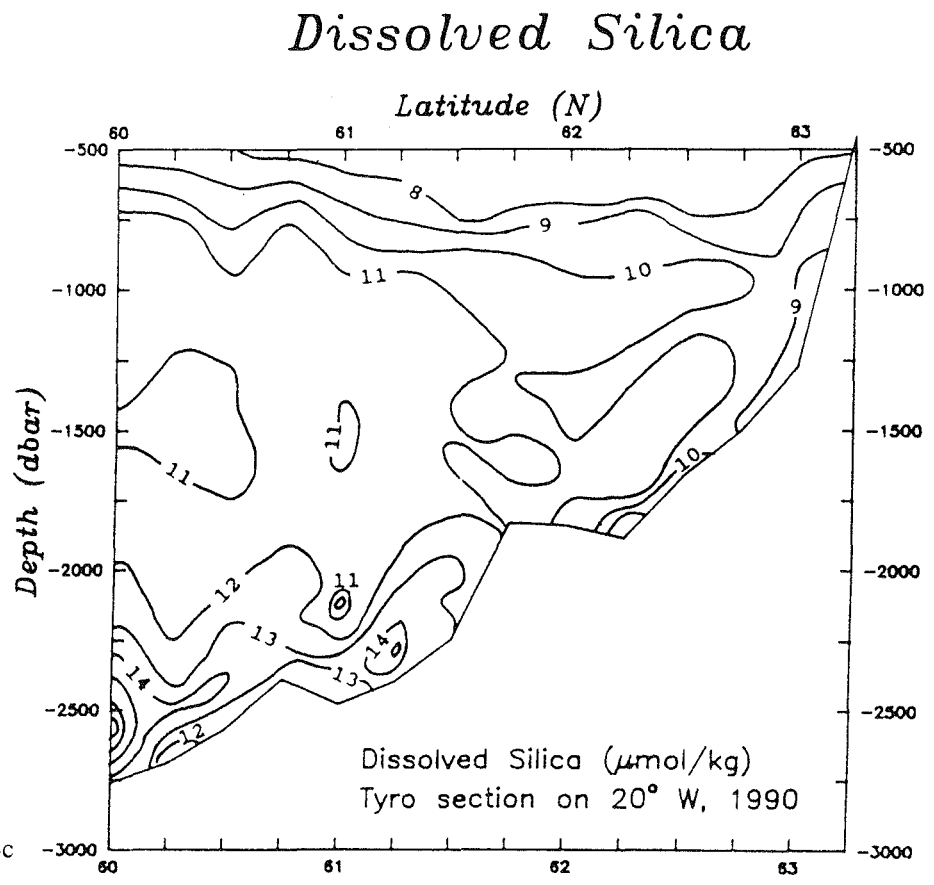

Figure 4c

Figure 4 Continued. As Figure 2 along 20°W from Tyro, 1990.

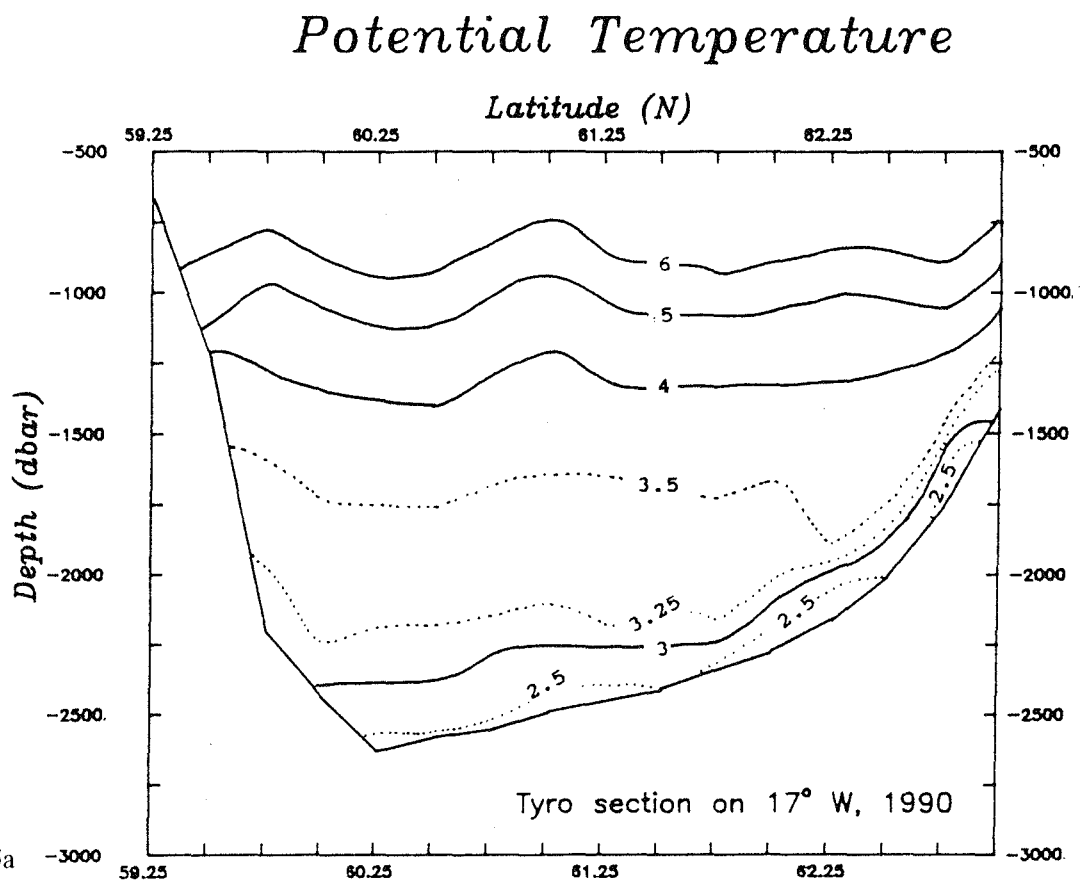

Figure 5a

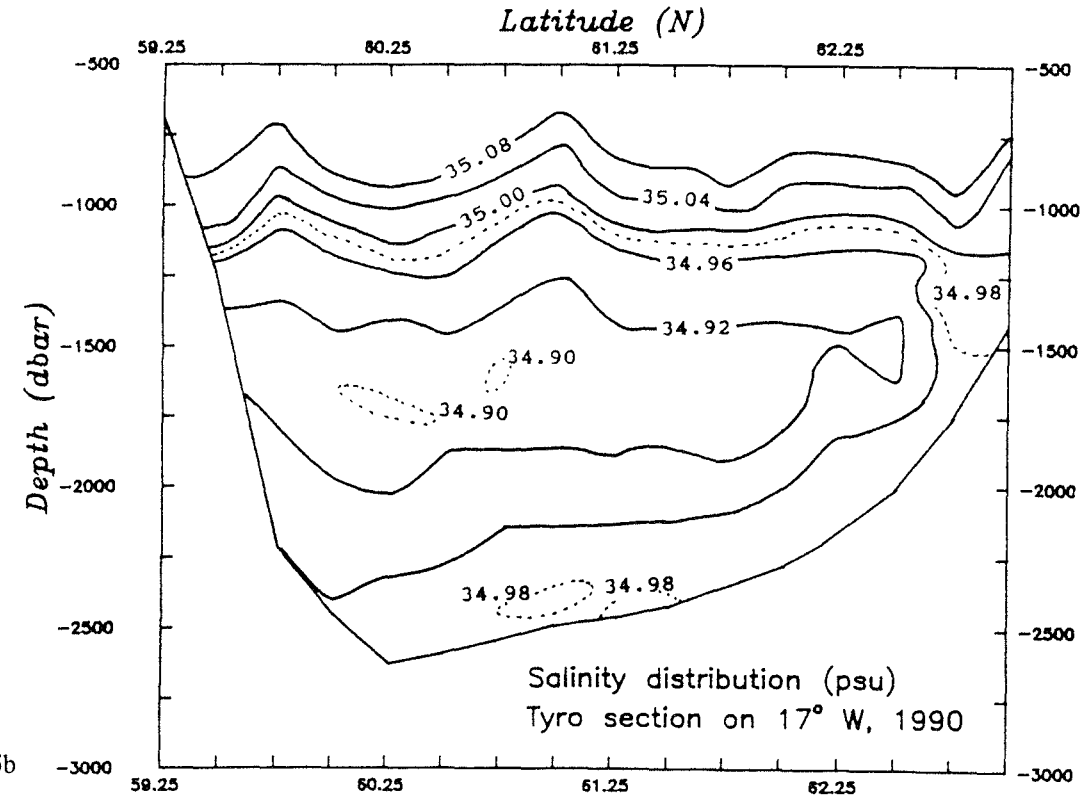

Figure 5b

Figure 5. As Figure 2 along 17°W from Tyro, 1990.

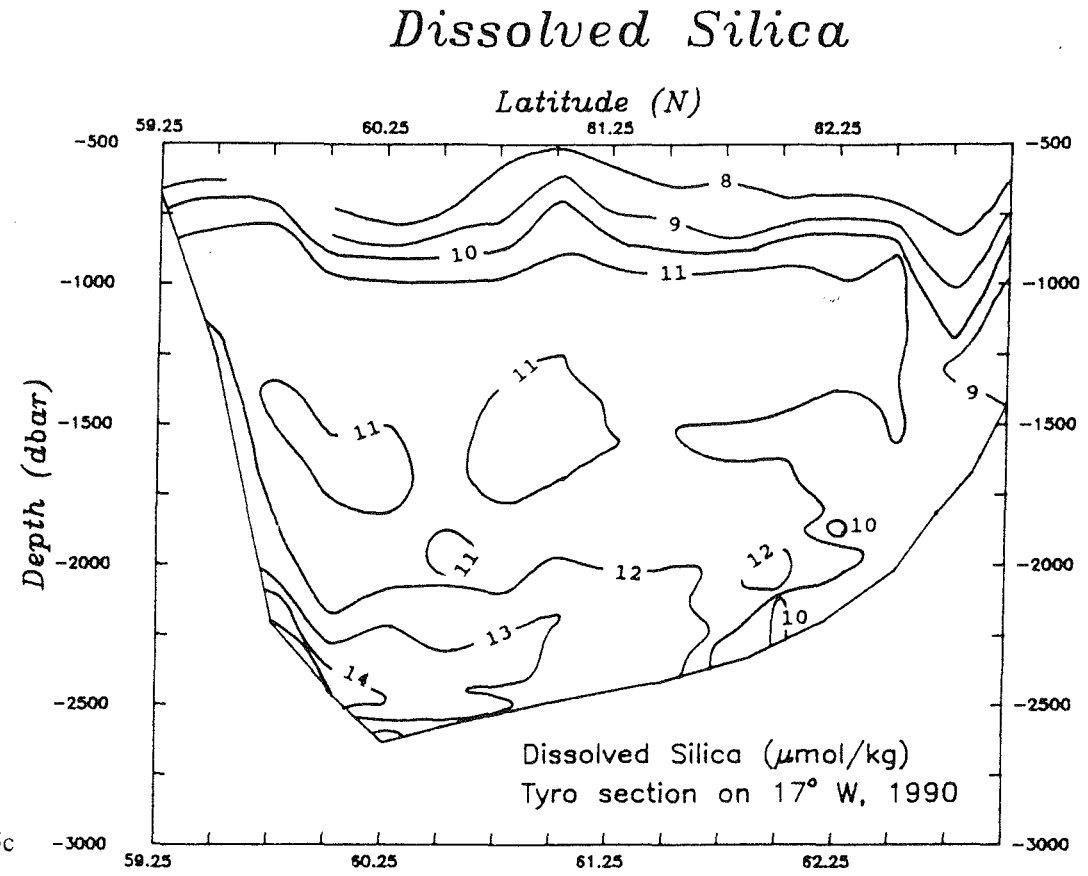

Figure 5c

Figure 5 Continued. As Figure 2 along 17°W from Tyro, 1990.

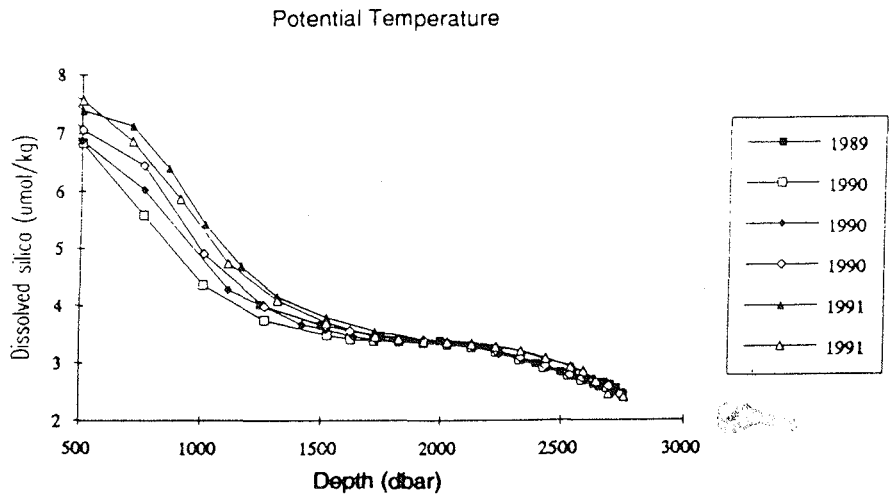

Figure 6. Vertical distribution of potential temperature (°C) at 60°N 20°W from Tyro cruises in 1989, 1990 and 1991.

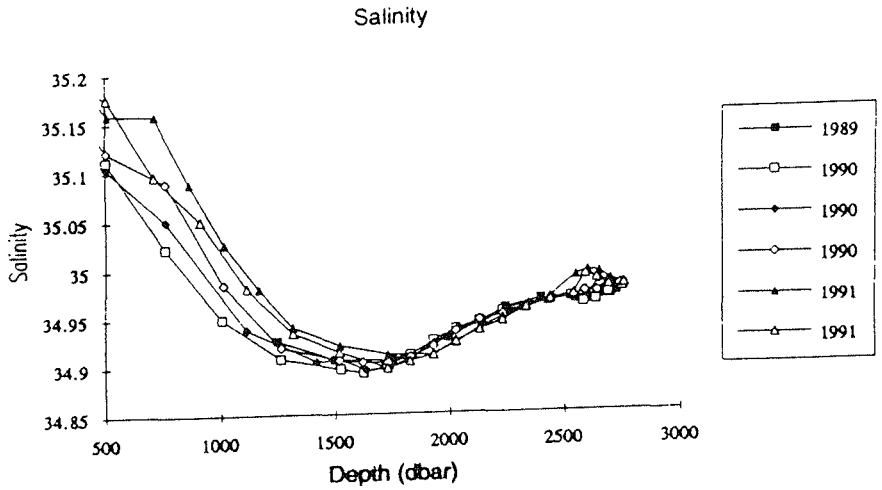

Figure 7. Vertical distribution of salinity (psu) at 60°N 20°W from Tyro cruises in 1989, 1990 and 1991.

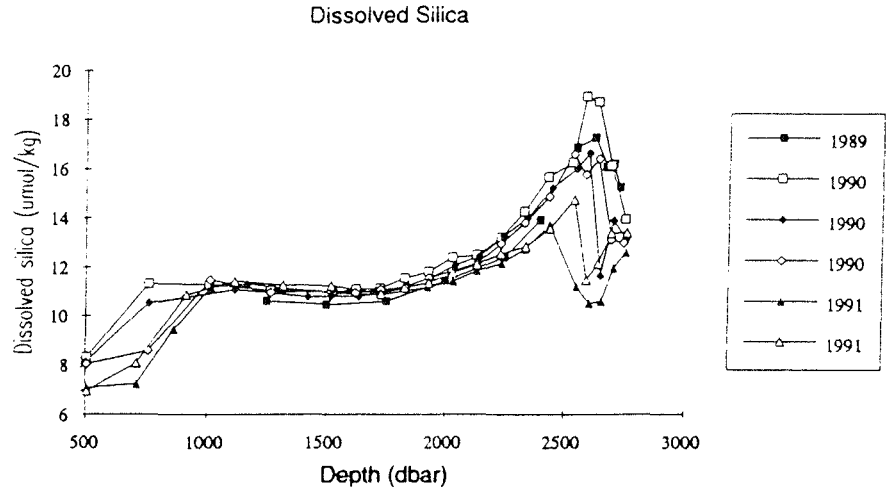

Figure 8. Vertical distribution of dissolved silica (μmol kg^{-1}) at 60°N 20°W from Tyro cruises in 1989, 1990 and 1991.

Satellite-tracked drogue paths over Faroe Bank and the Iceland-Faroe Ridge

Bogi Hansen[1], David Meldrum[2] and David Ellett[2]

[1]Fiskirannsóknarstovan, P.O. Box 3051, FR-110 Tórshavn, Faroe Islands. [2]Dunstaffnage Marine Laboratory, Oban, Argyll, Scotland.

Based on a paper presented to the ICES Hydrography Committee as ICES CM 1991/C:25

Satellite-tracked drogues have confirmed the existence of an anticyclonic circulation around Faroe Bank during three periods of 1986–89, and also showed a predicted self-contained circulation in the upper waters of the Faroe Bank Channel. Upon the Iceland-Faroe Ridge, drogues mainly followed the isobaths and were largely consistent with the classical circulation schemes for the area. The four drogues observed to cross the ridge did so through two channels, both of them on the southeastern half of the ridge.

Keywords: Faroe Bank, Iceland-Faroe Ridge, Drogues, Anticyclonic circulation

Introduction

In 1986 the SMBA Dunstaffnage Marine Laboratory in Oban, Scotland and the Fisheries Laboratory in the Faroe Islands initiated a joint project to study the upper-water flow over Faroe Bank and in Faroese waters using satellite tracked drogues. Originally the project was concentrated on the Faroe Bank (Figure 1) and the first results were reported to the ICES statutory meeting in 1986 (Hansen *et al.*, 1986). Together with evidence from hydrographic surveys and a current meter mooring these first results from the tracked drogues provided convincing evidence for a semi-closed anticyclonic circulation over the bank consistent with biological evidence indicating a fair amount of isolation of the bank water.

Since then the two drogues have been redeployed a number of times until they were both lost in 1989. The emphasis on the Faroe Bank circulation has continued; but in addition two other regions have been studied partly by design and partly by drogues drifting into the region after leaving the Faroe Bank. The two regions are the Iceland-Faroe Ridge and the Faroe Bank Channel (Figure 1).

Over the Iceland-Faroe Ridge, warm and saline water from the Atlantic flows into the Norwegian Sea and shortly after passing the ridge it encounters the colder and less saline waters from the East Icelandic Current in the Iceland-Faroe Front. The distribution of temperature and salinity makes it evident that there is a resulting eastward water transport over the ridge; but what is the flow pattern in more detail and where does the water cross the ridge? These are questions which as yet have been largely unanswered and were the reason for some of the drogue deployments.

The flow field of the Faroe Bank Channel has also been much discussed. In the deeper layers of the channel there can be no doubt about the direction of the flow of the cold "Overflow" water from the Norwegian Sea into the Atlantic; but how do the upper layers flow? The upper 300–500 meters of the channel are dominated by Modified North Atlantic Water (MNAW), which is found over large areas west of the Faroe Bank (Becker and Hansen, 1988); but this water could come either from north of the channel or from south of it and it has even been suggested that at least parts of this water could derive from the Faroe-Shetland Channel having passed over the Iceland-Faroe Ridge and flowed southward east of the Faroes. In 1988–1989 one of the drogues made a round-trip through the Faroe Bank Channel and combined with the available hydrographic evidence the drogue track does give some insight into the circulation of the Faroe Bank Channel.

Material and Methods

The two satellite-tracked buoys used in these experiments, labelled 3973 and 3979, were developed at the SMBA Laboratory (Booth and Ritchie, 1983). They

Table 1 Time and position of deployment for each experiment as well as the time of end either by recovery, by loss of drogue or by the drifter leaving the area. The columns labeled Day give the day number in the year.

	Start of Experiment			End of Experiment		
Drifter	Date	Day	Position	Date	Day	Status
3973	10 Mar 1986	69	60°50'N 8°45'W	3 May 1986	123	Recovered w. drogue
3979	10 Mar 1986	69	60°57'N 9°01'W	22 Mar 1986	81	Lost drogue
3973	25 Apr 1987	114	60°54'N 8°59'W	31 May 1987	151	Recovered w. drogue
3979	25 Apr 1987	114	60°50'N 8°44'W	31 May 1987	151	Recovered w. drogue
3973	31 May 1987	151	62°01'N 10°00'W	3 Jul 1987	184	Recovered w. drogue
3973	21 May 1988	142	62°00'N 10°59'W	27 Nov 1988	331	Recovered w. drogue
3979	21 May 1988	142	61°30'N 11°00'W	15 Nov 1988	320	Recovered w. drogue
3973	30 Nov 1988	335	61°24'N 7°59'W	18 Feb 1989	49	Left region w. drogue
3979	1 Dec 1988	336	61°08'N 9°31'W	11 Feb 1989	42	Lost drogue

were drogued with a square sail having an area of 5x12 m^2 at a depth of 60 meters as described in more detail in Hansen *et al.* (1986). Experience in North European offshore waters (Booth and Meldrum, 1985) has indicated that the direct wind effect on the buoys is small and the first deployment on Faroe Bank gave very convincing evidence for that (Hansen *et al.*, 1986).

The drogue deployments discussed in this paper were all made from the Faroese research vessel Magnus Heinason and usually the drogues were picked up by this vessel at the ends of the experiments. In the end, however, both drifters were lost as one of them went aground on the Faroes after having lost its drogue while logistical difficulties prohibited the recovery of the other drifter before it drifted too far from the area. In some cases the drogue has been lost during an experiment; but the change in behaviour and in the response to winds makes it fairly easy to establish the time at which the drogue was lost. If each deployment of a drifter is considered an experiment, a total of 9 experiments were made. In Table 1 we summarize these.

Drogue tracks on Faroe Bank

During 1986–89, satellite-tracked drogues were released on Faroe Bank during three periods, April-May 1986, April-May 1987 and December 1988-February 1989. The tracks of the two drogues released in April-May 1986 are shown in Figure 2, and have previously been described by Hansen *et al.* (1986), where the net anticyclonic drift around the bank was noted to have been interrupted in the case of drogue 3973 by a period of southerly movement outside the 200 m isobath to the west of the bank, and an excursion to the northwest towards the end of the drift. No obvious connection was seen between these movements and local winds.

The releases of the following year (Figures 3 and 4) were more regular, although a diversion into deeper water off the northwestern quadrant of the bank was again apparent in the path of drogue 3979. Within the 200 m isobath, it took 30 days for drogue 3973 to return to its starting point. Drogue 3979 spent 15 days in rounding the southern fringes of the bank and then travelled northwestwards in depths of 200–400 m during another 15 days.

In December 1988 (Figure 5), a drogue was launched to the west of the bank over soundings of 700-800 m. Within a few days the drogue had begun a southward movement over the 500 m isobath, which continued for about a week and which compares closely with the southward drift of 3973 in the same locality in 1986 (Figure 2). Subsequently it reversed its course and moved into shallower water and began an anticyclonic circulation around the bank, reaching the northeast corner after 30 days, passing down the east side over the course of about 25 days. The drogue continued along the western side of the bank, but by day 42 of 1989, detacment of the drogue was indicated by an abrupt increase in drift speed.

All five of the drogue tracks on the bank gave clear evidence of an anticyclonic circulation and suggest a residence time for water upon the bank which is in excess of 30–40 days. In two cases one of the drogues completed more than a complete circle around the bank. Drogue 3973 in April-May 1987 (Figure 3) used 30 days for this while drogue 3979 in December 1988 to February 1989 (Figure 5) used 45–60 days for the roundtrip depending upon where the starting point is chosen. There may be various explanations for this difference. For one thing the track in 1987 was over shallower parts of the bank than in 1988-89; but also this later track is rather anomalous. The drogue in this case started west of the bank, was advected onto the

bank and crossed over the shallowest part instead of following the isobaths round the northeastern corner. One reason for this anomalous behaviour may be wind. Just before Christmas in 1988 the most severe storm in recent times struck the Faroe Islands with extremely strong winds. The fact that the drogue kept over the bank during and after this storm says much for the persistence of the circulation.

On Figure 6, smoothed drogue tracks from all five experiments on Faroe Bank are plotted on the same map. The smoothing was done by eye. If the bank is divided into two halves by the length axis shown roughly on Figure 6, then we may divide each drogue track into southwest-going and northeast-going subtracks. The figure gives the impression that the northeast-going subtracks generally were over deeper water outside the 200 m isobath compared to the southwest-going subtracks which generally were within that isobath. Especially the first (western) part of the northeast-going subtracks seems to have been over fairly deep water. This indicates that the circulation may be non-symmetric and displaced towards the northwest with respect to the topography. A radial component of the flow, positive out from the bank may, however, also contribute.

A further asymmetry may be seen in the mean velocities. On the northeast-going subtracks the drogues generally seem to have moved about twice as fast as on the southwest-going subtracks. Thus in April-May 1987 drogue 3973 used 20 days for the southwest-going part of the roundtrip and 10 days for the northeast-going part. This implies mean residual velocities on the order of 5 cm s^{-1} on the southwest-going part and 10 cm s^{-1} on the northeast-going. The difference could be due to the difference in water depth along the two subtracks if the speed of the circulation increases from the crest outward. The southwest-going flow may, however, in general be slower than the northeast-going flow taking into account that the main flow in the region is eastward. Between September 1987 and June 1988, current meters moored at 275m depth at a position in 700 m soundings on the southern flank of Faroe Bank (60° 17.4' N, 8° 46.4' W) showed steady eastward currents apart from short west-going periods in early March and early June 1988 (Ellett, 1991).

Anticyclonic semi-diurnal tidal ellipses clearly traced by drogue 3973 at a time of spring tides (from 26 April 1987) indicated speeds in excess of 50 cm s^{-1} upon the bank top in soundings of about 100 m. In 1913 Jacobsen (1915) measured tidal currents on the Faroe Bank at a bottom depth of 110 m, close to the crest. He found anticyclonic tides with velocities approaching 1 m s^{-1} during neap tides. His measurements lasted only about a day, however, and should not be used uncritically. A moored current meter on the easternmost edge of the bank with bottom depth of about 120 m gave M_2 amplitudes of 26 and 28 cm s^{-1} respectively for the two velocity components (Hansen, unpubl. data).

Drogue tracks in the Faroe Bank Channel

Drogue 3793 was launched towards the northern exit of the Faroe Bank Channel in December 1988 (Figure 7). It travelled southwards to the region of divergent and deepening topography between the southern end of the Faroe Plateau, the Wyville-Thomson Ridge and Faroe Bank, where it made two large cyclonic circuits. Upon completing a smaller circuit in early January 1989 (Figure 8), it returned northwards in cyclonic paths which were north-going on the eastern side and south-going on the western side of the Faroe Bank Channel. Hansen (1985) has shown from temperature-salinity characteristics that there is little exchange of upper water between the Faroe-Shetland and Faroe Bank channels, with evidence indicating that water which enters the latter at the northwestern end travels southwards along the western side of the channel and recirculates northwards along its eastern flank. To some extent, the drogue paths of Figures 7 and 8 support this, but they also seem to indicate changes in the Faroe Bank Channel flow pattern over timescales of weeks to months.

Semi-diurnal tidal rotation of this drogue was anticyclonic along most of its track as for the drogues on Faroe Bank. While travelling north through the Faroe Bank Channel, cyclonic paths were traced; but these were on timescales of a few days and non-tidal. Certainly Sætre (1967) found anticyclonic tidal current ellipses in the Faroe Bank Channel using moored current meters.

Drogue tracks over the Iceland-Faroe Ridge

Four drogue drifts traced flow from the Atlantic to the Norwegian Sea across the Iceland-Faroe Ridge. The first of these was 3973, released in late May 1987 at 62° N, 10° W, over soundings of about 750 m west of the Faroe Plateau (Figure 9). This drogue moved northeastwards onto the ridge and then for a week travelled northwestwards along the 500–600 m isobaths. It then moved northeastwards to the crest of the Iceland-Faroe Ridge, where it spent a further 10–12 days before moving west then north, to be recovered upon the Norwegian Sea flank of the ridge 32 days after being launched.

In the following year, drogues released at 11° W showed much more reluctance to cross the ridge, requiring 150-170 days for the crossings (Figures 10 and 11). Despite spending about 40 days in June-July in the vicinity of the eastern ridge crest, drogue 3973 (Figure 10) remained over the Atlantic flank and subsequently moved northwestwards along the 500 m isobath towards the north-western low point of the ridge.

Returning more slowly and irregularly to the east, it remained here until early November, when it moved northwards to spend a week in soundings of 500 m on the Norwegian Sea flank of the ridge before moving more rapidly east and north into deep water.

Drogue 3979, launched 30 nautical miles to the south of 3973, had a similarly protracted journey (Figure 11). After 60 days spent to the west of the Faroe Bank Channel, it followed the 600-800 m isobaths northwestwards to the Icelandic end of the ridge where it stayed for a month, returning thereafter to the southeast and crossing the ridge-crest slowly over the course of some 14 days, after which it moved eastward into deep water.

The paths of these two drogues are consistent with the flow pattern suggested by Helland-Hansen and Nansen (1909) who in their Figure 39 (p.136) show some of the Atlantic water moving nortwestwards towards Iceland before crossing the ridge and then returning southeastwards. This semi-closed anticyclonic circulation is fairly well represented by the behaviour of the two drogues during August 1988 when they were moving in opposite directions along the ridge axis (Figure 12). It should, however, be stressed that drogue 3973 did not follow this path during its earlier crossing in June-July 1987 (Figure 9) and none of the drogues crossed the ridge crest in the Icelandic end of the ridge. Thus the circulation was rather over the western flank of the ridge than over the crest.

The fourth drogue to cross the Iceland-Faroe Ridge was drogue 3973 in February 1989. The earlier path of this drogue in the Faroe Bank Channel has been described. After reaching 62° N (Figure 8), it turned northeastwards and in the following 15 days crossed the ridge close to the northern slope of the Faroe Plateau. It continued to follow the 400 m isobath until mid-February 1989. Its further path is not shown here, but it moved eastward into deeper water at the north-western entrance to the Faroe-Shetland Channel where it made two anticyclonic circuits before moving off northeastwards into the Norwegian Atlantic Current.

Thus, only one (Figure 8) of the four drogues released west of Faroe reached the Norwegian Sea by rounding the slope adjacent to the Faroe Plateau. This was the one released closest to the Faroe Plateau. The remaining three drogues all eventually crossed the crest of the Iceland-Faroe Ridge close to 63° N, 9° 30' W, where the chart of Fleischer *et al.* (1974) shows the 500 m isobath penetrating well across the ridge from a northeasterly direction. The drogue launched at 10° W showed the least diversion in its course to this crossing point, whilst those from 11° W contoured the southern slopes of the ridge in both directions before finally entering the Norwegian Sea.

Comparing the various drogue tracks, it may be noted that one drifter may cross a point on the track of a previous drogue; but continue along a quite different path. This demonstrates clearly the variability of the flow across the ridge. In spite of this variability the four drogues crossed the ridge, not at four distinct sites; but through the two channels over the ridge closest to the Faroes.

Acknowledgements

The two buoys and satellite transmitters were kindly provided by the UK Department of Energy, after use in earlier DML drogue tracks. The recovery of drogues under often bad weather conditions requires exceptional eyesight and experience for which the authors want to compliment the crew of the RV "Magnus Heinason".

References

Becker, G., and Hansen, B. 1988. Modified North Atlantic Water. ICES CM 1988/C:17, 16 pp.

Booth, D. A., and Meldrum, D. T. 1985. Northeast Atlantic satellite-tracked buoy drifts. U.K. Department of Energy Offshore Technology Reports.

Booth, D. A., and Ritchie, D. 1983. SMBA Satellite Tracked Buoy and Drogue. SMBA Marine Physics Group Report, 22, 15 pp.

Ellett, D. J. 1991. Norwegian Sea Deep Water overflow across the Wyville-Thomson Ridge during 1987-88. ICES CM 1991/C:41, 11 pp.

Fleischer, U., Holzkamm, F., Vollbrecht, K., and Voppel, D. 1974. Deutsche Hydrographische Zeitschrift, 27, 3.

Hansen, B. 1985. The circulation of the northern part of the North Eastern Atlantic. Rit Fiskideildar, 9: 110-126.

Hansen, B., Ellett, D., and Meldrum, D. 1986. Evidence for an anticyclonic circulation on Faroe Bank. ICES CM 1986/C:15, 15 pp.

Helland-Hansen, B., and Nansen, F. 1909. The Norwegian Sea. Report on Norwegian Fishery and Marine Investigations, II (2), 390 pp.+suppl.

Jacobsen, J. P. 1915. Hydrographical investigations in Faeroe waters. Meddelelser fra Kommisionen for Havundersøgelser. Serie: Hydrografi, 2 (4). Copenhagen.

Sætre, R. 1967. Report on the Norwegian investigations in the Faeroe Channel 1964–65. NATO Subcommittee on Oceanographic Research. Technical Report No. 38. Bergen.

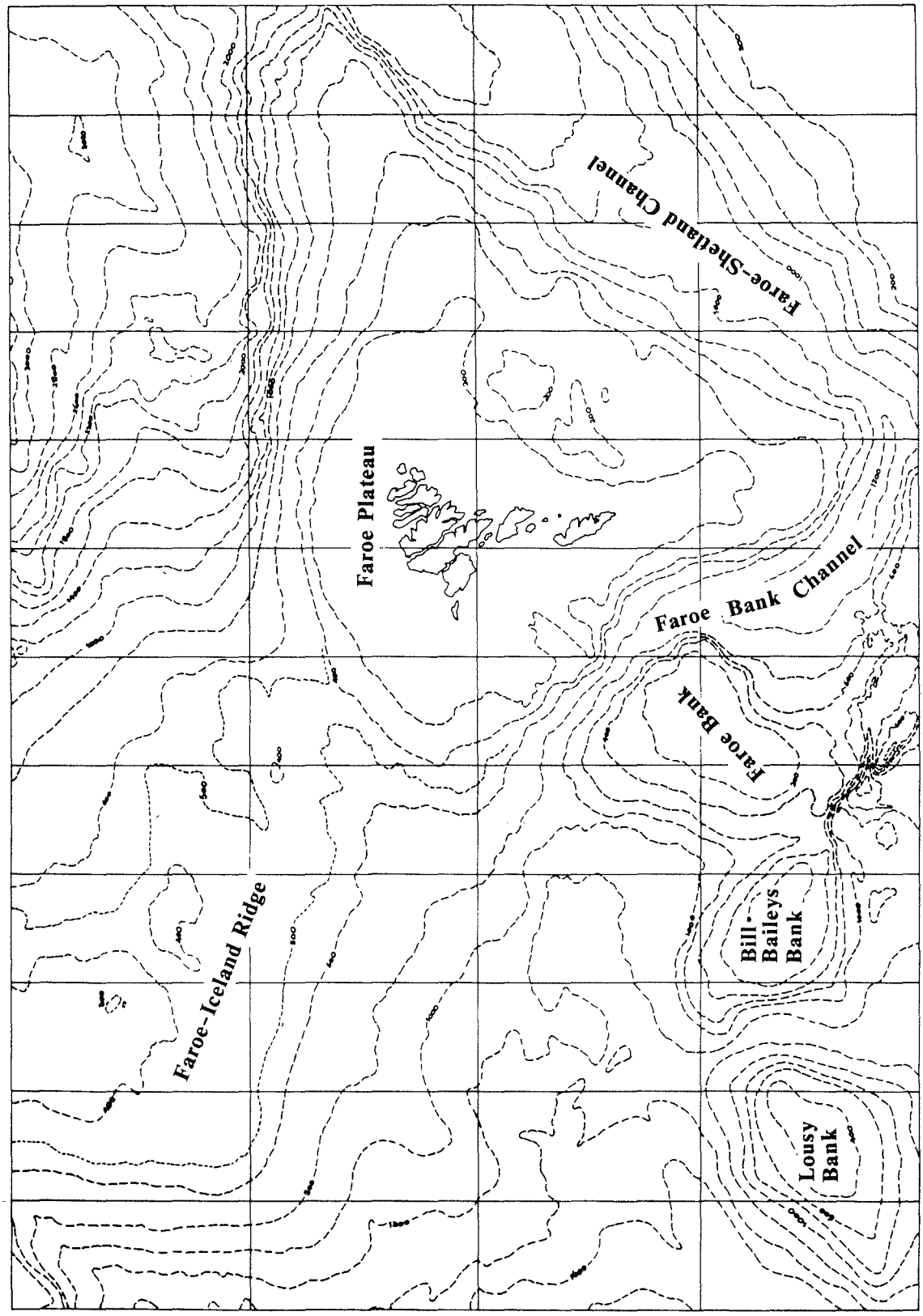

Figure 1. Bottom topography of the area investigated.

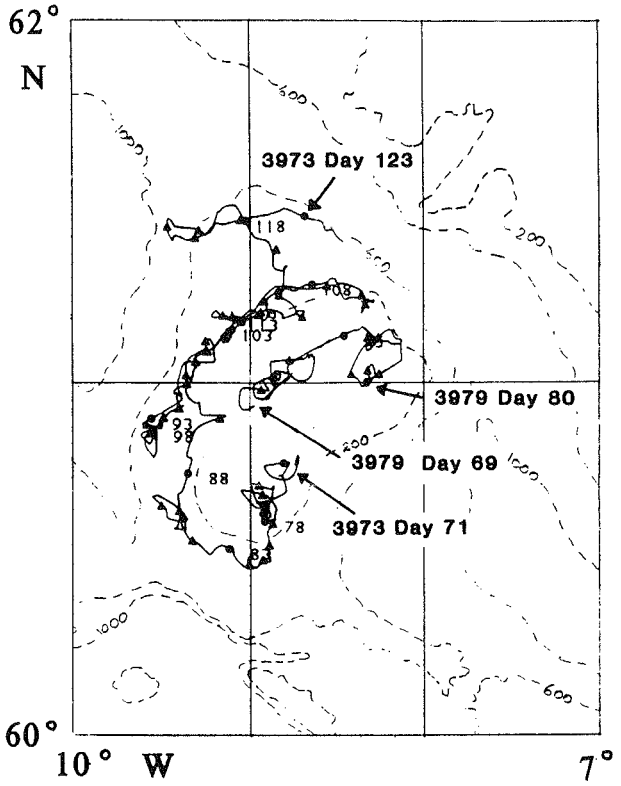

Figure 2. Drogues 3973 and 3979 during April - May 1986. Drogue tracks are indicated by continuous lines with arrows to indicate direction and filled circles every 5th day day number in 1986. Beginning and end of each drogue track is indicated. Broken lines are isobaths.

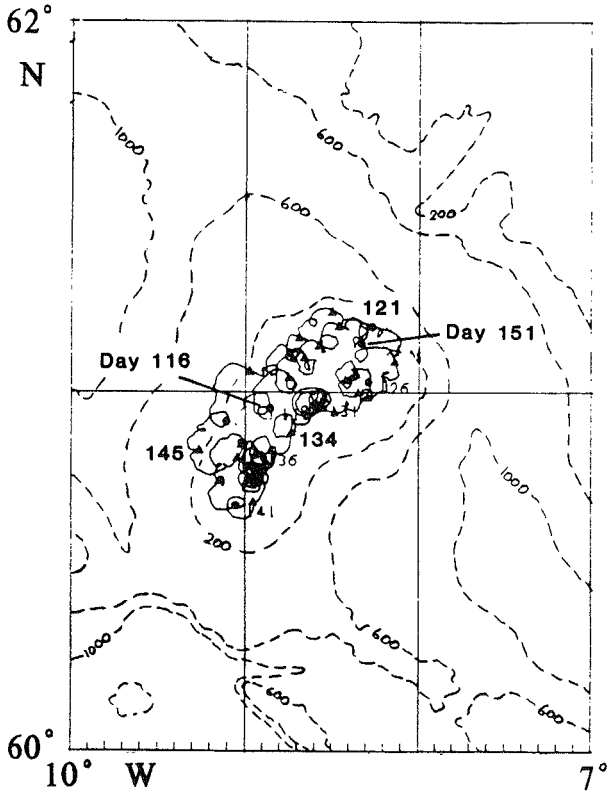

Figure 3. Drogue 3973 during April - May 1987. Drogue track is indicated by a continuous line with numbers indicating day number in 1987. Broken lines are isobaths.

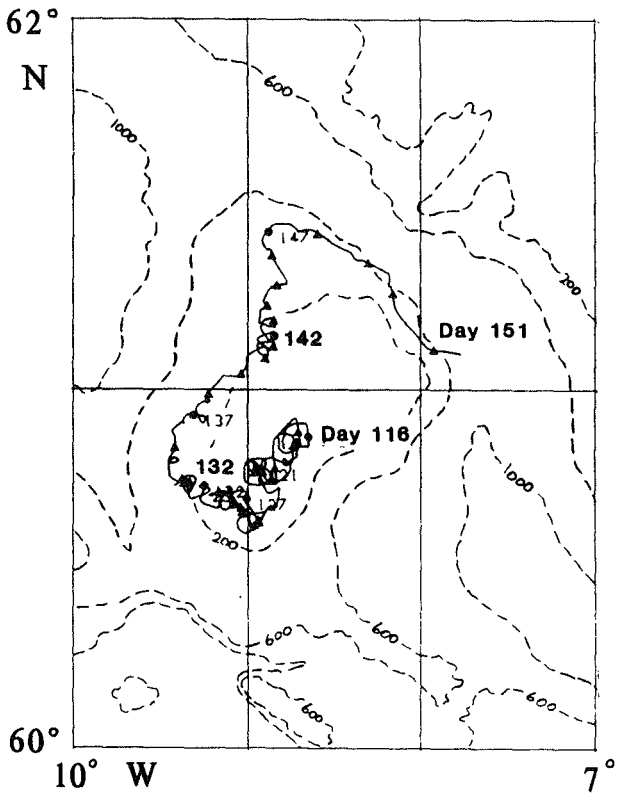

Figure 4. Drogue 3979 during April - May 1987. Drogue track is indicated by a continuous line with numbers indicating day number in 1987. Broken lines are isobaths.

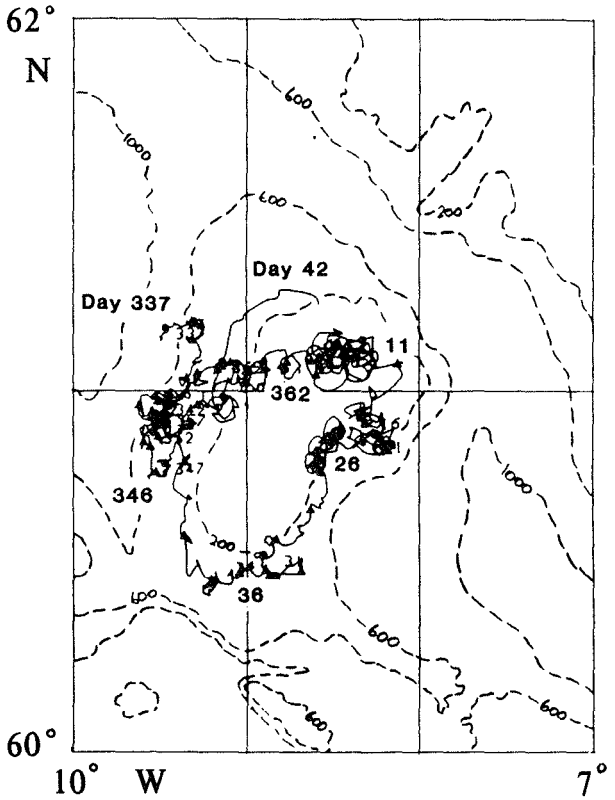

Figure 5. Drogue 3979 during December 1988 - February 1989. Drogue track is indicated by a continuous line with numbers indicating day number in 1988 and 1989. Broken lines are isobaths.

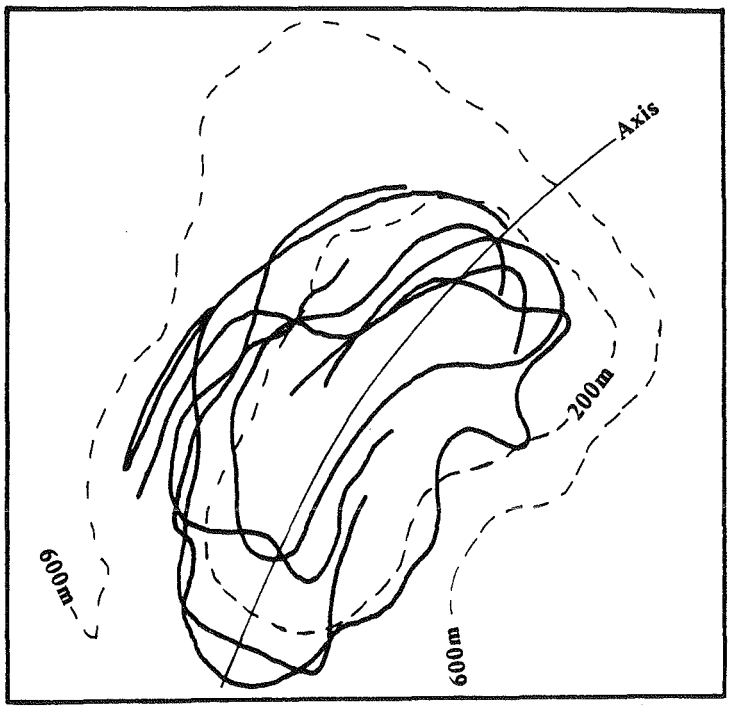

Figure 6. Smoothed tracks from the five drogue experiments on Faroe Bank (full lines) superposed on bottom topography (broken lines).

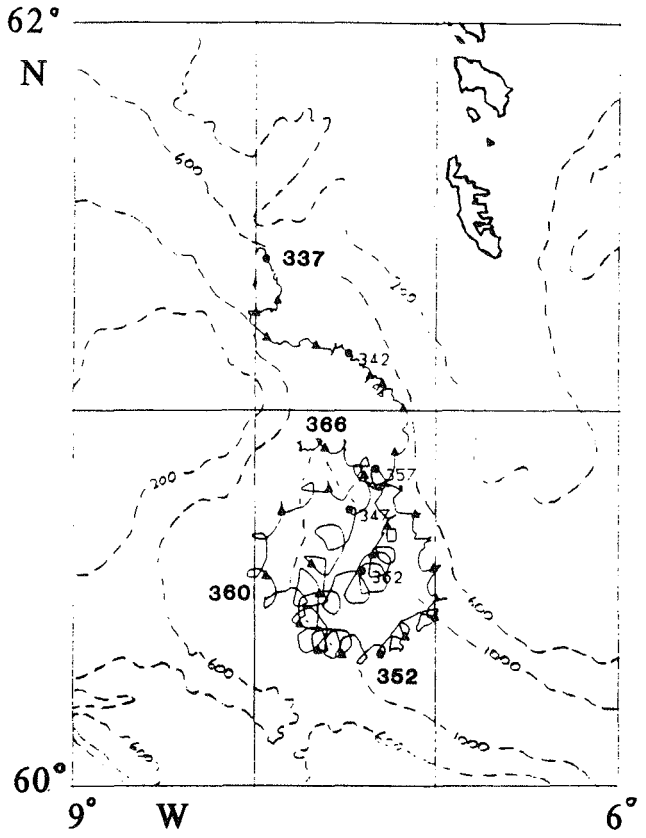

Figure 7. Drogue 3973 during December 1988. Drogue track is indicated by a continuous line with numbers indicating day number in 1988. Broken lines are isobaths.

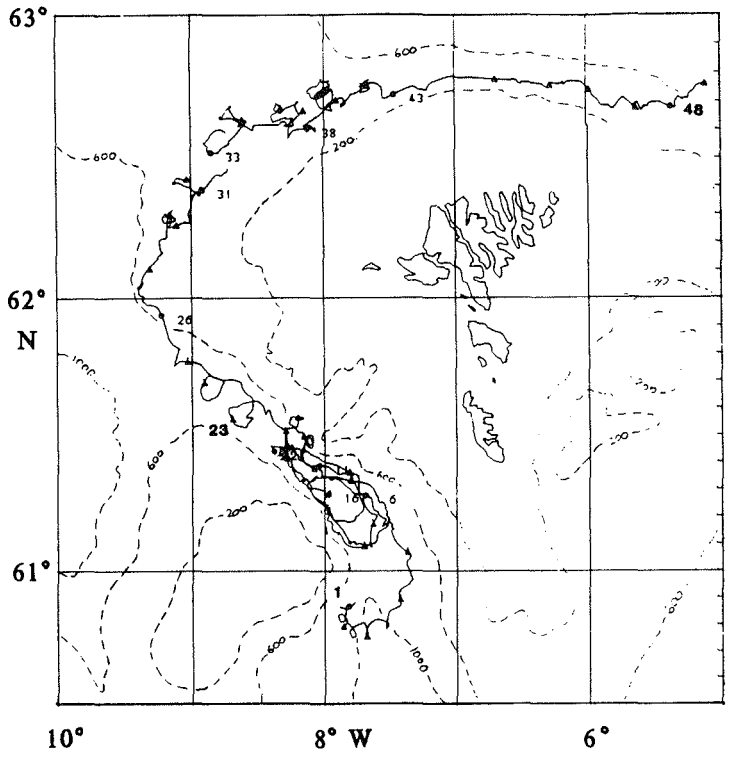

Figure 8. Drogue 3973 during January - February 1989. Drogue track is indicated by a continuous line with numbers indicating day number in 1989. Broken lines are isobaths.

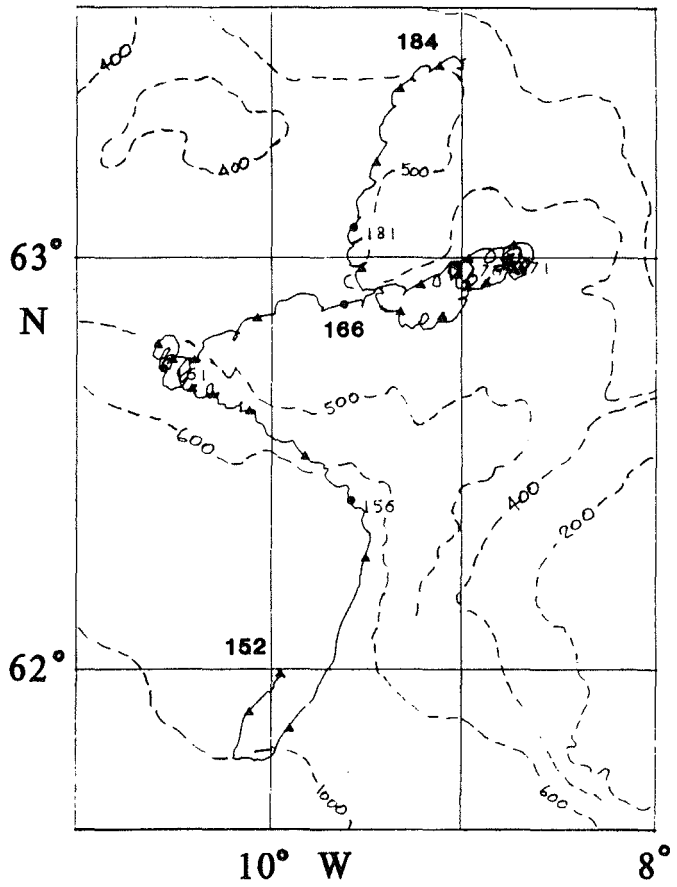

Figure 9. Drogue 3973 during June - July 1987. Drogue track is indicated by a continuous line with numbers indicating day number in 1987. Broken lines are isobaths.

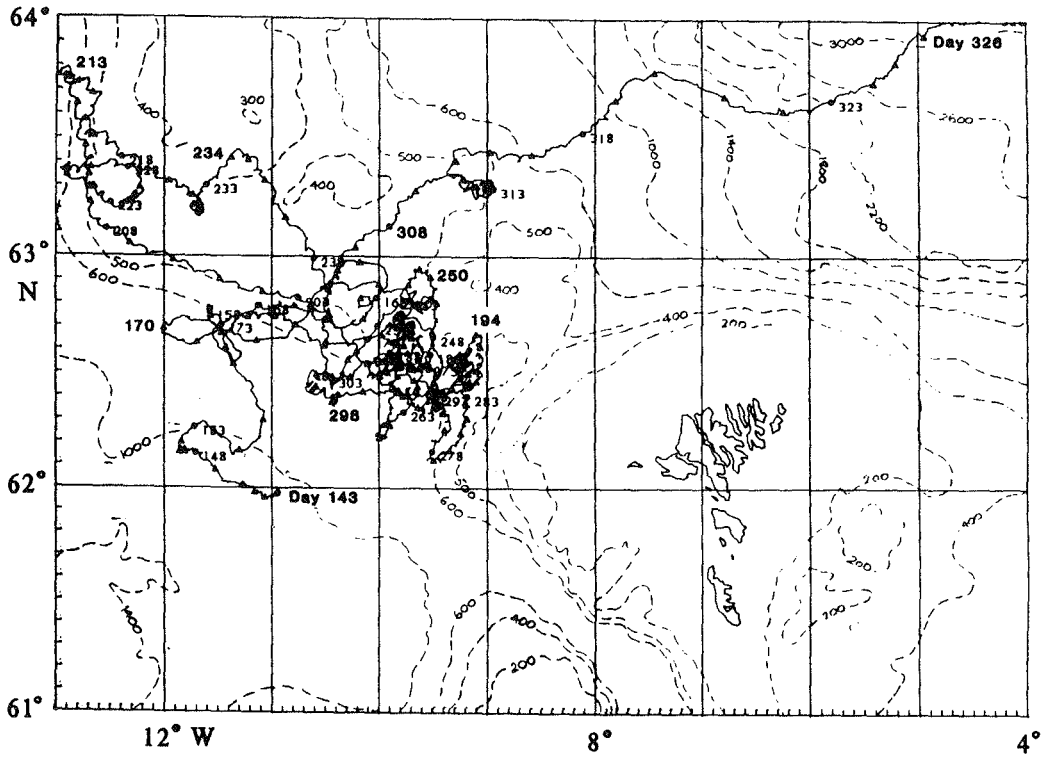

Figure 10. Drogue 3973 during May - November 1988. Drogue track is indicated by a continuous line with numbers indicating day number in 1988. Broken lines are isobaths.

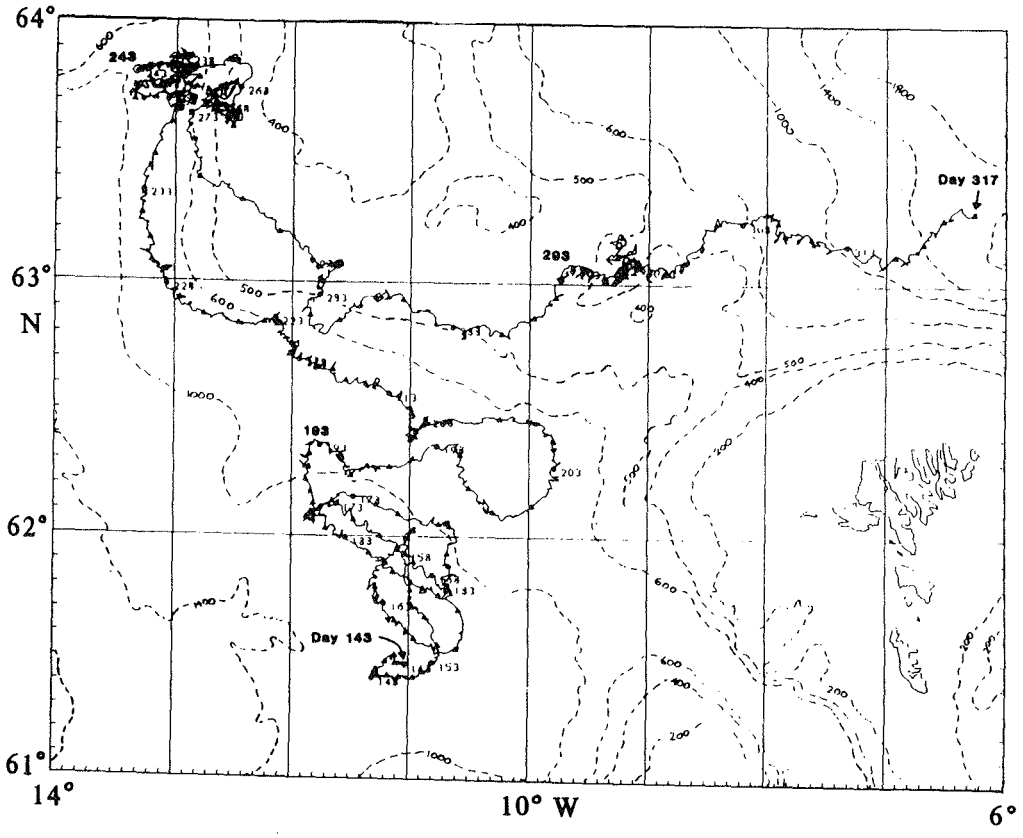

Figure 11. Drogue 3979 during May - November 1988. Drogue track is indicated by a continuous line with numbers indicating day number in 1988. Broken lines are isobaths.

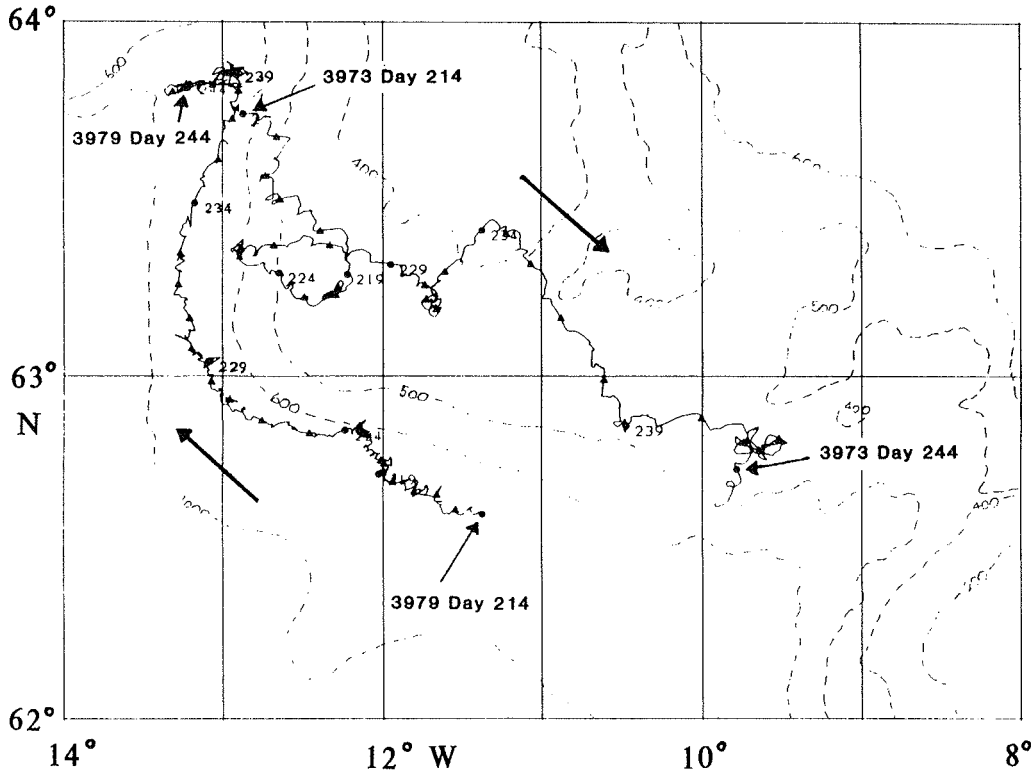

Figure 12. Drogues 3973 and 3979 during August 1987. Drogue tracks are indicated by continuous lines with numbers indicating day number in 1987. Beginning and end of each drogue track is indicated. Broken lines are isobaths.

Observations of radioactive tracers in Faroese waters

Henning Dahlgaard[1], Bogi Hansen[2] and Hans Pauli Joensen[3]

[1]Risø National Laboratory, Denmark. [2]Fiskirannsóknarstovan, P.O.Box 3051, FR-110 Tórshavn, Faroe Islands. [3]Fróðskaparsetur Føroya, Faroe Islands.

Based on a paper presented to the ICES Hydrography Committee as ICES CM 1991/C:26

In August 1990 levels of Cs-137 and Sr-90 were measured in different water masses surrounding the Faroe Islands together with hydrographic parameters. In the upper layers which are of Atlantic origin the influence of the Sellafield discharge and the Chernobyl release were found to be minor; but in the colder and less saline waters north of the islands higher levels of Cs-137 and Sr-90 were found. The highest levels were those of the Arctic Intermediate Water deriving from the Greenland Sea. This water is one of the components of the overflow of cold water from the Seas north of the Greenland Scotland Ridge into the world ocean and the observations showed increased Cs-137 levels, deriving from Sellafield and/or Chernobyl, in the overflow through the Faroe Bank Channel.

Keywords: Radioactivity, Norwegian Sea, Overflow, Sellafield, Chernobyl

Introduction

In later years there has been considerable interest in measurements of radioactive tracers in the sea. Partly this is due to environmental concern and partly due to the fact that radioactive tracers in some cases give unique opportunities for tracing water masses.

In the waters surrounding the Faroe Islands, radioactivity has been measured in the surface for many years as reported annually from the Risø Laboratory. These measurements have shown small levels of certain isotopes like Cs-137 which seem mostly to derive from fallout (Figure 1). There have also been sporadic measurements of radioactivity at greater oceanic depth (Livingston, 1985); but a comprehensive survey of levels to be found in the different water masses in the Faroe region is lacking and this is a drawback because some of these water masses play a very significant role in the "overflow" of cold dense water from the Nordic Seas (Norwegian, Greenland, Iceland Seas) and the Arctic Ocean to the North Atlantic.

This overflow is one of the key processes in the formation of North Atlantic Deep Water (NADW), the major deep water mass of the World Ocean. It occurs at three locations along the Greenland-Scotland Ridge. One of these is the Denmark Strait. The other two are on each side of the Faroes and consist of water masses discussed in this paper. Much of this water appears to get concentrated along the deep slope off East Greenland, south of the Denmark Strait where it seems to be very constant in transport value (Dickson *et al.*, 1990). The processes creating the different overflow components are, however, not necessarily the same. Thus the Faroe Bank Channel overflow has a large component of Norwegian Sea Deep Water (NSDW) which has formation processes quite different from those of the Greenland Strait overflow. It is therefore of importance to be able to separate the different components of the overflow and in order to succeed in that task all possible tracers should be considered.

As was mentioned, the surface levels of radioactivity around the Faroes are small indicating that the Sellafield discharge has not significantly contaminated these waters. This is not surprising since these waters derive mainly from the open Atlantic; but at deeper layers water masses are found which derive from the Greenland Sea and other northern regions and these could be expected by now to have been affected by the Sellafield discharge and other sources. Since these water masses contribute to the overflow their levels of the important radioactive isotopes should be determined.

With this motivation measurements of radioactivity were included in the NORDIC WOCE program which hopefully will run from 1993 to 1997. In order to ensure adequate sampling, however, it was considered helpful to do a pilot project with a much reduced sampling scheme to get initial indications of levels to be expected. This paper presents results from that pilot project. It was a joint effort by the Faroese Fisheries Laboratory (Fiskirannsóknarstovan), the science department of the University of the Faroe Islands, Náttúruvísindadeildin (NVD) and the Risø National Laboratory in Denmark. The original intention was to analyse the collected

samples for Cs-137, Cs-134, Sr-90 and Tc-99 so that the origin of the radioactivity could be traced. Unfortunately a contamination accident at the Risø Laboratory destroyed the Cs-134 and Tc-99 analyses, so only Cs-137 and Sr-90 will be reported here.

Material and methods

The observations reported in this paper were collected during a cruise with the Faroese research vessel Magnus Heinason in the period 17–21 August 1990. The observations include hydrographic casts with CTD and associated Rosette sampler and water samples taken by a large-volume sampler for radioactive analysis.

A total of 32 hydrographic stations were occupied as shown on Figure 2. Except for the last one (station No. 32) the stations are part of a set of standard sections which are occupied about four times a year. The station numbers shown on Figure 2 are the standard station numbers and were not occupied chronologically on this cruise. The standard sections cross all the major water masses in the Faroese region. In addition to these stations, station 32 was chosen for its position on the Iceland-Faroe Ridge at a location where overflow is considered to occur frequently.

The CTD used on the cruise was an EG&G Mark V unit with a 12 bottle G.O. Rosette sampler attached. The maximum depth sampled was 1300 meters. Water samples were taken regularly and analysed on an Autosal salinometer for salinity calibration. Unfortunately the CTD was one of the first of the Mark V units produced and an intermittent instrument failure reduced the data quality considerably. After intense editing, temperature and salinity profiles of reasonable quality were, however, obtained for all the stations observed except two stations on the section going north from the Faroes (section N on Figure 2).

Water samples for radioactive analysis were obtained with a Hydro-Bios water sampler with a capacity of 270 litres operated from a hydrographical winch. As the sampling is fairly time-consuming, only 14 samples were obtained at four different stations. Half of these were, however, double samples so that a total of 14 samples were available for analysis at NVD (Náttúruvísindadeildin, Faroe Islands) and 7 samples at Risø (Denmark), all of these comprising 250 litres each. No processing was performed on the ship. The depth of the large-volume water sampler was determined by a meter wheel. For the station in the Faroe Bank Channel (station 27 on Figure 2) the strong bottom currents in the overflow current could conceivably have given a false indication of the depth; but salinity samples taken from the water sampler confirm that the sampler was in the correct water mass when triggered.

The 7 water samples analysed in Denmark were transported to Risø in 50 l plastic containers. The 250 l samples were split into a 50 l and a 200 l sample. The 50 l samples were analysed for Sr-90 and Cs-137 by first precipitating strontium as carbonate, and later precipitating caesium on Ammonium Molybdo Phosphate (AMP) at pH 2.2. Strontium was isolated from the carbonate precipitate by the fuming nitric acid method, and Sr-90 was estimated from measurements of its short lived daughter Y-90 eliminating the possibility of contamination with other beta emitters. The concentration of Cs-137 was measured directly on the AMP precipitate by high resolution gamma spectroscopy on a Ge detector. The 1 st.dev. counting error is reported for the Cs-137 data. For Sr-90, the counting error was less than 3%, but the total analytical error is larger. The 200 l samples were pumped through an anion exchange resin for isolation of Tc-99 followed by AMP precipitation of caesium, in order to get material enough for the determination of Cs-134. Due to a contamination accident in the laboratory, the very low levels of both radionuclides were unfortunately lost in these samples.

The 14 samples analysed at NVD were transported ashore in 25 l plastic containers. 200 l of each sample were used for the Cs-137 analysis while the remaining 50 l were stored for a possible future analysis for Sr-90 and Tc-99. A caesium carrier (CsCl) was added to the 200 l and pH adjusted to 1.5–2.0. Caesium was then precipitated on AMP for 24 hours. The precipitate was vacuum filtered and washed with 0.025 M NH_4NO_3 and with 0.01 M HNO_3, whereupon it was dried at 105 degrees Celsius for 24 hours. The dried material was analysed with gamma spectroscopy using a Ge-detector and the software OMNIGAM from E&G Ortec. The Cs-137 concentrations are reported with 1 st.dev. counting error.

Results

The results of the CTD observations are summarised in Figure 3 showing temperature and salinity along the two standard sections (N and W) on which water was sampled for radioactive analysis. The positions and depths of the radioactivity samples are shown on the sections except for the last station. The hydrographical situation depicted on these sections is fairly normal. Between station 7 and 9 on section N is seen the Iceland-Faroe Front separating the warm and saline Atlantic waters from the colder and less saline waters to the north and east.

Table 1 Results of radioactivity measurements of seawater performed at NVD (Tórshavn) and at Risø (Denmark). All activities in Bq m^{-3}. The last column shows the ratio of Cs-137 to Sr-90 levels.

Station data				NVD analysis		Risø analysis			
Station	Position	Bottom	Sample	Cs-137		Cs-137		Sr-90	Cs-137
No.	Lat./ Long.	depth	depth	Act	st.d.	Act.	st.d.	Act.	Sr-90
1	62°20'N 6°05'W	81	50	2.4	0.4	2.4	0.2	1.34	1.8
10	63°50'N 6°05'W	2400	50	3.5	0.4	3.5	0.2	1.45	2.4
10	63°50'N 6°05'W	2400	200	3.7	0.4	3.7	0.2	1.48	2.5
10	63°50'N 6°05'W	2400	400	4.9	0.4	5.1	0.2	1.70	3.0
10	63°50'N 6°05'W	2400	700	3.6	0.4	3.6	0.4	1.35	2.7
10	63°50'N 6°05'W	2400	1000	0.2	0.3	2.7	0.2	1.28	2.1
27	61°20'N 7°53'W	810	50	2.8	0.4				
27	61°20'N 7°53'W	810	200	2.8	0.3				
27	61°20'N 7°53'W	810	500	3.7	0.4				
27	61°20'N 7°53'W	810	780	2.5	0.4	2.1	0.2	0.85	2.4
32	62°30'N 9°00'W	552	50	2.5	0.4				
32	62°30'N 9°00'W	552	200	2.3	0.3				
32	62°30'N 9°00'W	552	350	2.3	0.3				
32	62°30'N 9°00'W	552	520	2.7	0.4				

The results of the radioactivity measurements are shown in Table 1. The station numbers referred to in the table are those shown in Figure 2 and on the sections. The last column in Table 1 was obtained by dividing the Cs-137 activity measured at Risø by the Sr-90 activity. From the table it may be noted that for the 7 samples analysed for Cs-137 at the two different laboratories the correspondence is well within the specified standard deviations. Thus we feel confident that these values are reliable.

Discussion

Looking at Table 1, one sees variations especially in the activity of Cs-137 that are well outside the error bars. Two questions immediately arise: Are the variations systematic and tied to water mass variations? Where does the radioactivity come from? In the following we discuss these two questions.

Cs-137 content of different water masses. As regards Cs-137 the first question may be answered affirmatively. On Figure 4 we show temperature, salinity and Cs-137 activity profiles for the four stations sampled. The activities plotted are those measured by NVD which are more complete. The most notable feature is the maximum at 400 meters depth on station 10. It seems natural to link this Cs-137 maximum either to the salinity maximum somewhat above or to the salinity minimum somewhat below which can be seen both in Figure 3 and Figure 4. The salinity maximum does, however, coincide almost with the sample at 200 m depth where the Cs-137 level was considerably less than at 400 m, so the Cs-137 maximum is most likely associated with the salinity minimum at 500–600 m depth. This minimum with a salinity below 34.90 and temperature around 0 °C is a common feature in this area and is indeed usually much more prominent on this section than during the present cruise. The salinity minimum is associated with a water mass termed Arctic Intermediate Water (AIW) (Stefánsson, 1962; Blindheim, 1990). It derives from the Greenland Sea and also to a less degree, probably, from the Iceland Sea and it enters the southern Norwegian Sea in the deeper layers of the East Icelandic Current (Blindheim, 1990).

As mentioned in the introduction, the most likely route of Cs-137 rich waters to the Faroe area is through the Greenland Sea and thus it is by no means surprising that the highest Cs-137 values were observed in a water mass which is mostly formed in the Greenland Sea. In 1988, during the Greenland Sea Project, Cs-137 was measured on a section along 71 °N, and at depths, where the AIW is found, values of 5–8 Bq m^{-3} were obtained for Cs-137 with Cs-137/Sr-90 ratios of 2.3–3.2 (Dahlgaard *et al.*, 1991). A value of 5 Bq m^{-3} for the AIW in the southern Norwegian Sea two years later is therefore not unexpected; but it should be noted that we did not measure Cs-137 in the core of the AIW, thus somewhat higher values might well have been found with a denser vertical sampling on station 10. On the other hand, station 10 seems from the salinity section on Figure 3 to

have been the station with the most clearly expressed occurrence of AIW during this cruise.

Turning now to the other Cs-137 values, they also exhibit a clear correspondence to water mass origin. In Figure 5 we have plotted the TS-curves for the four stations where radioactivity samples were collected and the samples are shown on the plot with filled circles corresponding to their TS characteristics and with the Cs-137 activity noted. The main water masses have furthermore been shown on the figure as TS regions. The water masses in this area and especially those north of the Iceland-Faroe Front, are a rather complicated subject which can not be considered resolved and it is not made less complicated by the fact that different authors use different names and definitions for the water masses.

For the present paper we will not discuss the water masses in any detail; but restrict ourselves to the designations in Figure 5. In addition to AIW these are: Modified North Atlantic Water (MNAW), Shelf water, North Icelandic Water (NI) and Norwegian Sea Deep Water (NSDW). The boundaries between different water masses must always be somewhat ambiguous. It may, f.i., be discussed where the low-temperature limit of MNAW should be set. In spite of these ambiguities we get a fairly consistent picture of the Cs-137 activity in the different water masses.

The main water occupying the upper parts of the Faroese region is the MNAW and the five samples from this water mass have overlapping Cs-137 values within one st. dev. with a mean value around 2.5 Bq m^{-3}. Faroese surface water samples from 1973–1985 (Figure 1) have in that period shown an effective half life of 10 years for Cs-137 and 13 years for Sr-90, (Aarkrog, 1989). Extrapolating these pre-Chernobyl data to 1990 gives expected concentrations of 2.0 for Cs-137 and 1.5 for Sr-90. A small input of Sellafield/Chernobyl Cs-137 to MNAW on the order of 25% thus can not be excluded.

The one sample on the Faroe shelf had a Cs-137 level consistent with the MNAW values which is not surprising as that water must be mostly MNAW which has been slightly modified by contact with the atmosphere and runoff from land. The three uppermost samples on station 32 also had a Cs-137 level of the same magnitude. These samples consisted mostly of MNAW, while the deepest sample at station 32 from the TS characteristics contained more water of northern origin, consistent with a slightly increased Cs-137 level.

The other upper layer water mass, which is found north of the Iceland-Faroe Front has been termed NI in Figure 5 in order to be consistent with the traditional notation NI/AI for the combination of various upper-layer water masses north of the Iceland-Faroe Front and the AIW. This water had somewhat higher Cs-137 levels than the MNAW which again is consistent with its formation area receiving input from the Greenland Sea.

The Norwegian Sea Deep Water with temperatures below -0.5°C showed Cs-137 levels of the same magnitude as the MNAW or perhaps a bit smaller. Above the NSDW, Cs-137 values of 3.5–3.7 Bq m^{-3} were found both north of the Faroes at station 10 and in the Faroe Bank Channel at station 27. North of the Faroes we would expect a mixing layer between the NSDW and the AIW with Cs-137 levels between those of the two parent water masses. That a Cs-137 maximum also occurs in the Faroe Bank Channel between the MNAW and the NSDW reflects the fact that parts of this mixing layer follow the NSDW in the overflow out through the Faroe Bank Channel.

The origin of the radioactive tracers. The strontium analysis was carried out only on the 7 samples sent to Risø. On Figure 4 the Sr-90 levels can be compared to the hydrography and to the Cs-137 levels. The Cs-137 maximum in the AIW is found for Sr-90 also; but it is not as pronounced. Comparing the levels of the two tracers we may get an indication of the sources.

The global fallout from atmospheric nuclear test explosions contaminated the world ocean with several long lived radionuclides during the 1950's and 1960's with a distinct peak in 1962–1965. Throughout the 1970's and 1980's the Polar surface water in the East Greenland Current has shown higher concentrations of Cs-137 and Sr-90 than the central North Atlantic in spite of the fact that high latitude global fallout was smaller than mid latitude fallout. This is probably due to a local contamination of the Arctic Ocean with direct fallout from the Novaya-Zemlia nuclear test site. During the 1970's and early 1980's, this Polar water anomaly included excess Sr-90 relative to Cs-137 as compared to the general global Cs-137/Sr-90 fallout ratio of about 1.5, probably due to runoff with the Siberian rivers, including the River Ob, that drains the heavily contaminated Cheliabinsk nuclear weapons production area in the Urals.

Another large contributor to North East Atlantic anthropogenic radioactivity is controlled release from the Sellafield (formerly Windscale) nuclear fuel reprocessing plant in UK discharging to the Irish Sea. The Cs-137 discharges to the Irish sea reached about 1 PBq yr^{-1} (10^{15} Bq yr^{-1}) in 1970–1973, and peaked at about 4 PBq yr^{-1} in 1974–1978 after which they gradually decreased to less than 0.1 PBq yr^{-1} from 1986 and onwards. Throughout the 1980's the Sellafield contribution has gradually increased the Cs-137/Sr-90 ratio in the North East Atlantic including the East Greenland Current (Livingston 1985, Aarkrog *et al.*, 1987).

Finally, the Chernobyl Nuclear Power Plant accident gave significant injections of Cs-137 and Cs-134 to the Baltic Sea and to various locations throughout the North East Atlantic including Faroese waters (Aarkrog *et al.*, 1988; Aarkrog *et al.*, 1989). When the samples, discussed in this paper, were obtained this direct Chernobyl contamination of Faroese waters had been transported away. Most of the North East Atlantic region has, however, by now apparently been contaminated with Chernobyl caesium resulting in a general Cs-137/Sr-90 ratio larger than the global fallout ratio of 1.5.

In the Greenland Sea Project data set from 1988, previously cited (Dahlgaard *et al.*, 1991), a significant increase in the concentration of Cs-137 in several Greenland Sea water masses could partly be explained by Sellafield, partly by the Chernobyl accident. The highest concentrations of Chernobyl related caesium were found in the AIW flowing below the Polar Water in the East Greenland Current.

The Cs-137/Sr-90 ratios in the last column of Table 1 may thus give some indications of the relative importance of the various sources although more isotopes are needed to resolve the problem completely. For the Faroe Shelf water the value 1.8 for the Cs-137/Sr-90 ratio is just above the global fallout value indicating a small contribution by Sellafield and/or Chernobyl to the fallout levels in accordance with the above conclusion.

For the other samples the Cs-137/Sr-90 ratio ranges from 2.1 to 3.0 corresponding to increasing contribution from Sellafield/Chernobyl to the fallout levels. The highest ratio is found for the peak at 400 m depth at station 10 and this is consistent with its source in the Greenland Sea as previously mentioned. The lowest ratio except for the Shelf water was found in NSDW at 1000 m depth at station 10. A value of 2.1 for this water might still be considered high compared to the fallout value as this water can not have been recently in contact with the atmosphere; but the turnover time for NSDW is not considered to be much above 15 years (Heinze *et al.*, 1990) and in 1981 the Cs-137/Sr-90 ratio for the Lower Deep Water of the Greenland Sea was estimated to be close to 2 (Livingston, 1985).

Conclusion

Although limited by a relatively coarse sampling and a laboratory accident, the data set obtained does present a consistent picture of the occurrence of Cs-137 and to a smaller degree Sr-90 in Faroese waters. Although surface levels have not been much affected by contamination since the global fallout from nuclear test explosions, other sources have increased the Cs-137 level at intermediate depths around the Faroes especially in the Arctic Intermediate Water north of the islands; but also in the overflow water passing out of the Faroe Bank Channel. In spite of its limitations the data set obtained has demonstrated the potential utility of these and similar isotopes as tracers for the water masses of this region and of the overflow.

References

Aarkrog, A., 1989. Chernobyl related monitoring and comparison with fallout data. Proc. Sem. on The Radiological Exposure of the Population of the European Community from Radioactivity in North European Marine Waters, Project "MARINA", Bruges 14–16 June 1989. Commission of the European Communities, XI/4669/89-EN, 229–249.

Aarkrog, A., Boelskifte, S., Dahlgaard, H., Duniec, S., Hallstadius, L., Holm, E., and Smith, J. N. 1987. Technetium-99 and Cesium-134 as long Distance Tracers in Arctic Waters. Estuarine, Coastal and Shelf Science, 24: 637–647.

Aarkrog, A., Buch, E., Chen, Q. J., Christensen, G. G., Dahlgaard, H., Hansen, H., Holm, E., and Nielsen, S. P. 1988. Environmental Radioactivity in the North Atlantic Region including the Faroe Islands and Greenland 1986. Risø-R-550, Risø National Laboratory, Roskilde, Denmark.

Aarkrog, A., Buch, E., Chen, Q. J., Christensen, G. G., Dahlgaard, H., Hansen, H., Holm, E., and Nielsen, S. P. 1989. Environmental Radioactivity in the North Atlantic Region including the Faroe Islands and Greenland 1987. Risø-R-564, Risø National Laboratory, Roskilde, Denmark.

Blindheim, J. 1990. Arctic Intermediate Water in the Norwegian Sea. Deep-Sea Research, 37 (9): 1475–1489.

Dahlgaard, H., Chen, Q. J., and Nielsen, S. P. 1991. Radioactive tracers in the Greenland Sea. RADSTOMP'91: Radionuclides in the study of marine processes, 9–14 September 1991, Norwich, UK.

Dickson, R. R., Gmitrowicz, E. M., and Watson, A. J. 1990. Deep-water renewal in the northern North Atlantic. Nature, Vol. 344, No.6269, pp. 848–850.

Heinze, Ch., Schlosser, P., Koltermann, K. P. and Meincke, J. 1990. A tracer study of the deep water renewal in the European polar seas. Deep-Sea Research, 37 (9): 1425–1453.

Livingston, H. 1985. Anthropogenic radiotracer evolution in the Central Greenland Sea. Rit Fiskideildar, 9: 43–54.

Stefánsson, U. 1962. North Icelandic Waters. Rit Fiskideildar Vol. III, 269 p.

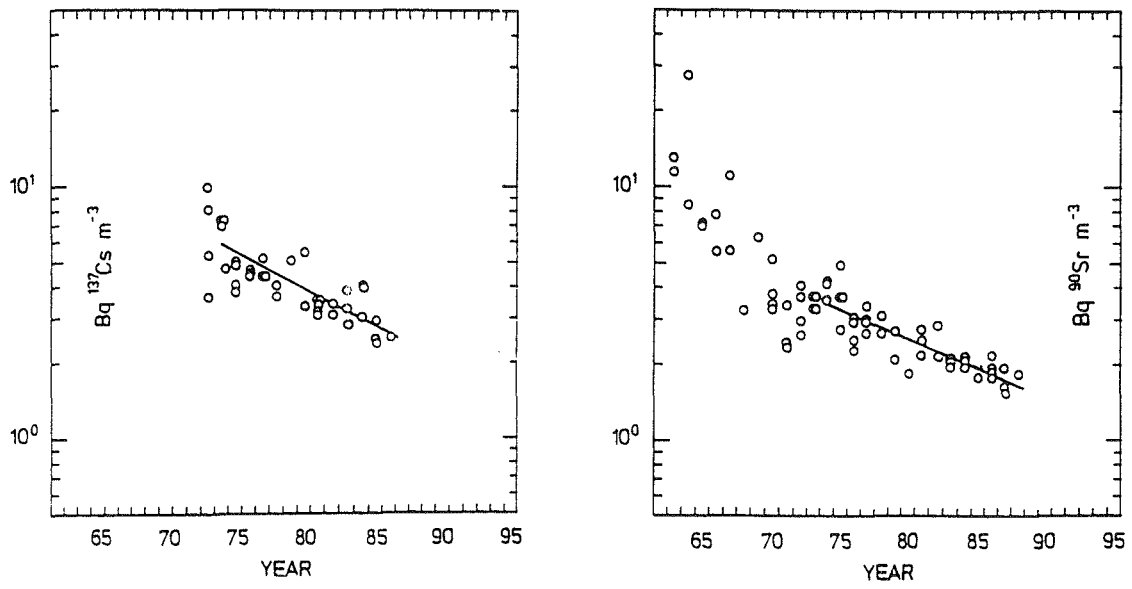

Figure 1. Levels of Cs-137 (left) and Sr-90 (right) in Faroese surface waters (Aarkrog, 1989).

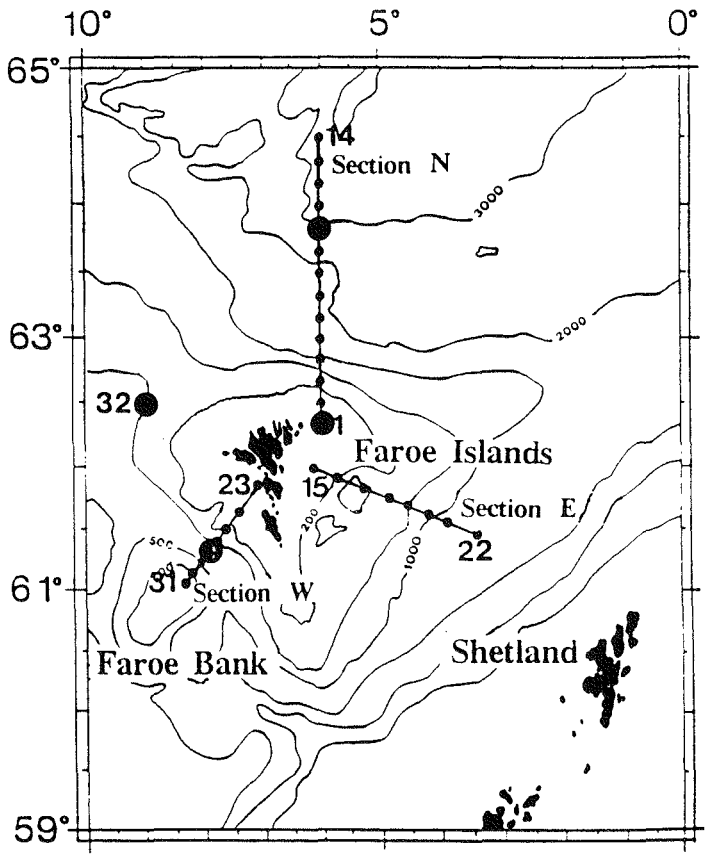

Figure 2. Map showing stations occupied by R/V Magnus Heinason 17 – 21 August 1990. Small dots indicate hydrographic stations. Large filled circles indicate stations where samples for radioactive analysis were obtained.

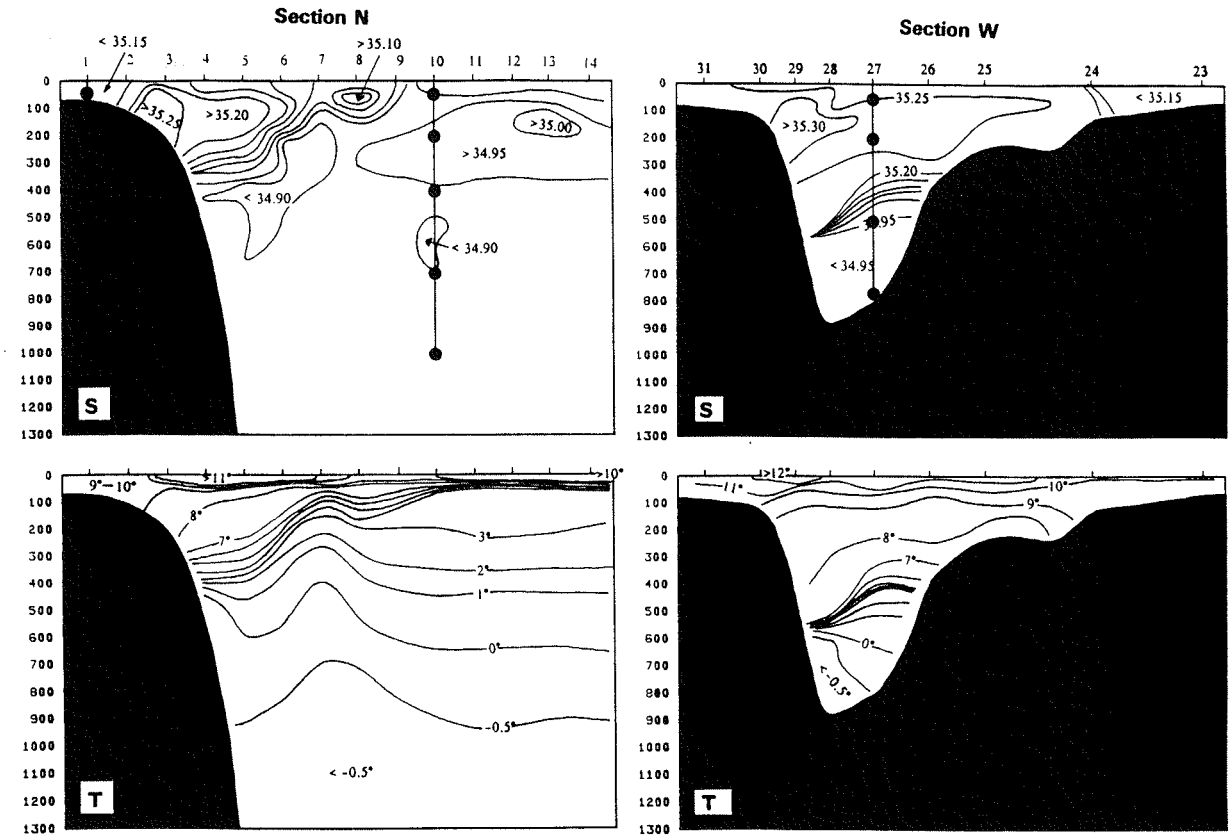

Figure 3. Temperature (T) and salinity (S) along two vertical sections (from the surface down to 1300 meters depth) shown in Figure 2. Numbers above the sections denote standard station numbers. Vertical lines denote those stations of these sections on which radioactivity samples were taken and filled circles on these lines indicate depths of samples.

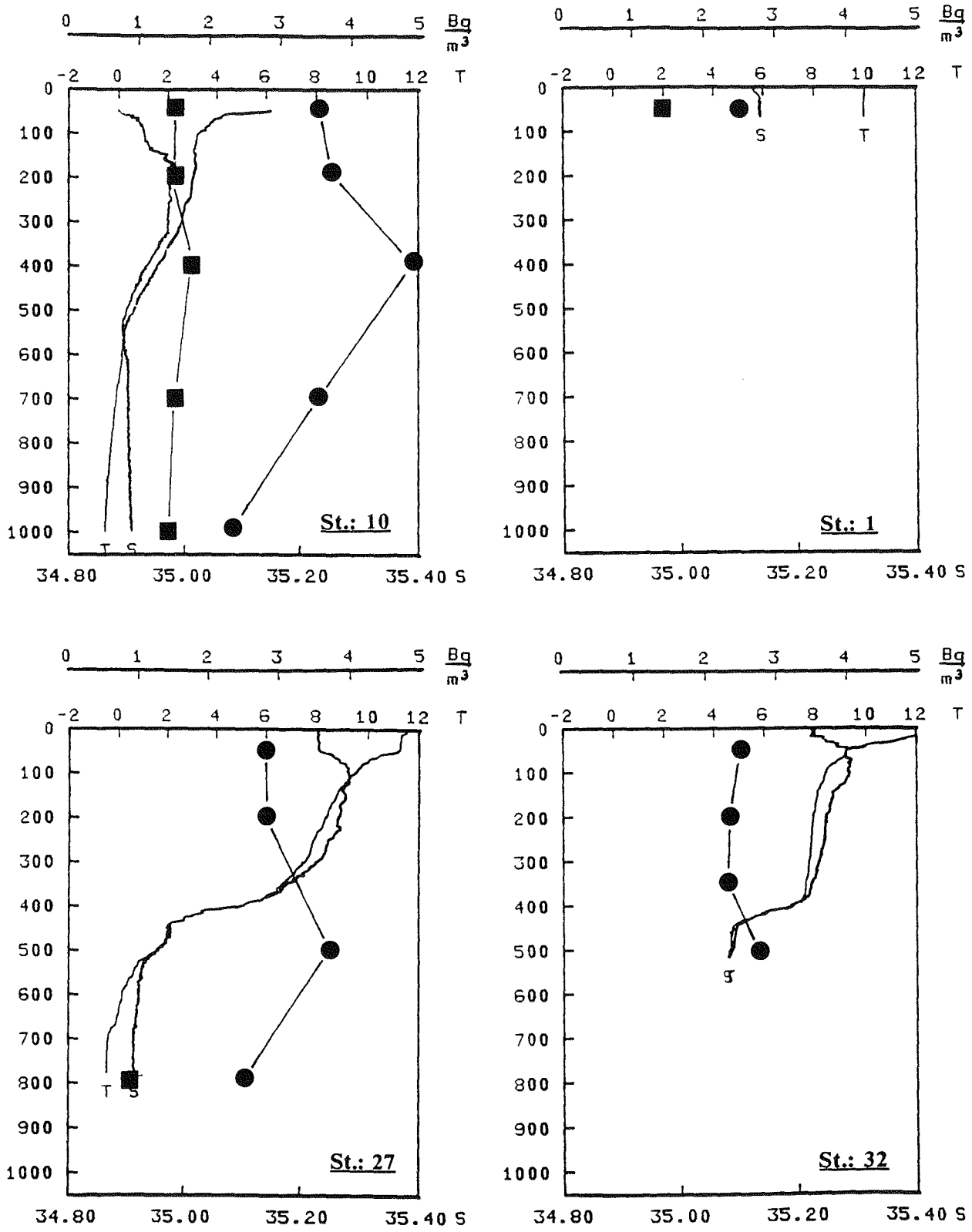

Figure 4. Vertical profiles for the four stations on which radioactivity was measured. Continuous lines show temperature (T) and salinity (S). The filled circles show Cs-137 and the filled squares show Sr-90 levels. The station positions are seen on Figure 2.

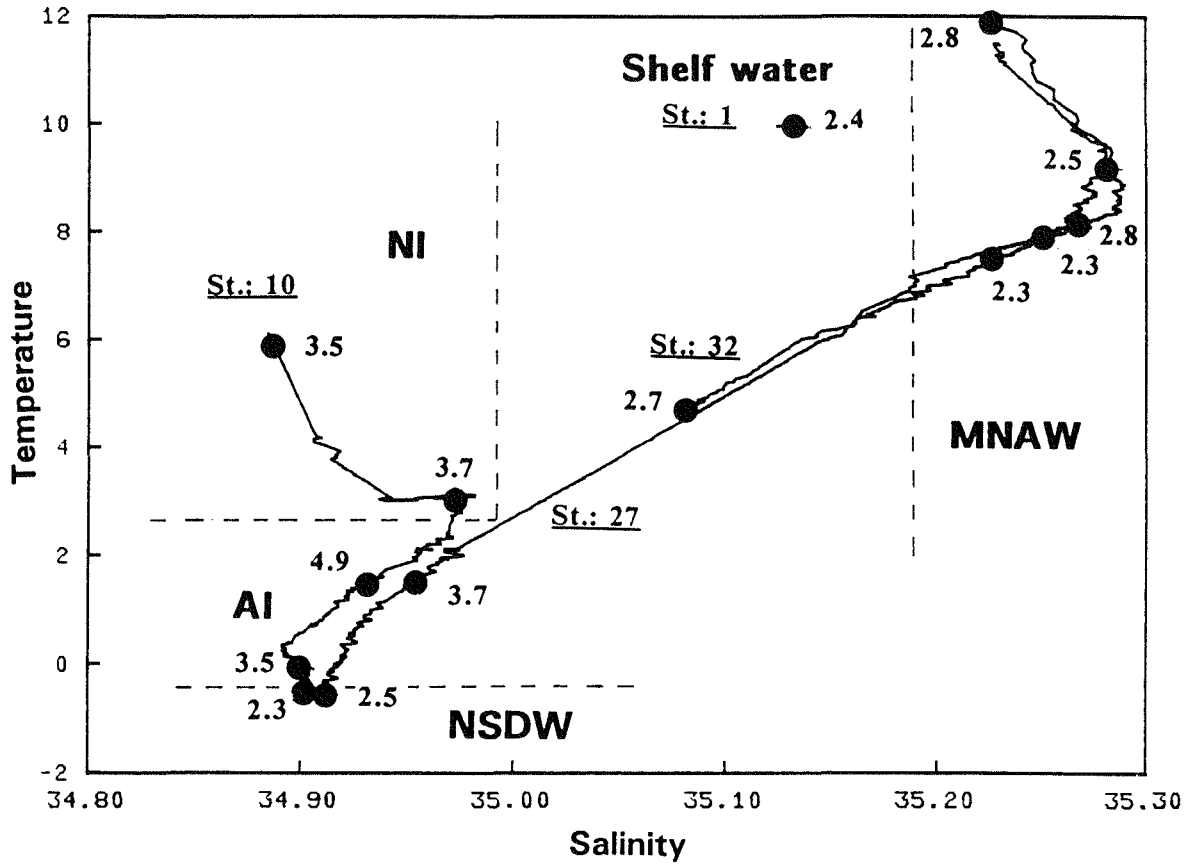

Figure 5. Temperature-Salinity (TS) diagram. Continuous curves show TS curves for the four stations on which radioactivity was measured. Filled circles on the TS curves indicate where samples were taken for Cs-137 analysis and the numbers by the circles indicate the Cs-137 levels. Regions bounded by broken lines indicate water masses.

The Arctic Ocean Deep Water component in the Greenland-Scotland overflow

Bert Rudels[1] Detlef Quadfasel[2]and Hans Friedrich[2]

[1]Alfred-Wegener Institut für Polarforschung, Bremerhaven, Germany. [2]Institut für Meereskunde der Universität Hamburg, Germany.

Based on a paper presented to the ICES Hydrography Committee as ICES CM 1991/C:30

Recent observations have shown that the Arctic Ocean deep waters are ventilated, not by advection from the Greenland Sea, but by shelf-slope convection occurring within the Arctic Ocean. In recent years the convective activity in the Greenland Sea has diminished and dense waters originating in the Arctic Ocean have become prominent also in the deeper layers of the Nordic Seas south of Fram Strait. The water transformations in the Arctic Mediterranean Sea are related to the boundary current of the Atlantic Water, which crosses the Greenland-Scotland ridge from the North Atlantic into the eastern Norwegian Sea. By examining how the properties of the boundary current evolve, it is possible to document the changes imposed upon its waters by the processes active in the Arctic Ocean. It is also possible to follow how the Arctic Ocean deep waters spread into the Nordic Seas and provide a substantial fraction of the overflow water which supply the North Atlantic Deep Water.

Keywords: Arctic Ocean, Overflow, Convection, Deep Water

Introduction

The Arctic Mediterranean Sea (Sverdrup *et al.*, 1942), comprising the Arctic Ocean and the three "Nordic Seas": the Greenland, Iceland and Norwegian Sea, is separated from the North Atlantic by the Greenland-Iceland-Scotland Ridge. The deepest passages are the Faeroe-Shetland Channel (850 m) to the east and the Denmark Strait (600 m) to the west. The ridge splits the North Atlantic Circulation. The northward flowing warm water bifurcates south of the ridge. One part crosses the ridge and flows northward as the Norwegian Atlantic Current. The second part turns westward forming the Irminger Current, the northern limb of the North Atlantic subpolar gyre.

The poleward sides of the oceanic circulation gyres are regions of deep winter convection (McCartney, 1977, 1982) and the winter homogenisation of the subpolar gyre in its north-western part, the Labrador Sea, might reach deeper than 2000 m (Dickson *et al.* 1997; Lazier, 1973, 1988) and is the source of the Labrador Sea Water (Talley and McCartney, 1982). The Labrador Sea Water constitutes the less dense part of the North Atlantic Deep Water, the main deep water mass of the world ocean.

That an outflow of dense water from the north across the Greenland-Scotland Ridge existed was recognised by Nansen (1912), but he did not believe that it could contribute significantly to the North Atlantic Deep Water (Warren, 1981). For a long time the main source of the North Atlantic Deep Water was supposed to lie south of Greenland (Sverdrup *et al.*, 1942) which would make the Arctic Mediterranean an isolated cul-de-sac extending to the Pacific Ocean. With several overflow experiments in the late 1950s and early 1970s (Dietrich 1956; Meincke, 1983) the importance of the Nordic Seas and primarily the Greenland Sea for supplying dense water to the North Atlantic was again appreciated. Worthington (1976) lists the Faeroe-Shetland Channel and the Denmark Strait overflows among the three most important northern components of the North Atlantic Deep Water, and Reid and Lynn (1971) follow the NADW on its route to supply deep water to all remote corners of the world ocean.

The characteristics of the overflow water are different for the two main passages. The Faeroe-Shetland outflow consists mainly of cold (Θ<-0.5°C) water from the Norwegian Sea and ultimately from the Greenland Sea (Swift, 1986; Smethie and Swift, 1989). The Denmark Strait overflow is assumed to involve intermediate waters formed in the Iceland Sea (Swift *et al*, 1980). Strass *et al.* (1993) examined the Θ-S characteristics on several sections across the Greenland Sea slope and found that isopycnal mixing between the water of the Atlantic Return Current RAC (Bourke *et al.*, 1986) and the Arctic Intermediate Water formed in the Greenland Sea would provide a water mass with similar characteristics as the Arctic Intermediate Water of the Iceland Sea.

This would imply that the deepest circulation of the Arctic Mediterranean is confined to north of the ridge. In fact, the internal circulation scheme between the two source areas, the Arctic Ocean and the Greenland Sea, proposed by Aagaard *et al.* (1985) excluded the Iceland Sea. Estimates of the strength of this deep circulation

have been obtained by Rudels (1986) from Θ-S analysis and by Smethie *et al.* (1988) and Heinze *et al.* (1990) using anthropogenic tracers. These studies all indicated a deep exchange through Fram Strait of 1-2Sv and estimated the deep water production in both the Greenland Sea and in the Arctic Ocean to be 0.5 to 1Sv. A production requires a corresponding sink. Rudels (1986) assumed that the low salinity upper part of the deep Arctic Ocean outflow crosses the Jan Mayen Fracture Zone and ultimately exits through Denmark Strait. The box models by Smethie *et al.* (1988) and Heinze *et al.* (1990) either postulate upwelling out of the deep water box or an outflow from the Norwegian Sea box, presumably through the Faeroe-Shetland Channel.

Smethie and Swift (1989) found that the deeper part of the Denmark Strait overflow is considerably older than the main outflow and concluded that this part originated from the Greenland Sea rather than the Iceland Sea. Danish and Icelandic oceanographers have observed what they consider Arctic Ocean Deep Water in the western Iceland Sea on their yearly cruises between 1987 and 1992 (Buch *et al.*, 1992, 1996) and Aagaard *et al.* (1991) state, based upon observation in the Greenland Sea, that about 1Sv of Arctic Ocean Deep Water crosses the Jan Mayen Fracture Zone. These studies then show that the Denmark Strait overflow contains a substantial fraction of water originating outside the Iceland Sea, and the deep circulation in the Arctic Ocean-Greenland Sea might not be as restricted as previously believed. Such ideas are not new. Stefánsson (1962) leaves the question open whether the Iceland Sea deep water is supplied from the north or from the east. The reason is obvious. The then existing techniques were not capable of distinguishing the small differences in the characteristics of the water masses involved.

This is, also today, not easy and several suggestions as to the origin of the overflow waters have been offered. The present work discusses the circulation and the transformations, in the Arctic Mediterranean, of the Atlantic Water entering as a boundary current through the Faeroe-Shetland Channel. This will take us on a journey beginning at the first splitting of the boundary current west of the Bear Island Channel and ending where the Canadian Basin derived deep water enters the Norwegian Sea, over the Iceland Sea, north-east of Iceland (Figure 1).

The study concerns contributions of the Arctic Ocean to the Greenland-Scotland overflow. It is a summary of recent ideas of water mass formation and circulation in the Arctic Ocean. It relates these ideas to the flow of the East Greenland Current through Fram Strait and to the transformations occurring in and south of Fram Strait. Observations from several cruises are considered. Some of these, especially the Oden-91 and the Lance-84 cruises, are presented in more detail elsewhere (Anderson *et al.*, 1994; Friedrich *et al.*, 1995; Houssais *et al.*, 1995). Additional observations are taken from the University of Hamburg Valdivia Cruise 104 to the Iceland Sea (1990) and the Norwegian Polar Research Institute Lance Cruise in 1988 to Fram Strait and the Greenland Sea.

The Arctic Ocean

The Atlantic Water of the Norwegian Atlantic Current follows the continental slope northward. It loses heat and the upper 600 m become homogenised by thermal convection in winter (Clarke *et al.*, 1990). When it reaches the latitude of the Barents Sea the current splits. One part continues northward as the West Spitsbergen Current, while the rest enters the shallow Barents Sea (Rudels, 1987; Blindheim, 1989).

As the West Spitsbergen Current reaches Fram Strait a second splitting occurs. About half of its water re-circulates to the west, while the remaining part enters the Arctic Ocean (Bourke *et al.* 1986; Rudels, 1987). The entering "Fram Strait branch" encounters and melts sea ice north of Svalbard (Untersteiner, 1988). A deep, less saline surface layer is formed and the lower part of the Atlantic Layer becomes shielded from the atmosphere and further cooling is reduced. (Steele *et al.*, 1995; Rudels *et al.*, 1996). The Fram Strait Branch continues eastward as a boundary current along the Eurasian continental slope (Aagaard *et al.*, 1989).

The branch crossing the Barents Sea is less deep and travels a longer distance, before it enters the Kara Sea between Novaya Zemlya and Franz Josef Land (Blindheim, 1989; Loeng *et al.*, 1993; Rudels, 1987). It interacts with the low salinity Norwegian Coastal Current and with cold, brine enriched water, formed above the shallower banks, which penetrates laterally into and cools the Atlantic Water (Nansen, 1906; Midttun, 1985; Quadfasel *et al.*, 1992). The Barents Sea inflow then becomes colder and less saline than the Fram Strait branch and its density range expands towards lighter as well as towards denser values.

The Barents Sea inflow enters the Arctic Ocean down the St. Anna Trough, and it encounters the warmer and more saline Fram Strait branch. After the merging of the two branches north of the Kara Sea the boundary current broadens as it approaches the Lomonosov Ridge (Schauer *et al.*, 1997). One part enters the Canadian Basin, while the main flow returns toward Fram Strait within the Eurasian Basin (Rudels *et al.*, 1994).

The Barents Sea inflow dominates the transformations of the Eurasian Basin water column. It cools the Atlantic Layer and creates a cold, low salinity intermediate depth water mass, which is found in the Amundsen Basin below the Atlantic Layer (Rudels *et al.*, 1994; Schauer *et al.*, 1997). The merging of the two branches also leads to strong interleaving and the

created inversions appear to be advected with the main flow and can be observed in the Atlantic and intermediate depth layers in the Amundsen Basin and over the Nansen-Gakkel Ridge (Rudels *et al.*, 1994).

Whereas the St. Anna Trough outflow is a permanent feature, a second transformation mechanism for the Atlantic and deeper layers is apparently intermittent: the sinking of brine enriched, dense shelfwater as boundary plumes down the continental slope into the deep basin. The plumes become warmer because of entrainment as they sink. Plumes only dense enough to reach and enter the Atlantic Layer cool the water at this level (Rudels, 1986; Schauer *et al.*, 1997), while plumes sinking into the intermediate and deep water could have entrained so much Atlantic Water that, when they merge with the water column, they make it warmer and more saline. (Rudels, 1986; Rudels *et al.*, 1994). The slope convection thus redistributes heat downward from the Atlantic Layer. To be sufficiently dense to reach the deepest layers, the initial salinity of the plumes must be high and the salinity increase observed in the deep layers of the Arctic Ocean is due to the brine export from the shelves, and is not caused by the removal of salt from the Atlantic Layer (Figure 2). The effects of the slope convection is primarily seen in the deepest layer, where the constant temperature and increasing salinity most readily can be explained by saline, entraining plumes passing through the intermediate layers. Dense, saline slope plumes have so far only been observed in Fram Strait and have been traced back to Storfjorden in the south of Svalbard (Quadfasel *et al.*, 1988; Schauer, 1995).

In the Canadian Basin only shelf processes can modify the waters of the boundary current entering along the Eurasian slope, and evidence of slope convection is clearly seen. The Atlantic Layer core is cooled still further, while the temperature and salinity of the intermediate and deep waters increase. The deepest part of the Canadian Basin is isohaline and a small decrease in temperature with depth is observed (Figure 2). Such structure cannot arise from slope convection alone. One possible explanation is a spill over of colder EBDW across the Lomonosov Ridge through gaps in the central parts of the ridge (Jones *et al.*, 1995). Because of the non-linearity of the equation of state of sea water, the Eurasian Basin Deep Water spilling over the Lomonosov Ridge becomes dense enough to sink to the deepest parts of the almost homogenous deep Canadian Basin water column. By contrast the Eurasian Basin is stratified below the sill depth of the Lomonosov Ridge and an overflow of warmer, more saline water from the Canadian Basin would remain at the level of the sill depth.

The strongest evidence of CBDW is seen in the western Eurasian Basin, where the CBDW shows up as an intermediate depth (1800m) salinity maximum. This indicates that the principal return flow from the Canadian Basin occurs as a boundary current along the slope of the Canadian Arctic Archipelago and Greenland. The boundary current does not only involve the deep water, but also carries water of the halocline, the Atlantic and the intermediate layers (Rudels *et al.*, 1994). The different return streams from the Canadian Basin and the Eurasian Basin, converge north of Fram Strait to form the Arctic Ocean outflow of the East Greenland Current.

The Arctic Ocean has acted as a separator for the entering Atlantic Water (Rudels and Quadfasel, 1991; Rudels, 1995). Through interactions with river runoff and through freezing and melting a less dense, low salinity surface water is formed. The rejection of brine and the induced slope convection transform the Atlantic Water into water masses which are in the density range of, or denser, than the overflow water supplying the North Atlantic Deep Water $27.95<\sigma_\Theta<28.00$ (Strass *et al.*, 1993): the modified Atlantic Water, historically defined as warmer than 0°C; the upper Polar Deep Water (uPDW) distinguished by its stable slope in the Θ-S diagrams, where the temperature decreases and salinity increases with increasing depth; the CBDW which is found as a salinity maximum in the Eurasian Basin; the Eurasian Basin Deep and Bottom Waters (EBDW, EBBW) occupying the deepest layers. The boundaries between the Atlantic Layer, the uPDW, the CBDW and the EBDW are somewhat arbitrary and we shall here follow the definitions given by Friedrich *et al.* (1995).

The lower limit of the Atlantic Layer is taken to be 0°C and the uPDW then becomes bounded above by the zero isotherm, and below it is separated from the CBDW by the $\sigma_{0.5}=30.444$ isopycnal. The boundary between CBDW and the EBDW is defined by the $\sigma_2=37.435$ isopycnal, which roughly corresponds to the sill depth of the Lomonosov Ridge (Aagaard *et al.* 1985). The Canadian Basin Bottom Water does not cross the Lomonosov Ridge and we have identified this water mass with the isohaline deep part of the water column with densities higher than $\sigma_2=37.435$. In the Eurasian Basin the layers below the isopycnal $\sigma_3=41.991$, corresponding to the sill depth of Fram Strait, are defined as the Eurasian Basin Bottom Water.

Fram Strait

As the boundary current approaches Fram Strait, it meets and mixes with the re-circulating branch of the West Spitsbergen Current. The nature and intensity of the resulting interactions can be inferred from temperature and salinity profiles and Θ-S curves from stations in the western Fram Strait (Figure 3). Below the Polar Surface Water the warm water of the Atlantic return flow completely absorbs the upper part of the Arctic outflow, the Modified Atlantic Water and part of the upper Polar Deep Water. The lower part of the upper

Polar Deep Water, while still recognised by its Θ-S slope, now shows up as a salinity minimum in profiles and Θ-S curves. Inversions found in the Atlantic and intermediate layers in the Eurasian Basin become wiped out and replaced by newly formed intrusions and interleaving between the Atlantic Water and the outflow.

Intrusions are also seen in the uPDW, CBDW and EBDW ranges. These indicate the presence of colder, less saline water, which must originate from the second main deep water formation area in the Arctic Mediterranean, the Greenland Sea. In the density range of the CBDW colder, less saline Arctic Intermediate Water (AIW) is seen while closer to the bottom the denser Greenland Sea Deep Water (GSDW) is found. Waters from the Greenland Sea thus penetrate northward into the western and central part of Fram Strait. The mixing is primarily isopycnal and the strong, sharp jumps suggest the existence of a narrow, perturbed frontal zone close to the boundary current. The interleaving structure is, however, not as regular as in the Nansen and Amundsen Basin (Figure 4). The mixing weakens the Arctic Ocean water mass properties and creates derived waters with characteristics of the NSDW (Norwegian Sea Deep Water).

It should be realised that the differences between warmer, more saline Arctic Ocean deep waters from the north and colder, less saline waters from the Nordic Seas in the south is not just a question of geography but of different formation processes. The shelf convection occurring on the right hand side of the boundary current redistributes heat downwards and increases the salinity of the deeper layers. The slope of the Θ-S curves then becomes more perpendicular to the isopycnals and the water column appears more stable. The open ocean convection in the Greenland Sea to the left of the boundary current (section 4) homogenises the water column making it colder, less saline and decreases the stability.

The Greenland Sea

The East Greenland Current, as it enters the Greenland Sea, also carries the modified Atlantic Water of the Atlantic Return Current. The AW has been substantially cooled not only by heat loss in the Norwegian Sea but also by mixing with colder and less saline modified Atlantic Water and upper Polar Deep Water in Fram Strait. Part of the Atlantic Water appears to leave the boundary current at the Greenland Fracture Zone and enters the Boreas Basin (Isert, 1996), which could account for some of the observed temperature decrease of the Atlantic Water between 79 N and 75 °N (Meincke *et al.*, 1997). The deeper part of the boundary current survives the mixing in Fram Strait and uPDW and Canadian Basin Deep Water are still to be seen on the Greenland slope. The EBDW maximum is more difficult to distinguish on the slope, but a deep salinity maximum in the Greenland Sea basin indicates that EBDW is found in the central Greenland Sea. The interaction between the outflowing Arctic Ocean deep waters and the waters formed in the Greenland Sea continue along the Greenland slope (Figures 5, 6).

This is in accordance with the circulation scheme proposed by Aagaard *et al.* (1985) and Swift and Koltermann (1988), where the high salinity Arctic Ocean deep water outflow was supposed to incorporate, by isopycnal mixing, the Greenland Sea Deep Water on its transit along the Greenland slope. It then gradually acquires the characteristics of the NSDW, and becomes short-circuited along the Jan Mayen Fracture Zone into the Norwegian Sea.

In a later work Aagaard *et al.* (1991) question details in this interpretation. On several stations along the Greenland Slope they observed three salinity maxima and found that the regression line through these maxima pointed toward the Greenland Sea Deep Water type (Swift and Koltermann, 1988). Their interpretation was that three different types of Arctic Ocean deep waters, all recognised by a salinity maximum, entered the Greenland Sea through Fram Strait. In the Greenland Sea a diapycnal mixing process then transformed the Arctic Ocean deep waters into Greenland Sea Deep Water. Secondly they noticed that the high salinity core on the continental slope appeared to cross the Jan Mayen Fracture Zone into the Iceland Sea, and they took the upper salinity maximum in the Norwegian Sea observed by Clarke *et al.* (1990) as evidence that the high salinity core enters the Norwegian Sea over the Iceland Sea.

Strass *et al.* (1993) reported isopycnal mixing between the RAC and Arctic Intermediate Water in the upper part of the water column. The intrusions on the different stations along the Greenland slope (Figures 5, 6) suggest isopycnal rather than diapycnal mixing. It is an exchange between the boundary current and the interior leading to a cooling and freshening of especially the CBDW on the slope and to an increase in salinity and temperature in the central Greenland Sea. In Figure 6 an isopycnal exchange of waters has occurred in the CBDW density range and the different depths of the intrusions on the two stations is consistent with the strong sloping of the isopycnals between the centre and the rim of the Greenland Sea.

Rudels (1986) distinguished just two maxima between CBDW and EBDW in the Arctic Ocean outflow and assumed that the CBDW remains at the slope and becomes transformed into NSDW by isopycnal mixing with Greenland Sea Deep Water. The EBDW is taken to enter directly into the Greenland Sea, where it was considered an integral part in forming the Greenland Sea Deep Water. The Greenland Sea then constitutes an equilibrium state between advection and convection

(Meincke *et al.*, 1997). The EBDW penetrates toward the centre, heating the Greenland Sea Deep Water and making it more saline. The plumes in the open ocean convection of the Greenland Sea entrain and redistribute ambient water and merge with the water column at the terminal depth and density of the convection. The introduction of colder, less saline convecting water causes the Greenland Sea Θ-S curve to contract, while the influx of EBDW into the central gyre tries to expand the characteristic hook shape of the Greenland Sea Deep Water Θ-S curve.

The Θ-S curves and profiles shown in Figure 6 indicate that the second dense water mass produced in the Greenland Sea, the Arctic Intermediate Water (Swift and Aagaard, 1981; Blindheim, 1990) is as dense or denser than the CBDW. The observations shown in Figures 3, 5 and 6 were taken in 1984 and 1988 respectively. Recent observations (GSP, 1990; Schlosser *et al.*, 1991; Rhein, 1991; Meincke *et al.*, 1997) suggest that presently the Greenland Sea deep water formation is greatly reduced and mainly Arctic Intermediate Water is produced. The presently formed Arctic Intermediate Water is less dense than the CBDW, which now penetrates into the central Greenland Sea gyre, adding a warmer "cap" to the Greenland Sea Deep Water (Figure 7).

The Iceland Sea

The hydrographic structure of the Iceland Sea can be seen on an east-west section (Figure 8) taken by RV Valdivia in October 1990 (Figure 1). The central part is enclosed by two streams of Atlantic Water. To the east the AW of the Norwegian Sea, which has recently crossed the Greenland-Scotland Ridge, is seen. Above the Greenland continental slope to the west the Atlantic Return Current is found. Below the return current the isotherms and the isohalines bend downward to the west and the spacing between the –0.2 and –0.5 isotherms increases as compared to the eastern part of the section. Below this level the isotherms still point downward, while the isohalines rise toward the slope. This again indicates that the deep waters of the western basin are different from those of the central Iceland Sea.

The higher temperatures and salinities in the deepest part imply that CBDW is present. The larger spreading of the isotherms and the lower salinities found in the west show that the water mass above the CBDW is less saline and has a weaker vertical temperature gradient than water of similar density to the east. These differences are more clearly seen on a Θ-S diagram showing stations from the western and the eastern basins of the Iceland Sea and from the Norwegian Sea (Figure 9). The Θ-S curves from the western basin resemble those from Fram Strait and suggest that both uPDW and CBDW enters the western Iceland Sea from the north. The uPDW is, as expected from the section, less saline and spans a smaller temperature interval than the corresponding water mass in the central Iceland Sea. The density increase with depth is caused by the increasing salinity and the western basin becomes more saline when the CBDW range is reached. These two waters are likely to have incorporated AIW as they pass the Greenland Sea.

The Arctic Intermediate Water of the Greenland Sea is colder and less saline than the uPDW. It therefore cannot constitute the source for the upper part of the central Iceland Sea deep water, which has characteristics more akin to the water below the Atlantic Layer in the Norwegian Sea. In particular the salinity minimum of the Norwegian Sea and the temperature maximum in the central Iceland Sea have similar Θ-S properties (Figure 9)

Stefánsson (1962) has shown that a weak cyclonic circulation exists in the Iceland Sea and Swift and Aagaard (1981) reported an increase in salinity and temperature in the upper layers between August and October on a repeated station in the north-eastern Iceland Sea. If Atlantic Water from the Norwegian Sea enters the Iceland Sea south of Jan Mayen, it will dominate the surface water. In winter it is cooled and may be transformed into water similar to the present temperature maximum layer. The lower salinity would be caused by the incorporation of the low salinity surface layer injected from the Jan Mayen Current. This newly formed, lower Arctic Intermediate Water (Swift and Aagaard, 1981) would then spread into the Norwegian Sea, creating the intermediate salinity maximum and also spill over into the western part of the Iceland Sea.

The idea that the Iceland Sea is the origin of the wide spread salinity minimum in the Norwegian Sea is old. Stefánsson (1962) proposed that the salinity minimum was formed south of Jan Mayen and Swift and Aagaard (1981) single out this area as one source for their "lower" Arctic Intermediate Water. We then have two source areas of AIW. The Greenland Sea forms a colder, denser type of AIW. The spreading of this water mass has been discussed by Blindheim (1990). In the Iceland Sea cooling and thermal convection form both upper and lower AIW in the Swift and Aagaard (1981) terminology.

We have chosen not to consider the water of the Atlantic Return Current as AIW. It comprises Atlantic Water of the West Spitsbergen Current cooled in the Atlantic domain during winter (Swift, 1986). As it recirculates in Fram Strait it incorporates mAW and uPDW exiting from the Arctic Ocean. Both these waters are created by processes different from the open ocean convection forming the AIW. Not until the Atlantic Return Current passes the Greenland Sea will it, by isopycnal mixing, absorb AIW (Strass *et al.* 1993).

The low salinity uPDW is not identified in the central and eastern Iceland Sea and must continue along the Greenland slope to the Denmark Strait, where it crosses the sill into the North Atlantic. The interactions between CBDW and AIW in the Greenland Sea reduce the salinity and temperature of the CBDW. It would normally be too dense to cross the sill in Denmark Strait, but water with CBDW as well as with uPDW characteristics has been observed at the sill in Denmark Strait (Buch *et al.* 1992, 1996).

To examine, if the CBDW is confined to the Greenland-Iceland Channel to the west, a north-south section across the gap between the Iceland continental slope and the Western Jan Mayen Ridge was occupied by RV Valdivia (Figure 10). With the disappearance of the uPDW the distinct "Arctic" shape of the Θ-S curves is lost, but the CBDW can be identified on the southern stations by the deepening of the isotherms and by the presence of salinities above 34.92 on the deepest station. Water with similar high salinities was also found from 1300m to the bottom in a 2300m deep depression east of the gap. This suggests that CBDW moves into the central Iceland Sea from the west.

High salinities of the deep waters north of Iceland have been reported by Malmberg (1983) and CBDW can be identified on the Valdivia stations along the Iceland continental slope toward the Norwegian Sea (Figure 11). The upper part of the Arctic Ocean deep outflow has retained its character of a boundary current through the Greenland and Iceland Seas. It is thus possible to trace the CBDW from the Canadian Basin into the Norwegian Sea just by their characteristics.

Fluxes

Transports have, so far, not been considered. Several attempts to provide mass balances for the Arctic Mediterranean have been undertaken. They range from overall estimates considering the Arctic Mediterranean as a cul-de-sac of the North Atlantic (Worthington, 1970, 1976; McCartney and Talley, 1984) down to detailed estimates of the different part of this Mediterranean Sea (Mosby, 1962; Vowinckel and Orvig, 1970; Aagaard and Carmack, 1989). Budgets only concerned with the Arctic Ocean have been offered by Aagaard and Greisman (1975) and Rudels (1987). Box modelling, often using anthropogenic tracers, has been applied to obtain balances for different parts of the water column like the deep water circulation in the Arctic Ocean and the Nordic Seas (Smethie *et al*, 1988; Heinze *et al.* 1990; Bauch *et al.*, 1995; Bönisch and Schlosser, 1995) or the upper layers in the Arctic Ocean (Östlund and Hut, 1984; Schlosser *et al.*, 1994). A comprehensive inverse modelling work using heat and salt balances and geostrophy focusing on the Nordic Seas has recently been completed by Mauritzen (1996a, b).

We shall proceed very much along the lines of classical budget estimates like those provided by Aagaard and Carmack (1989) and Mosby (1962). However, we shall try to integrate the knowledge of the processes affecting the boundary current with information about the fluxes through some key passages. Accordingly, we assume that the transports of the boundary current from the Norwegian Sea to the Arctic Ocean over the Barents and Kara seas and through Fram Strait are sufficiently known to be used.

Rudels (1987) estimated the net inflow to the Barents Sea to be 1.2 Sv using crude heat balance arguments. Blindheim (1989) analysing current measurements in the Bear Island Trough found a net inflow of 1.9 Sv, which eventually would enter the Kara Sea and the Arctic Ocean sinking down the St. Anna Trough. This value has been supported by year-long current measurements between Franz Josef Land and Novaya Zemlya (Loeng *et al.*, 1993) which indicated that about 2Sv entered the Kara Sea. In Fram Strait Rudels (1987) estimated that 1.9Sv of Atlantic Water in the West Spitsbergen Current crossed the 79 °N latitude. About half of this transport (1Sv) re-circulated in the strait while the rest would supply the boundary current flowing eastward along the Eurasian continental slope. Bourke *et al.* (1986) found based upon geostrophic calculations on a section along 80°N that the amount of Atlantic Water entering the Arctic Ocean was about 0.6Sv, and in their mass budget Aagaard and Carmack (1989) adopted 1Sv for the Atlantic inflow. These estimates suggest that 2Sv over the Barents Sea and 1Sv through Fram Strait entering the Arctic Ocean are reasonable estimates.

Atlantic Water not only supplies the Atlantic Layer of the Arctic Ocean. It also provides water to the upper layers by mixing with the river run off and, at least close to the inflow area north of Svalbard, by the melting of sea ice. The freshwater interacting with the Atlantic Water mainly derive from the Siberian rivers and according to Aagaard and Carmack (1989) the runoff from Ob, Yenisey and Lena is about 0.075Sv. Most of the river run off is exported as ice and if we adopt the figure 75% provided by Aagaard and Carmack (1989) 0.02Sv of freshwater dilutes the Atlantic Water.

The core of the Atlantic Water in the West Spitsbergen Current is about 500m thick and has a salinity of 35. North of Svalbard a 100m deep mixed layer with a salinity of approximately 34.3 is formed from ice melt and winter convection (Rudels *et al.*, 1996). Assuming a constant velocity in the upper 500m this implies that about 0.2 Sv of the Atlantic water of the Fram Strait Branch is transformed into a winter mixed layer north of Svalbard. This winter mixed layer is assumed to be advected along with the boundary current and will later provide water to the lower part of the halocline (Rudels *et al.*, 1996).

The mean salinity of the upper layers (mixed layer and halocline) in the Eurasian Basin is about 33.7 (Rudels *et al.*, 1996). This implies (with an AW salinity of 35) that 0.6 Sv of Atlantic Water is transformed into lighter waters. West of the Laptev Sea the mixed layer salinity is higher and the freshening is caused primarily by ice melt. This implies that the remaining part 0.4Sv of low salinity water originates from the Barents Sea Branch mixing with river runoff. To summarise: 0.2 and 0.4 Sv of Fram Strait and Barents Sea branch water respectively are transformed into Polar surface water.

Observations by Schauer *et al.* (1997) indicate that the Barents Sea branch can penetrate at least down to 1200m. Most of the Barents Sea branch is therefore likely to sink below the core of the Fram Strait inflow. Some interactions between the branches must occur because of the strong interleaving seen in the Atlantic core in the Nansen and Amundsen Basins (Rudels *et al.*, 1994). We therefore propose the 0.6Sv of the Barents Kara Sea inflow merge with the 0.8Sv of the Fram Strait Branch to form modified Atlantic Water (mAW) while the rest (1Sv) directly enters the intermediate layers.

Most of the mAW re-circulates in the Eurasian Basin and a smaller part enters the Canadian Basin in the boundary current. The slope convection in the Canadian Basin entrains water from the boundary current and redistributes it to deeper levels. About 0.2Sv will be transferred from the Atlantic layer into the intermediate and deep waters by this process (Jones *et al.*, 1995; Rudels, *et al.*, 1994). Furthermore, the inflow from the Bering Strait is smaller than the outflow through the Canadian Arctic Archipelago and 0.2Sv has to be supplied from the Atlantic inflow (Rudels, 1987). We assume that 0.1Sv from the upper layers and 0.1Sv from the mAW exit through the Canadian Arctic Archipelago.

The considerations above then imply that the water exiting Fram Strait would be distributed as 0.5Sv Polar Surface Water, 1.1Sv mAW and 1.2Sv intermediate and deep waters e.g uPDW, CBDW and EBDW. Hence, at this point, 2.3Sv are dense enough to provide water for the overflow from the Arctic Ocean.

In the second deep water formation area, the Greenland Sea, the estimate of deep water formation ranged in the mid-80s between 0.35 and 1Sv. (Smethie *et al.*, 1988; Heinze *et al.*, 1990; Rudels, 1986). Considering the present day situation with little or no renewal this is most likely an overestimate (Bönisch and Schlosser, 1995; Schlosser, 1991). If no Greenland Sea Deep Water is formed, more Arctic Intermediate Water should be created. Rudels (1986) estimated the formation of AIW to 1Sv in the Greenland Sea in the mid-80s and if we add the Boreas Basin we would expect a total of 2Sv of AIW and GSDW to form. The GSDW can only escape towards the east, and Blindheim (1990) has related the salinity minimum of the Norwegian Sea to the formation of AIW in the Greenland Sea. AIW also interacts with the East Greenland Current and we shall assume that 1Sv of the waters formed in the Greenland Sea enters the Norwegian Sea and 1Sv joins the East Greenland Current

The surface water which is being transformed in the Greenland Sea could be provided by the RAC. It is closest to the central gyre and a part of it has been seen entering the Boreas Basin (see above). The re-circulating of 1Sv at 79°N assessed by Rudels (1987) is not enough for the water transformations in the Greenland Sea but that value could well be an underestimate. Moreover, AW is recirculating south of Fram Strait (Gladfelder, 1964; Quadfasel and Meincke, 1987) and the total strength of the RAC is probably closer to 3Sv. These 3Sv would then be transformed into primarily AIW (2Sv) but it is also likely that some part will be diluted by ice melt as the RAC encounters the East Greenland Current. If we assume 0.5Sv lost to ice melt, the East Greenland Current would consist of 1Sv upper water, 0.5Sv RAC, 1.1Sv mAW, 1Sv AIW and 1.2Sv of Arctic Ocean deep water, when it reaches the Jan Mayen Fracture Zone. Except for the upper waters all water masses can here supply water to the overflow.

Not much has so far been said about the Arctic Ocean deep water but for simplicity we assume that it consists of 0.4Sv UPDW, 0.4Sv CBDW and 0.4Sv EBDW, 3.4Sv of the dense waters can then cross the Jan Mayen Fracture Zone into the Iceland Sea while the EBDW remains in the Greenland Sea. Further south, at the Denmark Strait the CBDW is too dense to cross the sill and will continue into the Norwegian Sea. 3.0Sv then remain for the overflow water in the Denmark Strait.

The remaining part of the boundary current, 0.4Sv, would then reach the Norwegian Sea north of Iceland. However, the Norwegian Sea will also receive the 0.4Sv EBDW and 1Sv of AIW and GSDW from the Greenland Sea providing 1.8Sv for the overflow east of Iceland.

How does this compare with recent estimates of the overflow? Dickson and Brown (1994) have estimated that 2.9Sv of overflow water are passing through the Denmark Strait and that 1Sv crosses between Iceland and the Faeroe Islands and 1.7Sv through the Faeroe-Shetland Channel This makes a total of 5.6Sv of overflow water. Only 0.8Sv is not accounted for by the boundary current.

This volume could be provided by Atlantic Water that re-circulates east and south of the Greenland Sea. Such a re-circulation, which is already indicated in Helland-Hansen and Nansen (1909) could then directly supply water for the formation of the Arctic Intermediate Water that is expected to take place in the north-eastern Iceland Sea (Swift and Aagaard, 1981). Most of this

dense water would then cross the sill between Iceland and the Faeroe Islands.

The discrepancies between the obtained total outflow and the proposed inflow are still greater. Worthington (1970, 1976) assumed that 8Sv of Atlantic Water enter the Arctic Mediterranean in the boundary current and that in addition 1Sv flows north in the west of Iceland. Of these 9Sv, 6Sv were taken to return as dense water to supply the North Atlantic Deep Water, while 3Sv consisted of the lighter Polar Surface Water of the East Greenland Current. 4Sv of the deep outflow pass through the Denmark Strait, 1Sv between Iceland and the Faeroe Islands and 1Sv through the Faeroe-Shetland Channel.

The deep outflow is, apart from details, close to that given by Dickson and Brown (1994). However, 2Sv of water leaving in the upper layers are not in our estimate. Because of the constraint with the ice export through Fram Strait (Aagaard and Carmack, 1989) it is difficult to form much more low density water in the Arctic Ocean, perhaps another 0.2–0.3Sv. 1Sv, the inflow west of Iceland, could re-circulate in the Iceland Sea and re-cross the sill east of Iceland. The rest could conceivably also leave the boundary current at about 70°N toward Jan Mayen. Another and perhaps more likely possibility is that the West Spitsbergen Current and the RAC are still stronger than assumed above and that not 0.5 but 1.5Sv of the RAC interact with sea ice and add to the upper part of the East Greenland Current.

These considerations show that the assessed fluxes are not completely unrealistic. More is not to be expected. It should be kept in mind that the different water masses do not flow in tubes and much interaction and mixing occur between the different deep and intermediate waters. A further point to emphasise is that there are several sources of about equal strength, which can contribute to the overflow, either directly or, in the case of water masses to be too dense to cross the sill, by replacing less dense water upwards.

Summary

We have followed the boundary current of the Arctic Mediterranean Sea, through its bifurcations and mergings, along the Eurasian and American continental slopes, and we have seen its density range expand. Some less saline and less dense waters have been formed, but mostly colder and denser water masses have been created. Even though the densest waters are formed by freezing and the injection of brine into the water column, the large, overall density increase is due to the removal of heat from diluted Atlantic Water. Several of the water masses are so dense that they become isolated from the World Ocean by the Greenland-Scotland Ridge and only take part in a deep circulation internal to the Arctic Mediterranean (Aagaard *et al.*, 1985; Rudels and Quadfasel, 1991).

At present the Arctic Ocean appears to contribute about half of the overflow water. This is surprising considering the age estimates for the Denmark Strait overflow water given by Smethie and Swift (1989). They find that the less dense water, which comprises 80 % of the Denmark Strait overflow, is 3–5 years old, which implies that the source area would be the Iceland Sea. The denser 20 % were established to be about 15 years old and assumed to have originated in the Greenland Sea.

The less dense overflow water would, in the present work, correspond to the water of the Atlantic Return Current, formed in Fram Strait and modified by mixing with AIW as it passes along the perimeter of the Greenland Sea. The denser part implies the uPDW and also CBDW, which is likely to have spent a considerable time in the Arctic Ocean. The incorporation of newly formed Arctic Intermediate Water into the boundary current in the Greenland and Iceland Seas may, however, cause an increase in the concentrations of the anthropogenic tracers upon which these time estimates are based. This would give the Arctic Ocean water masses an appearance of being "younger" and more recently ventilated and lead to erroneous conclusions about their origin.

The existence of an extended and persistent boundary current supplied by waters from several source areas increases the stability of the rate of the overflow of dense water to the North Atlantic and diminishes the possibility that the global conveyor belt should dry up (Rudels, 1995). Figure 13 shows the boundary current and the main source areas for dense water: The inflow to the Arctic Ocean in the St. Anna Trough, and the shelf seas; the open ocean convection in the Greenland and Iceland Seas; and the open ocean convection in the Norwegian Sea, preconditioning the inflow to the Arctic Ocean (Mauritzen, 1996a, b), and supplying the dense water of the Atlantic Return Current.

Two recently reported changes, the higher temperatures observed in the Arctic Ocean (Quadfasel *et al.* 1991; Carmack *et al.* 1995) and the reduction of the convection in the Greenland Sea (Dickson *et al.*, 1997) pose some interesting problems. The cause for the higher temperatures in the Arctic Ocean is most reasonably sought in a stronger or a warmer inflow of Atlantic Water into the Arctic Ocean. This could be due to a smaller than normal heat loss in the Greenland Sea, but also to a warmer Atlantic inflow to the Arctic Mediterranean.

The higher temperatures in the Arctic Ocean may also be due to variations in the relative density distributions between the Fram Strait and the Barents Sea branches of

the inflow to the Arctic Ocean. If the Barents Sea inflow becomes denser, it would enter the Arctic Ocean beneath the Fram Strait branch, which then could flow unobstructed along the slope into the Canadian Basin supplying the observed warm Atlantic Layer. Is this the case, fluctuations in the Atlantic Layer temperature in the Arctic Ocean should be rather common.

A second possibility is that the inflow through Fram Strait is linked to the convection in the Greenland Sea. When deep convection is reduced the lower part of the Greenland Sea is renewed by Arctic Ocean deep waters instead of transformed Atlantic Water. No GSDW flows northward into Fram Strait, which further facilitates the outflow of the Arctic Ocean deep waters. It could also mean that a part of the Atlantic Water, instead of re-circulating in Fram Strait, now more easily enters the Arctic Ocean. Such changes could reinforce themselves. More and warmer Atlantic Water in the Arctic Ocean leads to weaker ice formation, which in turn implies less dense water formed on the shelves and a weaker slope convection. More freshwater in the upper layers will lead to a lower density and salinity of the surface water leaving the Arctic Ocean. In combination with less re-circulating Atlantic Water this leads to less dense surface water input to the Greenland Sea and the deep convection is weakened still further.

Acknowledgement

This work has been supported by the Deutsche Forschungsgemeinschaft (SFB 318) and by the European Union under the MAST III ESOP project.

References

Aagaard, K. 1989. A synthesis of the Arctic Ocean circulation. Rapports et Procès-Verbaux des Réunions du Conseil International pour l'Exploration de la Mer, 188: 11–22.

Aagaard, K., and Greisman, P. 1975. Towards new mass and heat budgets for the Arctic Ocean. Journal of Geophysical Research, 80: 3821–3827.

Aagaard, K., Swift, J. H., and Carmack, E. C. 1985. Thermohaline circulation in the Arctic Mediterranean Seas. Journal of Geophysical Research, 90: 4833–4846.

Aagaard, K., and Carmack, E. C. 1989. The role of sea ice and other fresh water in the Arctic circulation. Journal of Geophysical Research, 94: 14485–14498.

Aagaard, K., Fahrbach, E., Meincke, J., and Swift, J. H. 1991. Saline outflow from the Arctic Ocean: Its contribution to the deep waters of the Greenland, Norwegian and Icelandic seas. Journal of Geophysical Research, 96: 20433–20441.

Anderson, L. G., Björk, G., Holby, O., Jones, E. P., Kattner, G., Koltermann, K.-P., Liljeblad, B., Lindegren, R., Rudels, B., and Swift, J. H. 1994. Water masses and circulation in the Eurasian Basin: Results from the Oden 91 Expedition. Journal of Geophysical Research, 99: 3273–3283.

Bauch, D., Schlosser, P., and Fairbanks, R. G. 1995. Freshwater balance and sources of deep and bottom waters in the Arctic Ocean inferred from the distribution of H_2O^{18}. Progress in Oceanography, 35: 53–80.

Blindheim, J. 1989. Cascading of Barents Sea bottom water into the Norwegian Sea. Rapports et Procès-Verbaux des Réunions du Conseil International pour l'Exploration de la Mer, 188: 49–58.

Blindheim, J. 1990. Arctic Intermediate Water in the Norwegian Sea. Deep-Sea Research, 37: 1475–1489.

Bönisch, G., and Schlosser, P. 1995. Deep water formation and exchange rates in the Greenland/Norwegian Seas and the Eurasian Basin of the Arctic Ocean. Progress in Oceanography, 35: 29–52.

Bourke, R. H., Weigel, A. M., and Paquette, R. G. 1988. The westward turning branch of the West Spitsbergen Current. Journal of Geophysical Research, 93: 14065–14077.

Buch, E., Malmberg S.-A., and Kristmannsson, S. S. 1992. Arctic Ocean deep water masses in the western Iceland Sea. ICEM CM 1992/C:2, 18 pp.

Buch, E., Malmberg, S.-A., and Kristmannsson, S. S. 1996. Arctic Ocean deep water masses in the western Iceland Sea. Journal of Geophysical Research, 101: 11965–11973.

Carmack, E. C., Macdonald, R. W., Perkin, R. G., McLaughlin, F. A., and Pearson, R. J. 1995. Evidence for warming of Atlantic Water in the southern Canadian Basin of the Arctic Ocean: Results from the Larsen-93 expedition, Geophys. Res. Letters, 22: 1061–1064.

Clarke, R. A., Swift, J. H., Reid, J. L., and Koltermann, K.-P. 1990. The formation of Greenland Sea Deep Water: double-diffusion or deep convection? Deep-Sea Research, 37: 687–715.

Dickson, R. R., and Brown, J. 1994. The production of North Atlantic Deep Water: Sources, rates and pathways. Journal of Geophysical Research, 99: 12319–12341.

Dickson, R. R., Lazier, J., Meincke, J., Rhines, P., and Swift, J. H. 1997. Long-term coordinated changes in the convective activity of the North Atlantic. Progress in Oceanography, 38: 241–295.

Dietrich, G. 1956. Überströmung des Island-Faröer Rückens in Bodennähe nach Beobachtungen mit dem Forschungsschiff "Anton Dohrn" 12955–56. Deutsche Hydrografische Zeitschrift, 9: 78–89.

Friedrich, H., Houssais, M.-N., Quadfasel, D., and Rudels, B. 1995. On Fram Strait Water Masses. Extended Abstract, Nordic Seas Symposium, Hamburg 7/3-9/3 1995: 69–72.

GSP-Group (J. Meincke chairman) 1990. Greenland Sea Project – A venture toward improved understanding of the oceans' role in climate. EOS, 71: 750–755.

Gladfelder, A.G. 1964. Oceanography of the Greenland Sea. RV Atka (AGB-3) survey summer 1962. U.S. Navy Ocean. office. Washington, 120 pp.

Isert, K. 1996. Untersuchungen der Hydrographischen Struktur der Grönlandsee im Frühjahr 1993 mit besonderem Hinblick auf die großskalige Zirkulation und die Tiefenwasserventilation. Diplom-Arbeit, Universität Hamburg, 114 pp.

Heinze, Ch., Schlosser, P., Koltermann, K.-P., and Meincke, J. 1990. A tracer study of the deep water renewal in the European polar seas. Deep-Sea Research, 37: 1425–1453.

Helland-Hansen, B., and Nansen, F. 1909. The Norwegian Sea. Ist physical oceanography based upon the Norwegian researches 1900–1904. Report on Norwegian Fishery and Marine Investigations, II(1), Kristiania.

Jones, E. P., Rudels, B., and Anderson, L. G. 1995. Deep Waters of the Arctic Ocean: Origins and Circulation. Deep-Sea Research, 42: 737–760.

Lazier, J. R. N. 1973. The renewal of Labrador Sea Water. Deep-Sea Research, 20: 341–353.

Lazier, J. R. N. 1988. Temperature and salinity changes in the deep Labrador Sea, 1962–1986. Deep-Sea Research, 35: 1247–1253.

Loeng, H., Ozhigin, V., Ådlandsvik, B., and Sagen, H. 1993. Current Measurements in the north-eastern Barents Sea. ICES CM 1993/C:41, 22pp.

Malmberg, S. A. 1983. Hydrographic investigations In the Iceland and Greenland Seas in late winter 1971. "Deep Water Project". Jökull, 33: 133–140.

Mauritzen, C. 1996a. Production of dense overflow waters feeding the North Atlantic across the Greenland Sea-Scotland Ridge. Part 1: Evidence for a revised circulation scheme. Deep-Sea Research, 43: 769–806.

Mauritzen, C. 1996b. Production of dense overflow waters feeding the North Atlantic across the Greenland Sea-Scotland Ridge. Part 2: An inverse model, Deep-Sea Research, 43: 807–835.

McCartney, M. S. 1977. Subantarctic Mode Water. *In* A Voyage of Discovery: The George Deacon 70th Anniversary Volume, pp. 103–119. Ed. by M. V. Angel. Oxford University Press.

McCartney, M. S. 1982. The subtropical re-circulation of Mode waters Journal of Marine Research, 40 (suppl): 427–464.

McCartney, M. S., and Talley, L. D. 1984. Warm-to-Cold Water Conversions in the Northern North Atlantic Ocean. Journal of Physical Oceanography, 14: 922–935.

Meincke, J. 1983. The modern current regime across the Greenland-Scotland Ridge. *In* Structure and Development of the Greenland-Scotland Ridge, pp. 637–650. Ed. by Bott, Saxov, Talwani and Thiede, Rds., Plenum Publ. Co.

Meincke, J., Rudels, B., and Friedrich, H. 1997. The Actic Ocean - Nordic Seas Thermohaline System. ICES Journal of Marine Science (in press).

Midttun, L. 1985. Formation of dense bottom water in the Barents Sea, Deep-Sea Research, 32: 1233–1241.

Mosby, H. 1962. Water, mass and heat balance of the North Polar Sea and of the Norwegian Sea. Geofysiske Publikationer 24(II): 289–313.

Nansen, F. 1906. Northern Waters. Captain Roald Amundsen's oceanographic observations in the Arctic seas in 1901. Vid-selskap Skrifter I, Mat.-Naturv. kl. Dybvad Christiania, 1 (3), 145 pp.

Nansen, F. 1912. Das Bodenwasser und die Abkühlung des Meeres. Internationale Revue der Gesamten Hydrobiologie und Hydrographie, 5 (1), 42 pp.

Östlund, H. G., and Hut, G. 1984. Arctic Ocean water mass balance from isotope data, Journal of Geophysical Research, 89: 6373–6381.

Quadfasel, D., and Meincke, J. 1987. Note on the thermal structure of the Greenland Sea gyres. Deep-Sea Research, 34: 1883–1888.

Quadfasel, D., Rudels, B., and Kurz, K. 1988. Outflow of dense water from a Svalbard fjord into the Fram Strait. Deep-Sea Research, 35: 1143–1150.

Quadfasel, D., Sy, A., Wells, D., and Tunik, A. 1991. Warming in the Arctic. Nature, 350, 385.

Quadfasel, D., Rudels, B. and Selchow, S. 1992. The Central Bank vortex in the Barents Sea: water mass transformation and circulation. ICES Marine Science Symposia, 195: 40–51.

Reid, J. L., and Lynn, R. S. 1971. On the influence of the Norwegian-Greenland and Weddell Seas on the bottom waters of the Indian and Pacific Oceans. Deep-Sea Research, 18: 1063–1088.

Rhein, M. 1991. Ventilation rates of the Greenland and Norwegian Seas derived from distributions of the chlorofluoromethanes F11 and F12. Deep-Sea Research, 38: 485–503.

Rudels, B. 1986. The Θ-S relations in the northern seas: Implications for the deep circulation. Polar Res. 4 n.s. 133–159.

Rudels, B. 1987. On the mass balance of the Polar Ocean, with special emphasis on the Fram Strait. Norsk Polarinstitutt Skrifter, 188. 53pp.

Rudels, B. 1995. The thermohaline circulation of the Arctic Ocean and the Greenland Sea. Philosophical Transactions of the Royal Society of London, A, 352: 287–299.

Rudels, B., and Quadfasel, D. 1991. Convection and deep water formation in the Arctic Ocean-Greenland Sea System. Journal of Marine Systems, 2: 435–450.

Rudels, B., Jones, E. P., Anderson, L. G., and Kattner, G. 1994. On the intermediate depth waters of the Arctic Ocean. *In* The role of the Polar Oceans in Shaping the Global Climate, pp. 33–46. Ed. by O. M. Johannessen, R. D. Muench and J. E. Overland. American Geophysical Union, Washington.

Rudels, B., Anderson, L. G., and Jones, E. P. 1996. Formation and evolution of the surface mixed layer and the halocline of the Arctic Ocean, Journal of Geophysical Research, 101: 8807–8821.

Schauer, U. 1995. The release of brine-enriched shelf water from Storfjord into the Norwegian Sea. Journal of Geophysical Research, 100: 16015–16028.

Schauer, U., Muench, R. D., Rudels, B., and Timokhov, L. 1997. The impact of eastern Arctic shelf water on the Nansen Basin intermediate layers. Journal of Geophysical Research, 102: 3371–3382.

Schlosser, P., Böhnisch, G., Rhein, M., and Bayer, R. 1991. Reduction of deep water formation in the Greenland Sea during the 1980s: Evidence from tracer data. Science, 251: 1054–1056.

Schlosser, P., Bauch, D., Fairbanks, R. G., and Bönisch, G. 1994. Arctic river-runoff: mean residence time on the shelves and in the halocline. Deep-Sea Research, 1053–1068.

Smethie, W. M., Chipman, D. W, Swift, J. H., and Koltermann, K.-P. 1988. Chlorofluoromethanes in the Arctic Mediterranean seas: evidence for formation of bottom water in the Eurasian Basin and the deep-water exchange through Fram Strait. Deep-Sea Research, 35: 347–369.

Smethie, W. M., and Swift, J. H. 1989. The tritium:krypton -85 age age of the Denmark Strait overflow water and Gibbs Fracture zone water just south of Denmark Strait. Journal of Geophysical Research, 94: 8265–8275.

Strass, V. H., Fahrbach, E., Shauer, U., and Sellmann, L. 1993. Formation of Denmark Strait overflow water by mixing in the East Greenland Current. Journal of Geophysical Research, 98: 6907–6919.

Steele, M., Morison, J. H., and Curtin, T. B. 1995. Halocline formation in the Barents Sea, Journal of Geophysical Research, 100: 881–894.

Stefánsson, U. 1962. North Icelandic Waters. Rit Fiskideildar, Reykjavik, 269 pp.

Sverdrup, H. U., Johnson, M. W., and Fleming, R. H. 1942. The Oceans: Their Physics, Chemistry and General Biology. Prentice-Hall, New York, 1042 pp.

Swift, J. H. 1986. The Arctic Waters. *In* The Nordic Seas, pp. 129–153. Ed. by B. G. Hurdle. Springer-Verlag, Heidelberg.

Swift, J. H., Aagaard, K., and Malmberg, S.-A. 1980. The contribution of the Denmark Strait overflow to the deep North Atlantic. Deep-Sea Research, 27: 29–42.

Swift, J. H., and Aagaard, K. 1981. Seasonal transitions and water mass formation in the Icelandic and Greenland Seas. Deep-Sea Research, 28: 1107–1129.

Swift, J. H., and Koltermann, K.-P. 1988. The origin of the Norwegian Sea deep water. Journal of Geophysical Research, 93: 3563–3569.

Talley, L. D., and McCartney, M. S. 1982. Distribution and circulation of Labrador Sea Water. Journal of Physical Oceanography, 1189–1205.

Untersteiner, N. 1988. On the ice and heat balance in Fram Strait. Journal of Geophysical Research, 92: 527–532.

Vowinckel, E., and Orvig, S. 1970. The climate of the North Polar Basin. *In* World Climate survey, vol. 14: Climates of the polar regions. Ed. by S. Orvig. Elsevier, Amsterdam, 370 pp.

Warren, B. A. 1981. Deep Circulation of the World Ocean. *In* Evolution of Physical Oceanography, pp. 6–40. Ed. by B. A. Warren and C. Wunsch . MIT press

Worthington, L. V. 1970. The Norwegian Sea as a mediterranean basin. Deep-Sea Research, 17: 77–84.

Worthington, L. V. 1976. On the North Atlantic Circulation. Johns Hopkins Oceanographic Studies No. 6., The Hopkins University Press, 110 pp.

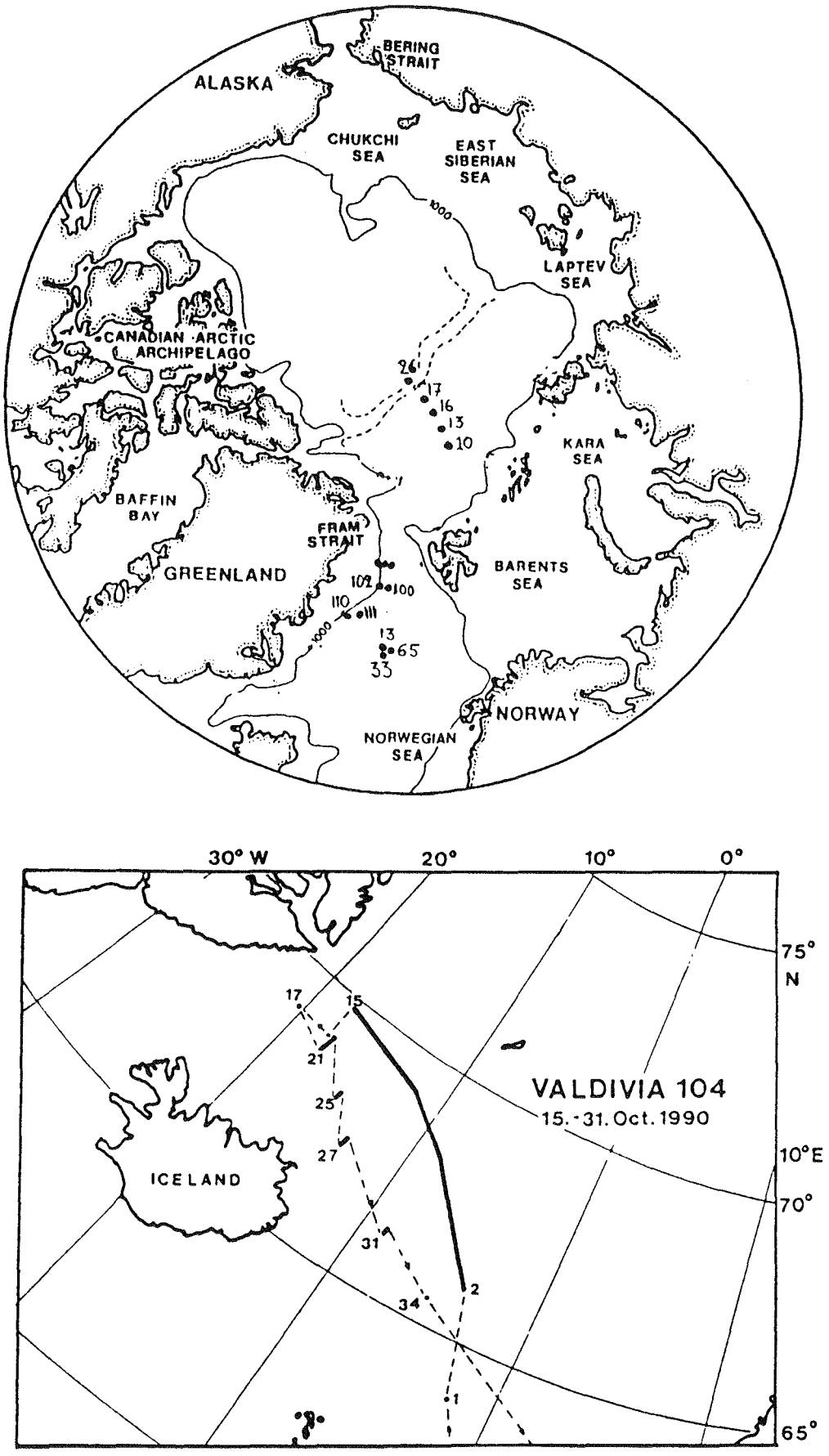

Figure 1. Maps and station positions. Top; the Arctic Mediterranean, bottom; the Iceland Sea.

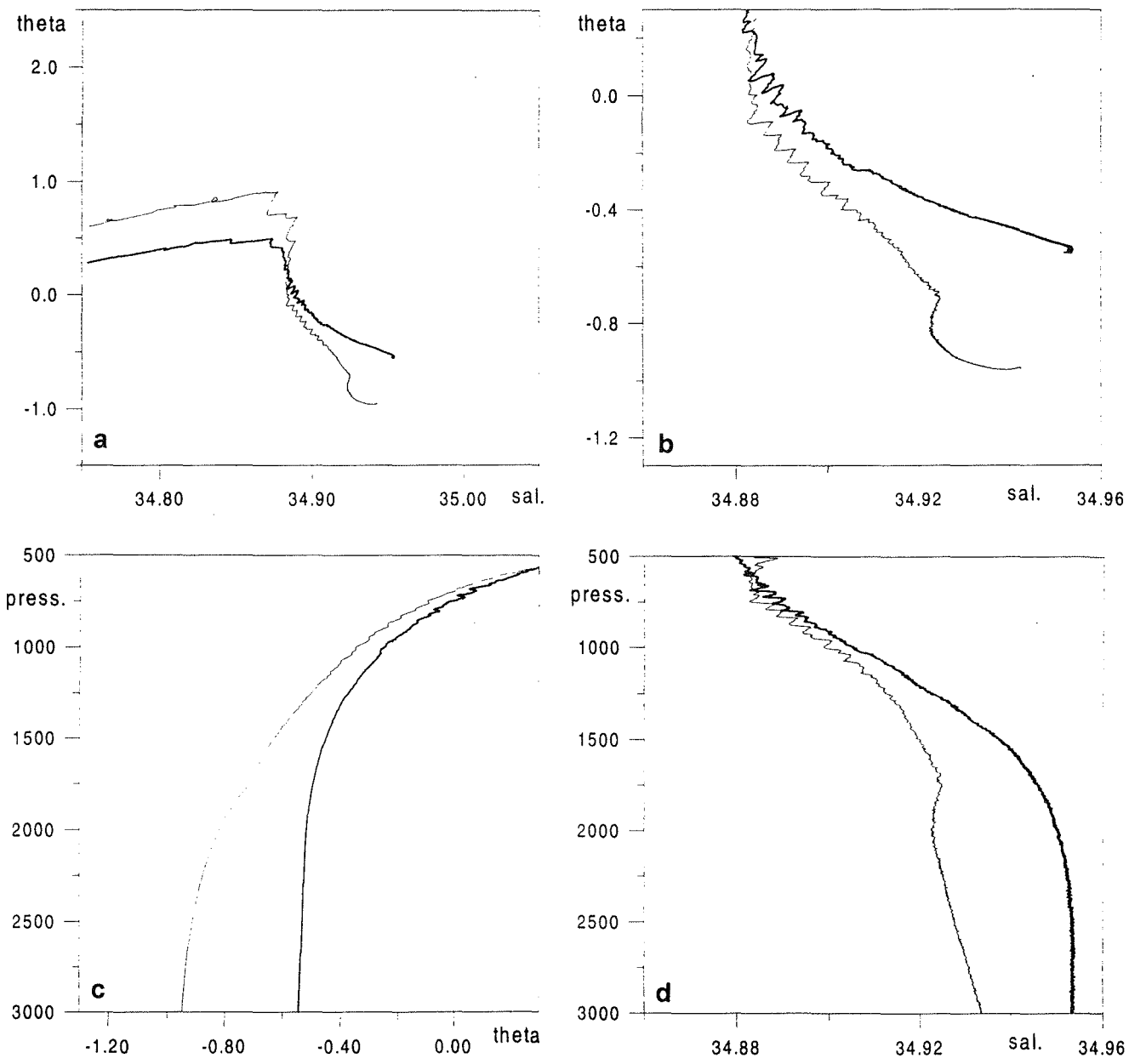

Figure 2. a) Θ-S curves, b) Θ-S curves (blow-up), c) potential temperature profiles, d) salinity profiles from Oden stations 16 and 26 (bold).

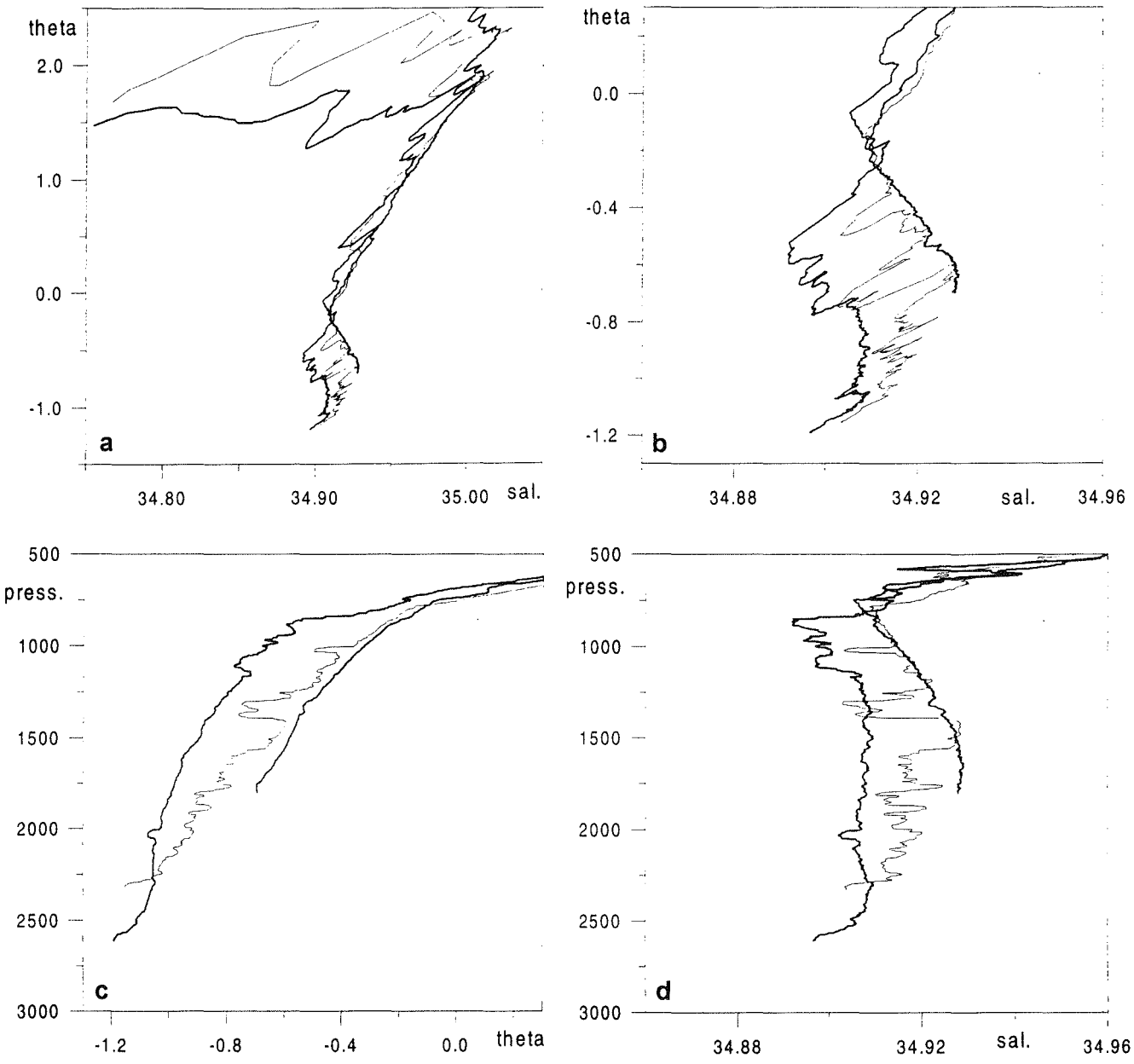

Figure 3. a) Θ-S curves, b) Θ-S curves (blow-up), c) potential temperature profiles, d) salinity profiles from 3 stations on the Greenland continental slope in Fram Strait (Lance 84).

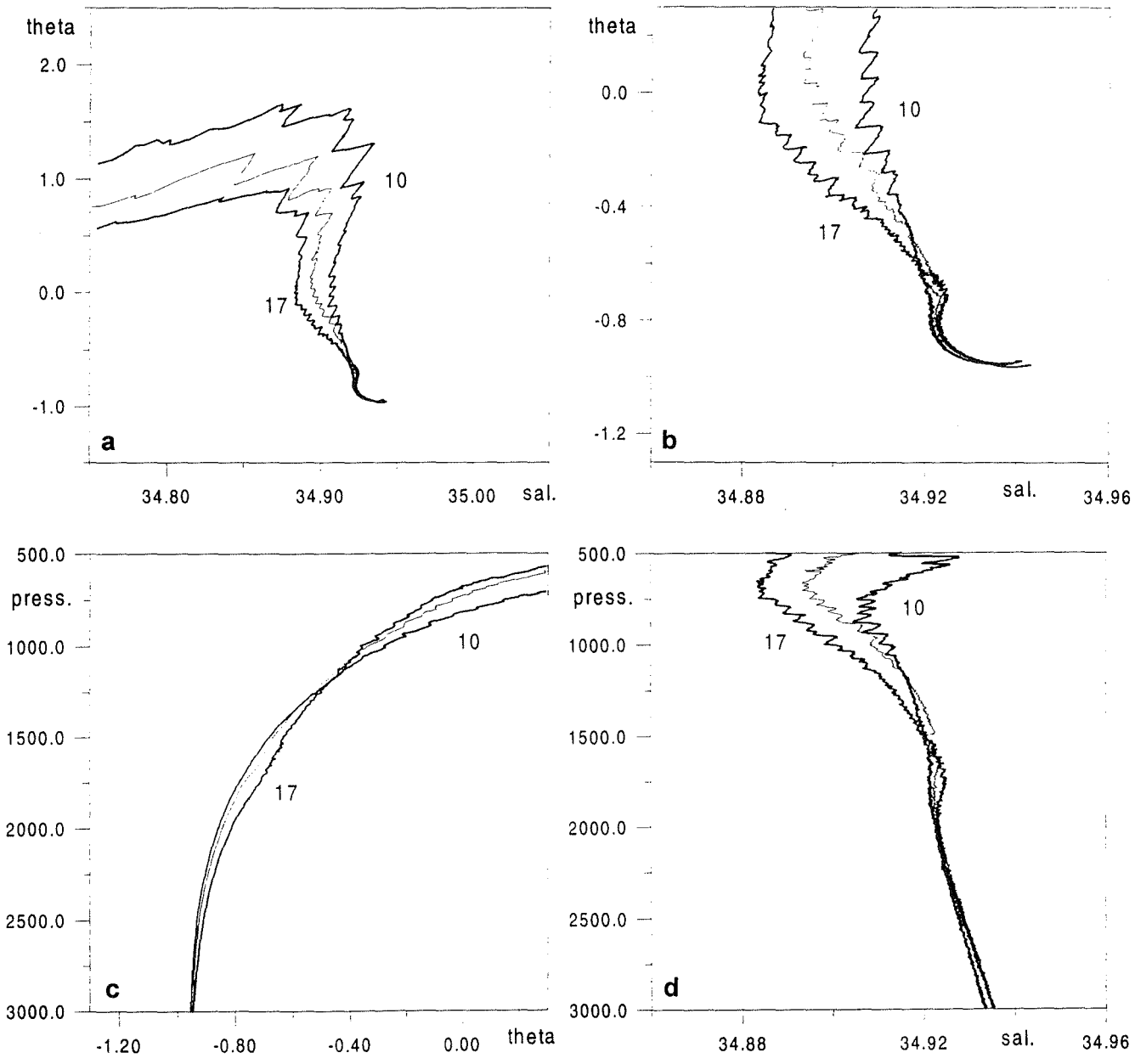

Figure 4. a) Θ-S curves, b) Θ-S curves (blow-up), c) potential temperature profiles, d) salinity profiles from Oden stations 10, 13 and 17 in the Nansen and Amundsen basins.

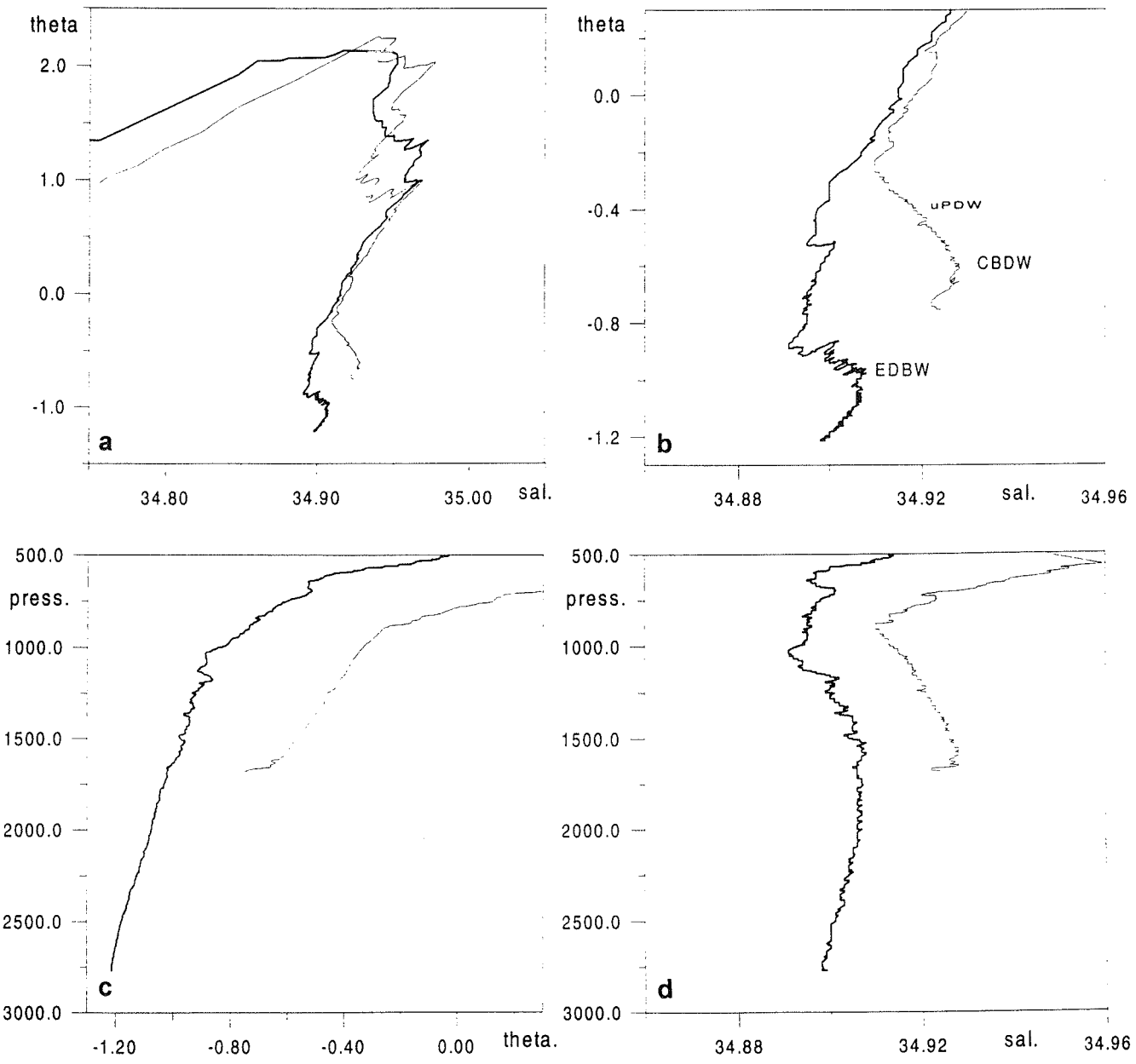

Figure 5. a) Θ-S curves, b) Θ-S curves (blow-up), c) potential temperature profiles, d) salinity profiles from stations 100 (bold) and 102 in the Boreas Basin slope (Lance 88).

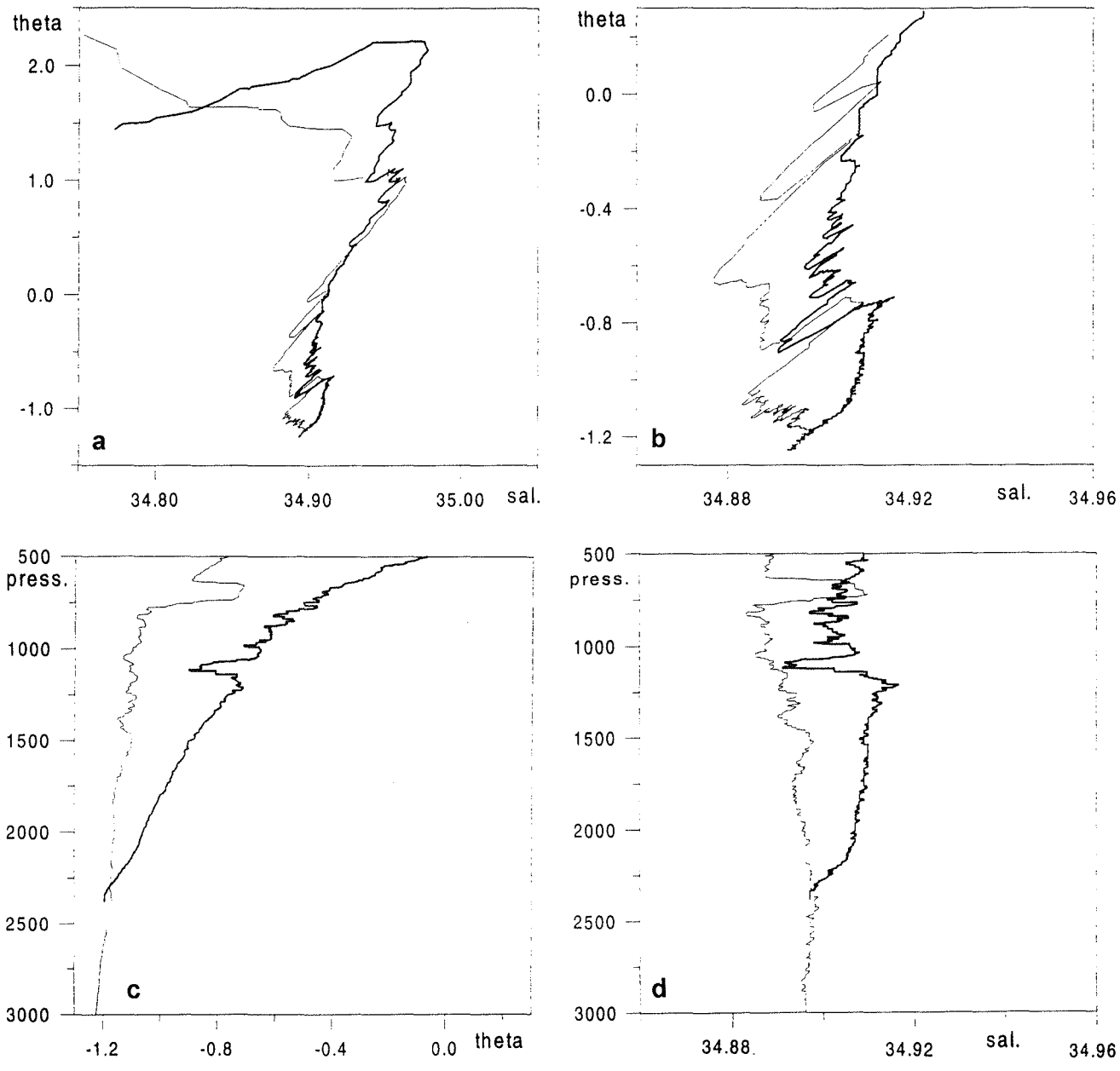

Figure 6. a) Θ-S curves, b) Θ-S curves (blow-up), c) potential temperature profiles, d) salinity profiles from stations 110 and 111 (bold) on the Greenland Sea slope (Lance 88). Notice the difference in depth of the isopycnal exchange on the two stations.

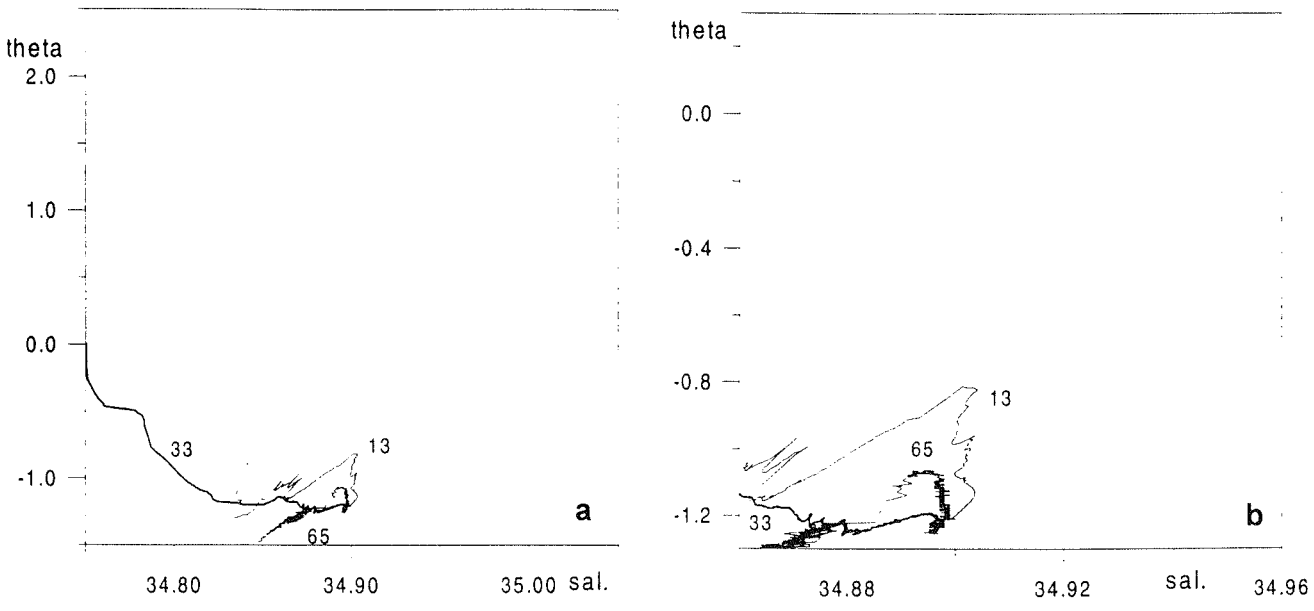

Figure 7. a) Θ-S curves, b) Θ-S curves (blow-up) from 3 stations in the central Greenland Sea: 65 (Valdivia 67), 33 (bold) (Valdivia 71) and 13 (Valdivia 136) showing the increased temperature and salinity of the Greenland Sea Deep Water.

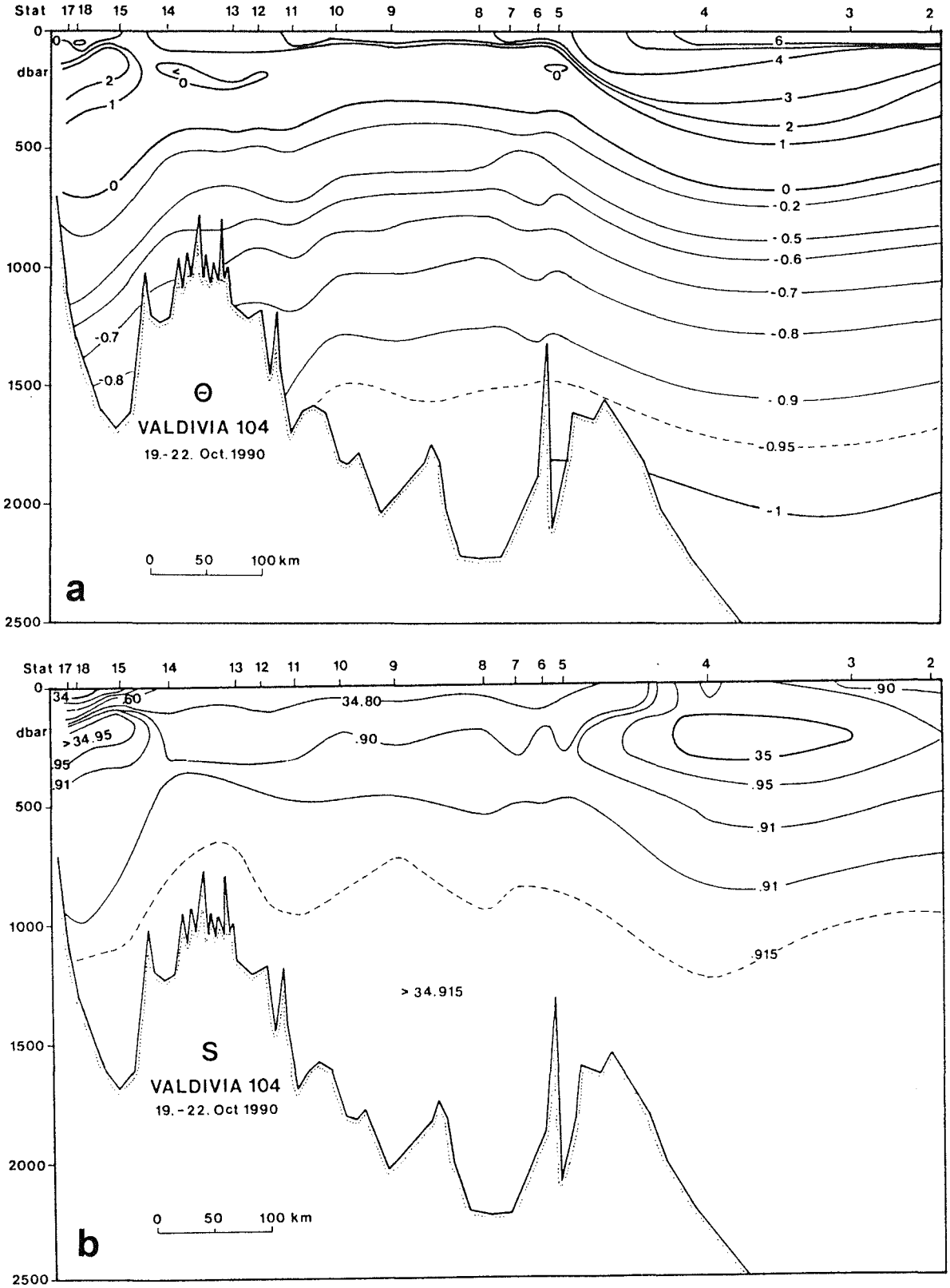

Figure 8. East-west vertical sections of a) potential temperature and b) salinity across the northern Iceland Sea (Valdivia 104). The section is composed of one long northerly section and one further to the south reaching the continental slope (see Figure 1)

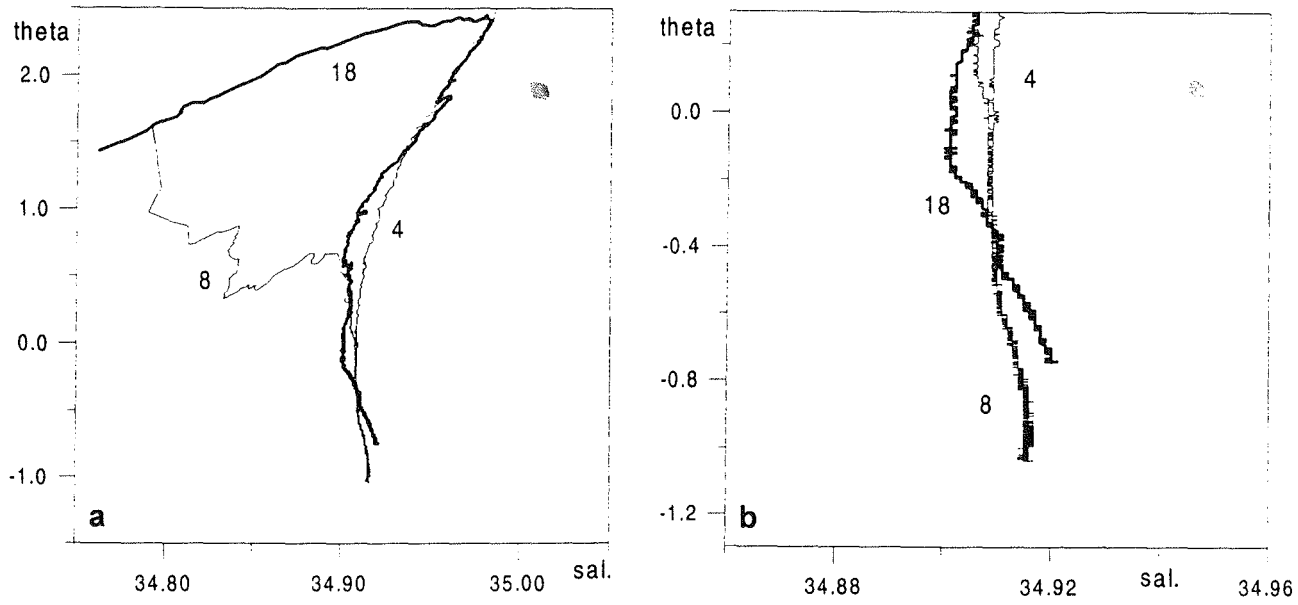

Figure 9. Θ-S curves from 3 stations, 18 at the slope, 8 from the eastern part of the Iceland Sea and 4 from the Norwegian Sea (Valdivia 104).

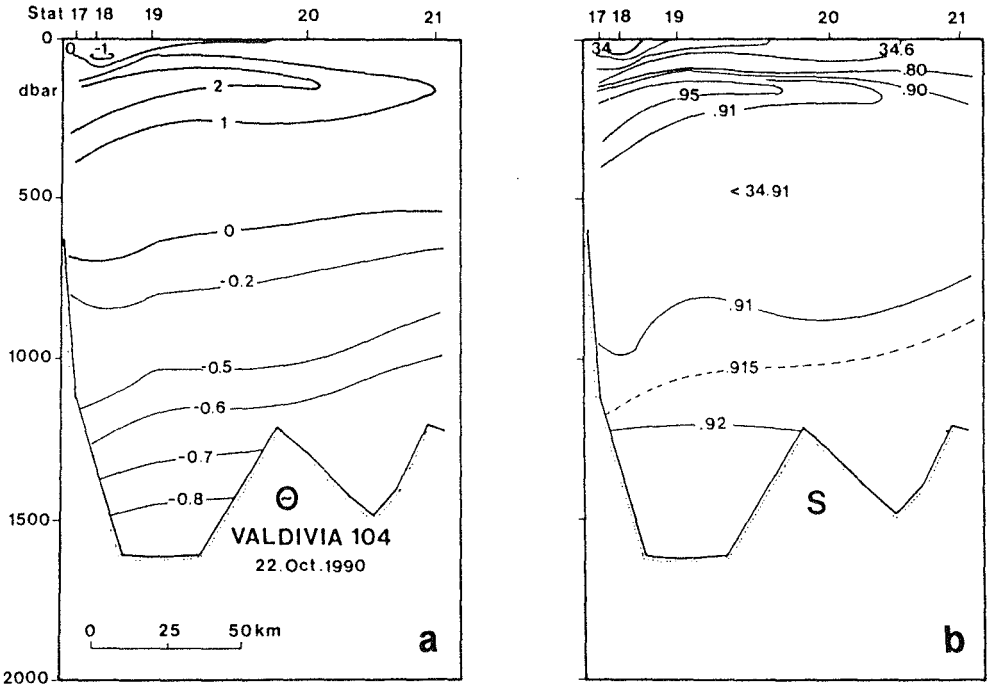

Figure 10. North-south vertical sections of a) potential temperature and b) salinity from Iceland to the western Jan Mayen Ridge across the northern Iceland continental slope (Valdivia 104).

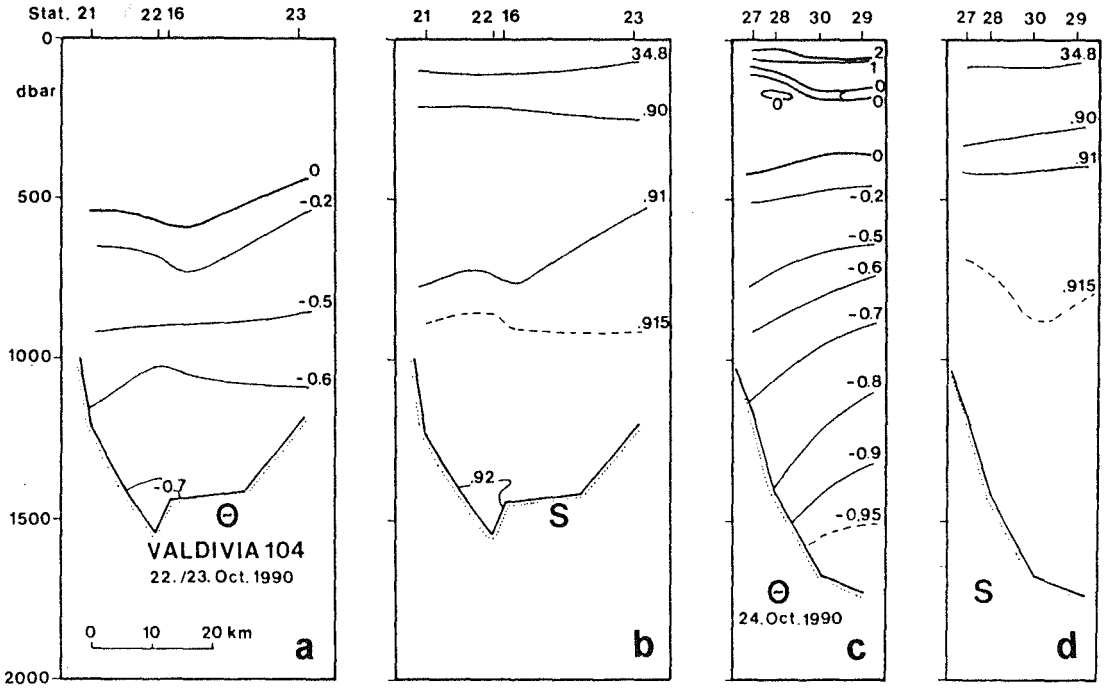

Figure 11. North-south vertical sections of a) and c) potential temperature and b) and d) salinity at the Iceland continental slope (Valdivia 104).

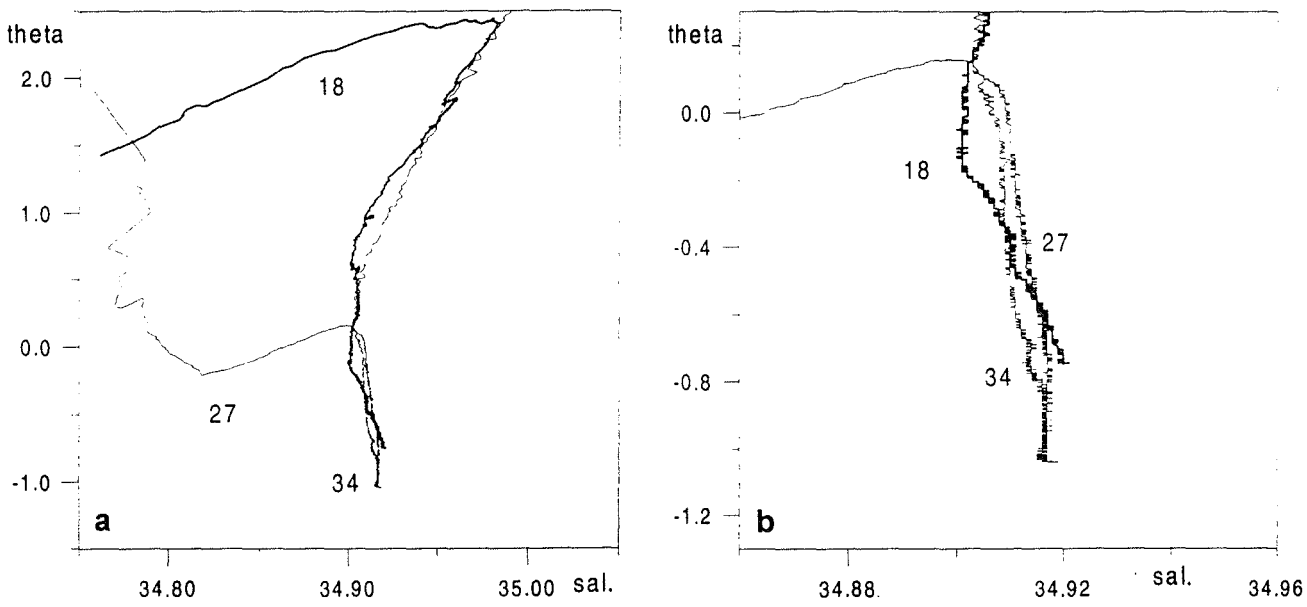

Figure 12. Θ-S curves from 3 stations, 18 from the western part of the Iceland Sea, 27 from north of Iceland and 34 from the southern Norwegian Sea (Valdivia 104).

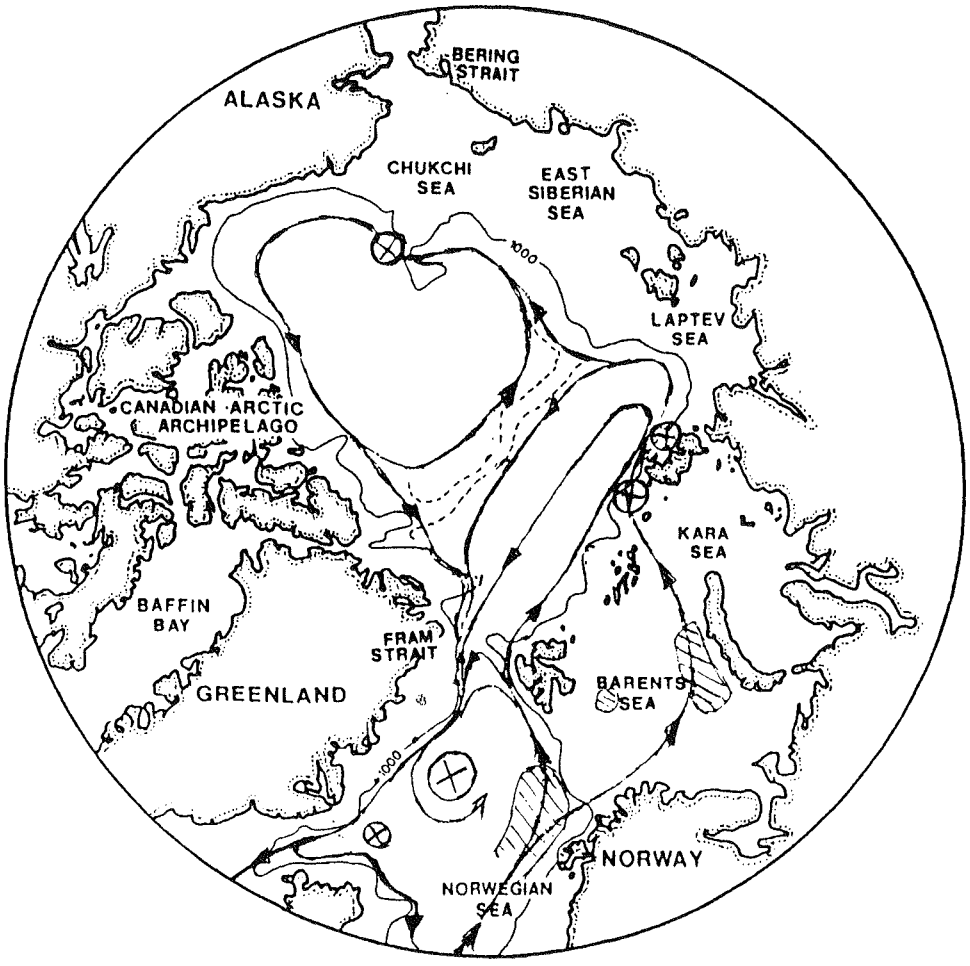

Figure 13. Map of the Arctic Mediterranean showing the path of the boundary current and the main source areas of dense water: The shelf contributions, the Barents - and Kara Sea outflow at the St. Anna Trough, the open ocean convection in the Greenland and Iceland Seas and the open ocean convection in the Norwegian Sea and the re-circulating West Spitsbergen Current.

Norwegian Sea Deep Water overflow across the Wyville Thomson Ridge during 1987–1988

D. J. Ellett

Scottish Association for Marine Science, P.O. Box 3, Oban, Argyll, Scotland, United Kingdom.

Based on a paper presented to the ICES Hydrography Committee as ICES CM 1991/C:41

As part of the ICES NANSEN investigations of Atlantic - Norwegian Sea exchange, current meters were deployed to the west of the Wyville-Thomson Ridge between September 1987 and June 1988. CTD surveys of the area and of Faroe Bank were also made in these two months. A rather steady westward flow of varying temperature and salinity characteristics was found throughout the period at the lowest levels and it is suggested that this was partly a result of entrainment driven by the lower part of the west of Scotland slope current, diverted to the west by the topography of the ridge. A variable eastward flow found at 275m depth represents the currents of the upper layers, but mid-water currents changed from weak easterlies in autumn and early winter, to episodes of strong westerlies in late winter and spring. The latter could be due to westward movement, as a result of the relaxation of winter wind forcing, of a cyclonic gyre situated at the southern entrance to the Faroe Bank Channel.

Keywords: Overflow, Wyville-Thomson Ridge, Transport

Introduction

Overflow of Norwegian Sea Deep Water (NSDW) across the Wyville-Thomson Ridge was first documented in 1972 (Ellett and Roberts, 1973), and short-term current measurements were made during the ICES Overflow '73 Expedition by J. Crease in a narrow gully west of the ridge. When combined with CTD data for a day (28 August 1973) when the mean current velocity was about 10% higher than the 25-day mean, the results gave a total westward flow of 1.2 Sv below a reference level of about 350 m depth, of which the NSDW component was 0.33 Sv (Ellett and Edwards, 1978). Subsequently, long-term current measurements were made some 75 km downstream from the ridge-crest by J. Gould during 1978–83, and at the lowest point of the ridge crest and upon the southeastern part of the ridge during 1982–83 by H. D. Dooley. Some results from these deployments are given by Dickson *et al* (1986). The Overflow '73 surveys had confirmed that overflow was not confined to the lowest part of the ridge-crest, but takes place along all the northwestern half of the ridge and Dooley's observations showed that short-term flows of water from intermediate levels of the Norwegian Sea occurred at approximately 30-day intervals at the southeastern end of the ridge. The fate of the latter overflow is unknown; it is not apparent upon water-bottle sections taken by the Aberdeen Laboratory immediately to the south of this position during 1927–52 (Tait, 1957), and in view of its intermittent nature it will not be considered here. Overflow northwestwards from the lowest point of the ridge-crest in about 7° 45'W, however, is trapped by topography and descends into the Rockall Channel by a narrow channel between Faroe Bank and the northern end of the Ymir Ridge (Figure 1). Because of this constriction of the flow, it was apparent that long-term monitoring of the Wyville-Thomson overflow could be carried out more readily in this vicinity than in upstream or downstream areas, and a programme of current measurements and CTD sections was executed between September 1987 and November 1988.

Current Meter Observations

Two current meter mooring sites were selected with regard to detailed sounding surveys made over a decade (Ellett, 1988). Earlier work, borne out by subsequent CTD surveys of the area, showed that the core of the overflow water was centred upon the lower southern slopes of Faroe Bank, extending upwards from the gulley between the bank and the Ymir Ridge. The sites, N1 and N2, were respectively in the centre of the gully in soundings of 1115 m and upon the slope in 710 m (Figure 2), and both were deployed on 6 September 1987. From this first deployment 177 days' records were obtained from N2, but N1 failed to surface on command,

releasing itself later only to be broken up in a gale. It was suspected that the strong currents in the gully had delayed release by leaning the mooring out of the vertical, so the replacement mooring, N3, was laid in 900 m depth at the head of the gully where currents might be expected to be less. 100 days' records were obtained from each of the five current meters of this deployment. A further deployment at these two sites was unsuccessful due to fishing activity, a single meter and release being returned from N2 by a trawler a few weeks after deployment.

Results

Figure 3 shows daily mean vectors at N2 in soundings of 710 m for September 1987 to June 1988. The vectors are presented relative to the trend of the 700 m isobath at the position, 078° – 258°T, westward (258°T) flowing vectors showing above the axes, and eastwards (078°) vectors below the axes. They show strong westerly flow immediately above the bottom on all but four days of the 9 months' record, mostly easterly flow in mid-water until March, when west to southwest periods occurred, and more persistent eastward flow in the upper water column, although with two periods of westerly currents in March and May-June. The data have been smoothed in Figure 4 which shows 10-day means of the easterly components. This emphasises the anomalous mid-water westerly flow during March to June, and shows that bottom currents on the whole were somewhat less at this time than in earlier months. Figure 4 also shows that the available records from N3 in the centre of the western exit from the Ymir Trough have very similar features to N2 records from the slope of Faroe Bank, although with generally lower current speeds. A high degree of coherence is particularly apparent in the 10-day mean temperatures of Figure 5, where closely similar variations occurred at the mid-water and bottom levels of both moorings. It had been anticipated that the two principal sources of coldest overflow, the col in the Wyville-Thomson Ridge crest in 7° 35'W and the northern sector of the crest, might produce differing signals at the two mooring sites, but upon the 10-day time scale both seem equally affected by events from either source.

CTD profiles upon a north-south section through the position of mooring N2 are shown in Figure 6a-e, and show the way in which water with a Norwegian Sea Deep water (NSDW) content blankets the lower Faroe Bank slopes. Short-term variations in the mode of overflow are evident; In September 1987 and February 1988 lowest temperatures were found at the bottom of the gully running from the Ymir Trough to the Cirolana Deep, but on 10 June 1988 the lowest values were in depths of 500 m on the bank slope, with a second cold core of slightly higher temperature below at 700 m. The position of the upper core was not sampled four days later, but the lower had disappeared at this time. Cold water was at about 540 m upon the slope in early November 1988, but sampling on this cruise (upon a chartered ship) was limited to 600 m depth. This random CTD sampling shows considerable short-term variability, possibly connected with alternative routes for overflow across the Wyville-Thomson Ridge, as mentioned above, but detailed CTD surveys of the area in September 1987 and June 1988 proved insufficiently synoptic to trace these cores back to the ridge crest.

An estimate of the total mean volume of overflow

Despite this short-term variability, the good correlations of currents and temperature on the 10-day time scale make it not unreasonable to attempt estimation of the volume of NSDW entering the Rockall Channel, using the mean east-west velocities and mean temperatures at the current meters over the deployment periods. Figure 7 shows these values and the approximate profiles they suggest for the two N2 records and the single N3 deployment. Since the flow at both positions was predominantly east-west, a zero level separating the overflow and the Atlantic inflow to the Norwegian Sea above it can be estimated for N2 and extrapolated with a degree of confidence for N3. For the 100 days for which data are available for both sites the mean westward bottom currents were 37 and 27 cm/sec for N2 and N3 respectively. At both moorings the mean thickness of the westerly flow was about 250 m, and the difference in latitude, projecting both onto a common north-south section was 7.2 km. These values, since we are neglecting overflow to north and south of the moorings, give us a minimum estimate of westward transport from the Ymir Trough of 0.3 Sv for the 100-day period 2 March – 10 June 1988, and is composed of water with a temperature (from both mean profiles) below 8°C. This is much below the estimate of 1.2 Sv total westward flow made from short-term measurements during Overflow '73, and which was regarded as near-maximal by Ellett and Edwards (1978), who suggested a minimal transport of 70% of this value (i.e., 0.8 Sv) for the period 11 August – 4 September 1973. The CTD data suggest that differences of this order are unlikely to have arisen from neglected overflow to north and south of the moorings, and must reflect the random nature of short-term determinations. The September to March N2 velocity and temperature profiles of Figure 7 appear to indicate a lesser mean transport value for the autumn-winter period, but this is an unsafe assumption without data from the lower current meter position.

Estimating the NSDW content

The mean temperatures from the lower current meters indicate a relatively low content of NSDW. The June 1988 CTD data allow us to establish a mixing line between the Atlantic water at crest-depth (500–600 m) approaching the Wyville-Thomson Ridge from the southwest and water at similar depth in the Norwegian

Sea to the north of the ridge. These values are 8.25°C, 35.255 psu and –0.30°C, 34.910 psu respectively (Figure 8). Mean temperatures for the overflow were 5.4°C (bottom) to 7.8°C (zero velocity level) at N2 and 4.0° to 7.6°C at N3 (Figure 7), giving an approximate overall mean of 6.2°C. From Figure 8, this implies a NSDW admixture of 6–8% at the zero velocity level and 33–50% at the bottom, with an overall value of 25%.

Discussion

These figures emphasise the importance of entrainment and mixing in the Wyville-Thomson overflow, and show that it may often be composed of mixed water from intermediate depths north of the ridge rather than of pure NSDW. The relatively steady flow of this water suggests the possibility that it could be entrained through the agency of the deeper part of the slope current previously running along the continental margin northwest of Scotland. Whereas the upper 500–550m of the slope current can cross the Wyville-Thomson Ridge, to continue northwards along the Norwegian Sea slope, water below this depth must be diverted westwards by the Ymir Ridge. There is evidence from the UK CONSLEX (Continental Slope Experiment) of 1982–83 of northerly mean currents to depths of 900–1000m immediately to the south of the ridge (CONSLEX Group, 1984), and topography dictates a necessary diversion to the west for this.

If such entrainment could account for the steadiness of the overflow, conditions to the north of the ridge seem likely to control the type of water entrained. Density sections across the ridge from the September 1987 and June 1988 cruises are given in Figure 9, where large horizontal increases in density at 400–500 m levels north of the ridge can be seen. Regular or irregular movements such as tidal cycles, spring/neaps cycles or internal waves may allow some of this water to reach the south side of the ridge crest. A general relaxation of the predominating winter southwesterly wind forcing in spring, by allowing some of this intermediate mixed water to cross the ridge, may account for the outbreaks of westerly flow seen at this season in the mid-water current records.

A related point concerns the irregular appearance of low temperature water at relatively shallow depths upon the southern Faroe Bank slope, as at station A8 in Figure 6c. As noted earlier, short-term variability made it impossible to trace this water back to the ridge crest, though it is probable that it came from the junction of the ridge and Faroe Bank. Its shallow depth is anomalous in comparison with all the nearest Norwegian Sea stations, and Figure 10 shows that shallower cold water was found only in the middle of the entrance to the Faroe Bank Channel. In December 1988 a satellite-tracked drogue confirmed the existence of a cyclonic gyre in this area (Hansen *et al*, 1991), which connects well with the doming of the isopycnals in the sections of Figure 9. Displacement of this gyre may be the mechanism which brings shallow cold water to the northwestern ridge crest.

The discrepancies between the long-term estimate of volume transport westwards from the ridge during March-June 1988 (0.3 Sv below 8°C) and Ellett and Edwards' (1978) estimates of a near-maximal value of 1.2 Sv total and 0.33 Sv NSDW have been mentioned above. Two other short-term determinations have been made by Saunders (1990), of 0.35 Sv on 1 June 1987 and 0.3 Sv on 21 May 1988, which though of similar magnitude to the long-term value, differ completely in composition. Saunders' estimates are for water of temperature below 3°C, whereas only one 10-day period at N2 (1–10 May 1988) and two at N3 (21 April – 10 May 1988) had mean temperatures of this order (see Figure 5). Calculations from the current meter data for 1–10 May 1988, the coldest period and shortly before Saunders' second determination, give a mean total transport westwards of 0.61 Sv, of which 0.08 Sv was water of temperature less than 3°C. For 21 May an estimate of 0.44 Sv is obtained, with mean temperatures for the day at the current meters not falling below 5.95°C, and the highest of the daily estimates for the next few days, that for 24 May, is 0.60 Sv, with west-going currents extending through most of the water column on the Faroe Bank slope and daily mean temperatures not below 3.35°C. The central site of Saunders' observations is some 50 km from the current meter positions, apparently giving sufficient distance for mixing processes to smooth out the extreme characteristics of the NSDW, although continuity of the volume of water descending into the Rockall Channel, and at times an increase in volume from entrainment, seem likely from these estimates. Thus Saunders' determinations and the current meter estimates are not incompatible, but the former may represent an upper value for overflow of 3°C water across the Wyville-Thomson Ridge, whereas the March-June mean of 0.3 Sv provides a general estimate of cold, intermediate and entrained water descending into the Rockall Channel at this season.

The study demonstrates the value of an extended period of observations of this overflow. The short-term data of Ellett and Edwards (1978) and Saunders (1990) appear to have been taken at times of high NSDW overflow and, in the former case, high entrainment. Such episodes are obviously not infrequent, and other brief and more extreme Wyville-Thomson overflow events are suggested by data from the JASIN surveys (Zenk, 1980) and especially by the dense water encountered upon one of four repeated sections across Rosemary Bank in 1965 by Elder (1970), but comparison with the relatively long-term mean currents presented here puts these into context.

Conclusions

1) Current measurements made about 50 km west of the Wyville-Thomson Ridge for 9 months at one site and 3 months at a second show a relatively steady westward flow at the lowest levels, a general eastward flow interrupted and sometimes reversed in spring in mid-water, and a variable easterly flow at the upper level.

2) For the 100 days in March-June 1988 when data for two moorings are available the westward flow descending into Rockall Channel was estimated to have a minimum mean value of 0.3 Sv, with a 25% content of NSDW.

3) Although dense water may cross the ridge at a number of points, currents upon the south slope of Faroe Bank and those in the westward-leading trough are coherent upon a 10-day time scale.

4) The relatively steady bottom overflow of variable characteristics possibly arises from entrainment by the lower part of the continental slope current northwest of Scotland, which is prevented by topography from entering the Norwegian Sea and must be diverted westwards. If this is so, the slope current west of Britain may have the same role in assisting this easternmost overflow of sub-thermocline water as is postulated in the case of the deeper Faroes – Greenland overflows by McCartney (1992) for a deep northerly flow in the eastern North Atlantic.

5) The movements in relation to wind forcing of a cyclonic gyre at the southern entrance to the Faroe Bank Channel to the northeast of the ridge may be an important factor upon the seasonal and short-term variability and the composition of the overflow.

Acknowledgements

This work was funded jointly by the UK Natural Environment Research Council and the Ministry of Defence. The contributions of Dr. J. M. Graham, C. R. Griffiths, N. McDougall and colleagues are gratefully acknowledged.

References

CONSLEX Group 1984. The UK Continental Slope Experiment: IOS and SMBA current meter data. IOS Internal Doc., (217), 239pp.

Dickson, R. R., Gould, W. J., Griffiths, C., Medler, K. J., and Gmitrowicz, E. M. 1986. Seasonality in currents of the Rockall Channel. Proceedings of the Royal Society of Edinburgh, 88B: 103–125.

Elder, R. B. 1970. Oceanographic observations between Iceland and Scotland, July-November 1965. US Coast Guard oceanogr. Rept, (28), 118pp.

Ellett, D. J. 1988. Bottom topography to the west of the Wyville-Thomson Ridge. Deutsche Hydrografische Zeitschrift, 41: 23–33.

Ellett, D. J., and Edwards, A. 1978. A volume transport estimate for Norwegian Sea overflow across the Wyville-Thomson Ridge. ICES CM 1978/C:19, 12pp.

Ellett, D. J., and Roberts, D. G. 1973. The overflow of Norwegian Sea Deep water across the Wyville-Thomson Ridge. Deep-Sea Research, 20: 819–835.

Hansen, B., Meldrum, D. T., and Ellett, D. J. 1991. Satellite-tracked drogue paths over Faroe Bank and the Faroe-Iceland Ridge. ICES CM 1991/C:25.

McCartney, M. S. 1992. Recirculating components to the deep boundary current of the northern North Atlantic. Progress in Oceanography, 29: 283–383.

Saunders, P. M. 1990. Cold outflow from the Faroe Bank Channel. Journal of Physical Oceanography, 20: 29–43.

Tait, J. B. 1957. Hydrography of the Faroe-Shetland Channel, 1927–1952. Marine Research, 1957 (2), 309 pp.

Zenk, W. 1980. Advected near-bottom temperature structures at the FIA? JASIN News, 17: 8–9.

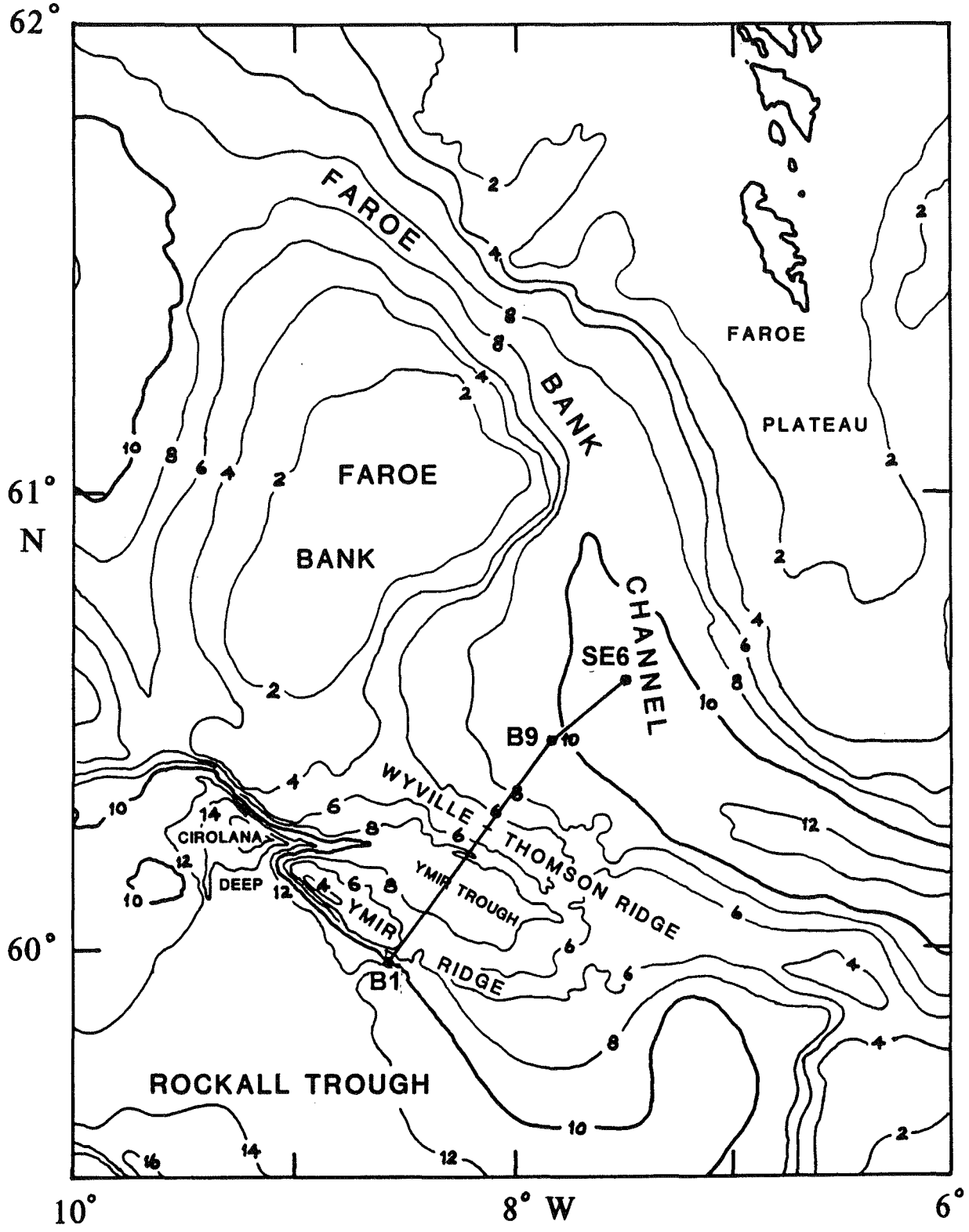

Figure 1. General topography of the area. Isobaths in hectometers.

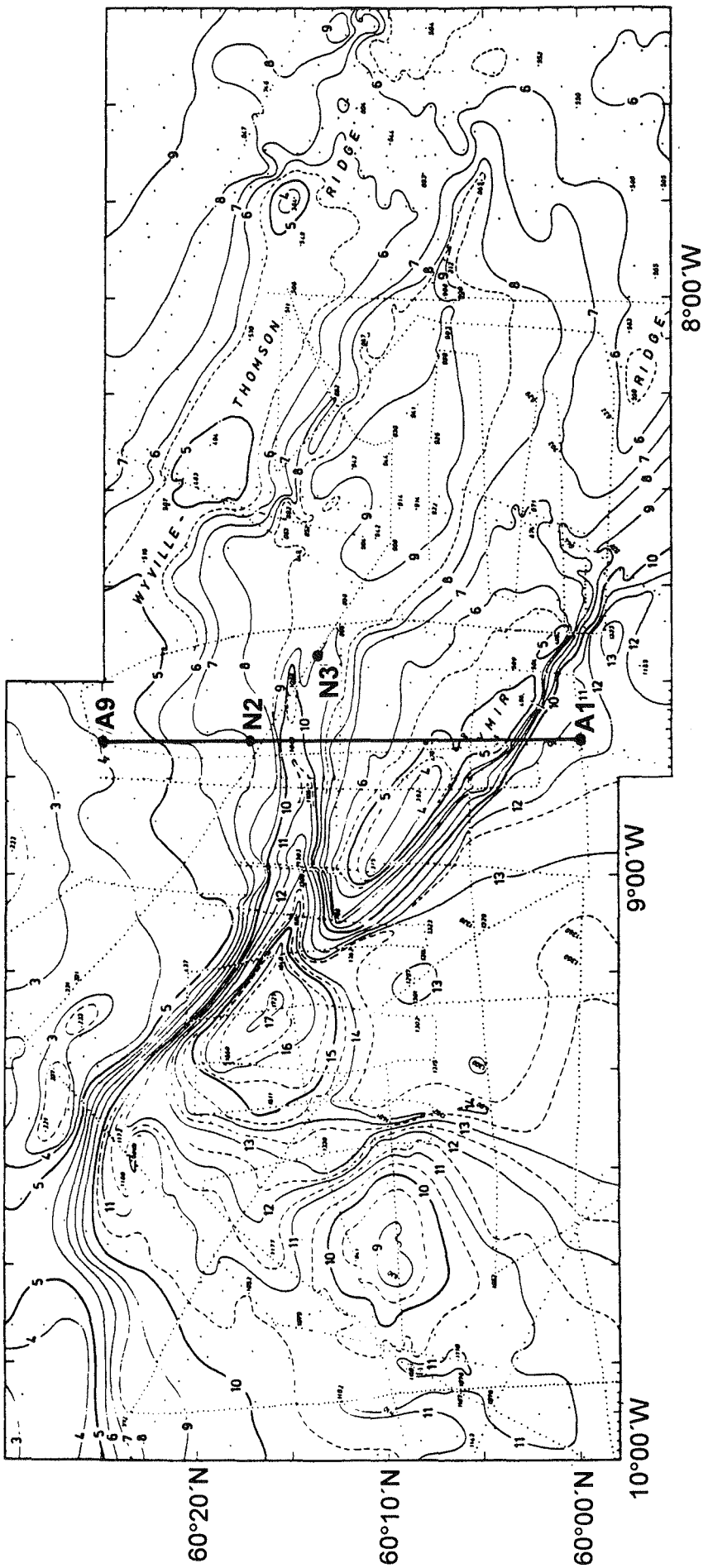

Figure 2. Current meter mooring positions and bottom topography (Ellett,1988) to the west of the Wyville-Thomson Ridge. Isobaths labelled in hectometers.

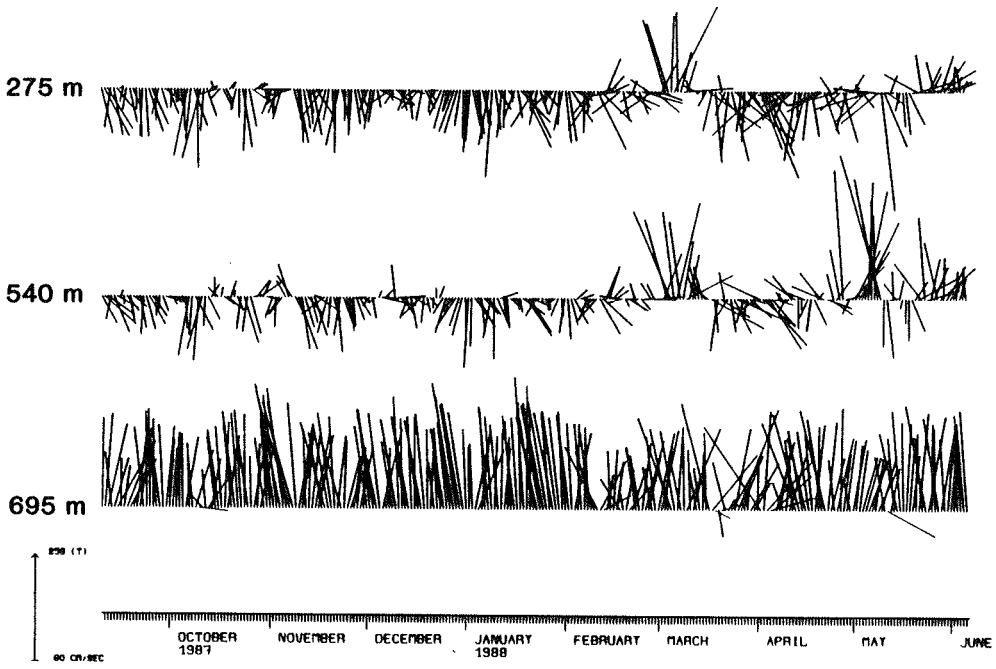

Figure 3. Daily current vectors at mooring N2, September 1987 - June 1988, relative to the trend of the 700m isobath. (The arrow, bottom left, points towards 258°T and represents 60 cm sec^{-1}).

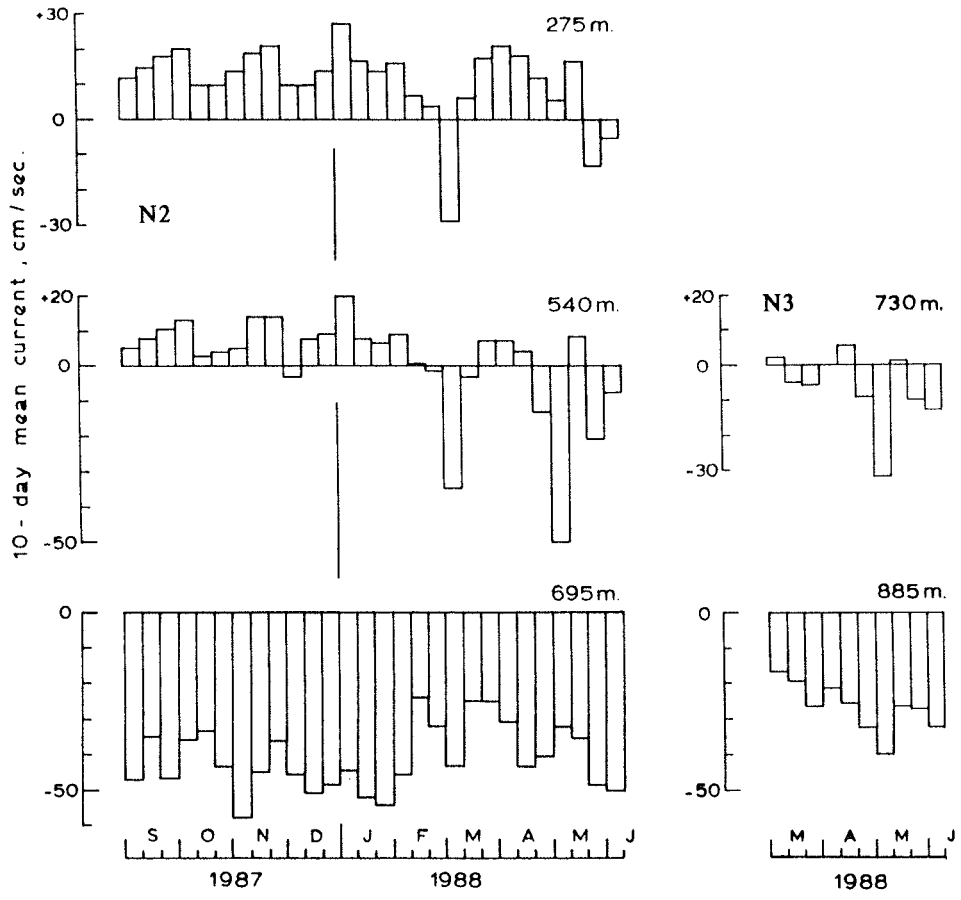

Figure 4. 10-day mean easterly (090 °T) current components at N2 and N3. (Easterly components positive, and westerly negative).

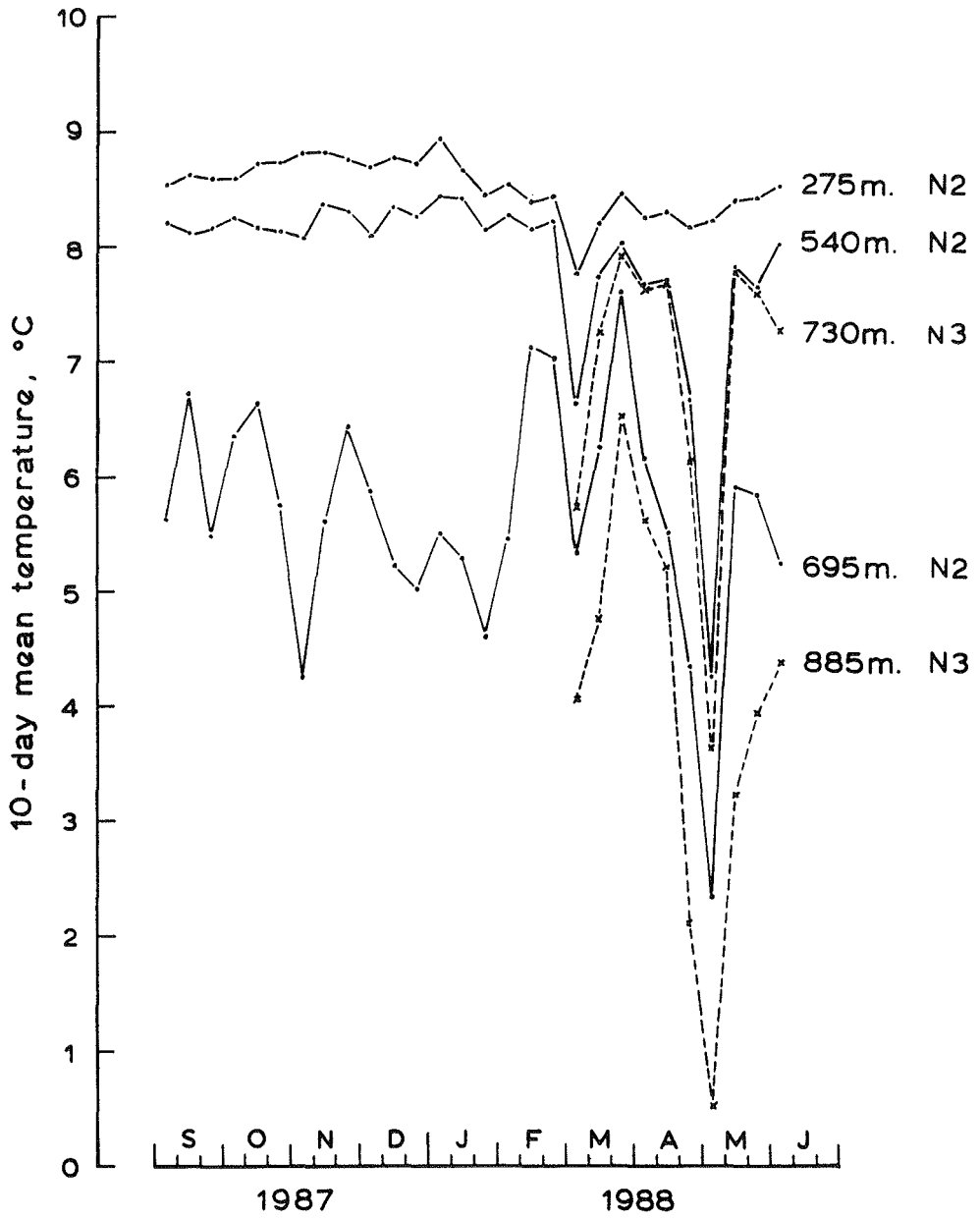

Figure 5. 10-day mean temperatures at the current meters.

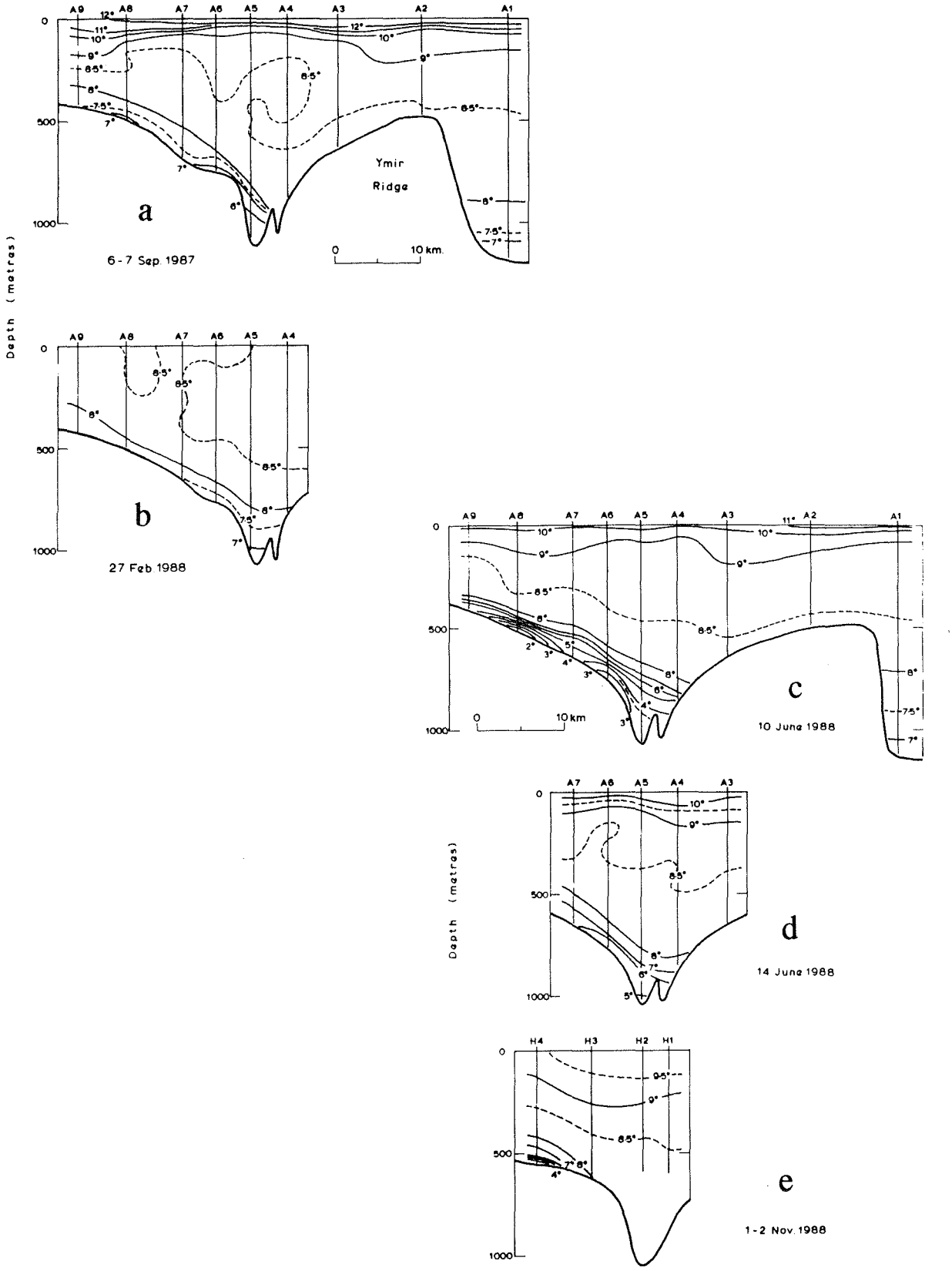

Figure 6a-e. Temperature sections across the channel between the Faroe Bank slope and the Ymir Ridge. Position of section A1 - A9 is shown on Figure 2. The stations H1 - H4 on Figure 6e are on the same longitudinal line, but have slightly different latitudes.

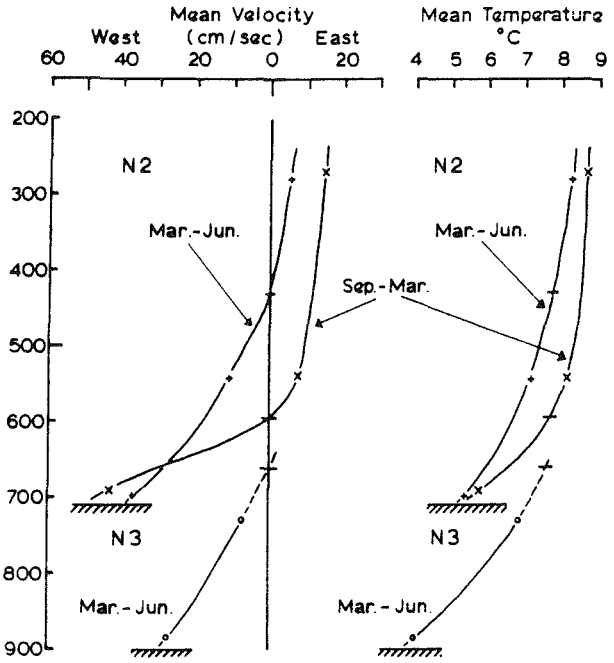

Figure 7. Mean E-W velocity components and temperatures from the current meter deployments.

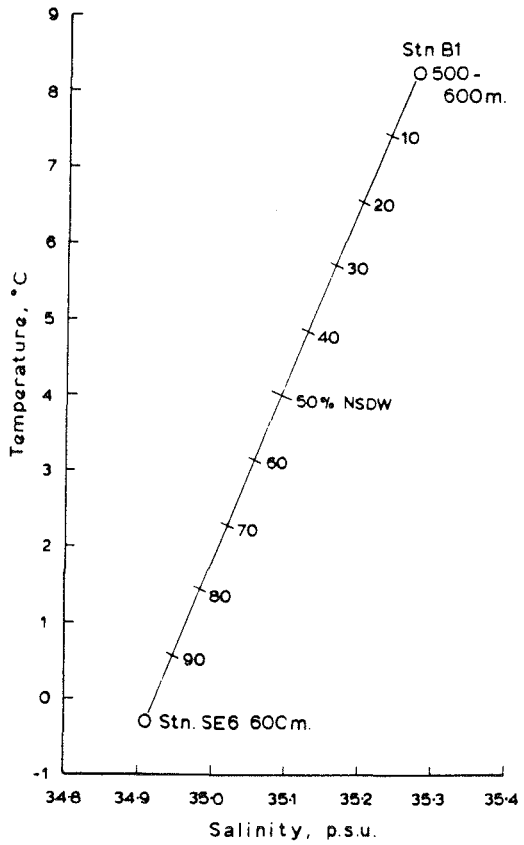

Figure 8. Temperature - salinity mixing diagram for the overflow, June 1988.

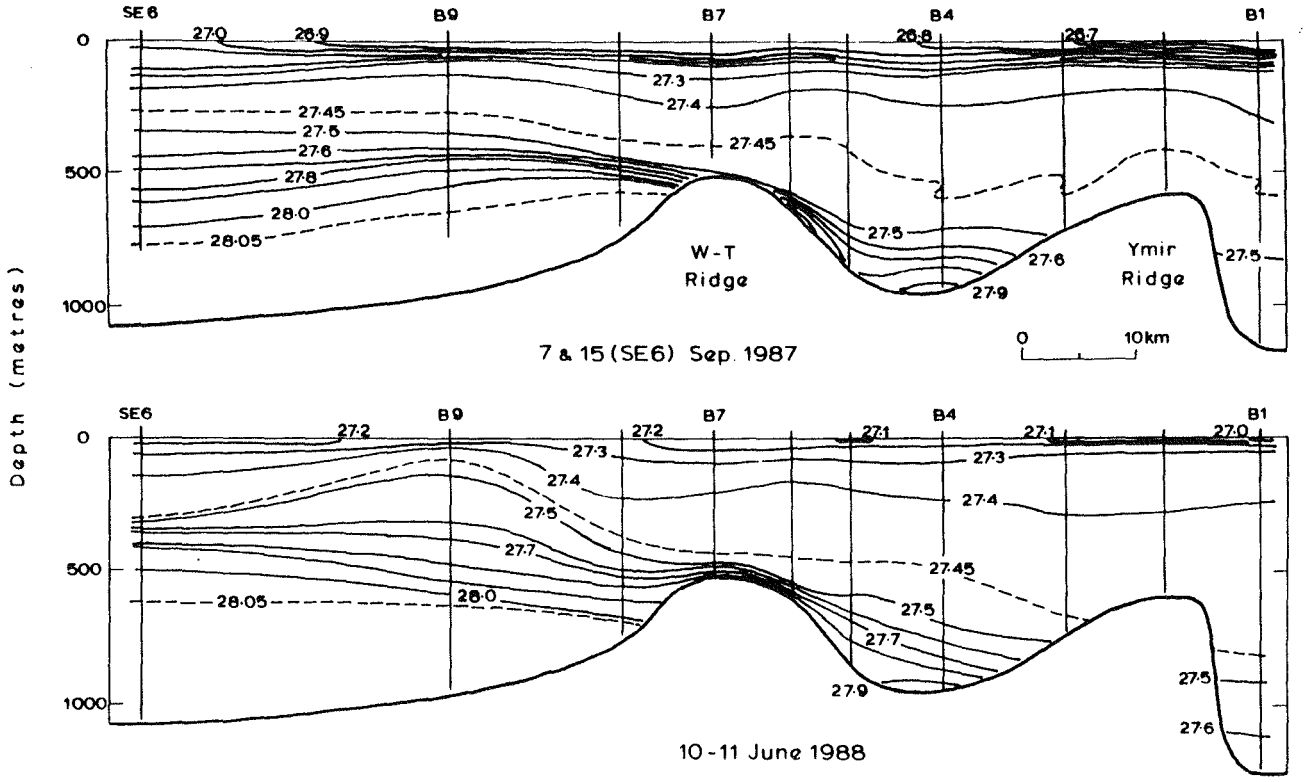

Figure 9. Density (σ_t) sections northeast-southwest across the ridges. Position of section shown on Figure 1.

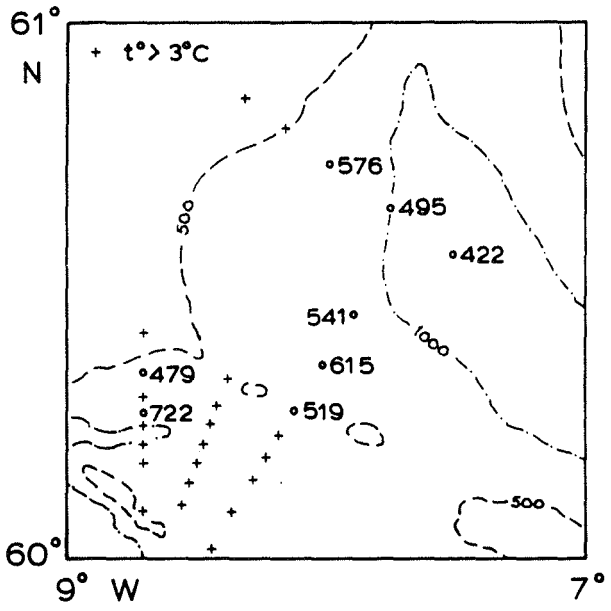

Figure 10. Depth (m) of the 3°C surface, 10–14 June 1988. (+ indicates stati8ons with no water below 3°C).

Subarctic Intermediate Water in the eastern North Atlantic

J. F. Read and D. J. Ellett

[1]Southampton Oceanography Centre, Empress Dock, Southampton, SO14 3ZH, UK. [2]Dunstaffnage Marine Laboratory, Oban, Argyll, UK.

Based on a paper presented to the ICES Hydrography Committee as ICES CM1991/C:42

Data from the eastern North Atlantic collected in 1989 were examined to identify the upper and intermediate water masses. Subarctic Intermediate Water (SAIW) and Mediterranean Water (MEDW) lay between a surface layer, 400–600 m thick of North Atlantic Central Water and a deep layer, below 1800 m, of Labrador Sea Water. The θ/S characteristics of the layer between 600–1800 m varied. To separate the influences of SAIW and MEDW a standard θ/S curve was defined from which a salinity anomaly could be calculated. Vertically contoured sections of the salinity anomaly showed MEDW centred at about 1000 m in the southern part of the region to 48°N. SAIW occurred at shallower depths, centred upon 600 m, and was concentrated between 49–54°N at 20°W. Calculations of geostrophic flow showed the strongest movement of SAIW to be at about 52°N, around the southern edge of the Rockall Bank. Part of this flow recirculated to the north and west and part was recirculated around the entrance to the Rockall Channel.

Keywords: North Atlantic, Subarctic Intermediate water, Rockall Channel

Introduction

The eastern North Atlantic, away from the major oceanic gyres, is a relative backwater, where the general circulation remains poorly defined. During 1989 several cruises surveyed the region in the vicinity of the 20°W meridian. In an attempt to clarify a small part of the picture we examine the hydrographic data with particular reference to the upper and intermediate waters.

Data

Hydrographic data were collected on four different cruises and combined to form four sections (Figure 1). Two sections along 20°W (section 1) and across the southern entrance to the Rockall Channel (section 3) were worked during late winter on RRS Discovery cruises 180 (Ellett *et al.*, 1989) and 181 (Pollard *et al.*, 1989; Read *et al.*, 1991). The data were collected between 1 – 3 February on cruise 180 and 13 – 22 April on cruise 181.

Two other sections were worked during summer along approximately 20°W (section 2) and approximately 58°N (section 4) on RRS Discovery cruise 184 between 22 July – 10 August (McCave *et al.*, 1989), and on the Lough Foyle DML cruise 2/89 between 5 – 6 August .

Vertically contoured sections of temperature (Figure 2) show the difference between summer (Figures 2b and 2d) and winter (Figures 2a and 2c) in the seasonal thermocline as opposed to the winter mixed layer.

Water masses

A θ/S scatter plot of the data from the four cruises shows the water masses of the area (Figure 3). They have been described by various authors and we can summarise their characteristics briefly.

North Atlantic Central Water (NACW) formed a surface layer 400–600 m deep and capped by the seasonal thermocline during summer (Figures 2b and 2d). We define NACW after Harvey (1982) as centred along a line between 10°C, 35.40 – 12°C, 35.65, but we extend the line to 9.5°C, 35.30 – 14.0°C, 35.875.

Subarctic Intermediate Water (SAIW) is formed as a winter mode water in the Labrador Basin of the western North Atlantic (Bubnov, 1968; Arhan, 1990). Core characteristics fall between $35.45 \leq S + 0.16 * \theta \leq 35.82$ and $27.3 \leq \sigma_\theta \leq 27.65$ (or $27.3 \leq \sigma_\theta$, $\sigma_1 \leq 32.25$) (Harvey and Arhan, 1988). However in our data set SAIW appears only as a much modified and mixed fresh end point below NACW.

Mediterranean Water (MEDW) also has characteristics originating from outside the eastern North Atlantic. It spreads northwards from the Straits of Gibraltar and is modified as it does so, mixing with NACW (above) and Labrador Sea Water (below), hence gradually becoming

cooler and fresher along a θ/S curve defined by Wüst (1935) as the Atlantic Intermediate Salinity Maximum line (ISM). MEDW tends to be restricted to the south of the region although it is carried northwards in the eastern slope current, and Reid (1979) suggests that it can be traced into the Norwegian and Greenland Seas.

Labrador Sea Water (LSW) forms a deep fresh layer centred upon about 1800 – 2000 m in the eastern basin. Like SAIW it is formed in the Labrador Basin, where Talley and McCartney (1982) define it as having a potential temperature and salinity of 3.3 – 3.4°C, 34.84 – 34.89. In the eastern North Atlantic it is slightly modified and for our data set we define it as having θ = 3.5°C, salinity = 34.90.

Below LSW are two deep waters. North Atlantic Deep Water (NADW) forms a widespread homogeneous mass throughout the Northeast Atlantic and is defined by Saunders (1986) as lying on the curve S = 34.698 + 0.098 θ. Iceland - Scotland Overflow water (ISOW) from the Norwegian Sea was seen at six stations in the Iceland Basin with a potential temperature and salinity of 2.4°C, 34.97.

SAIW and MEDW are both found below NACW and above LSW. MEDW tends to be restricted to the south, except in the eastern slope current and SAIW is found to the north. There appears to be interaction and interleaving between them and Harvey (1982) described a mixed water mass of intermediate salinity between MEDW and SAIW which he called Eastern North Atlantic Water (ENAW). To distinguish between the influence of MEDW and SAIW the procedure of Harvey (1982) was adopted. A standard θ/S curve was defined (Figure 3) from which a salinity anomaly could be calculated. The line chosen, defined by the points

14.0°C, 35.875; 9.5°C, 35.3 and 3.5°C, 34.90

followed the core of NACW and from NACW to LSW. The end point of NACW (9.5°C, 35.3) was chosen arbitrarily to suit this data set, given the restricted geographical region from which it was taken. Surveys from other areas of the Northeast Atlantic would probably show a different end point.

Water within ±0.05 of the standard θ/S curve is taken to be ENAW, while water with a negative anomaly less than –0.05 is of SAIW origin, and that with a positive anomaly greater than +0.05 indicates the influence of MEDW. The results are contoured in Figure 4.

Results

The work of Harvey (1982) showed the longitude of 20°W to be an area of change between MEDW and SAIW. His Figure 6 showed little, or no, SAIW at 46 – 48°N, 20°W and a considerable quantity of MEDW. Further north in Harvey's (1982) section along 53°N the influence of MEDW is restricted to the continental slope and SAIW, subducting from the west, extends across 20°W to about 18°W. Ellett and Martin (1973) have drawn attention to the fact that the closest approach of the Oceanic Polar Front to the European shelf occurs in 52° – 53°N, and Figure 2a, section 1 shows a frontal feature between these latitudes at 20°W. A satellite-tracked drogue launched here moved east-northeastwards at 30 cm s^{-1} during its first week (Pollard *et al.*, 1989), and it was in this vicinity that the lowest surface salinities (<35.2) were found on the previous cruise 180 in January.

Sections of the salinity anomaly down 20°W show MEDW centred at about 1000 dbar depth reaching as far as 48°N, while SAIW was found north of 49°N centred upon approximately 600 dbar depth. Section 2 showed the greatest amount of SAIW but was up to 200 km west of 20°W (Figure 1), whereas section 1 was closer to the 20°W meridian and here the core of SAIW was smaller and more broken. Section 1 ended at the tip of the Rockall Plateau and there was no SAIW at this point, presumably because of the current flowing westwards out of the Rockall Channel. Section 2 showed the main core of SAIW lying between 49 – 54°N and spreading as far as 57°N. Section 4 at 58°N showed no concentrated core of SAIW although the salinity anomaly still suggested that it was present. In contrast the section across the Anton Dohrn Seamount showed no sign of SAIW and appeared to be influenced by MEDW. Ellett, Edwards and Bowers (1986) found that evidence of SAIW tended to be removed by deep winter mixing and by enhanced mixing at the southern entrance of the Rockall Channel. Section 3 across the entrance to the Rockall Channel showed SAIW centred at about 400 dbar at 20°W and 600 dbar on the eastern side of the Channel, but with a core of MEDW in the slope current against Porcupine Bank.

Calculations of geostrophic velocity were made using a reference level of 3500 dbar or the deepest common level between pairs of stations. Contoured sections of geostrophic velocity (Figure 5) show the main core of SAIW on section 2 to lie in a region of weak eastward flow. The flow in section 1 was stronger but only two of the three cores of SAIW were moving eastwards. In section 3 geostrophic flow was northwards at the western end but southwards across the eastern side of the Rockall Channel, except for the slope current. This agrees with Ellett, Edwards and Bowers (1986) that there is northerly flow on the west side of the Rockall Channel and southerly flow on the east side.

Geostrophic velocities at 620 dbar relative to 3500 dbar or the deepest common level were extracted and plotted (Figure 6) together with the main cores of SAIW to show the pattern of circulation. (The geostrophic velocity at 420 dbar and shallower was almost identical

in pattern to that at 620 dbar but of order 0 – 5 cm s^{-1} stronger). It is seen that SAIW lay between 49° and 53°N flowing from the west and circulating around the entrance to the Rockall Channel. Between 53 – 57°N on section 2, geostrophic flow was weak but there was some movement westwards implying the recirculation of SAIW. This pattern, of water dividing around the southern tip of the Rockall Plateau, appears to confirm an inference from subsurface weather station data of a general northwesterly divergence of warmer water between 52°N and 59°N along 20°W (Ellett, 1968).

In summary it appears that the SAIW reaching the eastern boundary of the North Atlantic Ocean crosses 20°W at about 52°N, around the southern edge of the Rockall Bank. Some part of this inflow appears to re-circulate northwards and to the west while the main part appears to be circulated around the entrance to the Rockall Channel.

Acknowledgements

We would like to thank the Principal Scientists of the cruises: Professor Nick McCave, Mr David Meldrum, and Dr Raymond Pollard for making their data available for this study.

References

Arhan, M. 1990. The North Atlantic Current and Subarctic Intermediate Water, Journal of Marine Research, 48: 109–144.

Bubnov, V. A. 1968. Intermediate Subarctic Waters in the Northern Part of the Atlantic Ocean, Okeanologicheskiye Issledovaniya, 19: 136–153.

Ellett, D. J. 1968, Subsurface temperature and salinity conditions at Ocean Weather Stations, ICES, CM1968 / C:22, 16 pp.

Ellett, D. J., and Martin, J. H. A. 1973. The physical and chemical oceanography of the Rockall Channel, Deep-Sea Research, 20: 585–625.

Ellett, D. J. *et al.*, 1989. RRS Discovery Cruise 180 20 January – 4 February, SMBA Report, 4 pp.

Ellett, D., Edwards, A., and Bowers, R. 1986. The hydrography of the Rockall Channel, Proceedings of the Royal Society of Edinburgh, 88B: 61–81.

Harvey, J. 1982. θ - S relationships and watermasses in the eastern north Atlantic, Deep-Sea Research, 29 (8A): 1021–1033.

Harvey, J. and Arhan, M. 1988. Watermasses of the central North Atlantic in 1983–84, Journal of Physical Oceanography, 18 (12): 1855–1875.

McCave, I. N. *et al.*, 1989. RRS Discovery cruise 184 14 July – 14 August 1989. BOFS 1989 Leg 3. Benthic studies of the Biogeochemical Ocean Flux Study between 47°N and 60°N along 20°W in the northeast Atlantic Ocean, University of Cambridge, Department of Earth Sciences, 55 pp.

Pollard, R.T. *et al.*, 1989. RRS Discovery cruise 181 1 April – 3 May 1989. Circulation and structure of the Bay of Biscay and Northeast Atlantic out to 20°W and 41°N, IOSDL Cruise Report No 210, 51 pp.

Read, J. F., Pollard, R. T., and Hirst, C. 1991. 'CTD data from the north east Atlantic Ocean in April 1989 collected on RRS Discovery cruise 181' IOSDL Report No 285, 157 pp.

Reid, J. L. 1979. On the contribution of Mediterranean Sea outflow to the Norwegian-Greenland Sea, Deep-Sea Research, 26: 1199–1223.

Saunders, P. M. 1986. The Accuracy of Measurement of Salinity, Oxygen and Temperature in the Deep Ocean, Journal of Physical Oceanography, 16 (1): 189–195.

Talley, L. D., and McCartney, M. S. 1982. Distribution and Circulation of Labrador Sea Water, Journal of Physical Oceanography, 12: 1189–1205.

Wûst, G., 1935. 'The stratosphere of the Atlantic Ocean. Scientific results of the German Atlantic Expedition 'Meteor' 1925–27' vol 6, section, 1. English translation W. J. Emery (ed).

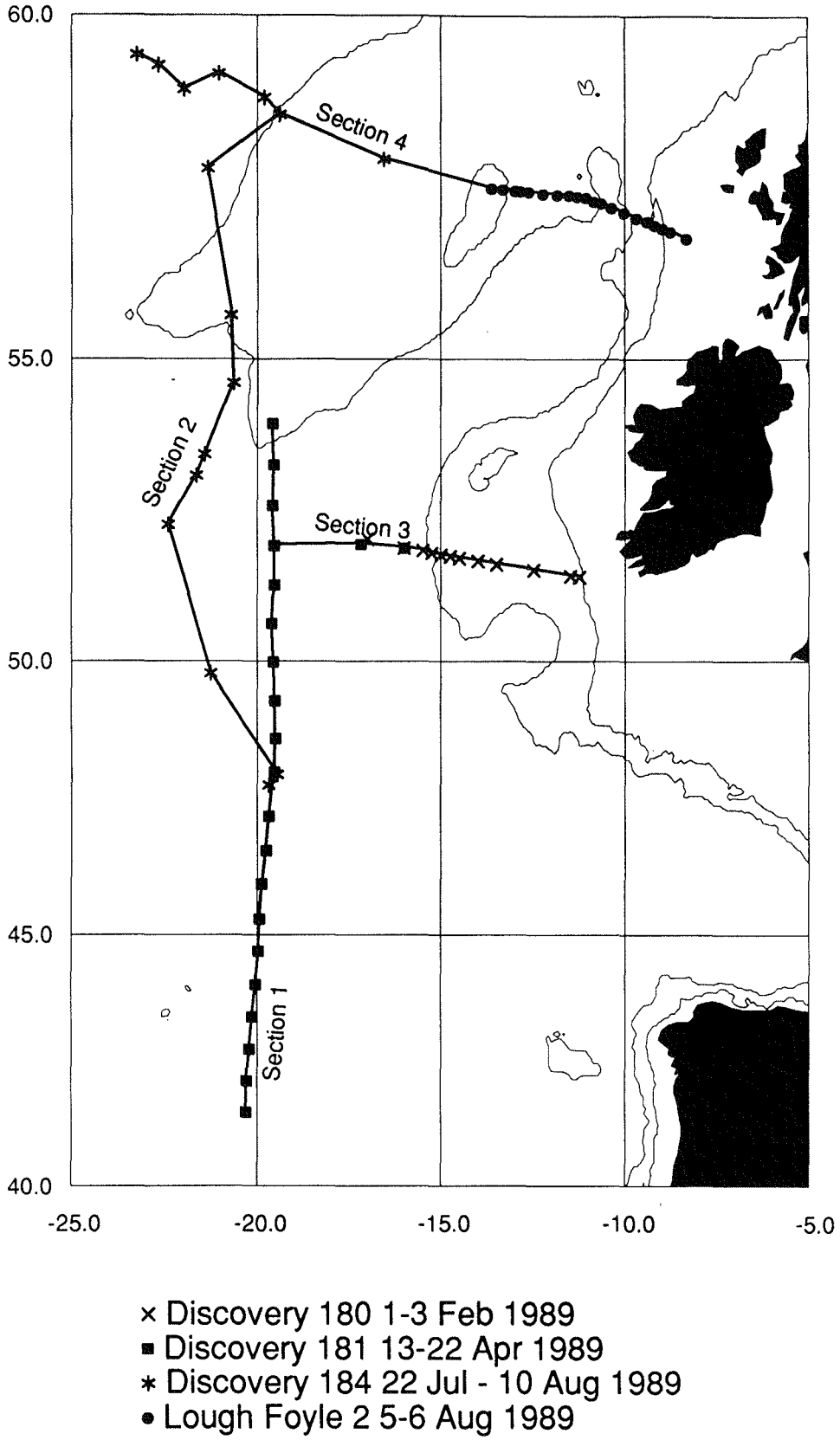

Figure 1. Location of the CTD stations worked on four cruises during 1989. The 200m and 2000m isobaths are shown.

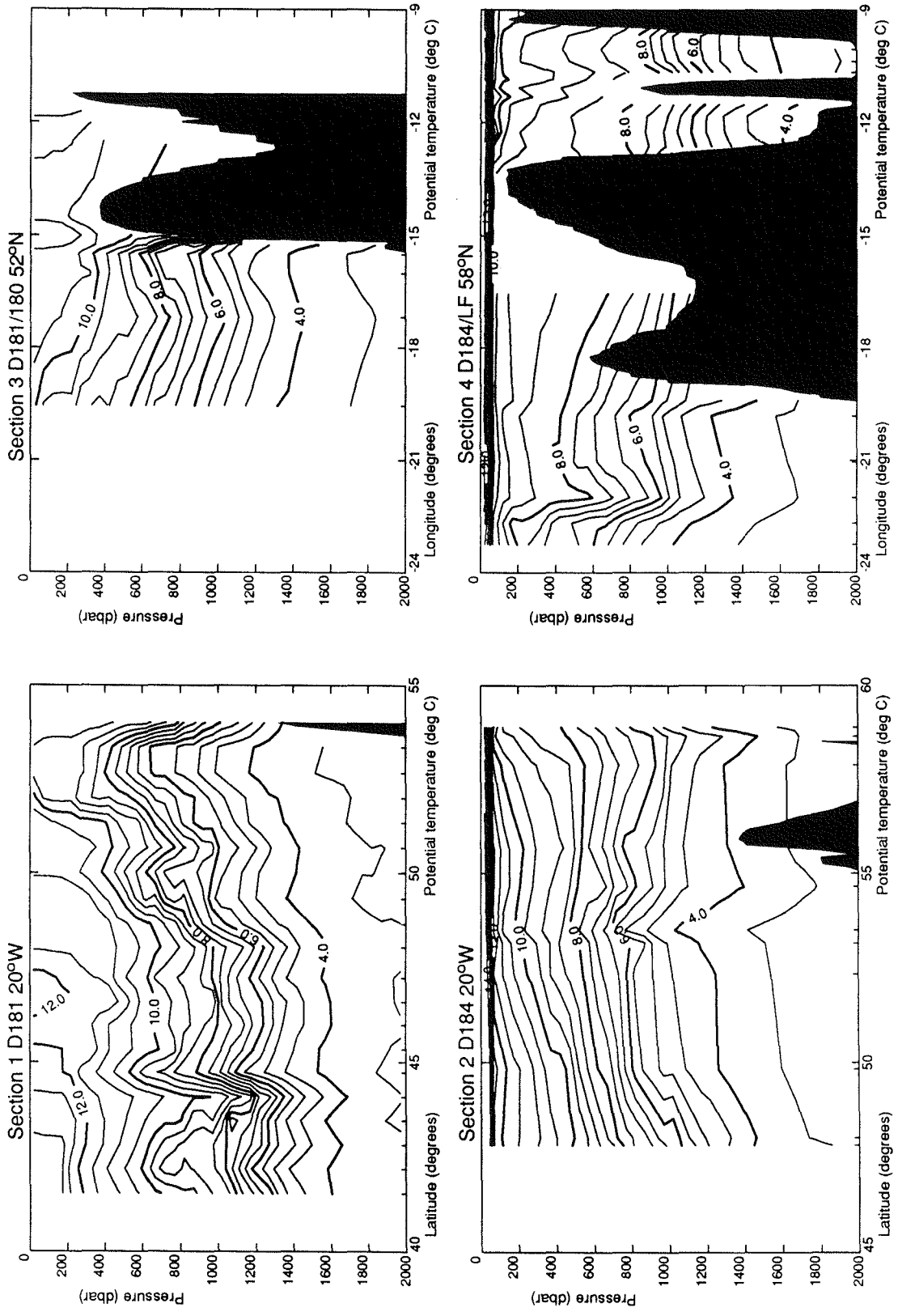

Figure 2. Potential temperature on the four sections shown in Figure 1.

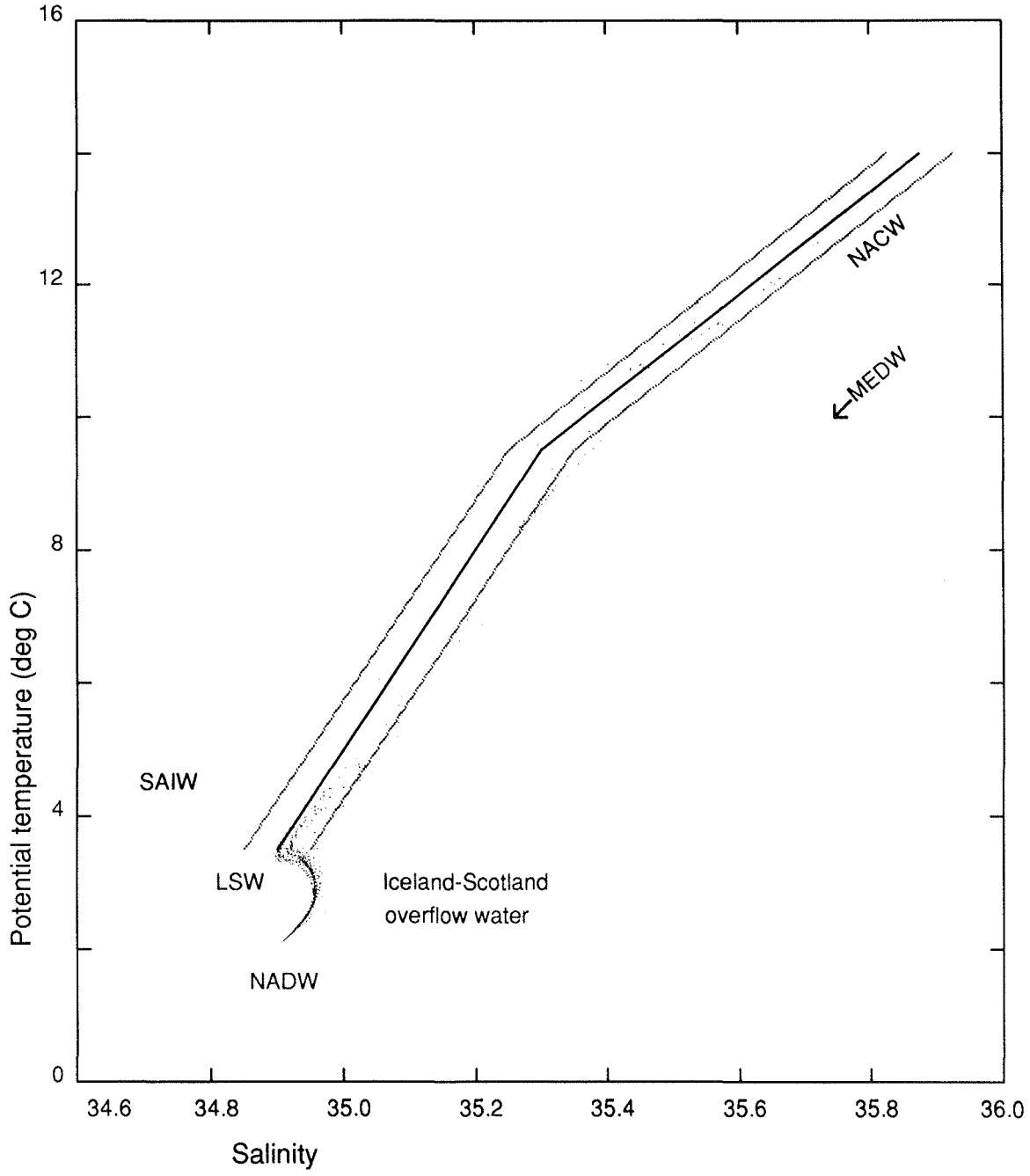

Figure 3. Potential temperature/salinity data at 50m intervals from all four sections. North Atlantic Central Water (NACW) lies in the upper layers, beneath which are Subarctic Intermediate Water (SAIW) and Mediterranean Water (MEDW). Below 4°C are Labrador Sea Water (LSW), Iceland-Scotland Overflow Water and North Atlantic Deep Water. The standard θ/S line is shown with the ±0.05 limits for eastern North Atlantic Water.

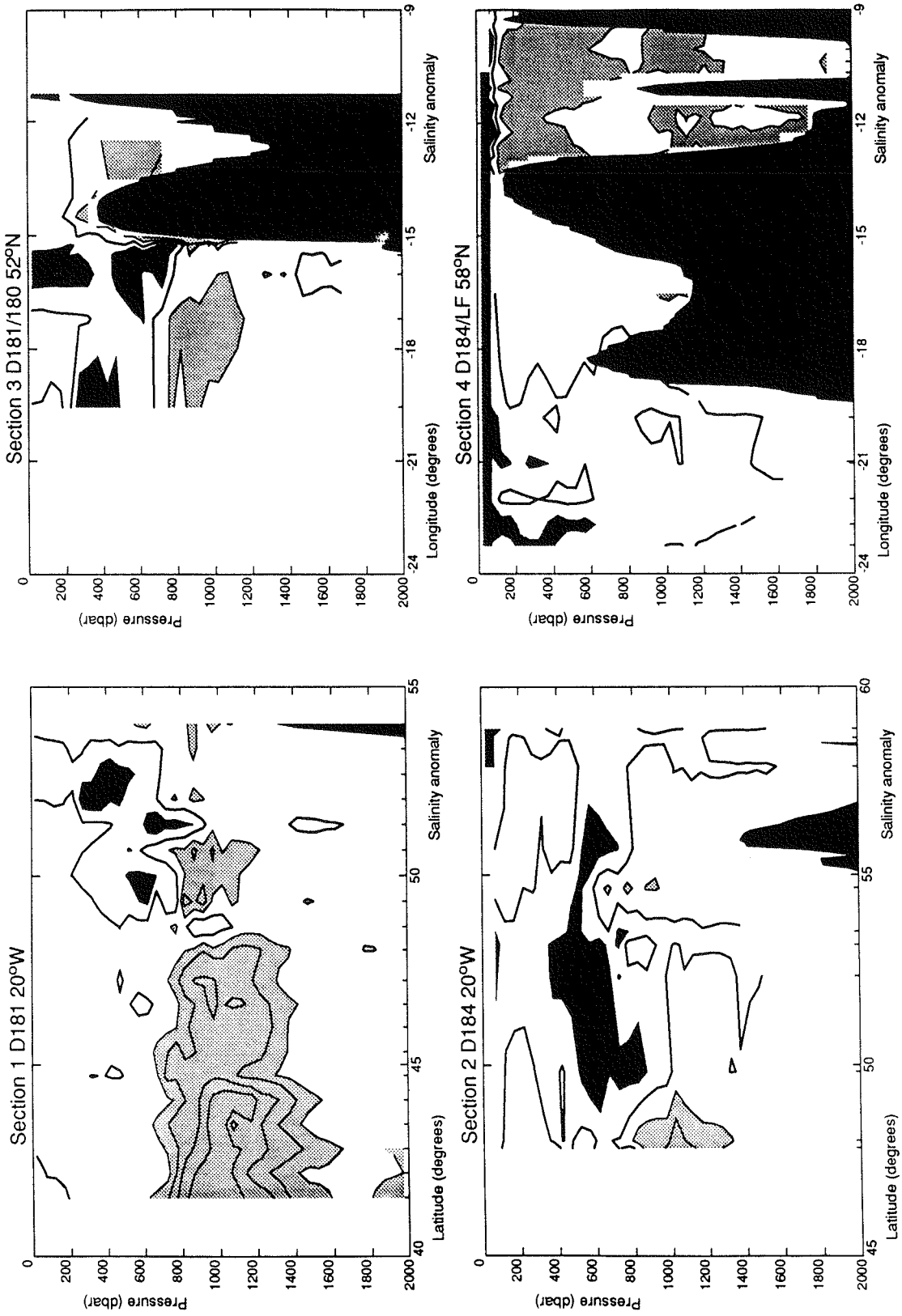

Figure 4. Salinity anomaly for the four sections shown in Figure 1. A positive anomaly, indicating Mediterranean Water, is shown by light grey shading while dark grey shading represents a negative anomaly indicating Subarctic Intermediate Water. The bold line represents a zero anomaly indicating eastern North Atlantic Water.

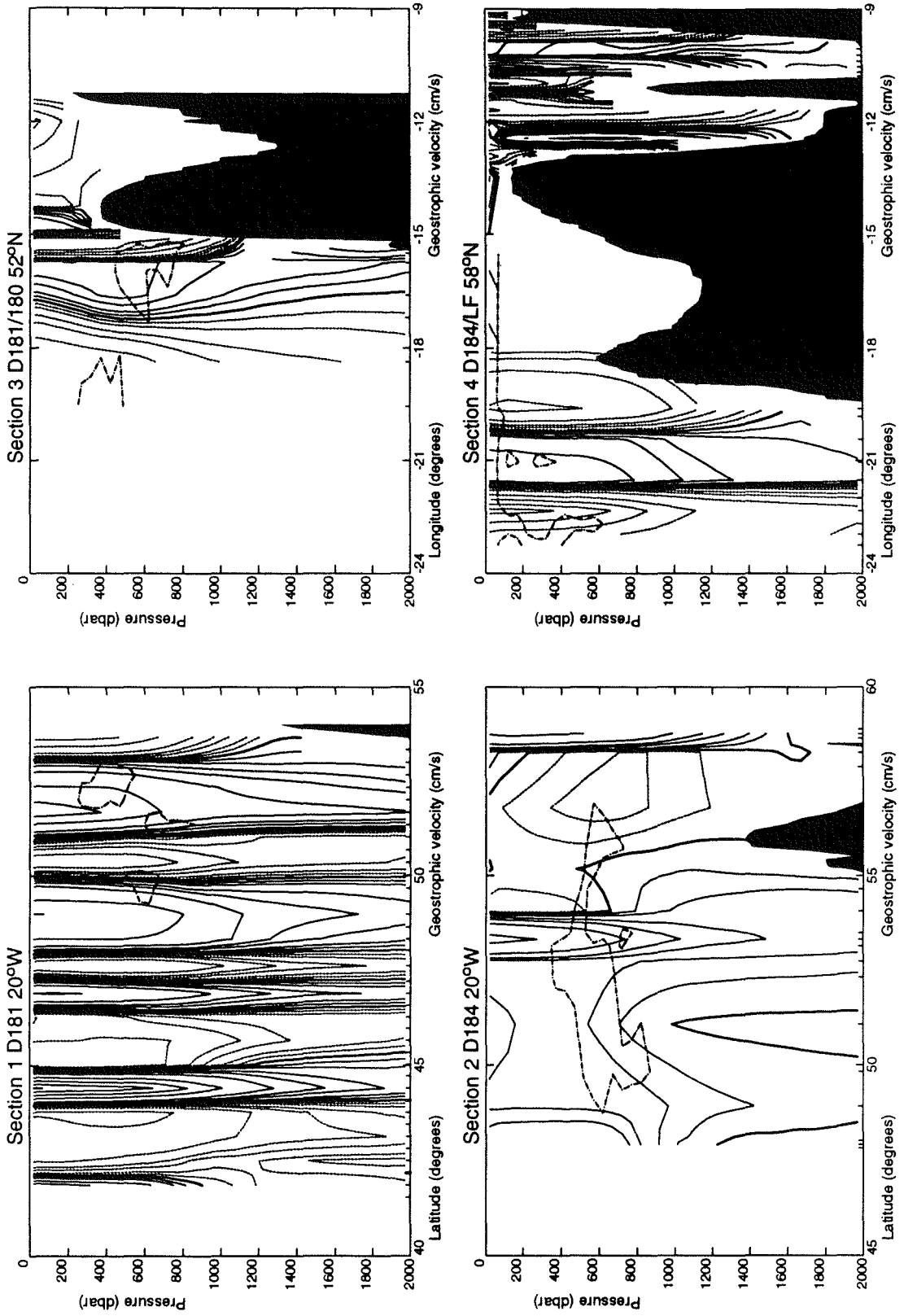

Figure 5. Geostrophic velocity calculated with a zero reference level of 3500 db or the deepest common level between pairs of stations. North or westwards flow is shown by a dashed line, south or eastwards flow is shown by a thin solid line. The bold solid line indicates zero flow. Cores of Subarctic Intermediate Water, as represented by the salinity anomaly from Figure 4, are outlined by a bold dash/dot line.

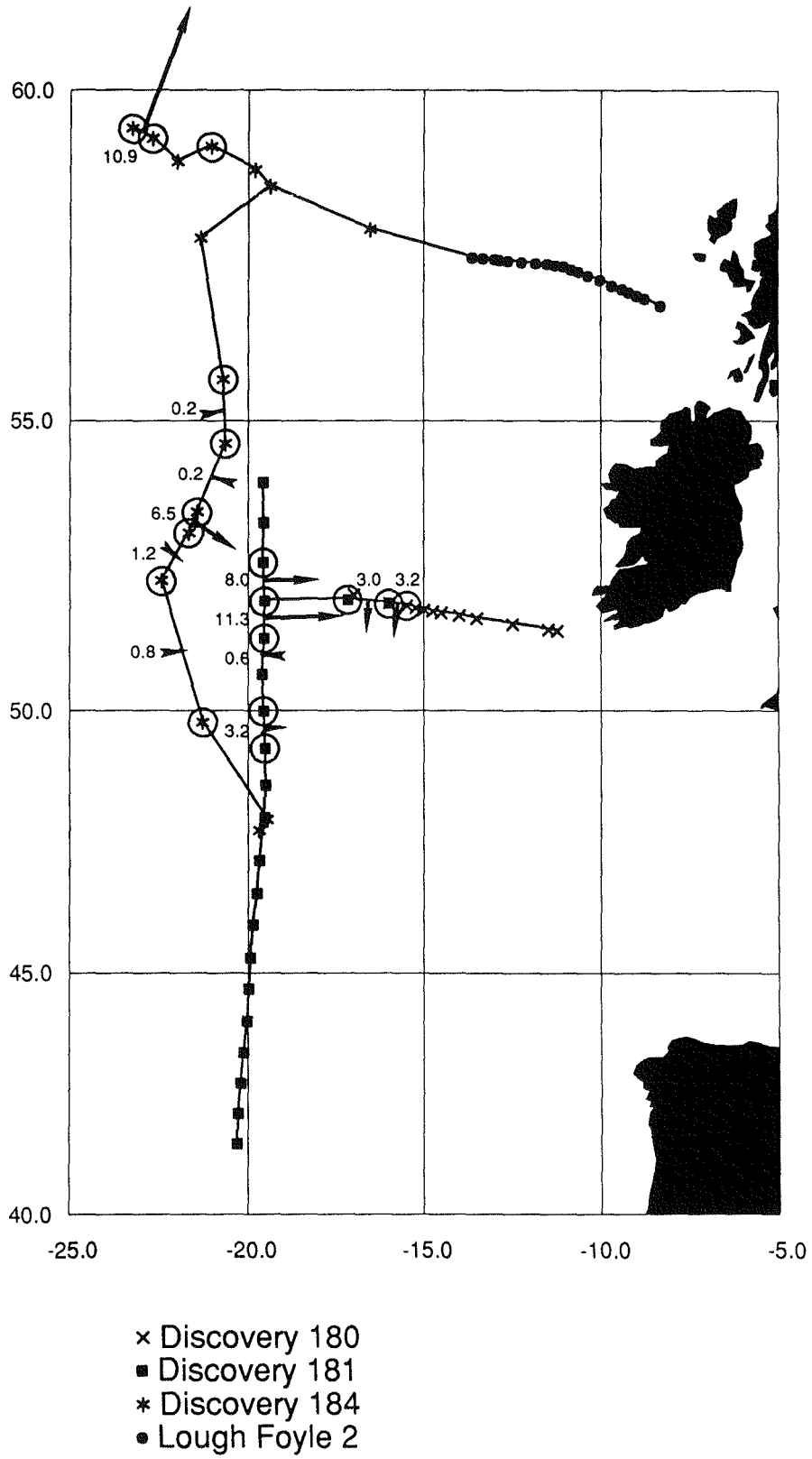

Figure 6. Geostrophic velocity (cm s^{-1}) from 620m. The arrows show the direction of flow and circles around the station symbol indicate the presence of Subarctic Intermediate Water.

Current measurements in the Iceland Basin

Hendrik M. van Aken

Netherlands Institute for Sea Research P.O. Box 59, 1790AB Den Burg/Texel, the Netherlands.

Based on a paper presented to the ICES Hydrography Committee as ICES CM 1993/C:11

Long term (6 months) current measurements from 5 moorings in the Iceland Basin have been analysed for the mean circulation and the structure of the variable current components. The flow at all 5 moorings had a strong baroclinic character. The mean circulation in the Sub-Polar Mode Water appears to have a general north-eastward direction with maximum mean velocities of 6–7 cm s^{-1}. Over the Icelandic slope mean velocities of the order of 10–20 cm s^{-1} have been observed where the Iceland-Scotland Overflow water flows westward along the topography. Near the bottom of the slope of the Hatton Bank water entered the Iceland Basin in a branch of the Deep Northern Boundary Current which has a cyclonic rotation sense in the Iceland Basin. The variable part of the current was analysed by means of principal component analysis. The current variations over the Icelandic slope appear to have a mainly barotropic character while variations in the baroclinic flow of Iceland-Scotland Overflow Water contribute 10% or less to the total energy of the variable deep flow. Over the slopes of the Hatton Bank and the Reykjanes Ridge the variable currents had a clear baroclinic character with shear in both speed and direction.

Keywords: Iceland Basin, Current measurements, Overflow

Introduction

The Iceland Basin is a choking point for the global thermohaline circulation. Through this basin Sub-Polar Mode Water (SPMW) from the North Atlantic Current with high temperature and salinity flows to the Faroese waters where it enters the Norwegian Sea, while cold waters, formed in the Nordic seas enter the Iceland Basin through the Faroe Bank Channel and across the Iceland-Faroe Ridge as Iceland Scotland Overflow Water (ISOW) (Schmitz and McCartney, 1993). The circulation in the Iceland Basin is assumed to be influenced strongly by the topography which guides the ISOW along the Icelandic slope toward the slope of the Reykjanes Ridge (McCartney, 1992; van Aken and de Boer, 1995). Along the slope of the Hatton Bank Lower Deep Water (LDW) is assumed to flow into the Iceland Basin in a branch of the Deep Northern Boundary Current (DNBC) (McCartney, 1992). In the Iceland Basin this LDW is entrained in the underlying ISOW and contributes to the total transport of the DNBC along the Icelandic and Reykjanes slopes (van Aken and de Boer, 1995). Because of tracer distributions the DNBC is assumed to have a cyclonic circulation in the Iceland Basin (McCartney, 1992; Tsuchiya *et al.*, 1992). Only few current meter observations have been reported from the Iceland Basin, mainly concentrated on the flow of ISOW in the bottom layer (Shor *et al.*, 1977).

In order to study the barotropic and baroclinic structure of the circulation in the Iceland Basin current meter mooring were deployed in 1989 and 1990 at strategic points in the Iceland Basin (Figure 1, Table 1). This current meter programme was additional to hydrographic surveys, carried out in 1990 and 1991 as part of the DUTCH-WARP research programme (van Aken and de Boer, 1995). Over the steep slope south of Iceland moorings IB89/1 and IB90/1 were deployed in 2 consecutive years at approximately the same position. Moorings IB90/3 and IB90/4 were situated over the slopes of the Hatton Bank and the Reykjanes Ridge respectively, while IB90/2 had a position in the deeper central part of the northern Iceland Basin. All moorings contained 4 current meters, of which 2 were mounted at 40 and 200 m from the bottom (Table 2).

In this paper the mean currents are described in terms of mean currents, their directional stability and variance. The structure of the variable part of the flow is studied by means of principal component analysis.

Table 1 Geographical mooring information.

Mooring	Latitude	Longitude	Water depth (m)
IB89/1	61° 33.1' N	20° 00.8' W	2120
IB90/1	61° 34.1' N	19° 57.8' W	2118
IB90/2	60° 59.6' N	19° 59.3' W	2388
IB90/3	59° 16.1' N	18° 24.7' W	1906
IB90/4	58° 45.1' N	28° 39.6' W	1923

The observations

The geographic position of the moorings is shown in Figure 1. The position of the current meters in the temperature field as observed along a nearby CTD section is shown in Figure 2. The uppermost current meters at moorings IB90/2, IB90/3 and IB90/4 were located above the permanent thermocline in the SPMW. The lowest 2 current meters at moorings IB89/1, IB90/1 and IB90/2 were located in the ISOW layer.

For this study NBA DNC-2M current meters were used. Data were recorded every 30 minutes. The data recovery was on average slightly over 6 months per current meter while 3 current meters failed (Table 2). A detailed description of the data and data processing is given by van Aken and Ober (1991; 1992).

In order to eliminate tidal motion the velocity components were low-pass filtered by the consecutive application of running averages with widths of 12.5 h, 24 h and 25 h. These low-pass filtered data were used for further processing, described below. Their data statistics are shown in Table 2.

The mean currents

The mean current components from the 5 moorings as well as the mean temperature are listed in Table 2. Added to this Table is also the Neumann/Weyers stability parameter B, defined by:

$$B = 100\ \underline{c}/c\ (\%) \qquad (1)$$

with $\underline{c}$ being the averaged vectorial velocity and c the averaged arithmetical velocity. This parameter can vary between 0% and 100% and is assumed to be a good measure of the directional stability of the current (Neumann, 1968). With a uni-directional flow B will amount to 100%.

In Figure 3a the current vectors in the upper 1520 m are shown, while Figure 3b shows the current vectors in the lowest 200 m. It is clear from Figure 3 and Table 2 that the mean current is strongly baroclinic at all mooring positions since the shear vector between the lowest and uppermost current meter has a magnitude of the order of the mean current velocity.

In the upper part of the water column the currents have a direction in the north to east quadrant at moorings IB90/2, IB90/3 and IB90/4 (Figure 2a). This indicates a general north-eastward flow of the thermocline water and the Sub-Polar Mode Water (SPMW) over a large part of the deep Iceland Basin. Over the steep South-Icelandic slope at moorings IB89/1 and IB90/1 the current has a mean west to north direction between 1318 and 1520 m. At this position and depth interval the water mainly consists of a mixture of SPMW, Labrador Sea Water (LSW) and Iceland Scotland Overflow Water (ISOW). Probably part of the north-eastward flowing surface water re-circulates in a cyclonic way close to the Icelandic shelf, in agreement with the hydrographic evidence which suggests a westward flow this slope water over the steep Icelandic slope (van Aken and de Boer, 1995). This circulation scheme agrees with the Lagrangean surface drifter tracks, reported by Otto *et al.* (1992) who observed a general north-eastward surface drift as well as some cyclonic re-circulation along the Icelandic and Reykjanes slopes. The direction stability in the upper 1500 m is of the order of 50 % or less (Table 2), indicating considerable eddy activity relative to the mean motion.

The flow in the bottom layer (Figure 3b) shows large mean currents, O(10–20 cm s^{-1}), over the steep Icelandic slope, where ISOW flows westwards in the DNBC. This order of magnitude is comparable with the order of magnitude of the short-term mean currents, reported by Shor *et al.* (1977) from positions 100–150 km up-stream. The current direction more or less agrees with the direction of the isobaths, indicative for topographic steering of this strong baroclinic flow. The difference in direction between the mean currents 200 m from the bottom at moorings IB89/1 and IB90/1, only a few miles apart (Table 1), is probably due to small-scale local topographic features. A considerable mean shear is observed between 40 and 200 m from the bottom at mooring IB90/1. The shear in velocity is assumed to be due to local horizontal density gradients. In order to check whether the southward veering of the current

Table 2 Mean currents meter readings (standard deviation in brackets), direction stability B and number of days, recorded.

Moring ident.	Depth (m)	Distance to bottom (m)	East comp. (cm s^{-1})	North comp. (cm s^{-1})	Stability %	Days recorded
IB89/1	1320	800	-1.2 (7.8)	1.6 (7.2)	19	147
IB89/1	1520	600	-2.3 (7.9)	0.7 (7.7)	21	145
IB89/1	1920	200	-12.8 (7.4)	1.4 (5.7)	85	140
IB89/1	2080	40	no data recorded			
IB90/1	1318	800	no data recorded			
IB90/1	1518	600	-3.9 (9.0)	1.0 (8.3)	36	173
IB90/1	1918	200	-15.2 (7.8)	-1.5 (3.1)	96	198
IB90/1	2078	40	-17.7 (8.0)	-7.2 (5.0)	96	212
IB90/2	488	1900	6.1 (7.7)	2.6 (8.7)	54	213
IB90/2	1388	1000	6.2 (8.0)	1.7 (11.2)	48	183
IB90/2	2188	200	4.6 (6.6)	-2.9 (7.7)	49	182
IB90/2	2348	40	3.1 (6.3)	-4.7 (6.4)	52	210
IB90/3	306	1600	1.9 (7.8)	5.9 (9.2)	52	202
IB90/3	1006	900	-0.4 (3.7)	1.4 (3.2)	28	186
IB90/3	1706	200	2.4 (4.6)	2.2 (4.6)	48	198
IB90/3	1866	40	3.9 (4.8)	3.0 (3.9)	58	192
IB90/4	323	1600	0.4 (5.2)	0.5 (5.1)	14	205
IB90/4	1023	900	1.4 (4.5)	1.3 (2.9)	34	192
IB90/4	1723	200	-0.5 (2.2)	0.4 (1.5)	19	169
IB90/4	1883	40	no data recorded			

direction is due to friction effects, the thickness of the bottom Ekman layer was estimated according to Weatherly and Martin (1978) to be of the order of 20 to 30 m. This agrees with observations by Williams and Armi (1991) in the deep boundary current near Newfoundland and rules out frictional effects as cause of the observed directional shear. Most probably local density gradients in the flow direction, caused by the containment of the baroclinic flow in the irregular topography of the Icelandic slope causes the vertical veering of the mean current direction.

If we take the mean near bottom velocities, observed at IB89/1 and IB90/1 as characteristic for the steep slope between 60°30'N and 60°45'N, we can derive a westward transport of water below σ_θ =27.8 kg m^{-3}, that is the ISOW below the LSW, to be 1.5 Sv for this narrow stretch of only 15 n. miles. Given the temperature and therefore density gradients between 60°45'N and 60°15'N (280 and 360 km in Figure 2a) we can expect the total transport of ISOW to be at least double this estimate.

The near-bottom current from mooring IB90/2, about 65 km south of IB89/1 and IB90/1 shows a mean south-eastward flow (Figure 3b). Because of the larger bottom depth (Table 1) and the lower bottom temperature at mooring IB90/2 (Table 2), it can be concluded that at mooring IB90/2 also ISOW is transported in the bottom current, in an even less diluted form than at IB90/1. This is confirmed by the hydrographic surveys, described by van Aken and de Boer (1995). The lateral veering of the flow direction is attributed to topographic steering by an extension of the West Katla Ridge (Malmberg, 1975). A similar, although less extensive lateral veering was observed by Shor *et al.* (1977) near the East Katla Ridge. Tracer distributions in the ISOW, as described by van Aken and de Boer (1995) confirm the flow of ISOW around the extension of the West Katla Ridge rather than across it.

The different orientations of the observed near-bottom baroclinic flow directions at IB89/1, IB90/1 and IB90/2 are probably due to a change in orientation of the near-bottom horizontal density gradient. The isopycnals and isotherms in the lowest 500 m follow the bottom contours quite closely (Figure 3a).

At mooring IB90/3, positioned on the north-western slope of the Hatton Bank, a mean north-eastward current with the maximum velocity close to the bottom was observed, closely following the isobaths (Figure 3b). The mean directional shear between 40 and 200 m from the bottom was small, compared to the moorings over the Icelandic slope, discussed above. Probably the flow along the more regular topography of the north-western Hatton Bank is less well able to generate density gradients in the flow direction compared to the South Icelandic slope with it's many ridges and canyons. The north-eastern flow along the Hatton Bank is probably part of the DNBC which transports water of southern origin, among which LDW, into the Iceland Basin. This

deep boundary current has also been observed along the edges of the Porcupine Abyssal Plain (Dickson *et al.* 1985). LDW transported in this eastern boundary current is assumed to re-circulate in the Iceland Basin and to modify ISOW properties (McCartney, 1992; van Aken and de Boer, 1995). With an inflow along the Hatton Bank and a westward flow along the Icelandic slope the deep circulation of the Iceland Basin has a cyclonic character.

The deep flow observed at mooring IB90/4 is extremely small (Table 2) and does not show any southward flow as expected by van Aken and de Boer (1995). Probably the south flowing bottom waters originating from ISOW mixed with SPMW, which follows the topographic contours, was diverted here, due to the rough topography of the Reykjanes slope, with numerous isolated peaks and ridges.

The directional stability B (Table 1) appears to be highest where strong baroclinic currents are found, subject to topographic steering. In the bottom layer at moorings IB89/1 and IB90/1 B is of the order of 90%. The lowest B values (O[20–30%]) are found over the Reykjanes Ridge (mooring IB90/4) and between 1318 and 1520 m over the steep Icelandic slope (moorings IB89/1 and IB90/1). There the flow is irregular with no clearly prevailing flow direction. The B values from the other current meters are of the order of 50 %.

The vertical distribution of the magnitude of the mean flow velocity (Figure 4) suggests a minimum in the energy of the mean flow to be found between close to 1000 m in between the main thermocline and the layer of Labrador Sea Water (van Aken and de Boer, 1995). For dynamic computation of the geostrophic circulation the reference level should be chosen at about this level.

The structure of low frequency variations

The low-pass filtered currents were de-trended by subtracting a least squares approximation. The resulting currents present the variable part of the current with time scales of 1 day to about half a year. Not any significant correlation was observed between the variations of the current components of current meters, mounted in different moorings, not even between moorings IB90/1 and IB90/2, only 65 km apart. This indicates that the variability of the currents is mainly caused by eddies with horizontal scales less than 65 km.

In order to study the vertical structure of the current variations, principal component analysis (Preisendorfer, 1988) was performed on the variable current components within a single mooring. Several methods exist for the principal component analysis of vector series (Kundu *et al.*, 1975; Mercier and Colin de Verdiere, 1985; Owens, 1985; Lippert and Briscoe, 1990). Here we have incorporated the velocity components as individual real valued scalar quantities, $q_i(t)$ (i=1–2N), where N is the number of current meters in a mooring. With principal component analysis an empirical orthogonal presentation of the data is generated, where the original data are represented by:

$$q_i(t) = \sum_{j=1}^{2N} e_{ij}\lambda_j(t) \qquad (2)$$

Here e_{ij} are the empirical orthogonal functions (EOF) and $\lambda_j(t)$ are the corresponding amplitudes. Since the amplitudes are not correlated, that is

$$\langle \lambda_i \lambda_j \rangle = l_j \delta_{ij} \qquad (3)$$

where the angle brackets represent the ensemble average over t, l_j is the variance of amplitude λ_j, and δ_{ij} is the Kronecker delta. This implies that the variance of a scalar parameter can be written as

$$\langle q_n q_n \rangle = \sum_{j=1}^{2N} l_j e_{nj}^2 \qquad (4)$$

From (4) it appears that the variance of q_n is formed by the addition of the contributions of the different EOFs. If there is some structure in the relation between the variables q_n usually a few EOFs can account for most of the variance of q. Therefore the EOFs are ordered for decreasing variance. For this study the EOFs and their amplitudes were determined according to the methods described by Preisendorfer (1988).

An EOF, based on a series of N current vectors, can be represented as a vector in a 2N-dimensional space, but also as a series of N 2-dimensional vectors. Each of these 2-D vectors can be related to one of the current meters. We will use this property to present the structure of each EOF as a series of N 2-D vectors.

Mooring IB90/2 in the centre of the northern Iceland Basin and mooring IB90/3 over the Hatton slope covered a large part of the water column (Figure 3a). The current components from IB90/2 and IB90/3 (N=4) were developed into EOFs.

The cumulative contribution of the EOFs to the total variance or energy at the levels of the current meters at IB90/2 (Figure 5, full line) shows that the first 2 EOFs account for 81% (EOF1 56%, EOF2 25%) of the total energy while the remaining EOFs each contribute only a few percent to the total energy. EOF1 of IB90/2, when plotted as a series of 4 current vectors (Figure 6a), shows nearly parallel vectors with only a small shear. Also EOF2 is presented by nearly parallel vectors with low shear, more or less perpendicular to the vectors representing EOF1 at all 4 current meter levels (Figure

6a, dashed lines). By determining the variable barotropic current from an average of the current components of all 4 current meters the contribution of the barotropic current to the total eddy energy was determined to be 75%. This suggests that the current variance at the site of mooring IB90/2 mainly is formed by nearly barotropic eddies or waves, generating a NW-SE oriented variance ellipse. No predominant rotation sense of the barotropic current vector could be determined by means of a rotary-component spectral analysis (Gonella, 1972).

For mooring IB90/3 it appeared, from the cumulative contributions to the total energy (Figure 5, dashed line) that the first 2 EOFs contributed 66% to the total energy. But for IB90/3 both EOF1 and EOF2 showed a strong shear in direction as well as in velocity, concentrated in the main thermocline (Figure 6b). This implies that along the Hatton Bank not only the mean current, but also the variable part of the current has a mainly baroclinic character.

The variable current at IB90/4 (N=3), shows an EOF structure with a maximum shear in both EOF1 and EOF2 in the permanent thermocline (Figure 7b). These 2 empirical modes explain 70% of the total eddy energy (Figure 7a). This implies that the eddy energy over the Reykjanes slope mainly can be attributed to baroclinic eddies, similar to the slope of the Hatton Bank.

In order to study the structure and relative importance of the variations in the flow of ISOW, the data from the deepest 3 current meters from moorings IB89/1, IB90/1 and IB90/2 were analysed by means of principal component analysis. Since here no data from the permanent thermocline or shallower levels are involved it is expected that the analysis will combine the barotropic mode and the first baroclinic mode into single EOFs, while the EOFs with baroclinic character are expected to be caused by variations in the overflow. The resulting EOF1 and EOF2 represent in all 3 cases well over 80% of the total energy (Figure 8), while their structure is mainly barotropic with low shear in direction and velocity (Figures 9a, c, e). EOF3 and EOF4 had a clear baroclinic character with the shear concentrated above 200 m from the bottom at moorings IB89/1 and IB90/1 and at about 200 m at mooring IB90/2 with EOF3 more or less perpendicular to EOF4 (Figures 9b, d, f). These EOFs are clearly connected with the baroclinic variations in the flow of ISOW relative to the overlying water. However, the total energy, involved in these baroclinic modes contributes only of the order of 10% or less to the total energy (Figure 8), as measured with the lowest 3 current meters.

Summary and conclusions

Current observations from 5 moorings in the Iceland Basin have been analysed to determine the structure of the mean circulation as well as the structure of the variable or eddy part of the motion.

The mean flow, as observed with the current meter moorings in the Iceland Basin has a strong baroclinic character with shear in direction as well as in velocity. The mean currents in the SPMW above the permanent thermocline have a general north-eastward direction. At deeper levels, in the DNBC, the flow is cyclonic, with a north-eastward inflow along the slope of the Hatton Bank and a westward outflow over the steep Icelandic slope. Especially in the lowest 200 m at moorings IB89/1 and IB90/1 the mean flow transports cold ISOW with mean velocities of the order of 10–20 cm s^{-1} and with very high (>90%) directional stability. Irregularities in the topography like ridges appear to guide the baroclinic near bottom flow by influencing the density field. Such a topographic effect is assumed to be responsible for the south-eastward flow of ISOW as observed at IB90/2, in the centre of the northern Iceland Basin. Over the slope of the Reykjanes Ridge the mean currents were very weak and had a low directional stability.

The current variations, analysed by means of a principal component analysis, appear to be mainly barotropic in the centre of the Iceland Basin (IB90/2) while over the slopes of the Hatton Bank and the Reykjanes Ridge these variations have a strong baroclinic character with maximum shear in the permanent thermocline. Over the Icelandic slope, where ISOW is found near the bottom, the main variations of the current below the permanent thermocline presented by EOF1 and 2 reveal a low shear in direction and velocity. There EOF3 and 4 represent variations in the baroclinic flow of ISOW along the bottom. However these baroclinic modes only contribute of the order of 10% to the total eddy energy.

Acknowledgements

This research was carried out as part of the DUTCH-WARP programme. This programme was supported by the Foundation of Marine Research (SOZ) of the Dutch National Science Foundation (NWO).

References

Dickson, R. R., Gould, W. J., Müller, T. J., and Maillard, C. 1985. Estimates of the mean circulation in the deep (>2000 m) layer of the Eastern North Atlantic. Deep-Sea Research, 14: 103–127

Gonella, J. 1972. A rotary-component spectral method for analysing meteorological and oceanographic vector time series. Deep-Sea Research, 19: 833–846

Kundu, P. A., Allen, J. S., and Smith, R. L. 1975. Modal decomposition of the velocity field near the Oregon coast. Journal of Physical Oceanogrography, 5: 683–704

Lippert, A., and Briscoe, M. G. 1990. Observations and EOF analysis of low-frequency variability in the western part of the Gulf Stream re-circulation. Journal of Physical Oceanogrography, 20: 646–656

Malmberg, Sv.-A. 1975. A note on the deep water south of Iceland - Overflow '73. ICES CM 1975/C:32

McCartney, M. S. 1992. Recirculating components to the deep boundary current of the northern North Atlantic. Progress in Oceanogrography 29: 283–383

Mercier, H., and Colin de Verdiere, A. 1985. Space and time scales of meso-scale motions in the eastern North Atlantic. Journal of Physical Oceanogrography, 15: 171–183

Neumann, G. 1968. Ocean Currents, Elsevier Scientific Publishing Company, Amsterdam, 352 pp.

Otto, L., van Aken, H. M., and de Koster, R. X. 1992. Use of drifters in the "DUTCH-WARP" programme, 1990 and 1991. Programme description and preliminary results. NIOZ Data-Report 1992–2, NIOZ, Texel, 22 pp.

Owens, W. B. 1985. A statistical description of the vertical and horizontal structure of eddy variability on the edge of the Gulf Stream re-circulation. Journal of Physical Oceanogrography, 15: 195–205

Preisendorfer, R. W. 1988. Principal component analysis in meteorology and oceanography. Elsevier, Amsterdam. 425 pp.

Schmitz, W. J., and McCartney, M. S. 1993. On the North Atlantic circulation. Reviews on Geophysics, 31: 29–49

Shor, A., Muller, D., and Johnson, D. 1977. Transport of Norwegian Sea Overflow. ICES CM 1977/C:44

Tsuchiya, M., Talley, L. D., and McCartney, M. S. 1992. An eastern Atlantic section from Iceland southward across the equator. Deep-Sea Research, 89: 1885–1917

van Aken, H. M., and de Boer, C. J. 1995. On the synoptic hydrography of intermediate and deep water masses in the Iceland Basin. Deep-Sea Research, 42: 165–189

van Aken, H. M., and Ober, S. 1991. A compilation of moored current meter data from the Iceland Basin (DUTCH-WARP 89, mooring IB89/1). NIOZ Data-Report 1991–2, NIOZ, Texel, 8 pp.+ Figures.

van Aken, H. M., and Ober, S. 1992. A compilation of moored current meter data from the Iceland Basin (DUTCH-WARP 90, moorings IB90/1, 2, 3 and 4). NIOZ Data-Report 1992–1, NIOZ, Texel, 16 pp.+ figs.

Weatherly, G. L., and Martin, P. J. 1978. On the structure and dynamics of the oceanic bottom boundary layer. Journal of Physical Oceanogrography, 8: 557–570

Williams, R., and Armi, L. 1991. The planetary boundary layer of the deep western boundary undercurrent. Deep-Sea Research, 38: 393–399

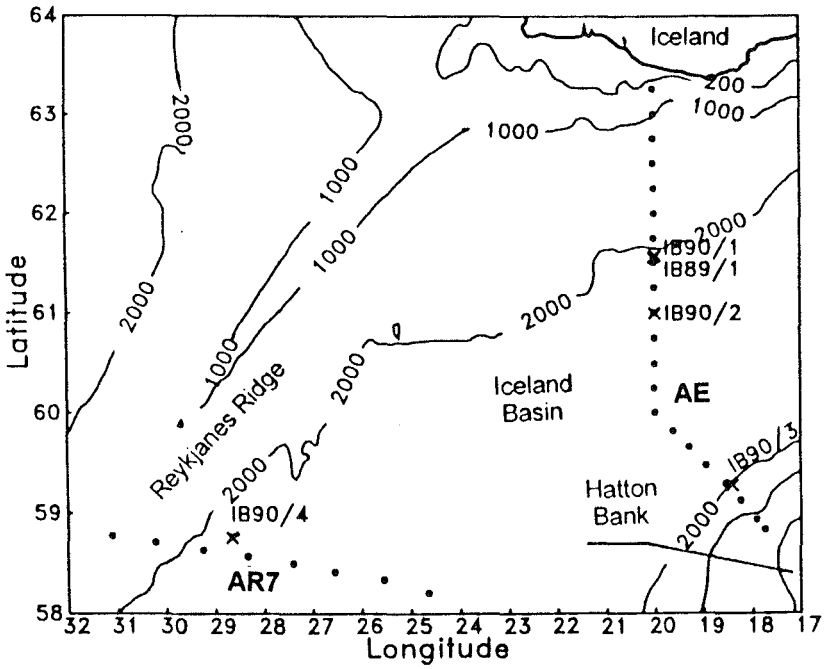

Figure 1. Topography of the Iceland Basin (depth in m) with the positions of the moorings indicated with crosses (x). The dots indicate the positions of CTD stations along 2 hydrographic survey lines (AE and AR7), occupied in April 1991.

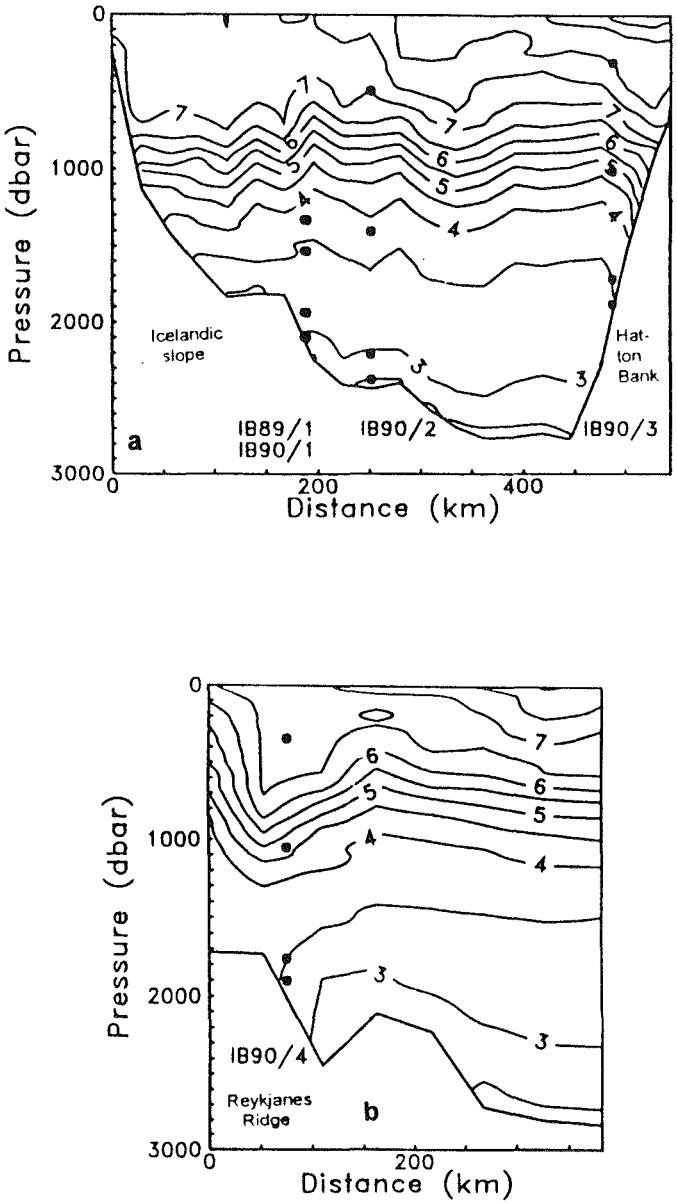

Figure 2. Position of the moored current meters, projected on the potential temperature field from the nearby CTD sections. a) section AE; b) section AR7.

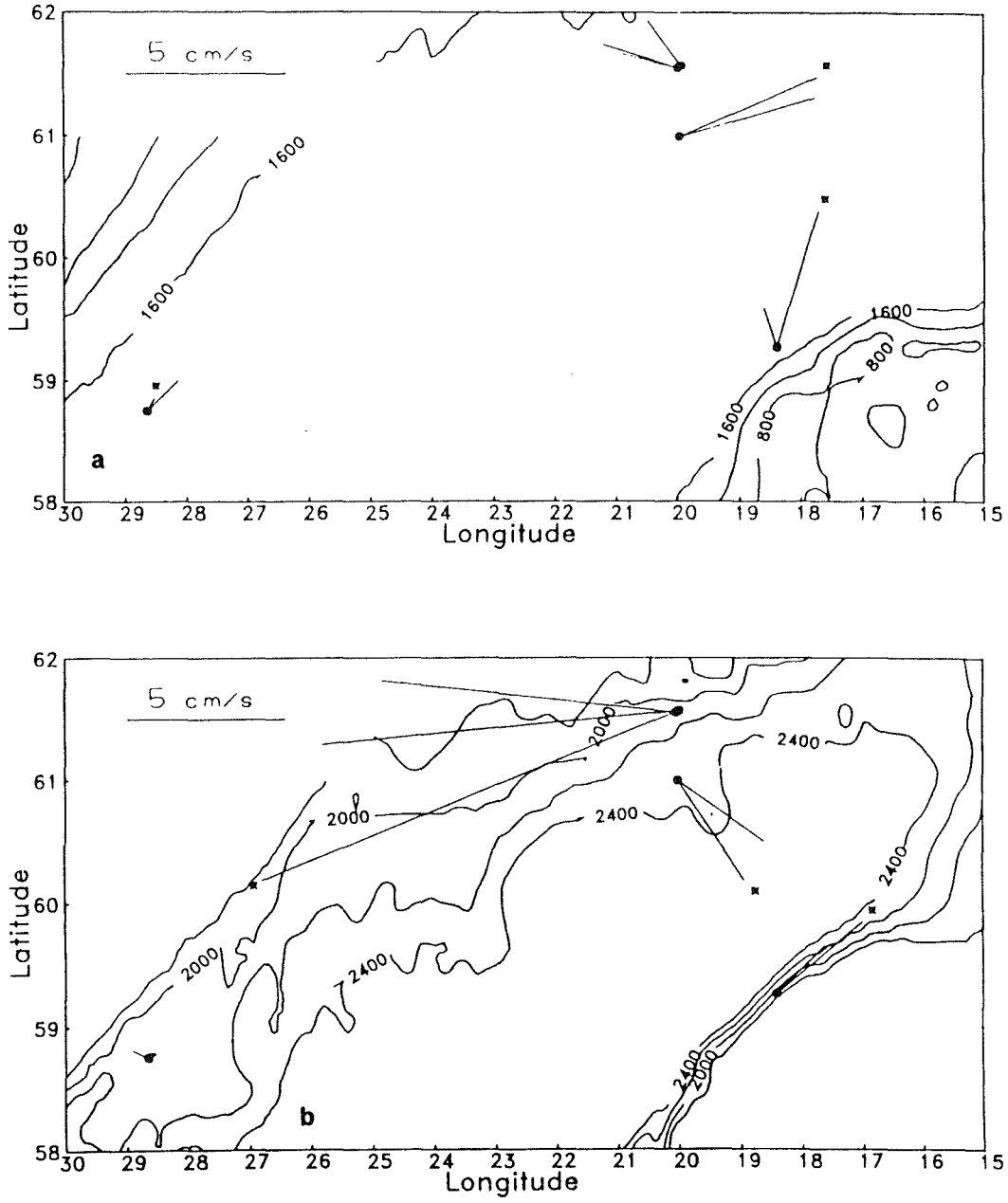

Figure 3. Mean current vectors with the surrounding topography. a) current vectors in the upper 1520 m. The current vectors in the SPMW are marked with an asterisk (*); b) current vectors from the lowest 200 m above the bottom. The currents at 40 m from the bottom are marked with an asterisk (*).

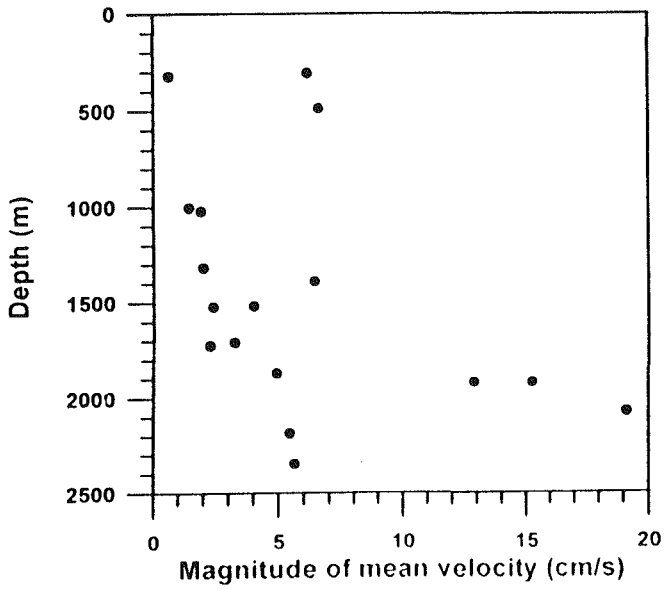

Figure 4. Magnitude of the mean current vectors, plotted versus the depth.

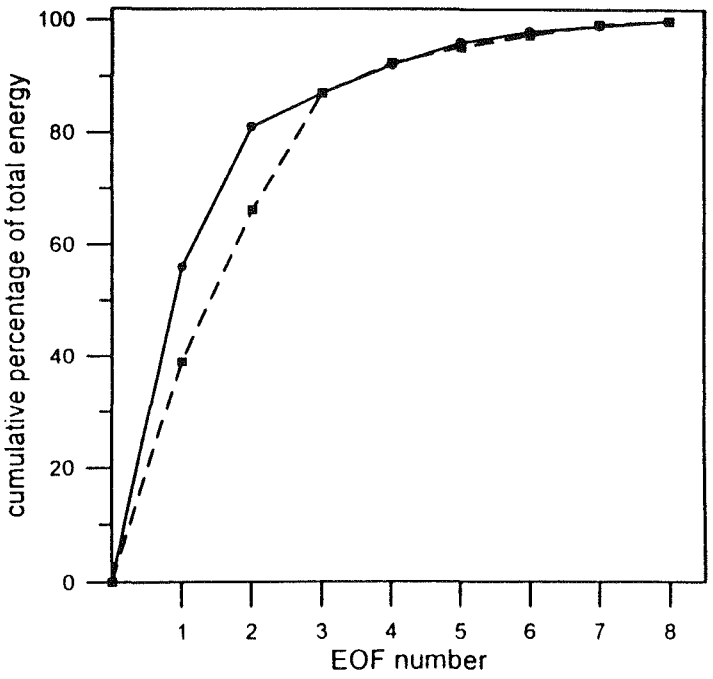

Figure 5. Cumulative contribution (%) of the EOFs to the total energy of the variable motion. IB90/2 full line, IB90/3 dashed line.

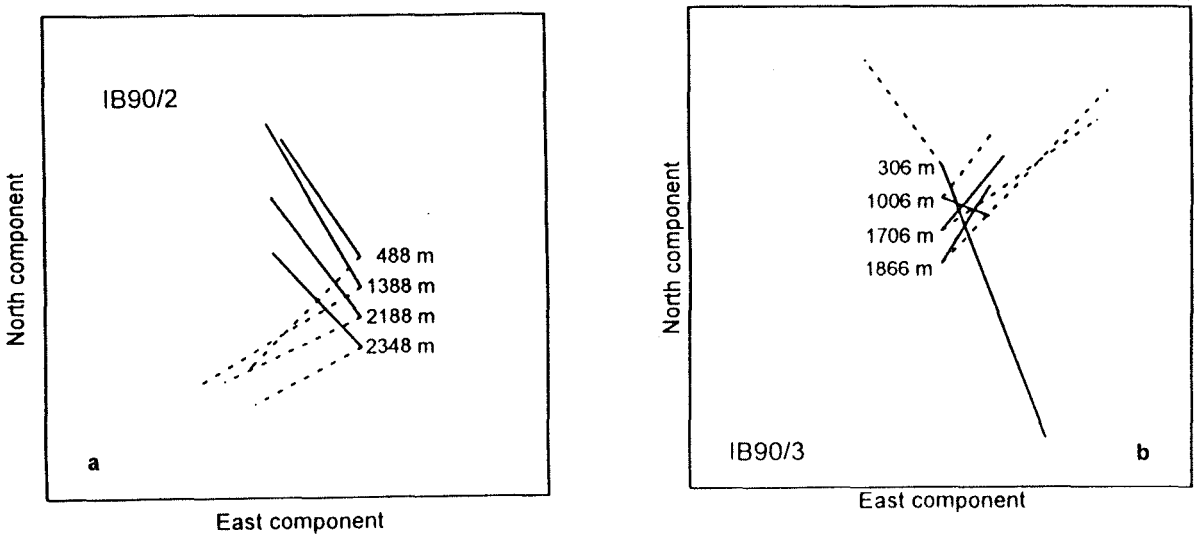

Figure 6. Vectors at 4 levels, representing EOF1 (full lines) and EOF2 (dashed lines) for IB90/2 (a) and IB90/3 (b).

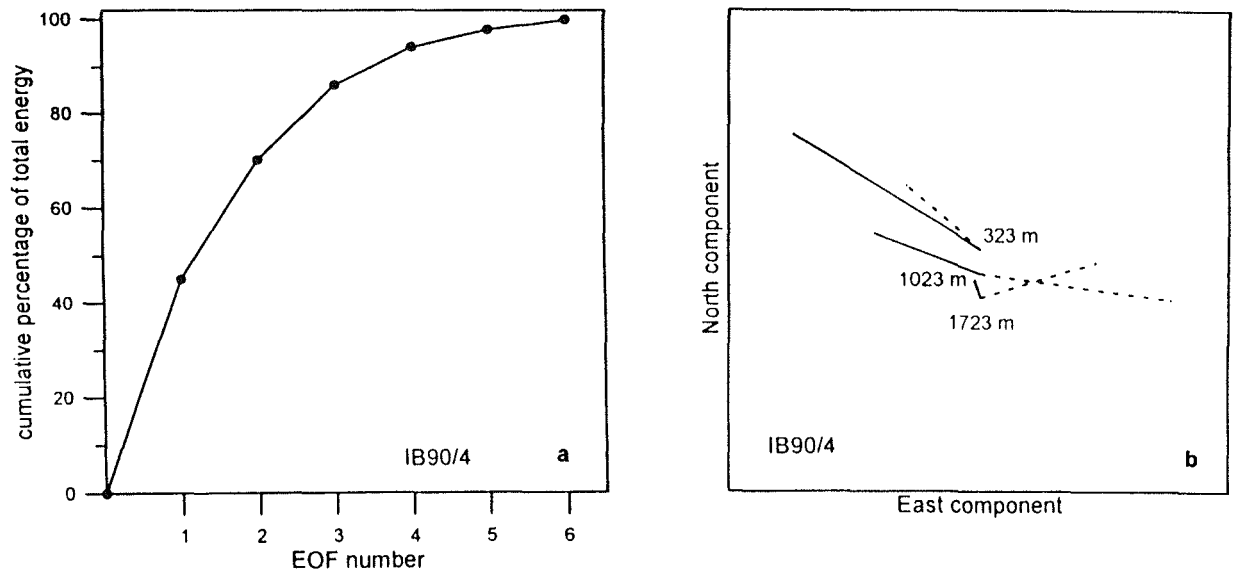

Figure 7. EOF properties for IB90/4. a) cumulative contribution (%) of the EOFs to the total energy of the variable motion; b) vectors at 3 levels, representing EOF1 (full lines) and EOF2 (dashed lines).

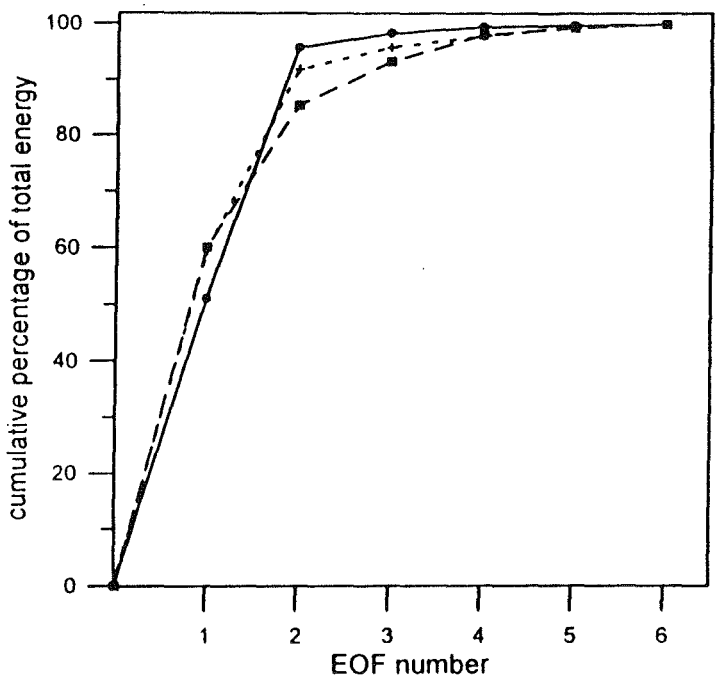

Figure 8. Cumulative contribution (%) of the EOFs to the total energy of the variable motion. IB89/1 full line, IB90/1 short dashes and IB90/2 long dashes.

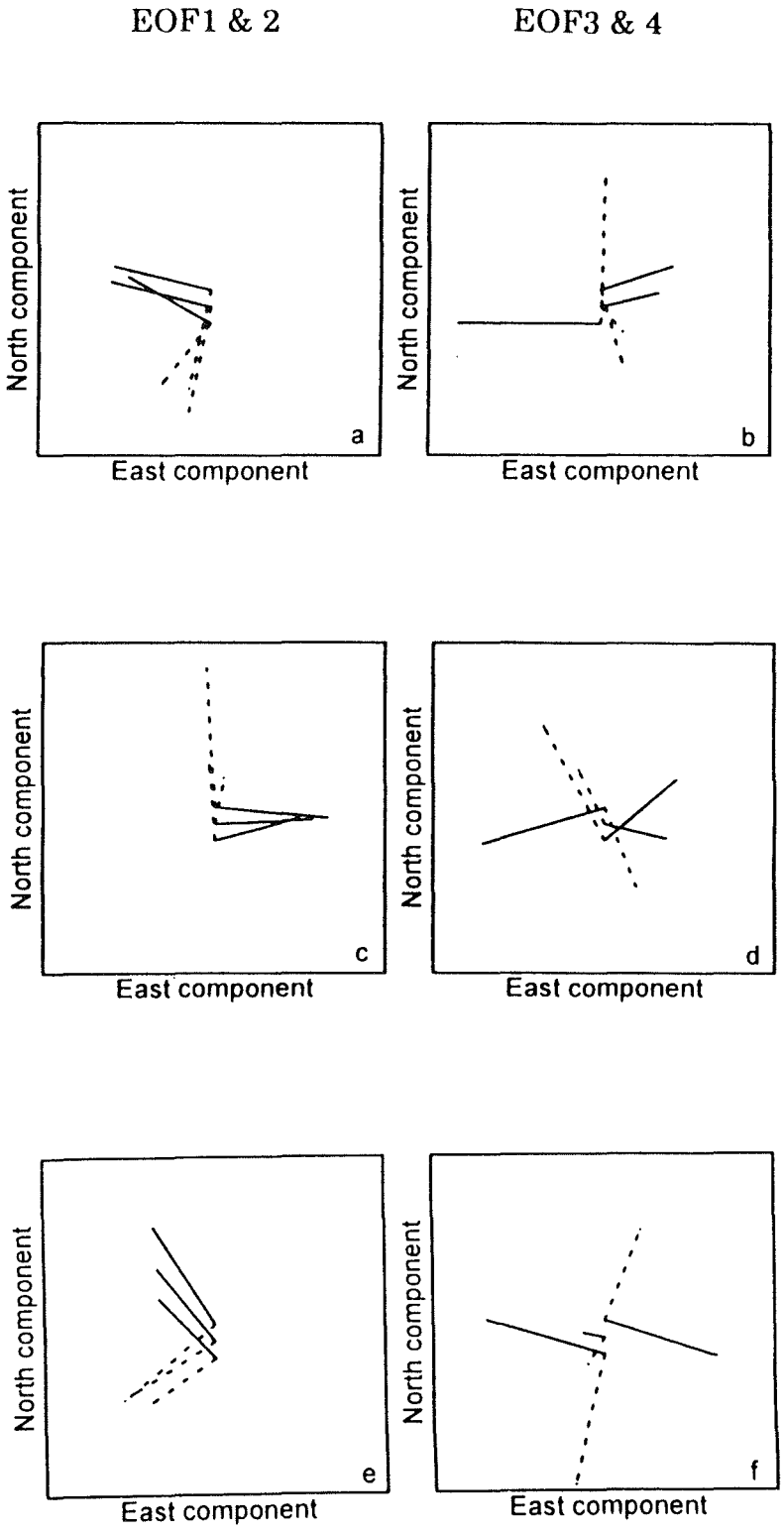

Figure 9. Vectors at 3 levels, representing the EOF structure for the lowest 3 current meters at IB89/1 (a, b), IB90/1 (c, d) and IB90/2 (e, f). EOF1 and EOF3 are drawn in full lines, EOF2 and EOF4 are dashed.

Water mass distribution in the Iceland Basin calculated with an Optimal Parameter Analysis

C. J. de Boer

Nuwendoorn 40, 1613 LD Grootebroek, The Netherlands

Based on a paper presented to the ICES Hydrography Committee as ICES CM 1993/C:16

An optimal multiparameter (water mass) analysis was applied upon data collected during the DUTCH-WARP cruises in 1990 and 1991 containing the tracers salinity, potential temperature, oxygen, silicate and nitrate. The method was tested for the influence of measurement errors and the errors in the characteristics. The individual contributions were calculated with a standard deviation of less than 0.05 and the volume percentages with a standard deviation of less than 2.8%. The contributions of the two years were compared. Intermediate Water occupied a larger volume in 1991 than in 1990. In 1990 the IW contribution changed strongly (from 500 to 1000 dbar) in 9 days. It is suggested that this was caused by Sub Polar Mode water (SPMW) brought to this depth. Multiparameter analysis shows that IW is a biochemically determined water mass instead of Antarctic Intermediate Water or Africa Water. Lower deep water (LDW) was found 100 dbar above the bottom at 60°N 20°W in 1990 but not in 1991. LDW seems to recirculate in the Iceland Basin. High Iceland-Scotland Overflow Water was found at the slope of the Hatton Bank.

Keywords: Iceland Basin, Water masses, Optimal Parameter Analysis

Introduction

In the oceans tracer concentrations are mainly determined by advection and diffusion. The sinks and sources of the tracers are found at the boundaries (land, bottom and surface) and form distinctive source water types. The mixture of source water types that form a water parcel can be used to find the spread, entrainment and diffusion of the source waters and relate these with transport to give insight into the dynamics of the oceans.

Classic water mass analysis is primarily based on a mixing triangle in θ-S space (Mamayev, 1975). A limitation of the method is that maximally 3 source water types can be used to calculate the compositions. In the Iceland Basin at least 4 water types are present (Emery and Meincke, 1986; McCartney, 1992), and only with extra assumptions can the mixing triangle be used. Tomzcak (1981), Thompson and Edwards (1981) introduced a method, also based on linear mixing, which allowed more than 3 source water types. They used more tracers than salinity and temperature. A disadvantage of the method was the negative contributions. Menke (1984) and Mackas *et al.* (1987) introduced a method to move a point outside the mixing triangle (causing the negative contribution) to the nearest mixing line or plane. In this paper this method is used to find the distribution of the different source water types. A stability analysis of the method is performed, to get an impression of the influences of measurement errors and errors in the characteristics of the contributions. The variability in and between two years is investigated at 60°N 20°W.

Data

The data used in this paper were collected by the RV Tyro in the Iceland Basin, during the DUTCH WARP programme (Deep and Upper Transport, Circulation and Hydrography WOCE Atlantic Research Programme) carried out in 1990 and 1991. The CTD measurements were calibrated, averaged and interpolated to give results at 1 dbar pressure intervals. This gave a precision of 0.0015 for salinity (PSS 1978) and 1.7 mK for temperature and 3 pMol kg^{-1} for the oxygen. In this paper the potential temperature (ITS 1990) is used, for shortness it is called temperature. From the samples taken with the bottles in the rosette sampler, the nutrients NO_3, PO_4 and SiO_4 were measured giving a precision of 0.1, 0.06, 0.08 μMol kg^{-1}, respectively. The PO_4 concentration was not used because it is highly linear correlated with NO_3 (Redfield *et al.*, 1963).

For the calculations from the 1990 data no oxygen values were used because the oxygen sensor failed during that cruise and very few oxygen determinations from the samples were obtained. The bottle data were interpolated to give samples every 25 meters. Only data east of 30°W and below 500 dbar were used. For a more detailed description of the data see Van Aken (1992).

Figure 1 shows the topography of the Iceland Basin together with the stations occupied in 1990 and 1991. The sections in 1990 and 1991 are at the same positions, except the AR7 sections. The names are the same for both years. The distance between stations was 15 miles on sections A, B, C, E, F (1990) and A to J (1991) and 30 miles on section D and the AR7 sections. Section D was only measured in 1990. Sections B and E are put together to give section BE. Section BE is oriented East West and section F is oriented North South. In Figure 6 stations 46 and 47 are both measured at 60°N 20°W.

Optimal parameter analysis

If it is assumed that a water sample i is formed by linear mixing, this means for sample i defined by:

$$x_i = (S_i \quad \theta_i \quad O_{2i} \quad SiO_{4i} \quad NO_{3i}) \qquad i = 1,\ldots,n \qquad (1a)$$

where S_i is the salinity, θ_i the temperature, O_{2i} the oxygen, SiO_{4i} the silicate, NO_{3i} the nitrate concentration of sample i and n the number of samples, and using the following definitions

$$b_i = (b_{i,1}, b_{i,2}, \ldots\ldots, b_{i,p}) \qquad (1b)$$

$$k_j = (S_{swt_j}\theta_{swt_j}O_{2swt_j}SiO_{4swt_j}NO_{3swt_j})$$
$$j = 1,\ldots,p \qquad (1c)$$

$$K = (k_1 k_2 \ldots k_p)' \qquad (1d)$$

that

$$x_i = b_i K \qquad (2)$$

b_i is the composition of sample i with $b_{i,j}$ the contribution of source water type j to sample i. k_j the characteristic tracer vector of source water type j, S_{swt_j} the characteristic salinity of source water type j, etc. and K the characteristic matrix. p is the total number of source water types. The implementation of mass conservation is easily done, by adding an extra column with value 1 to the characteristic vector k_j and to the data vector x_j. This is a multiparameter extension of the classic mixing triangle (Tomzcak, 1981).

Figure 2 shows various property-property plots, and the characteristic values of the source water types are indicated. The few oxygen values of 1990 are used to obtain the characteristic values. The characteristic values of Intermediate Water (IW) are determined on the base of the nitrate maximum instead of on the oxygen minimum. In this paper 5 source water types are used (p=5). If oxygen is used then 5 tracers are used (m=5), otherwise 4 tracers are used (m=4). The following source water types are present: Sub Polar Mode Water (SPMW), Intermediate Water (IW), Labrador Sea Water (LSW), Lower Deep Water (LDW) and Iceland-Scotland Overflow Water (ISOW). For more details see later. If $m+1 < p$, there are more unknowns than equations (m+1 because of mass conservation), and the system is underdetermined. When $m+1 > p$ the system is overdetermined. In this case the method minimizes the square residual. The residual for sample i is defined by:

$$R_i = x_i - b_i K \qquad (3)$$

and gives the difference between the calculated and the measured tracer value. The residual will be zero when there is exact linear mixing, no measurement errors occur, the tracers behave conservatively and the characteristics of the source water types are correct.

The different tracers used to calculate the contributions have different ranges; therefore the data are standardised. In this paper a standardisation is used that gives every tracer range 1.

$$x^*_{i,l} = \frac{\left[x_{i,l} - \min_i\left(x_{i,l}\right)\right]}{\left[\max_i\left(x_{i,l}\right) - \min_i\left(x_{i,l}\right)\right]} \quad l = 1,\ldots,m \qquad (4a)$$

$$k^*_{i,l} = \frac{\left[k_{i,l} - \min_i\left(x_{i,l}\right)\right]}{\left[\max_i\left(x_{i,l}\right) - \min_i\left(x_{i,l}\right)\right]} \quad l = 1,\ldots,m \qquad (4b)$$

$$K^* = (k_1^* \; k_2^* \ldots k_p^*)' \qquad (4c)$$

with $x_{i,l}$, $k_{j,l}$ the value of tracer l of sample i or source water type j, $x^*_{i,l}$, $k^*_{j,l}$ the standardised value of tracer l of sample i or source water type j and $max_i(x_{i,l})$ and $min_i(x_{i,l})$ are respectively the maximum and minimum value of tracer l over all the i samples. The contributions are now calculated while minimising the residuals of the standardised data and characteristics. The calculated distributions can be negative and due to the mass conservation other contributions can become greater than 100 %. This is physically unrealistic and is caused by points outside the mixing triangle. Menke (1984) and Mackas *et. al.* (1987) introduced a method that always calculates positive contributions, and by virtue of the mass conservation also contributions smaller or equal to 1. The method moves a sample outside the mixing triangle to the nearest mixing line or

Table 1 Characteristic values of the source water types.

Source water type	Salinity	Pot. Temp (°C)	Oxygen μmol kg^{-1}	SiO_4 μmol kg^{-1}	NO_3 μmol kg^{-1}
SPMW	35.640	12.0	270	3.6	12.0
IW	34.976	4.8	246	11.2	20.1
LSW	34.887	3.4	280	10.6	17.2
LDW	34.905	2.1	239	45.5	22.2
ISOW	34.985	2.0	280	10.0	15.2

mixing plane, giving a zero contribution instead of a negative contribution, but giving larger residuals than without the moving. For a detailed description of the procedure see Mackas *et al.* (1987) and Maamaatuaiahutapu *et al.* (1992). If errors in the measurement of salinity are less possible than for example in temperature, then, by the calculation of the residuals, salinity must gain a higher weight, resulting in a lower difference between measured and calculated salinity. This is achieved if equation 2 is solved while minimising the square residual where the residual is defined by:

$$R_i = [x^*_i - b_i K^*] W \quad (5)$$

with W a diagonal matrix with $W_{i,i}$ the weight for tracer i. This means that, with the highest weight on salinity, a point outside the mixing triangle is moved more or less isohaline to the nearest mixing line or plane. In Figure 3 this is demonstrated with 3 source water types, and the tracers temperature and salinity. Point 1 is calculated with a 10 times higher weight on salinity than on temperature, point 2 the other way around. Mass conservation always gets the same weight as the highest weight. Point 2 is moved along isotherms to the mixing line in contrast of point 1 which is moved along isohalines. The weighting influences the calculated contributions; point 1 contains 48% SPMW and 52% ISOW while point 2 contains 30% SPMW and 70% ISOW, but both are the results of 1 data point. A weighting matrix can be defined as:

$$W_{l,q} = \frac{\sigma_l}{\Delta swt_l} \delta_{l,q} \quad (6)$$

with σ_l the standard deviation of tracer 1 and Δswt_l the highest uncertainty of tracer 1 in the determination of the characteristic values of the source water types (in standardised units) and $\delta_{l,q}$ the kronecker delta (1 if $l=q$ else 0). This weighting matrix gives a higher weight to tracers with a high standard deviation (= high ability to discriminate between water types) and a low uncertainty in the characteristic tracer values. This weighting is based on Tomzcak and Large (1989). This gives for my data set 23.6, 4.2, 1.0, 17.0, and 10.0 for salinity and the mass conservation, temperature, oxygen, silicate and nitrate respectively. There are other definitions possible; instead of the uncertainty in the characteristics the measurement precision, or the expected non conservative behaviour of a tracer can be used. Mackas *et al.* (1987) used a non diagonal matrix W to take into account the covariance in the tracer characteristics.

Stability of the method

The contributions calculated by this method will be influenced by measurement errors and errors in the determination of the characteristic tracer values of the different source water types. The influences were investigated with stability tests. For this stability test only section A of 1991 was used.

Influence of errors in the characteristic valucs. The largest uncertainties for tracer characteristics were 0.01 for salinity, 1 °C for temperature, 5 μmol kg^{-1} for oxygen, 1 μmol kg^{-1} for silicate and nitrate both. To test the influence each characteristic tracer value was changed with the uncertainty of that tracer. The characteristic salinity of SPMW is normally 34.640 (Table 1), now the contributions were calculated once with a value of 34.630 and once with 34.650. The other tracer values remain unaltered. For each tracer and each source water type this was done giving 50 sets of contributions. The difference between the normal contributions and the "disturbed" contributions were calculated and summarised in Table 2. The overall influence can be calculated with the volume percentages occupied by the 5 water masses. These results are listed in test A in Table 3. The difference between the normal percentages and the mean percentages indicates that decreasing a value does not have the opposite effect of increasing the value. The highest differences are caused when the characteristics of LSW are changed. The used uncertainties are uncertainties in the determination of the SPMW characteristics, and these are much larger than the uncertainties in the determination of the characteristics of for example LSW. Therefore these results can be considered as "worst case" results. If for

Table 2 Difference between contributions calculated with changed and unchanged characteristics. ΔB means the difference between the contributions calculated with changed and unchanged characteristics. $B_{i,j}$ is between 0 and 1. The results obtained in test A are calculated with the maximal uncertainty for a tracer, and each tracer of each source water type is changed separately. The results of test B are obtained with the uncertainties of each tracer belonging to the source water type (separately), and the results of test C are obtained while using the uncertainties of B but every tracer is changed simultaneously. See text for more details.

test	Water mass	max(| ΔB |)	mean(ΔB)	std(ΔB)
A	SPMW	0.06	-0.001	0.007
	IW	0.29	0.002	0.033
	LSW	0.40	-0.006	0.047
	LDW	0.03	0.000	0.004
	ISOW	0.34	0.004	0.040
B	SPMW	0.02	0.000	0.002
	IW	0.04	0.000	0.005
	LSW	0.11	0.000	0.010
	LDW	0.00	0.000	0.001
	ISOW	0.09	0.000	0.008
C	SPMW	0.04	-0.004	0.007
	IW	0.11	0.011	0.025
	LSW	0.23	-0.021	0.049
	LDW	0.09	0.000	0.002
	ISOW	0.25	0.014	0.039

Table 3 Volume percentages calculated from the contributions which are calculated with the changed characteristics. For the explanations of the tests A, B, and C see Table 2.

test	water mass	unchanged	min %	max %	mean %	std %
A	SPMW	11.4	10.0	12.5	11.4	0.4
	IW	14.0	5.9	25.0	14.4	2.3
	LSW	55.7	45.3	60.3	54.9	2.8
	LDW	1.9	1.0	3.3	1.9	0.3
	ISOW	17.0	11.1	27.3	17.3	2.7
B	SPMW	11.4	11.2	11.7	11.5	0.09
	IW	14.0	13.0	15.3	14.2	0.32
	LSW	55.7	53.7	56.9	55.5	0.58
	LDW	1.9	1.7	2.0	1.9	0.03
	ISOW	17.0	15.4	18.7	16.9	0.46
C	SPMW	11.4	10.4	12.0	11.2	0.44
	IW	14.0	11.5	17.2	14.7	1.6
	LSW	55.7	48.7	58.2	54.2	2.7
	LDW	1.9	1.6	2.1	1.8	0.14
	ISOW	17.0	14.4	22.4	18.0	2.1

Table 4 Difference between contributions calculated with disturbed and undisturbed data. ΔB means the difference between the contributions calculated with disturbed and undisturbed data. $B_{i,j}$ is between 0 and 1.

Water mass	max(| ΔB |)	mean(ΔB)	std(ΔB)
SPMW	0.20	-0.0003	0.0039
IW	0.13	-0.0011	0.0253
LSW	0.16	-0.0019	0.0284
LDW	0.01	0.0000	0.0028
ISOW	0.17	0.0011	0.0187

Table 5 Volume percentages calculated from the contributions which are calculated with the disturbed data sets.

water mass	undisturbed	min %	max %	mean %	std %
SPMW	11.4	11.5	11.5	11.5	0.02
IW	14.0	14.0	14.5	14.3	0.10
LSW	55.7	55.1	55.6	55.3	0.10
LDW	1.9	1.8	1.9	1.9	0.01
ISOW	17.0	16.9	17.1	17.0	0.01

Table 6 Volume percentages calculated with (1991) and without oxygen (1990, 1991). Water masses: 1=SPMW, 2=IW, 3=LSW, 4=LDW, 5=ISOW.

	1990 Water mass					1991 (incl. O_2) Water mass					1991 (excl. O_2) Water mass				
section	1	2	3	4	5	1	2	3	4	5	1	2	3	4	
A	10.7	12.8	54.9	2.6	19.1	11.4	14.0	55.7	1.9	17.0	11.5	13.4	56.5	1.9	17.0
B	8.7	9.1	59.3	3.3	19.6	7.2	13.9	56.7	3.5	18.6	7.3	13.3	57.5	3.5	18.4
C	25.0	8.1	65.7	1.1	0.1	27.8	0.6	67.6	0.0	3.9	27.8	0.5	67.8	0.0	3.9
D	11.2	11.0	57.4	1.9	18.6										
E	11.0	13.0	60.0	3.6	12.4	9.3	19.7	53.9	3.9	13.2	9.4	18.9	54.7	3.9	13.0
F*	11.1	13.3	59.9	2.8	13.0	10.8	19.4	52.6	2.2	15.0	10.9	18.8	53.4	2.3	14.7
G						18.4	14.6	49.7	0.7	16.5	18.5	14.2	50.3	1.3	14.9
H						16.0	17.9	49.6	1.3	15.3	16.1	17.2	50.5	1.3	14.9
I						24.9	19.3	39.9	1.3	14.6	25.0	18.4	41.3	1.3	14.0
J						37.0	15.3	43.4	0.8	3.5	37.1	14.4	44.5	0.8	3.2
AR7**	5.7	11.6	48.0	17.5	17.2	12.1	20.4	45.5	5.7	16.4	12.2	19.5	46.8	5.6	15.9

*Section F in 1990 was 1 station (15 miles) less to the north.

**AR7 section had different positions in 1990 and 1991.

every source water type its own uncertainty in its tracer characteristic was used, the influence is much less (test B). When these uncertainties were used to disturb the characteristics all together randomly (with a random number for every tracer and every source water type, with a standard deviation equal to the tracer uncertainty of that specific tracer of that source water type) the influence increased (test C). Summarising the table shows that the individual contributions are estimated with a standard deviation of 0.01, 0.03, 0.05, 0.004 and 0.04 for respectively SPMW, IW, LSW, LDW and ISOW and the volume percentages are calculated with a standard deviation of 0.4 %, 2.3 %, 2.8 %, 0.3 %, and 2.7 %.

Influence of measurement errors. Besides the uncertainty in the characteristic values, also the measurement errors influence the calculated contributions. The influence of the measurement errors was tested by disturbing the normal data with random

noise of a standard deviation equal to measurement precision (see the Data section, for the nutrients 0.1 μmol kg^{-1} was used) and zero mean. All tracers were disturbed at the same time, but the disturbance for each tracer in a sample was uncorrelated. This was done 25 times. Table 4 summarises the differences between the contributions calculated with the disturbed and undisturbed data. The standard deviations of the differences indicate that the overall influence is small (<0.03). The volume calculations were only slightly influenced (Table 5).

Influence of oxygen. For the calculations of the 1990 data no oxygen was used. To find the influence of oxygen on the calculations, the contributions of 1991 were calculated with and without oxygen. The volume percentages of the different sections are listed in Table 6. The maximal difference between the calculated volume percentages is 1.4%. The small influence of oxygen is due to its low weight (1 vs. 23.6). Differences between the years 1990 and 1991 larger than 1.4% are significant and not due to the absence of oxygen in the calculations.

Water masses in the Iceland Basin

Tracer distributions. Figures 4a, 5a, 6a, 7a show the spatial distribution of the different tracers at section F and BE. Figures 4a and 6a show the data of 1990 on section F and BE. No Oxygen is shown here. Figures 5a and 7a show the data on the sections F and BE in 1991.

The salinity distribution (I in the Figures 4a, 5a, 6a and 7a) shows a salinity minimum with values below 34.92 and oxygen values above 275 μmol kg^{-1} indicating Labrador Sea Water (LSW) (Talley and McCartney, 1982). Sub Polar Mode Water (SPMW), formed by winter time convection in the North Atlantic Ocean (McCartney and Talley, 1982) can be found above 750 meters. Between this layer and LSW there was an oxygen minimum (subfigure III in the figures) and an NO_3 maximum (subfigure V). These extremes were not on the same depths. To obtain a characteristic value, the nitrate maximum is used. The water mass responsible for these extreme values is tentatively called Intermediate Water (IW) (Van Aken and de Boer, 1995). Its origin is not quite clear. Tsuchiya *et al.* (1992) suggest that it is Antarctic Intermediate Water (AAIW), although they did not find a continuous core so far north. Kawase and Sarmiento (1986) found a layer with corresponding characteristics which they call Africa Water (AW). McCartney (1992) suggests that the oxygen minimum is caused by an oxygen flux to the sediments of the Rockall Hatton Plateau, but in my data the oxygen minimum at the Rockall Hatton Plateau appears to be 200 dbar above the bottom (AR7 section 1991, not shown in this paper). IW can also be determined biochemically. Near the bottom below the layer of LSW, two cold water masses were found. In Figure 2d Lower Deep Water (LDW) is apparent with its high silicate concentrations (van Bennekom, 1985; de Boer *et al.*, 1991). This water mass is influenced by Antarctic Bottom Water which gives it its high silicate concentrations. LDW is transported by the Deep Northern Boundary Current (DNBC) westward looping through the Rockall Through, west across the south flank of the Rockall Plateau, north along the Hatton Bank into the Iceland Basin, where it turned westward with the ISOW along the Reykjanes Ridge. In the subfigures II and III Iceland-Scotland Overflow Water (ISOW) with its low temperature and high oxygen concentration (Lee and Ellet, 1965) is apparent. This water flows to the south-west, along the Icelandic slope and the Reykjanes Ridge.

Water mass distributions. With the characteristics from Table 1 the contributions of the source water types were calculated. Figures 4b–7b show the distributions of the contributions. Subfigure I shows SPMW. On the section BE a lower concentration of SPMW was found in 1991 than in 1990 and than on other sections. SPMW is found near the surface. On sections BE and F a relative SPMW maximum was found at 1800 dbar. It was brought to this depth by entrainment in ISOW at the Iceland-Faroe Ridge (van Aken and de Boer, 1995). In subfigure II the IW distribution is shown and it appears that IW does not reach the Icelandic shelf at section F. Between 1990 and 1991 great differences occurred in the IW distributions. In 1991 it reached almost to the bottom at the sections A, B, E, F and AR7, this was not the case in 1990 (except at section AR7).

High LSW contributions are found at 500 dbar, due to the high temperature and salinity characteristics of the SPMW. The minimum of the LSW and the maximum of the IW contribution at 1000 dbar (also shown in Figure 8c) suggests that IW divides the water mass formed by mixing of SPMW and LSW into two parts. Looking at the characteristics of IW, comparing them with the characteristics of AAIW as found by Tsuchiya *et al.* (1992) and using them in a mixing triangle containing LSW, AAIW and SPMW, it is not possible to obtain the characteristics of IW without negative contributions. This means that with the available water masses to modify AAIW it is not possible to obtain IW, and therefore it is not likely that IW is diluted AAIW. The same reasoning holds for Africa Water (AW). This water is suggested to be the source of IW by Kawase and Sarmiento (1986). With SPMW, LSW, AW and MOW (Mediterranean Outflow water) it is again not possible to obtain the characteristics of IW without negative contributions (M. H. C. Stoll, personal communication). This leads to the conclusion that IW is a biochemical water mass. The highest contributions of LSW are found at 1700 dbar.

Subfigure IV presents the LDW distribution. There was a clear difference between 1990 and 1991 and between the sections. In 1991 on section F the LDW distribution

showed 2 cores. This supports the recirculation pattern of LDW as suggested by McCartney (1992). In 1991 the LDW had equal in– and outflow surfaces (nothing is said about transports), while in 1990 the inflow seems to be much more confined to the Hatton Bank while the outflow is much broader. In the latter case the density suggests that the inflow velocity is much higher than the outflow velocity. At section BE only one core was found in 1990.

The ISOW distribution is shown in subfigure V with the highest values near the bottom. High ISOW contributions at 1000 dbar depth are found on the Icelandic shelf. ISOW is found over the whole section, also in the south (F) and east (BE). With the DNBC flowing along the Hatton Bank to the north, this means that part of the ISOW is recirculated into the Iceland Basin (Harvey and Theodorou, 1986). On the BE section ISOW was found on the whole section. Although the highest values were found near the Reykjanes Ridge, values over 50% were found at the Hatton Bank.

Variability in water mass compositions in the Iceland Basin

Variability at 60°N 20°W. In 1990 and 1991 60°N 20°W was visited 5 times. In Figure 8 the contributions from the different source water types are plotted against the depth. The +++ and xxx lines are the results from 1991. The contribution of SPMW and ISOW appears to be similar in the two years. In IW, LSW and LDW contributions there were larger differences within a year (see ooo, □, □, □, and ◊◊◊ all measured in 1990) and between the years. The IW maximum dropped, i.e. the oxygen minimum and nitrate maximum became less extreme. This can be seen in Figure 6b V. Stations 46 and 47 are both on 60°N 20°W, only 9 days apart (47 was done first!). Station 46 corresponds with the ◊◊◊ in Figure 8 and 47 corresponds with ooo. The squares were done 4 days after station 47. The maximum nitrate concentration was lower at station 46 than at 47, while the temperature and salinity were higher at station 46. In Figure 8a it appears that the SPMW contribution is higher at station 46. This suggests that SPMW is brought to this depth.

The LSW contribution also changed. In 1990 the maximum contribution of LSW was higher than in 1991 (10% more), and shallower (1700 dbar vs. 1800 dbar). The difference was caused by IW: in 1991 the nitrate maximum was larger and thicker than in 1990, and this caused LSW contribution to be smaller in 1991 than in 1990. This means that biochemical processes (e.g. remineralisation) were higher in 1991. In Figure d the contribution of LDW is plotted. In 1991 (+++ and xxx) there was a minimum at 2700 dbar while in 1990 there was a maximum. This means that LDW is sometimes present at this position and sometimes not. This could also be seen in silica plots (de Boer and van Aken, 1991) of that position. LDW was not found near the bottom, but about 100 dbar above the bottom. Below the core of LDW, ISOW is found.

Variability between the sections and the years. Table 6 summarises the volume percentages of the water masses of the different sections. It is not possible to compare the sections because the depth influences the percentages. If the largest depth of a section is only 750 dbar, no LDW and ISOW are available, and therefore the other percentages increase. On all sections LSW was the most dominant water mass and LDW the least. The percentage SPMW did not change much (less than ±3%). The IW volume increased by 1.2%—6.7% except on section C, where it vanished. On section C ISOW increased (found at the surface), due to significantly lower nutrient concentration in 1991 than in 1990. This caused the nitrate maximum to be lower and the IW volume to be smaller. The decrease in nutrients on section C is in contrast with the measurements at 60°N 20°W. The LSW volume percentage changes about ±7% at sections E and F.

The LDW volume stayed the same in both years, although the distribution differed. Although a large amount of LDW was found only at section AR7 in 1990, LDW can be found at section H and I, so LDW reached far into the Iceland Basin. From the AR7 section to these sections LDW is much diluted. The ISOW volume percentage decreased at the south-west part of the basin, and increased in the north-east part.

Conclusions

The optimal parameter analysis is a useful tool for water mass analysis. According to the stability tests the results are not much influenced by measurement errors or errors in the characteristics. The individual contributions are estimated with a standard deviation of less than 0.05 and the volume percentages are calculated with a standard deviation of less than 2.8%. The effect of not using oxygen is very small due to the low weight of oxygen gained from the weighting matrix. A disadvantage of the method is the dependency of the results on the weighting matrix. The weighting can change the contributions significantly when only salinity and temperature are used. If other tracers are used this influence becomes less.

IW was much stronger in 1991 than in 1990, while LSW was weaker. LDW was not found near the bottom but 100 dbar above (60°N 20°W). From the multiparameter analysis it appeared that IW is a biochemically obtained water mass. In 1990 a maximum of LDW was found, in 1991 it was absent. LDW reaches far into the Iceland Basin. On the F section two cores were present suggesting recirculation of LDW. High contributions of ISOW were found at the slope of the Hatton Bank.

Perhaps it is possible to relate the residuals of the samples at the surface to surface cooling or precipitation and the residuals near the bottom to fluxes from the bottom. This paper does not consider residuals. Further research is needed to address the question. Linear mixing is assumed in this method. There is no specific model behind this linear mixing; nothing is said about processes such as advection, diffusion etc. Therefore care must be taken when physical processes are deduced from the contributions calculated in this way.

Acknowledgements

The research reported here was supported by the Working Community of Meteorology and Oceanography (MFO) with financial aid from the Netherlands Organization for Advancement of Research (NWO) and from the Netherlands Foundation for Marine Research (SOZ/NWO). I thank M. H. C. Stoll for the fruitful discussions we had.

References

de Boer, C. J., van Aken, H. M., and van Bennekom, A. J. 1991. Hydrographic variability of the overflow water in the Iceland Basin. ICES CM 1991/C:13.

Emery, W. J., and Meincke, J. 1986. Global water masses: summary and review. Qceanologica Acta, 9: 383–391.

Harvey, J. G., and Theodorou, A. 1986. The circulation of Norwegian Sea overflow water in the eastern North Atlantic. Oceanologica Acta, 9: 393–402.

Kawase, M., and Sarmiento, J. L. 1986. Circulation and nutrients in mid depth Atlantic Waters. Journal of Geophysical Research, 91: 9749–9770.

Lee, A., and Ellett, D. 1965. On the contribution of overflow water from the Norwegian sea to the hydrographic structure of the North Atlantic Ocean. Deep-Sea Research, 12: 129–142.

Maamaatuaiahutapu, K., Garcon, V. C., Provost, C., Boulahdid, M., and Osiroff, A. P. 1992. Brazil-Malvinas Confluence: water mass composition. Journal of Geophysical Research, 97: 9493–9505.

Mackas, D. L., Denman, K. L., and Bennett, A. F. 1987. Least squares multiple tracer analysis of water mass composition. Journal of Geophysical Research, 92: 907–2918.

Mamayev, O. I. 1975. Temperature-Salinity Analysis of world ocean waters. Elseviers oceanography series 11, 374 pp.

McCartney, M. S. 1992. Recirculating components to the deep boundary current of the northern North Atlantic. Progress in Oceanography, 29: 283–383.

Menke, W. 1984. Geophysical Data Analysis: Discrete Inverse Theory. Academic Press, 260 pp.

Redfield, A. C., Ketchum, B. H., and Richards, F. A. 1963. The influence of organisms on the composition of sea water. *In* The Sea, vol. 2, pp. 26–77. Ed. by H. M. N. Hill. Interscience Publishers, NY.

Thompson, R. O. R. Y., and Edwards, R. J. 1981. Mixing and water mass formation in the Australian subantarctic. Journal of Physical Oceanography, 1: 1399–1406.

Tomczak, M. 1981. A multiparameter extension of temperature/salinity diagram techniques for the analysis of non-isopycnal mixing. Progress in Oceanography, 10: 147–171.

Tomczak, M., and Large, D. G. B. 1989. Optimum multiparameter analysis of mixing in the thermocline of the eastern Indian Ocean. Journal of Geophysical Research, 94: 16141–16149.

Tscuchiya, M., Talley, L. D., and McCartney, M. S. 1992. An eastern Atlantic section from Iceland southward across the equator. Deep-Sea Research, 39: 1885–1917.

van Aken, H. M. 1992. DUTCH-WARP 91, R.V. Tyro cruise 91/1 part 1, WOCE Hydrographic Programme section AR7E (cruise report) NIOZ, Texel, 34 pp.

van Aken, H. M., and de Boer, C. J. 1995. On the synoptic hydrography of intermediate and deep water masses in the Iceland Basin. Deep-Sea Research, 42: 165–189.

van Bennekom, A. J. 1985. Dissolved Silica as an indicator of Antarctic Bottom water penetration, and the variability in the bottom layers of the Norwegian and Iceland basin, Rit Fiskideildar, 9: 101–109.

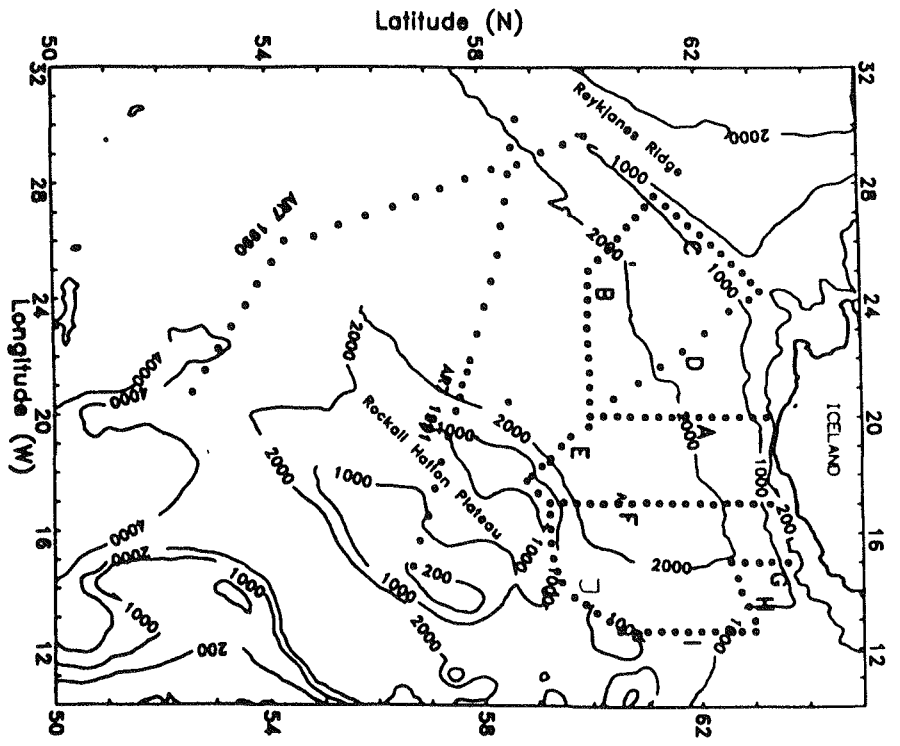

Figure 1. A subset of the hydrographic stations occupied during the DUTCH-WARP cruises in 1990 and 1991. The sections in 1990 and 1991 had the same names. Sections A, B, C, E and F were done in both years; section D was only done in 1990 (station distance 30 nautical miles), and sections G, H, I and J were only done in 1991. For all these sections the station distance was 15 naut. miles. The AR7 sections were different in 1990 an 1991 (station distance was 30 nautical miles). The western boundary of the Iceland Basin is formed by the Reykjanes Ridge, while the eastern boundary is formed by the Rockall-Hatton Plateau and the Iceland-Faroe Ridge.

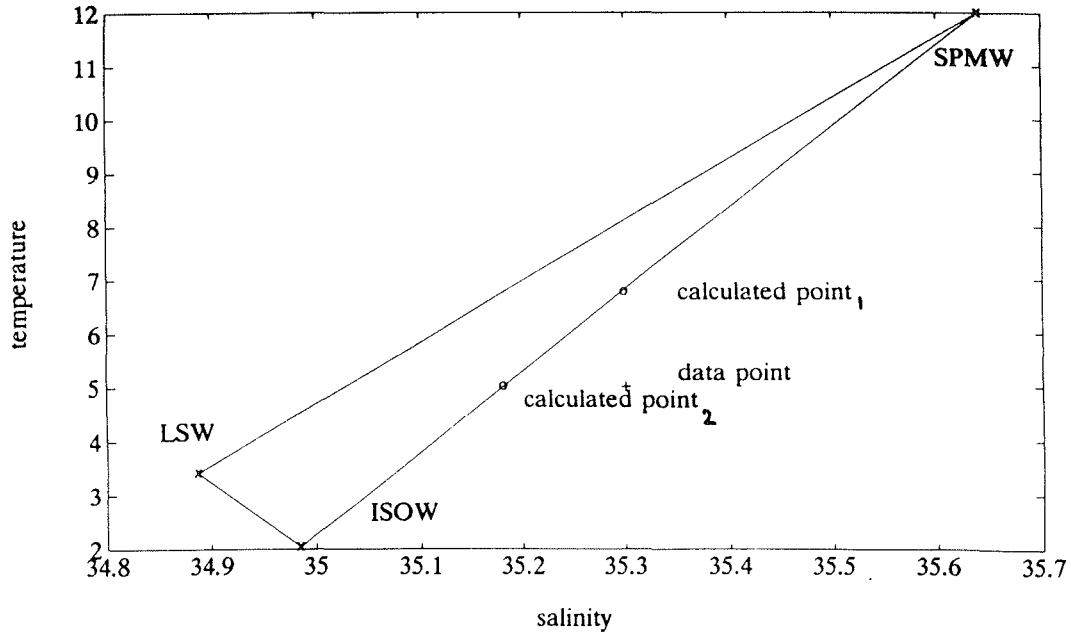

Figure 2. Property-property plots. All the samples measured in 1990 and 1991 are plotted. a: salinity-potential temperature; b: salinity-oxygen; c: salinity-silicate; d: nitrate-silicate. The silicate, nitrate and oxygen units are μmol kg^{-1}.

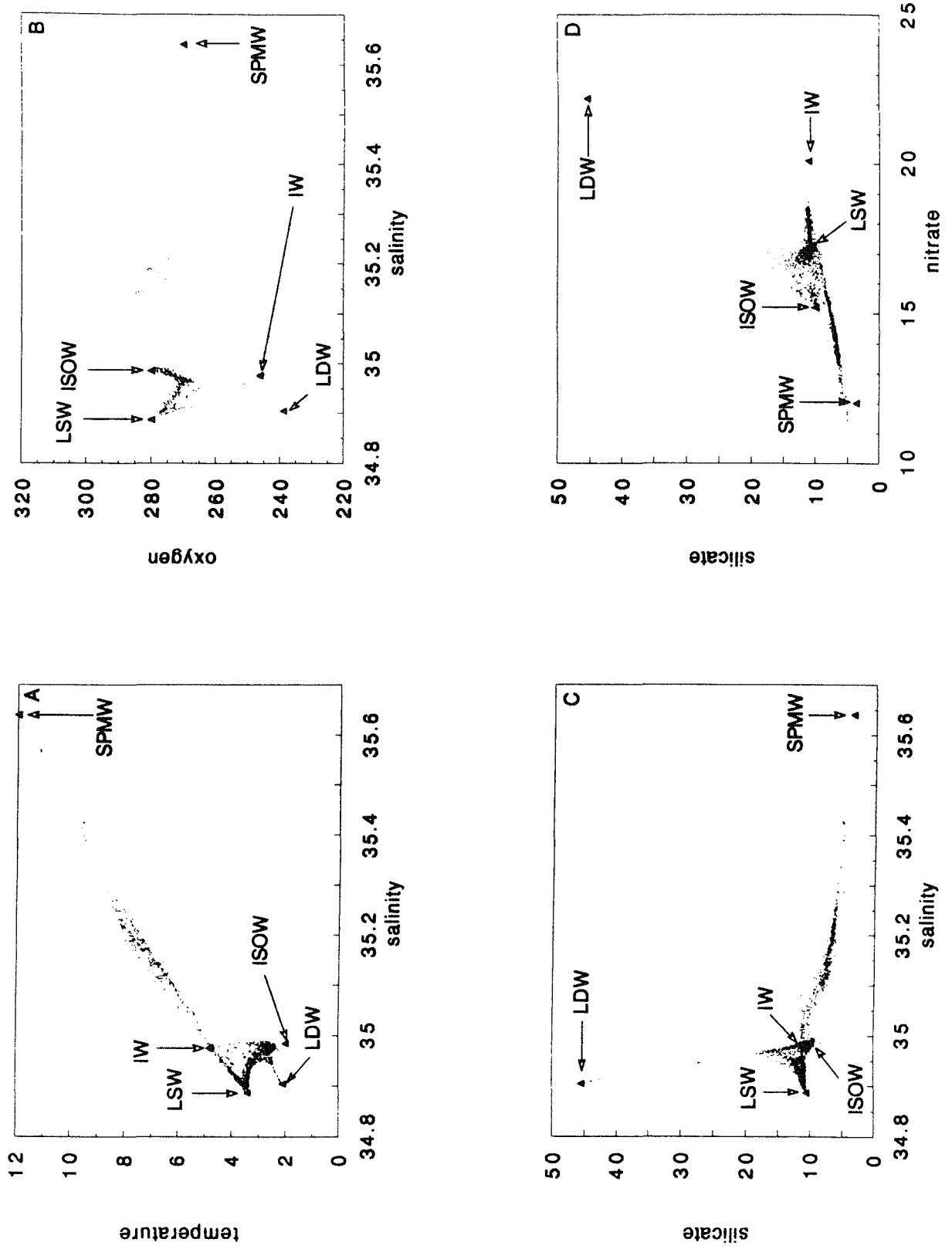

Figure 3. A hypothetical mixing triangle, with only SPMW, LSW and ISOW to show the influence of the weighting matrix. P is the original data point, point 1 is the resulting data point when a 10 times higher weight on salinity is used than on temperature, and point 2 is the resulting data point if a 10 times higher weight is used on temperature. In Table 2 the calculated contributions are listed.

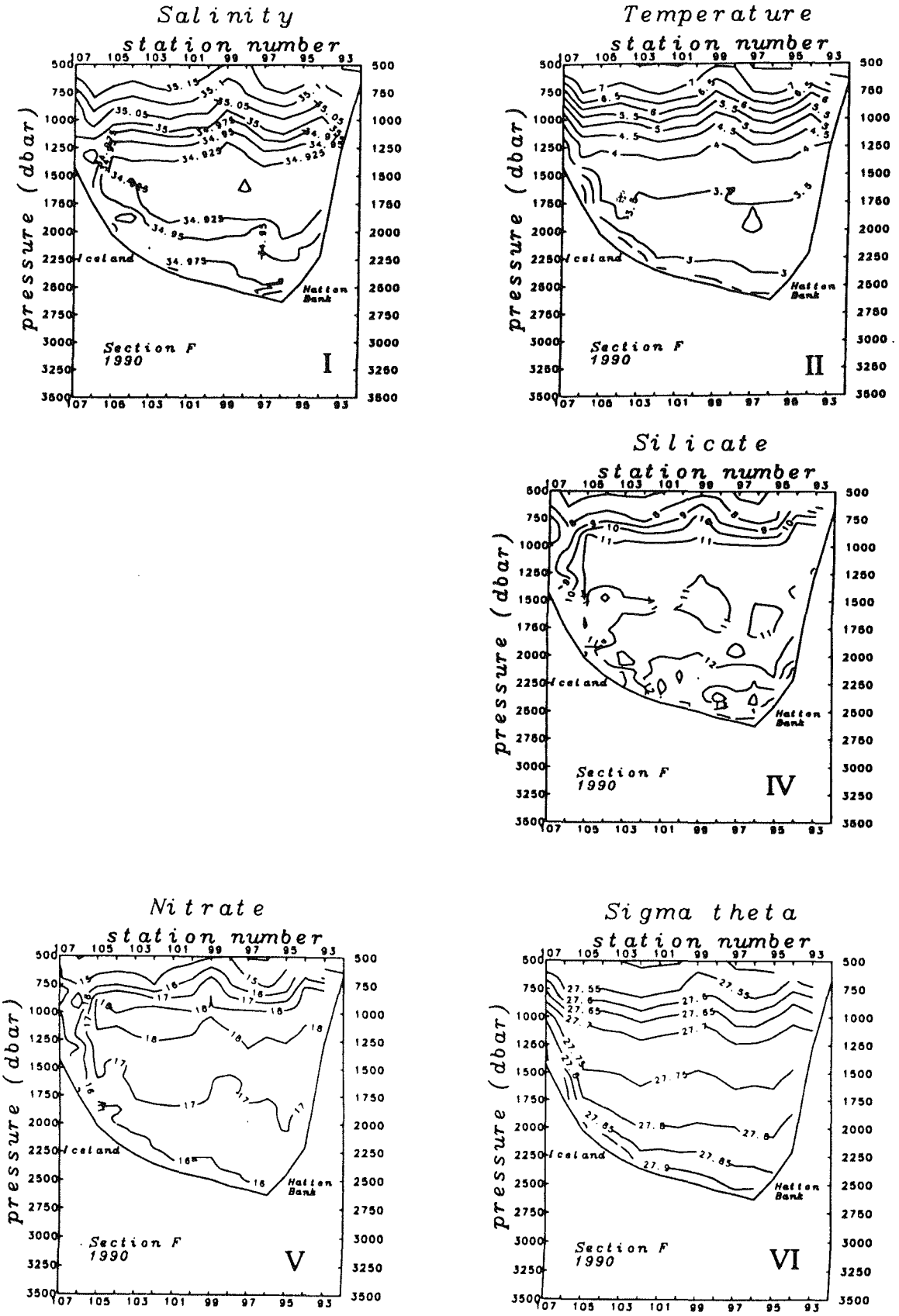

Figure 4 - Figure 4a. shows the tracer distributions on section F in 1990. Subfigure I shows the salinity distribution, subfigure II the (potential) temperature distribution, subfigure III the oxygen distribution (not in 1990), subfigure IV the silicate distribution, subfigure V the nitrate distribution and subfigure VI the sigma theta distribution. The silicate, nitrate and oxygen units are μmol kg^{-1}.

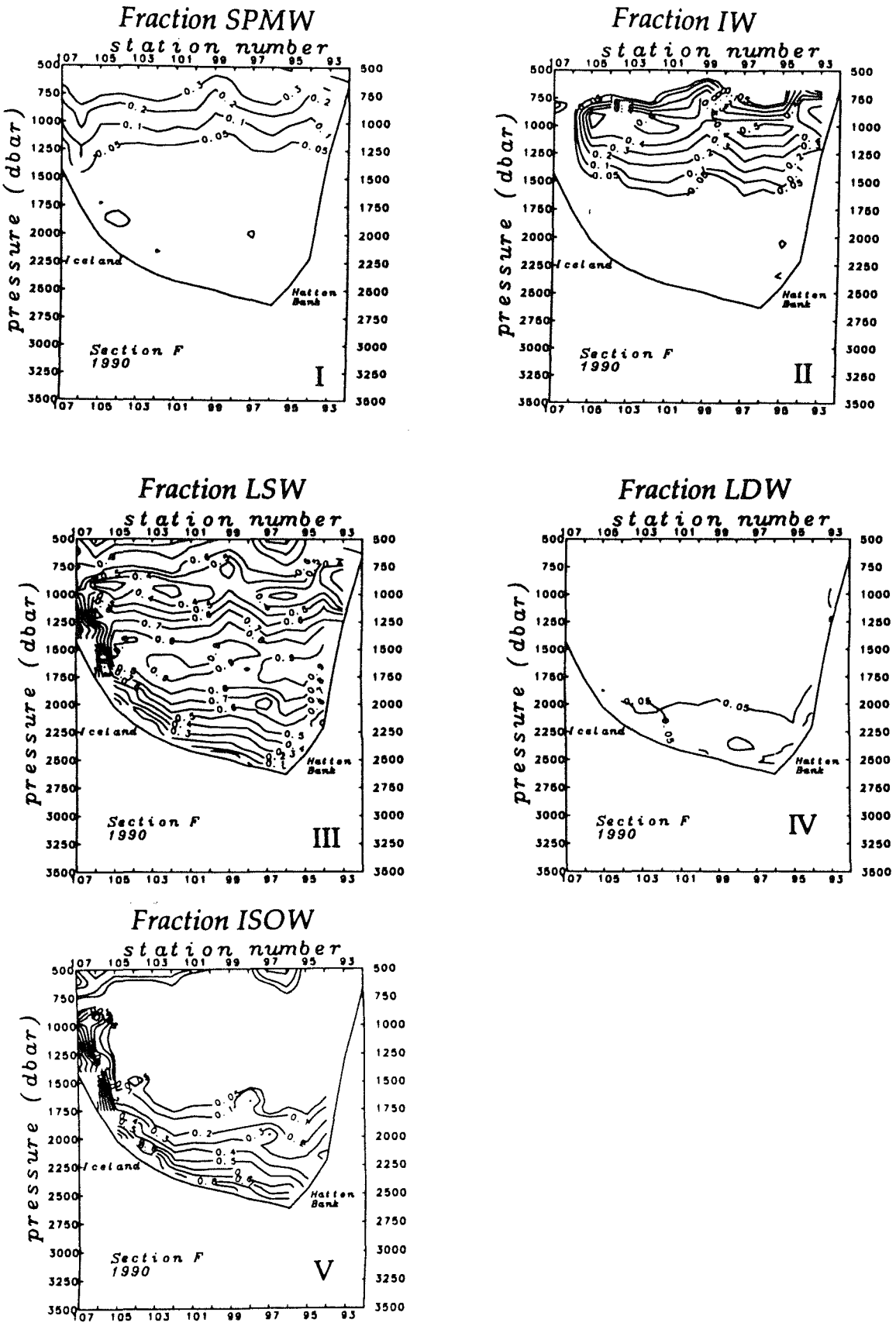

Figure 4b. shows the distribution of the contributions of the different source water types. Subfigure I shows the SPMW contribution, subfigure II the IW contribution, subfigure III the LSW contribution, subfigure IV the LDW contribution and subfigure V the ISOW contribution.

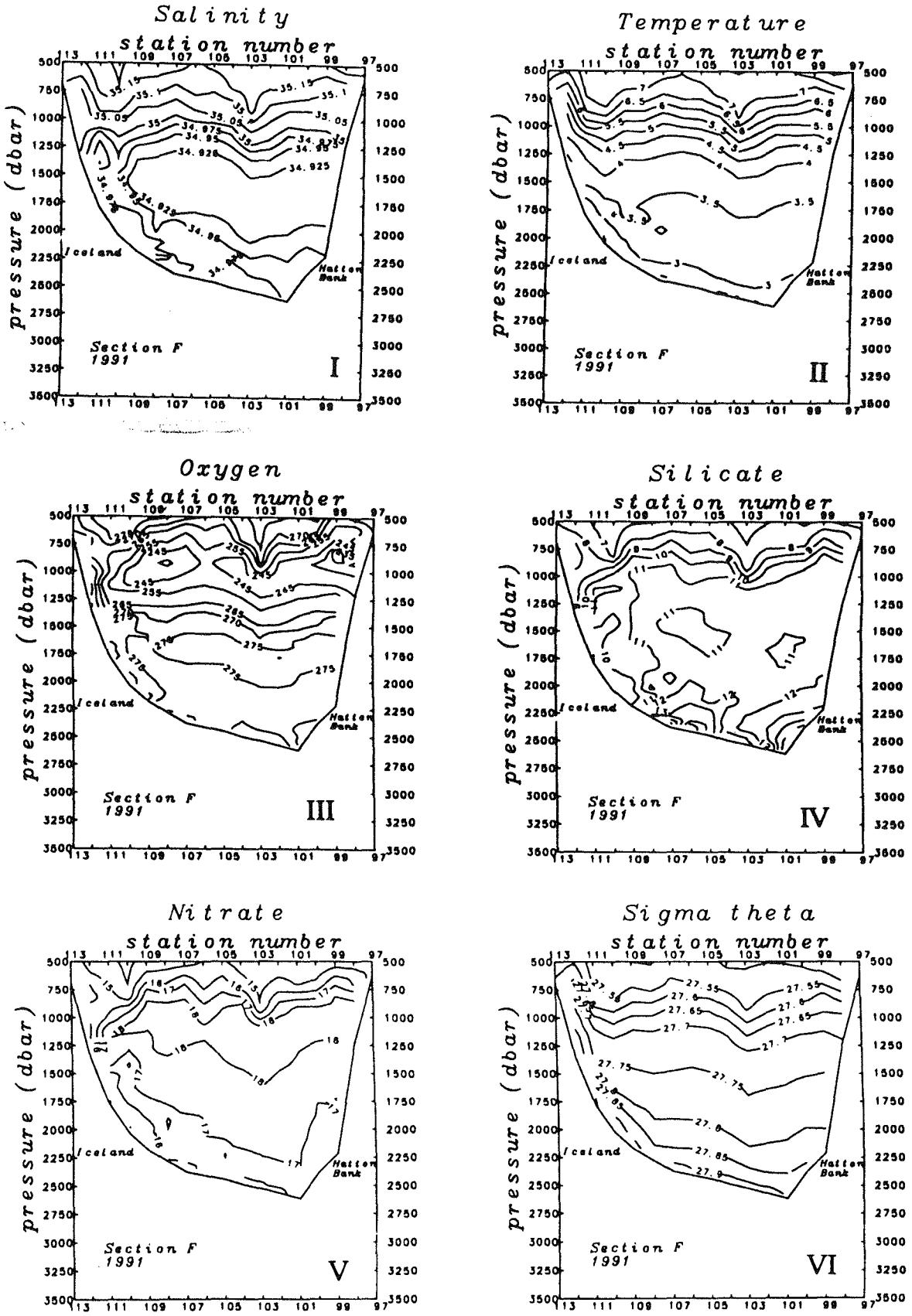

Figure 5 - Figure 5a. As Figure 4 with the data on section F in 1991.

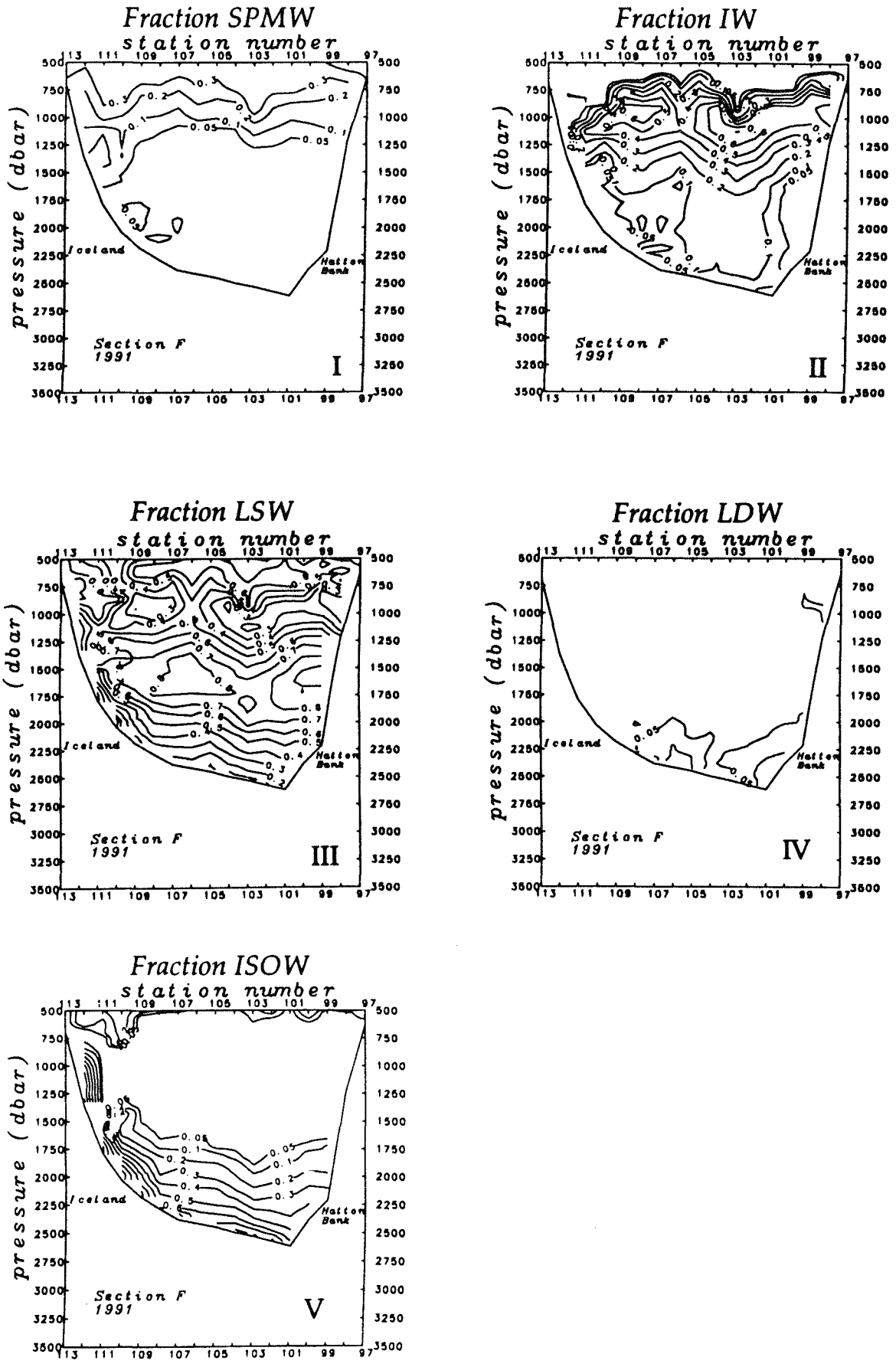

Figure 5b. As Figure 4 with the data on section F in 1991.

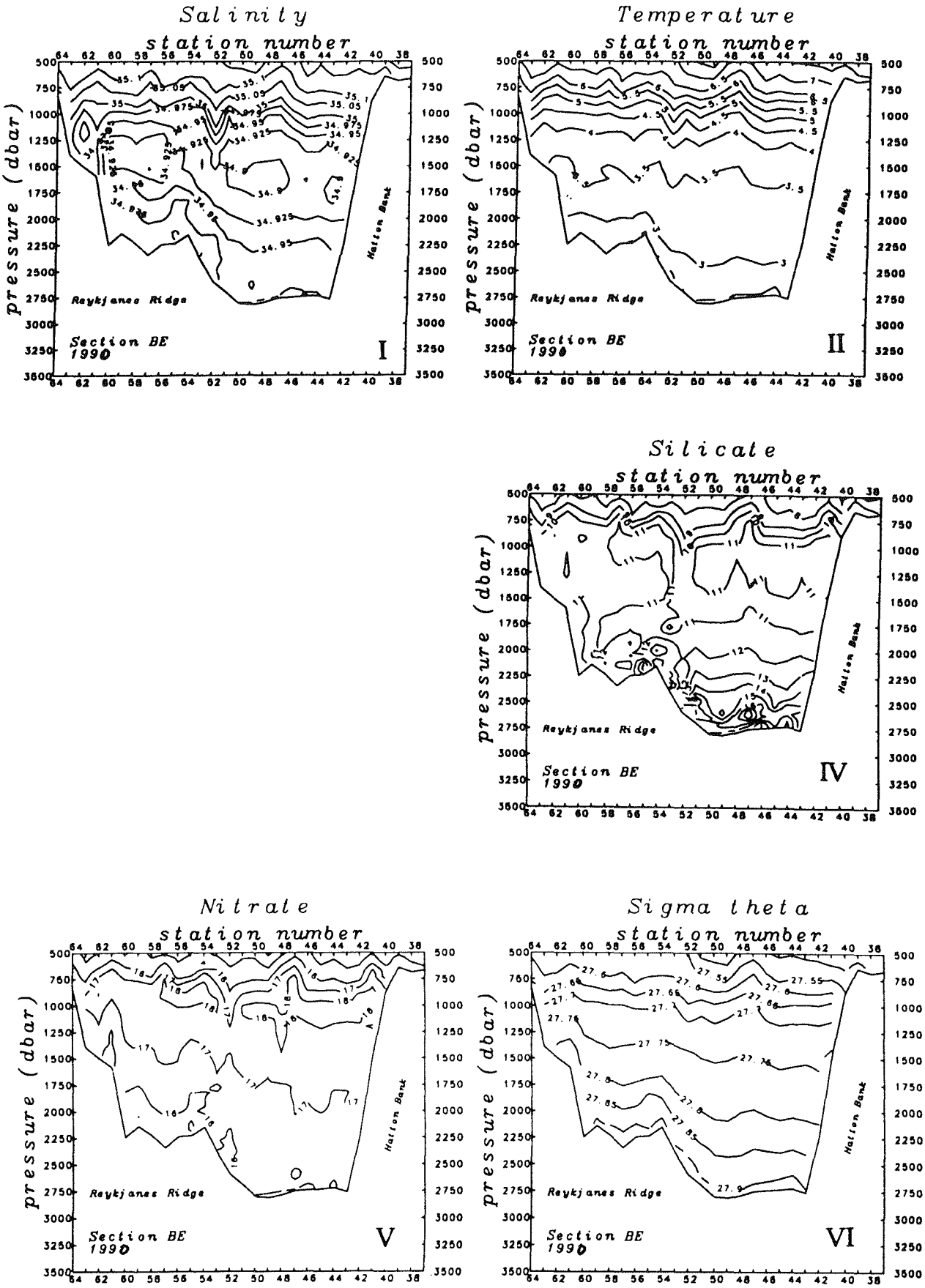

Figure 6 - Figure 6a. As Figure 4 with the data on section BE in 1990.

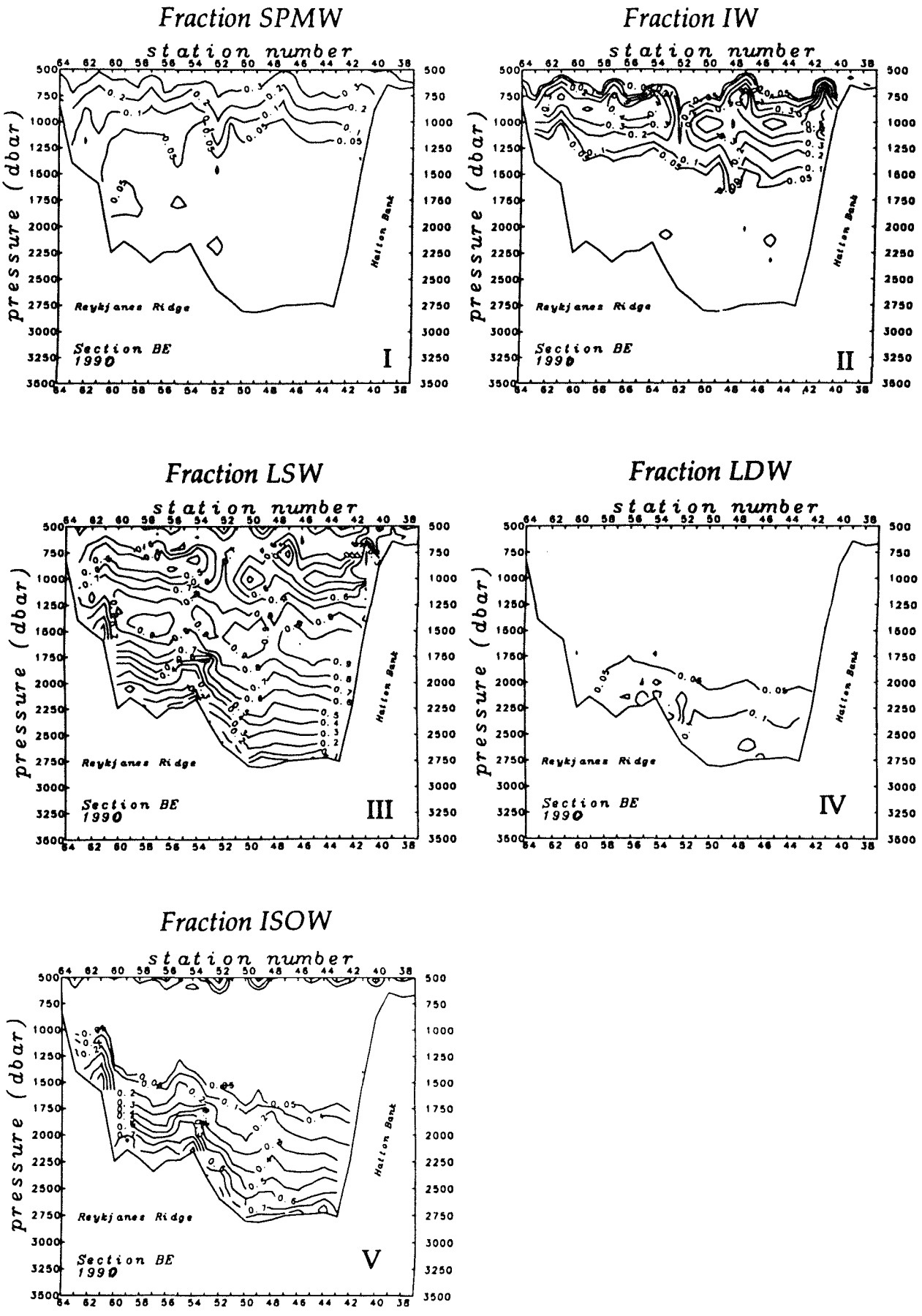

Figure 6b. As Figure 4 with the data on section BE in 1990.

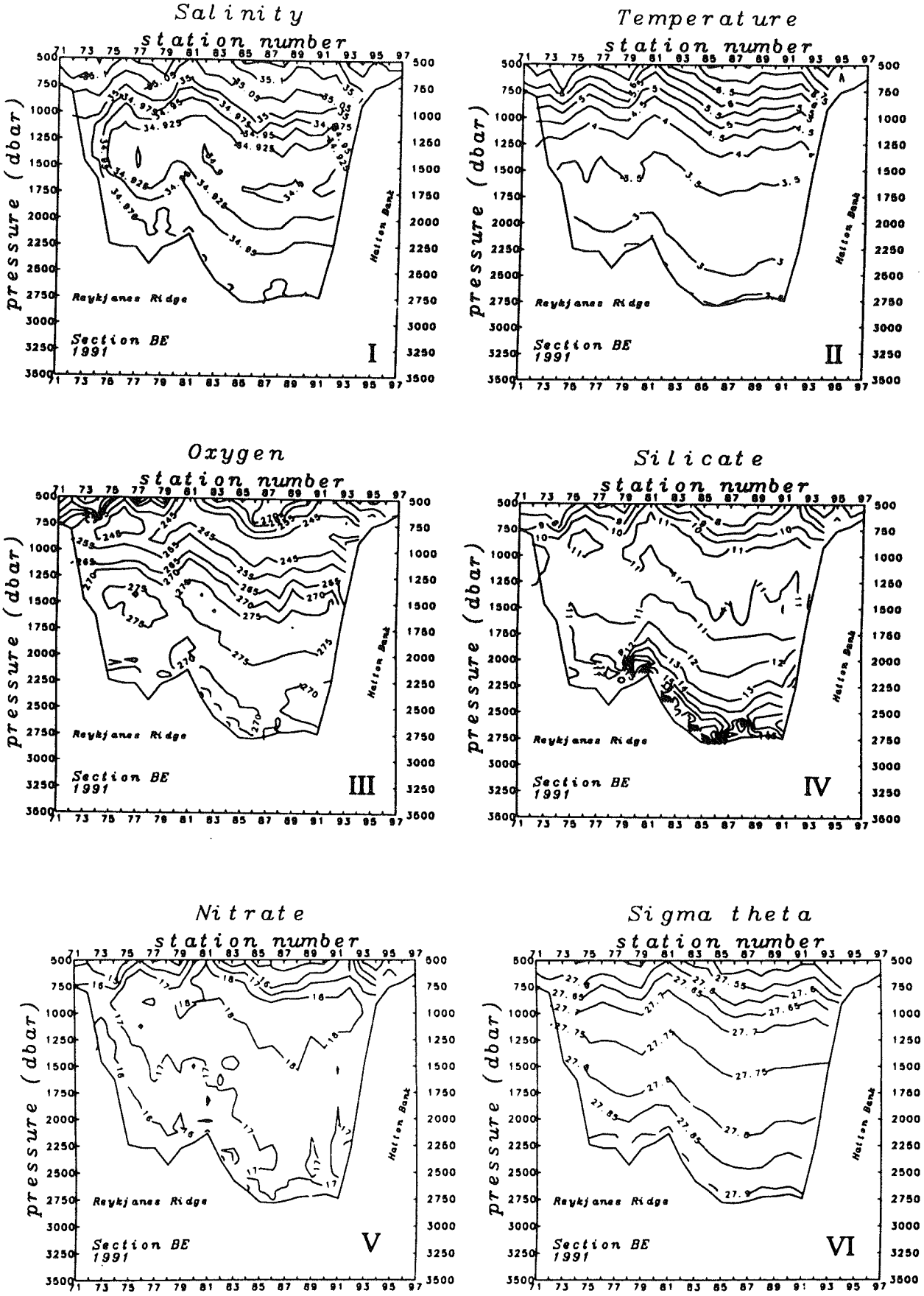

Figure 7 - Figure 7a. As Figure 4 with the data on section BE in 1991.

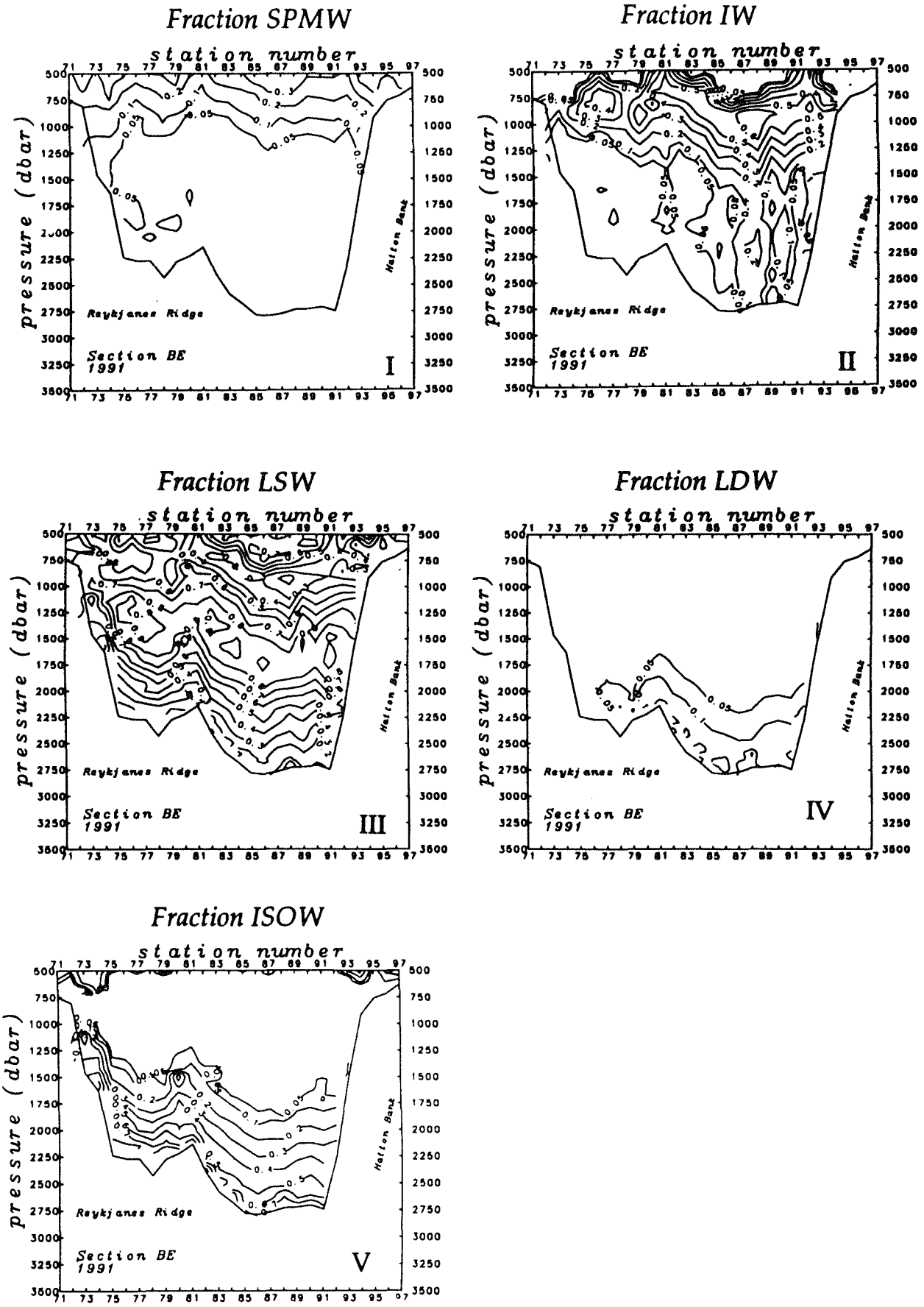

Figure 7b. As Figure 4 with the data on section BE in 1991.

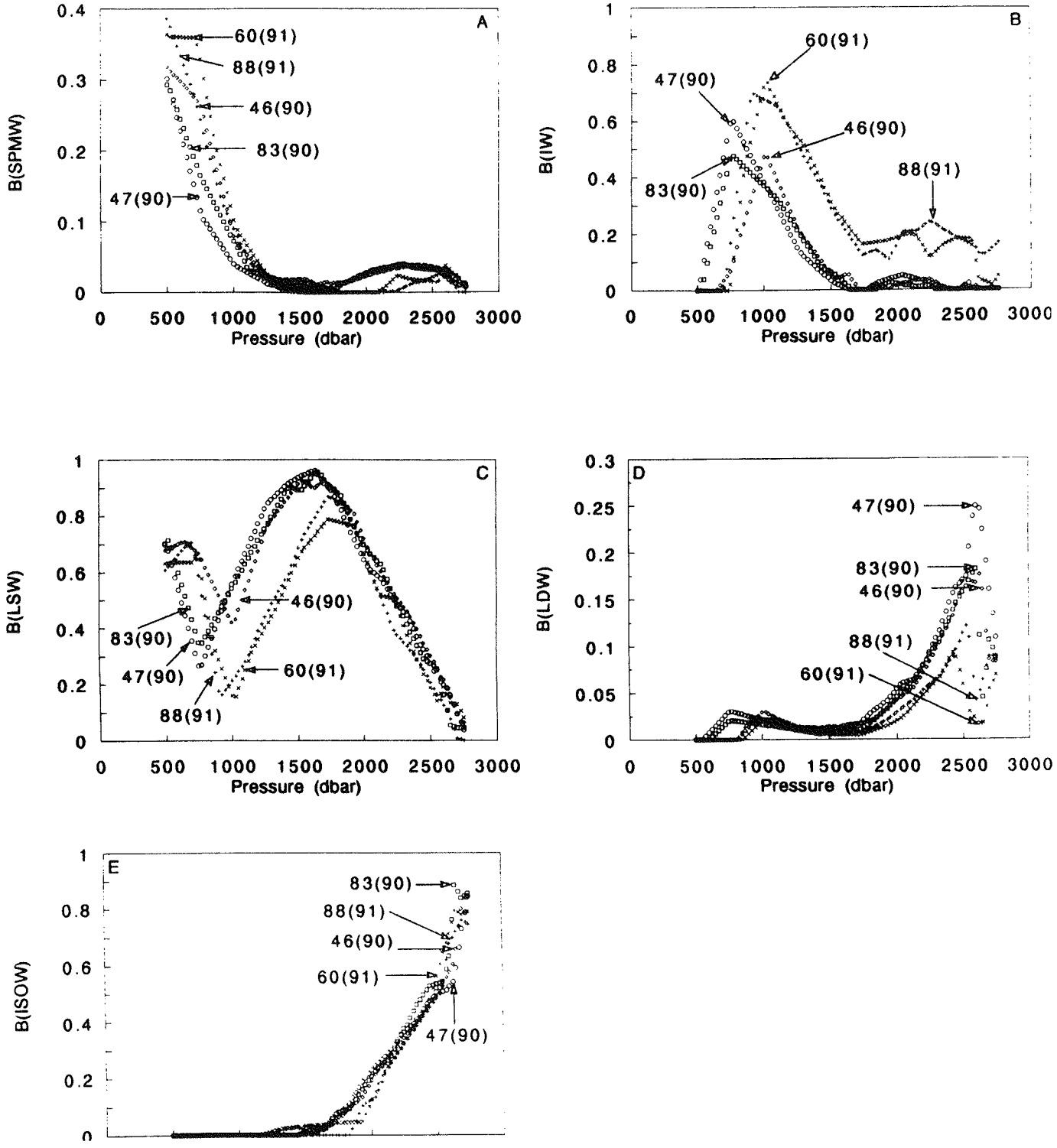

Figure 8. The contributions of the source water types on 60°N 20°W. Figure a shows the SPMW contribution, Figure b the IW contribution, Figure c the LSW contribution, Figure d the LDW contribution and Figure e the ISOW contribution. The +++ and xxx belong to the measurements in 1991. Station 88 in Figure 5 and 7 corresponds with the +++. The ooo, ◊◊◊ and □□□ are measured in 1990. The ooo corresponds with station 47 of Figure 4 and 6, the ◊◊◊ correspond with station 46 Figure 4 and 6. □□□ were measured 4 days after station 47 and 5 days before station 46. 47(90) was measured 17 July 1990; 83(90) was measured 21 July 1990; 46(90) was measured 26 July 1990; 60(91) was measured 29 April 1991 and 88(91) was measured 6 May 1991.